



**HAL**  
open science

# Asymmetric Sequential Cross-Coupling Reactions with Prochiral Zinc-Based C(sp<sup>3</sup>)-gem-Bimetallic Reagents

Federico Banchini

► **To cite this version:**

Federico Banchini. Asymmetric Sequential Cross-Coupling Reactions with Prochiral Zinc-Based C(sp<sup>3</sup>)-gem-Bimetallic Reagents. Organic chemistry. Sorbonne Université, 2024. English. NNT : 2024SORUS007 . tel-04949267

**HAL Id: tel-04949267**

**<https://theses.hal.science/tel-04949267v1>**

Submitted on 15 Feb 2025

**HAL** is a multi-disciplinary open access archive for the deposit and dissemination of scientific research documents, whether they are published or not. The documents may come from teaching and research institutions in France or abroad, or from public or private research centers.

L'archive ouverte pluridisciplinaire **HAL**, est destinée au dépôt et à la diffusion de documents scientifiques de niveau recherche, publiés ou non, émanant des établissements d'enseignement et de recherche français ou étrangers, des laboratoires publics ou privés.



SORBONNE UNIVERSITÉ

École Doctorale de Chimie Moléculaire de Paris Centre – ED406

*Institut Parisien de Chimie Moléculaire / Equipe ROCS*

## **Asymmetric Sequential Cross-Coupling Reactions with Prochiral Zinc-Based C(sp<sup>3</sup>)-Gem-Bimetallic Reagents**

Présentée par

**Federico BANCHINI**

Thèse de Doctorat de Chimie

Dirigée par le Prof. Fabrice CHEMLA et co-encadrée par le Dr. Olivier JACKOWSKI

Présentée et soutenue publiquement le 14 février 2024

Devant un jury composé du:

Dr. Jean-Luc VASSE	Université de Reims C.-A.	Rapporteur
Prof. Guillaume PRESTAT	Université Paris Cité	Rapporteur
Prof. Erwan LE GALL	Université de Paris-Est Créteil	Examinateur
Dr. Emmanuelle SCHULZ	Université Paris-Saclay	Examinatrice
Dr. Amandine GUÉRINOT	ESPCI Paris - PSL	Examinatrice
Prof. Virginie MANSUY	Sorbonne Université	Présidente du jury
Dr. Olivier JACKOWSKI	Sorbonne Université	Co-Encadrant de thèse
Prof. Fabrice CHEMLA	Sorbonne Université	Directeur de thèse



*Dedicato ai miei Genitori:*

*Se siete orgogliosi di me, siatelo soprattutto di voi stessi come genitori.  
Oltre ad avermi donato la vita, il dono più bello è stato  
avervi sempre lì accanto a me, come mio punto di riferimento.  
Tutto ciò che ho compiuto nella mia esistenza sarebbe stato nulla senza il vostro supporto.  
Questa tesi è il regalo che io faccio a voi.*

*Dedicated to my parents:*

*If you are proud of me, be proud first and foremost of yourselves as parents.  
Besides giving me life, the most beautiful gift has been  
having you always there by my side, as my true North.  
Everything I have achieved in my existence would have meant nothing without your support.  
This thesis is my gift to you.*



*"...All we have to decide is what to do  
with the time that is given to us."*

–Gandalf  
(The Lord of the Rings)





# ACKNOWLEDGEMENTS

Firstly, I would like to acknowledge the members of the jury for honouring me by accepting to examine and evaluate my work.

Afterwards, I want to express my sincere appreciation to my three supervisors, **Prof. Fabrice Chemla** and **Dr. Olivier Jackowski** and **Dr. Alejandro Perez-Luna**. Without their guidance, none of this would have been achievable. I am grateful for the opportunity they provided me to undertake this project and to be a part of their research group. Our discussions over these three years have significantly contributed to my growth, not just as a scientist, but primarily as an individual.

A heartfelt acknowledgment is reserved for **Alejandro**, who consistently made time for everyone. Your leadership of this group, always accompanied by patience, kindness, and your fantastic sense of humor, has consistently contributed to creating a serene atmosphere in the lab.

I would like to also thank **Prof. Erwan Le Gall**, **Dr. Marc Presset**, and **Baptiste Leroux** at the *Institut de Chimie et des Matériaux Paris-Est* (ICMPE), for their collaboration on our project. I appreciate all the meetings we have had and the collaborative efforts in advancing our mutual research together.

I am extremely grateful to all my current and past lab mates of the ROCS Team, my dearest friends during my PhD. Their presence significantly enriched my experience, making it truly special. **Ruben** (Rubenito), my Spanish friend. Thank you for all the moments we spent together, booking both the GC and HPLC for each other. I never surpassed your outstanding enantiomeric excess, but in the end, it does not even matter because neither of us succeeded in publishing in *Angewandte Chemie*. Thanks for introducing me to Bad Bunny and all your reggaeton music. **Gredy**, my partner in late-night work. Thank you for your hilarity and your nonsensical humor that perfectly complemented mine. Together, we laughed like crazy over the silliest things, just like kids. I'll never forget the first time I rode a roller coaster, with you sitting next to me, laughing so hard throughout the entire ride because I was screaming and swearing out of fear. **Tingting** (Ting<sup>2</sup>), my Chinese mate. Your daily smile and kindness brightened our office. I truly missed you in the recent period when you returned to China. The office seemed a bit dimmer without your light. I genuinely hope for the chance to see you again one day, perhaps sharing a meal in Beijing. **Jassmin**, **Anna**, and **Simona**, my Italian "3 Marie". I cherished the time when all three of you were here; I fondly call that time 'The Golden Age.' We were incredibly happy together, sharing wonderful moments both in and outside the lab. Thank you for the times we spent at "La Fac", and then moving to other places to continue our gatherings. I still deeply miss you all, and I often find myself longing to go back to those days. Anyway, thank you for sweetening this nightmare called PhD. **Alessia**, now a part of the new \$CASCH\$ Team. Despite occasional disagreements, I appreciate all the moments we shared in the labs, complaining about the dirty



glassware and the greasy contaminations in our NMR spectra. **Lorenzo**, the quiet boy. You are one of the most laid-back people I have ever met, and honestly, that is a great attitude. But trust me, try speaking a little louder sometimes! Thank you for all the breaks we have had together, always with your cup of tea. I will never forget your fantastic pumpkin costume at Mika's Halloween Party. I hope you will excel in your germanium chemistry, even if it is not as good as the zinc one! **Arturo** (Arturito), my memes mate, now part of the \$CASCH\$ Team. Thank you for sharing the most hilarious and ridiculous memes with me, the ones I enjoyed the most. Also, thanks for always messing around with me, especially when it came to the spicy food I cannot handle. I hope you will achieve excellent results for your project, you truly deserve it. **Fabio**, my Italian friend in the MACO team. Thank you for your kindness and availability, especially when I constantly came to you to ask for chemicals. Thanks for everything, particularly for listening to all my bulls\*\*t. **Valentin**, my multilingual mate. Keep practicing your Italian because it is superb; you speak it better than many native Italians! You have just embarked on the (scary) adventure of the PhD, so good luck! I am sure you will do great. Without naming specific individuals due to the multitude, I would like to sincerely thank all the interns who contributed to our labs. However, I do want to express special gratitude to **Erwan** and **Charis** for their remarkable contributions to my project. Thank you both for your hard work. Lastly, I want to extend my deepest appreciation to the following three individuals who mean a lot to me, and without whom this adventure would not be so extraordinary. **Ichrak**, your presence in the office has meant more than just having a colleague – it has been a shared journey packed with debates, laughter, and chaos. Thank you for writing our manuscripts together, because with you in the office, the hell of editing became a bit more bearable. Of course, thank you for all the silly questions you asked, which demanded equally silly answers from me... good job, you f\*\*ked up my mental health. I will admit, at times, you pushed me to the brink of burnout, and for a moment, I contemplated stabbing you with the nearest pen on my desk. Nevertheless, together we have formed this wonderfully nonsensical and unique friendship. Of course, I will miss you immensely, but as everything in life, good things must come to an end. Zoe and I will plan to visit Tunisia as soon as we can, so just wait for us! **Marco** (Markito), you were the very first person I met when I arrived in Paris. Right from the start, I considered you my closest lab mate. I genuinely value every moment we shared discussing our chemical queries and supporting each other. With you in the lab, I really improved as chemist. Thank you for your kindness in and outside the lab, you have been a pillar for both. Thank you also for the countless beers you offered and the times you nudged me to go to the pub, even when I was hesitant. I will always remember our Friday evenings at “La Fac”, where we drank and laughed so hard. I wish you all the best for your future, and please, next time do not rent an apartment without asking first if there is already a family of rats living there! **Mikaël**, my zinc-mate. Firstly, thank you for being the sole companion sharing a similar project in zinc chemistry with me. We both comprehend the challenges of this particular branch of organometallic chemistry, but I firmly believe that it has been an incredible learning experience, especially for you. Keep persisting, despite the numerous hurdles you might encounter while chasing your dreams. I have

no doubt that one day you will become an outstanding researcher and professor. Moreover, thank you for all the French insights you have shared, be it about language, food, or more. If more French people were like you, France would undoubtedly be the best country in the world (even though I am aware you already believe it is!). I also love our discussions about anime during our lab work and the fantastic music we listened to. I could not have wished for a better lab mate.

My also want to express my appreciation to all the permanent members of the ROCS Team, including **Giovanni, Julie, and Myriam**. In this context, special thanks to **Alexandre**, who consistently provided support to everyone and for everything. His extensive knowledge in chemistry, coupled with his immense kindness, was a constant presence that made a significant impact. Thank you, Alexandre, for contributing to maintaining a positive and joyful atmosphere in the laboratory.

I would like to extend my appreciation to the staff of the experimental platform at the institute. With their kindness, they have consistently been incredibly helpful and accommodating, always available to address my inquiries and meet all my measurement requirements. For these reasons, special thanks go to **Omar Khaled, Claire Troufflard, Règina Maruchenko, and Gilles Clodic** for their exceptional support.

To all my friends in Livorno (Italy): **Lorenzo, Ginevra, Marco, Sara B., Checco, Flavio, Sara N., Tommaso** (Pisto), **Alessio** (Berto), **Beatrice, Matilde** and **Fonzie**. It would take too long to adequately express my gratitude to this group, and truthfully, you already know how much each of you means to me. From the depths of my heart, thank you for everything you have done for me. Even though we did not get to see each other frequently over these three years, I deeply appreciate that every time I returned to Livorno, even for a brief visit, you always made time to spend with me.

To the main pillar of my life... **my family**. Thanks to my grandparents and uncles who have always believed in me and encouraged me to give my best, no matter what. To my loving (?) siblings **Iacopo, Cristina, Matteo, and Tommaso**, with whom I share a beautiful relationship of both love and hate. Thank you for your affection and your teasing sarcasm, for growing up with me and giving me priceless memories of my childhood and adolescence. And obviously an immense thank you goes to my **Parents**, for their unconditional love and unwavering support. You have given me everything, sparing nothing for yourselves, always placing me at the center of your lives. I can never repay all that you have done for me, but if this thesis makes you proud of me, perhaps it can be a small beginning. I could not have wished for better parents than you. If, one day, I were to become a parent, I could only aspire to be like, knowing that I would never match up to your example.

Finally, I want to take a moment to acknowledge and commend the person who has undoubtedly been my greatest support during these challenging three years. Moving forward, I will write in Italian, unconcerned by whether others understand or not, because the following words are solely for you, **Zoe:**

*Da quando ho deciso di venire a Parigi per intraprendere questo dottorato, ti ho coinvolto in una relazione a distanza. Un tipo di relazione che non avresti mai voluto, e una distanza che ti ha sempre spaventato. Ma hai saputo farti carico di questo fardello e mi hai promesso che ci avremmo provato insieme, e che saresti stata al mio fianco pronta a supportarmi da oltre 1000 km di distanza. Non solo hai mantenuto la tua promessa, ma hai fatto molto di più. Sei stata le fondamenta di questa mia esperienza. Nei giorni più bui eri l'unica in grado di strapparmi un sorriso. E nei momenti di gioia, quando i miei sforzi davano frutto, eri la prima persona a cui mi rivolgevo, perché eri la prima che volevo rendere orgogliosa. Solo tu sapevi dare un tocco speciale alle mie vittorie. Ogni volta che potevi, non hai esitato a fare le valigie e venire a trasferirti da me per mesi, nonostante tutta la tua vita fosse a Livorno. E quando eri qui, Parigi diventava splendida, colorata, e radiosa ai miei occhi. Ma quando ripartivi, tornava ad essere grigia, sterile, e monotona. Hai messo da parte, o perfino rinunciato, ad impegni e passioni che amavi. Hai sempre voluto mettermi al primo posto, e l'hai sempre fatto di tua spontanea volontà, a prescindere da tutto. In questi tre anni mi hai reso una persona migliore, e il solo stare con te mi sprona ad esserlo. Non basterebbe tutta la carta di questo mondo per mettere nero su bianco quanto il tuo supporto in questa avventura abbia significato per me. Se potessi scrivere un secondo autore su questa tesi, non esiterei a scrivere il tuo nome. Per tutto quello che mi hai aiutato, questo lavoro è in parte anche tuo. Spero un giorno di riuscire a ripagarti di tutto l'affetto e la fiducia che hai riposto in me. Per ora posso solo dirti: grazie infinite.*





# LIST OF PUBLICATIONS

Parts of this Ph.D. thesis have been published:

1) **"Enantioselective Sequential Catalytic Arylation-Fukuyama Cross-coupling of 1,1-Biszincioalkane Linchpins"**

Federico Banchini, Baptiste Leroux, Prof. Dr. Erwan Le Gall, Dr. Marc Passet, Dr. Olivier Jackowski,\* Prof. Dr. Fabrice Chemla,\* Dr. Alejandro Perez-Luna,\* *Chem. Eur. J.* **2023**, *29*, e202301084.

2) **"Stereoselective Double Functionalization of Geminated C(sp<sup>3</sup>)-Organodimetallic Linchpins"**

Federico Banchini, Baptiste Leroux, Prof. Dr. Erwan Le Gall, Dr. Marc Passet, Dr. Olivier Jackowski,\* Prof. Dr. Fabrice Chemla,\* Dr. Alejandro Perez-Luna,\* *ChemCatChem* **2024**, *16*, e202301495.







# TABLE OF CONTENTS

ACKNOWLEDGEMENTS.....	7
LIST OF PUBLICATIONS .....	13
LIST OF ABBREVIATIONS.....	22
<b>GENERAL INTRODUCTION</b> .....	25
<b>PART I: BIBLIOGRAPHIC OVERVIEW</b> .....	31
1. C(sp <sup>3</sup> )-Geminated Organobimetallics Overview.....	33
1.1. C(sp <sup>3</sup> )-Geminated Organobimetallics Introduction.....	33
1.2. Enantioselective Sequential Reactions of <i>Gem</i> -Bimetallic Reagents: An Underexplored World.....	35
1.3. <i>Gem</i> -Diboryl Reagents.....	36
1.3.1. Chiral Non-Racemic <i>Gem</i> -Diboryl Reagents.....	36
1.3.2. Achiral <i>Gem</i> -Diboryl Reagents.....	39
1.4. <i>Gem</i> -Borylsilyl Reagents.....	45
1.4.1. Racemic <i>Gem</i> -Borylsilyl Reagents.....	45
1.4.2 Chiral Non-Racemic <i>Gem</i> -Borylsilyl Reagents .....	45
1.5. <i>Gem</i> -Silyl Grignard Reagents.....	50
1.6. <i>Gem</i> -Borylzirconio Reagents .....	51
1.6.1. Racemic <i>Gem</i> -Borylzirconio Reagents.....	51
1.6.2. Chiral Non-Racemic <i>Gem</i> -Borylzirconio Reagents.....	52
1.7. <i>Gem</i> -Borylzinc Reagents.....	53
1.7.1. Racemic <i>Gem</i> -Borylzinc Reagents .....	53
1.7.2. Chiral Non-Racemic <i>Gem</i> -Borylzinc Reagents .....	58
1.8. <i>Gem</i> -Zinczirconio Reagents .....	59
1.9. <i>Gem</i> -Dizinc Reagents.....	60
1.9.1. Synthesis of <i>Gem</i> -Dizinc Reagents.....	61
1.9.1.1. Synthesis <i>via</i> Gaudemar/Normant Carbometallation Coupling .....	61
1.9.1.2. Synthesis <i>via</i> Metal Insertion of <i>Gem</i> -Dihalogen Compounds .....	67
1.9.1.2.1. Synthesis of Bis(iodozincio)methane.....	67
1.9.1.2.2. Synthesis of <i>Gem</i> -Dizincioalkanes .....	69
1.9.1.2.3. Synthesis of Heteroatom-Substituted <i>Gem</i> -Dizincio Reagents.....	71
1.9.1.3. Synthesis <i>via</i> Metal–Halogen Exchange.....	72
1.9.2. Reactivity of <i>Gem</i> -Dizinc Reagents.....	72
1.9.2.1. Olefination Reaction .....	73
1.9.2.1.1. Methylenation .....	73

1.9.2.1.2. Alkylidenation with <i>Gem</i> -Dizinc Reagents Synthesized <i>via</i> Metal Insertion of <i>Gem</i> -Dihalogen Compounds .....	75
1.9.2.1.3. Alkylidenation with <i>Gem</i> -Dizinc Reagents Synthesized <i>via</i> Carbometallation.....	76
1.9.2.4. Nucleophilic Cyclopropanation .....	76
1.9.2.4.1. Nucleophilic Cyclopropanation with <i>Gem</i> -Dizinc Reagents Synthesized <i>via</i> Carbometallation.....	77
1.9.2.4.2. Nucleophilic Cyclopropanation with Bis(iodozincio)methane .....	77
1.9.2.4.3. Nucleophilic Cyclopropanation with Bis(iodozincio)iodomethane .....	81
1.9.2.3. Sequential S <sub>N</sub> i–Eletrophilic Substitution .....	82
1.9.2.2. Sequential Reactions with Two Electrophiles .....	83
1.9.2.2.1. Sequential Reactions of <i>Gem</i> -Dizinc Reagents Prepared <i>via</i> Carbometallation .....	83
1.9.2.2.2. Sequential Reactions with Bis(iodozincio)methane .....	84
1.9.2.2.3. Sequential Reactions with 1,1-Bis(iodozincio)ethane .....	92
1.9.2.2.4. Sequential Reactions with $\alpha$ -Hetero-substituted <i>Gem</i> -Dizinc Reagents.....	94
2. Configurational Stability of Organozinc Compounds .....	95
2.1. General Dynamic Behaviour of Organozinc Compounds .....	95
2.2. Inversion of Carbon–Zinc Bond .....	96
2.2.1 Primary Alkylzinc Compounds .....	97
2.2.2. Secondary Alkylzinc Compounds.....	99
2.2.3. Secondary Benzylzinc Compounds .....	103
2.2.4. C(sp <sup>2</sup> )–Zn Bond: Vinylzinc Compounds.....	105
2.2.5. Allyl- and Propargylzinc Compounds.....	105
3. Conclusion .....	107
<b>PART II: RESULTS AND DISCUSSION</b> .....	109
1. Enantioselective Sequential Catalytic Arylation-Fukuyama Cross-coupling of 1,1-Bis(zincio)alkanes .....	111
1.1. Purpose and Objective of the Project.....	111
1.2. Synthesis of 1,1-Bis(iodozincio)ethane.....	114
1.3. Synthesis of Thioesters.....	115
1.4. Synthesis of Ligands.....	116
1.4.1. Synthesis of P[3,5-(CF <sub>3</sub> ) <sub>2</sub> C <sub>6</sub> H <sub>3</sub> ] <sub>3</sub> (L17) for the Arylation Reaction .....	116
1.4.2. Synthesis of Enantiopure L21 for the Enantioconvergent Fukuyama Cross-Coupling .....	116
1.5. Preliminary Studies.....	117
1.6. Optimization Pd-Catalyzed Arylation Reaction of 1,1-Bis(iodozincio)ethane .....	120
1.7. Concluding Remarks on the Pd-Catalyzed Arylation Reaction of 1,1-Bis(iodozincio)ethane.....	126
1.8. Optimization of the Enantioselective Sequential Arylation/Fukuyama Cross-Coupling Reaction of 1,1-Bis(iodozincio)ethane .....	127

1.9. Scope of the Enantioselective Sequential Arylation/Fukuyama Cross-Coupling Reaction of 1,1-Bis(iodozincio)ethane .....	133
1.9.1. Variation of (Hetero)Aryl Iodide .....	133
1.9.2. Variation of Thioester .....	135
1.10. Mechanistic Studies: KR or DKR? .....	136
1.11. Potential Pharmaceutical Application: Naproxen Synthesis .....	141
1.12. Enantioselective Sequential Arylation/Fukuyama Cross-Coupling Reaction with Other 1,1-Biszincioalkanes .....	144
1.12.1. Enantioselective Sequential Arylation/Fukuyama Cross-Coupling Reaction with Silyl-Substituted <i>Gem</i> -Dizincio Reagents .....	150
1.13. Enantioselective Sequential Intramolecular Arylation–Fukuyama Cross-Coupling Reaction .....	151
1.14. Partial Conclusion .....	156
2. Enantioselective Sequential Double Allylation of $\alpha$ -Silyl-Substituted <i>Gem</i> -Dizinc Reagents .....	157
2.1. Asymmetric Allylation: Introduction .....	157
2.2. Asymmetric Allylation of Organozinc Reagents .....	158
2.3. Enantioselective Allylation of <i>Gem</i> -Dizinc Reagents .....	162
2.4. Objectives and Purpose of the Project .....	163
2.5. Synthesis of 1,1-Bis(bromozincio)trimethylsilylmethane .....	164
2.6. Preliminary Studies .....	165
2.7. Screening of Chiral Ligands for the Pd-Catalyzed Allylation of $\text{Me}_3\text{SiCH}(\text{ZnBr})_2$ with Cinnamyl Chloride .....	166
2.8. Screening of Chiral Ligands for the Pd-Catalyzed Enantioselective Allylation of $\text{Me}_3\text{SiCH}(\text{ZnBr})_2$ with Ethyl 2-(Bromomethyl)acrylate .....	168
2.9. Screening of Cu-Salts for the Enantioselective Allylation of $\text{Me}_3\text{SiCH}(\text{ZnBr})_2$ with Ethyl 2-(Bromomethyl)acrylate .....	170
2.10. Investigation on the Complete Absence of Enantiomeric Excess .....	172
2.10.1. Investigation of the Metal/Ligand-Free Nature of Allylation Reaction of $\text{Me}_3\text{SiCH}(\text{ZnBr})_2$ .....	172
2.10.2. Investigation on the Stereospecificity of Iodination Reaction .....	173
2.10.3. Investigation on the Configurational Stability of the $\alpha$ -Silyl Organozinc Intermediate .....	175
2.10.3.1. Negative Hyperconjugation Effect .....	175
2.10.3.2. Effect of $\alpha$ -Heteroatoms on Configurational Stability in Organolithium and Organozinc Compounds .....	176
2.10.3.3. Preliminary Studies .....	177
2.10.3.4. Investigation Using NMR Spectroscopy and Chiral Solvating Agents .....	178
2.10.3.5. Racemisation Rate .....	182
2.11. Partial Conclusion .....	184
<b>GENERAL CONCLUSION AND PERSPECTIVES .....</b>	<b>186</b>

<b>PART III: EXPERIMENTAL SECTION</b> .....	193
3.1. General Information .....	195
3.2. Preparation of Inorganic Salts in THF Solution .....	196
3.3. Preparation of 1,1-diiodo alkanes .....	197
3.4. Preparation of 1,1-Bis(iodozincio)alkanes.....	206
3.4.1. General Procedure for the preparation of 1,1-Bis(iodozincio) Alkanes (GP1) .....	206
3.5. Synthesis of Ligands.....	208
3.6. Preparation of secondary Benzylzinc Halides <i>via</i> Reductive Zincation .....	212
3.7. Preparation of Thioesters .....	216
3.7.1. General Procedure for the Preparation of Thioesters (GP2).....	216
3.8. Preparation of Aryl Iodides.....	222
3.9. Racemic Sequential Catalytic Arylation–Electrophilic Substitution of 1,1-Bis(iodozincio)alkanes ....	224
3.9.1 Catalytic Arylation–Iodolysis of 1,1-Bis(iodozincio)ethane .....	224
3.9.2. Catalytic Arylation–Cu-Mediated Allylation .....	225
3.9.2.1. General Procedure for the Sequential Pd-Catalyzed Arylation–Cu-Mediated Allylation of 1,1- Bis(iodozincio)alkanes (GP3) .....	225
3.9.3. Synthesis of Enantioenriched $\alpha$ -Disubstituted ketones .....	228
3.9.3.1. General Procedure for the Pd-Catalyzed Enantioselective Sequential Arylation–Fukuyama Cross-Coupling of 1,1-Bis(iodozincio)alkanes (GP4) .....	228
3.10. Synthesis of Bis(bromozincio)trimethylsilylmethane .....	263
3.11. General Procedure for the Enantioselective Sequential Allylation–Iodolysis (GP5) .....	264
3.12. General Procedure for the Enantioselective Sequential Double Allylation (GP6).....	266
3.13. Preparation of $\alpha$ -Silyl Organozinc ( $\pm$ )-240-I in THF- <i>d</i> 8 .....	270
REFERENCES.....	271





## LIST OF ABBREVIATIONS

Ac	acetyl
aq	aqueous
Ar	aryl
APCI	atmospheric pressure chemical ionization
ATR	attenuated total reflection
B(dan)	naphthalene-1,8-diaminoboryl
B(mac)	<i>syn</i> -1,2-dimethyl-1,2-dihydroacenaphthylene-1,3,2-dioxaboryl
Bn	benzyl
B(nep)	5,5-dimethyl-1,3,2-dioxaboryl
Boc	<i>tert</i> -butyloxycarbonyl
B(pin)	4,4,5,5-tetramethyl-1,3,2 dioxaboryl
<sup>n</sup> Bu	buthyl
<sup>t</sup> Bu	<i>tert</i> -buthyl
Cbz	benzyloxycarbonyl
CuTC	copper(I) thiophene-2-carboxylate
<i>m</i> -CPBA	<i>m</i> -chloroperoxybenzoic acid
DABCO	1,4-diazabicyclo- [2.2.2]octane
DCM	dichloromethane
dba	dibenzylideneacetone
DBU	1,8-diazabicyclo- [5.4.0]undec-7-ene
DCE	1,2-dichloroethane
DIBAL-H	diisobutylaluminium hydride
DIAD	diisopropyl-azodicarboxylate
DKR	dynamic kinetic resolution
DME	1,2-dimethoxyethane
DMF	dimethylformamide
DMI	1,3-dimethyl-2-imidazolidinone
DMSO	dimethyl sulfoxide
dr	diastereomeric ratio
ee	enantiomeric excess
equiv	equivalent
er	enantiomeric ratio
es	enantiospecificity
ESI	electrospray ionization
Et	ethyl
FGI	functional group interconversion
GC	gas chromatography
GP	general procedure
h	hour
HMPA	hexamethylphosphoramide

HPLC	high-performance liquid chromatography
HRMS	high resolution mass spectrometry
Hz	Hertz
IR	infra-red
KR	kinetic resolution
LDA	lithium di-isopropylamide
LED	light emitting Diodes
LG	leaving group
LiDBB	lithium di- <i>tert</i> -butylbiphenylide
LiHMDS	lithium bis(trimethylsilyl)amide
M	molarity
Me	methyl
<i>n.d.</i>	not detected
<i>n.r.</i>	no reaction
<sup>n</sup> Pr	propyl
<sup>i</sup> Pr	iso-propyl
min	minute
MOM	methoxymethyl
m.p.	melting point
MTBE	methyl <i>tert</i> -butyl ether
MW	molecular weight
NaHMDS	sodium bis(trimethylsilyl)amide
NMO	N-methylmorpholine-N-oxide
NMR	nuclear magnetic resonance
OTf	trifluoromethanesulfonyl
PCC	pyridinium chlorochromate
Ph	phenyl
ppm	parts per million
rt	room temperature
TBAF	tetrabutylammonium fluoride
TBS	<i>tert</i> -butyldimethylsilyl
THF	tetrahydrofuran
THT	tetrahydrothiophene
TLC	thin layer chromatography
TM	transition metal
TMEDA	tetramethylethylenediamine
TMS	trimethylsilyl
TS	transition state
Ts	4-toluenesulfonyl
UV	ultraviolet
9-BBN	9-Borabicyclo[3.3.1] nonane





# **GENERAL INTRODUCTION**

---



Nature is capable to build highly complex natural products in iterative manner and with superlative efficiency and perfect stereochemical control, from very simple molecules. Chemists all over the world have tried to mimic the extreme synthetic ability of nature for more than a century. Nevertheless, the weakness and imperfection of classical synthetic procedures lie in the multistep sequences using monofunctional reagents, which usually lead to a slight molecular structure augmentation of the starting compounds, together with isolation and purification at each stage of the synthesis, leading to feeble material improvement and to the contrary large amounts of organic waste.

Anyway, the pursuit of creating tools for the streamlined and selective construction of intricate molecular structures with minimal chemical steps is a fundamental goal in organic synthesis, and it offers promising prospects for addressing the synthetic inefficiencies mentioned above. In this context, the application of specific synthetic linchpins, which are chemical species with multiple reactive sites, facilitating a series of consecutive reactions without the need for isolation and purification at each stage of the synthesis, stands out as one of the most potent strategies. In the specific, organo-multi-metallic compounds capable of participating sequentially in multiple electrophilic substitution reactions seem exceptionally well-suited for this purpose.

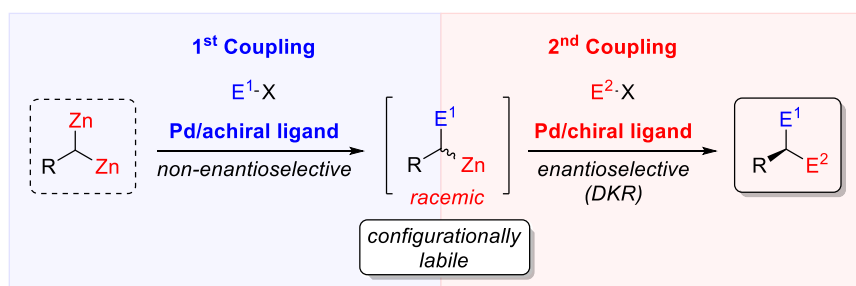
In this diversity-oriented synthesis, there has been a notable focus on geminated C(sp<sup>3</sup>)-organodimetallic species. They are anticipated to serve as bis-nucleophilic components in various reaction pathways, enabling the formation of densely 1,1-disubstituted carbon centers through sequential interactions with two electrophilic partners. While this type of organobimetallic compounds have been known for a long time, it is only in recent decades that their reactivity has gained significant attention. Nowadays, the opportunity for them to participate in consecutive reactions with electrophiles is well-established and has been reported for various di-nucleophilic reagents, such as 1,1-diborioalkanes and 1,1-dizincioalkanes, which have been particularly well-utilized. To a lesser extent, mixed 1,1-borylzirconioalkane, and 1,1-borylzincioalkanes have also been well-explored. Conversely, achieving these sequences in enantioselective fashion remains a major challenge. While various examples of enantioselective bifunctionalization have been reported for the *gem*-bimetallic compounds mentioned above, only one example has been reported for *gem*-dizinc reagents before this work, and the enantiomeric excess (ee) of the final product is very low.

Within this framework, the specific aim of this project was to bridge this significant gap in the literature and *develop novel, highly efficient enantioselective sequential cross-coupling reactions using prochiral gem-dizinc compounds.*

The initial segment of this manuscript is devoted to a thorough and inclusive literature review on the chemistry of geminated C(sp<sup>3</sup>)-organobimetallic reagents in asymmetric organic synthesis, placing special emphasis on their sequential bifunctionalization. It also explores the potential for post-functionalization to create complex molecules of interest with biologically relevant applications, such as pharmaceuticals and agrochemicals. In addition, a dedicated part on the configurational behaviour of organozinc compounds is discussed.

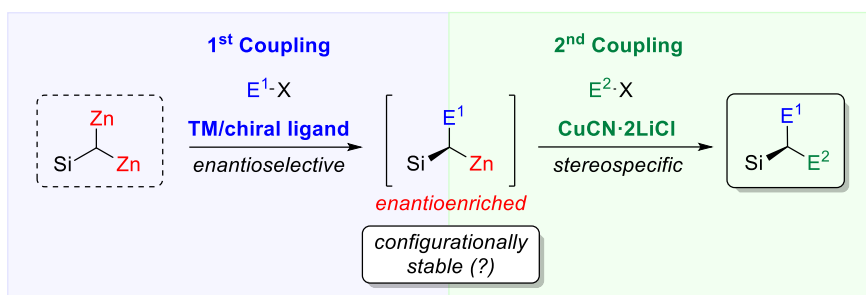
The second part of the manuscript is divided into *two distinct sections, both focusing on the development of enantioselective sequential cross-coupling reactions using gem-dizinc reagents.*

In the first section, we investigate two catalytic C–C bond-forming reactions employing prochiral 1,1-bis(iodozinc)alkanes in the same pot, utilizing two distinct palladium-based catalytic systems. The first reaction, non-enantioselective, results in the formation of configurationally labile secondary benzylzinc species from an achiral precursor, while the second reaction is enantioconvergent, effectively achieving a highly efficient dynamic kinetic resolution (DKR) of racemic intermediates (**Scheme GI-1**). This strategy, new in the area of asymmetric synthesis through two consecutive electrophilic substitution reactions of geminated C(sp<sup>3</sup>)-organobimetallics, provides a valuable methodology for producing complex molecules with high enantiomeric purity in a modular fashion, serving as interesting building blocks.



**Scheme GI-1.** Enantioselective sequential cross-coupling reaction of prochiral *gem*-dizinc alkanes in one pot through two distinct palladium-based catalytic systems.

In the second section, a leap forward is introduced by using a hetero-substituted *gem*-dizinc reagent. These hetero-substituted *gem*-dizinc reagents can be viewed as *gem*-trimetallic compounds, opening up a fascinating avenue for achieving three sequential cross-coupling reactions in a single pot. In this context, we investigated the development of enantioselective sequential cross-coupling reactions with silyl-substituted *gem*-dizinc compounds, entailing an initial enantioselective step, followed by a stereospecific copper-mediated cross-coupling (**Scheme GI-2**).



**Scheme GI-2.** Enantioselective sequential cross-coupling reaction of prochiral silyl-substituted gem-dizincio reagents (TM: transition-metal).



**PART I:**  
**BIBLIOGRAPHIC OVERVIEW**

---



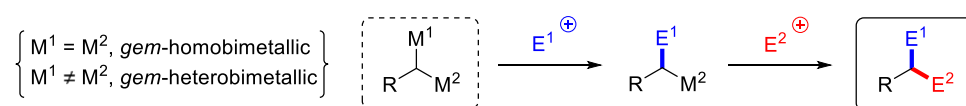


# 1. C(sp<sup>3</sup>)-Geminated Organobimetallics Overview

## 1.1. C(sp<sup>3</sup>)-Geminated Organobimetallics Introduction

Due to the overpopulation of the globe combined with persistent changes in environment and medicine, over the years there has been an increasing need of developing new synthetic strategies to produce agrochemical products and materials as well as pharmaceuticals for the humankind, in the most environmentally friendly way possible. For instance, developing tools to achieve the efficient and selective assembly of complex molecular structures with a minimum of chemical steps is a key endeavour in organic synthesis. Organo-*multi*-metallic compounds capable to react sequentially in multiple electrophilic substitution reactions, avoiding isolation and purification at each stage of the synthesis, appear ideally suited for this purpose.

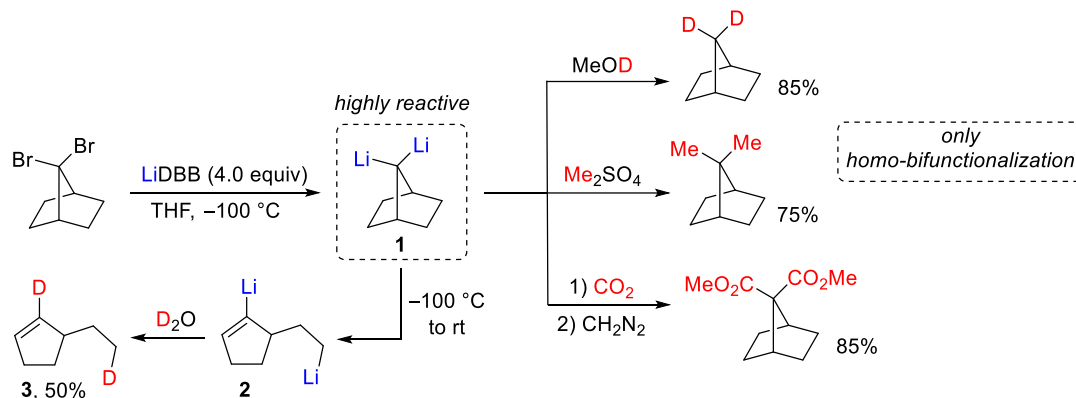
In this context, geminated C(sp<sup>3</sup>)-organobimetallics attract pursued interest. Although *gem*-organobimetallic compounds have been known for a long time, it is only in recent decades that their reactivity has garnered significant attention as powerful and versatile tools.<sup>[1]</sup> As doubly nucleophilic species (formal geminal dianion), the opportunity to be engaged in consecutive reactions with two different electrophiles and form a couple of new bonds is well established (**Scheme I-1**).



**Scheme I-1.** Consecutive reactions of C(sp<sup>3</sup>)-geminated organobimetallics with two electrophiles (*M* = metal; *E* = electrophile).

The field of geminated bimetallic organic compounds took its roots in the 1950's with the pioneering work of Wittig, West, and Ziegler in the first preparations of dilithiomethane,<sup>[2-4]</sup> although it would take a few more decades for the full chemical behaviour of these compounds to truly develop. Initially, a few examples of non-stabilized aliphatic geminal dilithium compounds, like dilithiomethane<sup>[5]</sup> and 7,7-dilithionorbornane<sup>[6]</sup> (**1**) were synthesized. These compounds were prepared by subjecting the corresponding di-haloalkanes to lithium 4,4'-di-*tert*-butylbiphenylide (LiDBB) at extremely low temperatures (−100 °C). However, these early geminal dilithium compounds posed significant challenges due to their high instability. No sequential reactions with two distinct electrophiles were reported, and only simple quenched with MeOD, CO<sub>2</sub> (followed by esterification with diazomethane), dimethyl sulfate and trimethyltin chloride were performed (**Scheme I-2**).<sup>[5,6]</sup> These reactions led to homo-bifunctionalization, limiting the synthetic versatility of these reagents. Furthermore, when these *gem*-bimetallic species were heated, they underwent degradation, such as **1**

which underwent ring opening, resulting in the formation of lithio-(lithioethyl)cyclopentene (**2**), as evidenced by the creation of the corresponding dideuterated ethylcyclopentene (**3**).



**Scheme 1-2.** Simple reactivity of non-stabilized aliphatic gem-dilithio compounds.

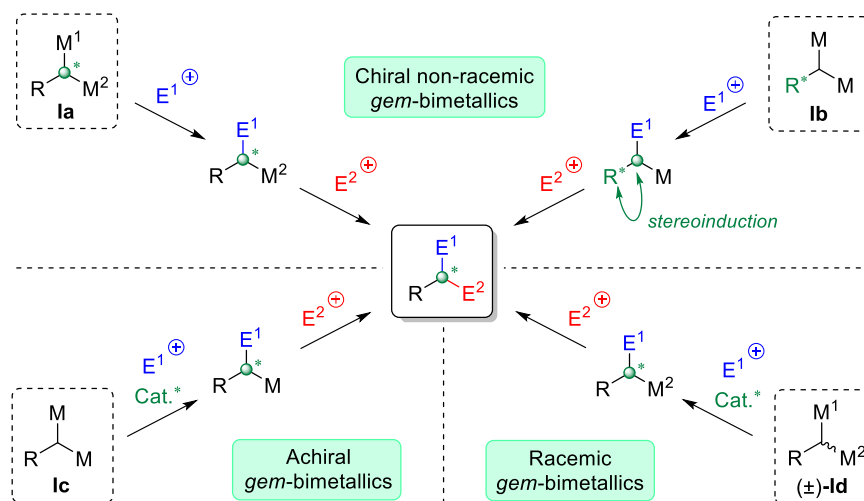
Due to the necessity of carrying out reactions at extremely low temperatures, combined with the limited reactivity observed, interest in working with compounds began to wane. However, the synthesis of *gem*-dilithio alkanes gained attention by metalating derivatives containing acidic hydrogen atoms. In this approach, strongly electron-withdrawing groups like high-valent phosphorus moieties, phenylsulfones and their derivatives, cyanide groups, etc., became essential, stabilizing the corresponding *gem*-dilithio reagents. Here, an entire world opens up, as over the years, countless examples and procedures in literature have documented this type of stabilized *gem*-dianions species in organic synthesis.<sup>[7-9]</sup> Nonetheless, the presence of these substituents in close proximity to the geminal site restricts in some way the potential versatility of these reagents in organic synthesis. Indeed, some reaction may not be possible due to the compatibility with the other reagents or the conditions of the reaction, and if these groups are unwanted in the final product, after the desired bifunctionalization they had to be converted or removed, leading to an increase in chemical step number, materials, financial resources invested, and a higher ecological impact.

In light of these considerations, the bibliography of this manuscript will not focus on stabilized *gem*-bimetallic reagents containing strongly electron-withdrawing groups, and thus completely avoiding them. Instead, it will focus on non-stabilized or poorly-stabilized *gem*-bimetallics characterized by the presence of simple hydrocarbon substituents such as alkyl, allylic, benzyl, etc. In this scenario, the field of non-stabilized geminated bimetallic organic compounds started in the 1970's with the introduction of *gem*-dizinc reagents. Subsequently, a large range of 1,1-organobimetallic species have been developed and successfully applied in various useful applications in synthetic organic chemistry. It is well established that the different reactivity and selectivity of these reagents strongly depends on the character of the metal-carbon bond providing many possibilities of organic transformation sequences beyond our imagination.

## 1.2. Enantioselective Sequential Reactions of *Gem*-Bimetallic Reagents: An Underexplored World

Enantioselective reactions constitute a vibrant domain within modern organic chemistry, and their importance cannot be emphasized enough. They play a pivotal role in the total synthesis of natural products, pharmaceuticals, and agrochemicals, all of which frequently feature multiple stereocenters.<sup>[10-12]</sup> However, the successful achievement of enantioselective reactions can be extremely complex, and harmonizing the precise construction of these stereocenters with the goal of minimizing the number of chemical steps can present significant challenges.

Building upon the earlier discussion, *gem*-bimetallic compounds could be ideal candidates for serving as building blocks in enantioselective synthesis. In fact, utilizing bifunctionalization reactions with *gem*-bimetallic compounds may offer a promising avenue for generating enantiomerically enriched products. Specifically, enantioselective tandem cross-coupling reactions with these reagents are highly sought after, as they provide a straightforward method for creating stereogenic carbons in stereocontrolled configurations. The main strategies developed so far for the development of asymmetric double electrophilic substitution employing these reagents are depicted in **Scheme I-3** and can be classified in two general groups.



**Scheme I-3.** General strategies for the asymmetric double electrophilic substitution of *gem*-bimetallic reagents.

A first group concerns the use of chiral non-racemic *gem*-bimetallic reagents; it includes derivatives chiral at the carbon bearing the geminated carbon-metal bonds (**Ia**) or reagents with stereogenic centers on the carbon backbone (**Ib**) that induce stereocontrol during electrophilic substitution reactions of prochiral *gem*-bimetallic units. For this first group, the stereoselective preparation of the requisite 1,1-bimetallic reagents has attracted most of the research efforts. The second group is the realm of asymmetric catalysis and concerns the use of achiral (**Ic**) or racemic ((±)-**Id**) derivatives

engaged in catalytic enantioselective desymmetrization or resolution reactions. These tactics rely exclusively on catalyst-controlled transformations.

However, despite these potential advantages, the use of *gem*-bimetallic reagents in enantioselective bifunctionalization reactions remains a notable challenge, with few documented examples in the literature. In the following sections, we will list and discuss these examples, categorized by the type of bimetallic compounds, with a particular focus on the potential synthetic applications that these reagents could offer.

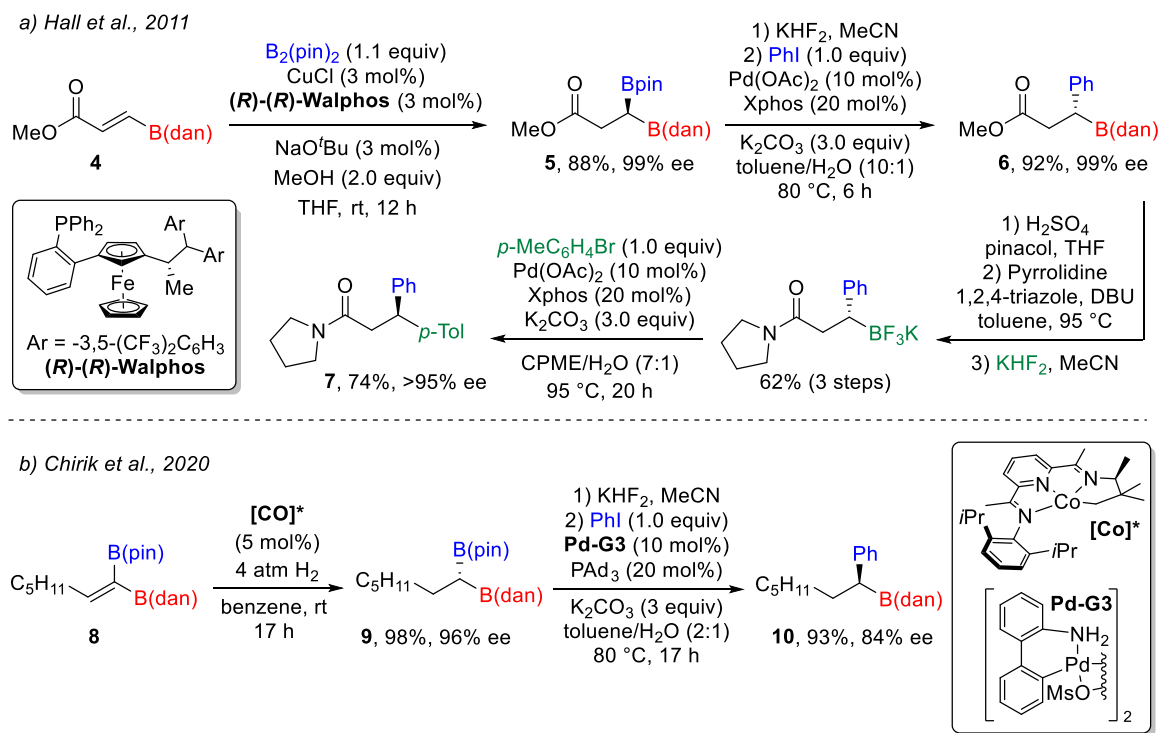
## 1.3. Gem-Diboryl Reagents

In the last decades *gem*-diborylalkanes have emerged as a distinct and promising class of bifunctional reagents capable of being engaged in a broad spectrum of chemical processes, including both transition-metal-catalyzed and transition-metal-free cross-coupling reactions, as well as other functional-group transformations.<sup>[13-15]</sup> Their chemical stability and non-toxicity allows to operate simple and safe manipulation and long-term storage.<sup>[16]</sup> However, it is worth mentioning that when employing these *gem*-bimetallic reagents, most of the bifunctionalization reactions reported in the literature are not sequential. After the first functionalization, the monometallic intermediate is isolated and purified. This leads to greater consumption of solvents, materials, and financial resources, ultimately increasing the ecological impact.

### 1.3.1. Chiral Non-Racemic Gem-Diboryl Reagents

Only a limited number of transformations involving enantiomerically enriched *gem*-diboryl alkanes have been reported. This is due to the fact that is not so easy to prepare these bimetallics in high enantiomeric purity. The first groundbreaking in this context was made by Hall, who accomplished the first efficient synthesis of a highly optically enriched *gem*-bis(boronate) reagent (**Scheme I-4a**).<sup>[17]</sup> This innovative reaction was possible through a Cu(I)-catalyzed enantioselective conjugate borylation addition of  $\beta$ -boronylacrylate **4** with bis(pinacolato)diboron, leading to the formation of 1,1-diboronate species **5** bearing two different boronyl units and exhibiting an outstanding 99% ee. With this enantiopure reagent in hands, the authors performed a chemical transformation of the B(pin) moiety by a stereospecific and chemoselective Suzuki-Miyaura coupling with aryl bromides leading to access to benzylic boronic esters **6** with inversion of configuration. Subsequently, the benzylic boronates, after necessarily converting the carboxyester unit into amide and the -B(dan) group into -BF<sub>3</sub>K, was engaged in a cross-coupling reaction with *p*-bromotoluene, leading to an enantioenriched 1,1-diarylalkane **7** (fundamental pharmacophore or bioactive module

in pesticides)<sup>[18,19]</sup> in good overall yield and excellent enantiopurity. However, in this case the bifunctionalization is tedious as it requires several manipulations of the boron substitution.

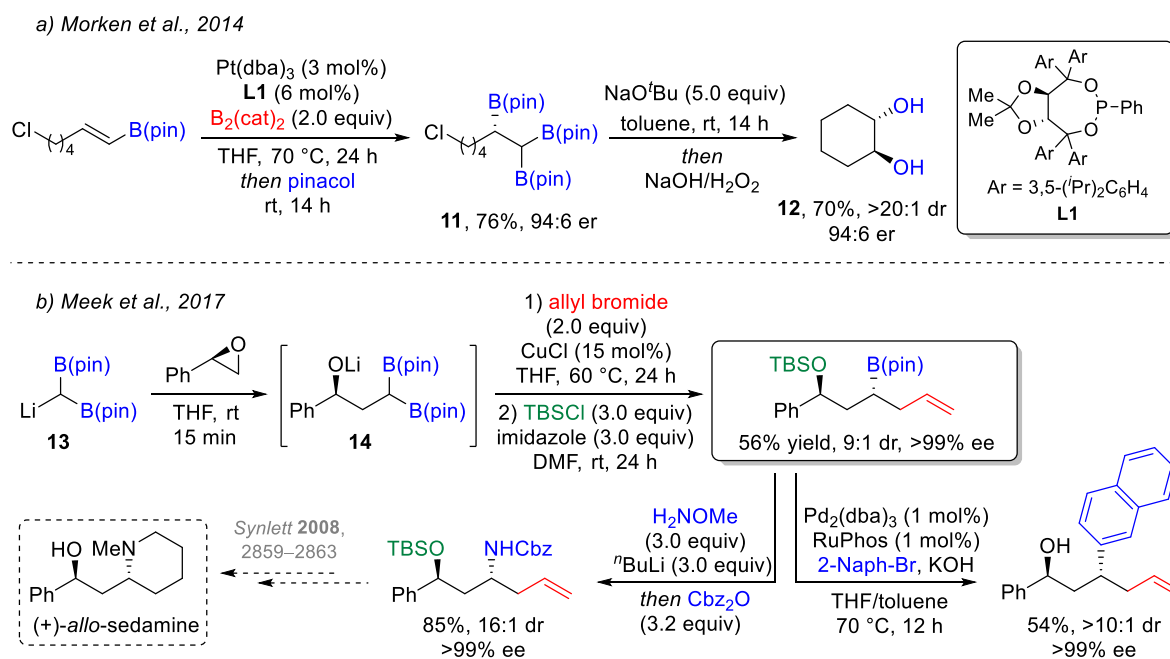


**Scheme I-4.** a) Synthesis of the first optically pure *gem*-diborylalkane via enantioselective borylation addition, and subsequent stereospecific di-arylation. b) Enantioselective hydrogenation of a 1,1-diborylalkene and subsequent stereospecific monoarylation.

Recently, Chirik reported a versatile procedure for asymmetric hydrogenation of *gem*-diborylalkenes **8** (Scheme I-4b).<sup>[20]</sup> Excellent yields and enantioselectivity of the corresponding *gem*-diborylalkanes **9** were achieved utilizing the C<sub>1</sub>-symmetric pyridine(diimine) cobalt complex **[Co]\*** along with low pressure of H<sub>2</sub>. After manipulation of the boron substitution, the authors performed a first chemoselective arylation (with stereoinversion), albeit with a small loss of enantiomeric purity (**10**). However, the authors never mentioned a second functionalization.

An alternative approach for creating chiral non-racemic *gem*-diboryl compounds involves the generation of a stereogenic center in close proximity to the geminated prochiral pattern. By leveraging this nearby stereogenic center, it becomes possible to selectively functionalize one of the boryl groups in a diastereoselective fashion. It is worth illustrating in particular two works where the potential of the bifunctionalization of these *gem*-bimetallics was well demonstrated. The first one has been developed by Morken, who enabled the production of enantioenriched 1,1,2-tris(boronates) **11** *via* Pt-catalyzed enantioselective diboration of alkenylboronic esters (Scheme I-5a).<sup>[21]</sup> A substrate-controlled stereoselective intramolecular deborylative alkylation reaction was performed, resulting in the formation of *syn*-diol **12** upon alkaline oxidation with very good diastereo- and enantioselectivity.

However, following this strategy, only one new C–C bond was formed, and the second functionalization was limited to a simple oxidation. The second work was reported by Meek who achieved the synthesis of enantioenriched boronic esters **14** through the reaction of **13**, with chiral non-racemic epoxides (**Scheme I-5b**).<sup>[22]</sup>



**Scheme I-5.** Synthesis of chiral nonracemic gem-bisboranyl compounds via generation of a stereogenic center in close proximity to the geminated prochiral pattern, followed by bifunctionalization.

The resulting enantiomerically enriched *gem*-bis(boronates) were not isolated and engaged *in situ* in a copper-catalyzed allylation. Various subsequent functionalizations were documented, such as the amination of the remaining boron motif in order to synthesize the piperidine alkaloid, such as (+)-*allo*-sedamine, or Pd-catalyzed arylation coupling.

Within the realm of literature, alternative studies have employed this approach to achieve the synthesis of geminated bis(boronates) with stereogenic center at the  $\alpha$ -position, followed by diastereoselective transformations.<sup>[23–25]</sup> Nonetheless, none of these studies fully harnessed the potential of the bifunctionalization of these reagents, rendering their efforts in achieving difficult enantioselective synthesis somewhat futile.

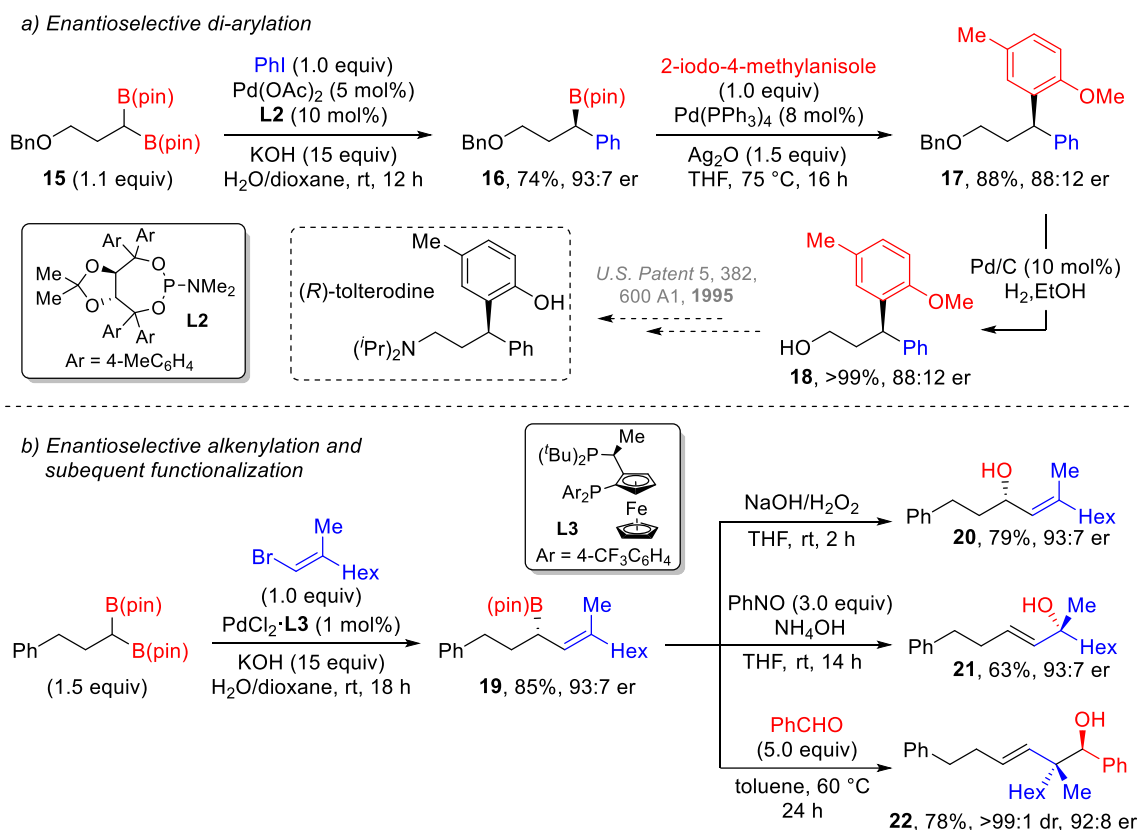
### 1.3.2. Achiral *Gem*-Diboryl Reagents

So far, we have described all the enantioselective bifunctionalization reactions of enantiomerically enriched *gem*-diboryl linchpins and illustrated their synthetic value with the possible applications in synthesis. As we have seen, in some instances, the preparation of the starting material has proven to be laborious due to the multiple manipulations required for the different boron substituents. In this way the recognized benefit of this bimetallic species in asymmetric catalysis are subject to intrinsic limitations. In this context, thanks to the ease preparation of prochiral geminal bisboryl species from commercially available precursors such as methylenebis(boronates),<sup>[26–28]</sup> *gem*-dihalides,<sup>[29,30]</sup> alkynes,<sup>[31–38]</sup> alkenes,<sup>[39–41]</sup> carbonyls compounds,<sup>[42]</sup> carbamates,<sup>[43]</sup> esters,<sup>[44]</sup> diazo compounds,<sup>[45–48]</sup> alkyl halides,<sup>[28,49]</sup> allylic ethers,<sup>[50]</sup> and boryl alkenes<sup>[51]</sup> the approach of developing stereoselective reactions of these type of linchpins have steadily expanded over the past decade, significantly broadening the scope of synthetic applications of this type of reagent. For this reason, we will not focus on the synthesis of such reagents, but we will privilege their asymmetric transformations. However, since the literature in this field is much more extensive, we will try to make a selection based on the importance and synthetic impact of the applications reported up to the present day.

In 2014, Morken presented the first enantioselective bifunctionalization of achiral *gem*-bis(boronate) **15** (**Scheme I-6a**).<sup>[52]</sup> The initial step entailed an enantioselective Suzuki-Miyaura cross-coupling with aryl halides utilizing a Pd(OAc)<sub>2</sub> catalyst in conjunction with phosphoramidite ligand **L2**, leading to the production of highly optically enriched (93:7 er) secondary benzylic boronates **16**. Then, a stereoretentive cross-coupling with 2-iodo-4-methylanisole was executed, albeit with a slight decrease in enantiomeric purity (88:12 er). To enhance the versatility of this methodology, the deprotection of **17** led to the formation of **18**, a well-known precursor in the synthesis of (*R*)-tolterodine, a medication employed for the management of urinary incontinence.<sup>[53]</sup>

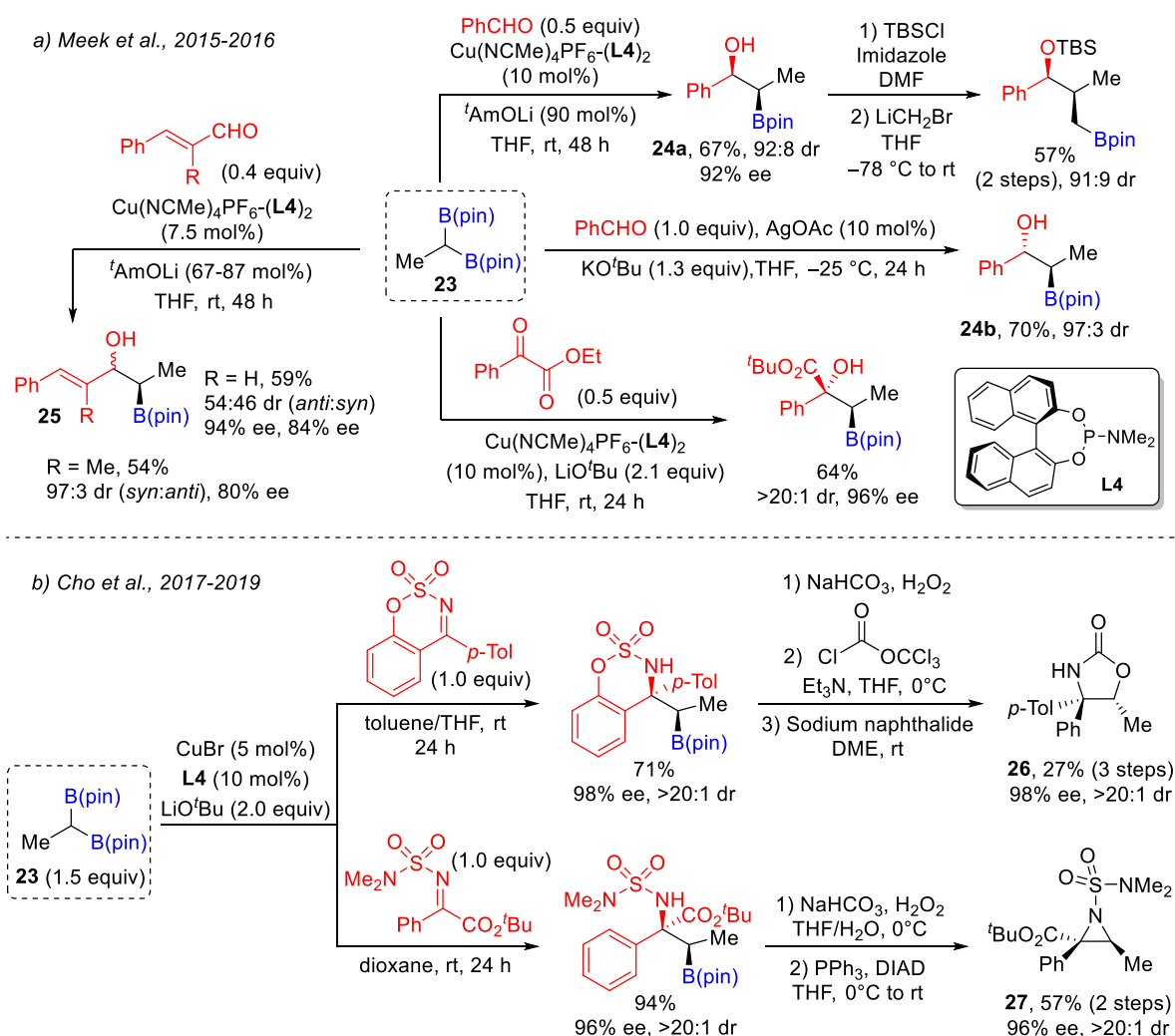
Subsequently, in reference to the first step, Morken expanded the range of electrophiles to encompass alkenyl bromides.<sup>[54]</sup> This was achieved by employing PdCl<sub>2</sub> precomplexed with **L3** (**Scheme I-6b**). This asymmetric cross-coupling resulted in the formation of enantiomerically enriched disubstituted allylic boronic esters **19**, which were readily converted into enantioenriched secondary and tertiary alcohols (respectively **20** and **21**). Furthermore, these boronates proved to be valuable in stereospecific carbonyl allylations, facilitating the creation of stereogenic quaternary carbon centers (**22**).





**Scheme I-6.** First asymmetric bifunctionalization of prochiral gem-bis(boronates): a) enantioselective di-arylation, b) enantioselective alkenylation and subsequent various functionalizations.

The success achieved in the field of asymmetric palladium catalysis prompted exploration of *gem*-bis(boronates) reactivity with various other transition-metals. In this context, Meek and colleagues developed a chiral copper complex-catalyzed *syn*-enantioselective 1,2-addition of 1,1-bis(boryl)ethane **23** to aryl (i.e. **24a**) and alkenyl aldehydes (i.e. **25**), resulting in good yield and excellent selectivity (**Scheme I-7a**).<sup>[55]</sup> When cinnamaldehydes non-substituted in  $\alpha$ -position were used, good enantioselectivity (94% ee, and 84% ee) but (basically) no diastereoselectivity (*anti:syn*, 54:46) were observed. Interestingly, by employing AgOAc as the catalyst source, Meek changed the stereoselectivity of reaction, leading to the formation of *anti*- $\beta$ -hydroxyboronates **24b**.<sup>[56]</sup> Subsequently, Meek broadened the range of electrophiles to encompass  $\alpha$ -keto esters while achieving consistent levels of yield and selectivity.<sup>[57]</sup> Examples of the second C–B bond stereoretentive elaboration were accomplished by transformation into alcohols or amines or *via* homologation reactions.



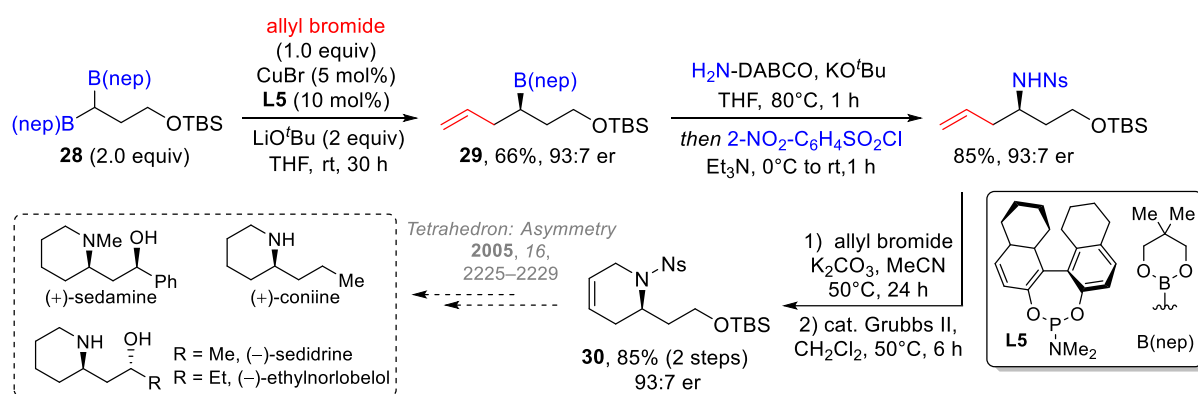
**Scheme I-7.** Cu-catalyzed *syn*-enantioselective 1,2-addition of 1,1-bis(boryl)ethane to: a) aldehydes and  $\alpha$ -keto esters, b) ketimines and  $\alpha$ -imino esters.

Advancements have been made also in coupling of *gem*-bis(boronates) with aldimines and ketimines. Cho described the copper-catalyzed enantioselective 1,2-addition to cyclic aldimines,<sup>[58,59]</sup> ketimines and  $\alpha$ -imino esters,<sup>[60]</sup> enabling the synthesis of interesting products as building blocks for asymmetric synthesis (**Scheme I-7b**). These reactions proceeded with outstanding yields and selectivity, and the presence of ester groups facilitated the transformation of the products into various chiral highly functionalized heterocycles like oxazolidinones **26** and aziridines **27**, upon alkaline oxidation of the boron moiety.

Allylic substitution reactions have also been well-documented. In 2016, Shi and Hoveyda introduced a Cu-NHC-catalyzed enantioselective allylic substitution of allylic phosphates, although it was limited to reactions with non-substituted bis[(pinacolato)boryl]methane.<sup>[61]</sup> This method exhibited remarkable regioselectivity ( $S_N2'$ : $S_N2$ , up to >98:2), leading to the formation of branched homoallylic boronic esters that could subsequently be transformed into optically active alcohols (up to 98% *ee*). In

the same year and using the same non-substituted *gem*-bis(boronate), Niu presented an alternative approach for asymmetric allylation by utilizing a well-established iridium-catalyzed enantioselective allylic substitution reaction allylic carbamates, achieving the same level of selectivity and efficiency.<sup>[62]</sup>

More recently, Cho and Baik developed a copper-catalyzed enantiotopic-group-selective allylation reaction for prochiral *gem*-bis(boryl)alkanes **28** (**Scheme I-8**).<sup>[63]</sup> This method yielded functionalized homoallylic boronic esters **29** in good yields (66%) and high enantiomeric purity (93:7 er). DFT calculations indicated that the initial formation of a cyclic Lewis acid–base pair intermediate occurred between LiO<sup>t</sup>Bu and <sup>t</sup>BuO–Cu. This species plays a key role, promoting simultaneously the C–B bond cleavage and C–Cu bond formation processes. Various second functionalizations were showcased to enhance the versatility of this procedure. In particular, **29** were applied for the synthesis of enantiomerically enriched piperidine derivatives like **30**, which present a foundational structure commonly found in numerous piperidine alkaloids,<sup>[64]</sup> such as coniine, sedridine, sedamine and ethylnorlobelol.<sup>[65]</sup>

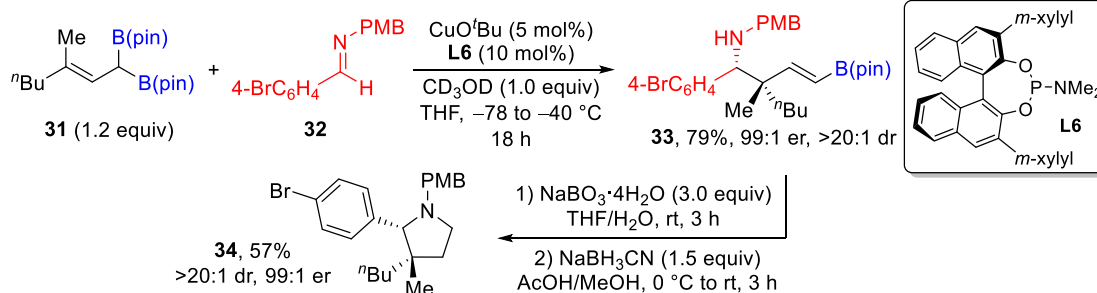


**Scheme I-8.** Cu-catalyzed enantiotopic-group-selective allylation reaction of prochiral *gem*-bis(boryl)alkanes, and subsequent functionalization of the resulting homoallylic boronic esters for the synthesis of enantiomerically enriched piperidine derivatives.

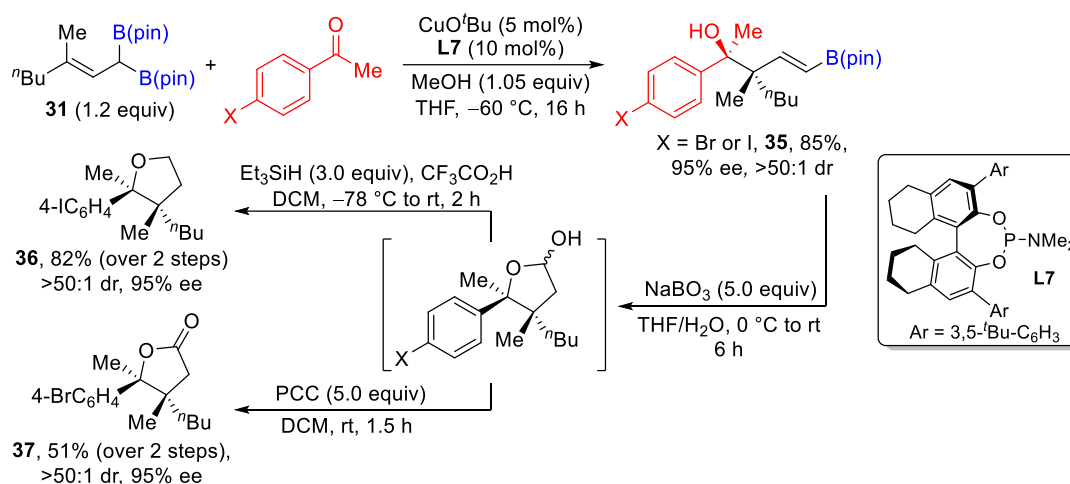
In 2020, Meek reported a successful copper-catalyzed allylboration reaction involving protected imines **32** and  $\gamma$ -disubstituted allyl *gem*-bis(boronates) **31** (**Scheme I-9a**).<sup>[66]</sup> This reaction yielded highly pure homoallylic amines **33** containing quaternary carbon centers in good yields (79%) and outstanding diastereo- and enantiocontrol (dr >20:1, 99:1 er). A subsequent functionalization of the resulting alkenyl boronic ester was performed, synthesizing in this way pyrrolidine derivatives such as **34**.

In the same year, Zanghi and Meek extended the application of the allylboration method to include carbonyl electrophiles (**Scheme I-9b**).<sup>[67]</sup> The allyl addition of **31** to various sterically hindered ketones was developed, generating tertiary alcohols **35** featuring neighbouring quaternary carbon centers in excellent diastereo- and enantioselectivity (dr >20:1, 95% ee).

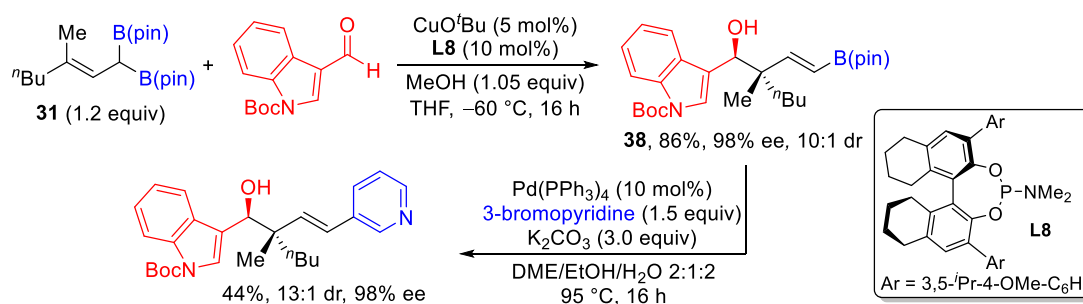
## a) Allylboration reaction of protected imines



## b) Allylboration reaction of ketones



## c) Allylboration reaction of aldehydes



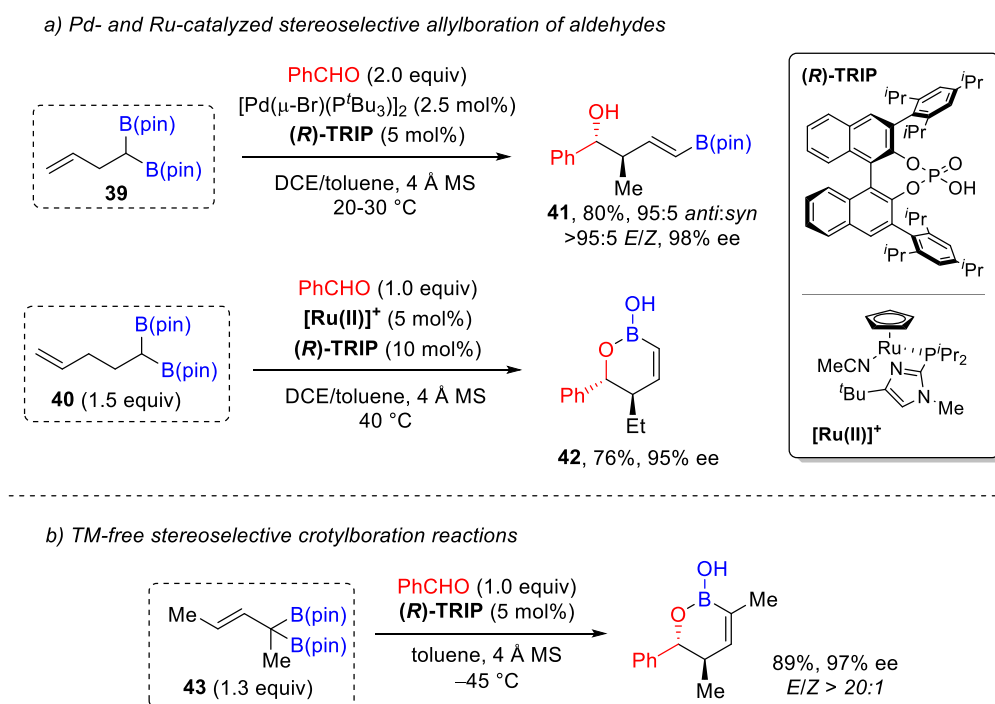
**Scheme I-9.** Cu-catalyzed enantioselective allylboration reaction involving  $\gamma$ -disubstituted allyl *gem*-bis(boronates) and: a) PMB-protected imines; b) ketones; c) aldehydes.

The stereoselectivity was attributed to a proposed six-membered transition state, which minimized steric interactions between the ligand and the ketone by placing the larger substituent on the ketone in a pseudoequatorial position. The reaction displayed a wide range of compatible substrates, and the resulting alkenyl boronates **35** were then transformed into highly substituted tetrahydrofuran **36** and  $\gamma$ -lactone **37**. Meek and Liang also illustrated that  $\alpha,\beta$ -unsaturated ketones could serve as valid electrophiles for allylic *gem*-bis(boronates).<sup>[68]</sup> However, this conjugate addition was only diastereoselective and not enantioselective. Finally, Meek also achieved allyl addition to aldehydes (**Scheme I-9c**).<sup>[69]</sup> This process was effective for alkyl, alkenyl, and alkynyl aldehydes, leading to the

production of homoallylic alcohols like **38** with high yields (86%) and enantioselectivity (98% ee), and good diastereoselectivity (10:1 dr). In addition to being transformed into substituted tetrahydrofuran and  $\gamma$ -lactone compounds (similar to the reaction with ketones), **38** was engaged in further functionalizations such as Suzuki cross-coupling with 3-bromopyridine.

Other allylboration reactions were reported with other TM-catalysts. For example, Murakami documented a highly stereoselective allylboration of aldehydes by constructing an allylic *gem*-diboryl species *in situ* through an alkene transposition reaction of 1,1-bis(boryl)alk-*n*-enes like **39** and **40** catalyzed by palladium or ruthenium, affording respectively alkenyl boronates **41** and *anti*-1,2-oxaborinan-3-enes **42** (**Scheme I-10a**).<sup>[70-73]</sup>

Additionally, Chen synthesized  $\alpha$ -disubstituted *gem*-diboryl **43** and successfully devised a range of stereoselective crotylboration reactions without the use of any TM-catalyst (**Scheme I-10b**).<sup>[74]</sup>



**Scheme I-10.** Stereoselective allylboration of aldehydes with prochiral 1,1-bis(boryl)alk-*n*-enes: a) Pd- and Ru-catalyzed, b) transition-metal free.

## 1.4. *Gem*-Borylsilyl Reagents

*Gem*-borylsilyl alkanes represent a distinctive and unique class in the realm of geminated bimetallic compounds. Thanks to their robust configurational stability and excellent orthogonal reactivity, wherein the C–B bond selectively engages in electrophilic substitution reactions while leaving intact the C–Si bond for subsequent transformations, this family of reagents has been extensively utilized in the development of asymmetric reactions. However, in practice, the implantation of the second functionalization step has rarely been documented.

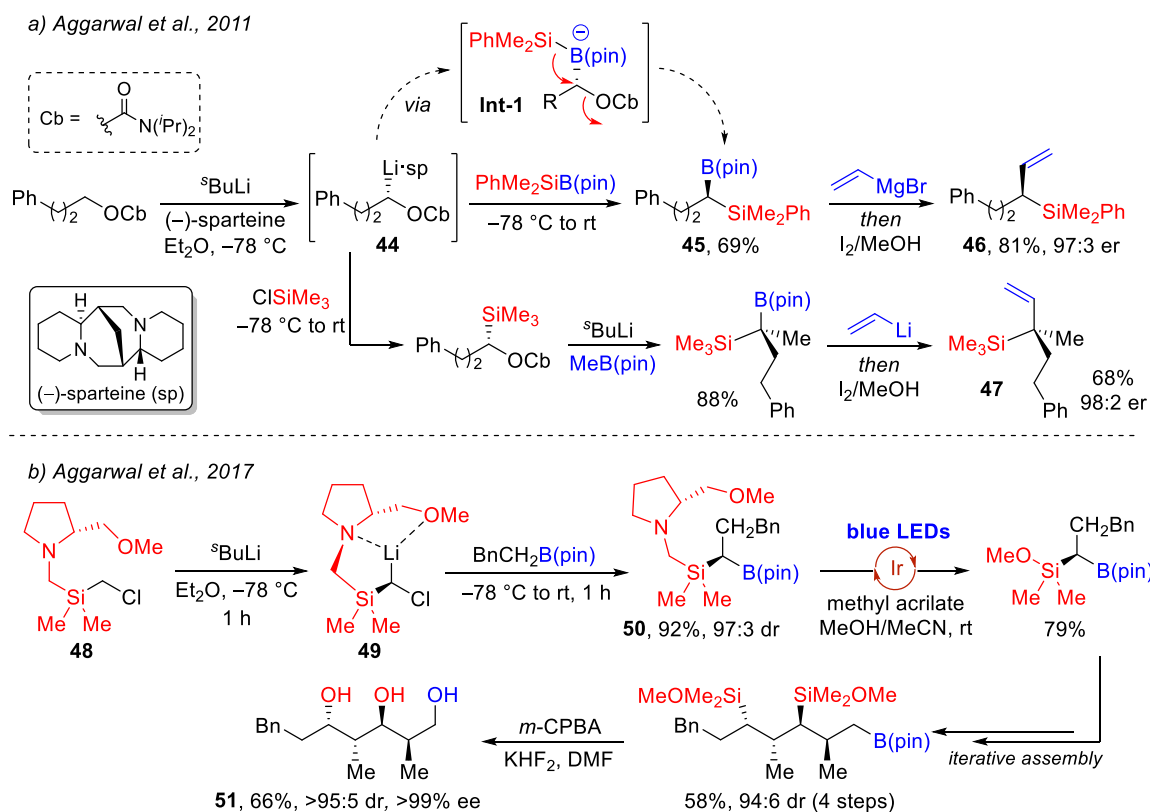
### 1.4.1. Racemic *Gem*-Borylsilyl Reagents

Various strategies have been explored in the extensive investigation of chiral racemic  $\alpha$ -borylsilyl alkanes synthesis.<sup>[48,75–78]</sup> However, to the best of our knowledge, there are no enantioselective reactions reported in the literature so far that employ racemic 1,1-borylalkyl silanes.

### 1.4.2 Chiral Non-Racemic *Gem*-Borylsilyl Reagents

Over the years, numerous research groups all around the globe tried to accomplish the preparation of enantiomerically enriched geminated silylboronates for stereospecific transformations to achieve complex architectural products. In this context, different synthetic strategies and reactions have been developed.

The first preparation of enantiomerically enriched *gem*-borylsilyl alkanes has been described in 1983 by Matteson and co-workers, using (+)-pinanediol-derived organoboronate esters with a homologation reaction with [chloro(trimethylsilyl)methyl]lithium carbenoid,<sup>[79]</sup> albeit with a mediocre enantioselectivity (46% ee). After nearly three decades, Aggarwal group reported the silaboration of chiral non-racemic lithiated carbamates **44**, previously generated through enantioselective deprotonation with (–)-sparteine (**Scheme I-11a**). In this context, after the formation of a boronate complex **Int-1**, a 1,2-metalate rearrangement provide *gem*-borylsilyl alkanes **45** in 69% yields and excellent enantioselectivity ( $\geq 97:3$  er).<sup>[80]</sup> Enantiomeric ratio was measured only after conducting a Zweifel olefination step, yielding synthetic useful tertiary allylsilanes **46** with 97:3 er. Additionally, the authors also developed a domino sequence beginning with the same enantioselective deprotonation with (–)-sparteine, and then involving a silylation and a subsequent Matteson homologation reaction, in order to provide enantiomerically enriched ( $>98:2$  er) quaternary allylsilanes **47**, upon final Zweifel olefination. However, the functionalization of the optically active organosilanes was not performed.



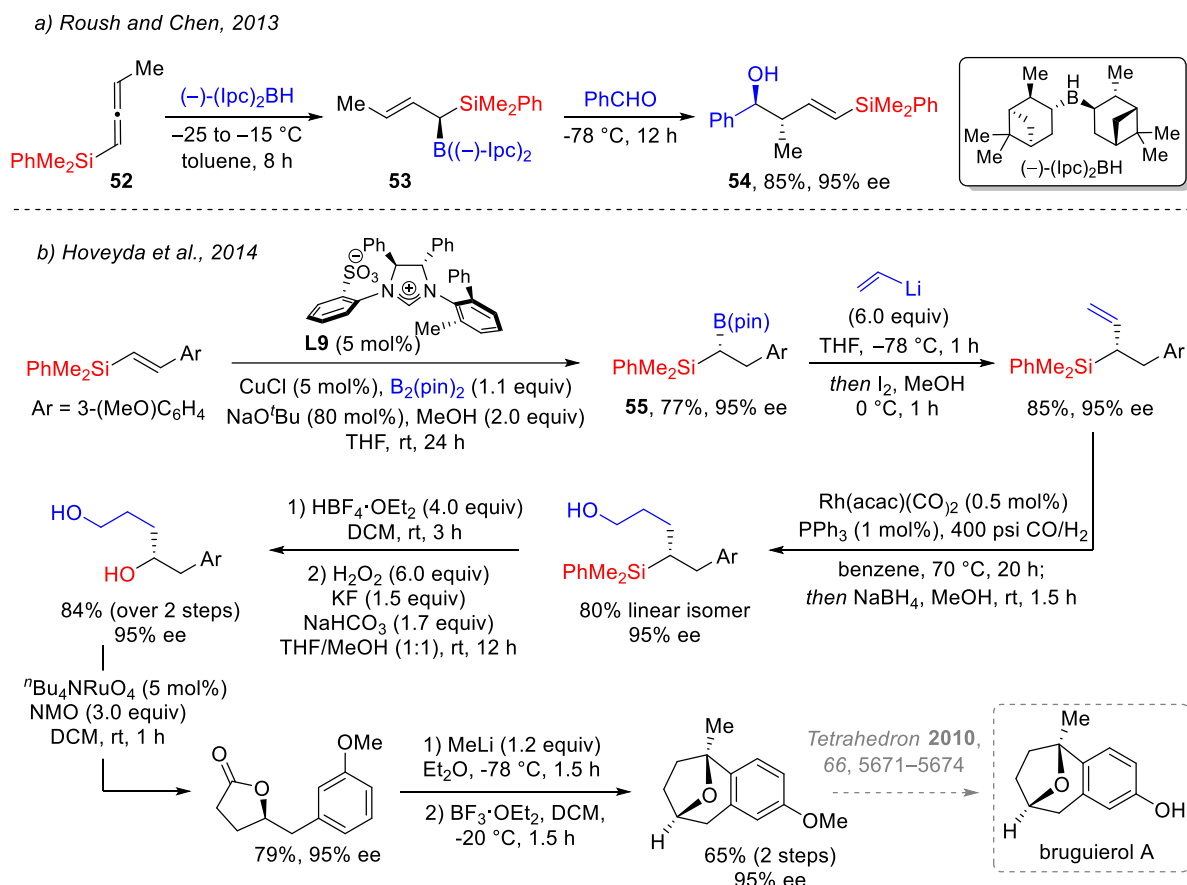
**Scheme I-11.** a) Synthesis of enantioenriched *gem*-borylsilyl alkanes from the chiral non-racemic lithiated carbamates, and subsequent stereospecific Zweifel olefination. b) Enantioselective synthesis of *gem*-borylsilyl alkanes starting from **48**, and stereoselective homologation reactions for the preparation of stereotetrads.

Interestingly, years after the same research group applied the same approach in the stereodivergent preparation of stereotriads and stereotetrads (respectively with three and four contiguous stereogenic centers).<sup>[81]</sup>

Recently, again Aggarwal reported a novel protocol for the enantioselective preparation of  $\alpha$ -silylboronates using the chlorosilyl compound **48** (Scheme I-11b).<sup>[82]</sup> A high diastereoselective control of the lithiation step was possible thanks to the chelating side arm of the proline derivative, allowing to obtain the related lithiated  $\alpha$ -silyl carbenoid **49** with excellent enantioselectivity. Subsequently, **49** was allowed to react with boronates in a stereo-controlled homologation, affording *gem*-borylalkyl silanes **50** in good to excellent yields and high degree of enantiopurity. The authors demonstrate that the directing group is not a problem for synthetic purposes, and it can be easily removed through an iridium-catalyzed photoredox cleavage. They thus performed iterative homologation transformation with chiral non-racemic lithiated carbenoids to afford the diastereoselective preparation of *anti*-polypropionate stereotetrads **51**, which are more challenging to synthesize since the classic aldol and crotylation methodologies are not stereoselectively efficient.<sup>[83–87]</sup>

In 2013, Roush and Chen prepared enantiomerically enriched geminated borylsilyl alkanes **53** by non-catalyzed hydroborylation strategy, involving (–)-diisopinocampheylborane and racemic

allylsilane **52** (Scheme I-12a).<sup>[88]</sup> Once the hydroboration was done, they subsequently performed *in situ* a crotylation of aldehydes. Using this strategy, (*E*)- $\delta$ -silyl-*anti*-homoallylic alcohols **54** was obtained in high yield (85%) and ee (95%). However, the second functionalization of the C–Si bond was not reported.

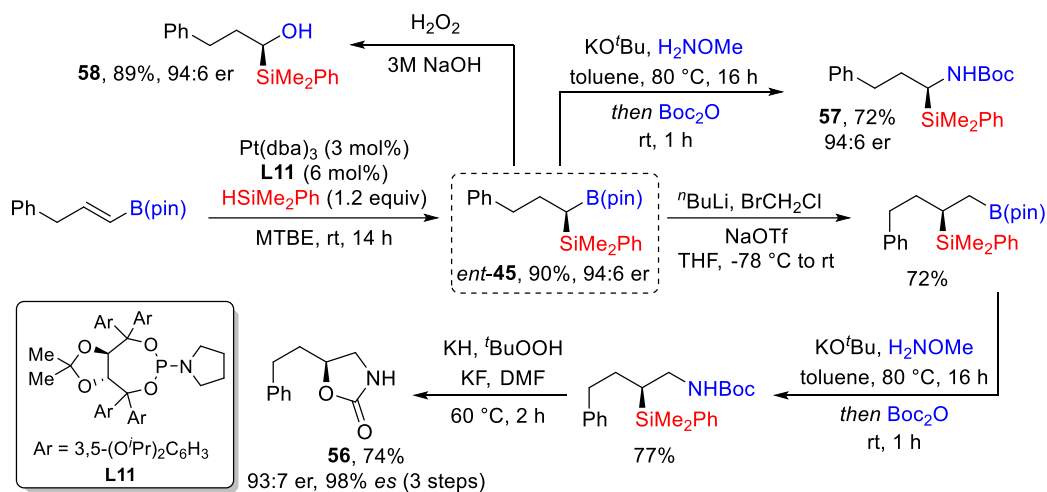


In the same year, Hoveyda described a novel efficient copper-NHC complex-catalyzed enantioselective proto-borylation of vinylsilanes to obtain chiral non-racemic *gem*-borylsilanes **55** (Scheme I-12b).<sup>[89]</sup> The exquisite regio- and enantioselectivity (95% ee) is dictated from the aromatic substituent stabilizing effect in synergy with the imidazolium scaffold of the ligand (**L9**). For this reason, in cases of alkyl substituents on the alkenylsilane, the  $\alpha$ -regioselectivity was completely inverted to the  $\beta$ -position. To probe the versatility of the transformation and explore synthetic valuable applications, the authors showcased the total synthesis of bruguirol A, a pharmacologically active natural product effective against Gram-positive and Gram-negative bacteria.<sup>[90,91]</sup>

Among all the methodologies for the synthesis of enantioenriched *gem*-borylsilyl alkanes, the hydrosilylation developed by Morcken is the only one that employs catalytic amounts of transition-



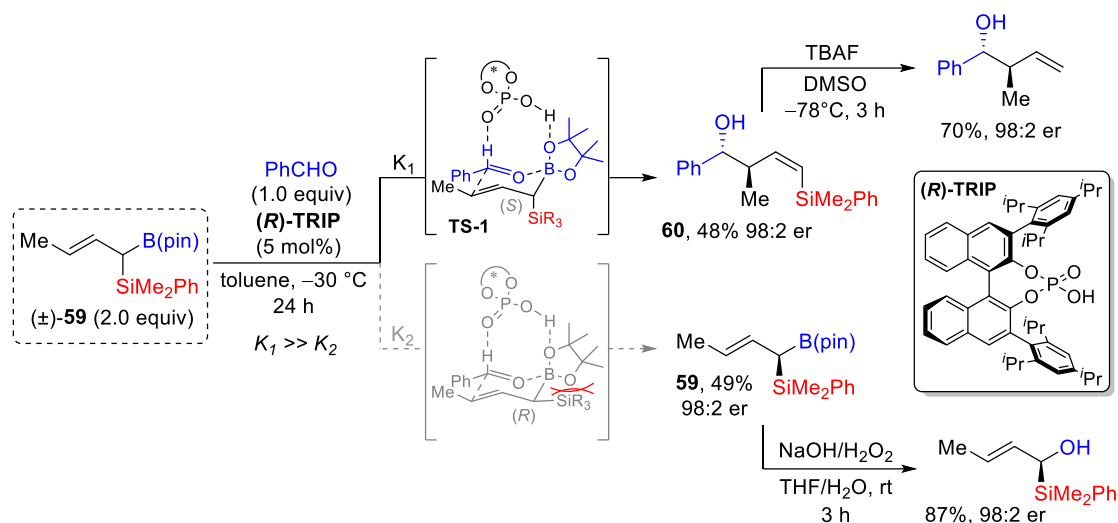
metal catalyst, achieving both high enantiomeric excess and yield without using  $\beta$ -aryl-substituted alkenylboronates.<sup>[92]</sup> Through the use of a platinum-phosphoramidite **L11** complex, a wide variety of differently functionalized vinylboronic esters were converted into chiral non-racemic *gem*-borylsilyl alkanes like *ent*-**45** with excellent yields and ee (**Scheme I-13**).



**Scheme I-13.** Preparation of enantiomerically enriched *gem*-borylsilyl alkane *ent*-**73** via Pt-catalyzed enantioselective hydrosilylation of alkenyl boronate **94**, and successive various functionalizations.

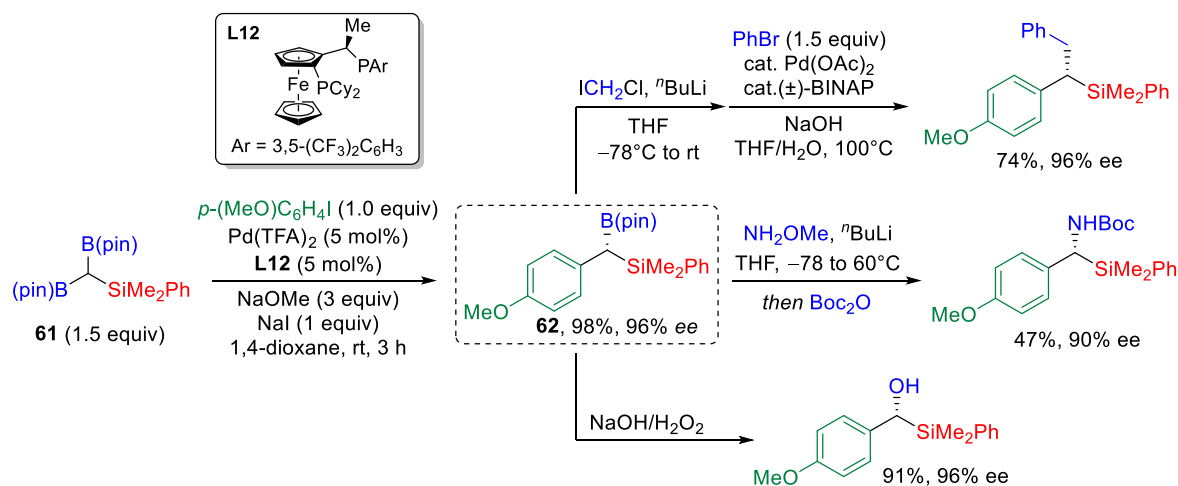
The synthetic potential of these reagents was illustrated through two key demonstrations: the total synthesis of oxazolidinone **56** in a telescope sequence with 98% es over 3 steps, and the transformation of the boron unit into an amine and hydroxy group, forming respectively  $\alpha$ -silyl amine **57** and  $\alpha$ -silyl alcohol **58**. In particular, these compounds have shown to have interesting application as amino acid bioisosteres,<sup>[93]</sup> and as chiral auxiliaries.<sup>[94]</sup>

Kinetic resolution was also employed as a synthetic route for enantiomerically enriched *gem*-boryl silanes. This approach was developed by Cho, who elegantly exploited the kinetic resolution of  $\alpha$ -silyl-substituted allylboronate ( $\pm$ )-**59** via a chiral phosphoric acid-catalyzed chemo-, diastereo-, and enantioselective allylboration of various benzaldehyde to furnish **60** (**Scheme I-14**).<sup>[95]</sup> The key step of the kinetic resolution relies on the chair-like transition state **TS-1** through coordination with the chiral phosphoric acid. In this context, the silyl unit occupies a pseudo-axial position to promote the minimal steric repulsion between silyl and boryl groups. The significant difference of the two rate constants facilitates an efficient kinetic resolution process. Various, albeit simple, functionalizations have been performed with both enantiomerically enriched species leading to interesting optically active compounds.



**Scheme I-14.** Kinetic resolution for the preparation of enantiomerically enriched *gem*-boryl silanes.

Finally, a few years ago, Cho described an interesting way to prepare enantiomerically enriched benzylic *gem*-silylboronates **62**.<sup>[96]</sup> They developed a highly efficient enantiotopic-group selective Pd-catalyzed Suzuki-Miyaura cross-coupling of *gem*-bis(boryl)methylsilane **61** and aryl iodides (**Scheme I-15**).



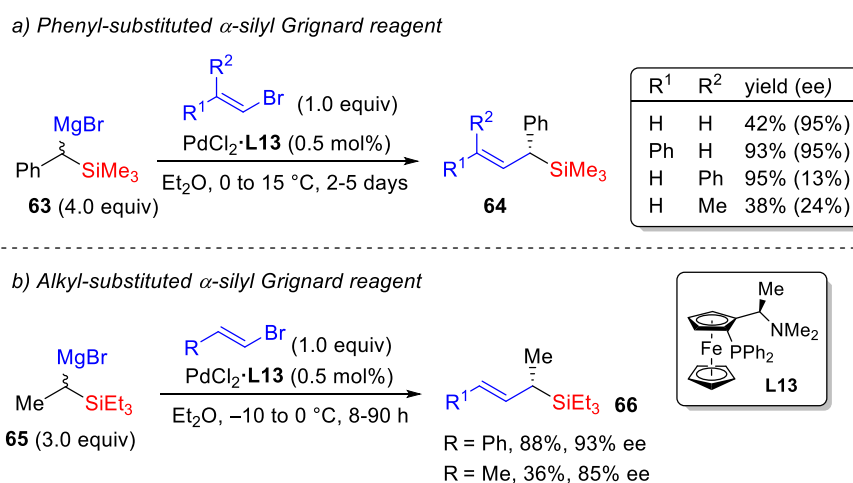
**Scheme I-15.** Enantiotopic-group selective Pd-catalyzed Suzuki-Miyaura cross-coupling of *gem*-bis(boryl)methylsilane for the synthesis of optically active benzylic *gem*-silylboronate, and subsequent various functionalizations of the C–B bond.

The *gem*-bimetallic species obtained were converted into other synthetically valuable products such *via* C–C and C–heteroatom bond-forming reactions, emphasizing the value of these building blocks in asymmetric synthesis. However, in none of these transformations the functionalization of the C–Si bond was performed.

## 1.5. Gem-Silyl Grignard Reagents

The use of *gem*-silyl Grignard reagents in enantioselective transformations can enable the synthesis of enantioenriched organosilanes, as intermediates after the first functionalization. These species hold a distinct position in the repertoire of organic chemists, serving as versatile reagents for the preparation of complex molecules, owing to the extensive range of transformations possible through the C–Si bond, along with the exceptional functional group tolerance they display.<sup>[97,98]</sup> Despite these premises, the *gem*-silyl Grignard reagents have received very few attentions and no enantioselective bifunctionalization reactions have been reported. However, it is worth mentioning what has been done in this context briefly.

Kumada reported the first enantioselective transformation of racemic  $\alpha$ -(trialkylsilyl)benzylmagnesium bromide **63** involving a Pd(II)-catalyzed alkenylation, leading to optically active allylsilanes **64** (**Scheme I-16a**).<sup>[99]</sup>



**Scheme I-16.** Enantioselective Pd-catalyzed alkenylation of: a) racemic  $\alpha$ -(trialkylsilyl)benzyl magnesium bromides, b) alkylmagnesium bromides.

However, it is worth noting that a significant amount of the  $\alpha$ -silyl Grignard reagent (4.0 equiv) was necessary to achieve good conversions, and allylsilanes **64** were obtained with high enantiomeric excess only when simple ethylene bromide or (*E*)-substituted vinyl bromides were employed. The authors did not perform any second functionalization. Unlike vinyl electrophiles, the use of the same catalytic system for the cross-coupling of phenylbromoacetylene with **63** did not produce good results, furnishing the corresponding propargylsilane with a very low enantiomeric excess (18% *ee*).<sup>[100]</sup>

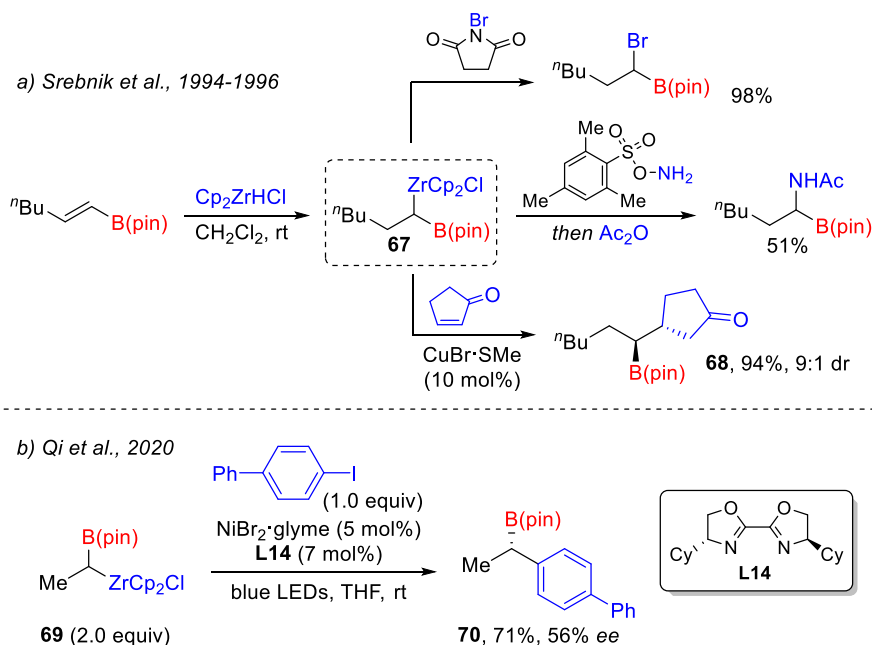
A few years later, in 1986, the same authors expanded the protocol to racemic alkyl-substituted  $\alpha$ -silyl Grignard reagent **65**,<sup>[101]</sup> although once again, no further functionalization of the optically active organosilane **66** was performed (**Scheme I-16b**).

## 1.6. Gem-Borylzirconio Reagents

The chemistry of C–B bond is well established, making the mono-organoboronates one of the main useful synthetic tools in the armoury of organic chemists. The chemistry of organozirconium reagents is also well-known and developed. Nevertheless, despite these premises, *gem*-borazirconocene alkanes have received very few attentions and remain so far largely underexplored (as their analogue *gem*-zincazirconocenes).

### 1.6.1. Racemic Gem-Borylzirconio Reagents

The addition of  $\text{Cp}_2\text{ZrHCl}$  (also known as Schwartz's reagent)<sup>[102–104]</sup> to B-alkenylborabicyclo-[3.3.1] nonanes (B-alkenyl-9-BBN)) resulted in the successful formation of the expected *gem*-bimetallic species. However, these compounds displayed significant instability and proved to be difficult to characterize.<sup>[105]</sup> On the contrary, alkenyl boronates has been employed to synthesize a fair variety of racemic *gem*-borylzirconocenes **67**, which proved to be considerably more stable than the aforementioned ones.<sup>[106]</sup> In this context, Srebnik explored the general reactivity, primarily of the zirconocene motif in the first functionalization, illustrating simple transformations such as halogenation and amination (**Scheme I-17a**).<sup>[107]</sup>



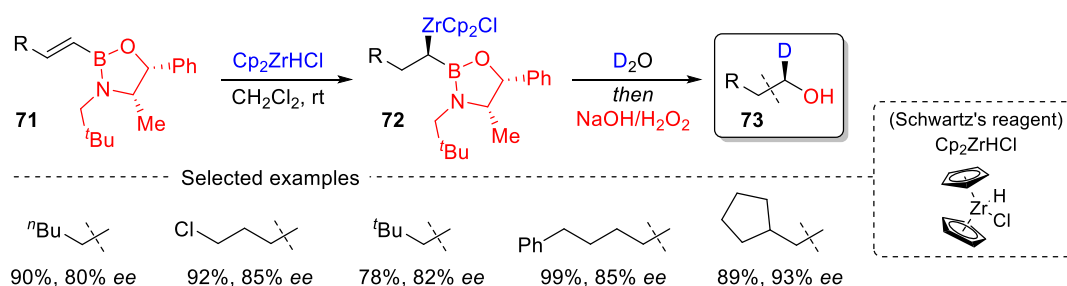
**Scheme I-17.** a) Synthesis of racemic *gem*-boryl zirconocene **117** and his general reactivity. b) Ni-photocatalyzed enantioselective arylation of racemic *gem*-borylzirconocene **124**.

Moreover, Cu-catalyzed nucleophilic substitution and addition reactions were also examined. In particular, under these conditions, the conjugate 1,4-addition to cyclic  $\alpha,\beta$ -unsaturated enone was observed to favor the *anti*-adduct **68** with good diastereoselectivity (9:1).<sup>[108]</sup> However, in all these examples the second functionalization was limited only to a simple oxidation of the C–B bond.

If we examine enantioselective transformation employing racemic *gem*-borazirconocene alkanes, only one has been reported in the literature so far, by Qi, who described a nickel-photocatalyzed, cross-coupling reaction of **69** with aryl halides (**Scheme I-17b**).<sup>[109]</sup> Nevertheless, while the protocol is well developed in racemic fashion employing a nickel-bipyridine complex, its operation in an enantioselective manner with the aid of a chiral bis(oxazoline) ligand **L14** resulted in only moderate enantiomeric purity (56% ee) of the product **70**. Additionally, the second functionalization was not performed.

## 1.6.2. Chiral Non-Racemic *Gem*-Borylzirconio Reagents

Only one method has been reported so far for the preparation of enantioenriched *gem*-borylzirconocene alkanes (**Scheme I-18**). In this context, Srebnik developed a diastereoselective hydrozirconation reaction of optically pure vinylboronic esters **71**.<sup>[110]</sup> After quenching the resulting  $\alpha$ -boryl zirconocenes **72** with D<sub>2</sub>O and oxidizing the boron unit, high yields (77–99%) and enantioselectivity (80–93% ee) of the corresponding  $\alpha$ -deuterated alcohols **73** were attained, indicating the high optical purity of the bimetallic species.



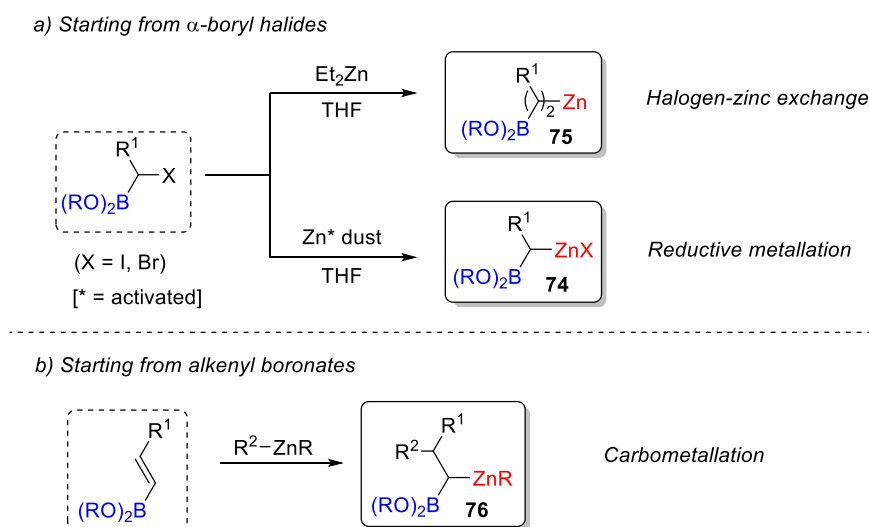
**Scheme I-18.** Diastereoselective hydrozirconation of optically pure vinylboronic esters for the preparation of enantioenriched *gem*-borylzirconocene alkanes: synthesis of optically active deuterated terminal alcohols.

This approach facilitates the straightforward synthesis of optically active deuterated terminal alcohols **73**, a category with limited representation in the literature,<sup>[111–113]</sup> thus significantly enhancing the value of this protocol. Nevertheless, this sequential reaction is the only one reported by the authors, which somewhat restricts the synthetic versatility of these bimetallic reagents.

## 1.7. Gem-Borylzinc Reagents

In the last few years, regarding the domain of  $\alpha$ -boryl organometallics, the popularity of  $\alpha$ -boryl zinc species as versatile reagents in asymmetric synthesis has increased considerably. In fact, given that the organozinc reagents undergo transmetalation with transition metal salts more readily than organoboranes, the C–Zn bond can participate in cross-coupling reactions with various electrophiles with high functional group tolerance, leaving the C–B bond intact for another C–C or C–heteroatom bond construction reactions. With this strategy, several chiral organoboron compounds can be potentially obtained, and most important, the resulting alkylboronic esters which are chemically and configurationally stable can be applied in a myriad of stereospecific transformations.<sup>[114–117]</sup>

The synthesis of racemic  $\alpha$ -boryl zinc reagents have been successfully achieved following three strategies (**Scheme I-19**). The initial two methods typically involve the transformation of  $\alpha$ -boryl halides, either *via* the oxidative addition of zinc metal to produce  $\alpha$ -borylzinc halides **74** or through halogen-zinc exchange with  $\text{Et}_2\text{Zn}$  resulting in di( $\alpha$ -boryl)alkylzincs **75**.<sup>[118–120]</sup> The third strategy instead entails a carbometallation reaction involving alkenylboronates and allylic zinc reagents to furnish *gem*-borylzinc reagents **76**.<sup>[121–123]</sup>

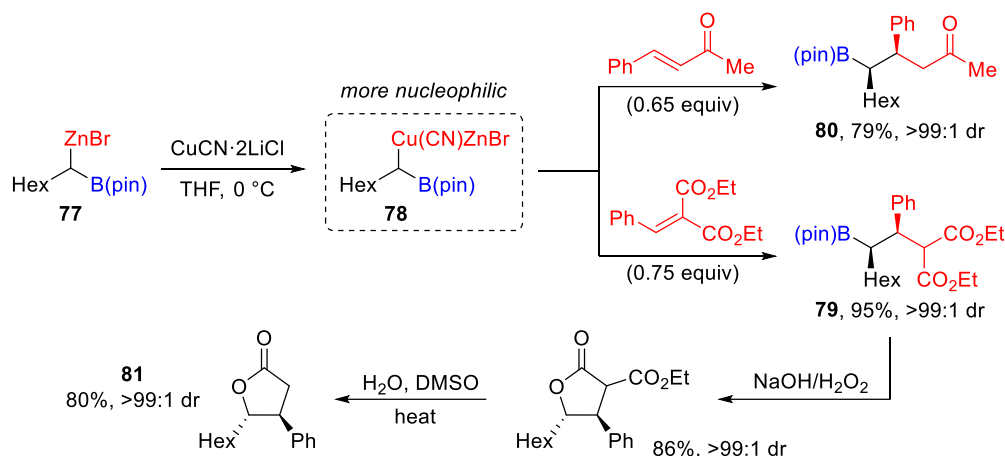


**Scheme I-19.** Strategies for the preparation of racemic *gem*-borylzinc reagents.

### 1.7.1. Racemic Gem-Borylzinc Reagents

The initial two approaches starting from  $\alpha$ -borylzinc halides were pioneered by Knochel.<sup>[118–120]</sup> With the synthesis of these unique building blocks in hands, in 1990 Knochel and co-workers achieved the first stereoselective transformation (**Scheme I-20**).<sup>[118]</sup> They made a significant breakthrough by discovering that the addition of stoichiometric quantities of  $\text{CuCN}\cdot 2\text{LiCl}$  to the resulting  $\alpha$ -boryl

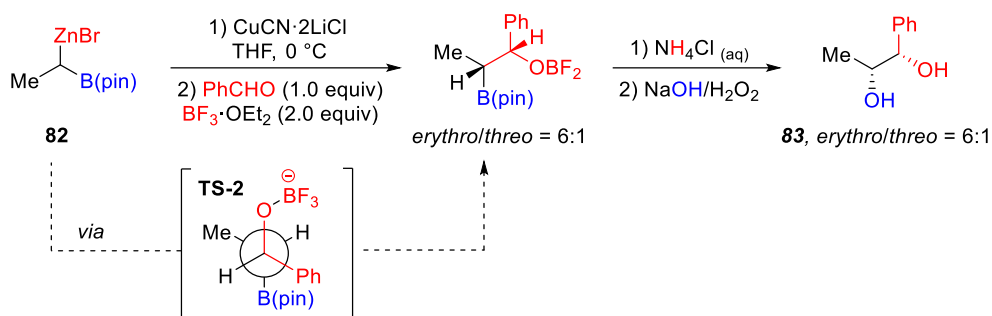
alkylzinc halides **77** substantially enhanced the nucleophilicity of organozinc reagents, leading to the creation of  $\alpha$ -boryl zinc-cuprates **78**.



**Scheme I-20.** 1,4-addition of *gem*-borylzinc-cuprate reagents to  $\beta$ -branched Michael acceptors and post-functionalizations.

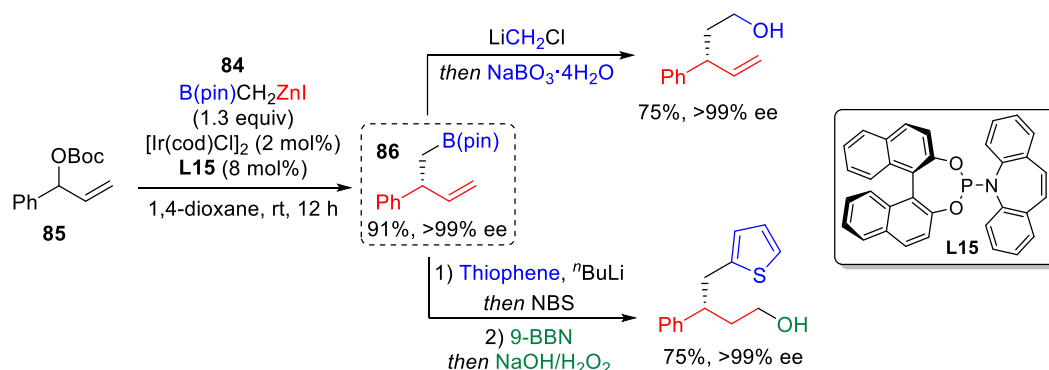
These intermediates were then allowed to react with a range of electrophiles. Notably, the transformations with  $\beta$ -phenyl-substituted Michael acceptors such as benzylidenemalonate and benzylideneacetone, displayed remarkable diastereoselectivity, predominantly yielding the *syn*- $\gamma$ -(dialkoxyboryl) 1,4-adducts (respectively **79** and **80** in good yields and outstanding diastereomic ratios (*syn:anti*, >99:1). Moreover, alkylboronic esters derived from this procedure possess significant synthetic versatility. For example, **79** was transformed by oxidation and subsequent decarboxylation to the corresponding *trans*-lactone **81** (attractive building block for the synthesis of natural products)<sup>[124]</sup> with complete stereoretention.

Years later, Miyaura and co-workers reported that the sequence of addition of the Knochel's copper(I)  $\alpha$ -borylzinc reagents **82** to benzaldehydes in the presence of BF<sub>3</sub>·OEt<sub>2</sub> takes place with good levels of diastereoselectivity (**Scheme I-21**). Interestingly, subsequent oxidation of the boronic ester group with alkaline hydrogen peroxide led to synthetically intriguing *anti*-diol **83**.<sup>[120]</sup> The *erythro*-selectivity can be aptly elucidated through the transition state **TS-2**, wherein the boronic ester moiety and the carbonyl oxygen are arranged in *anti*-positions to each other in order to minimize the steric hindrance, analogous to the configuration of methyl and phenyl groups.



**Scheme I-21.** Addition of the Knochel's copper(I)  $\alpha$ -borylzinc reagents to benzaldehyde.

The first enantioselective reaction employing non enantioenriched *gem*-borylzinc halides was reported only in 2021 employing the achiral  $B(\text{pin})\text{CH}_2\text{ZnI}$  (**84**) (**Scheme I-22**). Indeed, despite being the simplest *gem*-borylzinc halide to be prepared,<sup>[118]</sup> **84** has been underexploited until recently.<sup>[125-128]</sup> In this context, Zhan and Guo developed an iridium-catalyzed enantioconvergent cross-coupling of **84** with racemic branched allylic carbonates **85**.<sup>[129]</sup> Of course, using this *gem*-borylzinc reagent the stereogenic information is introduced at the electrophilic carbon of the allylic carbonate, leading to the formation of chiral homoallylic organoboronates **86**. The authors performed various functionalization of the boron moiety showcasing the synthetic utility of this procedure.



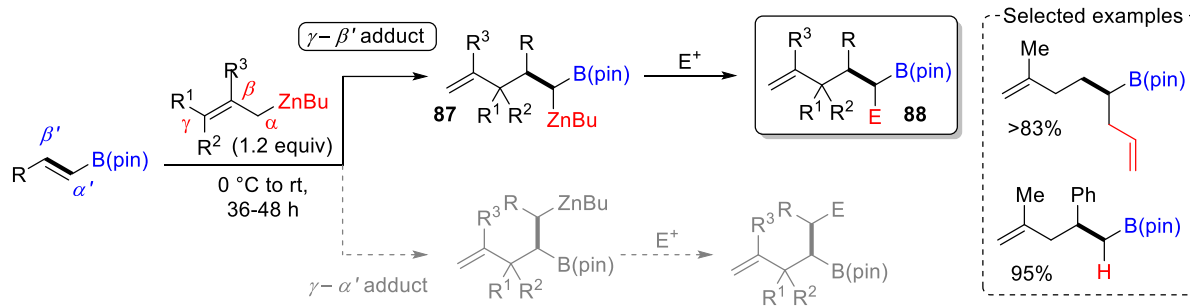
**Scheme I-22.** Ir-catalyzed enantioconvergent cross-coupling of  $B(\text{pin})\text{CH}_2\text{ZnI}$  and branched allylic carbonates, and subsequent C–B bond functionalization of the resulting enantioenriched homoallylic boronates.

In 2001, Nakamura and co-workers unveiled the versatile potential of alkenylboronic esters as starting materials for carbozincation reactions.<sup>[121]</sup> Within this framework, the addition of allylic zinc reagents to vinyl boronic esters demonstrated complete regioselectivity and quantitative conversion, yielding highly versatile geminated borylzinc compounds **87** (**Scheme I-23**). Subsequent electrophilic trapping of these intermediates led to a diverse array of organoboronates **88**, with good yields (83–95%). Following this synthetic methodology, only one attempt has been made in enantioselective fashion, involving the installation of a chiral bis-oxazoline motif in place of the butyl group on the

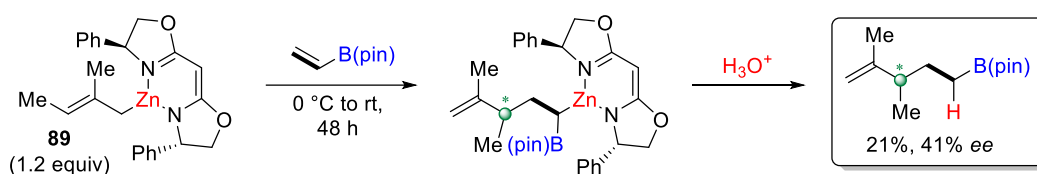


organozinc reagent **89** (Scheme I-23b). Unfortunately, the outcome displayed unsatisfactory reactivity (21% yield), and a mere chiral induction (44% ee).<sup>[121]</sup>

a) Allylzincation of vinylboronates

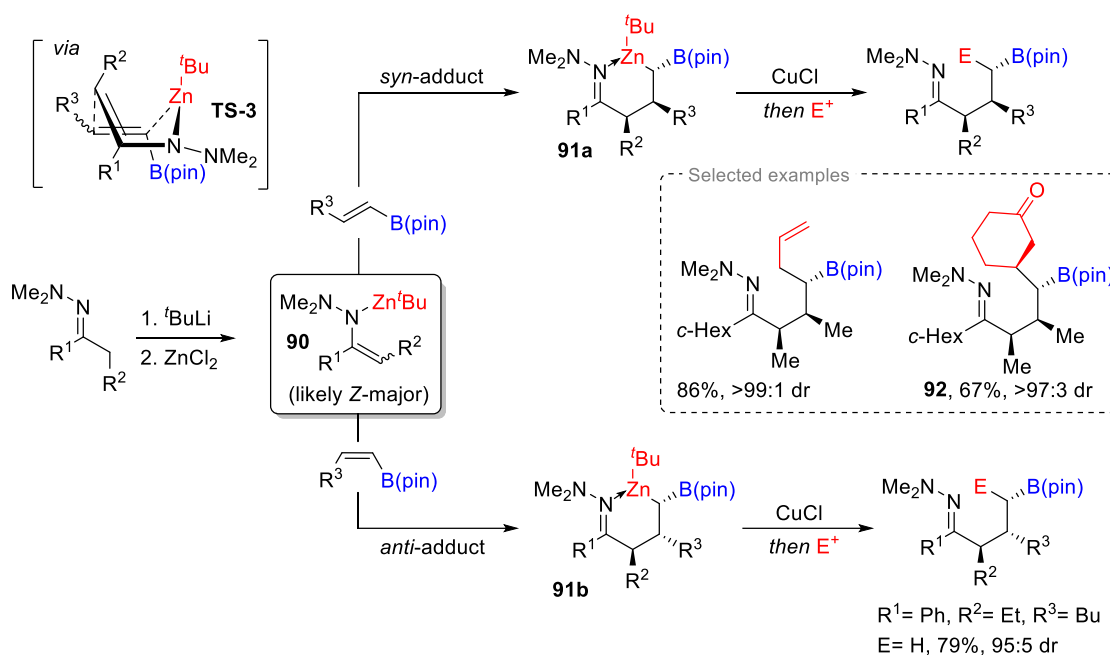


b) Asymmetric allylzincation of vinylboronates



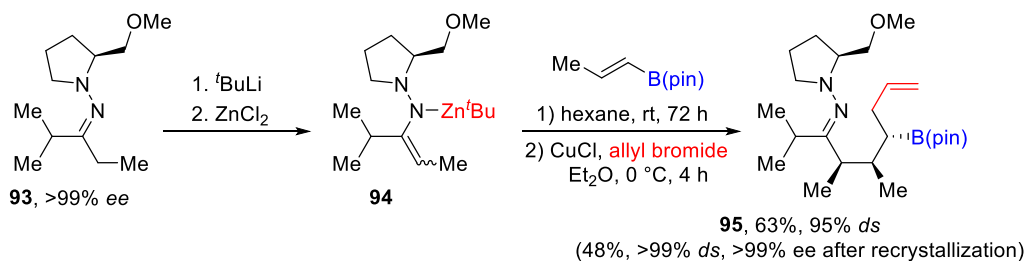
**Scheme I-23.** a) Regioselective carbometallation addition of allylic zinc reagents to alkenylboronic esters; b) asymmetric carbometallation of **89** to vinyl boronates.

Nevertheless, the significant synthetic value of these sequential reactions in asymmetric synthesis was established three years later by the same research group through the development of carbozincation reactions involving alkenylboronic esters and zincated hydrazones **90** (Scheme I-24).<sup>[122,123]</sup> In this elegant procedure, the *anti* (or *syn*) stereoselective 1,2-addition of **90** to respective 1,2-disubstituted *E*- (or *Z*-) alkenyl boronic esters was demonstrated to furnish three consecutive stereogenic carbon centers located at positions  $\alpha$ ,  $\beta$ , and  $\gamma$  to the imine carbon (i.e., **91a** or **91b**). The outstanding diastereoselectivity observed (up to  $>99\%$ ) is well rationalized by a six-membered boat-like transition state **TS-3**. Additionally, it is possible to generate an extra stereogenic center after cross-coupling of the  $\alpha$ -borylzinc intermediate with a carbon electrophile, such as compound **92**, thereby resulting in the formation of a consecutive series of four stereogenic centers.



**Scheme I-24.** Stereoselective anti (or syn) 1,2-addition of zincated hydrazones to respective 1,2-disubstituted E- (or Z-) alkenyl boronic esters.

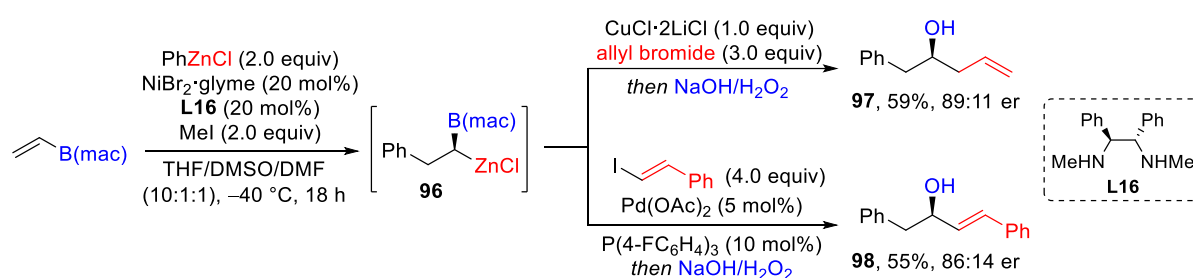
The same research group further highlighted the potential applications in asymmetric synthesis, employing the optically active (*S*)-1-amino-2-methoxymethylpyrrolidine (SAMP) hydrazone **93** (**Scheme I-25**).<sup>[123]</sup> The resulting chiral enantiomerically enriched zincated hydrazone **94** was then subjected to reaction with the alkenyl boronates, and subsequently trapped with allyl bromide furnishing the desired product **95** with satisfactory yields and excellent diastereoselectivity and enantioselectivity (48% yield, >99% *ds* and >99% *ee* after recrystallization). Worth noting is the fact that the absolute configuration of the  $\alpha$ -carbon contrasts with that observed at the  $\alpha$ -carbon of analogous products generated through the alkylation reaction of lithiated SAMP hydrazones with alkyl halides. This phenomenon underscores the promising utility of this synthetic sequence.



**Scheme I-26.** Enantioselective carbозincation reaction of (*E*)-alkenyl boronates with **94**.

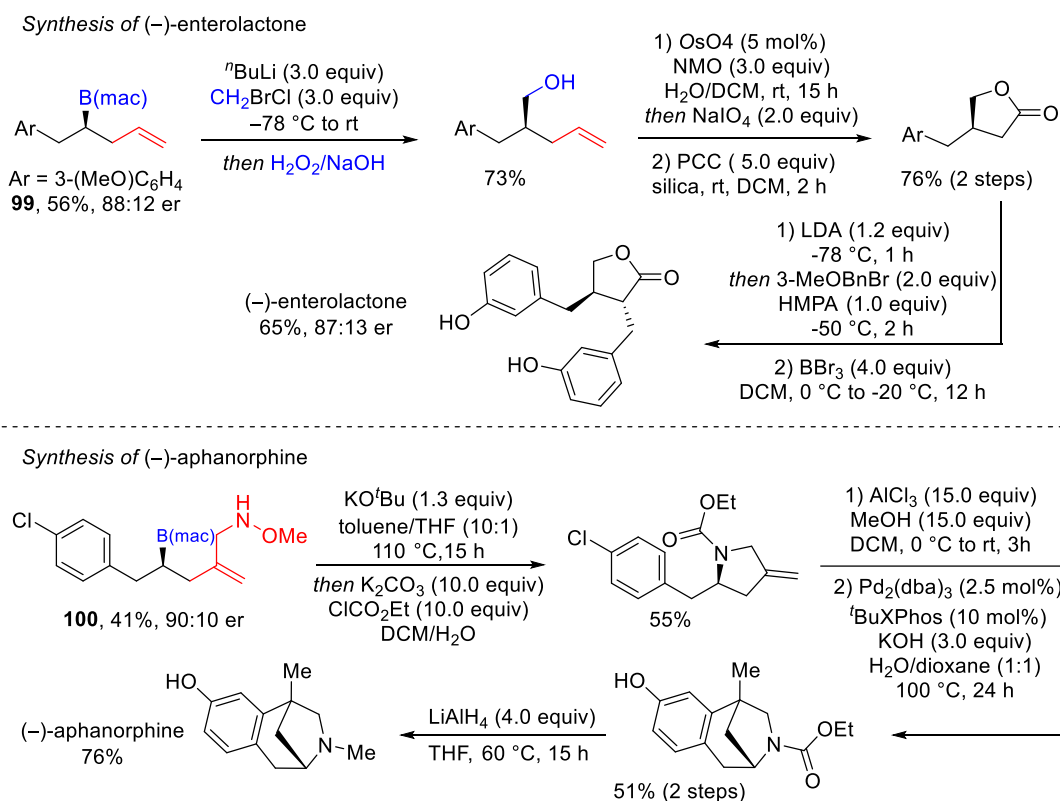
### 1.7.2. Chiral Non-Racemic *Gem*-Borylzinc Reagents

Despite their well-established reactivity enabling a sequential two-step procedure for the assembly of complex molecules in a straightforward manner, for the preparation of enantioenriched *gem*-borylzinc reagents only one method has been reported so far (**Scheme I-27**). In this context, Morken developed the synthesis of enantiomerically enriched, configurationally stable  $\alpha$ -borylzinc reagents like **96**, *via* catalytic enantioselective carbозincation of vinylboronic esters.<sup>[130]</sup> This process involved the use of a nickel-**L16** complex with arylzinc chlorides at low temperature ( $-40\text{ }^{\circ}\text{C}$ ), and stoichiometric amounts of methyl iodide. The latter one facilitates the oxidation of low-valent inactive Ni(II) species into the highly unstable Ni(III) species which is quickly converted into the active Ni(I) species. Subsequently these enantioenriched  $\alpha$ -borylzinc species were engaged in Cu(I)-mediated allylations and Pd(II)-catalyzed cross-coupling reactions in a stereospecific manner, affording enantioenriched secondary boronic esters, which were directly converted in the corresponding alcohols (i.e. **97** and **98**) with good yields and enantioselectivity.



**Scheme I-27.** Synthesis of enantioenriched *gem*-borylzinc compounds through Ni-catalyzed enantioselective carbозincation of vinylboronic ester with arylzinc chlorides, and sequential stereospecific reactions.

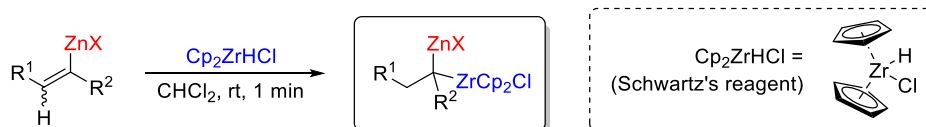
The authors highlighted the significant synthetic potential of the enantioenriched homoallylic boronates **99** and **100** obtained by this procedure, by applying it for the total synthesis of natural products of biological relevance such as (–)-enterolactone<sup>[131,132]</sup> and (–)-aphanorphine<sup>[133]</sup> (**Scheme I-28**). Note that in the latter synthesis, the authors do not report the enantiomeric purity of the obtained (–)-aphanorphine.



**Scheme I-28.** Valorization of the enantiomerically enriched homoallylic boronates **99** and **100**: total synthesis of (-)-enterolactone and (-)-aphanorphine.

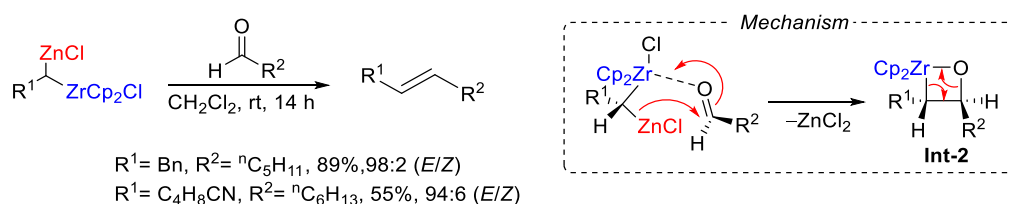
## 1.8. Gem-Zinczirconio Reagents

Despite their potential synthetic application as attractive synthons, *gem*-zinczirconio reagents have not received particularly attention, probably due to their high instability (decomposition after 10 minutes at room temperature).<sup>[134]</sup> For their preparation, as hydrozirconation of olefins has been employed for the synthesis of organozirconium compounds,<sup>[135-137]</sup> so the addition of  $\text{Cp}_2\text{ZrHCl}$  to alkenylzinc halides has been applied to synthesize a large variety of this type of *gem*-bimetallics (**Scheme I-29**).<sup>[138]</sup>



**Scheme I-29.** Preparation of *gem*-zinczirconocene alkanes by addition of  $\text{Cp}_2\text{ZrHCl}$  to alkenylzinc halides.

Although *gem*-zinczirconocene alkanes exhibit high instability, they have been used predominantly for the formation of functionalized alkenes (**Scheme I-30**). In fact, if a carbonyl compound is added immediately after the formation of the *gem*-bimetallic reagent, a stereoselective olefination reaction takes place affording prevalently (*E*)-alkenes like with good yields and satisfactory (*E*)-stereoselectivity.<sup>[135,136,139]</sup> The mechanism appears to be very similar to the Wittig-type reaction involving the formation of an ordered cyclic intermediate **Int-2**, which subsequently eliminates the zirconium oxide moiety, and effectively explaining the (*E*)-stereoselectivity of the transformation.<sup>[139]</sup>



**Scheme I-30.** Olefination reaction of *gem*-zinczirconocene alkanes with aldehydes.

However, it is important to note that to the best of our knowledge, no applications of *gem*-zinczirconio reagents in sequential reactions with two different electrophiles have been reported so far.

## 1.9. Gem-Dizinc Reagents

Since their discovery by Frankland in 1848,<sup>[140]</sup> organozinc compounds have proven to be highly valuable reagents for transition metal catalyzed cross-couplings and nucleophilic addition reactions.<sup>[141-144]</sup> Their ability to tolerate common electrophilic functional groups such as ketones, esters, and nitriles, coupled with the inherent reactivity of the carbon-zinc bond, positions them perfectly for synthesizing intricate functionalized products.<sup>[145-147]</sup> And what could be better than *one* organozinc functionality? Well, obviously the answer could be having *two* organozinc functionalities on the same carbon, enabling a straightforward way to construct very complex molecules. Notably, *gem*-dizinc compounds, which correspond to this characteristic, have exhibited remarkable efficacy in organic synthesis that surpass our expectations. Since the *mono* organozinc intermediate cannot be isolated after the first functionalization, it necessitates the execution and development of sequential reactions. These sequential bi-functionalization reactions are more environmentally friendly, as they require only one isolation and purification step, resulting in reduced consumption of solvents, materials, and resources.

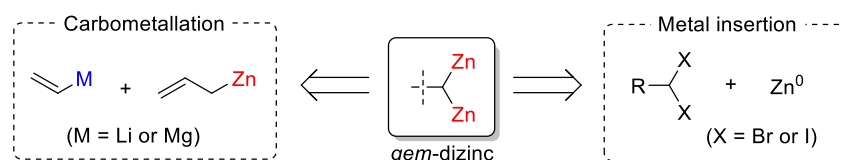
As this topic constitutes the primary focus of this Ph.D. research and manuscript, hereafter we will comprehensively detail the synthesis and the reactivity of *gem*-dizinc compounds, including in a

racemic manner, to truly grasp the synthetic potential and application of these intriguing building blocks.

### 1.9.1. Synthesis of Gem-Dizinc Reagents

The synthesis of C(sp<sup>3</sup>)-geminated organodizinc compounds has been accomplished through regioselective carbometallation of alkenylmetal compounds or metal insertion of *gem*-dihaloalkanes (**Scheme I-31**). A unique instance, not depicted in **Scheme I-31** but to be elucidated later, involves metal-halogen exchange for the creation of a particular *gem*-dizinc carbenoid.

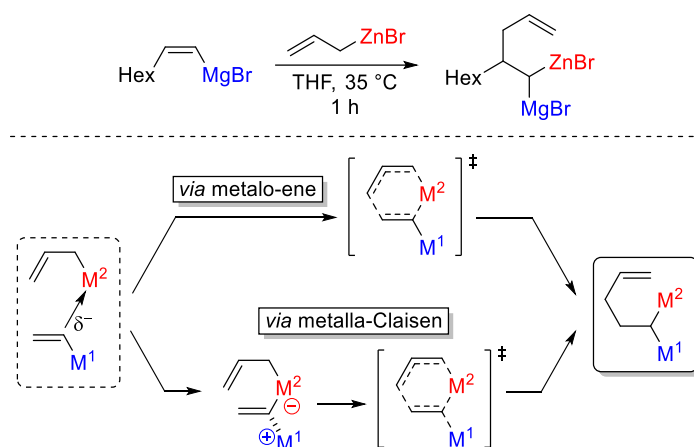
What the reader will discover is that, depending on the method of preparation, the nature of the *gem*-dizinc reagents changes completely, resulting in significant variations in their reactivity.



**Scheme I-31.** Two distinct methods for the synthesis of *gem*-dizinc reagents: carbometallation coupling from alkenyl metal compounds and allylzinc (left), and metal-insertion from corresponding *gem*-dihaloalkanes (right).

#### 1.9.1.1. Synthesis *via* Gaudemar/Normant Carbometallation Coupling

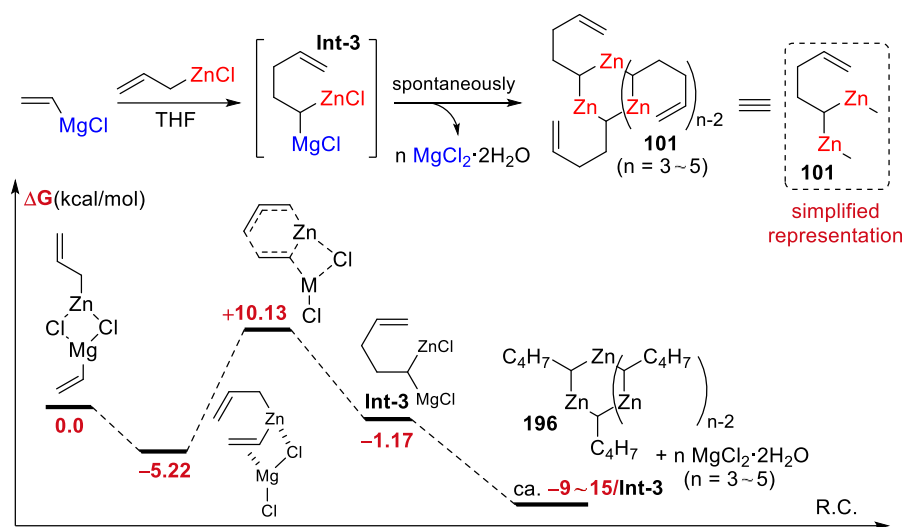
In 1971, Gaudemar made an impactful discovery wherein allylzinc bromide in THF solution was able to undergo carbometallation reactions with vinyl Grignard reagents (**Scheme I-32**).<sup>[148]</sup>



**Scheme I-32.** Gaudemar/Normant addition process to form *gem*-organobimetallic compounds.

Since then, this reaction has undergone substantial development,<sup>[149,150]</sup> and Normant and Knochel further developed it as a practical method for the preparation of geminated organobimetallic compounds.<sup>[151–155]</sup> To the reader, this phenomenon may appear counterintuitive, as the involvement of two nucleophiles yields a third nucleophile, albeit it is notably simpler than the allylzincation of simple olefins.<sup>[156,157]</sup> DFT calculations have played a significant role in effectively elucidating the favourable reaction between alkenyl metals and allylzinc halides, unveiling a mechanism that passes through two possible pathways involving in both cases a six-membered ring transition state (**Scheme I-32**).<sup>[158–160]</sup>

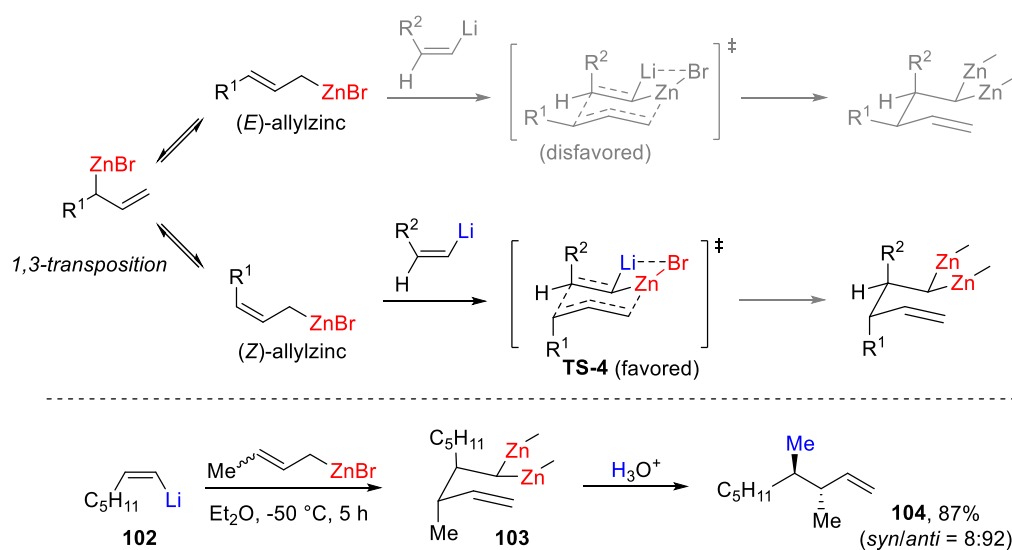
To this field, researchers such as Normant, Knochel, Marek, and Nakamura contributed the most. Their studies revealed that while lithium and magnesium could be independently use as alkenyl metal partner, zinc metal was essential as an allylic metal compound.<sup>[154]</sup> At the time, the true nature of these bimetallic reagents remained elusive and were often considered heterobimetallic, such as Zn/Li or Zn/Mg (see **Scheme I-32**). Consequently, in many of the cited papers on this subject, the bimetallic nature was left unspecified, with only "metal" indicated at the geminal site. In this context, in 1999 Nakamura conducted a DFT study that revealed the actual structure should consist of an oligomeric *gem*-dizinc species **101** (cyclic or linear) to gain the driving force of the reaction (**Scheme I-33**).<sup>[159]</sup>



**Scheme I-33.** DFT (B3LYP/631A) energy diagram for the Gaudemar/Normant coupling (only the metalla-claisen pathway is reported, since is the one with lowest energy) suggesting the formation of a *gem*-dizinc oligomer **101**.

Considering both enthalpic and entropic factors, it is highly probable that trimer and tetramer products are the most likely outcomes. Alongside with crystallographic structure of an analogue of **101**,<sup>[161]</sup> the existence of such oligomers was confirmed. However, such bimetallic compounds have never been crystallized, and their true nature remains unclear to date. For the sake of simplicity, from now on, we will refer to these bimetallic compounds as *gem*-dizinc monomers (see simplification in **Scheme I-33**).

Subsequently Marek and Normant have conducted extensive research on the diastereoselective formation of stereogenic centers in cases where both the alkenyl metal and the allylzinc halide are substituted.<sup>[1]</sup> Typically, in terms of stereochemical control, consideration should be given to the configurations of both reagents. Intriguingly, through the application of DFT calculations, a comparison among four potential chair-like transition states has led to the determination that the transition state **TS-4** involving (*Z*)-crotylzinc bromide is the most favourable due to the proximate effect (**Scheme I-34**).<sup>[158]</sup> Consequently, considering the stereochemistry of crotylzinc bromide becomes redundant, because its configuration changes through 1,3-transposition. Indeed, stereochemically defined alkenyllithium **102** reacts with stereochemically undefined crotylzinc bromide to furnish the desired product **104** with high yield and excellent *anti*-diastereoselectivity, upon quench of **103** with H<sub>3</sub>O<sup>+</sup>.<sup>[156]</sup> The crucial factor lies in the utilization of diethyl ether as a solvent, owing to its lower Lewis basicity compared to THF. This characteristic facilitates the zinc coordination with the electron-rich C–C bond. However, due to the inefficiency of zinc insertion into the allyl-halide bond in diethyl ether, the preparation of allylzinc reagents requires transmetalation from the corresponding allyl Grignards (synthesized in Et<sub>2</sub>O) with ZnBr<sub>2</sub>.



**Scheme I-34.** Diastereoselective formation of *gem*-dizinc compounds via Gaudemar/Normant addition process.

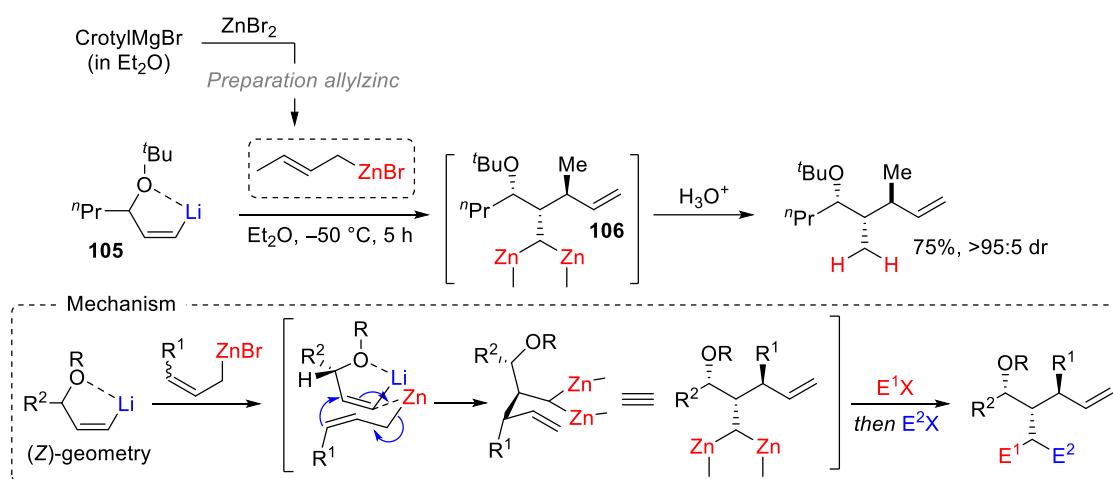
Significantly, this transmetalation reaction generates MgBr<sub>2</sub>, which could potentially expedite both the addition step and subsequent reactions of the *gem*-dimetallic compounds. Since then, based on this information, various highly diastereoselective reactions involving both functionalized the vinyl partner and the allylzinc reagent have been developed and well reported in literature.

Marek and Normant also documented a highly diastereoselective crotylzincation of (*Z*)-alkenyl lithium **105** bearing a *t*-butoxy substituent, resulting in the formation of *gem*-organodizinc species like **106** with remarkable stereocontrol (**Scheme I-35**).<sup>[156]</sup> When the allylic site of the vinylic partner is heterosubstituted (with O, N, or S), the effective preference for a particular diastereoisomer can be

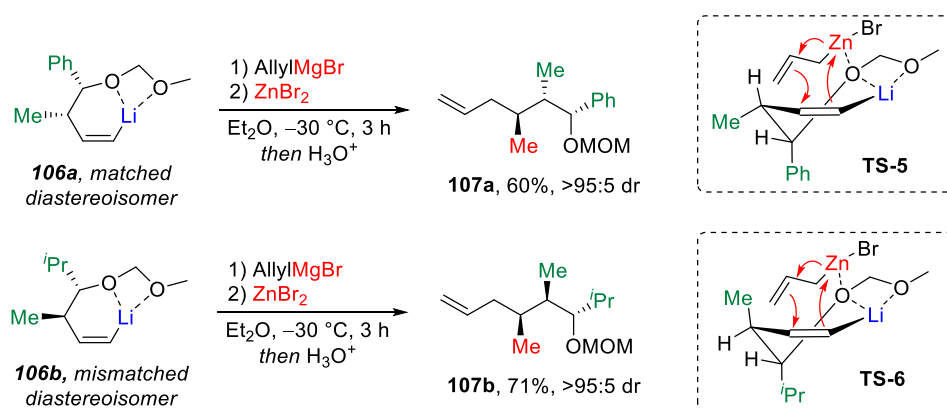


attributed to the internal coordination that occurs during the Gaudemar/Normant addition process.<sup>[162]</sup> This coordination specifically occurs on the *anti*-face in relation to the R<sup>2</sup> group with remarkable stereocontrol.<sup>[163]</sup> This scenario leads to the creation of three stereogenic centers, equating to six possible diastereoisomers, but promoting the formation of (basically) only one. On the other hand, since this coordination mechanism becomes possible only with (*Z*)-alkenyl lithium compounds (like **105**), when the  $\gamma$ -alkoxy vinyl lithium presents an (*E*)-geometry, the lack of chelation occurs, and the observed lower diastereoselectivity (76:24 dr)<sup>[164]</sup> is attributed to the allylic 1,3-strain effect mentioned above.

Instead of a *t*-butoxy substituent, the utilization of a MOM (methoxy methyl ether) group ensures better chelation, leading to enhanced diastereoselectivity (dr >98:2).<sup>[165]</sup>



When (*Z*)-vinyl lithium compounds originate from homoallylic ethers, the chelating group becomes more distantly positioned ( $\delta$ -position to the metal). Nonetheless, remarkable induction still takes place, yielding the desired product as a sole diastereoisomer (**Scheme I-36**).<sup>[166]</sup>



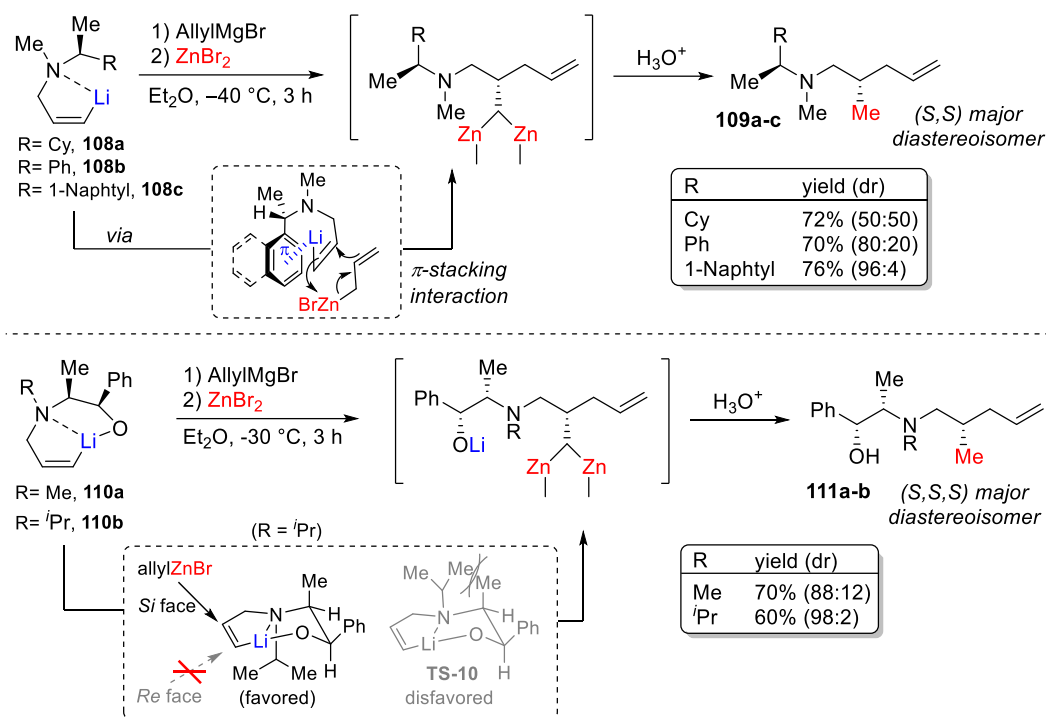
The presence of a substituent in the allylic position of the initial homoallylic ether results in the carbometallation yielding either a "matched" (**106a**) or "mismatched" (**106b**) diastereoisomer. The matched vinyl lithium **106a** generates **107a** with excellent diastereoselectivity (dr >95:5). Unexpectedly, the authors were surprised to find that the mismatched diastereoisomer **106b** also exhibited a highly diastereoselective carbometallation reaction (dr >95:5), wherein the allyl group added *syn* to the methyl group and *anti* to the *i*Pr substituent. This puzzling result can be explained by drawing parallels with addition to substituted cyclohexenes, with a chair-like conformation in the transition state. Considering that the six-membered heterocycle formed through chelation behaves similarly to a six-membered ring, the diastereoselectivity stems from a kinetically guided allylzinc addition directed by chelation toward the oxygen atom. This addition takes place on the energetically preferred conformation, which, in the case of *anti*-disubstituted homoallylic ethers **107a** is (easily comprehensible) represented by **TS-5**, while for *syn*-disubstituted homoallylic ethers **107b**, is the diaxial one (**TS-6**).<sup>[167]</sup>

This elegant approach to the preparation of *gem*-dizinc compounds stands as an efficient and direct process of generating multiple stereocenters within a single operation. If an effective way can be found to introduce asymmetry into this process, it could hold immense potential as a tactic for generating asymmetrical vicinal carbon atoms in one-pot reactions.

To this regard, Marek, Normant and their collaborators employed chiral auxiliaries such as chiral amines to induce the chirality transfer during the carbometallation reaction of allylzinc to alkenyl metal.<sup>[168,169]</sup> Nevertheless, when using the optically active (*Z*)-vinyl lithium **108a** the resulting product **109a** exhibited a disappointing 1:1 diastereomeric mixture (**Schem I-37, top**).<sup>[168]</sup>

In scenarios where the allylic carbon of the (*Z*)-vinyl metal partner is primary, inducing face selection becomes feasible by introducing an aromatic appendage to leverage  $\pi$ -cation interactions with the metal. Consequently, incorporating a 1-phenylethyl substituent onto the nitrogen such as **108b** facilitate the desired facial preference, yielding improved diastereoselective outcome of 80:20. To enhance the  $\pi$ -cation phenomenon, a chiral naphthylamine was employed (**108c**), leading to a significant increase in the diastereomeric ratio up to 96:4. However, the use of *N*-methyl-1-(naphthalen-1-yl)ethanamine as a chiral promoter is hindered by its significant cost,<sup>†</sup> which restricts its applicability on a larger scale. To address this limitation, incorporating an alcohol group, as in compound **110a**, results into **111a** with a favourable 88:12 dr, aided by chelation with the oxygen atom (**Scheme I-37, bottom**).<sup>[169]</sup> Enhancing the bulkiness of the *N*-alkyl group, such as *i*Pr (**110b**), further improves the outcome to a remarkable 98:2 dr. This improvement can be attributed to the reduced accessibility of the *Re* face of the favoured conformation during the carbometallation of the allylzinc partner.

<sup>†</sup> Price for Merck-Sigma Aldrich: (*R*)-*N*-Methyl-1-(naphthalen-1-yl)ethanamine (100 mg) - €82.55; (*S*)-*N*-Methyl-1-(naphthalen-1-yl) not available (updated 19.08.2023).



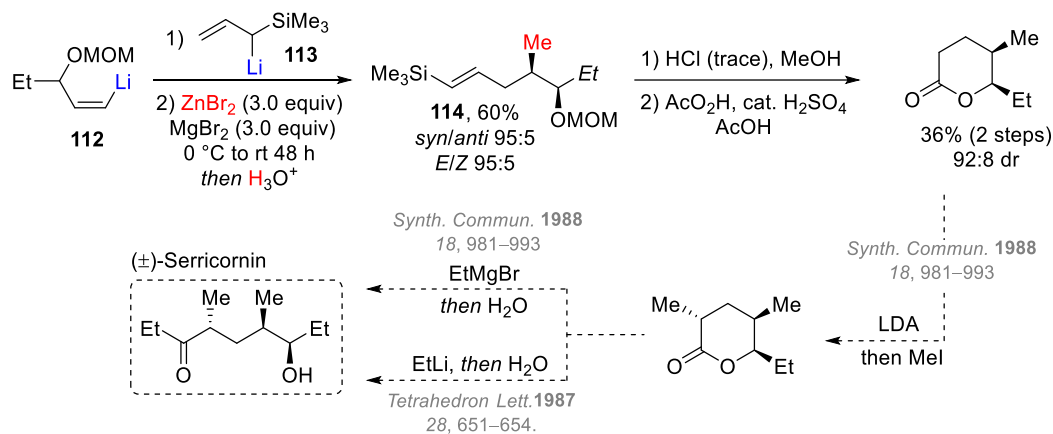
**Scheme I-37.** Stereoselective addition of allylzinc to optically active (*Z*)-vinyl lithium compounds.

Similarly, Marek, Normant and Alexakis also exploited this approach for enantioselective synthesis by derivatization of the vinyl partner into an optically active C<sub>2</sub>-symmetry aminal.<sup>[170]</sup> For instance, (*Z*)-β-iodoacrolein was converted into the aminal, and the carbometallation of the corresponding optically active vinyl lithium compound with crotylzinc bromide led to the formation of a single isomer (70%, dr >95:5), which was readily hydrolysed back to aldehyde.<sup>[168]</sup>

Ultimately, allenyl metal compounds also serve as counterparts for carbometallation reactions with allylzinc reagents. This coupling yields allylic *gem*-dizinc species that can undergo sequential reactions with different electrophiles such as aldehydes and ketones, enabling the synthesis of complex molecules through one-pot procedures.<sup>[171]</sup> However, an equimolar diastereomeric mixture (1:1) was consistently observed.

If a heteroatom is present in the allylzinc reagent, the potential chelation does not interfere and high diastereoselective ratios are observed.<sup>[156,172]</sup> In this scenario, metalated allyl silanes also have demonstrated interesting applications as precursors for the Gaudemar/Normant coupling, offering avenues for further functionalization through silicon chemistry.<sup>[173]</sup> For example, when lithiated allyl silane **113** is added to **112** in the presence of 2 equivalents of ZnBr<sub>2</sub> at rt, carbometallation occurs over the course of 92 hours (**Scheme I-38**). In the resulting carbometallation adduct **114**, the silicon motif ends up positioned at the vinylic site, displaying moderate stereoselectivity (*syn/anti*, 73:27) alongside a robust *E/Z* ratio (95:5). However, by utilizing 3 equivalents of ZnBr<sub>2</sub> and MgBr<sub>2</sub>, the coupling is expedited, and it can be carried out within 24 h at 0 °C. This modification yields excellent *syn* diastereoselectivity (95:5), although with a slightly reduced *E/Z* ratio (87:13). This later issue can be

addressed by allowing the reaction mixture to reach rt for an additional 24 hours after the initial addition process conducted at 0 °C. This maneuver prompts *Z*-to-*E* isomerization, culminating in the formation of a single *syn*-(*E*) isomer.



**Scheme I-38.** Metalated allyl silanes in Gaudemar/Normant coupling and potential synthetic applications: total synthesis of serricornin.

Armed with this refined transformation, the authors effectively showcased the practical utility of these substrates by orchestrating a novel total synthesis of serricornin, the female sex pheromone of *Lasioderma serricorne*.<sup>[174]</sup> Finally, also allenylzinc reagent are able to give the Gaudemar/Normant carbometallation with alkenyl metal to afford *gem*-bimetallic species that hold the potential for engagement with various electrophiles.<sup>[162]</sup>

### 1.9.1.2. Synthesis *via* Metal Insertion of *Gem*-Dihalogen Compounds

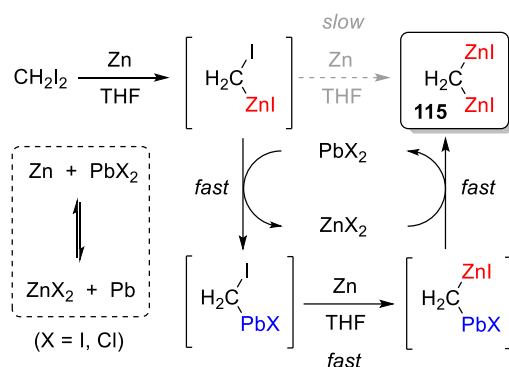
#### 1.9.1.2.1. Synthesis of Bis(iodozincio)methane

The synthesis of the simplest *gem*-dizinc compound, the bis(iodozincio)methane, has been accomplished through the process of halogen–metal exchange involving *gem*-dihaloalkanes, specifically by direct reduction of dihalomethane with zinc metal. It is noteworthy, however, that this technique is also recognized in the literature as the classical way of preparing halomethylzinc, famously referred to as the Simmons–Smith reagent.<sup>[175,176]</sup> Indeed, the conventional approach for generating the Simmons–Smith reagent involves treating diiodomethane with a zinc/copper couple in diethyl ether as solvent. However, pivotal investigations by Fried<sup>[177]</sup> and Miyano<sup>[178–180]</sup> in the context of their Wittig-type methylenation reaction revealed that when the same procedure is carried out employing THF as the solvent, a certain extent of *gem*-dizinc species formation occurs, albeit without delving further into its structural investigation.

In 1975 Nysted patent revealed the formation of a *gem*-dimetallic species from dibromomethane is possible when utilizing a zinc-lead combination.<sup>[181,182]</sup> The patent asserts that treating dibromomethane with a zinc/lead couple in THF at reflux results in the generation of a distinctive *gem*-dizinc species. However, the available evidence at the time was limited to <sup>1</sup>H NMR spectroscopic data, which did not suffice for a comprehensive structural determination. In this context, the proposed structure remained incompletely characterized and well-defined.<sup>‡</sup> Nonetheless, this reagent has shown effectiveness in the methylenation reaction of a large array of carbonyl compounds.<sup>[183-191]</sup>

Then, in 1978, Nozaki, Oshima, and Takai unveiled their findings, detailing the effectiveness of a reagent derived from the combination of diiodomethane, zinc, and either titanium(IV) chloride<sup>[192,193]</sup> or trimethyl aluminium<sup>[192]</sup> in the methylenation of carbonyl compounds. Their protocol encompassed the preparation of the reagent by adding diiodomethane to an excess of zinc dust and a sub-stoichiometric quantity of TiCl<sub>4</sub> (or Me<sub>3</sub>Al) in THF, followed by stirring for half an hour at rt. The emergence of Wittig-type olefins was attributed to the presence of the *gem*-bimetallic species, albeit the exact roles of Me<sub>3</sub>Al and TiCl<sub>4</sub> remain unclarified.

What was of utmost importance in these studies, is that the zinc powder employed was sourced from pyrometallurgy zinc, containing trace amounts of lead(II) (~ 0.04–0.07%). This minuscule catalytic quantity of lead played a pivotal role in facilitating the subsequent reduction of the Simmons–Smith reagent into *gem*-dizinc species, as later elucidated by Takai and Utimoto (**Scheme I-39**).<sup>[194]</sup>

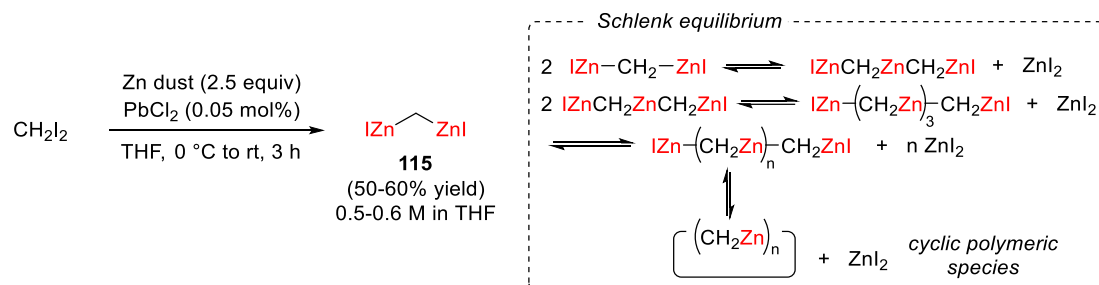


**Scheme I-39.** Proposed effect of lead(II) in the synthesis of *gem*-dizincio compounds [exemplified illustrated with bis(iodozincio)methane].

The proposed mechanism entails a transmetalation process wherein the zinc carbenoid interacts with lead(II), resulting in the formation of a lead carbenoid. This lead carbenoid is subsequently promptly reduced by zinc, leading to the creation of a geminal lead/zinc species. Ultimately, a further transmetalation from lead to zinc, by zinc halide, results in the desired bis(iodozincio)methane (**115**). Armed with these investigations, Utimoto and Matsubara accomplished a groundbreaking feat in 1998

<sup>‡</sup> The THF suspension is commercially accessible from Merck (Sigma Aldrich) under the name "Nysted reagent."

by presenting a general and reliable procedure for the synthesis of **115** as THF solution (**Scheme I-40**).<sup>[195]</sup>



**Scheme I-40.** Matsubara and Utimoto's procedure for the synthesis of bis(iodozincio)methane and its Schlenk equilibrium towards oligomeric/polymeric species.

Determining the structure of this *gem*-bimetallic in THF solution is not straightforward due to the potential involvement of Schlenk equilibria that could result in the formation of oligomeric/polymeric species. However, an in-depth structural analysis employing various X-ray techniques, revealed that the *gem*-dizinc compound prepared in this manner predominantly adopts a monomeric configuration.<sup>[196,197]</sup> Notably, the conditions outlined by Utimoto and Matsubara do not trigger the formation of polymethylene zinc *via* Schlenk equilibrium (**Scheme I-40**), a white solid that is generally insoluble in most solvents. Once prepared, a solution of **115** can remain unchanged for at least a month within a sealed vessel and inert atmosphere.

#### 1.9.1.2.2. Synthesis of *Gem*-Dizincioalkanes

By adhering to the procedure outlined above for the preparation of bis(iodozincio)methane, it is possible to effectively synthesize other *gem*-dizincioalkanes. For instance, 1,1-bis(iodozincio)ethane (**117**) can be successfully obtained with a yield of 50% by treating 1,1-diiodoethane (**116**) with zinc powder (activated through sonication) and a catalytic amount of lead chloride in THF at 0-25 °C (**Scheme I-41**).<sup>[195]</sup>

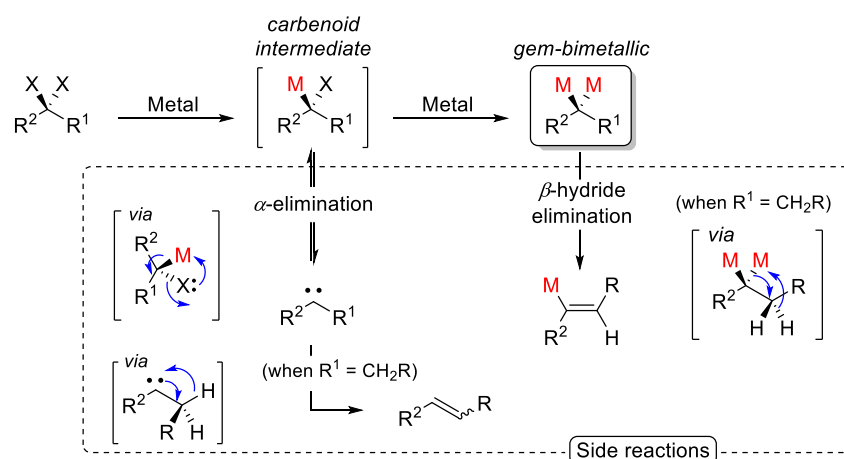


**Scheme I-41.** Preparation of 1,1-bis(iodozincio)ethane.

However, generating *gem*-dizincioalkanes from the corresponding 1,1-dihaloalkanes presents a greater challenge compared to the synthesis of **115**. This heightened complexity arises from the

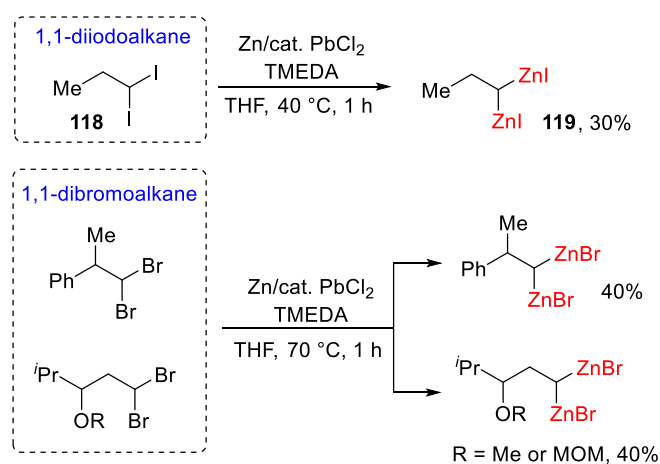
potential occurrence of  $\beta$ -hydride elimination during the reduction of *gem*-dihaloalkanes containing  $\beta$ -hydrogens, leading to the creation of alkene by-products (**Scheme I-42**).

Moreover, the stability of the carbenoid intermediate  $\alpha$ -haloalkylzinc compound is contingent on the substrate and is generally lower than that of  $\alpha$ -halomethylzinc, rendering it more susceptible to  $\alpha$ -elimination reactions.<sup>[198,199]</sup>



**Scheme I-42.** Potential side reactions during the reduction of *gem*-dihaloalkane into the *gem*-dizinc species.

However, the addition of TMEDA enables the successful preparation of various *gem*-dizinc reagents, such as **119** from **118**, with satisfactory yields, by suppressing these undesired reactions (**Scheme I-43**).<sup>[200]</sup> Through this approach, it becomes feasible to synthesize *gem*-dizincioalkanes even when they contain functional groups in the  $\beta$ -position, such as methoxy groups.

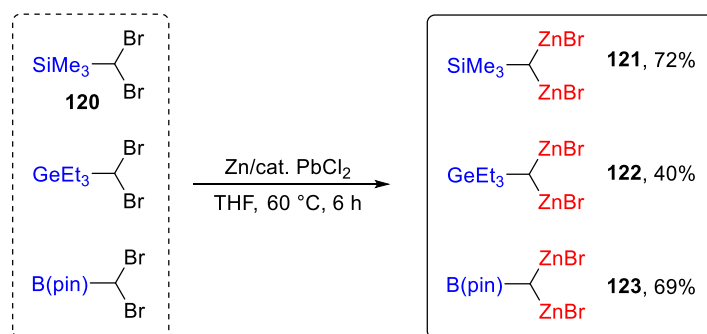


**Scheme I-43.** Procedure for the preparation of various *gem*-dizincioalkanes adding TMEDA as stabilizing agent to avoid undesired parasite reactions during the formation.

Nevertheless, the real structure of these bimetallic compounds in solution remains ambiguous and unclear. While  $^1\text{H}$  NMR analyses reveal the creation of  $\text{C}(\text{sp}^3)$ -geminated organodizinc species, it is crucial not to overlook the possibility of Schlenk equilibriums. Indeed, Nakamura and colleagues conducted computational investigations into the structure of 1,1-bis(iodozincio)ethane in solution (solvated model), suggesting that their true structure in ethereal solvents could be oligomeric.<sup>[160]</sup>

### 1.9.1.2.3. Synthesis of Heteroatom-Substituted *Gem*-Dizincio Reagents

Matsubara and co-workers reported that when trialkylsilyldibromomethanes like **120** are subjected to treatment with pyrometallurgical zinc (alternatively, with pure zinc, a catalytic amount of  $\text{PbCl}_2$  is required) in THF, the corresponding silyl-substituted *gem*-dizinc compounds **121** are obtained with significant yields (**Scheme I-44**).<sup>[201]</sup> The presence of the silyl group enhances the yield of the reduction of the C–Br bonds due to the absence of  $\beta$ -hydrogens, contributing to the notable stability observed in the resulting silyl-substituted *gem*-dizinc compounds. Although no investigations regarding the detailed structure of these organobimetallics in solution are documented in the literature, the possibility of its formation as oligomers cannot be ruled out. The only resemblance can be found in the research conducted by Raston, who synthesized trimethylsilyl(2-pyridyl)dizinciomethane and effectively isolated a tetrameric crystal structure that was identified through X-ray analysis.<sup>[161]</sup>



**Scheme I-44.** Procedure for the preparation of silyl, germyl, and boryl substituted *gem*-dizincio reagents.

Similarly, Matsubara also achieved the successful preparation of *gem*-dizinc species featuring a boryl (**123**),<sup>[202]</sup> and even a germyl group (**122**),<sup>[203]</sup> showcasing the extensive range of possibilities for the synthesis of these organobimetallic linchpins.



### 1.9.1.3. Synthesis *via* Metal–Halogen Exchange

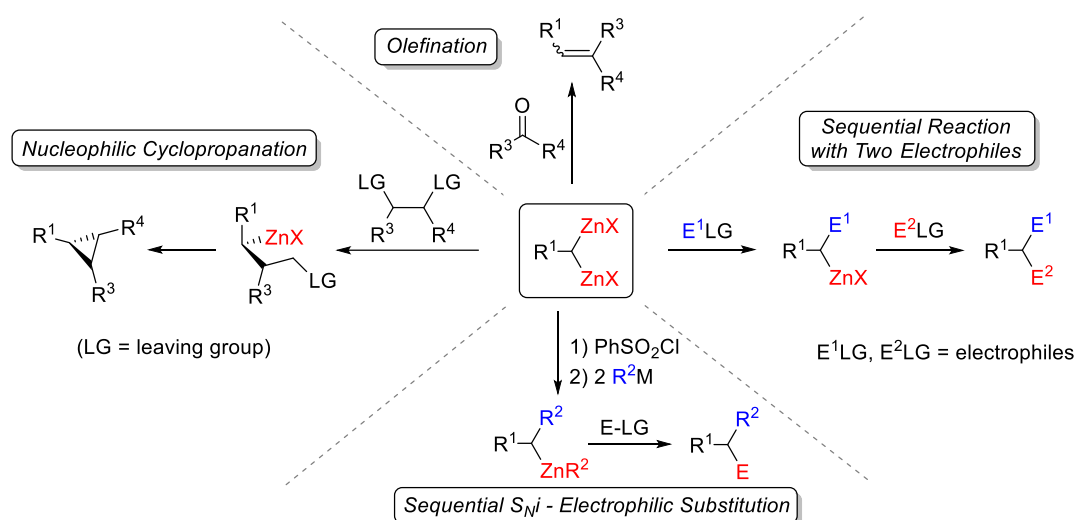
In 2004, Charette documented the synthesis of a *gem*-dizinc carbenoid **124**, bis(iodozincio)iodomethane, by metal–halogen exchange (**Scheme I-45**). This *gem*-dizinc reagent was rapidly prepared (within 5 minutes) by reacting EtZnI (2.0 equiv) and CHI<sub>3</sub> (1.0 equiv) at 0 °C.<sup>[204,205]</sup> Noteworthy is the fact that this particular reagent displays characteristics belonging to both a carbenoid and a *gem*-dizinc species, thereby serving as a zinciomethyl carbenoid.<sup>[204,205]</sup>



**Scheme I-45.** Preparation of bis(iodozincio)iodomethane.

### 1.9.2. Reactivity of *Gem*-Dizinc Reagents

When considering C(sp<sup>3</sup>)-geminated organodizinc compounds, an increase in nucleophilicity is expected in contrast to simple organomonozinc species. This arises from the substitution of carbon with a pair of electropositive metal atoms. The distinct structure of these reagents leads to distinct transformations, which can be schematically illustrated in **Scheme I-46**.



**Scheme I-46.** General reactivity of C(sp<sup>3</sup>)-geminated organodizinc reagent.

With different *gem*-dizinc alkanes in hands, a *plethora* of these synthetic transformations have been developed. In this section, we bring together all the existing literature that has been reported to date regarding the reactivity of these bimetallic species. Specifically, we will place a stronger emphasis and

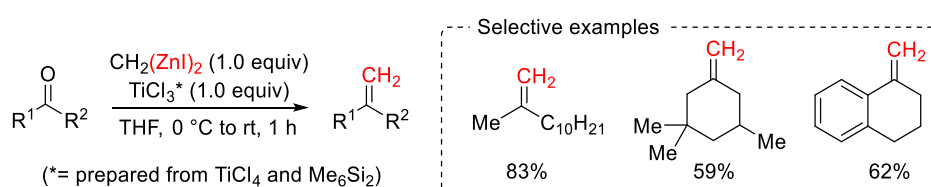
attention on examining the sequential reactions with two electrophiles, which constitute the core focus of this PhD project.

### 1.9.2.1. Olefination Reaction

The olefination reaction of carbonyl compounds can be achieved through diverse methods, with the Wittig reaction being the most renowned approach.<sup>[206,207]</sup> Nonetheless, despite the valuable attributes of the Wittig reaction, certain limitations are present. For instance, the ylide employed can display a degree of basicity that triggers enolization in the initial carbonyl compound.<sup>[208]</sup> Concurrently, it often exhibits limited nucleophilicity and fail to react with specific substrates. These factors have sparked renewed attention in the realm of *gem*-dizinc compounds for this purpose.

#### 1.9.2.1.1. Methylenation

As previously mentioned, preliminary studies on the methylenation reaction of aldehydes and  $\alpha$ -alkoxyketones were carried out using a combination of a zinc-copper mixture and dihalomethane.<sup>[177,179]</sup> The Nysted reagent, in conjunction with stoichiometric quantities of titanium(IV) chloride, also proved effective for achieving the same transformation, thereby broadening the applicability of this reaction.<sup>[183-191]</sup> Subsequently, different research teams explored the methylenation reaction involving dihalomethane and zinc in the presence of titanium salts. However, the role of titanium salts remained unclear, and the reported procedures often suffered from issues of experimental reproducibility on the preparation of the active species.<sup>[193,209]</sup> In response, Utimoto and Matsubara investigated the influence of titanium salts in the olefination reaction alongside with bis(iodozincio)methane in THF solution. With these investigations, they established a well-defined protocol for the methylenation reaction with satisfactory reproducible results (**Scheme I-47**).<sup>[195]</sup> à



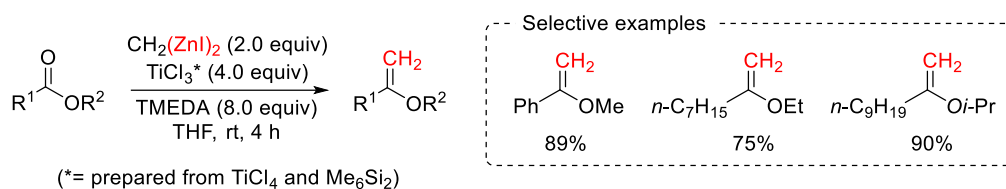
**Scheme I-47.** Methylenation reaction of cyclic and acyclic ketones with bis(iodozincio)methane.

Simple ketones does not undergo methylenation process in the absence of titanium salts. To this regard, a stoichiometric amount of active form of  $\text{TiCl}_3$  (according to Girolamis's correction in 1998, where the salt prepared from titanium(IV) chloride and hexamethyldisilane, was previously mistakenly interpreted as  $\text{TiCl}_2$ )<sup>[210]</sup> is necessary to yield favorable outcomes with numerous cyclic and

acyclic ketones. Through this approach, even highly enolizable ketones like  $\alpha$ -tetralone were methylenated, albeit with modest yields, an outcome unattainable *via* Wittig reaction. However, it is worth to note that aldehydes experience methylenation without the necessity of titanium salts.

Particularly noteworthy is the drastically enhanced nucleophilic attack of the bimetallic reagent on the carbonyl group in the presence of a heteroatom at the  $\alpha$ -position. Consequently, ketones containing an oxygen or nitrogen atom at the  $\alpha$ -position are transformed into methylenated products using bis(iodozincio)methane as the sole reagent, free from any additional additives.<sup>[211]</sup>

Furthermore, Matsubara and co-workers demonstrated that the methylenation reaction can be extended to esters to yield vinyl ethers (**Scheme I-48**).<sup>[212]</sup> However, achieving the desired methylenation requires the addition of an excess of TMEDA.

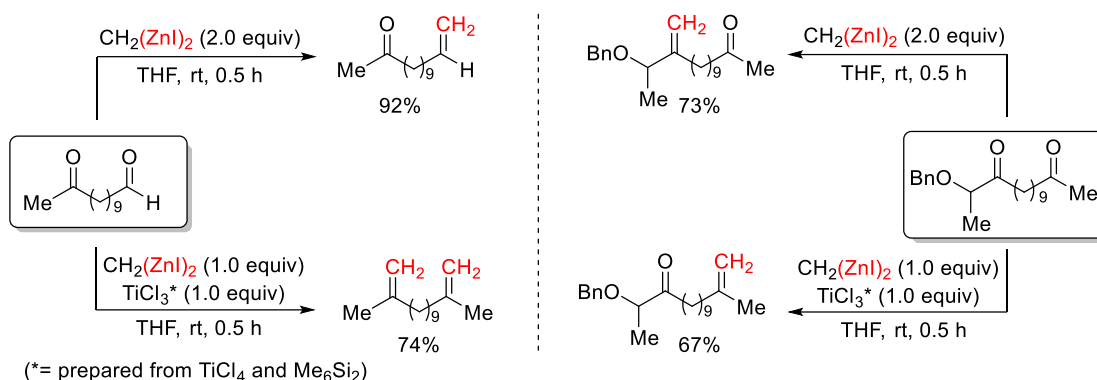


**Scheme I-48.** Methylenation reaction of various esters with bis(iodozincio)methane.

When dealing with simple ketones, one might consider an alternative approach. Instead of introducing  $\text{TiCl}_3$  (as a Lewis acid activator) to promote the nucleophilic attack, a straightforward heating process could potentially afford the desired transformation. However, what is actually observed is that increasing the temperature does not lead to improved reactivity. This is likely attributed to the structural change of the *gem*-dizinc compound into its polymeric form,<sup>[196,197]</sup> which displays lower reactivity for this reaction. This alteration in structure can be counteracted through the use of tetrahydrothiophene (THT)/THF as solvent mixture. Introducing THT, the reaction mixture was heated up to 60 °C and the yields of the corresponding alkenes were drastically enhanced. Nevertheless, the extremely pungent smell reminiscent of rotting eggs of this solvent makes the practical execution of larger-scale experiments (basically) impossible.<sup>§</sup> For this reason other solvents were tested and ionic liquids were found to mirror the function of THT.<sup>[213]</sup>

Chemoselective methylenation of substrates bearing multiple carbonyl groups have also been documented following Matsubara and Utimoto's procedure (**Scheme I-49**). For example, aldehydes are selectively methylenated by bis(iodozincio)methane in the presence of simple ketones. However, both aldehyde and ketone groups are subjected to methylenation when titanium(III) chloride is added.<sup>[195]</sup> Similarly, a keto group positioned in  $\alpha$ -position to a heteroatom experiences selective methylation respect to a simple ketone group, with the reverse chemoselectivity noted in the presence of  $\text{TiCl}_3$ .<sup>[211]</sup>

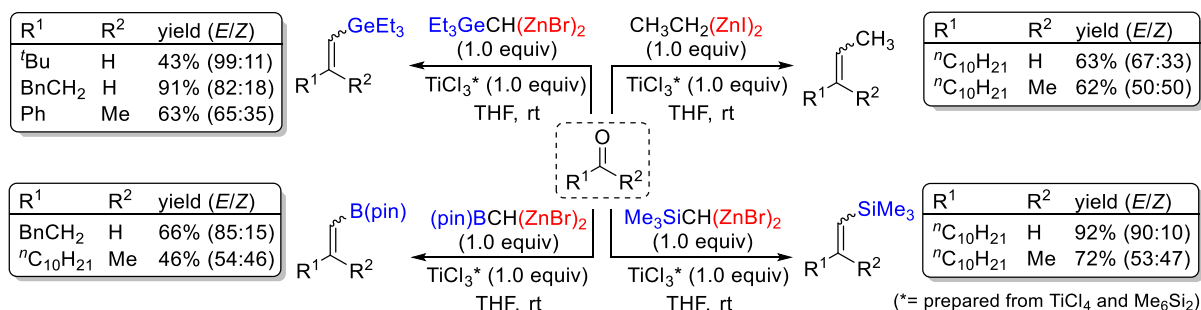
<sup>§</sup> THT presents an extremely low odour threshold at 1 ppb.



**Scheme I-49.** Chemoselective methylenation reactions of dicarbonyl compounds with bis(iodozincio)methane.

### 1.9.2.1.2. Alkylidenation with Gem-Dizinc Reagents Synthesized via Metal Insertion of Gem-Dihalogen Compounds

Treating aldehydes and ketones with 1,1-bis(iodozincio)ethane in the presence of active  $\text{TiCl}_3$  leads to the formation of the corresponding substituted alkenes with satisfactory yields.<sup>[195]</sup> However, the resulting mixture comprises equal amounts of both *E*- and *Z*-isomers (**Scheme I-50**).



**Scheme I-50.** Olefination reactions with 1,1-bis(iodozincio)ethane and hetero-substituted gem-dizinc reagents with aldehydes and ketones.

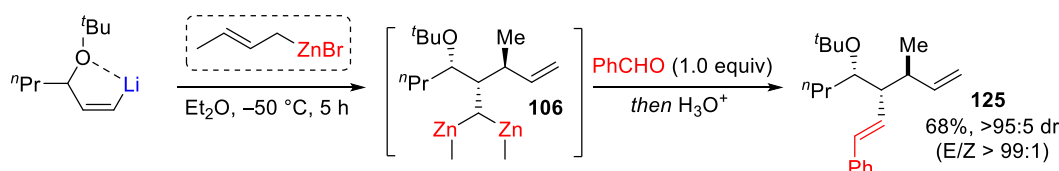
*Gem*-dizinc reagents bearing silyl, boryl, and germyl groups have also been tested for olefination reactions.<sup>[195,202,203]</sup> In cases where aldehydes are employed, the outcomes display high yields, accompanied by good stereoselectivity towards the *E*-isomers. Conversely, when ketones are subjected to the same treatment, the yields are comparatively lower, and the selectivity drops drastically.

Significantly, esters can be transformed into alkylidene compounds by reacting them with a mixture of pyrometallurgical zinc (otherwise a catalytic amount of  $\text{PbCl}_2$  is required), 1,1-dibromoalkanes,  $\text{TiCl}_4$ , and TMEDA. This process proceeds smoothly, yielding *Z*-isomers with

commendable stereoselectivity.<sup>[214]</sup> The methodology is also applicable for converting thioesters and amides into alkylidene derivatives.<sup>[215]</sup>

### 1.9.2.1.3. Alkylidenation with Gem-Dizinc Reagents Synthesized via Carbometallation

So far, only one example has been reported in the literature on the olefination reaction with *gem*-dizinc compounds prepared *via* Gaudemar/Normant carbometallation coupling (**Scheme I-51**). In this context, in 1996, Marek and Normant conducted a diastereoselective synthesis of *gem*-dizinc reagent **106**,<sup>[163]</sup> and engaged it with benzaldehyde, resulting in the production of **125** in 68% yield and high stereomeric purity (E/Z > 99:1, dr > 95:5). Notably, the corresponding olefination reaction was achieved without the need for titanium(III) salts.



**Scheme I-51.** Olefination of benzaldehyde with *gem*-dizinc **106**.

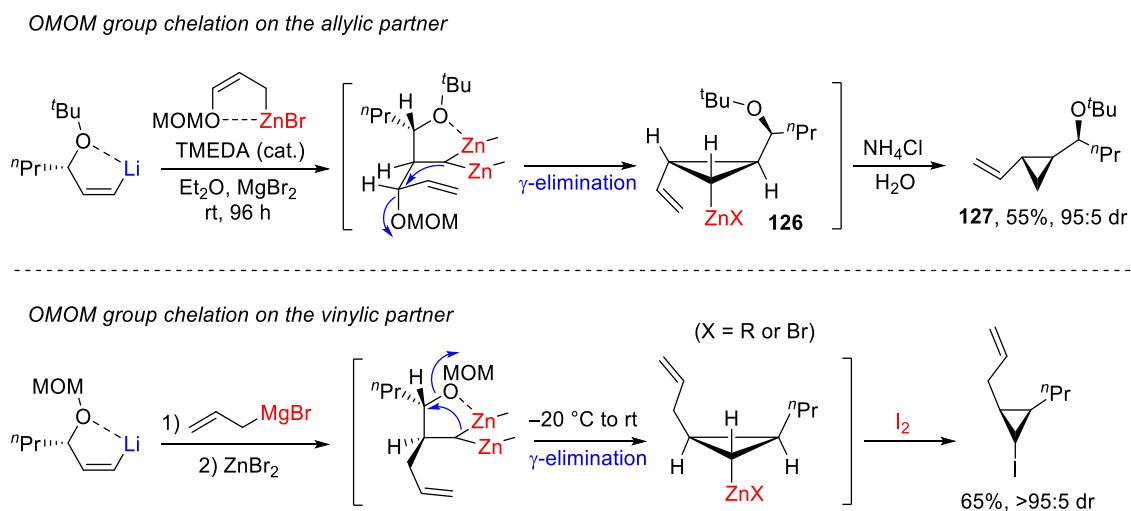
It is worth noting that although this reaction preceded before Matsubara's alkylidenation of *gem*-dizincio compounds chronologically,<sup>[195]</sup> we included this example here to demonstrate to readers how significantly the reactivity of these bimetallic reagents can vary with different preparations.

### 1.9.2.4. Nucleophilic Cyclopropanation

The cyclopropane skeleton is frequently encountered in a large array of natural products.<sup>[216–219]</sup> Several of these naturally occurring compounds containing cyclopropane exhibit significant biological activities and, on occasion, evolve into potential drugs or agrochemicals. Furthermore, the cyclopropane framework serves as versatile synthetic intermediates in organic synthesis.<sup>[220,221]</sup> The primary technique for synthesizing the cyclopropenyl motif involves the interaction between an electrophilic carbenoid and an olefin, as commonly observed in the literature.<sup>[222–227]</sup> However, C(sp<sup>3</sup>)-*gem*-dizinc compounds have been employed for this purpose with excellent results.

### 1.9.2.4.1. Nucleophilic Cyclopropanation with *Gem*-Dizinc Reagents Synthesized via Carbometallation

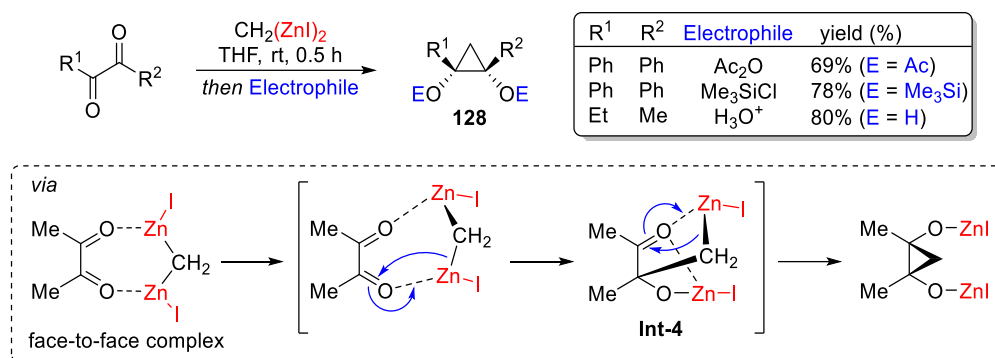
If a heteroatom is present in the allylzinc reagent involved in the Gaudemar/Normant carbometallation reaction with an alkenyl metal compound, the potential chelation does not interfere and high diastereoselective ratios are observed.<sup>[156,172]</sup> Nevertheless, when strong chelation is ensured through the utilization of an OMOM group, and the product of carbometallation addition is allowed to reach rt, it promptly undergoes  $\gamma$ -elimination of the OMOM group resulting in cyclopropylzinc derivative **126** (**Scheme I-52, top**). A simple protonolysis indeed provides direct access to **127**, which features three stereodefined consecutive centers.<sup>[228]</sup> This procedure is of significant interest due to the product pattern's resemblance to numerous metabolites with biological properties discovered in marine invertebrates and algae, which have been the focus of multiple synthetic endeavors during the past decades.<sup>[229–234]</sup> Notably, the same type of 1,3- $S_Ni$  have been observed also when the strong chelation with a OMOM group is present in the vinylic partner (**Scheme I-52, bottom**).<sup>[235,236]</sup> Hence, presence of the OMOM allows the cyclopropanation reaction at rt, whatever it's present on the allylic or vinylic partner.



**Scheme I-52.** Stereoselective cyclopropanation via OMOM group chelation-controlled Gaudemar/Normant carbometallation and subsequent  $\gamma$ -elimination process.

### 1.9.2.4.2. Nucleophilic Cyclopropanation with Bis(iodozincio)methane

$C(sp^3)$ -*gem*-dizinc species bear two nucleophilic sites on the same carbon atom, suggesting their potential to engage in nucleophilic [2+1] reactions with 1,2-diketones. Indeed, Matsubara and co-workers observed that the reaction between bis(iodozincio)methane and 1,2-diketones unveils a new [2+1] cycloaddition process, leading to the selective formation of *cis*-cyclopropanediol derivatives **128**, upon quench with various electrophiles (**Scheme I-53**).<sup>[237]</sup>

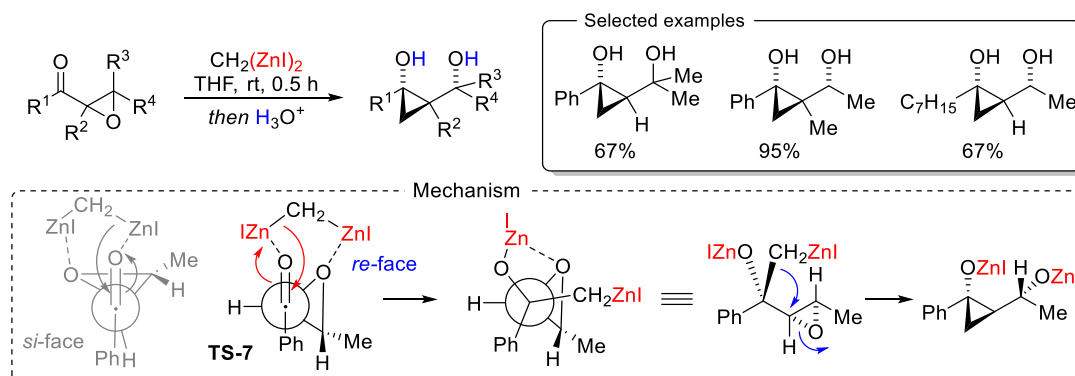


**Scheme I-53.** [2+1] Cycloaddition reaction of bis(iodozincio)methane with 1,2-diketones via face-to-face complex.

DFT calculations on the simple 2,3-diketobutane were used to map out the mechanism of the reaction. According to them, it was explained that the first interaction in this process involves a *face-to-face* complex, where the *gem*-dizinc plays a role as a bidentate Lewis acid.<sup>[238]</sup> Then, the *gem*-dizinc attacks the 1,2-diketone which is in the specific *s-cis* conformation. The alteration caused by the non-flat arrangement prevents the removal of a proton from the methyl group, which would have otherwise resulted in the undesirable conversion of the diketone into its enol form. The sole observed *cis*-product is likely attributed to chelation control originating from the *mono*-addition intermediate **Int-4**.

Interestingly, Matsubara, Nomura, and Oshima developed a similar reaction involving  $\alpha$ -ketoimine compounds to produce *cis*- $\alpha$ -aminocyclopropanol, exhibiting the same excellent diastereoselectivity.<sup>[239,240]</sup> Additionally, Matsubara and co-workers described the stereoselective cyclopropanation of divinyl-1,2-diketones with bis(iodozincio)methane to produce cycloheptane-1,3-diones via Oxy-Cope rearrangement of the zinc alkoxides of *cis*-divinylcyclopropane-1,2-diols.<sup>[241-243]</sup>

Matsubara and co-workers reported that also epoxyketones can serve as effective electrophiles for cyclopropane ring formation exploiting the dual Lewis acid property of the *gem*-dizinc reagents (**Scheme I-54**).<sup>[244]</sup>

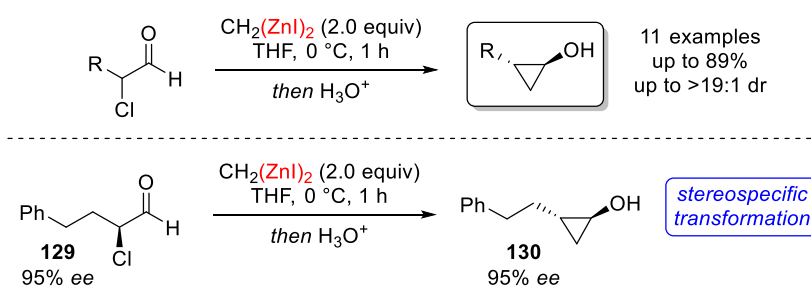


**Scheme I-54.** Reaction of  $\alpha,\beta$ -epoxy ketones with bis(iodozincio)methane and proposed mechanism for stereoselective product formation.

The interaction between these substrates and bis(iodozincio)methane comprises a diastereoselective attack on the ketone, succeeded by a stereospecific attack of the just formed alkylzinc halide into the epoxide. Notably, when employing an optically active epoxy ketone, the desired product is obtained without loss of the enantiomeric purity.<sup>[244]</sup>

The preference for specific stereoisomer can be clarified by considering the diastereoselective approach involving an attack on the *re*-face of the ketone substrate. This stands in contrast to certain prior instances where diastereoselective metal-mediated nucleophilic attacks occurred on an  $\alpha,\beta$ -epoxy ketones through a Cram-chelation model.<sup>[245,246]</sup> The nucleophilic attack is well explained through the presence of **TS-7** via a face-to-face coordination. The absence of the alternative attack is likely attributed to the increased energy associated with the eclipsed conformation of the epoxyketone, resulting in a greater hindrance from the steric interactions between bis(iodozincio)methane and the epoxide ring.

In 2007 the authors also extended the application of bis(iodozincio)methane's reactivity for the diastereoselective preparation of basic cyclopropanols structures from  $\alpha$ -tosylated ketones.<sup>[247]</sup> This process leads to *trans*-cyclopropanols with good diastereoselectivity, attributed to the same chelation face-to-face of the bimetallic compound with the  $\alpha$ -heteroatom and the oxygen of the carbonyl group before initiating the nucleophilic attack on this latter one. A few years later, Walsh replicated the synthesis of identical substrates, commencing with  $\alpha$ -chloroaldehydes and bis(iodozincio)methane (**Scheme I-55**).<sup>[248]</sup>

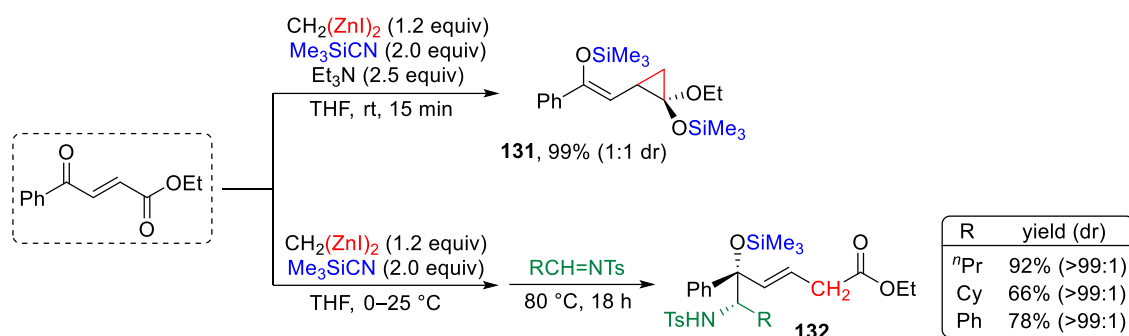


**Scheme I-55.** Cyclopropanation reaction with  $\alpha$ -chloroaldehydes and bis(iodozincio)methane.

However, when employing optically active  $\alpha$ -chloroaldehyde **129** in the reaction, it showcased the full retention of enantiomeric purity. This approach emerged as significantly more intriguing since it provides a reliable method for obtaining enantiomerically enriched cyclopropanols like **130**. This is particularly noteworthy considering that enantioenriched  $\alpha$ -chloroaldehydes can be readily prepared through organocatalytic electrophilic chlorination.<sup>[249,250]</sup>

Another noteworthy utilization of bis(iodozincio)methane in this context was also pioneered by Matsubara, involving its application in the 1,4-addition of  $\beta$ -acylcrotonates (**Scheme I-56**).<sup>[251]</sup>

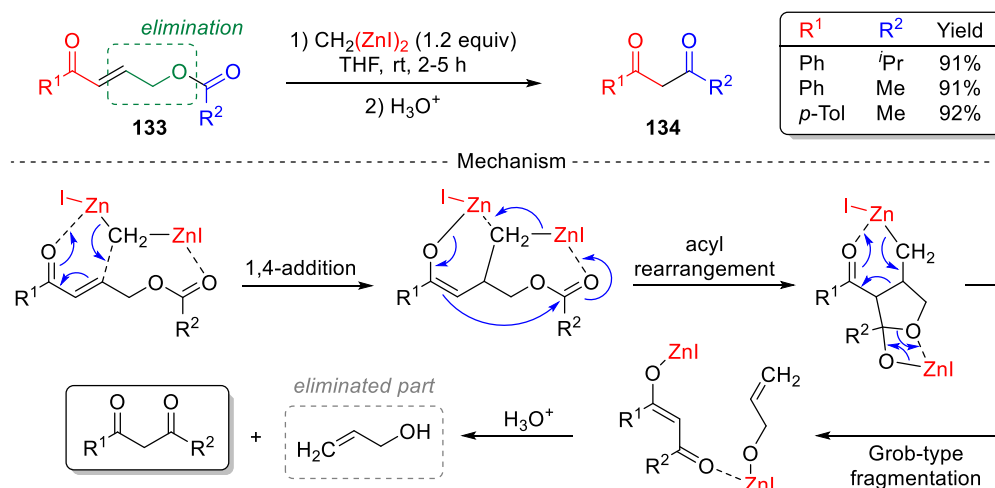




**Scheme I-56.** 1,4-addition of bis(iodozincio)methane to  $\beta$ -acylcrotonates in the presence of trialkylsilyl cyanide, and subsequent reaction with imines to afford  $\beta$ -aminoalkanol.

These types of substrates undergo Michael-addition upon activation with trialkylsilyl chloride or cyanides, leading to the formation of the corresponding homo-enolate. Sequential intramolecular nucleophilic addition to the ester group, followed by quench with another equivalent of trialkyl silyl cyanide (or chloride), yields O-silyl protected cyclopropanols **131** as a diastereomeric mixture. Additionally, the cyclopropane ring within this product is susceptible to opening and reacting with an imine, ultimately producing  $\beta$ -aminoalkanol derivatives **132** with remarkable diastereoselectivity.

When the silyl-based trapping reagent is excluded and substituted with an electrophilic group within the substrate, an intramolecular reaction can take place between the substrate and the zinc enolate that is formed *in situ* (**Scheme I-57**). To illustrate, compounds **133**, which carry an acyloxy group in the  $\gamma$ -position to the enone, undergo a reaction with the zinc enolate generated *in situ*, yielding diketones **134** with three fewer carbon atoms.<sup>[252]</sup> DFT calculations suggest a plausible mechanism involving a tandem reaction comprising three sequential steps.<sup>[253]</sup> The distinctive aspect of this reaction lies in the simultaneous elimination of three atoms. Consequently, this method finds interesting application in producing cyclic 1,3-diketones with medium-sized rings, achieved through the three-atom ring-contraction reaction of the corresponding lactones.<sup>[252]</sup>

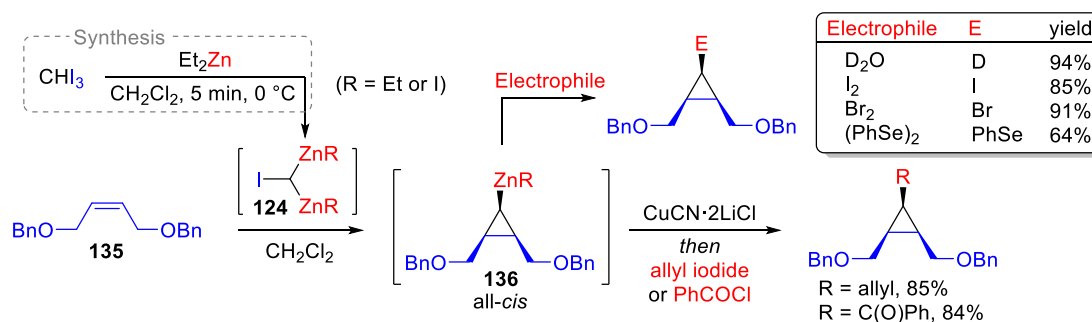


**Scheme I-57.** 1,3-Diketone preparation by the reaction of  $\gamma$ -acyloxy- $\alpha,\beta$ -unsaturated ketones with bis(iodozincio)methane and proposed mechanism.

#### 1.9.2.4.3. Nucleophilic Cyclopropanation with Bis(iodozincio)iodomethane

As mentioned earlier in the preparation section, Charette and colleagues successfully synthesized bis(iodozincio)iodomethane (**124**) by combining diethylzinc and iodoform.<sup>[204]</sup> The readily prepared reagent was employed in a reaction with **135** to generate a cyclopropylzinc intermediate **136**, which was subsequently engaged with various electrophiles (**Scheme I-58**). Notably, the resulting cyclopropyl derivatives exhibited an all-*cis* configuration.

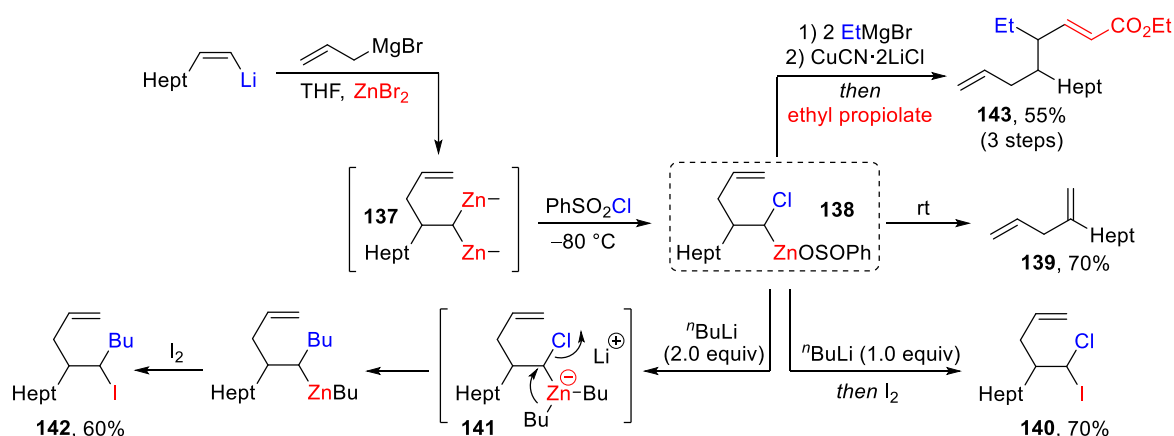
Furthermore, it was demonstrated that this reagent also reacts with other allylic ethers or alcohols, and the stereochemical outcome is significantly influenced by the nature of the proximal directing group,<sup>[204]</sup> and that the addition of 0.5 equivalents of  $\text{ZnI}_2$  into the reaction mixture was observed to enhance both the yield and the efficiency of the transformation.<sup>[205]</sup> While the exact role of  $\text{ZnI}_2$  remains undisclosed, it is hypothesized to serve one of two functions: either stabilizing bis(iodozincio)iodomethane by preventing its decomposition or reducing the transition state energy of the zinco-cyclopropanation step.



**Scheme I-58.** Diastereoselective zinco-cyclopropanation with bis(iodozincio)iodomethane.

1.9.2.3. Sequential S<sub>N</sub>i–Electrophilic Substitution

Since the last century, it has been well-established that the reaction between diethyl zinc and benzenesulfonyl chloride produces ethyl chloride and zinc phenylsulfinate.<sup>[254]</sup> When *gem*-dizinc reagents synthesized *via* the Gaudemar/Normant carbometallation method, are exposed to benzenesulfonyl chloride, an intriguing series of reactions unfolds (**Scheme I-59**).<sup>[255]</sup> When **137** encounter neat PhSO<sub>2</sub>Cl at a frigid temperature of -80 °C, they give rise to an α-chlorozinc carbenoid **138**, which remains stable at temperatures below -50 °C in a diethyl ether solution or below -20 °C when THF is added. Interestingly, at these temperatures, **138** does not react with I<sub>2</sub> but when it is warmed to rt, it undergoes a rapid α-elimination process and subsequent 1,2-H-migration to form **139**, which demonstrate its distinct carbenoid nature. However, when 1 equivalent of *n*-BuLi is added, followed by quench with I<sub>2</sub>, the expected di-halo compound **140** is obtained in a commendable 70% yield. This outcome can be explained by recognizing that the organozinc sulfinate exhibits limited nucleophilic character, rendering it unreactive with I<sub>2</sub> without first undergoing α-elimination. The addition of *n*BuLi transforms **138** into a diorganozinc more nucleophile, capable of reacting with iodine even at low temperature.



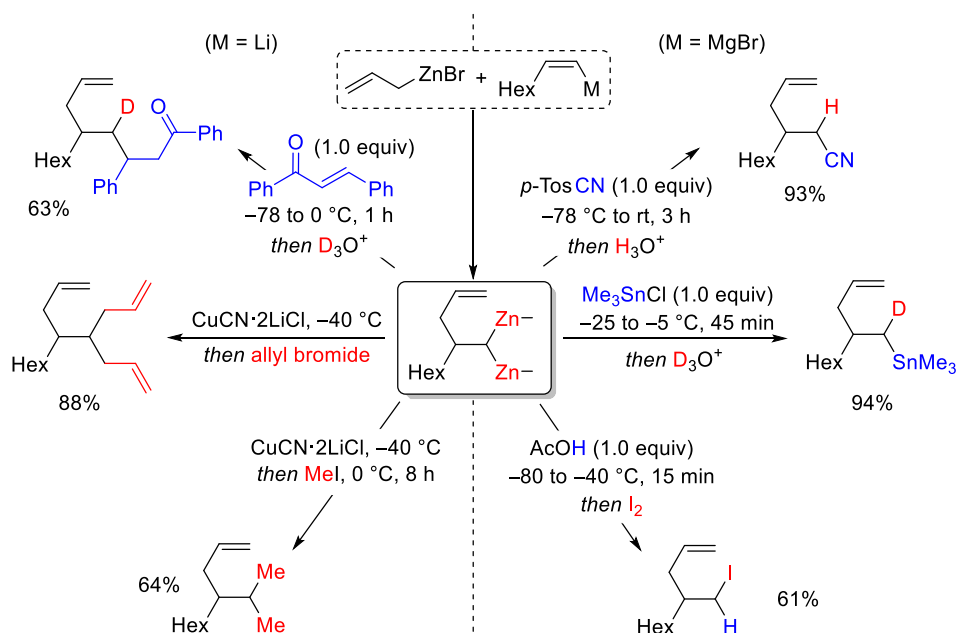
**Scheme I-59.** Selective monoalkylation of *gem*-dizinc reagents via an intramolecular nucleophilic substitution.

More intriguingly, when 2 equivalents of *n*-BuLi are introduced, an α-chloro-triorganozincate **141** is formed, which are well-documented for their propensity to engage S<sub>N</sub>i reactions.<sup>[256–260]</sup> Subsequently, reaction with iodine leads to the formation of **142**. Alkyl groups, both primary, secondary, and tertiary, can all be engaged in the S<sub>N</sub>i reaction, as well as lithium or magnesium organometallics. Instead of quenching with I<sub>2</sub>, which has limited utility in synthetic applications, the authors directed **138** into a copper-mediated conjugated addition with ethyl propiolate. This strategic maneuver resulted in the formation of **143** with an overall yield of 55% over three consecutive steps. This stands as single example where the *gem*-dizinc was not allowed to react with electrophiles only.

### 1.9.2.2. Sequential Reactions with Two Electrophiles

#### 1.9.2.2.1. Sequential Reactions of *Gem*-Dizinc Reagents Prepared via Carbometallation

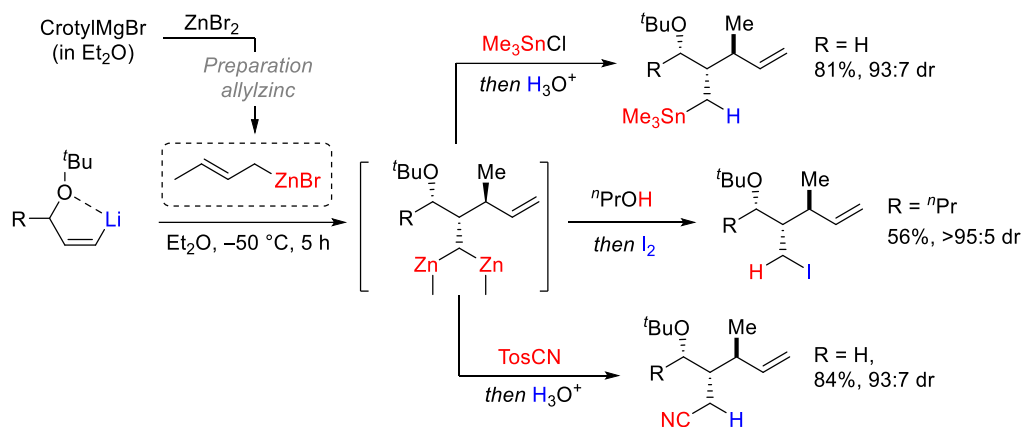
Knochel and Normant pioneered the sequential reactivity of the *gem*-dizinc compounds with distinct electrophiles.<sup>[151-155]</sup> The *gem*-dizinc reagents synthesized through the Gaudemar/Normant carbometallation, were exposed to numerous electrophiles (**Scheme I-60**). As already stated before, their studies revealed that the *gem*-dimetal species could be originated also from allylzinc and alkenyllithium and not only with alkenyl magnesium compounds.<sup>[154]</sup> All these reactions demonstrated very good reactivity towards the electrophiles tested, and since then, the synthetic potential of these organobimetallics could no longer be overlooked.



**Scheme I-60.** Various sequential reactions of *gem*-organodimetallic reagents prepared by the Gaudemar/Normant addition process.

In most of these reactions only one new C–C bond was formed, with the subsequent step involving a simple quench with  $H_2O$  (or  $D_2O$ ). However, the captivating characteristic of *gem*-dizinc compounds lies in their unique ability to simultaneously establish two C–C bonds. Recognizing this, Knochel and Normant converted the *gem*-dimetal compounds into the corresponding copper reagents and subjected them to a variety of electrophiles.<sup>[153]</sup> However, despite the good overall yields, the reactions furnished identical couplings on the two metals, such as bis-allylation and bis-methylation, displaying a limited interest in terms of synthetic applications.

Despite the various stereoselective preparations discussed thus far, only a handful of instances have been documented involving sequential functionalization (**Scheme I-61**).



**Scheme I-61.** Sequential bifunctionalization of diastereomerically enriched gem-dizinc reagents.

However, it is worth noting that both the first and second reactions consistently involved simple protonation, leading to a lack of true bifunctionalization. Furthermore, achieving stereoselectivity in double functionalization has never been accomplished.

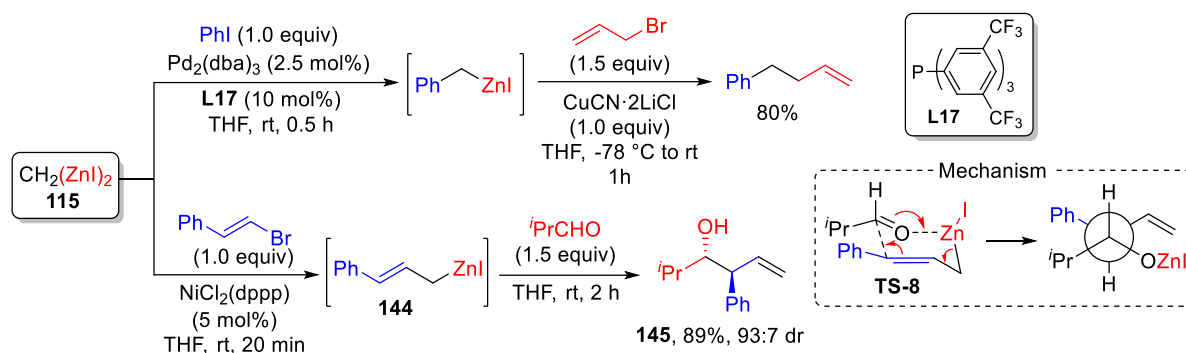
#### 1.9.2.2.2. Sequential Reactions with Bis(iodozincio)methane

Bis(iodozincio)methane, featuring dual nucleophilic sites on a single carbon, offers the potential for sequential reactions with two distinct electrophiles, acting as molecular linchpin. Matsubara for the first time noticed that the reactivity of the first carbon-zinc bond significantly surpasses the resultant methylzinc compound in reactions with D<sub>2</sub>O.<sup>[200]</sup> In fact, the first deuteration step occurs at -35 °C, whereas the subsequent step requires raising the temperature up to 0 °C. These findings, for the first time, implied the feasibility of employing these two C-Zn bonds independently in an orthogonal manner.

To achieve this purpose, the application of transition-metal-catalyzed cross-coupling reactions has paved the way. Matsubara, Utimoto, and their co-workers firstly developed the Pd-catalyzed coupling between bis(iodozincio)methane and allyl chlorides along with electron-deficient phosphine ligands.<sup>[261]</sup> Specifically, P[3,5-(CF<sub>3</sub>)<sub>3</sub>C<sub>6</sub>H<sub>3</sub>]<sub>3</sub> (**L17**) phosphine and tris(2-furanyl)phosphine, showed the best results. Rather than quenching with DCl-D<sub>2</sub>O, which is not synthetically interesting, the organomonozinc intermediate could serve as nucleophile for reacting with different allyl halides, propargyl bromide or acyl halides, leading to various functionalized scaffolds in one-pot.

In this particular context, Matsubara and co-workers expanded the range and variety of electrophiles involved in this type of transformation several years later. For instance, utilizing the same

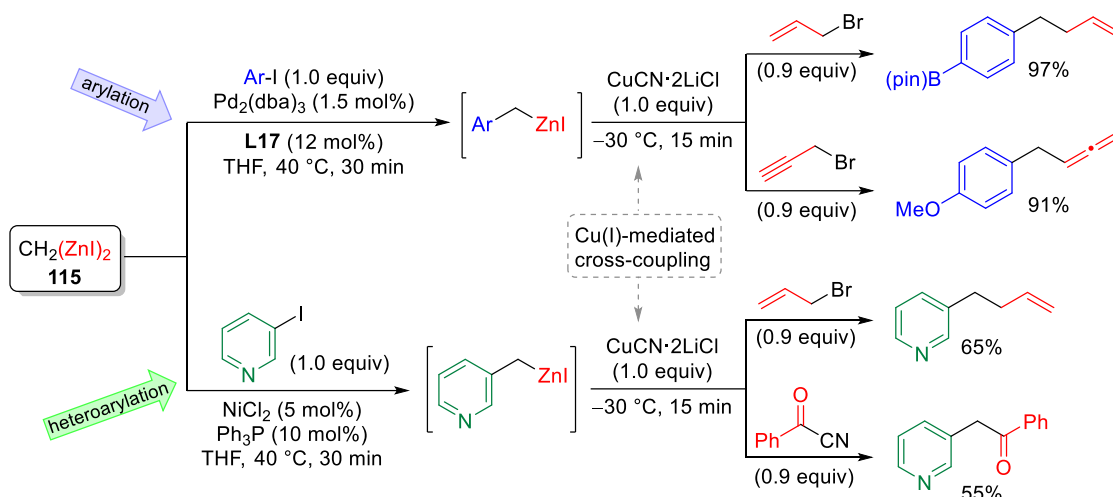
catalytic system, not only allylic halides but also aryl iodides were employed, although a stoichiometric amount of Cu(I) salts was necessary for the second step with allyl halides (**Scheme I-62**).<sup>[261]</sup>



**Scheme I-62.** Sequential cross-coupling reactions with bis(iodozinc)methane and various electrophiles.

They also illustrated the use of vinyl bromide as initial electrophile leading to a diverse array of possible product combinations. However, in this case, the  $\text{NiCl}_2(\text{dppp})$  catalyst proved to be much more efficient than the palladium catalyst, affording the desired cinnamylzinc iodide **144**. Then, **144** was allowed to react with isopropyl aldehyde as the second electrophile and the reaction yielded **145** with a good diastereoselective ratio (*anti/syn* = 93:7). This stereoselective outcome is attributed to a cyclic mechanism, which involves preferential equatorial substitution in the six-membered ring transition state **TS-8**.<sup>[262]</sup>

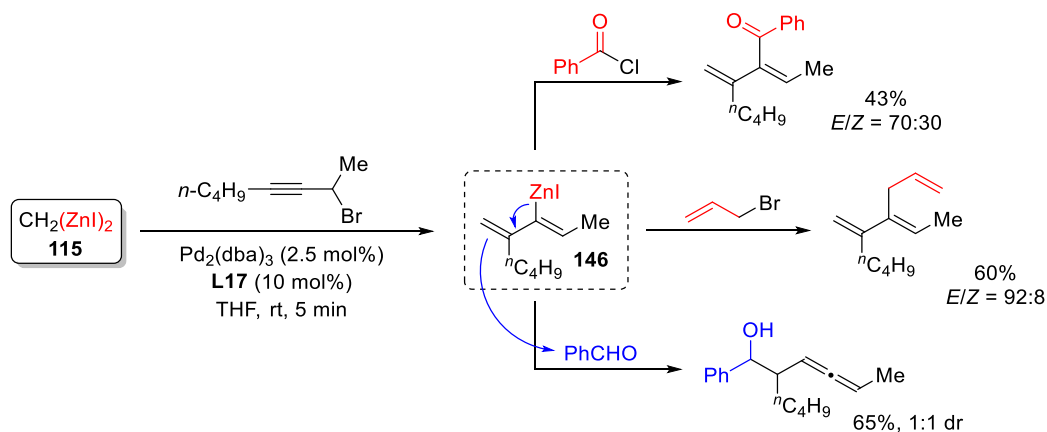
Several years later, the Matsubara group conducted further research on monoarylation as a first cross-coupling (**Scheme I-63**).<sup>[263]</sup> They managed to enhance the catalytic system's efficiency by reducing the amount of  $\text{Pd}_2(\text{dba})_3$  catalyst from 2.5% to 1.5%, and they significantly expanded the range of substrates that could undergo the process. Regardless the electronic properties of the substituents, those located in the *para*- and *ortho*-positions were successfully incorporated. This resulted in zinciomethylation with favourable yields, which were determined by quenching the reactions with  $\text{NH}_4\text{Cl}/\text{H}_2\text{O}$ . Additionally, the group extended their investigation to include a diverse set of iodopyridines as substrates for the cross-coupling reaction. Interestingly, when using Pd-catalyst in these cases, it was unsuccessful. However, the utilization of a nickel-catalyst proved to be highly efficient. For the second cross-coupling, they conducted a copper-mediated reaction with allyl and propargyl bromides as well as benzoyl cyanide.



**Scheme I-63.** Pd-catalyzed mono-arylation and Ni-catalyzed monoheteroarylation of bis(iodozincio)methane, and subsequent Cu-mediated cross-coupling reactions.

Through this approach, they successfully synthesized complex products in a practical manner, achieving outstanding yields (up to 97% over two reaction steps).

When propargyl bromides are used as electrophile for the first cross-coupling, the formation of a conjugated dienyl zinc reagent **146** occurs smoothly (**Scheme I-64**).<sup>[264]</sup>

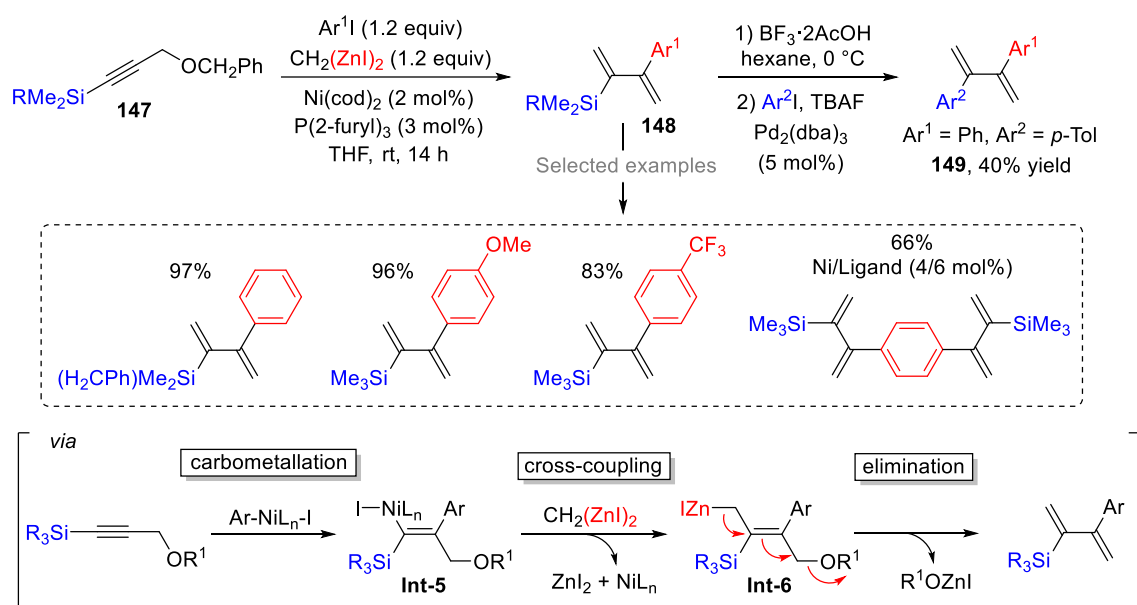


**Scheme I-64.** Formation of a conjugated vinylzinc reagent from Pd-catalyzed cross-coupling of bis(iodozincio)methane and propargyl bromides, and subsequent functionalization of the remaining C-Zn bond.

When this *mono*-organozinc species is allowed to react with allyl bromides or acyl chlorides, it functions as a vinylzinc reagent leading to a practical and straightforward method for producing 1,3-dienes.<sup>[264]</sup> Conversely, if this *mono*-organonometallic compound is exposed to aldehydes it acts as an allenylzinc reagent.

Regarding the synthesis of 1,3-dienes, Matsubara introduced an innovative approach in crafting 1,3-dienes **148** bearing aryl substituents through the reaction of bis(iodozincio)methane and propargyl ethers, bringing a major advancement in the valuable synthetic methodologies using the

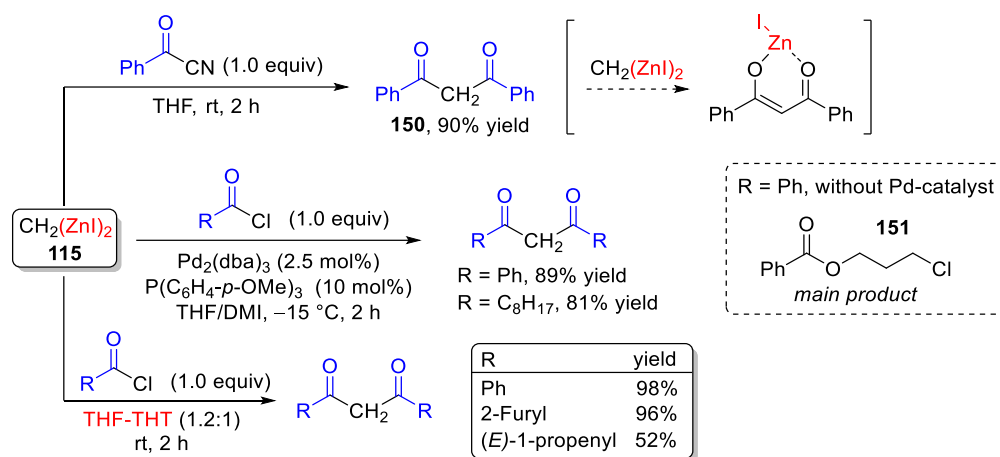
*gem*-dizinc reagent (**Scheme I-65**).<sup>[265]</sup> The reaction was carried out using a nickel catalyst derived from Ni(cod)<sub>2</sub> and (2-furyl)<sub>3</sub>P mixing together bis(iodozincio)methane, **147** and the aryl iodide, furnishing the desired product in very good yields. Treating **147** with bis(iodozincio)methane in the presence of the nickel catalyst, excluding the aryl iodide, resulted in the complete recovery of the ether. Based on this observation, the authors hypothesized that the initial step of the mechanism may involve the carbonickelation of the arylnickel iodide species (formed earlier through oxidative addition of the nickel catalyst to aryl halide), forming **Int-5**. Subsequently, the cross-coupling of this intermediate with the *gem*-dizinc compound generates an allylzinc **Int-6**, which upon the elimination of the zinc alkoxide is converted into the 1,3-diene product. This transformation proved to be versatile in scope, enabling the employ of various aryl iodides with either electron-donating or electron-withdrawing substituents with excellent outcomes (up to 99% yield).



The authors emphasized the potential value of the final product by conducting *via* Hiyama coupling and additional aryl functionalization through *via* Hiyama coupling on the silicon motif. This process provides versatile and efficient route for the synthesis of unsymmetrical 2,3-diaryl-1,3-butadienes **149**.

Since Matsubara and co-workers discovered that bis(iodozincio)methane readily responded to different electrophiles under Pd-catalysis, they proceeded to investigate the consecutive reaction involving it with two acyl groups. This investigation aimed to create a practical route for symmetric and asymmetric 1,3-ketones. Reaction of benzoyl cyanide (2 equiv) with **115** afforded **150** in 44% yield without the need for a Pd-catalyst (**Scheme I-66**).<sup>[266]</sup>



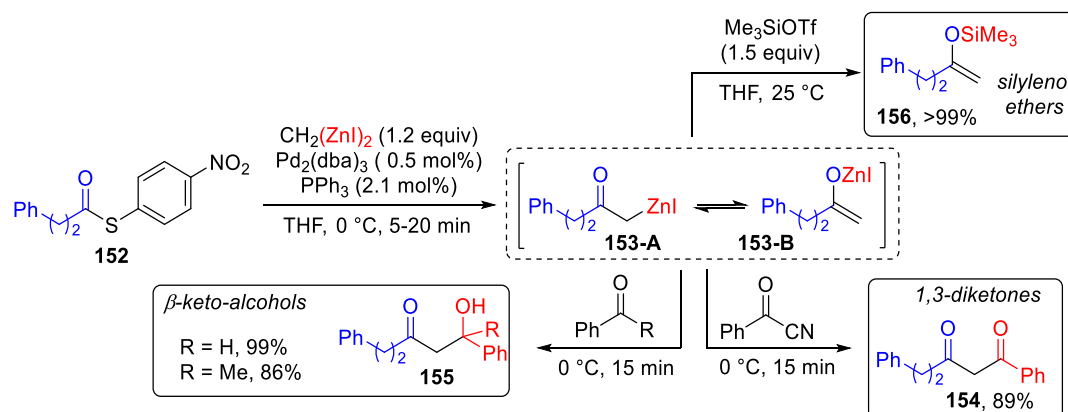


**Scheme I-66.** Reaction of bis(iodozincio)methane with acyl chlorides: synthesis of symmetric 1,3-diketones.

By modifying the molar ratio to 1:1, the yield was enhanced to 90%. This occurred because of the deprotonation of the methylene within the 1,3-diketone product by the *gem*-dizinc reagent, leading to the creation of the zinc-enolate and thus demanding excess quantity of the dizinc species. On the contrary, the use of benzoyl chloride (instead of benzoyl cyanides) lead to a THF-ring opening with acyl chloride, affording **151**, since in these conditions acyl chlorides react faster with THF than bis(iodozincio)methane. However, coupling reaction under Pd<sub>2</sub>(dba)<sub>3</sub>/P(C<sub>6</sub>H<sub>4</sub>-*p*-OMe)<sub>3</sub> catalysis in a mixture THF/DMI (1:1) proceeded smoothly, yielding symmetrical 1,3-diketones in high yields. (up to 89%).

To circumvent the need for Pd-catalysis, an alternative approach would involve identifying a suitable solvent capable of activating the nucleophilic attack of bis(iodozincio)methane on the carbonyl group of an acyl chloride. Among the solvents investigated by Matsubara, THT exhibited a good ability to activate and stabilize the *gem*-dizinc compound. The <sup>1</sup>H NMR spectroscopic data acquired in THF-THT solvent indicated a successful coordination of THT to the dizinc compound.<sup>[267]</sup> However, the correlation between reactivity and structural changes remains unclear. Consequently, this methodology enabled the preparation of symmetric 1,3-diketones all without necessitating the use of any TM-catalyst.

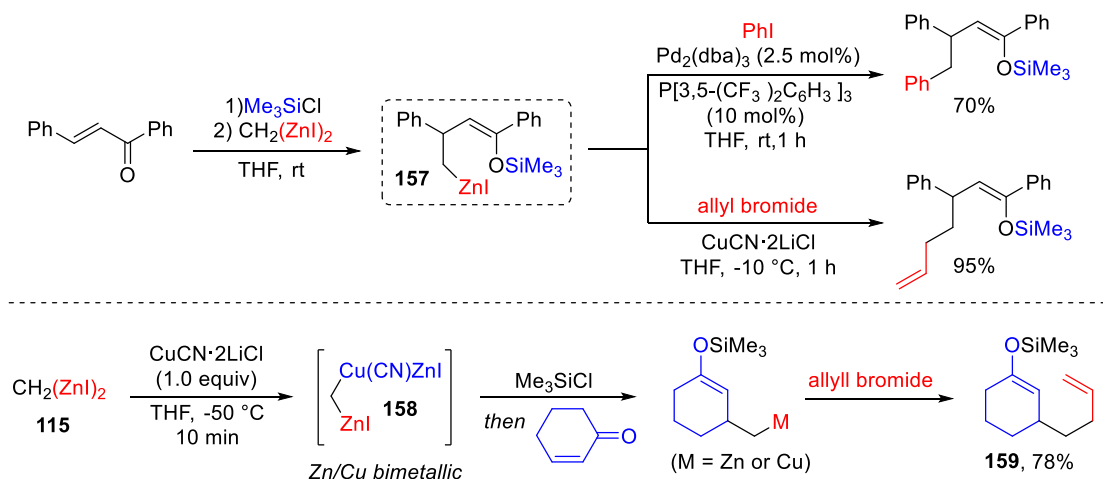
In order to synthesize non-symmetric 1,3-diketones, Matsubara exploited a Fukuyama cross-coupling<sup>[268,269]</sup> between bis(iodozincio)methane and thioesters as the initial step (**Scheme I-67**).<sup>[270,271]</sup> This was employed to generate a Reformatsky-type enolate **153**, capable of reacting with a distinct electrophiles.



**Scheme I-67.** Synthesis of non-symmetric 1,3-diketones, silylenol ethers and  $\beta$ -keto alcohols.

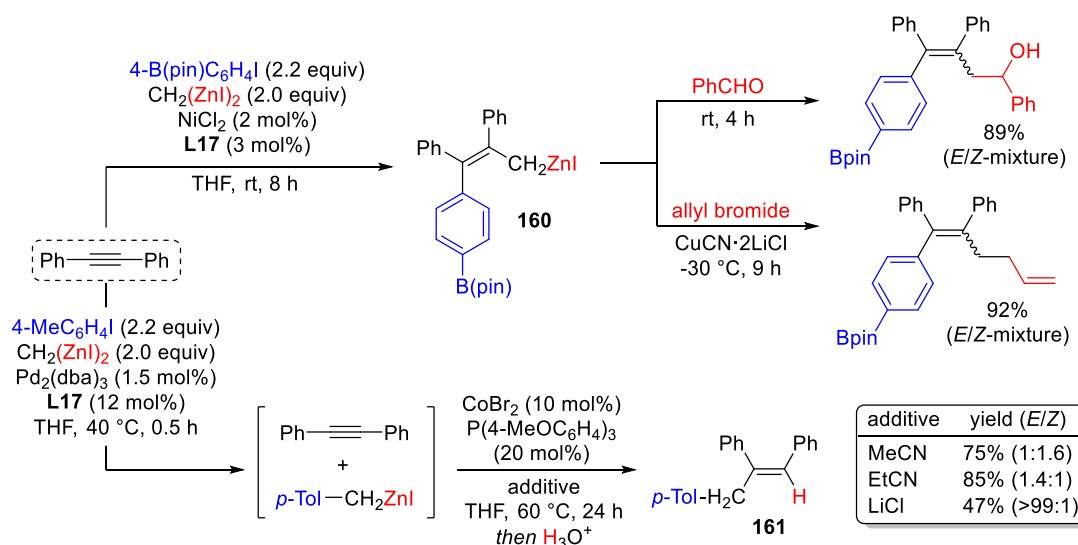
In this procedure they employed differently alkyl substituted 4-nitrobenzenethiol esters **152** along with the  $\text{Pd}_2(\text{dba})_3/\text{PPh}_3$  catalytic system. The electronic properties of the substituent attached to the aryl sulfide motif was crucial: only electron-withdrawing substituents promoted the complete formation of the kinetic enolate. The corresponding zinc-enolate was subsequently applied as nucleophile toward a wide range of acyl cyanides to furnish the desired 1,3-diketones **154** in excellent yields (89%). Moreover, within this protocol, aldehydes and ketones could also serve as second electrophiles to lead uniquely to the aldol product **155**. Interestingly, the reaction conditions also enabled the conversion of chiral thiol esters preserving the integrity of their chiral information. To expand the applicability of this method, by adding silylation reagents to the zinc-enolate intermediates, the researchers synthesized various silyl enol ethers like **156**,<sup>[271,272]</sup> which are very valuable reagents in organic synthesis, particularly for cycloadditions and cross-aldol reactions.<sup>[273-275]</sup>

As part of another utilization of the sequential reaction approach, Matsubara and Utimoto explored the interaction between *gem*-dizinc reagents and  $\alpha,\beta$ -unsaturated carbonyl compounds to execute 1,4-addition reactions (**Scheme I-68**).<sup>[276]</sup> In this context, the bis(iodozincio)methane reacted with chalcones, leading to the corresponding  $\gamma$ -zincio-enolate **157**, upon trapping *in situ* by chlorotrimethylsilane. This intermediate was then allowed to react with various organic halides. However, when subjecting 2-cyclohexen-1-one to treatment with bis(iodozincio)methane and chlorotrimethylsilane, the outcome did not lead to the desired enone compound, and no reaction occurred. In this circumstance, the researchers developed a tactic involving the creation of an organocopper species **158** using the *gem*-dizinc compound and a copper salt. The intention of this method was to augment nucleophilicity, thereby streamlining the 1,4-addition reaction process. Employing this strategy, the reaction with cyclohexanone proved successful, and subsequent reaction with allyl bromide produced **159** in 78% yield.



**Scheme I-68.** 1,4-Addition reactions of bis(iodozincio)methane with  $\alpha,\beta$ -unsaturated ketones and successive functionalization of the second C-Zn bond.

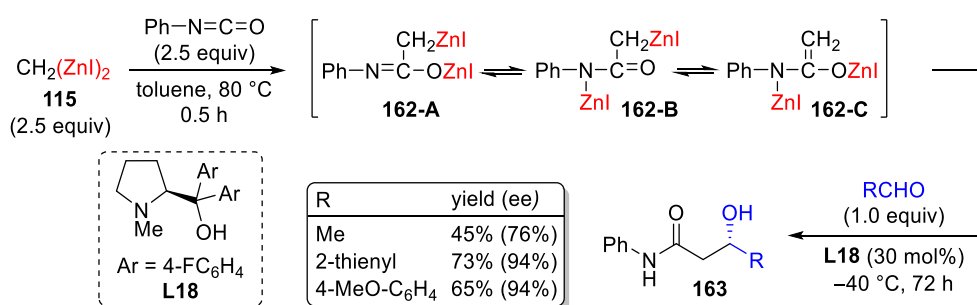
In a recent study, Shimada, Ikeda, and Matsubara introduced a novel three-component coupling reaction involving a symmetrical 1,2-diaryl substituted alkyne, iodoarene, and bis(iodozincio)methane (**Scheme I-69**).<sup>[277]</sup> In the presence of a nickel catalyst, this process yielded allylic zinc compounds **160** featuring a tetrasubstituted alkene moiety. Various combinations of  $\text{NiCl}_2$  and triarylphosphine ligands were explored, revealing that electron-deficient phosphines produced the most favorable yields. Among these ligands,  $\text{P}[\text{3,5-(CF}_3)_2\text{C}_6\text{H}_3]_3$  demonstrated the highest efficacy, as already depicted above (see **Schemes I-63/64**). According to the authors, the reaction takes place through the initial aryl nickelation of the alkyne, followed by a subsequent cross-coupling with bis(iodozincio)methane. **160** was further utilized in conjunction with a diverse array of electrophiles, such as aldehydes and allyl halides.



**Scheme I-69.** TM-catalyzed three-component coupling between 1,2-diaryl substituted alkyne, iodoarene, and bis(iodozincio)methane.

Conversely, when employing the same combination of reagents in the presence of a palladium and cobalt catalyst, the outcome leads to the formation of tetrasubstituted alkenylzinc compounds. This reaction is promoted by a two-step process: a palladium-catalyzed cross-coupling of iodoarene with bis(iodozincio)methane as first, followed by a cobalt-catalyzed benzylzincation of the alkyne. Interestingly the use of different additives comported different yield and regioselectivity of the final alkene product **161**. For instance, among the additives, LiCl resulted in the lowest yield (47%), but only the *E*-product was observed. Conversely, MeCN and EtCN yielded similar results (75% and 85% respectively), but with contrasting diastereoselective ratios of *E*- and *Z*-alkene.

In 2014, an intriguing study by Haraguchi and Matsubara unveiled a novel series of sequential reactions involving bis(iodozincio)methane. The *gem*-dizinc reagent, when treated with phenyl isocyanate, generates a zinciomethylenated product **162**, that functions as an amide-enolate equivalent (**Scheme I-70**).<sup>[278,279]</sup> This intermediate displayed limited reactivity with aldehydes in Reformatsky-type reactions, likely attributed to the “absence” of the *O*-enolate form **162-C**, and instead exhibited characteristics more aligned with alkylzinc forms **162-A** and **162-B**.<sup>[280]</sup> However, upon introduction of an aminoalcohol, the corresponding adducts **163** formed in noteworthy yields. This activation played a pivotal role in achieving asymmetric induction. In fact, the utilization of catalytic amounts of a chiral aminoalcohol **L18** derived from *L*-proline, drove the process toward catalytic asymmetric Aldol-type reactions, showcasing remarkable chiral induction (up to 93% ee).

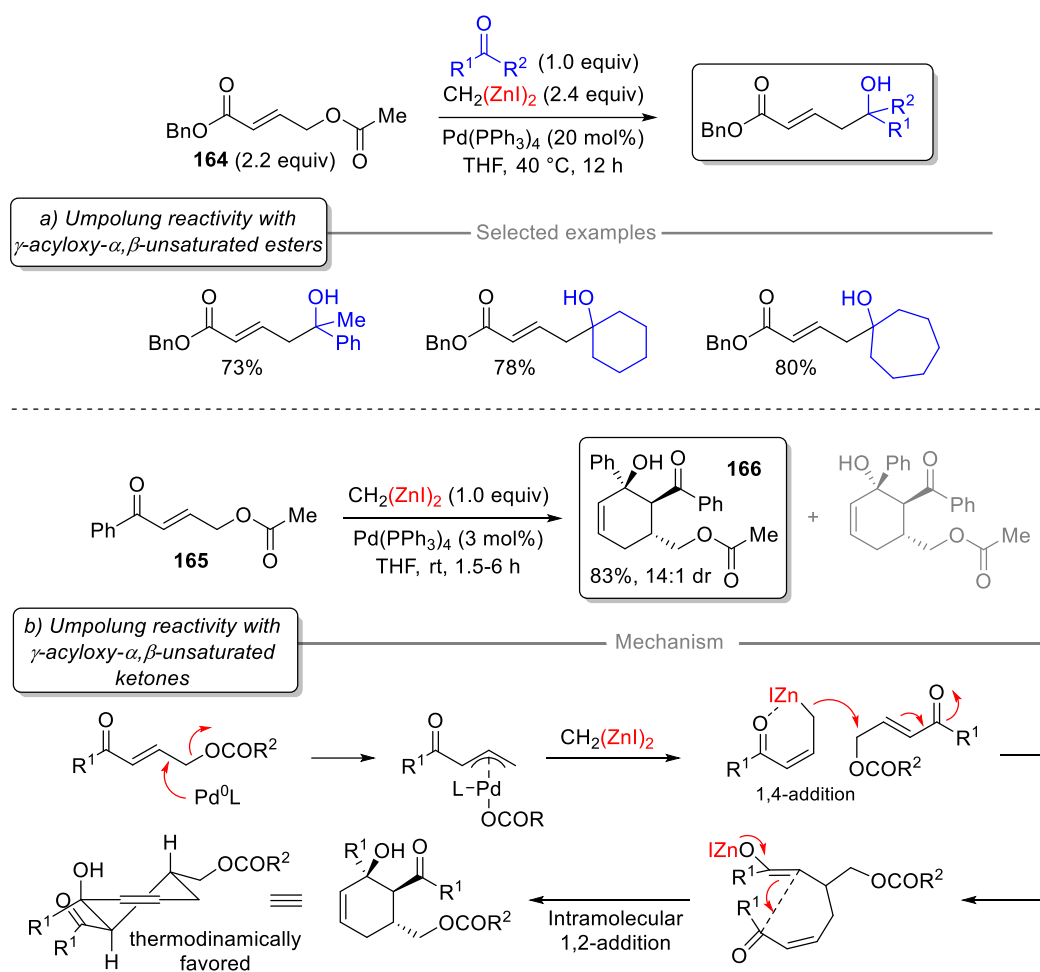


**Scheme I-70.** Formation of a zinc enolate equivalent of amides by reaction of bis(iodozincio)methane and isocyanates: aminoalcohol catalyzed enantioselective Reformatsky-type reaction.

Lastly, Matsubara detailed an effective method for allylating ketones through the umpolung reactivity of  $\pi$ -allyl-palladium intermediates with bis(iodozincio)methane (**Scheme I-71a**). This process involved generating an allylic zinc species *via* the reduction of the  $\pi$ -allyl-palladium compound using the *gem*-bimetallic, which acted as reducing agent. The allylic zinc species serves thus efficiently as allylating reagent for the  $\gamma$ -acyloxy- $\alpha,\beta$ -unsaturated esters **164**.<sup>[281]</sup>

However, extending this umpolung process to  $\gamma$ -acyloxy  $\alpha,\beta$ -unsaturated ketones like **165** resulted in a distinct reaction pathway (**Scheme I-71b**).<sup>[282]</sup> Treating **165** with bis(iodozincio)methane in the presence of a Pd(0)-catalyst produced the corresponding cyclohexene

derivatives **166** in a diastereoselective manner. The authors proposed a mechanism wherein the formation of the  $\gamma$ -keto allylic zinc, facilitated by the *gem*-bimetallic through the  $\pi$ -allyl-palladium species, underwent a 1,4-addition to the substrate. The emerging zinc enolate subsequently underwent an intramolecular addition to the keto group, yielding selectively the thermodynamically favoured isomer of the cyclohexene derivative.



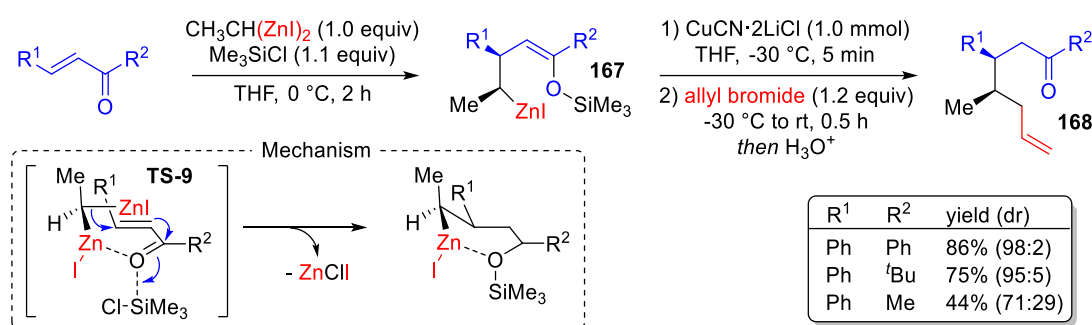
**Scheme I-71.** Umpolung reactivity of  $\pi$ -allyl-palladium intermediates with bis(iodozincio)methane employing a)  $\gamma$ -acyloxy  $\alpha,\beta$ -unsaturated esters, b)  $\gamma$ -acyloxy  $\alpha,\beta$ -unsaturated ketones.

### 1.9.2.2.3. Sequential Reactions with 1,1-Bis(iodozincio)ethane

The stereochemical aspects of the 1,4-addition of 1,1-bis(iodozincio)ethane (**117**) to  $\alpha,\beta$ -unsaturated ketones have been the focus of investigations (**Scheme I-72**). Matsubara observed that the diastereoselective conjugate addition of 1,1-bis(iodozincio)ethane resulted in the formation of the secondary organozinc reagent **167** with remarkable *cis*-diastereoselectivity.<sup>[283]</sup> It was suggested that when the reaction proceeds *via* the *s-cis* conformation, the 1,4-addition likely occurs through a six-

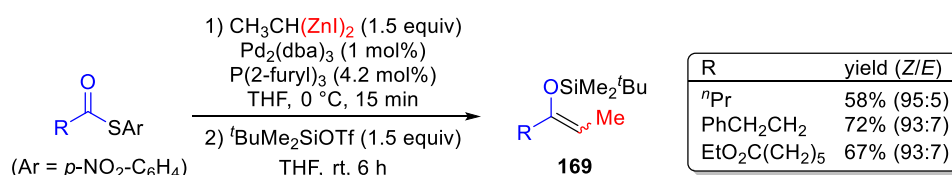
membered transition state **TS-9**, where the coordination of a zinc atom at the *endo* position of the carbonyl oxygen is deemed essential for diastereoselective outcome.

The bulkiness of the substituent  $R^2$  in compound plays a pivotal role in both the yield and diastereoselectivity by promoting the displacement of the coordinated *gem*-dizinc to the terminal position of the *s-cis* enone. Subsequently, the authors engaged the configurationally stable monorganozinc compounds into a copper-mediated allylation, leading to the stereospecific formation of **168** in good yields.



**Scheme I-72.** *cis*-diastereoselective 1,4-addition of 1,1-bis(iodozincio)ethane to  $\alpha,\beta$ -unsaturated ketones.

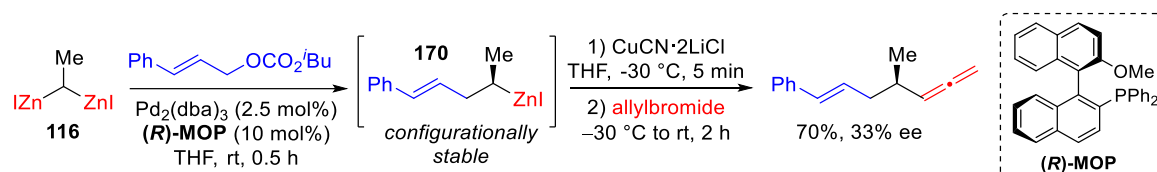
As mentioned before, the palladium-catalyzed Fukuyama reaction between thioesters and bis(iodozincio)methane produce  $\alpha$ -zincioketones, which isomerize to zinc enolates. Similarly, the employ of 1,1-bis(iodozincio)ethane led to the corresponding zinc enolate with remarkably *Z*-selectivity (**Scheme I-73**).<sup>[272]</sup> After silylation trapping of the zinc intermediate with *t*-BuMe<sub>2</sub>SiOTf, various silyl enol ethers **169** with *Z*-conformation were obtained in satisfactory yields.



**Scheme I-73.** *Pd*-catalyzed Fukuyama cross-coupling between 1,1-bis(iodozincio)ethane and alkyl thioesters.

The utilization of sequential cross-coupling reactions with *gem*-dizincioalkanes may offer a promising route for generating optically active organozinc compounds. In general, chiral enantioenriched organometallic species, are highly sought after they provide a straightforward method for constructing asymmetric carbons in optically active configurations.<sup>[284–288]</sup> In this context, Matsubara and coworkers embarked on the quest to synthesize a chiral *mono*-organozinc compound, through a desymmetrization strategy after the initial cross-coupling reaction.<sup>[289]</sup> Their approach involved the reaction of 1,1-bis(iodozincio)ethane (**117**) with cinnamyl electrophiles in the presence

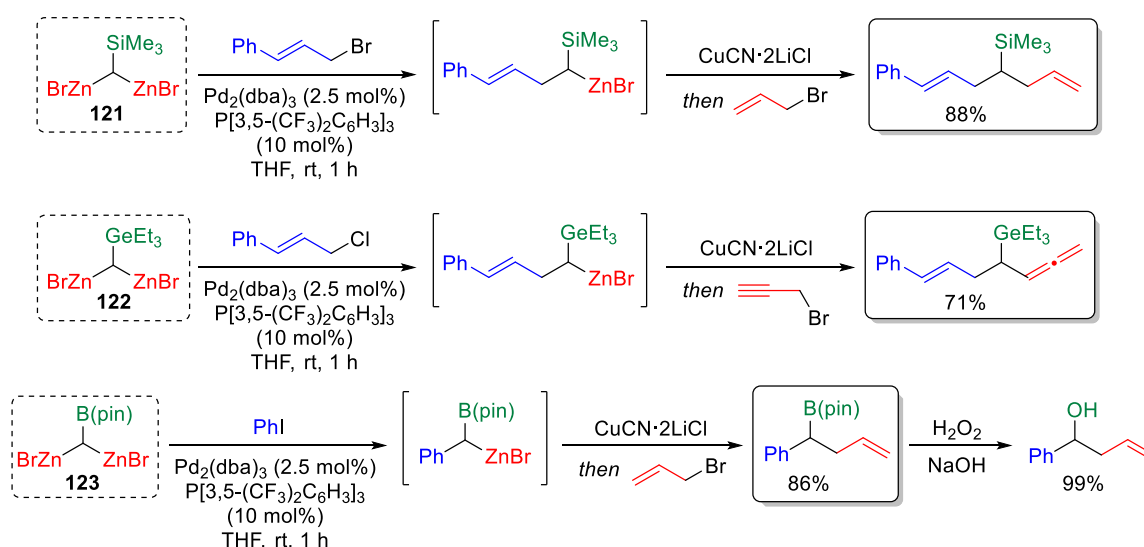
of a Pd(0) catalyst alongside a chiral phosphine ligand (**Scheme I-74**). The resulting organomonozinc intermediate **170**, configurationally stable, was subsequently engaged in a stereospecific copper(I)-mediated coupling reaction with propargyl bromide. However, it is noteworthy that the highest observed level of asymmetric induction in this endeavor reached a mediocre 33% ee when using cinnamyl carbonate as the electrophile and (**R**)-MOP as chiral ligand. To date, this stands as the sole exemplar of an enantioselective transformation involving a prochiral *gem*-dizincioalkane.



**Scheme I-74.** Synthesis of a chiral non-racemic mono-organozinc via desymmetrization of 1,1-bis(iodozincio)ethane, and subsequent copper-mediated cross-coupling with propargyl bromide.

#### 1.9.2.2.4. Sequential Reactions with $\alpha$ -Hetero-substituted *Gem*-Dizinc Reagents

The readily prepared silyl-, boryl-, and germyl-substituted *gem*-dizinc compounds can also undergo sequential cross-coupling reactions with a wide range of electrophiles (**Scheme I-75**).<sup>[201–203]</sup> However, while these sequential coupling reactions with *gem*-dizinc reagents offer the potential to produce chiral  $\alpha$ -functionalized organozinc compounds, stereoselective versions of these transformations have not yet been developed.



**Scheme I-75.** Sequential reactions of hetero-substituted *gem*-dizinc compounds with various electrophiles.

## 2. Configurational Stability of Organozinc Compounds

First of all, it is crucial to remind the reader that the term "*configurationally stable*" lacks specificity on its own. This concept becomes meaningful only when linked to both a specific temperature and a specific timeframe. In this framework, the configurational behaviour is a crucial aspect of asymmetric organic chemistry, and its understanding forms the bedrock of a solid theoretical foundation for research in enantioselective reactions. In fact, configurational stability (or lability) directly impacts the success of enantioselective transformations, and understanding how configuration can be either preserved or altered during a reaction is a pivotal aspect for optimizing experimental conditions to achieve maximum efficiency and selectivity.

As we discussed in the preceding section, the most employed *gem*-bimetallic compounds for the development of enantioselective sequential reactions have been *gem*-bis(boronates).<sup>[290]</sup> This preference stems from the fact that, whether starting with enantiomerically enriched reagents or racemic compounds, *mono*-organoboronates formed after the initial functionalization step, exhibit robust configurational stability.<sup>[291-293]</sup> This exceptional stability has enabled the development of a diverse array of bimetallic reagents and various subsequent sequential reactions, all without any loss of enantiomeric excess, even under harsh conditions.<sup>[290]</sup>

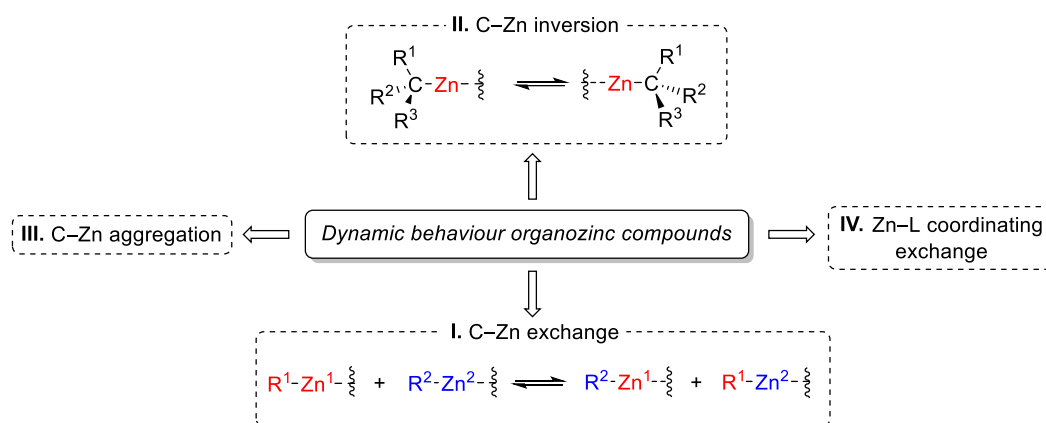
In contrast, the situation is very different for organozinc compounds. Unlike their boron counterparts, these organometallic reagents exhibit a configurational stability highly dependent on the nature of the reagent itself, and generally it undergoes rapid changes as temperature increases.<sup>[294]</sup> This characteristic sets organozinc compounds apart and has, until now, relegated them to the periphery of enantioselective sequential reactions. In fact, their utilization in this context has been largely disregarded. The only reported example of an enantioselective reaction with *gem*-dizinc prochiral compounds, dating back to 2000 by Matsubara,<sup>[289]</sup> relied on the assumption that the *mono*-organozinc intermediate after the first reaction was configurationally stable. Nevertheless, the achieved enantiomeric excess in this instance was rather modest, standing at a mere 33% ee. Therefore, if we aim to advance the development of new sequential reactions with *gem*-dizinc compounds, it becomes of paramount importance to ascertain whether the *mono*-organozinc intermediate will exhibit labile or stable configurational behaviour. For this reason, the analysis of the configurational stability of organozinc compounds will be comprehensively discussed in this section.

### 2.1. General Dynamic Behaviour of Organozinc Compounds

Conceptually the dynamic behaviour of organozinc compounds in solution can be examined by four distinct processes: exchange, inversion, aggregation, and coordinating-ligand exchange (**Scheme I-76**).<sup>[294]</sup> All of these mechanisms theoretically involve varying degrees of changes in the C–Zn bonds.



Nevertheless, while mechanisms such as coordinating-ligand exchange and aggregation primarily do not induce significant alterations in the C–Zn bond, exchange and inversion result in notable modifications to its structural integrity. As a result, among these mechanisms, only the dynamic of exchange and inversion have been extensively investigated by numerous research teams, focusing on their impact on the C–Zn bond.



**Scheme I-76.** Dynamic behaviour of organozinc compounds.

The aim of the next paragraphs is to provide a concise yet thorough analysis of the configurational stability of organozinc compounds in solution, examining all the factors which influence it. However, since the C–Zn exchange occurs with retention of the configuration, and aggregation and coordinating-ligand exchange do not affect (almost) at all the integrity of the C–Zn bond, only the inversion process will be considered and discussed.

## 2.2. Inversion of Carbon–Zinc Bond

The inversion of configuration in C–Zn bonds involves breaking and reassembling of the bond from the opposite side of the carbon atom, resulting in a complete modification of the bond's integrity. The speed of the inversion process is strongly influenced by the characteristic of the carbon atom bonded to zinc (substitution and hybridization). In this realm, comprehensive research and confirmation have been achieved mainly within primary, allylic, and benzylic organozinc systems. Secondary organozinc compounds, albeit to a minor proportion, also contribute to this body of knowledge. However, the precise mechanisms implicated in this process have not been entirely elucidated and continue to be uncertain.

## 2.2.1 Primary Alkylzinc Compounds

In the realm of organic chemistry, within the array of different organometallic compounds, organozincs hold a middle ground concerning the electronegativity of the metal. As a prevailing tendency, it is commonly acknowledged that for organometallic reagents without bearing additional functionalities, those with stronger covalent carbon-metal bond are prone to exhibit higher energetic barriers for the inversion at the carbon center (also known as topomerization barriers).<sup>[295]</sup> Conversely, the organometallic compounds with weaker covalent bond tend to display the opposite behaviour.

To study the configurational behaviour of primary organometallic reagents, in the specific case neohexylmetallic compounds (neohexyl = 3,3-dimethylbutyl) in dilute ether solutions, a comparative analysis of <sup>1</sup>H NMR spectra was conducted (**Table I-1**).<sup>[296]</sup>

**Table 1.** <sup>1</sup>H NMR spectra of different neohexylmetallic compounds in Et<sub>2</sub>O under slow inversion conditions.

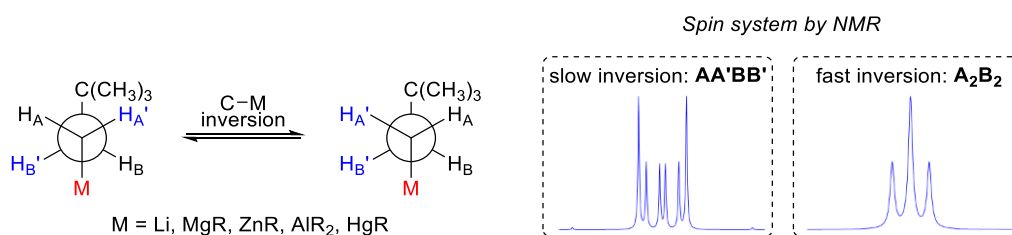
RM <sup>a</sup>	RLi	R <sub>2</sub> Mg	R <sub>2</sub> Zn	R <sub>3</sub> Al	R <sub>2</sub> Hg	
Temperature (°C)	-18	30	30	30	30	
M Electronegativity (Pauling)	1.0	1.2	1.6	1.5	1.9	
Conc. in Et <sub>2</sub> O (mol%)	5	5	1	1	15	
Chemical shifts: <sup>b</sup>	δ <sub>A</sub> (ppm)	-1.08	-0.68	+0.15	-0.20	+1.01
	δ <sub>B</sub> (ppm)	1.35	1.39	1.47	1.25	1.58
Coupling constants: <sup>b</sup>	J <sub>AB</sub> (Hz)	3.5	4.0	4.7	3.9	5.1
	J <sub>AB'</sub> (Hz)	15.5	14.2	13.3	14.2	11.8
	J <sub>AA'</sub> (Hz)	-12.1	-12.5	-12.4	-13.4	-12.5
	J <sub>BB'</sub> (Hz)	-13.05	-13.4	-13.6	-13.4	-13.6

<sup>a</sup> R = (CH<sub>3</sub>)<sub>3</sub>CCH<sub>2</sub>CH<sub>2</sub>. <sup>b</sup> (CH<sub>2</sub>CH<sub>2</sub>M)

At first sight, it was observed that the chemical shift of both methylene groups moves linearly towards lower frequencies as the electronegativity of the metal decreases, suggesting that the shielding effects primarily arise from the higher polarization of the C–M bond, while the influence of anisotropic effects from the metal orbitals is negligible.

In theory, in cases where the inversion process is slow compared to the NMR time scale, the CH<sub>2</sub>CH<sub>2</sub> group of neohexyl consistently exhibits an AA'BB' spin system, but if inversion at the α carbon occurs at a rate which is rapid on the NMR time scale, then the spectra show a simple A<sub>2</sub>B<sub>2</sub> system (**Scheme I-77**). The characteristic AA'BB' spin system is observed at room temperature for all organometallic reagents reported in **Table I-1**, except for neohexylLi, which requires lower temperatures for analysis. The values of the vicinal coupling constants indicate that the organometallic compound exist predominantly in the *anti*-conformation.<sup>[297]</sup> When the temperature of Et<sub>2</sub>O solutions containing

neohexylli, (neohexyl)<sub>2</sub>Mg, and (neohexyl)<sub>2</sub>Zn is increased, the AA'BB' spectral pattern gradually turns into the A<sub>2</sub>B<sub>2</sub> configuration for the CH<sub>2</sub>CH<sub>2</sub> group.<sup>[296]</sup> These changes occur due to the averaging of the vicinal coupling constants, which is consistent only with the inversion of the configuration at the  $\alpha$ -carbon. In the case of (neohexyl)<sub>3</sub>Al and (neohexyl)<sub>2</sub>Hg the AA'BB' spin system remains unchanged up to 150–160 °C, proving that these compounds are configurationally stable in Et<sub>2</sub>O (compared to the NMR time scale) under the given experimental conditions.<sup>[296]</sup>



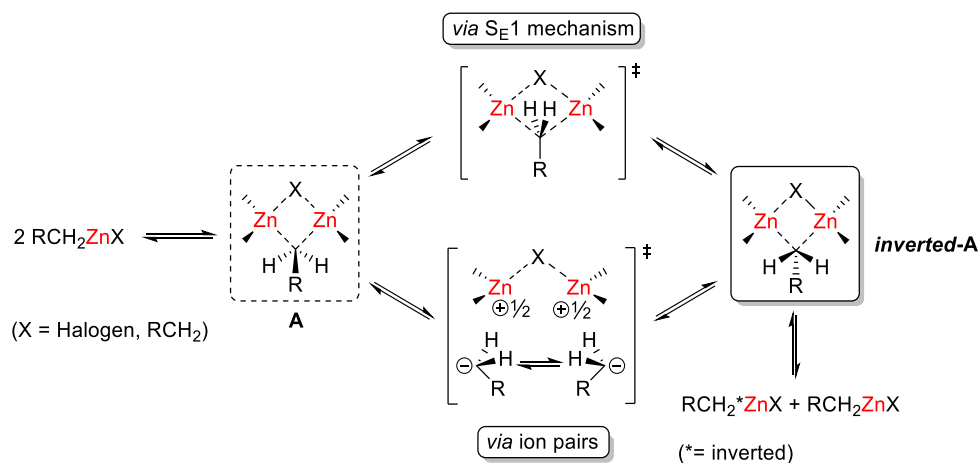
**Scheme I-77.** NMR spin systems with slow and fast inversion of the C-Metal bond in neohexylmetallic compounds.

The inversion rates of zinc compounds exhibit relatively linear Arrhenius plots. These plots allow for the determination of activation energy ( $E_a$ ) values. In particular, for the primary diorganozinc compounds (neohexyl)<sub>2</sub>Zn, activation parameters were assessed within the temperature range of 80–145 °C.<sup>[298]</sup> Extrapolating from these measurements, a value of  $\Delta G^\ddagger = 21.1$  kcal mol<sup>-1</sup> was obtained for the inversion process at 25 °C, indicating a slow inversion rate, compared to the corresponding organolithium and organomagnesium reagents, aligning with the anticipated effect of metal electronegativity.

Despite extensive investigations on inversion barriers in lithium and magnesium compounds, research on inversion barriers in organozinc reagents has remained limited. Nevertheless, an experimental case involving a  $\beta$ -(Boc)amino-substituted primary organozinc iodide was reported.<sup>[299]</sup> In this case, methylenic protons  $\alpha$  to the zinc were observed as the AB part of an ABC spin system, suggesting sluggish inversion rates. Through calculations involving shifts and coupling constants (which will not be discussed here), a lower limit of  $\Delta G^\ddagger \approx 15$  kcal mol<sup>-1</sup> at 25 °C was established. However, the authors refrained from pursuing additional efforts to reach the coalescence temperature.

A conceivable mechanism has been postulated to explain the inversion of primary alkylzinc compounds at higher temperatures (**Scheme I-78**).<sup>[294]</sup> This mechanism could involve a first-order process like dissociation–recombination (or S<sub>E</sub>1 mechanism). However, organozinc compounds might engage in pathways with lower energy requirements for inversion through the formation of aggregates. These aggregates could readily give rise to dimeric structures, which might even become the more stable species (depending on substituent characteristics), thus playing a crucial role in the exchange process. Consequently, an aggregate could provide opportunities for a carbanion to interact

with a metal cation from one face, or with another cation from the opposite face, facilitating inversion routes that are more accessible than  $S_{E1}$  process.



**Scheme I-78.** Postulated mechanism for the inversion of the C-Zn bond in primary organozinc reagents, involving aggregates via two pathways: a)  $S_{E1}$  mechanism; b) ion-pairs formation.

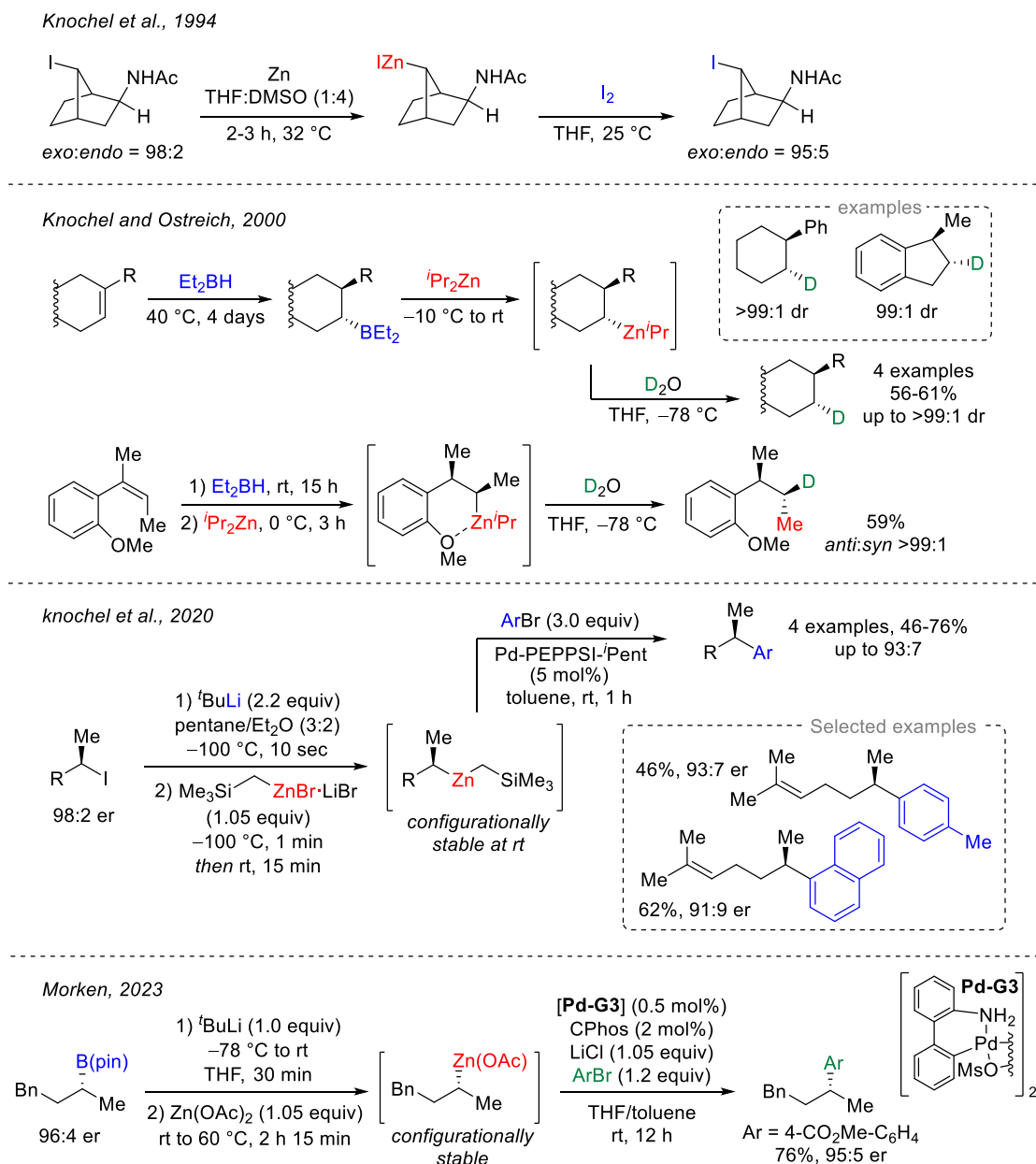
In **Scheme I-78**, a possible ionic mechanism for inversion is proposed, involving dimeric organozinc reagents. Through heterolytic cleavage of the C-Zn bond, a fast-inverting carbanion is generated, and its stability is ensured by ion-pair formation with a bimetallic cation displaying dispersed charge. The inversion of one of the two organozinc molecules occurs after dimer dissociation, as the inverted carbanion caves in conjunction with the back metal cation.

## 2.2.2. Secondary Alkylzinc Compounds

NMR spectroscopy is an immensely valuable analytical technique for investigating the dynamics (e.g., internal rotation, conformational exchanges, isomerization) of organic molecules and various systems with activation energies ranging approximately from 5 to 25 kcal/mol.<sup>[300]</sup> When experimental conditions permit the identification of peak coalescence, the spectroscopic information gained hold significant worth.<sup>[297,298]</sup> Nevertheless, challenges arise in instances where the dynamic process occurs slowly on the NMR time scale, such as the inversion of a C-metal bond. In these cases, a fundamental query arises regarding the preservation of the stereochemical integrity of the organometallic compound over a macroscopic time scale, and an answer to this query remains unsolved. This circumstance is particularly relevant to the majority of secondary organometallic compounds, which are more attractive than primary counterparts due to their potential in synthetic applications.

Various examples of the controlled manipulation of stereochemistry at the C-Zn center during the preparation and reactions of organozinc compounds have been reported (**Scheme I-79**). In this field,

diastereomeric cyclic secondary organozinc halides were synthesized in the form of isomeric mixtures, exhibiting configurational stability under the specific experimental conditions of the reactions.<sup>[301]</sup>

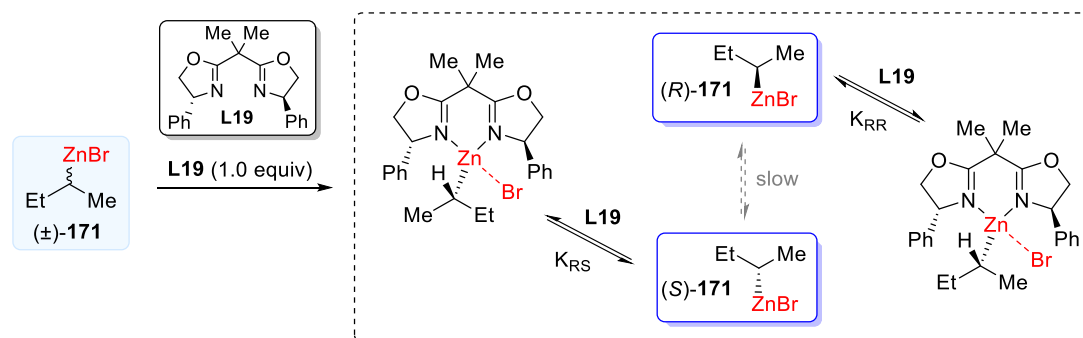


**Scheme I-79.** Examples of diastereomerically and enantiomerically enriched secondary cyclic and acyclic organozinc compounds.

Additionally, diverse cyclic and acyclic diastereomerically enriched mixed diorganozinc compounds,<sup>[302–305]</sup> and in one instances even enantiomerically enriched,<sup>[306]</sup> have been synthesized and subsequent exploration of their stereochemistry occurred following their interaction with electrophiles, where they showed a robust configurational stability. Additionally, Morken recently developed an enantioenriched alkyzinc acetate that exhibited considerable configurational stability

(Scheme I-79, bottom).<sup>[307]</sup> However, in all these cases a thorough investigation of the preservation of the stereochemical integrity of the organometallic compound during the time was lacking.

In this context, Guijarro and Rieke<sup>[308]</sup> directly investigated the configurational behavior of secondary alkyl organozinc halides directly using NMR spectroscopy along with chiral solvating agents.<sup>[309]</sup> This approach mirrors the methodology employed by Hoffman while investigating  $\alpha$ -seleno organolithium compounds.<sup>[310]</sup> The underlying concept of this method is that complexing the racemic organometallic compound with an enantiomerically pure chiral ligand leads to the formation of diastereoisomeric complexes. Among various chiral ligands, C<sub>2</sub> symmetrically substituted bis(oxazoline) ligands were identified as the optimal choice. Notably, (+)-2,2'-isopropylidene-bis[(*R*)-4-phenyloxazoline] **L19** displayed two sets of signals in a (surprisingly) very simple <sup>1</sup>H NMR spectrum of 2-butylzinc bromide ( $\pm$ )-**171** at room temperature (Scheme I-80).<sup>[308]</sup> The presence of two distinct signal sets in a 1:1 ratio, each representing one enantiomer of the organozinc reagent, means that the inversion proceeds slow within the NMR time scale. However, a deeper investigation is required to establish the extent of the stereochemical stability of the C–Zn bond in secondary alkylzinc bromides.



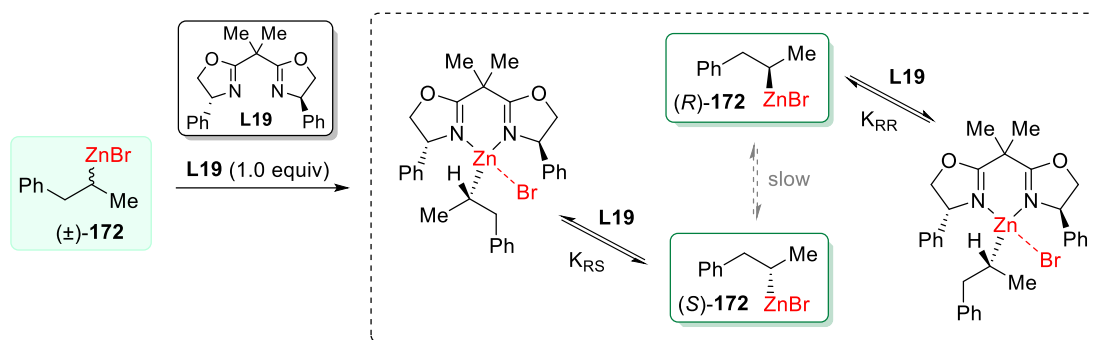
Scheme I-80. Equilibrium complexation of racemic 2-butylzinc bromide with **L19**.

If the organozinc species is in rapid equilibrium (within the NMR time scale), it will exhibit a single set of signals, even if it forms two diastereoisomers with the enantiopure ligand. Indeed, using the corresponding racemic ligand resulted in just one signal set, as expected.

Recording the same <sup>1</sup>H NMR spectrum experiment at  $-50\text{ }^{\circ}\text{C}$  the equilibrium can be frozen, leading to the re-emergence of two signals sets like those observed with the use of the enantiopure ligand. Nevertheless, these signal sets manifest in different proportions, aligning with the thermodynamic equilibrium constant, which is influenced by the compared stabilities of the diastereomeric complexes. In the specific case of ( $\pm$ )-**171** at  $-50\text{ }^{\circ}\text{C}$ , integration reaches the sensitivity threshold, resulting in a ratio of 1.01:1 due to the subtle steric hindrance discrepancy between the methyl and ethyl groups.<sup>[311-314]</sup>

By replacing the ethyl group with the more sterically hindered benzyl group, significant alterations are expected in the thermodynamic equilibrium composition, opening the possibility of

accurately gauging the rate of inversion of the secondary C–Zn bond (**Scheme I-81**). In the presence of one equivalent of **L19**, the spectrum of 1-phenyl-2-propylzinc bromide ( $\pm$ )-**172** revealed the expected occurrence: two signal sets in a 1:1 ratio, indicating the racemic character of the organozinc compound. However, given that this system does not represent a static state, the equilibrium composition will dynamically evolve based on the inversion rate of the C–Zn bond.

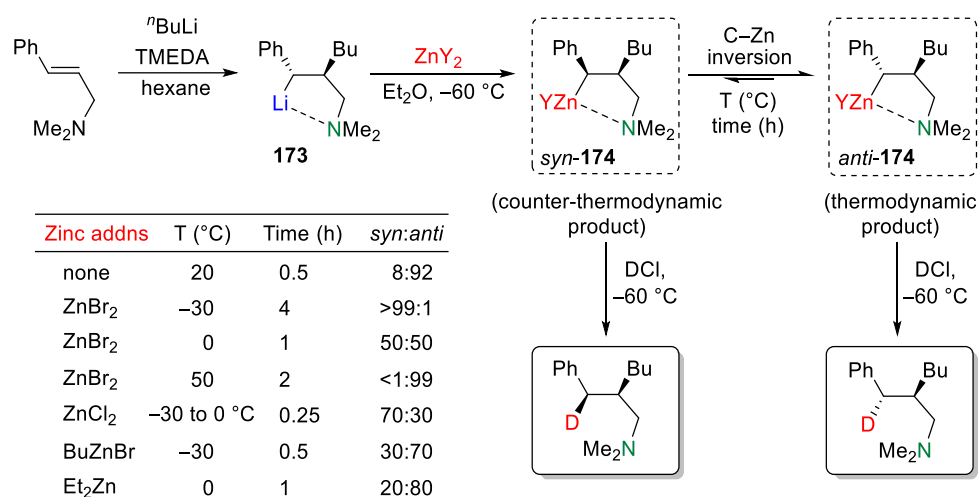


**Scheme I-81.** Equilibrium complexation of racemic 1-phenyl-2-propylzinc bromide with **L19**.

This evolution continues until the system reaches its thermodynamic equilibrium configuration. Therefore, the presence of the chiral ligand essentially induces a shift in the composition of the initial racemic mixture of the organozinc compounds, leading to a different final outcome. This value aligns with the new thermodynamic equilibrium in the chiral environment. By deriving the laws governing the interconversion rate of both enantiomers, the equations that depicts the exponential progression toward the ultimate equilibrium state can be readily deduced.<sup>[308]</sup> Over the course of 9 days, the observation of a sample containing ( $\pm$ )-**172** and **L19** through  $^1\text{H}$  NMR revealed a gradual yet discernible transformation of the diastereomeric ratio towards the projected one (approximately 2.7:1). Employing a logarithmic plot, the half-life of the C–Zn bond inversion was calculated, resulting in  $t_{1/2} = 4$  months, which corresponds to a free activation energy  $\Delta G^\ddagger = 27.2$  kcal mol $^{-1}$  at rt.<sup>[308]</sup> It is important to note that this data provides an approximation of the system's progression towards equilibrium, since the initial assumption of a monomolecular transition state do not take in account the aggregation processes, and, moreover, during the observation of the sample the presence of solids hindered a complete tracking of the reaction's progress. Worthy of note is also that the conclusion about the configurational stability concerns only the studied system, with a zinc atom complexed to a diamine ligand. However, this reliable strategy allows for the determination of the *ee* of organometallic compounds, bypassing the use electrophiles which could potentially cause unintended alterations.<sup>[315,316]</sup>

### 2.2.3. Secondary Benzylic Zinc Compounds

The configurational stability of secondary benzylic organozinc halides have been well investigated.<sup>[317,318]</sup> Organobenzyl zinc compounds with well-defined configurations can be readily synthesized from their corresponding benzyl lithium counterparts. These reagents are known to exhibit fluxional behaviour with low inversion barriers,<sup>[319,320]</sup> which allows them to predominantly exist as the thermodynamically most stable benzyl lithium epimer.<sup>[321,322]</sup> By exploiting this dynamic behaviour and selecting an appropriate organic substitution pattern, this equilibrium can be nearly completely shifted, resulting in practically a single diastereomer. This phenomenon is particularly noticeable in intramolecularly-chelated benzyl lithium reagents **173**, where the chelating amino group at the  $\gamma$ -position blocks the configuration of benzyl lithium, after thermodynamic equilibration, through coordination (**Scheme I-82**).



**Scheme I-82.** Investigation of the configurational behaviour of the benzylic organozinc reagent synthesized in diastereomerically pure form (syn:anti >99:1).

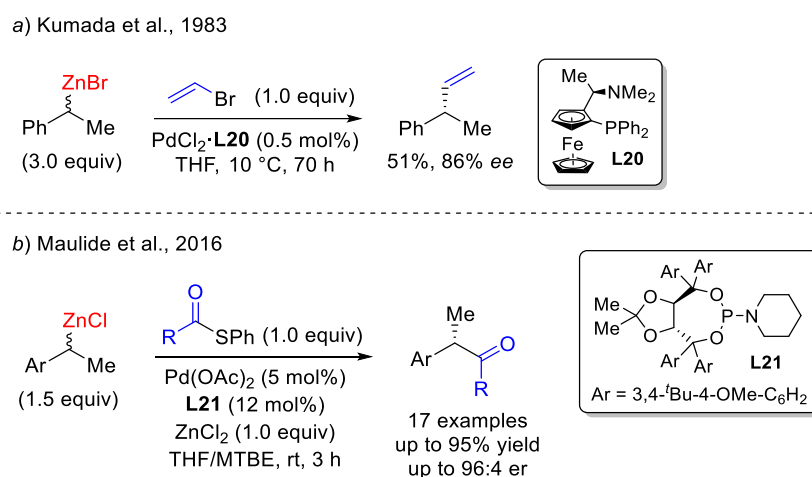
The key point is that with these reagents the Li–Zn transmetalation occurs with total inversion of the configuration at the benzylic carbon. Now, the resulting benzylic organozinc halides *syn*-**174** exhibits significantly higher inversion barriers compared to the corresponding benzyl lithium reagent, due to the increased covalent nature of the C–Zn bond.<sup>[323]</sup> However, since this species is thermodynamically unfavorable (Ph group *syn* to Bu) the benzylic organozinc reagent slowly epimerizes and the equilibrium between *syn*-**174** and *anti*-**174** will tend to re-equilibrate over time. This epimerization is remarkably slow enough to observe it on a macroscopic timescale, depending on temperature and time-before quenching. For the organozinc halide, at –30 °C the inversion process for *syn*-**174** essentially does not occur or is unnoticeable (syn:anti >99:1), whereas a 2 h period at 50 °C suffices for the equilibrium to entirely shift towards the thermodynamically more stable *anti*-**174** isomer (anti:syn >99:1). Notably, if an alkylzinc halide or a dialkylzinc is added instead of ZnBr<sub>2</sub> or ZnCl<sub>2</sub>, the lithium is



replaced by an alkylzinc group or zincate, leading to a preference for the thermodynamic product even at low temperatures. This indicates a significant difference in configurational stability between an organozinc halide and a bisorganozinc or zincate reagent.

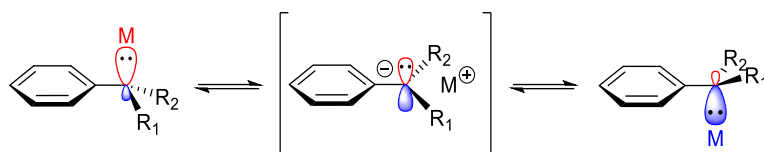
Noteworthy, the diastereoselectivity of the reaction was also influenced by the choice of solvent. For instance, in the more polar solvent THF, the oxygen atom competes effectively with the nitrogen atom of the amino group, resulting in minor diastereoselectivity (*syn:anti* = 40/60).<sup>[317]</sup> On the other hand, when the benzyl lithium reagent is prepared in hexane and quenched with DCl, no detrimental effects are observed (*anti:syn* = 92:8).

Further studies have confirmed the configurational lability of secondary benzylic organozinc halides.<sup>[324,325]</sup> In fact, a fluxional behaviour is imperative to explain the stereochemical results of certain chirally-induced Pd-catalyzed cross-coupling reactions conducted at room temperature. Starting from racemic benzylzinc halides, these reactions afforded the desired products with high enantioselectivity and excellent yield (**Scheme I-83**).



**Scheme I-83.** Enantioselective Pd-catalyzed cross-coupling reactions involving racemic benzylzinc reagents.

Although the configurational lability of these organozinc compounds has been well-established, the exact mechanism behind the stereochemical inversion is still unclear. However, a possible mechanism involving dimers, like the one proposed for primary organozinc halides, is theoretically possible (see **Scheme I-78**). Considering the stability of the benzyl carbanion, benzyl organozinc compounds might experience swift racemization in solution due to dissociation through an ion pair with a planar configuration (**Scheme I-84**), followed by subsequent rearrangement and resulting in the loss of chiral information (as proposed for chiral benzyl alkali metal derivatives).<sup>[326]</sup>



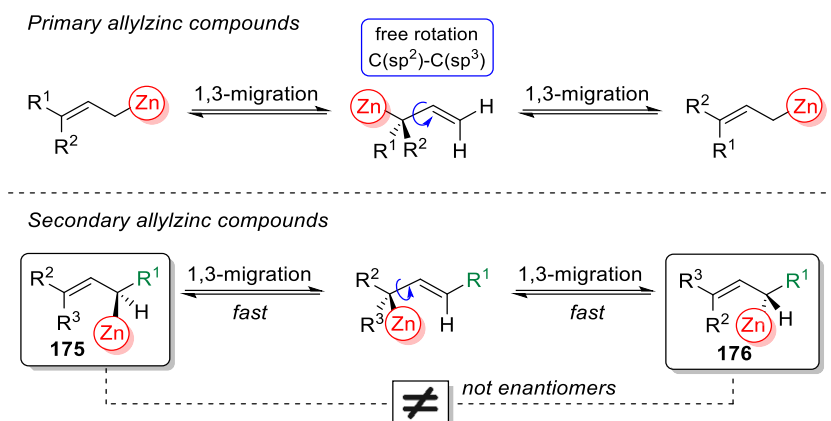
**Scheme I-84.** Possible mechanism of inversion of configuration for benzyl organozinc compounds via ion pair.

## 2.2.4. C(sp<sup>2</sup>)-Zn Bond: Vinylzinc Compounds

Alkenylzinc reagents generally exhibit robust configurational stability, showing defined *Z*- or *E*-configurations in their <sup>1</sup>H NMR spectra. For instance, divinylzinc produces a well-defined ABC spin system with distinct coupling constants.<sup>[327]</sup> According to the literature, alkenylzinc halides have been observed to retain their stereochemical configuration during reactions with electrophiles.<sup>[328]</sup> Moreover, strongly electron-poor polyfluorinated substituted vinylzinc halides,<sup>[329]</sup> as well as *Z*- or *E*-1,2-difluorovinylzinc halides,<sup>[330]</sup> have displayed exceptional configuration stability over a significant duration of time under laboratory conditions. However, to the best of our knowledge, the inversion barriers of these compounds remain unknown.

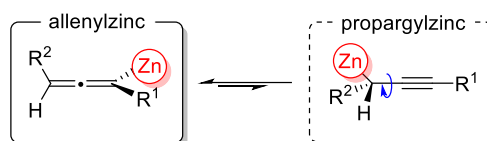
## 2.2.5. Allyl- and Propargylzinc Compounds

Allylzinc compounds present a fluxional behaviour inevitable due to two processes: 1) metallotropic shift (1,3-migration of the zinc atom), and 2) free rotation around the  $\sigma$  C(sp<sup>2</sup>)-C(sp<sup>3</sup>) bond, resulting in facile and thus rapid isomerization (**Scheme I-85, top**). To illustrate, even at -60 °C in THF, the isomerization of diallylzinc exhibits a  $\Delta G^\ddagger$  value around 9.6 kcal mol<sup>-1</sup>, leading to an astonishingly brief half-life of  $t_{1/2} = 10^{-3}$  s.<sup>[331]</sup> However, this fluxional behaviour does not affect the stereogenic information of the C-Zn bond. To illustrate, if a substituent is present on the carbon where the metal is attached, this fluxional behavior converts **175** to **176** (**Scheme I-85, bottom**). These two species are not enantiomers but diastereoisomers and repeating this "1,3-migration – free rotation" sequence reverts **176** back to **175**. Considering this fact and knowing from the literature (as mentioned before) that secondary alkylzinc compounds are not configurationally labile, it is anticipated that secondary allylzinc reagents should exhibit configurational stability. Nevertheless, to the best of our knowledge, to date there is no documented evidence of enantiomerically enriched secondary allylzinc compounds, thus leaving this question unanswered.



**Scheme I-85.** Fluxional behaviour of allylzinc compounds via 1,3-migration and free-rotation at the  $C(sp^2)$ - $C(sp^3)$  bond.

Within the propargyl–allenyl organozinc system, the allenyl form prevents the free rotation step, thus leading to significantly high inversion barriers, preventing racemization. It is widely recognized that the propargylzinc–allenylzinc equilibrium strongly favors the allenic structure (**Scheme I-86**). This deduction is based on the  $^1\text{H}$  NMR and IR spectral data of diallenylzinc and allenylzinc halides,<sup>[332]</sup> which exhibit distinct similarities with allenyllithium compounds.<sup>[333]</sup>



**Scheme I-86.** Propargylzinc–allenylzinc equilibrium.

Furthermore, this conclusion is bolstered by DFT calculations on allenylzinc halides, confirming the allenic nature of these organometallic reagents.<sup>[334]</sup> Consistently, various examples of chiral allenyl zinc reagents have showcased considerable configurational stability, although the limits of temperature and time are strongly influenced by the specific substituents incorporated.<sup>[335–339]</sup>

So far, no rates or kinetic reaction orders related to the potential mechanism of the propargyl–allenyl organozinc rearrangement have been reported, despite its intriguing conceptual nature. However, what can be affirmed is that eliminating a dissociative ionic pathway is possible as long as the configuration of the propargyl–allenyl system remains unchanged. Within this context, the metallotropic rearrangement could take place either antarafacially or suprafacially within the propargyl–allenyl subunit, but not both simultaneously. Otherwise, a different mechanism would unavoidably result in racemization.

### 3. Conclusion

Over the past decade, there has been a significant surge in advancing C(sp<sup>3</sup>)-geminated organobimetallics for asymmetric synthesis. Through the stepwise double functionalization of each carbon-metal bond, these compounds enable the straightforward and selective construction of complex molecules with a minimal number of chemical steps, which stands as a fundamental goal in the realm of modern synthetic chemistry. Diverse strategies, such as diastereoselective transformation of enriched chiral reagents or enantioselective conversion of achiral/racemic derivatives, have been employed. In most cases, desymmetrization systems aim for the initial electrophilic substitution to yield an enantioenriched, configurationally stable *mono*-organometallic intermediate, ready for subsequent stereospecific transformations.

So far,  $\alpha$ -metalated organoboronates have dominated this domain, owing to the chemical and stereochemical stability of both bimetallic and *mono*-organoboron derivatives, along with the convenient access they offer to a broad array of linchpins. This chemistry has found extensive use in various synthetic applications. However, limitations arise from the weak compatibility of secondary organoboronates in cross-coupling reactions, constraining the scope of the second functionalization step, which often occurs outside one-pot procedures.

Potential solutions lie in *gem*-dizinc compounds, showcasing a fundamental departure from  $\alpha$ -metalated organoboronates. Here, the consecutive functionalizations occur in a single pot, by-passing the isolation of the *mono*-organometallic intermediate. Furthermore, an additional advantage of zinc chemistry lies in the fact that cross-coupling reactions involving secondary organozinc reagents are frequently easier, requiring less harsh conditions, and encompass a broader range compared to those involving secondary organoboronates. Consequently, this widens the potential for double cross-coupling, as evidenced by the multitude of (non-enantioselective) reactions that have been developed. Yet, despite these advancements, the realm of enantioselective sequential electrophilic substitutions with *gem*-dizincio linchpins remains unexplored. This uncharted territory served as the driving force behind our interest in this Ph.D. project.



**PART II:**  
**RESULTS AND DISCUSSION**

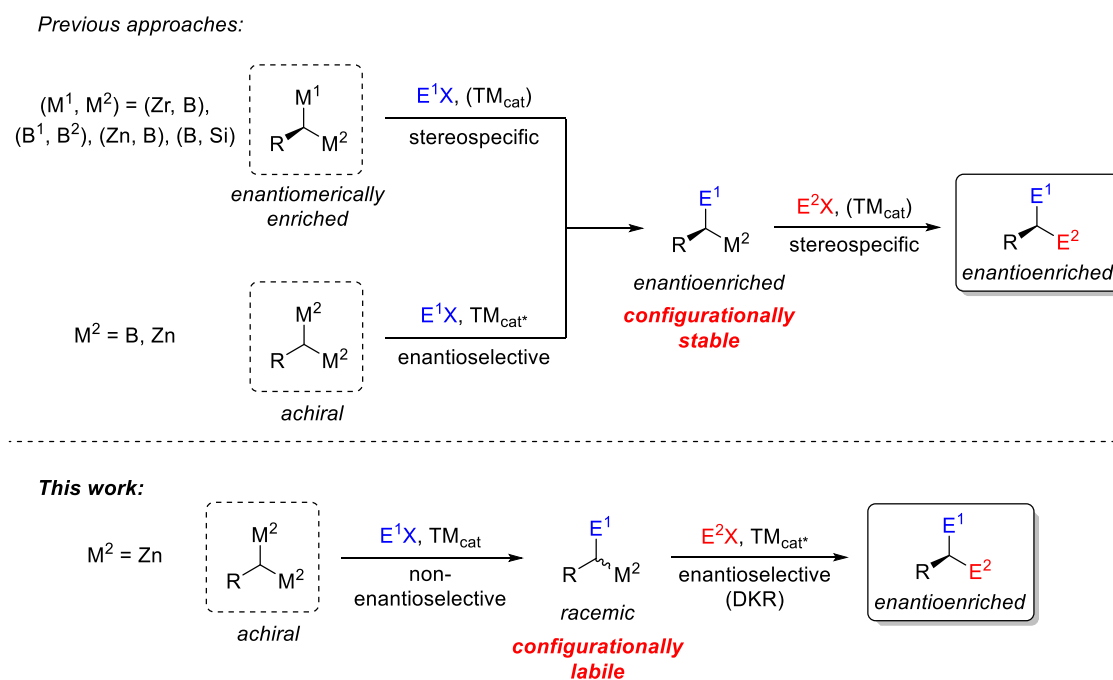
---



# 1. Enantioselective Sequential Catalytic Arylation-Fukuyama Cross-coupling of 1,1-Biszincioalkanes

## 1.1. Purpose and Objective of the Project

As mentioned in the previous section of the literature review, geminated C(sp<sup>3</sup>)-organobimetallics have proven to be invaluable tools for conducting consecutive reactions with two distinct electrophiles in an enantioselective manner. However, the development of new reactions in this context remains a challenging endeavor. Up to this point, the enantioselective sequential reactions we have outlined primarily rely on two fundamental strategies (**Scheme II-1, top**). The first approach entails the preparation of chiral enantiopure *gem*-bimetallic reagents, which are subsequently employed in two consecutive stereospecific reactions. This methodology has been extensively explored with *gem*-diborylalkanes, featuring two boron atoms differentiated by their substitution patterns, as well as with *gem*-boryl silanes.<sup>[290]</sup> Additionally, it has found application with mixed 1,1-borylzirconioalkanes<sup>[110]</sup> and 1,1-borylzincioalkanes.<sup>[130]</sup>



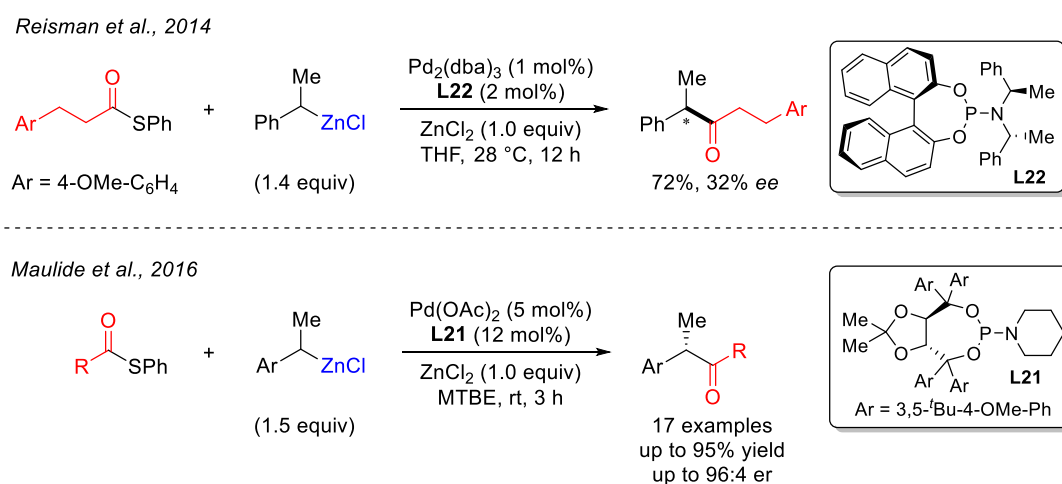
**Scheme II-1.** Asymmetric synthesis through two consecutive electrophilic substitution reactions of geminated C(sp<sup>3</sup>)-organobimetallics: previous approaches (top) and our work (bottom).

On the other hand, the second strategy involves the desymmetrization of achiral *gem*-bimetallic reagents through catalytic enantiotopic group-selective cross-coupling reactions. Subsequently, a chiral, enantioenriched *mono*-organometallic intermediate is obtained, which then undergoes



stereospecific transformation. For instance, 1,1-bis(pinacolboronate) esters have been employed in enantioselective palladium- or copper-catalyzed C–C bond-forming reactions, yielding enantioenriched secondary organoboranes suitable for (enantiospecific) C–B bond elaboration.<sup>[290]</sup> Additionally, 1,1-bis(iodozincio)ethane was used in a one-pot enantioselective Pd-catalyzed allylic alkylation/stereoretentive Cu-mediated allenylation sequence, albeit with low enantiomeric excess.<sup>[289]</sup> The key common feature in both strategies is the utilization of an *enantioenriched configurationally stable mono-organometallic* intermediate. However, it is important to note that these strategies may not be suitable for *gem*-bimetallics in which the corresponding *monometallic* intermediate is not configurationally stable upon the first functionalization. In such cases, the enantiomeric purity of the final product may decrease, or in the worst-case scenario, the stereogenic information could be completely lost.

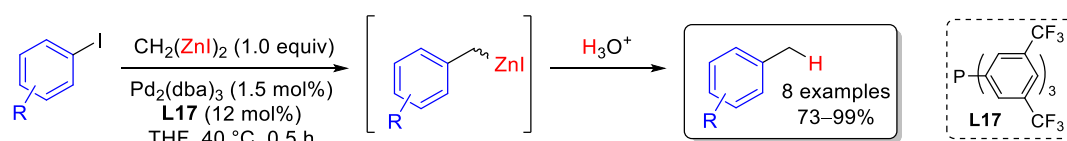
Alternatively, a different approach can be considered, utilizing a *racemic configurationally labile mono-organometallic* intermediate for the second step and implementing an enantioconvergent reaction to ensure dynamic kinetic resolution (DKR) (**Scheme II-1, bottom**). In this context, there is no longer a need to achieve the enantioselective desymmetrization of the initial achiral *gem*-dimetallic reagent. The inspiration for this novel approach comes from previous findings in stereoselective cross-coupling reactions involving configurationally labile secondary organozinc reagents.<sup>[340–345]</sup> To the best of our knowledge, this approach is unprecedented and ideally suited for 1,1-dizincio bimetallics, which in addition have proved so far poor substrates for enantioselective desymmetrization.<sup>[289]</sup> Our interest was piqued by reports of asymmetric Pd-catalyzed Fukuyama cross-coupling reactions between (1-arylethyl)zinc reagents and thioesters (**Scheme II-1**).<sup>[344,345]</sup> Specifically, under Maulide's developed conditions,<sup>[345]</sup> this reaction has the capability to yield  $\alpha$ -disubstituted ketones with high yields and remarkable enantiomeric purity, making them valuable synthetic intermediates for asymmetric synthesis.



**Scheme II-2.** Enantioselective protocol for the Pd-catalyzed Fukuyama cross-coupling between (1-arylethyl)zinc chlorides and thioesters.

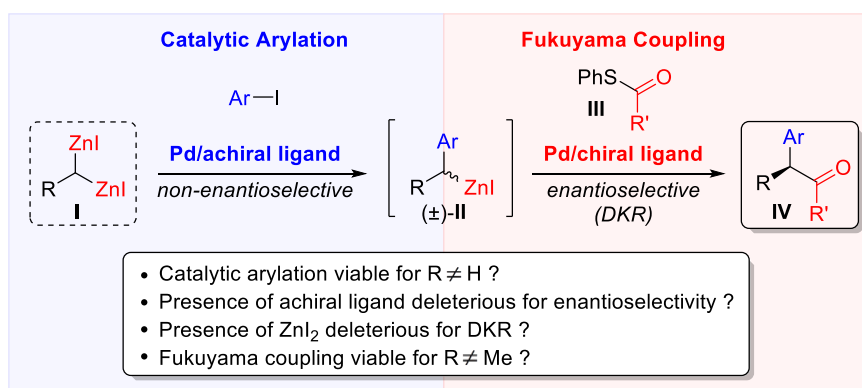
This process relies on the efficient DKR of (racemic) benzylic secondary organozinc nucleophiles. In the documented procedures, the organozinc reagents are prepared through the reductive zincation of the parent 1-(arylethyl)chlorides.<sup>[344,345]</sup>

Expanding on Matsubara's research involving the selective (mono)arylation of 1,1-bis(iodozincio)methane (**Scheme II-3**),<sup>[263]</sup> we reasoned that (1-arylethyl)zinc nucleophiles and other (1-arylethyl)zinc intermediates could likewise be accessed from 1,1-bis(iodozincio)ethane and potentially other (yet unknown) 1,1-bis(iodozincio)alkanes through a Pd-catalyzed arylation process using aryl iodides.



**Scheme II-3.** Matsubara Pd-catalyzed (mono)arylation reaction of bis(iodozincio)methane with aryl iodides.

The development of such a two-step, one-pot sequence represents a significant advancement in providing a more direct and modular approach to the same family of disubstituted ketones within a broader scope (**Scheme II-4**). This innovative method opens up opportunities on two fronts. Firstly, it allows for the incorporation of electron-rich aryl moieties, which were previously challenging to introduce as the requisite 1-(arylethyl)zinc reagents ( $\pm$ )-**II** were problematic to access. Secondly, it extends the applicability to ketones **IV** that feature an alkyl group R other than methyl.



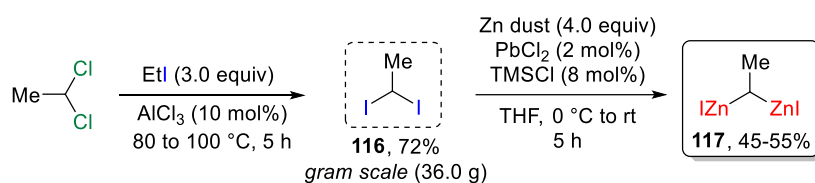
**Scheme II-4.** Enantioselective Pd-catalyzed sequenced arylation-acylation of 1,1-bis(iodozincio)alkanes in one pot and associated challenges.

Nevertheless, the sequential bidirectional coupling strategy faces however several challenges. First of all, it required the identification of suitable conditions to achieve the initial coupling while maintaining good selectivity for the mono-arylation product. This could be particularly challenging due to the presence of the alkyl group, which could trigger competing  $\beta$ -hydride elimination pathways.

Secondly, it demands a method to achieve stereodifferentiation during the second step, even in the presence of an achiral ligand necessary for the first catalytic system. Besides this, the strategy must efficiently accommodate DKR during the Fukuyama coupling, especially with benzylzinc *iodides*, which may exhibit slower racemization compared to the benzylzinc *chlorides* used previously.<sup>[317]</sup> Lastly, it is necessary to assess the effectiveness in terms of both yield and enantiomeric excess of the enantioselective acylation step for benzylzinc intermediates that featured alkyl groups at the benzylic position other than methyl.

## 1.2. Synthesis of 1,1-Bis(iodozincio)ethane

At the outset of our work, we chose to focus on 1,1-bis(iodozincio)ethane, a compound prepared through a straightforward two-step synthesis. In the first step, 1,1-diiodoethane (**116**) was conveniently synthesized using a modified literature procedure (**Scheme II-5**).<sup>[346]</sup> This was achieved by the reaction of aluminum chloride with a mixture of ethylidene chloride and ethyl iodide. The resulting crude product was easily purified via distillation at reduced pressure, yielding analytically pure **116** with a 72% yield. Importantly, the scalability of this reaction is a significant advantage, allowing for the efficient production and long-term storage of large quantities (36.0 grams, ~128 mmol) of the dihalide, since this compound has been demonstrated to be stable over time when stored at  $-20\text{ }^{\circ}\text{C}$  in the dark.

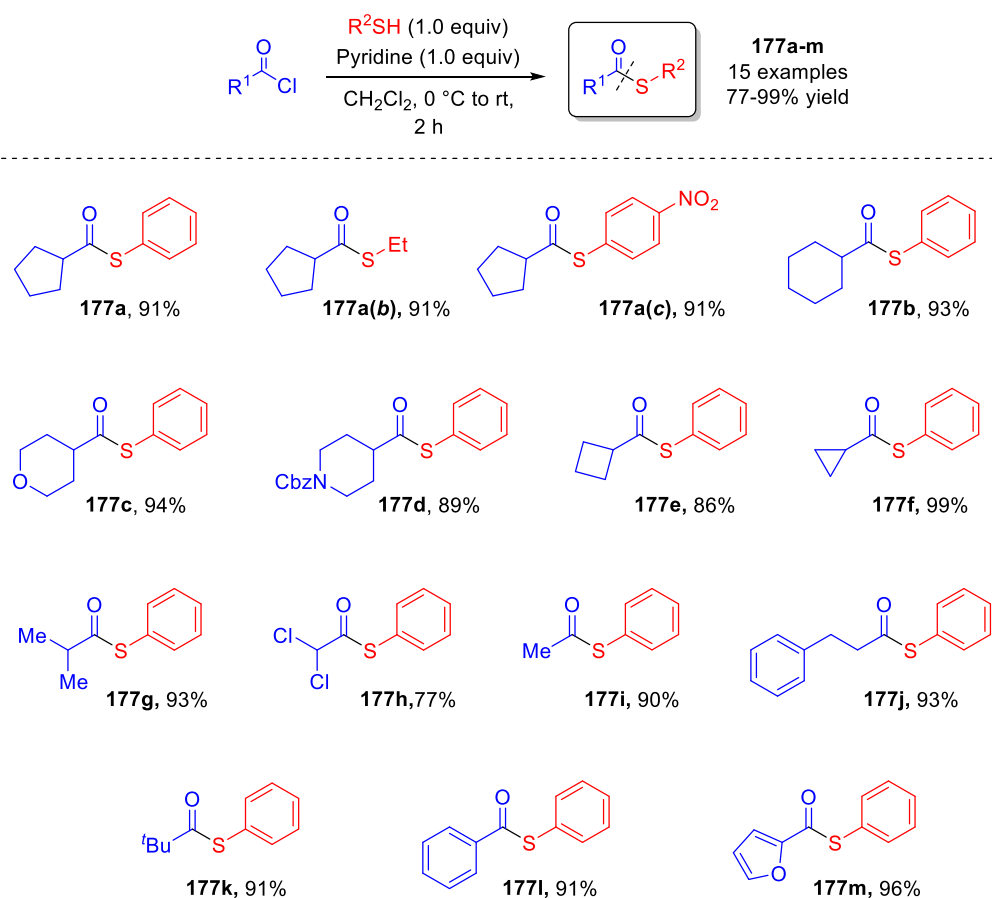


**Scheme II-5.** Gram scale preparation of 1,1-bis(iodozincio)ethane.

Subsequently, following a modified Matsubara's procedure,<sup>[289]</sup> 1,1-bis(iodozincio)ethane (**117**) was prepared through direct metal insertion after activating zinc with trimethylsilyl chloride. To accomplish this, 1,1-diiodoethane was treated with zinc powder (4 equiv) and a catalytic amount (2 mol%) of  $\text{PbCl}_2$  in THF at  $0\text{ }^{\circ}\text{C}$  for 2 h, followed by an additional 3 h at rt (**Scheme II-5**). Excess zinc was then removed by centrifugation, and the supernatant was transferred to another sealed flask. The yield of the bimetallic reagent was determined by titration with  $\text{I}_2$ ,<sup>[347]</sup> consistently resulting in concentrations of 0.45–0.55 M (45-55% yield). The solution of **117** could be stored under a positive pressure of argon at  $-20\text{ }^{\circ}\text{C}$  for at least 2 weeks with no noticeable loss of quality.

### 1.3. Synthesis of Thioesters

Regarding the enantioconvergent Fukuyama cross-coupling process, thioesters **177a-m** were utilized as electrophiles. Given their non-availability as commercially supplied substrates, here we outline the method for their preparation. In particular, they were successfully synthesized following a procedure reported in literature,<sup>[348]</sup> through the nucleophilic addition/elimination reaction involving acyl chlorides and thiol compounds, with the presence of stoichiometric amount of pyridine in dichloromethane for 2 h (**Scheme II-6**).



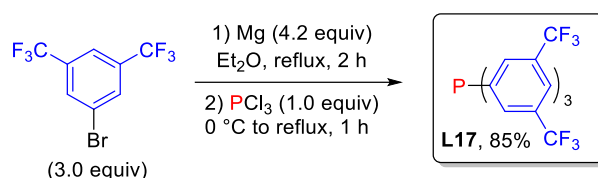
**Scheme II-6.** Thioester synthesis procedure and comprehensive chart of all thioesters prepared.

A wide variety of substrates was efficiently synthesized (15 examples, 77-99% yield). These thioesters had a broad spectrum of alkyl substituents, encompassing primary, secondary, and tertiary groups, along with some (hetero)aryl substituents.

## 1.4. Synthesis of Ligands

### 1.4.1. Synthesis of P[3,5-(CF<sub>3</sub>)<sub>2</sub>C<sub>6</sub>H<sub>3</sub>]<sub>3</sub> (L17) for the Arylation Reaction

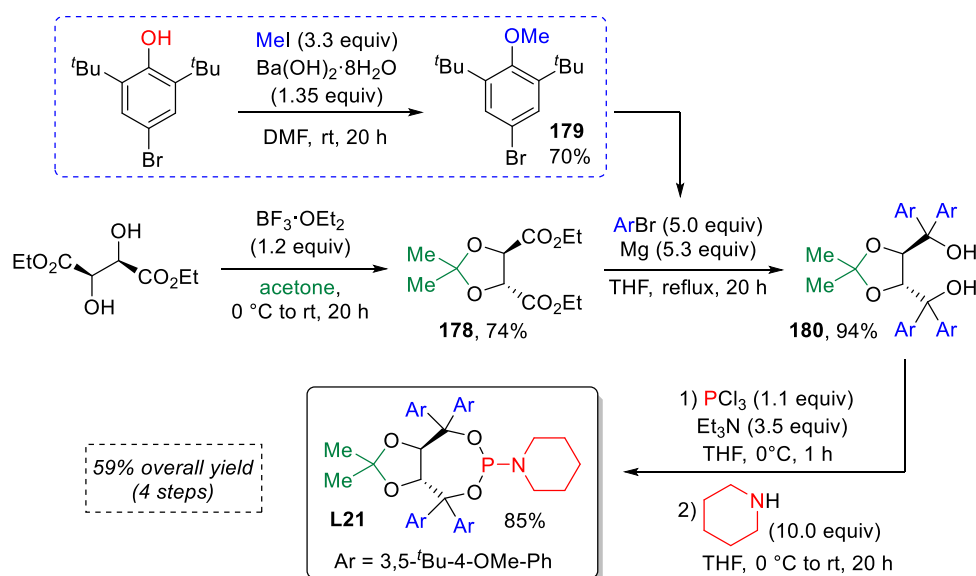
The trifluoromethylated phosphine ligand P[3,5-(CF<sub>3</sub>)<sub>2</sub>C<sub>6</sub>H<sub>3</sub>]<sub>3</sub> (**L17**) was synthesized through a reaction involving a Grignard reagent and phosphorous trichloride (**Scheme II-7**).<sup>[349]</sup> The Grignard reagent was prepared by reacting the corresponding trifluoromethylated bromo-aryl derivative with magnesium turnings in diethyl ether. Subsequently, the Grignard reagent was allowed to react with a solution of PCl<sub>3</sub> in the same ethereal solvent at 0 °C for 1 h, resulting in the desired trifluoromethylated triarylphosphine with an excellent 85% yield.



**Scheme II-7.** Synthesis of trifluoromethylated phosphine ligand P[3,5-(CF<sub>3</sub>)<sub>2</sub>C<sub>6</sub>H<sub>3</sub>]<sub>3</sub> (**L17**).

### 1.4.2. Synthesis of Enantiopure L21 for the Enantioconvergent Fukuyama Cross-Coupling

The chiral ligand **L21** used in the enantioconvergent Fukuyama cross-coupling<sup>[345]</sup> was synthesized according to the procedure outlined in **Scheme II-8**.

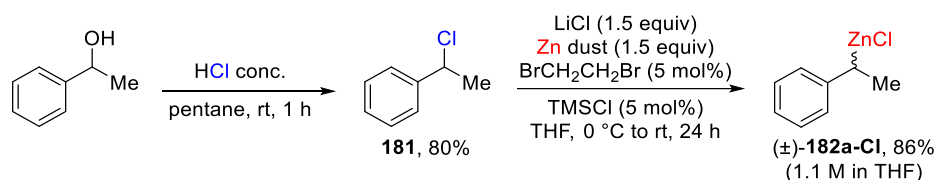


**Scheme II-8.** Synthetic sequence for the preparation of **L21**.

The synthesis commences with (+)-diethyl *L*-tartrate, which is commercially available. This compound is converted into the corresponding acetal **178** using acetone and  $\text{BF}_3 \cdot \text{OEt}_2$ , yielding a good 74%. Subsequently, the ester **178** is allowed to react with 5 equivalents of the Grignard reagent, prepared from the bromo-aryl derivative **179**, which is in turn obtained from a phenol derivative through methylation with methyl iodide and barium hydroxide in DMF. This reaction leads efficiently to the formation of the corresponding TADDOL derivative **180** in excellent yield (94%). The final step in the synthesis involves the creation of a cyclic phosphoramidite. This process begins with the formation of the  $(\text{RO})_2\text{P-Cl}$  intermediate in the presence of  $\text{Et}_3\text{N}$  to capture the generated HCl. Then, a substantial excess of piperidine is added to produce the TADDOL-derived phosphoramidite ligand **L21**, resulting in an 85% yield, and an overall satisfactory yield of 59%.

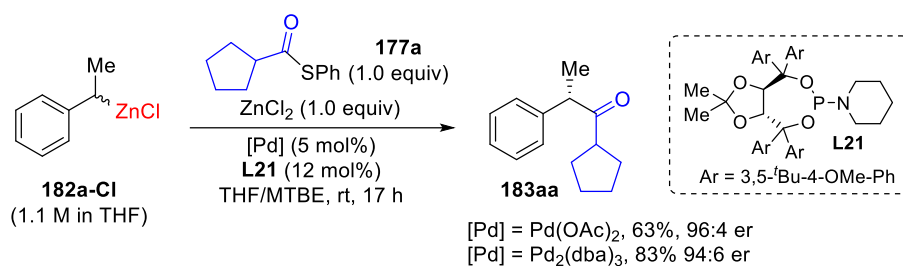
## 1.5. Preliminary Studies

The preliminary studies were undertaken with the primary objective of replicating Maulide's outcomes to assess the reproducibility of the enantioselective Fukuyama cross-coupling reaction with secondary benzylzinc chlorides.<sup>[345]</sup> Within this context, benzyl chloride **181** was synthesized from the corresponding alcohol through a simple  $\text{S}_{\text{N}}2$  halogenation reaction with HCl conc., and then by direct zinc insertion a solution of (1-phenylethyl)zinc chloride ( $(\pm)$ -**182a-Cl**) was prepared in  $\sim 1.1$  M in THF (**Scheme II-9**).



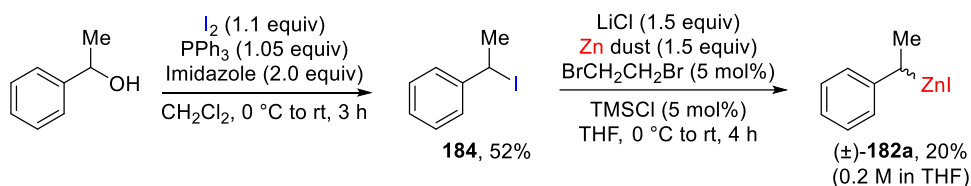
**Scheme II-9.** Preparation of (1-phenylethyl)zinc chloride in THF solution.

We endeavored to replicate the Maulide's benchmark reaction with the thioester **177a** (**Scheme II-10**).<sup>[345]</sup> Using  $\text{Pd}(\text{OAc})_2$  as the palladium source, our reaction yielded the desired product **183aa** with a 63% yield and a 96:4 enantiomeric ratio, mirroring Maulide's reported conditions.<sup>[345]</sup> However, we were unable to attain the same high yield (90%) he reported, and we encountered reproducibility issues, as some attempts yielded only 46%. In response, we explored  $\text{Pd}_2(\text{dba})_3$  as an alternative palladium source, which resulted in a 83% yield but with a slight decrease in enantioselectivity (94:6 er), as reported with this palladium source.<sup>[345]</sup>



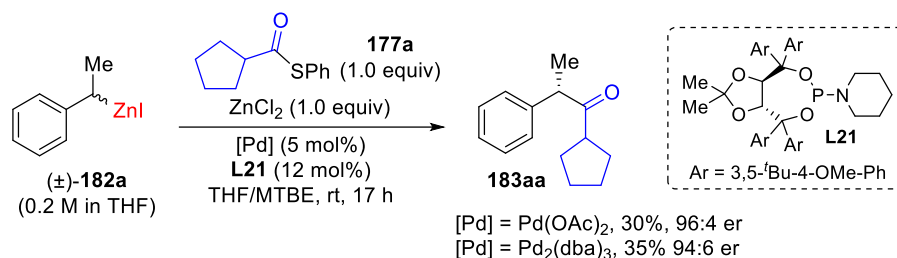
**Scheme II-10.** Replicating Maulide's enantioconvergent Fukuyama cross-coupling reaction.

In our sequential reaction, following selective monoarylation, a secondary benzylzinc iodide is generated. We aimed to investigate if the enantioconvergent Fukuyama cross-coupling reaction with (1-phenylethyl)zinc iodide (( $\pm$ )-**182a**) would yield comparable results. To explore this, we synthesized benzyl iodide **184** from the corresponding alcohol through the Appel reaction (**Scheme II-11**).<sup>[350]</sup> Subsequently, we prepared a solution of **182a** *via* reductive zincation, albeit with a relatively low concentration of  $\sim 0.2$  M in THF.



**Scheme II-11.** Preparation of (1-phenylethyl)zinc iodide in THF solution.

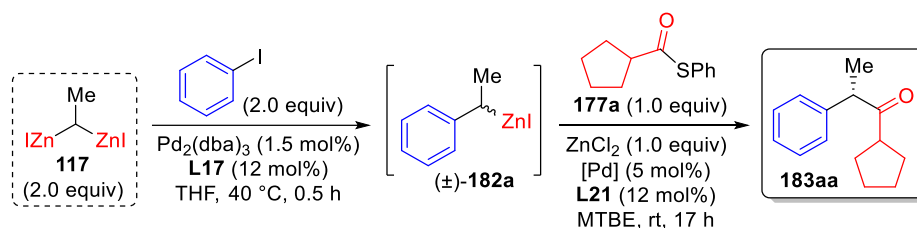
We performed the Fukuyama cross-coupling with  $\text{Pd}(\text{OAc})_2$  and  $\text{Pd}_2(\text{dba})_3$  (**Scheme II-12**). In both cases, we achieved approximately a 30-35% yield of the desired product. Remarkably, the enantiomeric ratio matched the values obtained with benzylzinc chloride ( $\pm$ )-**182a-Cl**. These findings suggest that the reaction is indeed viable with benzylzinc iodides, and more important, the enantioselectivity is not affected by the counter anion of the organozinc. However, it appears that the counter anion may have an impact on the efficiency of the reaction. Nevertheless, it is important to take into consideration that the benzylzinc iodide ( $\pm$ )-**182a** was present in a notably low concentration. While we aimed to maintain a consistent volume ratio of THF and MTBE, this approach inadvertently led to a substantial dilution of the reaction mixture, which may also have contributed to the observed lower yield.



**Scheme II-12.** Enantioconvergent Fukuyama cross-coupling reaction with (1-phenylethyl)zinc iodide.

Following these initial results, we embarked on a series of preliminary experiments to delve into the sequential bifunctionalization of 1,1-bis(iodozincio)ethane. We followed the specific conditions outlined by Matsubara for the Pd-catalyzed monoselective arylation,<sup>[263]</sup> and Maulide for the Pd-catalyzed enantioconvergent Fukuyama cross-coupling reaction.<sup>[345]</sup> In this exploration, we selected simple iodobenzene as the aryl iodide for the initial step and thioester **177a** for the subsequent one (**Table II-1**).

**Table II-1.** Preliminary experiments on the enantioselective sequential arylation-Fukuyama cross-coupling with 1,1-bis(iodozincio)ethane.



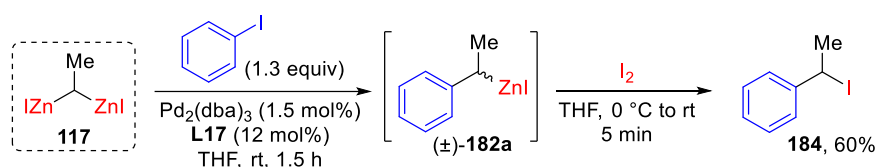
Entry	[Pd]	Yield <b>183aa</b> <sup>[a]</sup>	er <sup>[b]</sup>
1	Pd(OAc) <sub>2</sub>	<10% <sup>[c]</sup>	n.d.
2 <sup>[d]</sup>	Pd(OAc) <sub>2</sub>	<10% <sup>[c]</sup>	n.d.
3 <sup>[e]</sup>	Pd <sub>2</sub> (dba) <sub>3</sub>	50% <sup>[b]</sup>	94:6

<sup>[a]</sup> Yield measured prior to purification by <sup>1</sup>H NMR analysis using 1,3,5-trimethoxybenzene as internal standard. <sup>[b]</sup> Measured by chiral-phase GC. The absolute configuration was determined by comparison with literature data. <sup>[c]</sup> <sup>1</sup>H NMR yield only. <sup>[d]</sup> Second cross-coupling performed at 40 °C for 72 h. <sup>[e]</sup> Reaction performed without the addition of ZnCl<sub>2</sub>.

When utilizing Pd(OAc)<sub>2</sub> as catalyst for the Fukuyama cross-coupling, the sequential reaction did produce the desired compound, although with a very low yield, measuring less than 10% based on NMR analysis (entry 1, **Table II-1**). This discouraging outcome persisted even when we allowed the reaction to proceed over an entire weekend at 40 °C (entry 2, **Table II-1**). However, upon employing Pd<sub>2</sub>(dba)<sub>3</sub>, we achieved a notable improvement, with a 50% isolated yield of the desired compound (entry 3, **Table II-1**). Moreover, the enantiomeric ratio remained consistent at 94:6. This result revealed that in this particular scenario, the utilization of an achiral ligand for the first coupling *did not* negatively impact the enantioselectivity of the subsequent reaction. Nonetheless, it is worth noting



that the use of 2 equivalents of 1,1-bis(iodozincio)ethane appeared excessive, especially when considering that the yield based on this reagent is merely 25%. At this juncture, we were not aware of the yield of the first step. Consequently, we decided to repeat the (mono)arylation under the same conditions. After a half-hour reaction time at 40 °C, we quenched the benzylzinc intermediate ( $\pm$ )-**182a** with I<sub>2</sub> (**Scheme II-13**), as reported by Knochel for alkylzinc compounds.<sup>[347]</sup>



**Scheme II-13.** Pd-catalyzed (mono)arylation of 1,1-bis(iodozincio)ethane and subsequent iodolysis of the benzylzinc intermediate.

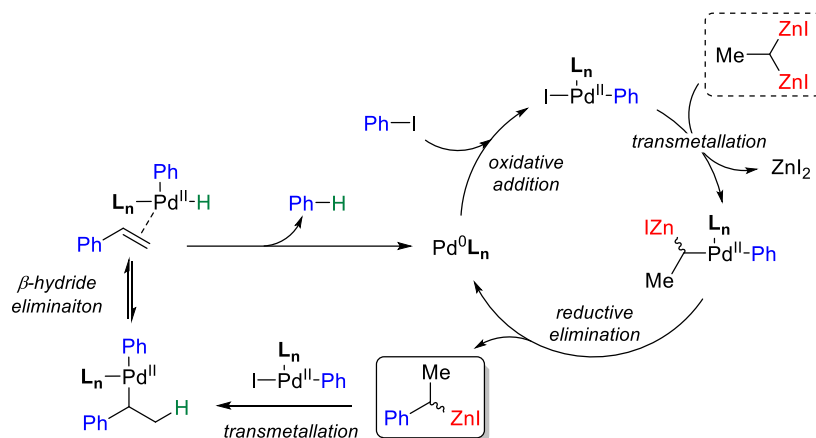
Our findings revealed that the yield of the initial step was a modest 60%. This prompted us to make the following decision. We opted to commence the optimization process by focusing on the first cross-coupling reaction. Our goal was to improve its efficiency and achieve a more satisfactory yield. Only after successfully optimizing the first step could we then proceed to optimize the second step.

## 1.6. Optimization Pd-Catalyzed Arylation Reaction of 1,1-Bis(iodozincio)ethane

As already mentioned before, at the outset of our work, the first reaction of 1,1-bis(iodozincio)ethane and phenyl iodide in THF at 40 °C, in the presence of Pd<sub>2</sub>dba<sub>3</sub> (1.5 mol%) and **L17** (12 mol%), followed by iodolysis, delivered benzyl iodide **184** in 60% yield along with 10–20% of styrene and 4–8% of ethylbenzene. This result demonstrated that substitution at the methylene carbon of the *gem*-bisorganozinc partner was well tolerated. Furthermore, no di-arylation was detected, substantiating exquisite chemoselectivity towards cross-coupling between the *gem*-dizinc and *mono*-zinc nucleophiles. However, 10–20% of styrene is a significant amount of byproduct, which could arise from the  $\beta$ -hydride elimination of an intermediate benzylic palladium complex (**Scheme II-14**).<sup>[351]</sup> Recalling the concept of  $\beta$ -hydride elimination, this reaction involves the transformation of an alkyl group, which possesses a  $\beta$ -hydrogen atom  $\sigma$ -bonded to a metal center, into two distinct products: a metal-bound hydride and a  $\pi$ -bonded alkene.<sup>[352]</sup> For this reaction to transpire, it is essential that the alkyl group in question has hydrogen atoms on the  $\beta$ -carbon atom and the metal complex must feature an vacant site, positioned in a *cis* orientation relative to the alkyl group.

Based on this, we decided to look first for suitable conditions to accomplish Pd-catalyzed (mono)arylation and achieve a more satisfactory yield of the corresponding ( $\pm$ )-**182a**, given that such

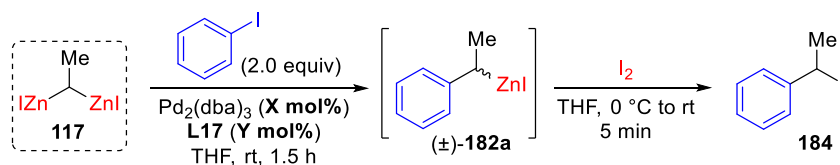
transformation had not been reported previously by Matsubara for 1,1-dizincio bimetallics having alkyl substituents.<sup>[261,263]</sup>



**Scheme II-14.** Possible simplified reaction course for the Pd-catalyzed cross-coupling of 1,1-bis(iodozincio)ethane with an aryl iodide.

First of all, we discovered that the reaction could also be carried out effectively at room temperature, yielding the same results, albeit requiring a longer time for completion (entry 1, **Table II-2**).

**Table II-2.** Influence of catalyst amount for the Pd-catalyzed (mono)arylation of 1,1-bis(iodozincio)ethane.



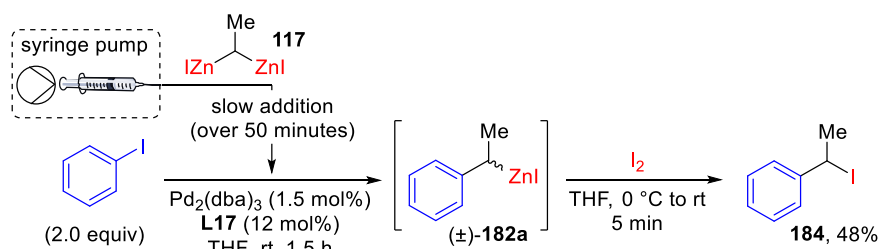
Entry	(X mol%)/(Y mol%)	Yield <b>184</b> <sup>[a]</sup>	Conversion <b>117</b> <sup>[a]</sup>
1	1.5/12 mol%	61%	>99%
2	4.5/36 mol%	35% <sup>[b]</sup>	91%
3	0.5/4 mol%	51%	>99%

[a] Determined by <sup>1</sup>H NMR analysis using 1,3,5-trimethoxybenzene as internal standard. [b] Average calculated from 2 experiments.

Subsequently, we decided to test the impact of tripling the amount of palladium and ligand in the reaction, with the aim of potentially improving the yield. Surprisingly, our endeavors led to an unintended outcome. Under these reaction conditions, we only managed to obtain 35% of the desired product as average of 2 experiments (respectively 27% and 43%), with nearly complete conversion of the *gem*-dizinc reagent and a 6% formation of styrene (entry 2, **Table II-2**). In the crude reaction

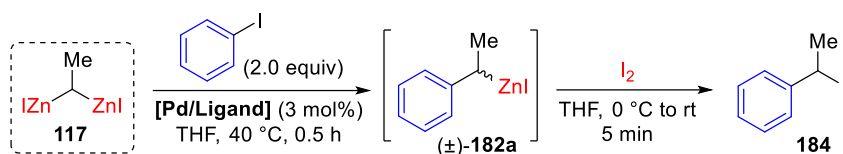
mixture, we observed no other byproducts, but an unexplained disappearance of material left us puzzled. The significant increase in catalyst quantity, as it turned out, had a detrimental effect on the arylation process. Recognizing this, we decided to revert to using a smaller amount of catalyst (entry 3, **Table II-2**). However, under these conditions the yield was slightly reduced to 51%. Considering that 1.5 mol% of  $\text{Pd}_2(\text{dba})_3$  is already a relatively small quantity, we opted to prioritize yield and continued with this catalytic amount. It is important to mention that a consistent loss of around 20% in recovery was observed in these reactions, and this trend continued throughout all the optimization study.

Our subsequent effort involved a dropwise addition of the *gem*-dizinc reagent into the reaction mixture (**Scheme II-15**). By adding the reagent gradually by the means of a syringe pump, we aimed to optimize the reaction conditions to achieve better control over the reaction sequence and improve the yield of the monozinc intermediate. Despite our effort, the outcome remained relatively modest, yielding only 48% with an 84% of conversion. Consequently, the rate of addition did not appear to exert a substantial influence on the results.



**Scheme II-15.** Dropwise addition of 1,1-bis(iodozincio)ethane for the Pd-catalyzed (mono)arylation.

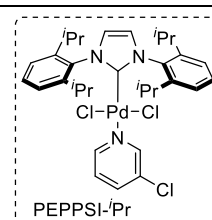
Subsequently, we carried out a brief screening process to assess how different palladium sources affected the reaction's efficiency. We sought to examine the performance of different Pd(II)-precatalysts, as outlined in **Table II-3**. Among the precatalysts tested,  $\text{PdCl}_2(\text{PPh}_3)_2$  emerged as a viable choice for facilitating the (mono)arylation process, resulting in a 59% yield of the corresponding *mono*-organozinc intermediate, alongside a 10% formation of styrene (entry 1, **Table II-3**). Nevertheless, it is worth noting that these findings did not exhibit any noticeable enhancement over the prior results. In contrast, when we employed the  $[\text{Pd}(\text{allyl})\text{Cl}]_2/\text{L17}$  combination, the yield of the desired product was only 38%, accompanied by just 6% styrene formation and 4% ethylbenzene (entry 2, **Table II-3**). In the final stage of this screening, we extended our investigations to include the PEPPSI-*i*-Pr precatalyst, which had previously demonstrated success in facilitating the second arylation of bis(iodozincio)methane.<sup>[263]</sup> Surprisingly, our efforts yielded no product formation, and in this context, we were also unable to achieve di-arylation (entry 3, **Table II-3**).

**Table II-3.** Screening of Pd(II) precatalyst for the Pd-catalyzed (mono)arylation of 1,1-bis(iodozincio)ethane.

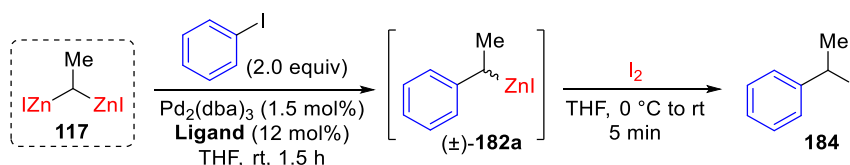
Entry	[Pd/Ligand]	Yield <b>184</b> <sup>[a]</sup>	Conversion <b>117</b> <sup>[a]</sup>
1	PdCl <sub>2</sub> (PPh <sub>3</sub> ) <sub>2</sub>	59%	>99%
2 <sup>[b]</sup>	[Pd(allyl)Cl] <sub>2</sub> /L17	38%	>99%
3	PEPPSI- <i>i</i> Pr	0%	33%

[a] Determined by <sup>1</sup>H NMR analysis using 1,3,5-trimethoxybenzene as internal standard.

[b] 12 mol% of P[3,5-(CF<sub>3</sub>)<sub>2</sub>C<sub>6</sub>H<sub>3</sub>]<sub>3</sub>.



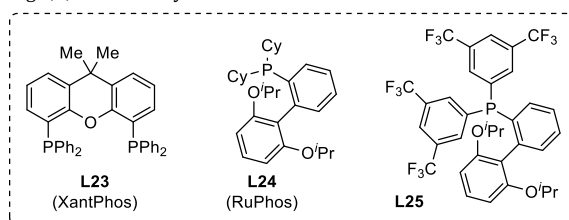
Given the substantial variations observed in our previous results, we made the decision to initiate a comprehensive screening of various ligands, utilizing Pd<sub>2</sub>(dba)<sub>3</sub> as the palladium source. The outcomes of this ligand screening are outlined in **Table II-4**. To begin, the use of the simple PPh<sub>3</sub> ligand produced results that closely mirrored those achieved with PdCl<sub>2</sub>(PPh<sub>3</sub>)<sub>2</sub>, which was somewhat expected (entry 2, **Table II-4**). Subsequently, we investigated electron rich phosphine ligands such as P(4-MeC<sub>6</sub>H<sub>4</sub>)<sub>3</sub> and P(4-OMeC<sub>6</sub>H<sub>4</sub>)<sub>3</sub>, yielding similar results of 58% and 54% yield, respectively (entries 3 and 4, **Table II-4**). However, it is essential to note that we encountered some issues with reproducibility, leading to occasional significantly lower yields. With no improvement in the yield of the monozinc intermediate observed, we explored the effectiveness of P(*o*-furyl)<sub>3</sub>, which exhibited efficient (mono)allylic alkylation with 1,1-bis(iodozincio)ethane.<sup>[261]</sup> Nonetheless, in our conditions it demonstrated poor results, achieving only a 26% yield (entry 5, **Table II-4**). Following this, we tested the bidentate phosphine ligand Xantphos (**L23**), but it exhibited very low efficiency for (mono)arylation, practically failing to form the benzylzinc intermediate (entry 6, **Table II-4**). Lastly, we evaluated **L24** with alkyl substituents, and **L25** characterized by electron-deficient and electron-neutral aromatic substituents (entries 7 and 8, **Table II-4**). The first one produced unsatisfactory result, while the other yielded results similar to those achieved with PPh<sub>3</sub> and **L17**.

**Table II-4.** Ligand screening for the Pd-catalyzed (mono)arylation of 1,1-bis(iodozincio)ethane.

Entry	Ligand	Yield <b>184</b> <sup>[a]</sup>	Conversion <b>117</b> <sup>[a]</sup>
1	<b>L17</b>	60%	>99%
2	PPh <sub>3</sub>	56%	>99%
3	P(4-MeC <sub>6</sub> H <sub>4</sub> ) <sub>3</sub>	58% <sup>[b]</sup>	>99%
4	P(4-OMeC <sub>6</sub> H <sub>4</sub> ) <sub>3</sub>	54% <sup>[b]</sup>	98%
5	P( <i>o</i> -furyl) <sub>3</sub>	26%	63%
6	<b>L23</b>	<3%	47%
7	<b>L24</b>	11%	70%
8	<b>L25</b>	56%	97%

[a] Determined by <sup>1</sup>H NMR analysis using 1,3,5-trimethoxybenzene as internal standard.

[b] Problems of reproducibility.



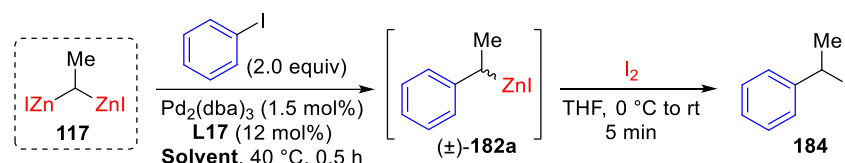
After the ligand screening, we decided to continue using **L17** and to start a comprehensive screening of solvent, which is summarized in **Table II-5**.

Initially, we began our investigation by utilizing the etheral solvent MTBE, which is employed in the enantioconvergent Fukuyama cross-coupling reaction.<sup>[345]</sup> However, our initial attempts resulted in a mere 40% yield, accompanied by 9% styrene and 12% ethylbenzene formation (entry 2, **Table II-5**). Subsequently, we explored the potential of polar solvents such as DMF and acetonitrile, but they yielded similar results, each with less than 50% yield and 10% styrene formation (entries 3 and 10, **Table II-5**). On the other hand, non-polar solvents like chloroform and 1,4-dioxane proved to be ineffective, if not entirely unsuitable for the reaction. Surprisingly, THT, which had demonstrated competence in activating and stabilizing bis(iodozincio)methane for synthesizing symmetrical ketones,<sup>[267]</sup> proved to be unsuitable under these circumstances (entry 11, **Table II-5**).

When we introduced halogenated solvents such as 1,2-dichloroethane and dichloromethane, the reactivity of the bimetallic reagent underwent a significant transformation. In fact, the reaction proceeded at a considerably slower rate, requiring significantly more time to reach completion. For instance, with 1,2-DCE, after 7 h at 40 °C, the conversion plateaued, and the yield only reached 42%, with a concurrent 4% styrene formation (entry 5, **Table II-5**). Degradation started occurring after this

extended duration. Conversely, in CH<sub>2</sub>Cl<sub>2</sub>, the reaction displayed a faster kinetic profile and greater efficiency, resulting in a satisfactory yield of 77% after just 4 h at 40 °C, with only 7% styrene detected. Conducting the reaction in dichloromethane the limited presence of styrene compared to the yield suggests that  $\beta$ -hydride elimination was not a competitive process.

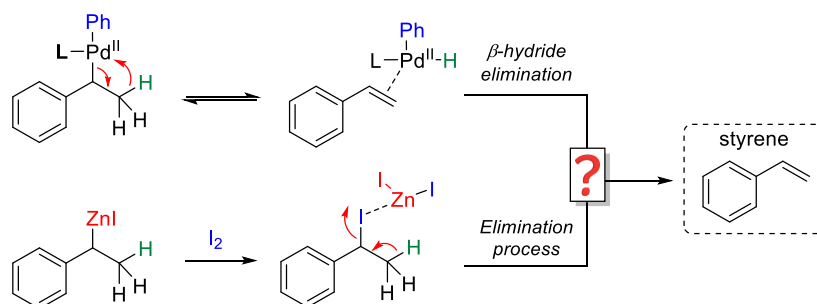
**Table II-5.** Solvent screening for the Pd-catalyzed (mono)arylation of 1,1-bis(iodozincio)ethane.



Entry	Solvent	Yield <b>184</b> <sup>[a]</sup>	Conversion <b>117</b> <sup>[a]</sup>
1	THF	60%	>99%
2	MTBE	40%	98%
3 <sup>[b]</sup>	DMF	48%	>99%
4 <sup>[c]</sup>	1,2-DCE	20%	40%
5 <sup>[d]</sup>	1,2-DCE	42%	65%
6 <sup>[b]</sup>	CH <sub>2</sub> Cl <sub>2</sub>	30%	50%
7 <sup>[e]</sup>	CH <sub>2</sub> Cl <sub>2</sub>	77%	95%
8	CHCl <sub>3</sub>	0%	>99%
9	2-Me-THF	3%	>99%
10 <sup>[c]</sup>	MeCN	31%	>99%
11	THT	4%	78%
12	1,4-dioxane	8%	98%

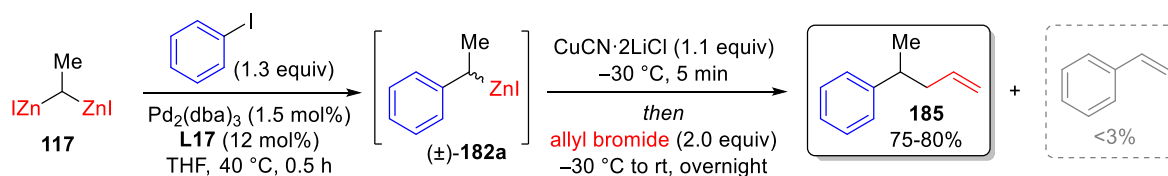
[a] Determined by <sup>1</sup>H NMR analysis using 1,3,5-trimethoxybenzene as internal standard. [b] Reaction time: 1 h. [c] Reaction time: 1.5 h. [d] Reaction time: 7 h. [e] Reaction time: 4 h.

At some point in our research, doubts emerged concerning the generation of styrene as an unintended byproduct. Notably, especially in the screening solvent and employing the same palladium-ligand complex, we consistently observed the formation of 10-15% styrene. As said before, this undesired outcome could potentially arise from the  $\beta$ -hydride elimination of an intermediate benzylic palladium complex. However, it could also originate from benzyl iodide **184** through an elimination process during the iodolysis step (**Scheme II-16**).



**Scheme II-16.** Possible causes of undesired styrene formation during our sequential arylation/iodolysis.

To shed light on this issue, we made the decision to conduct the reaction in THF, which routinely resulted in a 60% yield, accompanied by 13-18% styrene. Subsequently, we subjected compound ( $\pm$ )-**182** to a copper-mediated allylation reaction (**Scheme II-17**).

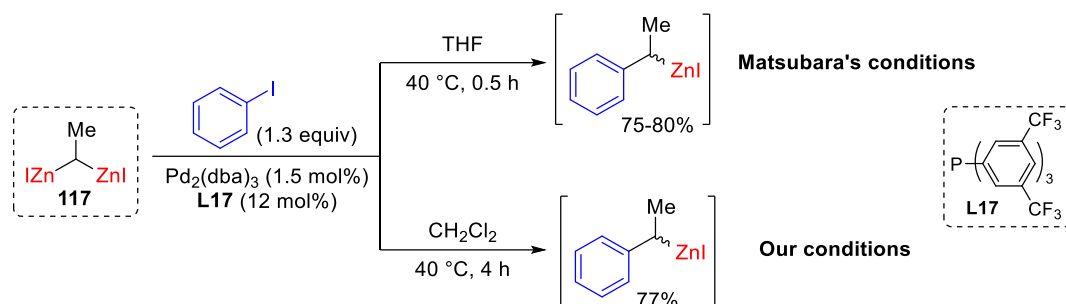


**Scheme II-17.** Sequential Pd-catalyzed arylation/copper-mediated allylation of 1,1-bis(iodozincio)ethane in one pot.

For our pleasure, we isolated product **185** with a remarkable 75-80% yield and only detected negligible traces of styrene (<3%). This outcome strongly suggests that the formation yield of ( $\pm$ )-**182a** from compound **117** is, at the very least, 75-80%, and further implies that  $\beta$ -hydride elimination is not a prominently competitive process under our specific reaction conditions.

## 1.7. Concluding Remarks on the Pd-Catalyzed Arylation Reaction of 1,1-Bis(iodozincio)ethane

To sum up, this optimization study has led us to identify reaction conditions that yield consistent results in the Pd-catalyzed (mono)arylation of 1,1-bis(iodozincio)ethane. Specifically, utilizing  $\text{Pd}_2(\text{dba})_3$  (1.5 mol%) and **L17** (12 mol%) in THF at 40 °C for 0.5 h (Matsubara's conditions),<sup>[263]</sup> the reaction between 1,1-bis(iodozincio)ethane and iodobenzene results in a selective (mono)arylation product with a yield of (at least) 75-80% (**Scheme II-18**). On the other hand,  $\text{CH}_2\text{Cl}_2$  can also be employed, yielding similar results of 77%, although the reaction time is significantly extended to 4 h to achieve completion.



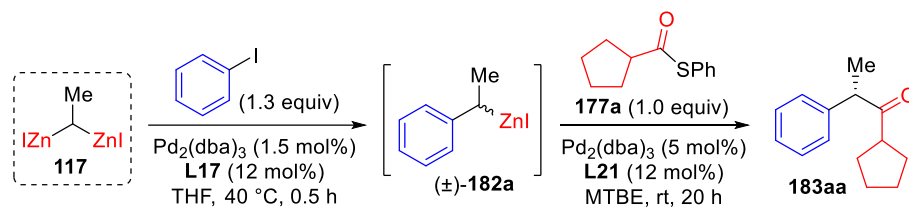
**Scheme II-18.** Pd-catalyzed (mono)arylation of 1,1-bis(iodozincio)ethane in THF and CH<sub>2</sub>Cl<sub>2</sub>.

Under these specific conditions, we have effectively demonstrated the compatibility of the Pd-catalyzed (mono)arylation process with *gem*-dizinc reagents that feature hydrogen atoms positioned  $\beta$  to the metal center. This essential insight expands the practicality of the transformation, making it readily applicable to 1,1-bis(iodozincio)alkanes like 1,1-bis(iodozincio)ethane, beyond its previous scope limited to bis(iodozincio)methane.

## 1.8. Optimization of the Enantioselective Sequential Arylation/Fukuyama Cross-Coupling Reaction of 1,1-Bis(iodozincio)ethane

Next in line was the optimization of the entire sequence of the (mono)arylation reaction, leading to the intermediate ( $\pm$ )-**182a**, followed by the subsequent Pd-catalyzed enantioselective cross-coupling reaction with thioesters using the chiral enantiopure ligand **L21**. Initial experiments involved the use of equimolar amounts of **117** and thioester **177a** (**Table II-6**). The first cross-coupling took place in THF at 40 °C, followed by the cross-coupling of ( $\pm$ )-**182a** and **177a**, which occurred under the conditions outlined in the preliminary study. This included the use of the catalytic system Pd<sub>2</sub>(dba)<sub>3</sub> (5 mol%)/**L21** (12 mol%) at room temperature, with MTBE as the solvent. Product **183aa** was successfully obtained in 33% yield with a remarkable enantiomeric excess of 94:6 (entry 1, **Table II-6**). This outcome aligns with our earlier observations in preliminary studies and underscores the fact that the presence of the achiral ligand **L17** in the reaction media does not preclude high enantiocontrol during the second step of the process. Our initial attempt to improve the efficiency of the process involved the use of THF as the sole solvent for the entire tandem reaction, but it proved to be somewhat less effective in terms of both yield and *er* (entry 2, **Table II-6**). In response, we decided to explore alternative solvent combinations (entries 3–5, **Table II-6**).



**Table II-6.** Optimization for the enantioselective sequential arylation/Fukuyama cross-coupling reaction of 1,1-bis(iodozincio)ethane

Entry	Variation 1 <sup>st</sup> coupling	Variation 2 <sup>nd</sup> coupling	Yield <b>183aa</b> <sup>[a]</sup>	er <sup>[b]</sup>
1	none	none	33%	94:6
2	none	THF instead of MTBE	28%	93:7
3	CH <sub>2</sub> Cl <sub>2</sub> (4 h) instead of THF (0.5 h)	none	35%	92:8
4	CH <sub>2</sub> Cl <sub>2</sub> (4 h) instead of THF (0.5 h)	CH <sub>2</sub> Cl <sub>2</sub> instead of MTBE	<5%	n.d.
5	CH <sub>2</sub> Cl <sub>2</sub> (4 h) instead of THF (0.5 h)	THF instead of MTBE	21%	n.d.
6	none	2.0 equiv of thioester	32%	94:6
7	none	Addition of LiCl (3.0 equiv)	17%	n.d.
8	none	Pd <sub>2</sub> (dba) <sub>3</sub> /L21(10/24mol%)	36%	94:6

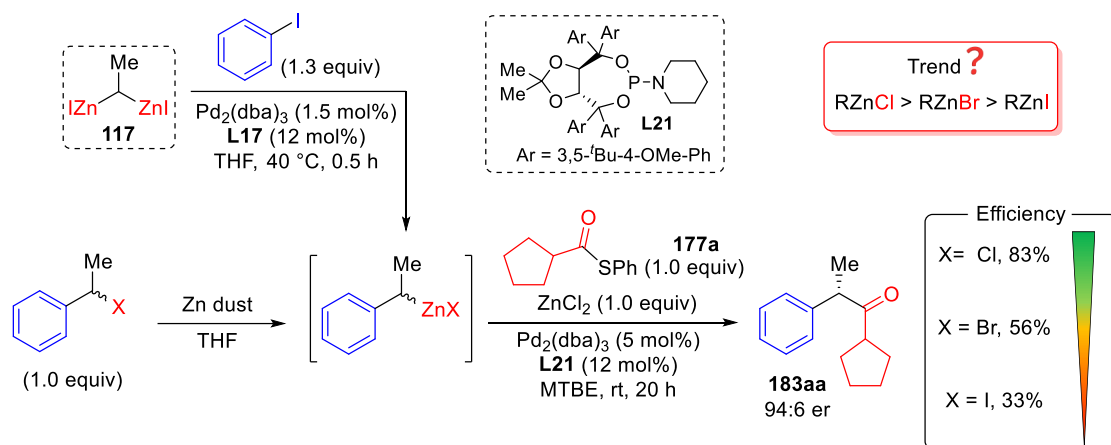
[a] Yield measured prior to purification by <sup>1</sup>H NMR analysis using 1,3,5-trimethoxybenzene as internal standard.

[b] Measured by chiral-phase GC. The absolute configuration was determined by comparison with literature data.

For these variations, we initiated the reaction with CH<sub>2</sub>Cl<sub>2</sub> as the solvent for the first coupling. However, despite our best efforts, none of the solvent combinations based on this approach proved to be more efficient or capable of enhancing the enantioselectivity in the second step of the reaction. Consequently, our initial strategy, employing THF for the acylation step, retained its position as the most efficient approach. Consequently, we made the decision to persist in optimizing the tandem reaction using this solvent. We also experimented with using a slight excess of thioester, but no notable differences were observed (entry 6, **Table II-6**). Subsequently, we introduced LiCl into the second coupling step (entry 7, **Table II-6**), a common additive in Negishi cross-couplings.<sup>[353,354]</sup> This additive is used to boost the reactivity of organozinc halides toward the transmetalation by promoting the formation of zincate complexes RZnX<sub>2</sub><sup>-</sup>.<sup>[355,356]</sup> However, in our case, this addition turned out to have a detrimental effect. Following that, we made an effort to double the amount of catalyst for the second step, although this adjustment resulted in only a marginal increase in yield, if any at all (entry 8, **Table II-6**).

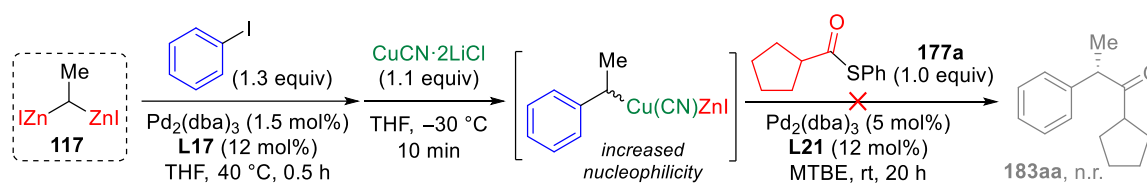
Based on these findings, we began to consider the possibility that, in the context of the Fukuyama cross-coupling, benzylzinc iodide may be less efficient than benzylzinc chloride. In fact, it is worth noting that with our tandem reaction, we achieved the same yield as when we used benzylzinc iodide prepared through zincation from the corresponding benzyl iodide (**Scheme II-19**). This led us to consider whether the choice of the organozinc halide's counter anion could influence the efficiency of the reaction. Additionally, to corroborate this hypothesis, Maulide's work indicated that when the

reaction was conducted with benzylzinc bromide, the product was obtained with identical levels of enantioselectivity but a reduced yield of 56% (**Scheme II-19**). This prompted us to question whether there might be a discernible trend with the counter anion of the benzyl zinc halide, with chloride being the most effective and iodide the least effective.



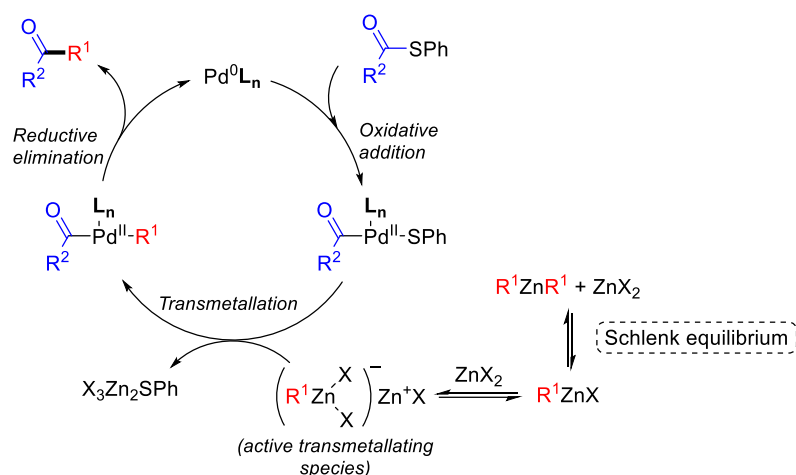
**Scheme II-19.** Potential impact of counter anion of the organozinc halide on Fukuyama cross-coupling efficiency.

Subsequently, our attempted approach involved introducing stoichiometric amount of a THF solution of CuCN·2LiCl before the second step (**Scheme II-20**). This was done to create the mixed organocopper-zinc reagent, recognized for its heightened nucleophilicity and increased reactivity.<sup>[153,357,358]</sup> Unfortunately, no reaction took place, and the thioester remained completely unreacted, resulting in its full recovery.



**Scheme II-20.** Attempt to bolster the efficiency of the Fukuyama cross-coupling by forming the mixed organocopper-zinc reagent.

At a certain point, we began to question the use of ZnCl<sub>2</sub> in our process. Previous research reports have highlighted the advantages of incorporating a stoichiometric amount of ZnCl<sub>2</sub> as an additive to enhance the efficiency of the Fukuyama cross-coupling.<sup>[344,345,359]</sup> This enhancement can be attributed to several factors. First, alkylzinc halides are known to undergo a Schlenk equilibrium with their dialkylzinc counterparts. The Fukuyama cross-coupling operates effectively with RZnX species but is less efficient with R<sub>2</sub>Zn reagents.<sup>[141,359]</sup> Second, ZnCl<sub>2</sub> likely enhances conversion and yield by facilitating the formation of zinc-ate complexes that are more amenable to transmetalation (**Scheme II-21**).<sup>[354,359]</sup>

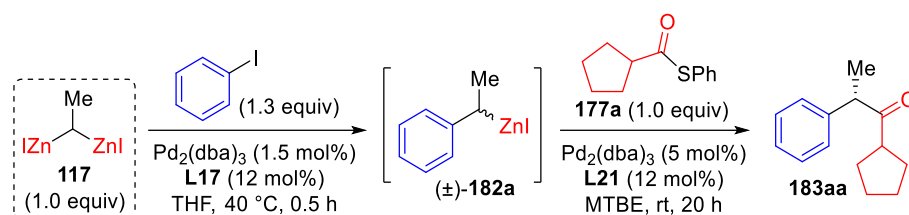


**Scheme II-21.** Catalytic cycle of Pd-catalyzed Fukuyama cross-coupling with zinc-ate complexes.

When we conducted the reaction using 1 or 2 equivalents of  $\text{ZnCl}_2$ , no noticeable changes were observed in terms of both yield and enantioselectivity (entries 1 and 2, **Table II-7**).

However, we discovered that the presence of  $\text{ZnCl}_2$  significantly improved the efficiency of our second coupling step, and consequently, the entire sequence, provided that at least 6.0 equivalents were used in relation to the *gem*-dizincio reagent (entry 3, **Table II-7**). With this amount of zinc salt, we managed to enhance the yield to a satisfactory 50%. Further increasing the quantity of  $\text{ZnCl}_2$  did not result in any additional improvements (entry 4, **Table II-7**). Additionally,  $\text{ZnCl}_2$  is also believed to accelerate the rate of racemization of the organometallic compounds with chiral secondary organozinc reagents.<sup>[304]</sup> In our system, this role seemed to be crucial because, on one hand, we observed no significant difference in *er* for reactions performed with or without the  $\text{ZnCl}_2$  additive. On the other hand, a substantial disparity in yield was evident between reactions using racemic or enantiopure ligands, when  $\text{ZnCl}_2$  was absent. However, for a more in-depth analysis of these mechanisms, we refer to paragraph <1.10. Mechanistic Studies: KR or DKR?>

While maintaining the very high levels of enantioselectivity, a synthetically valuable 75% yield in product **183aa** was achieved by increasing the amount of *gem*-dizincio reagent (**117**) to a slight excess of up to 1.5 equiv respect to **177a** (entry 6, **Table II-7**), which aligns with the typical substrate/reagent ratio employed in the Fukuyama cross-coupling. Further increasing the excess of bimetallic reagent did not result in any additional improvements (entry 7, **Table II-7**). Interestingly, the nature of the zinc counter-anion does not seem to have a decisive effect on the reaction outcome, given that quite similar results were obtained using  $\text{ZnI}_2$  or  $\text{ZnBr}_2$  as additives (entries 8 and 9, **Table II-7**). A series of inorganic salts, including  $\text{LiCl}$ ,  $\text{MgCl}_2$ , and  $\text{AlCl}_3$ , were tested in the course of the optimization (entries 10–12, **Table II-7**). The outcomes revealed that the inclusion of one of these chloride-based salts had an adverse influence on the reaction. The net result was a considerable drop in the yield of the desired product, and there was also a noticeable reduction in the level of *ee*.

**Table II-7.** Optimization for the enantioselective sequential arylation/Fukuyama cross-coupling reaction of 1,1-bis(iodozincio)ethane

Entry	Variation 1 <sup>st</sup> coupling	Variation 2 <sup>nd</sup> coupling	Yield <b>183aa</b> <sup>[a]</sup>	er <sup>[b]</sup>
1	none	+ ZnCl <sub>2</sub> (1.0 equiv)	33%	94:6
2	none	+ ZnCl <sub>2</sub> (2.0 equiv)	35%	94:6
3	none	+ ZnCl <sub>2</sub> (6.0 equiv)	50%	94:6
4	none	+ ZnCl <sub>2</sub> (10.0 equiv)	50%	94:6
5	1.25 equiv of <b>117</b> <sup>[c]</sup>	+ ZnCl <sub>2</sub> (7.5 equiv) <sup>[d]</sup>	63%	94:6
6	1.5 equiv of <b>117</b> <sup>[c]</sup>	+ ZnCl <sub>2</sub> (9.0 equiv) <sup>[e]</sup>	75%	94:6
7	2.0 equiv of <b>117</b> <sup>[c]</sup>	+ ZnCl <sub>2</sub> (12.0 equiv) <sup>[f]</sup>	76%	94:6
8	1.5 equiv of <b>117</b> <sup>[c]</sup>	+ ZnBr <sub>2</sub> (9.0 equiv) <sup>[e]</sup>	67%	95:5
9	1.5 equiv of <b>117</b> <sup>[c]</sup>	+ ZnI <sub>2</sub> (9.0 equiv) <sup>[e]</sup>	64%	94:6
10	1.5 equiv of <b>117</b> <sup>[c]</sup>	+ LiCl (9.0 equiv) <sup>[e]</sup>	18%	55:45
11	1.5 equiv of <b>117</b> <sup>[c]</sup>	+ MgCl <sub>2</sub> (9.0 equiv) <sup>[e]</sup>	24%	61:39
12	1.5 equiv of <b>117</b> <sup>[c]</sup>	+ AlCl <sub>3</sub> (9.0 equiv) <sup>[e]</sup>	10%	84:16
13	1.5 equiv of <b>117</b> <sup>[c]</sup>	+ ZnCl <sub>2</sub> (9.0 equiv) and SEt instead of SPh as leaving group <sup>[e]</sup>	62%	95:5
14	1.5 equiv of <b>117</b> <sup>[c]</sup>	+ ZnCl <sub>2</sub> (9.0 equiv) and S(4-NO <sub>2</sub> -C <sub>6</sub> H <sub>4</sub> ) instead of SPh as leaving group <sup>[e]</sup>	18%	n.d.
15	1.5 equiv of <b>117</b> <sup>[c]</sup>	+ ZnCl <sub>2</sub> (9.0 equiv) <sup>[g]</sup>	48%	94:6

[a] Yield measured prior to purification by <sup>1</sup>H NMR analysis using 1,3,5-trimethoxybenzene as internal standard. [b] Measured by chiral-phase GC. The absolute configuration was determined by comparison with literature data. [c] The amount of PhI and catalyst was adjusted to keep the ratios indicated in the scheme. [d] Pd<sub>2</sub>(dba)<sub>3</sub> (6.5 mol%)/L<sub>21</sub> (15 mol%). [e] Pd<sub>2</sub>(dba)<sub>3</sub> (7.5 mol%)/L<sub>21</sub> (18 mol%). [f] Pd<sub>2</sub>(dba)<sub>3</sub> (10 mol%)/L<sub>21</sub> (24 mol%). [g] Pd<sub>2</sub>(dba)<sub>3</sub> (3.75 mol%)/L<sub>21</sub> (9 mol%).

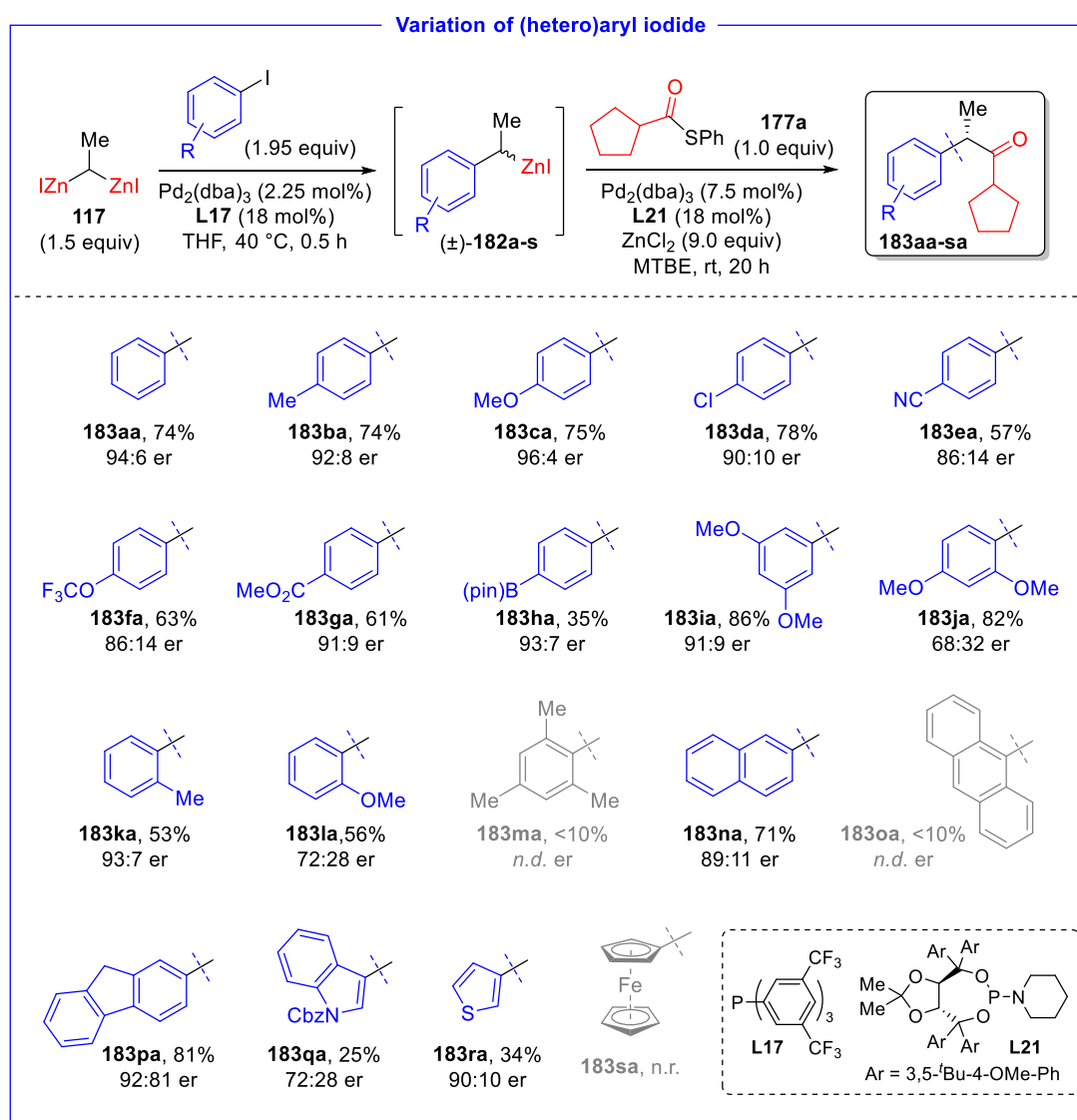
The thioester leaving group modulation was also explored within the scope of this protocol (entries 13 and 14, **Table II-7**). When ethyl was used in place of phenyl, a still respectable 62% yield with a 95:5 er was achieved. Conversely, when 4-nitrophenyl was employed, there was minimal reaction observed. This observation is especially intriguing since the oxidative addition was expected to be promoted by this particular leaving group, suggesting it should expedite the reaction.<sup>[360]</sup> Subsequently, an attempt was made to reduce the amount of palladium source (3.75 mol%) and **L21** (9 mol%) during the second step in order to make the entire protocol more valuable (entry 15, **Table II-7**). Unfortunately, this adjustment led to a moderate decrease in the yield to 48%, underscoring the necessity of using higher amounts of catalyst for optimal performance.

As further enhancements in the efficiency of the tandem reaction were not attainable, we opted for the conditions outlined in entry 6 of **Table II-7** and then commenced our exploration of the protocol's scope.

## 1.9. Scope of the Enantioselective Sequential Arylation/Fukuyama Cross-Coupling Reaction of 1,1-Bis(iodozincio)ethane

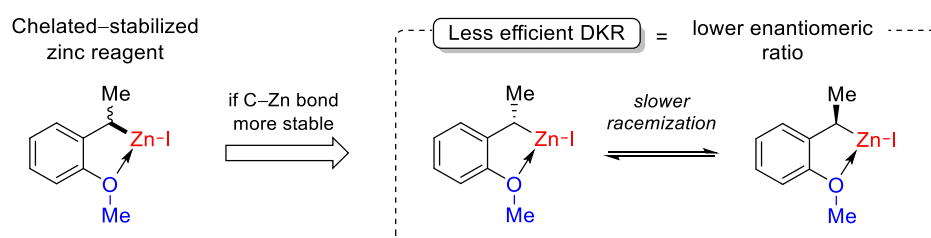
### 1.9.1. Variation of (Hetero)Aryl Iodide

With the best conditions identified in hand (entry 6, **Table II-7**), we then established the scope of the tandem reaction. Regarding the aryl iodide partner, *para*- and *meta*-substituted derivatives were well tolerated in the sequence, delivering ketones (**183aa-183ga**, and **183ia**) in 57–86% yield and with high er, regardless of the electronic character (electron-donating or electron-withdrawing) of the substituents.



**Scheme II-22.** Scope of (hetero)aryl iodides for the enantioselective sequential arylation/Fukuyama cross-coupling reaction of 1,1-bis(iodozincio)ethane.

Remarkably, even a chloride substituent (**183da**) was compatible with the reaction conditions, yielding product containing an aryl halide that could be further utilized in subsequent cross-coupling reactions. Additionally, the B(pin) group (**183ha**), which provides opportunities for further modifications as well, displayed excellent enantioselectivity (93:7 er), albeit with a modest reduction in efficiency (35%). Substitution in the *ortho* position of the aryl ring, which notably was not disclosed in the previous report,<sup>[345]</sup> was found to be possible (**183ja**, **183ka**, **183la**), albeit this led to a moderate reduction in yield (~55%). However, in the particular case of 2-methoxy-substituted aryl iodides (**183ja**, and **183la**), a lower enantioselectivity was also observed. This notable reduction in enantioselectivity observed may be attributed to a specific interaction occurring between the metal and the methoxy group. This interaction results in the formation of chelate-stabilized zinc reagent (**Scheme II-23**).<sup>[304]</sup> Through the formation of this chelate structure, the C–Zn bond may become more stable, causing a decrease in the rate of C–Zn bond inversion. Consequently, this slower racemization process leads to reduced efficiency in the dynamic kinetic resolution of the reaction, resulting in diminished enantioselectivity for the overall transformation.



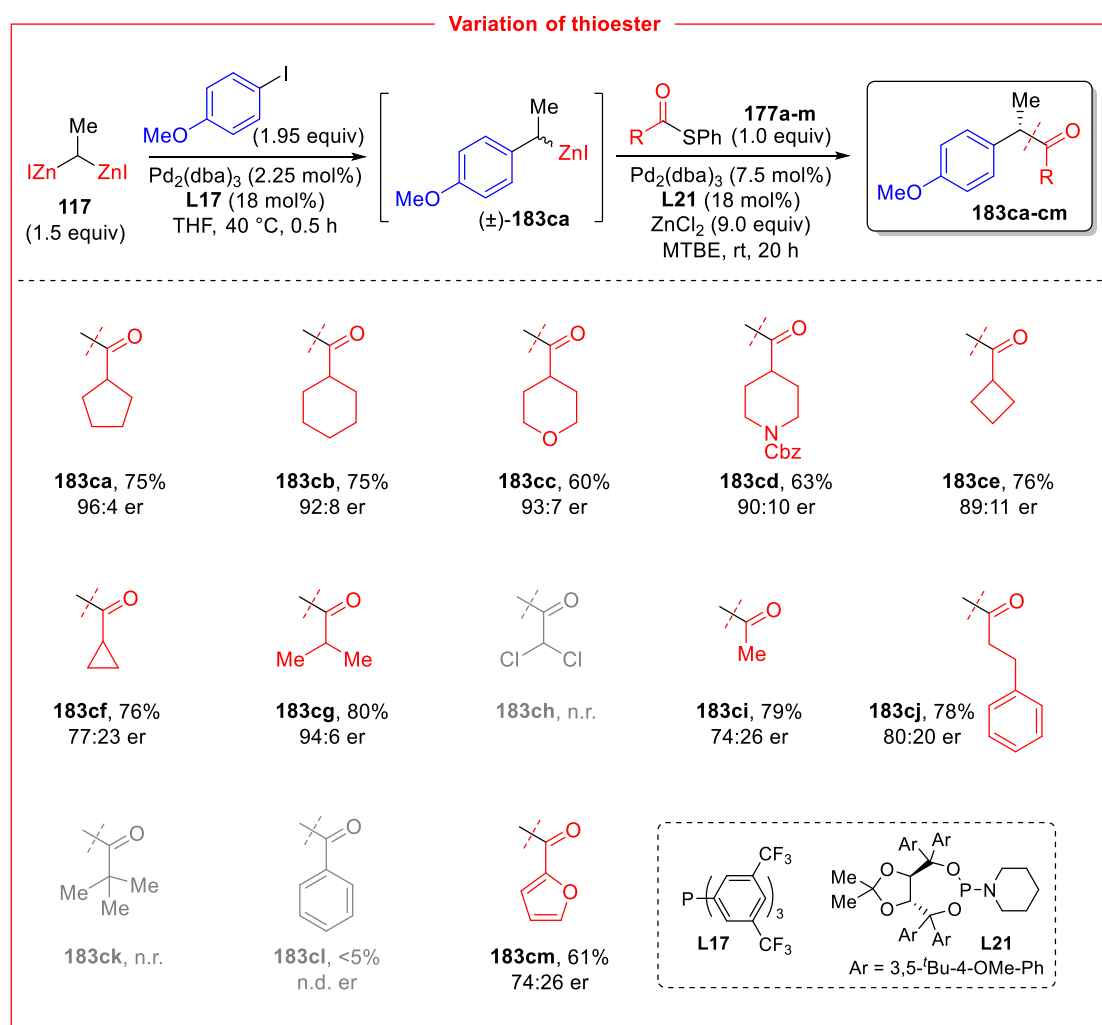
**Scheme II-23.** Potential methoxy group chelation-induced C–Zn bond stability.

In contrast, *ortho*-disubstituted aryl iodides proved to be ineffective (**183ma**), consistent with the observed decrease in the efficiency of the Fukuyama cross-coupling reaction due to increased steric hindrance. On the other hand, aryl iodides derived from more extended aromatic structures performed exceptionally well, yielding 2-naphthyl (**183na**) or 2-fluorenyl (**183pa**) products with high yields and enantioselectivity. However, the 9-anthracenyl product (**183oa**) was obtained in a very low yield, aligning with the outcomes observed for *ortho*-disubstituted aryl iodides.

The method was tested also with heteroaromatic iodides. Although the efficiency was somewhat reduced, the transformation remained viable, resulting in the formation of indolyl (**183qa**) or thiophen-3-yl (**183ra**) products. Lastly, the less frequently used ferrocenyl iodide was tested. Unfortunately, no product (**183sa**) was formed in this case.

### 1.9.2. Variation of Thioester

Variation of the thioester partner was also comprehensively explored (**Scheme II-24**). Thioesters containing secondary alkyl groups consistently delivered high yields (60-80%) and enantioselectivity ( $\geq 89:11$  er), exemplified by the formation of products **183cb-ce** and **183cg**. Cyclopropyl- (**183cf**), methyl- (**183ci**), and linear alkyl-substituted (**183cj**) ketones were produced with respectable yields (76-79%) but displayed only moderate enantiomeric ratios ( $\sim 75:25$ ). In contrast, more sterically hindered substrates, like *tert*-butyl ketone **183ck**, were either produced in very low yields or not at all. Interestingly, heteroaryl ketones like **183cm** were found to be compatible with the process, albeit with a modest enantioselectivity (74:26 er). Nonetheless, aromatic substrates, such as phenyl-ketone **183cl**, exhibited minimal reactivity in our conditions, yielding only trace amounts of the expected product. Lastly, the dichloro-substituent **183ch** was found to be entirely unsuitable for the reaction, resulting in the complete recovery of the substrate.



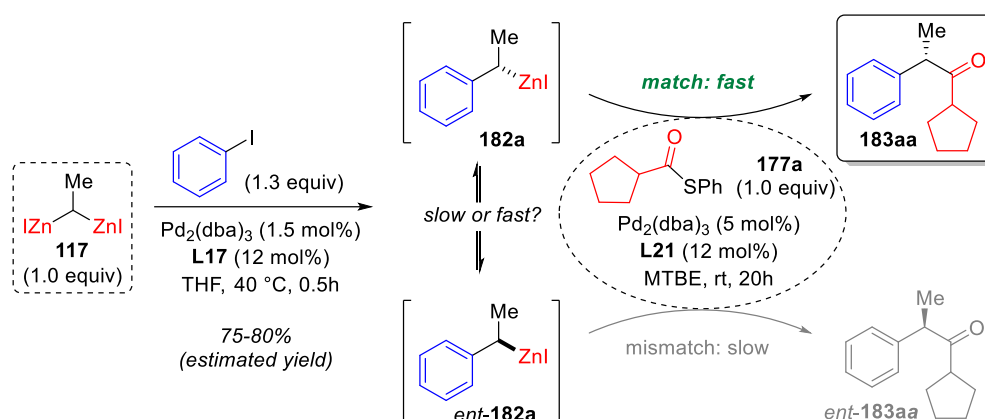
**Scheme II-24.** Scope of thioesters for the enantioselective sequential arylation/Fukuyama cross-coupling reaction of 1,1-bis(iodo)ethane.



## 1.10. Mechanistic Studies: KR or DKR?

As previously mentioned,  $\text{ZnCl}_2$  is believed to accelerate the rate of racemization in organometallic compounds when combined with chiral secondary organozinc reagents.<sup>[304]</sup> In our experimental system, the role of  $\text{ZnCl}_2$  appeared to be of paramount importance. Significantly divergent yields were observed between reactions involving racemic or enantiopure ligands when  $\text{ZnCl}_2$  was absent (entries 1 and 2, **Table II-8**). However, no discernible difference in yield was noted in reactions employing racemic or enantiopure ligands when  $\text{ZnCl}_2$  (6.0 equiv) was added (entries 3 and 4, **Table II-8**).

**Table II-8.** Sequential arylation/Fukuyama cross-coupling reaction of 1,1-bis(iodozincio)ethane in racemic and enantioselective fashion with or without  $\text{ZnCl}_2$ .



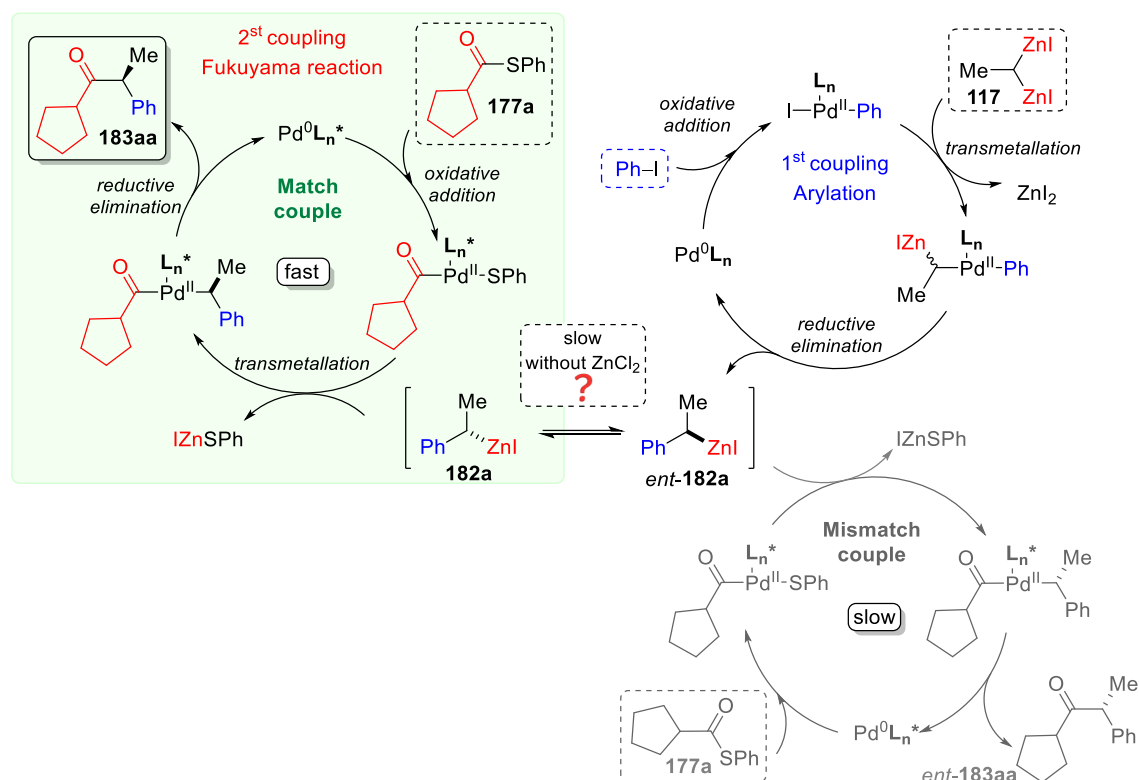
Entry	$\text{ZnCl}_2$ (equiv)	Ligand 2 <sup>nd</sup> coupling	Yield <b>183aa</b> <sup>[a]</sup>	er <sup>[b]</sup>
1	none	<b>L21</b>	33%	94:6
2	none	(±)- <b>L21</b>	53%	50:50
3	6.0	<b>L21</b>	50%	94:6
4	6.0	(±)- <b>L21</b>	52%	50:50

[a] Yield measured prior to purification by  $^1\text{H}$  NMR analysis using 1,3,5-trimethoxybenzene as internal standard. [b] Measured by chiral-phase GC. The absolute configuration of X was determined by comparison with literature data.

This led us to contemplate the possibility that the Fukuyama step might involve a kinetic resolution (KR) rather than a dynamic one. It is worth noting that while secondary benzylzinc halides are known to be configurationally labile according to existing literature,<sup>[317]</sup> no prior investigations have delved into the behavior of secondary benzylzinc iodides. The nature of the counteranion's size could potentially influence the inversion rate of the C–Zn bond, rendering it significantly slower.

In our specific context, taking into consideration that the initial coupling yielded ~75-80% of racemic benzylzinc iodide, theoretically, a maximum yield of ~40% for the desired enantioenriched product could be achieved in the Fukuyama coupling. Interestingly, this theoretical value closely aligned with

the yield obtained without the addition of  $\text{ZnCl}_2$  (entry 1, **Table II-8**). Consequently, we postulated that the primary role of  $\text{ZnCl}_2$  in the reaction medium was to expedite the racemization rate of benzylzinc iodide and facilitate an efficient DKR process (**Scheme II-25**), even though no significant disparity in er was observed between reactions conducted with or without the  $\text{ZnCl}_2$  additive. In simpler terms, the addition of  $\text{ZnCl}_2$  could have the power to switch from a KR to a DKR for the acylation step.

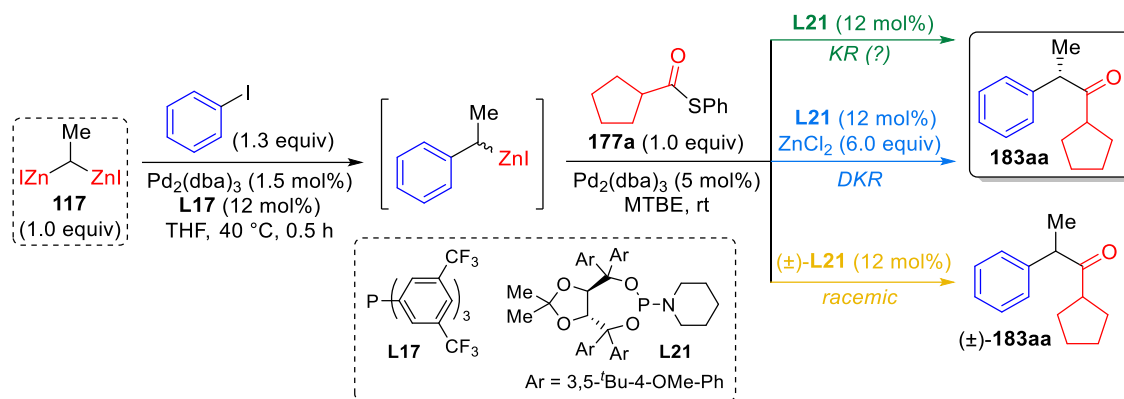


**Scheme II-25.** Proposed catalytic cycle of the Pd-catalyzed enantioselective sequential arylation/Fukuyama cross-coupling with 1,1-bis(iodozincio)ethane.

For a better understanding, we performed the kinetic profile of the tandem reaction under the following conditions: with enantiopure **L21** and no addition of  $\text{ZnCl}_2$  (**Figure II-1**, green line); with enantiopure **L21** and addition of  $\text{ZnCl}_2$  (**Figure II-1**, blue line); and with ( $\pm$ )-**L21** (**Figure II-1**, yellow line).

**Figure II-1** reveals an intriguing insight into the kinetic profiles of the three reactions during the initial 4 h of the Fukuyama cross-coupling process. During this period, the reactions exhibit a remarkable harmony. Subsequently, a notable divergence emerges. In one reaction employing enantiopure **L21** without the addition of  $\text{ZnCl}_2$ , it reaches a standstill at a 36% yield, forming a plateau (**Figure II-1**, green line). In contrast, the other two reactions conclude with final yields of 53-56%, and their profiles remain remarkably similar (**Figure II-1**, blue and yellow line). Furthermore, the enantioselective reaction employing enantiopure **L21** consistently maintains an enantiomeric ratio of 94:6. If our

hypothesis of a kinetic resolution mechanism without the involvement of the zinc salt holds true, it suggests that after the initial 4 h, the reaction essentially reaches completion.



### Kinetic Study of the Sequential Arylation/Fukuyama Coupling

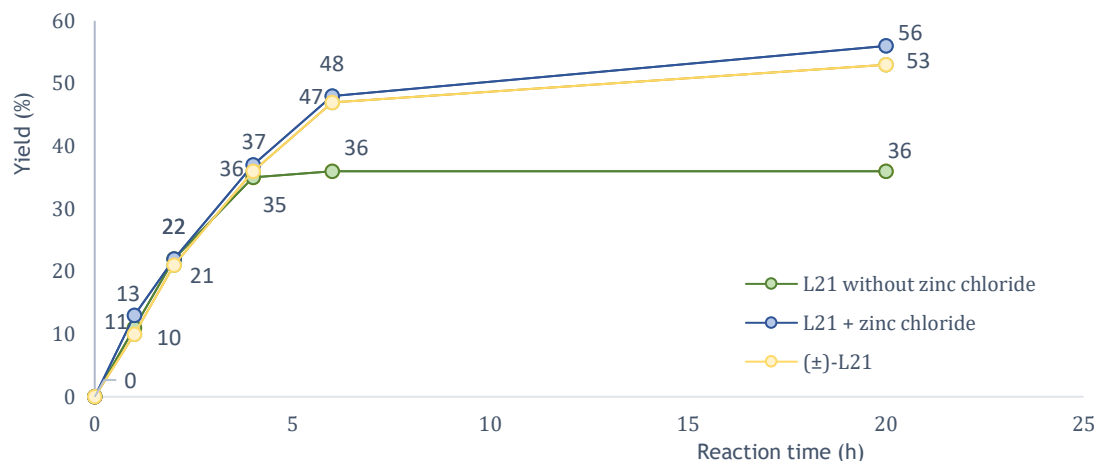


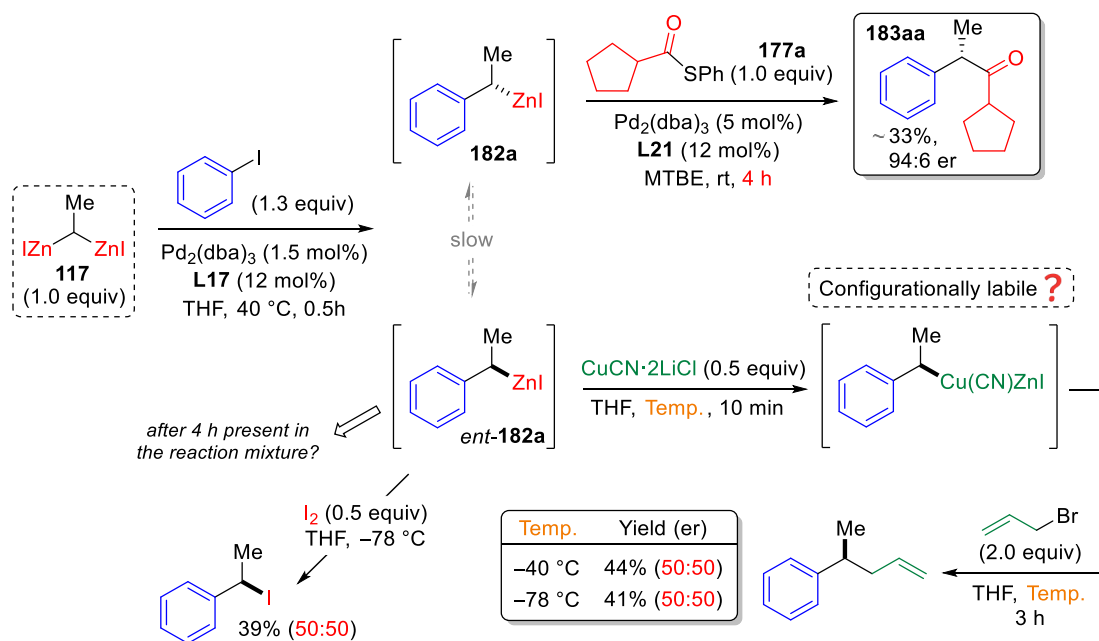
**Figure II-1.** Kinetic profiles of the Pd-catalyzed sequential arylation/Fukuyama coupling under different conditions: enantiopure **L21** and no addition of  $\text{ZnCl}_2$  (green line), with enantiopure **L21** and addition of  $\text{ZnCl}_2$  (blue line), and with  $(\pm)$ -**L21** (yellow line).

In this scenario, the reaction mixture should contain our enantioenriched product **183aa** (~33%, 94:6 er). Simultaneously, the mixture may contain the enantioenriched secondary benzylzinc iodides, with an enantiomeric ratio expected to be similar to that of the product. Therefore, if we can effectively engage the enantioenriched benzylzinc iodide in a stereospecific reaction, such as a copper-mediated allylation with allyl bromide, we should be able to obtain a highly enantioenriched adduct.

This rationale led us to conduct our tandem reaction in the presence of enantiopure **L21** and without the addition of  $\text{ZnCl}_2$  (**Scheme II-26**). According to our kinetic studies (**Figure II-1**), after 4 h, the Fukuyama coupling is expected to reach the plateau at ~35%. Consequently, we initiated the transmetalation of the benzylzinc intermediate with a THF solution of  $\text{CuCN}\cdot 2\text{LiCl}$  at low temperature ( $-40\text{ }^\circ\text{C}$ ), followed by the addition of allyl bromide (2.0 equiv) after a few minutes. We successfully obtained the desired product with a 44% yield, indicating that the unreacted benzylzinc was still

active. However, disappointingly, no enantiomeric excess was observed. We made another attempt at a lower temperature ( $-78\text{ }^{\circ}\text{C}$ ), but even then, a totally racemic mixture was obtained.

This raised questions about whether the mixed organozinc-copper reagent might be configurationally labile, potentially causing the complete loss of enantiomeric enrichment in the benzylzinc intermediate. Consequently, we decided to intercept the remaining enantiopure benzylzinc iodide through a reaction that does not involve other transition metals. To this end, we opted to perform iodolysis at  $-78\text{ }^{\circ}\text{C}$  (**Scheme II-26**). Once again, we achieved the desired product **184** with a comparable yield (39%), but no enantiomeric excess was observed.



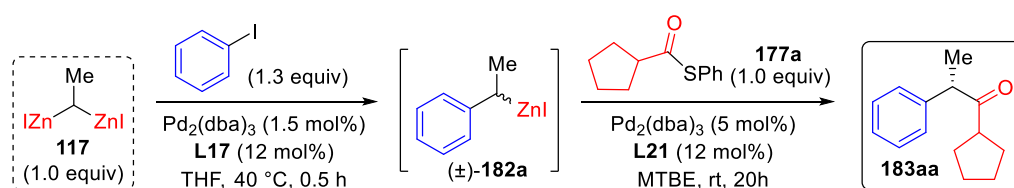
**Scheme II-26.** Alternative transformations to trap the remaining enantioenriched benzylzinc intermediate under the conditions of kinetic resolution (no addition of  $\text{ZnCl}_2$ ) of the Fukuyama cross-coupling.

With these results at our disposal, we have now verified that secondary benzylzinc iodides exhibit configurational lability at room temperature, in accordance with the existing literature.<sup>[317]</sup> This observation suggests thus the presence of a dynamic kinetic resolution within the Fukuyama process. However, since the substantial disparity between the reactions involving enantiopure and racemic ligands remains unclear, we made the decision to delve deeper into the matter (**Table II-9**).

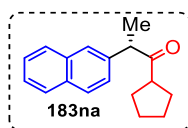
To initiate this investigation, we conducted the tandem reaction with twice the amount of  $\text{Pd}/\text{L21}$  (10/24 mol%) in two distinct approaches: once right from the start of the reaction (entry 1, **Table II-9**), and the second time adding new catalyst after 4 h when the conversion rate reaches a plateau (entry 2, **Table II-9**). Intriguingly, the two results yielded different outcomes. Having double amount of catalyst from the beginning produced no changing, resulting in 36% yield. On the contrary, when introducing new  $\text{Pd}_2(\text{dba})_3/\text{L21}$  (5/12 mol%) after 4 h, the system appears to rejuvenate its efficiency,

resulting in a final yield of 53% with 94:6 er (entry 2, **Table II-9**). In this case, it seems as though the chiral catalyst experiences a form of "poisoning," and only by adding fresh catalyst after 4 h can we attain the maximum yield. We were keen to investigate whether this type of poisoning was reversible. To explore this, we conducted the reaction solely with Pd<sub>2</sub>(dba)<sub>3</sub>/**L21** (5/12 mol%) and introduced ZnCl<sub>2</sub> after 4 h (entry 3, **Table II-9**).

**Table II-9.** Investigation of the low conversion of the Pd-catalyzed enantioselective arylation/Fukuyama coupling without ZnCl<sub>2</sub>.



Entry	Difference from above (2 <sup>nd</sup> coupling)	Yield <b>183aa</b> <sup>[a]</sup>	er <sup>[b]</sup>
1	Addition of Pd <sub>2</sub> (dba) <sub>3</sub> / <b>L21</b> (10/24 mol%)	36%	94:6
2	Addition of new Pd <sub>2</sub> (dba) <sub>3</sub> / <b>L21</b> (5/12 mol%) after 4 h	53%	94:6
3	Addition of ZnCl <sub>2</sub> (6.0 equiv) after 4h	50%	95:5
4	Addition of <b>183na</b> as additive (30 mol%)	37%	94:6

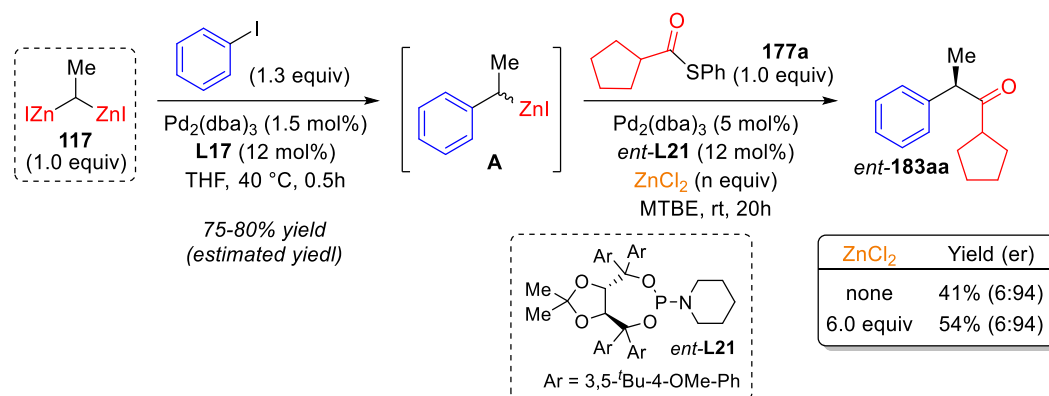


[a] Yield measured prior to purification by <sup>1</sup>H NMR analysis using 1,3,5-trimethoxybenzene as internal standard. [b] Measured by chiral-phase GC. The absolute configuration of X was determined by comparison with literature data.

Surprisingly, the yield increased to 50%, demonstrating the ability of ZnCl<sub>2</sub> to restore the catalyst's activity. Within this framework, we considered the possibility that the chiral product might be responsible for poisoning the chiral catalyst. As a result, we added **183na** (as similar product obtained from the scope) as a "poisonous additive" in 30 mol% (entry 4, **Table II-9**). However, in this case, without the addition of ZnCl<sub>2</sub>, the expected yield of 37% was achieved with the same er of 94:6.

At this point, since the preparation of the racemic ligand originated from a commercially available starting material different from that used for the enantiopure ligand (tartaric acid instead of (*L*)-diethyl tartrate), we entertained the idea that an invisible impurity, undetectable by NMR analysis, might be present in both the enantiopure and racemic ligands. This impurity could potentially influence the efficiency of the acylation step. Consequently, we synthesized the corresponding enantiomer of **L21** (*ent*-**L21**) using the same synthetic procedure used for the preparation of **L21** (see **Scheme II-8**) but starting from (*D*)-diethyl tartrate. With *ent*-**L21** in hand, we conducted the reaction both with and without ZnCl<sub>2</sub> (**Scheme II-27**). In one case, when we introduced ZnCl<sub>2</sub> into the reaction mixture, we achieved the expected outcome, yielding 54% of the *ent*-**183aa** with an er of 6:94 (**Scheme**

**II-27**). However, when we conducted the reaction without the addition of  $\text{ZnCl}_2$ , we obtained the same er (6:94) but with a yield of 41%. While a slightly higher yield (41% instead of 35%) was achieved with *ent*-**L21**, it remained lower than the yield obtained with the racemic version and the addition of zinc salt.



**Scheme II-27.** Pd-catalyzed enantioselective sequential arylation/Fukuyama coupling reaction using *ent*-**L21** as ligand for the acylation step and with/without  $\text{ZnCl}_2$ .

Finally, we conducted the tandem reaction using an authentic racemic ( $\pm$ )-**L21** prepared from equal amounts of **L21** and *ent*-**L21**. However, there was no noticeable difference between the two experiments, resulting in a 48% yield without  $\text{ZnCl}_2$  and a 52% yield with its inclusion. At this stage, despite our efforts to decipher the underlying reason for the discrepancy between eantiopure and racemic ligand without addition of  $\text{ZnCl}_2$ , we found ourselves at an impasse, unable to explain this particular phenomenon. Consequently, we made the decision to conclude this specific investigation and redirect our valuable time and resources toward the continuation of the project. However, it is worth noting that other investigations are ongoing in our laboratories.

## 1.11. Potential Pharmaceutical Application: Naproxen Synthesis

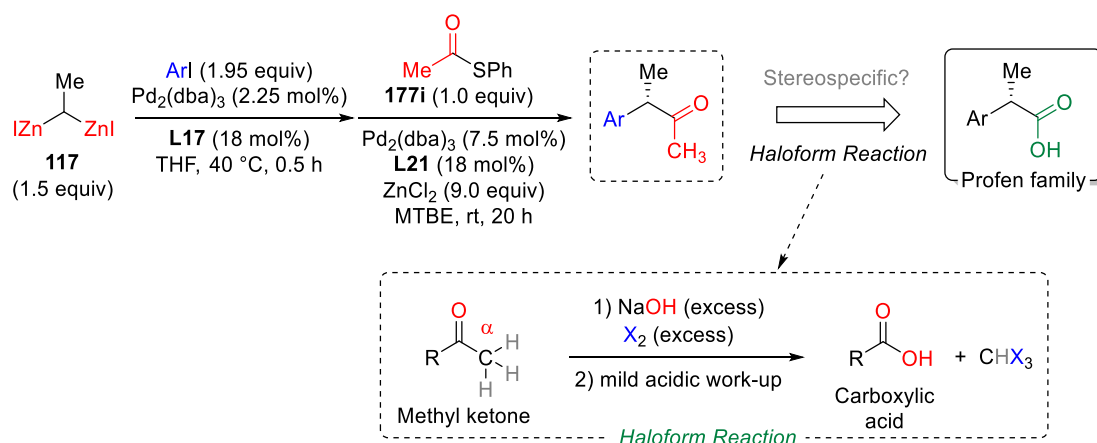
2-Arylpropionic acids, constitute a group of compounds (known as profen family) that have emerged as a cornerstone in the realm of non-steroidal anti-inflammatory drugs (NSAIDs), with ibuprofen and naproxen ranking among the most commonly used members. To put this into perspective, in 2020 ibuprofen alone was valued at approximately 300 million US dollars\*\* and was prescribed, just in the USA, over 16 million times.†† The pharmacological effects of these compounds stem from their ability to inhibit the binding of arachidonic acid to the cyclo-oxygenase subunit of

\*\* Ibuprofen market research report 2020 (<https://menafn.com/1099915665/Ibuprofen-Market-Research-Report-2020>)

†† The Top 300 of 2021 (<https://clincalc.com/DrugStats/Top300Drugs.aspx>).

prostaglandin synthetase. This inhibition, in turn, prevents the formation of various prostaglandins, consequently modulating the inflammatory response. Notably, only the (*S*)-profen enantiomer exhibits anti-inflammatory activity. Despite this knowledge, profen drugs were initially often marketed as racemic form, largely due to the presence of a 2-arylpropionyl-CoA epimerase in the human body, facilitating the interconversion of enantiomers.<sup>[361]</sup> Nonetheless, (*R*)-profen variants may give rise to health risks, including the possibility of accumulating in adipose tissues with unknown consequences.<sup>[362]</sup> These characteristics underscore the importance of developing efficient methods for producing enantiopure profens. However, despite their relatively small molecular structures, the asymmetric synthesis of (*S*)-profen derivatives remains a formidable challenge even if over the past decade, several procedures have been firmly established.<sup>[363,364]</sup>

To underscore the synthetic possibilities offered by our sequential asymmetric reaction, we aimed to identify potential applications for the straightforward synthesis of pharmaceutical compounds. Specifically, by employing *S*-phenyl ethanethioate (**177i**) as the thioester in the Fukuyama cross-coupling, we can obtain enantiomerically enriched  $\alpha$ -aryl methyl ketones. With these substrates, 2-arylpropionic acid derivatives could be synthesized through the haloform reaction (**Scheme II-28**).

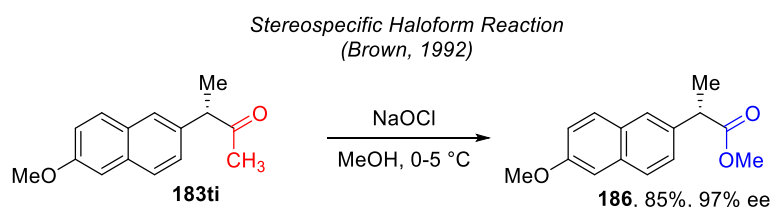


**Scheme II-28.** A synthetic way to achieve 2-arylpropionic acid derivatives from  $\alpha$ -aryl methyl ketones using the haloform reaction.

The haloform reaction is a rare example of ketone oxidation to carboxylic acids.<sup>[365]</sup> This very old reaction involves the treatment of a methyl ketone with an excess of base and halogen. The mechanism of this reaction involves a sequence of three consecutive cycles, involving deprotonation and halogenation at the  $\alpha$ -carbon, followed by the addition of a base to the carbonyl group and the expulsion of  $\text{CX}_3$  as a leaving group.

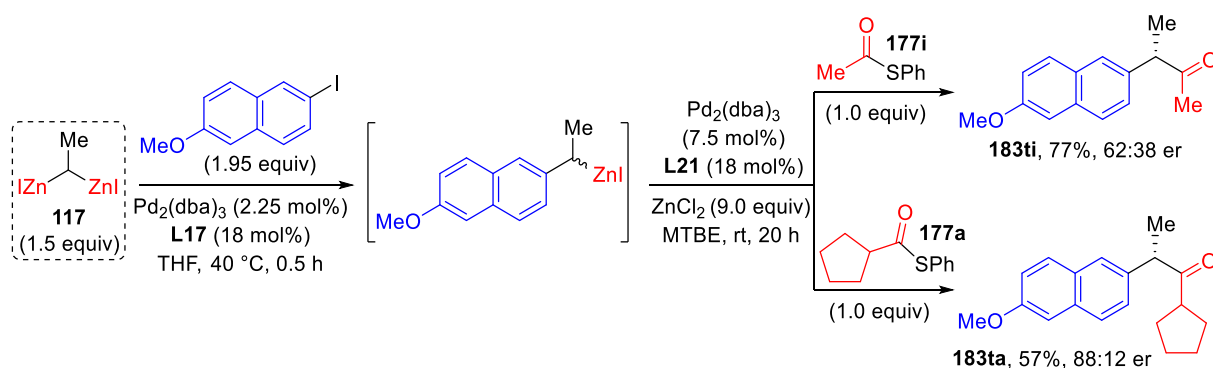
In our case the presence of an enolizable proton in the  $\alpha$ -position does not inherently ensure the stereospecificity of the haloform transformation. However, it has been reported more recently that this haloform reaction can be performed in a stereospecific manner on enantiopure substrates leading

to optically active 2-aryl propanoic acids.<sup>[366]</sup> Specifically, the author reported that the haloform reaction of ketone **183ti**, employing sodium hypochlorite in methanol at a temperature of 0-5°C, yielded (*S*)-methyl naproxen (**186**) in 85% yield and 97% ee (**Scheme II-29**).



**Scheme II-29.** Stereospecific example of haloform reaction.

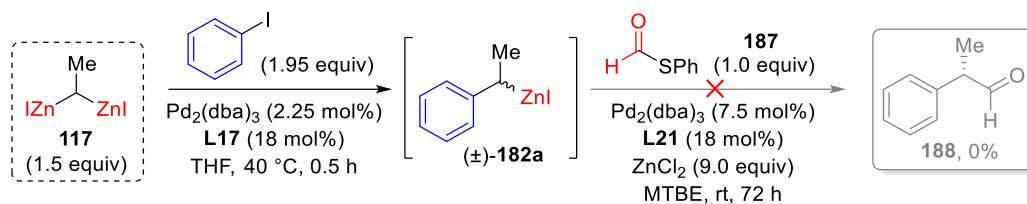
Therefore, we proceeded with our asymmetric sequential reaction to synthesize ketone **183ti**, with the intention of applying the stereospecific haloform reaction mentioned before,<sup>[366]</sup> to synthesize in straightforward manner the enantiomerically enriched (*S*)-Naproxen. Unfortunately, as anticipated, the presence of primary alkyl substituents on the thioester led to a reduction in enantiomeric excess, which was especially pronounced in this instance. When thioester **177i** was used, we achieved only a mediocre 62:38 enantiomeric ratio (**Scheme II-30**). However, when employing thioester **177a**, we were able to restore a more satisfactory enantiomeric ratio of 88:12, although it is worth noting that this product (**183ta**) is not compatible with the haloform reaction.



**Scheme II-30.** Enantioselective synthesis of (*S*)-Naproxen analogs.

Given this outcome, we chose to persist exploring different thiocarbonyl electrophiles for the subsequent step. Indeed, another way to prepare benzyl carboxylates could be via oxidation of the corresponding aldehyde. In line with this, inspired from the work by Haraguchi and Fukuzawa, who detailed the palladium-catalyzed formylation of alkenylzinc reagents with aryl thioformates,<sup>[360]</sup> we endeavored to assess phenyl thioformate **187** under our conditions (**Scheme II-31**). Regrettably, despite complete consumption of phenyl thioformate, no product **188** was observed under our experimental conditions. In this respect, additional studies are currently underway in our laboratories.

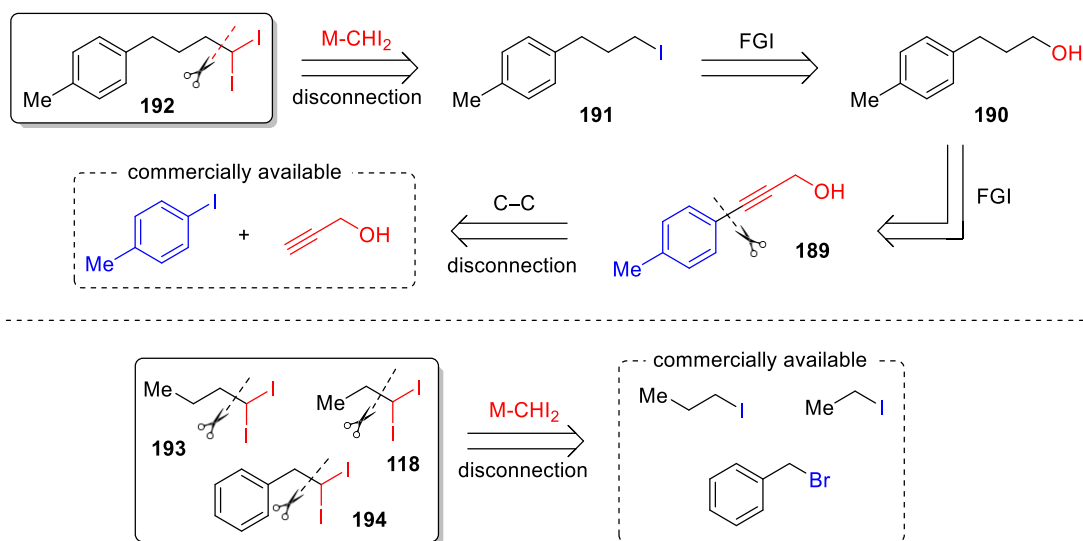




**Scheme II-31.** Unsuccessful attempt for the Pd-catalyzed enantioselective sequential arylation/formylation reaction using 1,1-bis(iodozincio)ethane.

## 1.12. Enantioselective Sequential Arylation/Fukuyama Cross-Coupling Reaction with Other 1,1-Biszincioalkanes

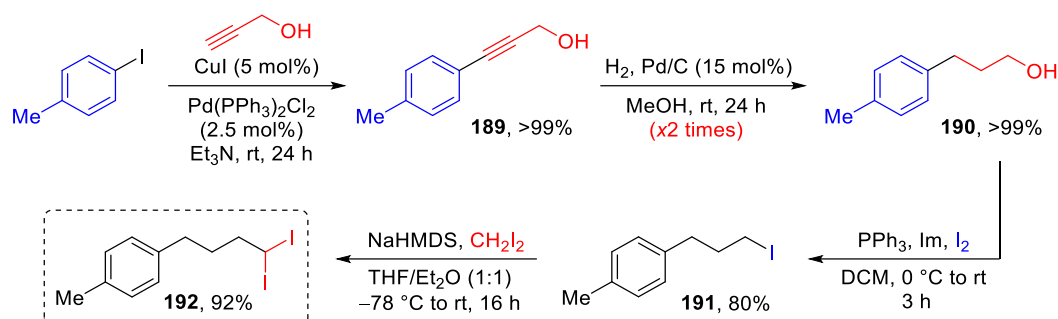
Reaching this stage, we decided to evaluate the potential as linchpins of 1,1-dizincio bimetallics featuring different primary alkyl substituents at the methylene carbon. To achieve this objective, our initial step was to create a new array of *gem*-diiodo compounds. We proceeded to synthesize the following compounds based on the retrosynthetic plan outlined in **Scheme II-32**.



**Scheme II-32.** Retrosynthesis of selected 1,1-diiodo compounds for various 1,1-bis(iodozincio)alkanes.

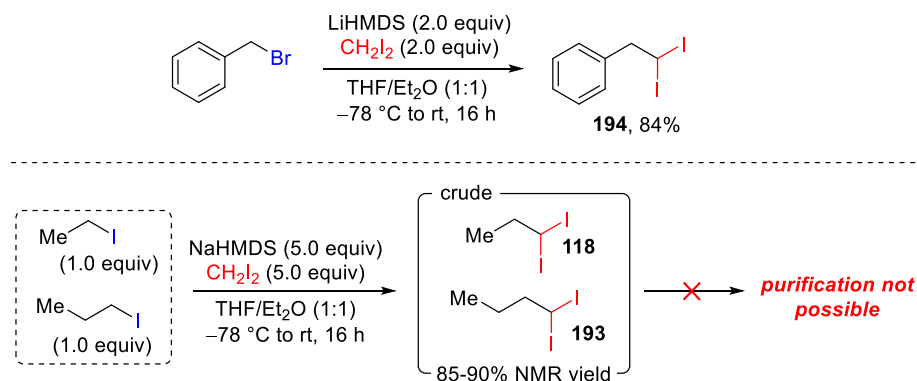
To prepare compound **192**, we initiated the synthesis with a simple Sonogashira reaction involving *p*-iodotoluene and propargyl alcohol (**Scheme II-33**). This step furnished the desired adduct **189** in quantitative yield. Subsequently, we conducted a reduction with hydrogen over Pd/C in methanol at room temperature for 24 hours, resulting in the corresponding alkene. To obtain the targeted alkane **190**, we repeated the same reduction. Following this, we employed an iodination reaction to convert efficiently (80% yield) the alcoholic group into an iodide (**191**).

Finally, we achieved excellent yields of the *gem*-diiodoalkane **189** using a practical procedure described by Charette for the alkylation of NaCHI<sub>2</sub> with alkyl iodides.<sup>[367]</sup>



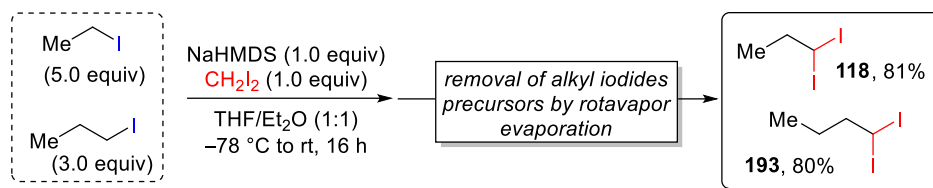
**Scheme II-33.** Preparation of *gem*-diiodo alkane **192**.

A similar alkylation approach using LiCHI<sub>2</sub> and the corresponding alkyl bromide was effectively applied to compound **194** (84% yield), as reported by Charette (**Scheme II-34**).<sup>[367]</sup>



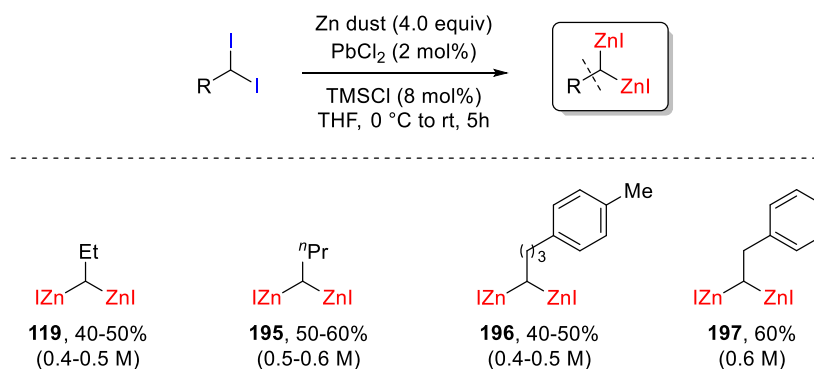
**Scheme II-34.** Application of Charette's alkylation procedure for the preparation of *gem*-diiodo compounds **118**, **193** and **194**.

In contrast, for *gem*-diiodo compounds **118** and **193**, the reaction produced excellent yields (~90-95%). Nevertheless, to attain such high yields, a significant excess (5 equiv) of diiodomethane was necessary. This presented a challenge due to the similar polarity and boiling points of **118** and **193** with the remaining diiodomethane, making the purification process quite arduous, and practically impossible to obtain pure products without diiodomethane contamination. However, by reversing the stoichiometry of the reaction, we still achieved a very satisfactory yield (**Scheme II-35**). This time, exploiting the substantial volatility difference between *gem*-diiodo compounds (boiling point >180°C) and alkyl iodides (69-73°C for 1-iodoethane and 101-102°C for 1-iodopropane), we successfully obtained analytically pure **118** and **193**.



**Scheme II-35.** Successful preparation of *gem*-diiodo compounds **118** and **193** using a modified version of Charette's alkylation procedure with reverse stoichiometry.

With our array of 1,1-diiodo compounds in hand, we synthesized the corresponding 1,1-bis(iodozincio)alkanes (**119**, and **195-197**) in THF solutions (**Scheme II-36**) by treatment with zinc dust in the presence of  $\text{PbCl}_2$  (2 mol%). It is important to highlight that we obtained satisfactory yields without requiring TMEDA, an additive that was previously necessary for achieving moderate yields in the Matsubara's procedure for *gem*-dizincio reagents other than 1,1-bis(iodozincio)ethane.<sup>[200]</sup>



**Scheme II-36.** Chart of 1,1-bis(iodozincio)alkanes prepared.

However, it should be mentioned that *gem*-dizinc reagents **196** and **197** exhibited a distinct deep red coloration (**Figure II-2, left**), unlike the others, which appeared pale in colour, akin to 1,1-bis(iodozincio)ethane (**Figure II-2, right**).



**Figure II-2.** THF solution of *gem*-dizincio **196** (left) and THF solution of 1,1-bis(iodozincio)ethane **117** (right).

Due to the intensity of this coloration, the colorimetric titration with iodine proved to be less precise, as the endpoint was not easily discernible. Consequently, we opted to quench the reaction with iodine in the presence of an internal standard (1,3,5-trimethoxybenzene) and subsequently calculate the NMR yield to determine the concentration of the solution (**Figure II-3, top**). However, it is important to note that the product of the iodolysis corresponded to the starting material for the zinc insertion process to form the *gem*-dizinc. To be sure of the complete consumption of the starting material in the zincation process and that the  $^1\text{H}$  NMR signals used for yield calculations exclusively originated from the titrated *gem*-dizincio **196**, we also conducted hydrolysis of the bimetallic reagent. After the hydrolysis, no  $^1\text{H}$  NMR signals were detected from the *gem*-diiodo compound, confirming that all of the starting material had been consumed (**Figure II-3, bottom**). Consequently, only the set of signals originating from the corresponding hydrocarbon were observed. The identical strategy was carried out for *gem*-dizinc **197**, furnishing the same result.

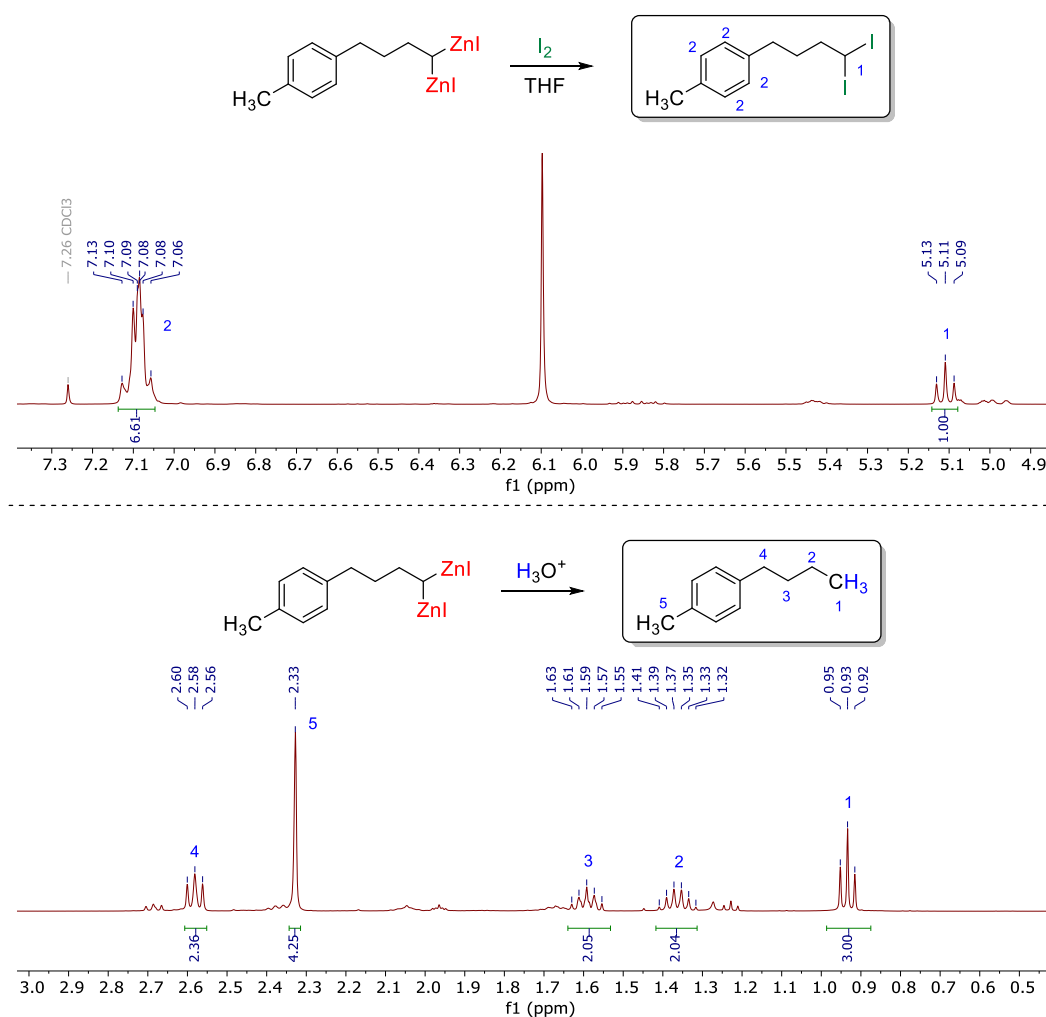
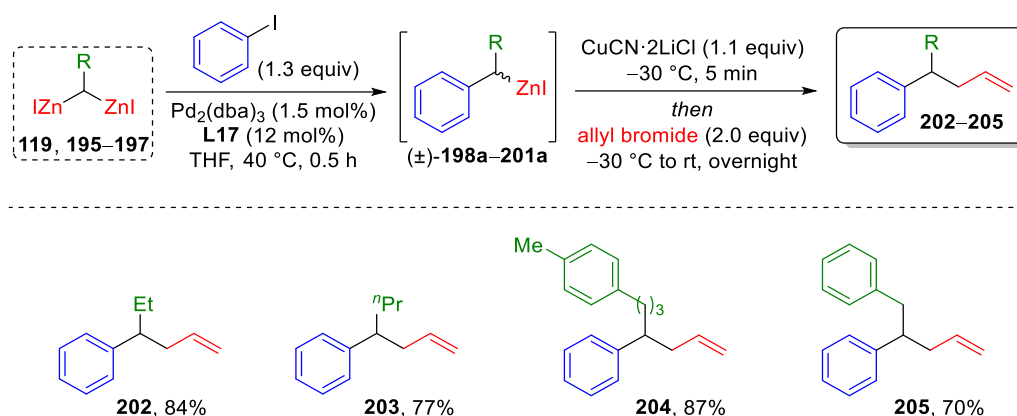


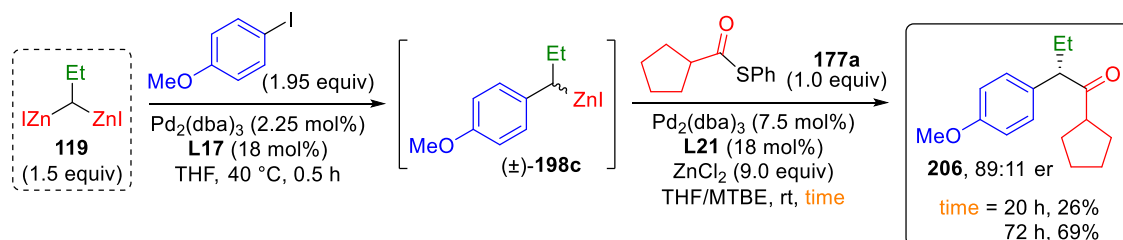
**Figure II-3.**  $^1\text{H}$  NMR spectra of iodolysis (top) and hydrolysis (bottom) of *gem*-dizincio **196**.

We were pleased to discover that the experimental conditions originally designed for the Pd-catalyzed (mono)arylation of 1,1-bis(iodozincio)ethane were not limited to that specific compound but also applied effectively to 1,1-bis(iodozincio)alkanes **119**, and **195–197** (**Scheme II-37**). When these compounds underwent cross-coupling reactions with phenyl iodide, they produced organozinc intermediates ( $\pm$ )-**198a–201a**. These intermediates were subsequently subjected to a copper-mediated allylation reaction, resulting in the synthesis of products **202–205** with impressive yields ranging from 70% to 87% (**Scheme II-37**). These yields provide a reliable estimate, at the lower limit, for the arylation reaction's efficiency.



**Scheme II-37.** Sequential Pd-catalyzed arylation/Cu-mediated allylation of gem-bis(iodozincio)alkanes in one pot.

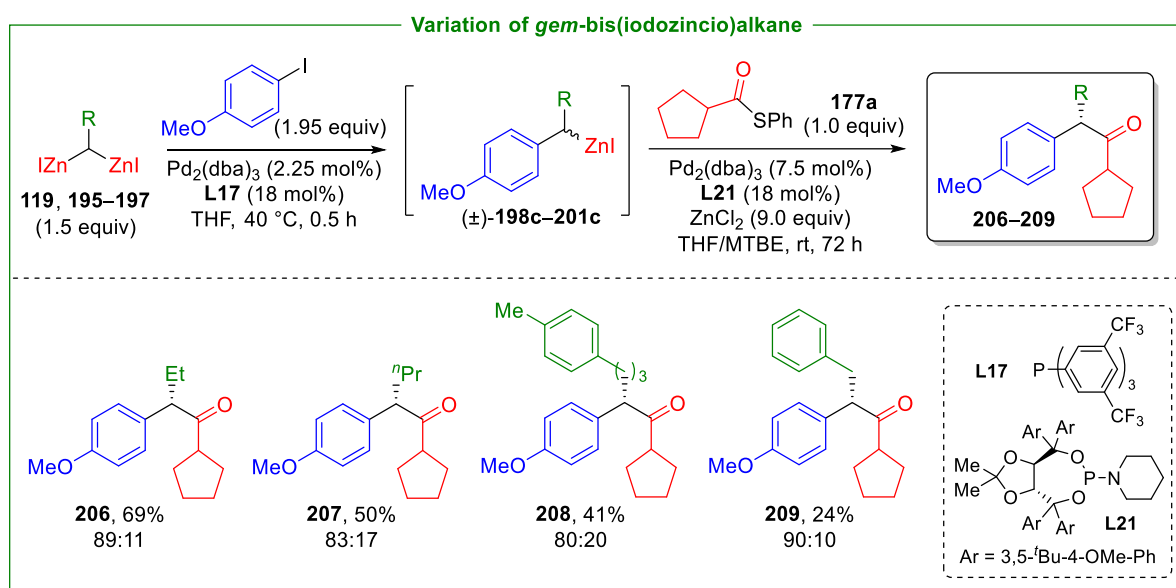
The protocol for enantioselective sequential arylation-acylation reaction was then applied to the Et-substituted linchpin **119**. In this procedure, we employed 4-methoxyiodobenzene and thioester **177a** as the electrophilic reagents (**Scheme II-38**). The desired product **206** was successfully obtained in high 89:11 er, but only a low 26% yield after 20 h of reaction time for the acylation step. Despite this initial setback, we were able to significantly enhance the yield, achieving a more satisfactory level of 69%, by extending the reaction time of the Fukuyama step to 72 h (**Scheme II-38**). This adjustment allowed us to maximize the efficiency of the acylation process, resulting in a higher overall yield of **206**.



**Scheme II-38.** Enantioselective sequential Pd-catalyzed arylation-Fukuyama cross-coupling reaction of **119**.

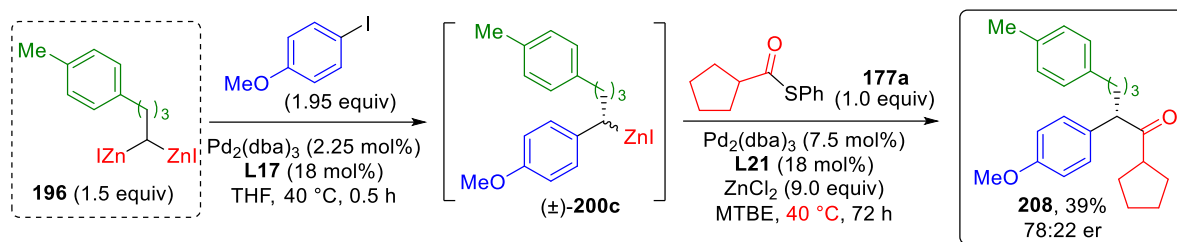
The same reaction conditions were applied to 1,1-bis(iodozincio)alkanes **195–196**, which feature longer alkyl chains. This led to the formation of coupling products **207–208**, which were obtained with respectable enantiomeric ratios and yields, in spite of a gradual erosion with increasing length of the alkyl substituents. In a contrast, when we performed the enantioselective sequential reaction with *gem*-bis(iodozincio)alkane **197**, we achieved the desired product **209** with a highly favorable enantiomeric ratio of 90:10 (**Scheme II-39**). However, the yield was limited to 24%. This outcome may be attributed to the presence of a proximal aromatic ring, which, despite the shorter alkyl chain, introduced significant steric hindrance which could affect the efficiency of the acylation step.

It is worth emphasizing that these findings hold great importance as they mark the initial instances of enantioselective Fukuyama cross-coupling using organozinc reagents other than (1-arylethyl)zinc derivatives.



**Scheme II-39.** Enantioselective sequential Pd-catalyzed arylation-Fukuyama cross-coupling reaction of 1,1-bis(iodozincio)alkanes **119, 195–197**.

An attempt was made to carry out the second step of the tandem reaction at 40 °C for 72 h, using *gem*-dizinc **196**, with the aim of potentially improving the efficiency of the Fukuyama cross-coupling while preserving enantiomeric control, or at most, causing a slight and tolerable decrease (**Scheme II-40**). However, after purification, we recovered only 39% of the product, accompanied by a marginal decrease in enantiomeric ratio to 78:22. This outcome underscores that elevating the reaction temperature does not enhance the acylation step but seems also not be detrimental for the enantioselectivity.

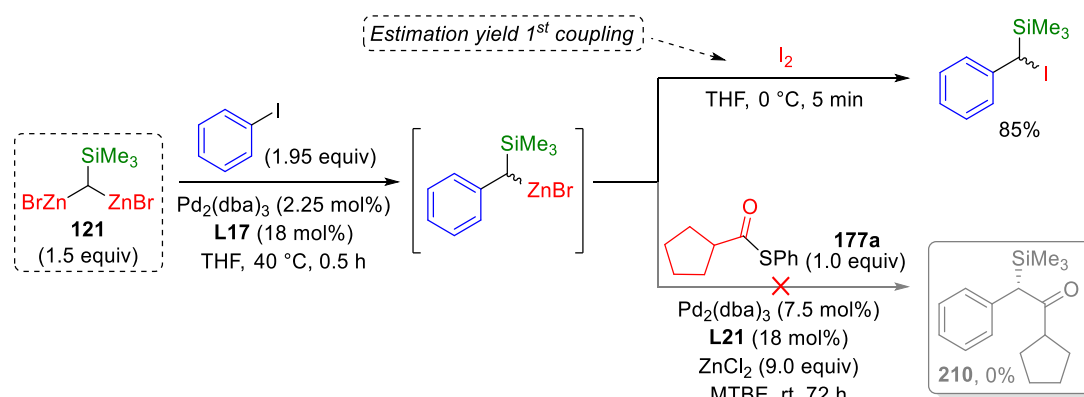


**Scheme II-40.** Effect of higher temperature in the Fukuyama cross-coupling step with *gem*-dizincio **196**.

### 1.12.1. Enantioselective Sequential Arylation/Fukuyama Cross-Coupling Reaction with Silyl-Substituted *Gem*-Dizincio Reagents

With our enantioselective sequential arylation/Fukuyama coupling procedure, we aimed to broaden the versatility of our protocol. In this pursuit, we sought to explore the use of hetero-substituted *gem*-dizinc reagents to have the possibility of another potential functionalization. Specifically, we selected a silyl-substituted *gem*-dizincio, in the specific trimethylsilylbis-(bromozincio)methane **121**, whose preparation is detailed in “Part II: Chapter 2” for dedicated study. The mono(arylation) process was executed, followed by a quench with iodine to approximate the yield of the initial step (**Scheme II-41**). To our satisfaction, an 85% yield was obtained. Encouraged by this outcome, we proceeded to attempt the entire enantioselective sequential arylation/acylation process in a single pot. Unfortunately, no product **210** was observed, together with no conversion of the thioester, leading to its complete recovery.

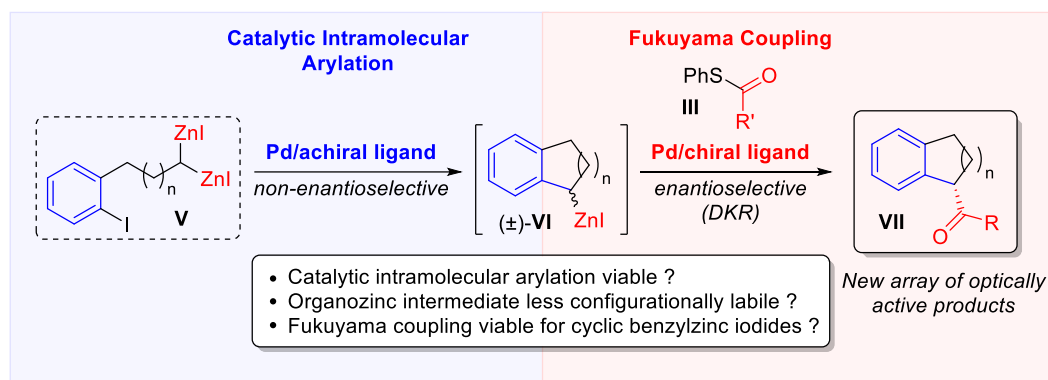
Although we had hoped for a different outcome, this result aligns with the inefficiency of the acylation step observed previously due to increased steric hindrance of the substituents on the secondary benzylzinc intermediate.



**Scheme II-41.** Unsuccessful attempt for the Pd-catalyzed enantioselective sequential arylation/Fukuyama cross-coupling reaction using trimethylsilylbis(bromozincio)methane.

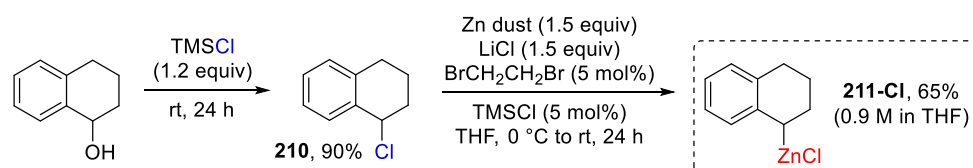
### 1.13. Enantioselective Sequential Intramolecular Arylation–Fukuyama Cross-Coupling Reaction

Having demonstrated our ability to synthesize *gem*-dizincio compounds with various alkyl substituents, we decided to embark on the synthesis of a bimetallic compound, akin to **V**, but featuring an iodide substituent in the *ortho*-positions of the aromatic ring (**Scheme II-42**). This modification would potentially enable an intramolecular arylation. In this context, the arylation/Fukuyama sequence, when performed intramolecularly, could evolve into a highly potent protocol for diversifying compound development. Indeed, this tandem process holds the promise of facilitating the straightforward construction of optically active complex cyclic structures **VII**.



**Scheme II-42.** Enantioselective sequential Pd-catalyzed intramolecular Arylation/Fukuyama cross-coupling reaction.

Prior to initiating the synthesis of the selected *gem*-dizinc reagent for the intramolecular arylation, we opted to explore if the enantioselective Fukuyama cross-coupling reaction was viable with cyclic benzylzinc halides. The objective was to assess whether, with our optimized conditions for the acylation step, we could achieve both high yields and precise enantiocontrol. To commence this investigation, we initiated the synthesis of our organomonozinc reagent, starting with the readily available 1,2,3,4-tetrahydronaphthalen-1-ol (**Scheme II-43**). After conducting halogenation with trimethylsilyl chloride at room temperature for 24 hours in neat conditions, we obtained the corresponding chloride **211-Cl** compound in 90% yield.

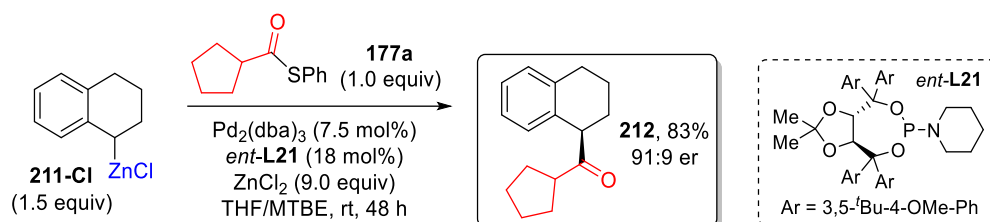


**Scheme II-43.** Synthesis of the organozinc reagent **211**.



Subsequently, we carried out the zinc insertion step, resulting in the successful generation of a THF solution containing the organometallic reagent with a high concentration (determined *via* titration with I<sub>2</sub>).<sup>[347]</sup>

With our organozinc compound readily available, we proceeded to execute the enantioconvergent Fukuyama cross-coupling reaction, employing our optimized conditions (**Scheme II-44**). It should be noted that this experiment was conducted with *ent*-**L21**, as **L21** was over.

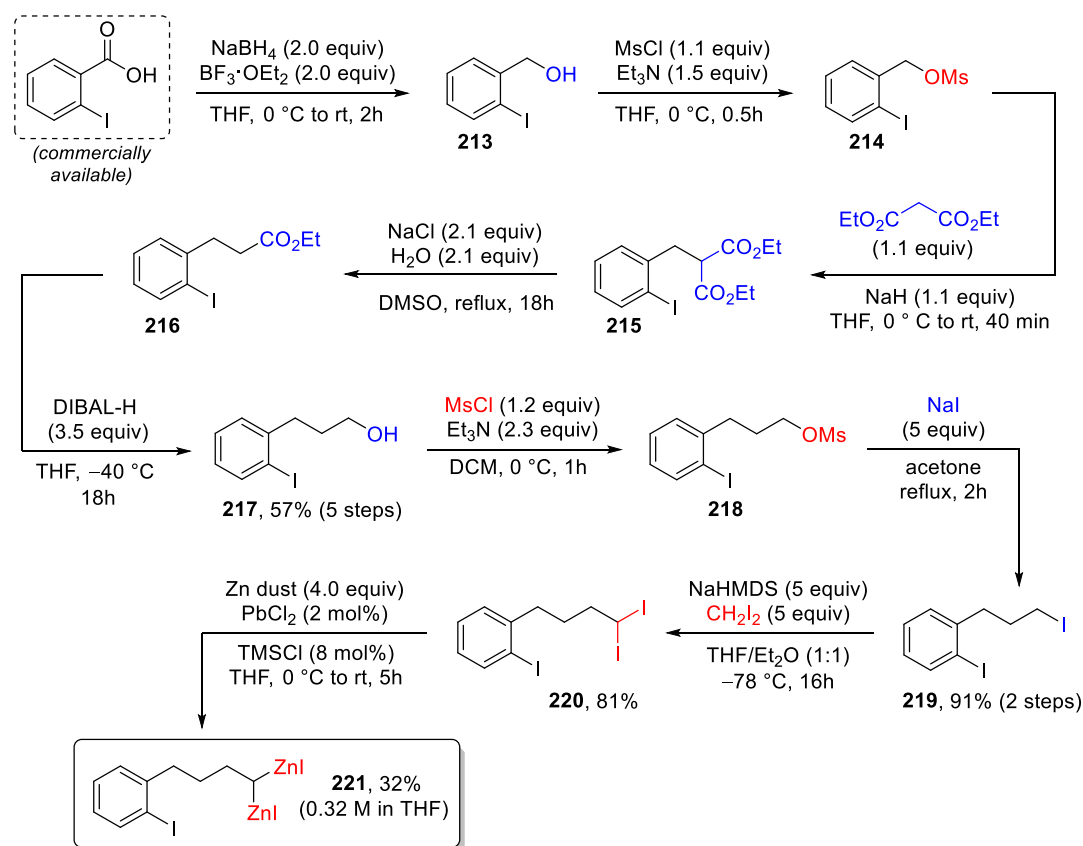


**Scheme II-44.** Enantioconvergent Pd-catalyzed Fukuyama cross-coupling reaction with cyclic organozinc chloride **211**.

To our satisfaction, we obtained the intended product **212** with high yield (83%) and enantiomeric ratio (91:9). This outcome highlights the feasibility of enantioselective acylation with cyclic secondary benzylzinc halides. Consequently, we planned and performed to synthesize *gem*-dizinc **221** (**Scheme II-45**), which serves as the precursor for the organomonozinc intermediate (**211-Cl**) *via* intramolecular arylation.

We initiated the synthesis by starting with the commercially available 2-iodobenzoic acid. Its carboxylic group was reduced to alcohol using NaBH<sub>4</sub> in combination with BF<sub>3</sub>·OEt<sub>2</sub> in THF. The resulting crude alcohol **213** was then treated with methanesulfonyl chloride in the presence of Et<sub>3</sub>N in THF to obtain the corresponding mesylate **214**. This mesylate was used in an S<sub>N</sub>2 reaction with deprotonated diethyl malonate to produce the desired compound **215**. Subsequently, a dealkoxycarbonylation was carried out by refluxing **215** in DMSO with the addition of water and NaCl, resulting in the formation of **216**. The crude ester was then reduced to alcohol using DIBAL-H in THF at a low temperature overnight. Afterward, purification through column chromatography provided the highly pure alcohol **217** with a 57% yield over the course of 5 steps. Then, the alcohol moiety was transformed into a mesylate (**218**) using methanesulfonyl chloride, followed by a nucleophilic substitution with sodium iodide to obtain the primary alkyl iodide **219**. Subsequently, we achieved a high yield of the *gem*-diiodoalkane **220** using the procedure (already mentioned) described by Charette for the alkylation of NaCHI<sub>2</sub> with alkyl iodides.<sup>[367]</sup> Therefore, after a series of eight synthetic steps, we obtained a significant quantity of **220** with an overall yield of 42%. Following this, we proceeded to synthesize the corresponding 1,1-bis(iodozincio)alkane **221** in a THF solution, using the same method involving zinc dust and PbCl<sub>2</sub> (2 mol%) that we had previously used to prepare other *gem*-dizincio reagents.

While the title of the bimetallic reagent did not yield exceptional results (0.32 M in THF), we successfully achieved zinc insertion exclusively at the geminal iodides and not at the aromatic one. This success serves as evidence that the preparation of this specific class of functionalized *gem*-dizinc compounds is indeed feasible.



**Scheme II-46.** Synthetic sequence for the preparation of *gem*-dizincio **221**.

However, the preparation of this specific bimetallic species proved to be exceptionally challenging, probably due to the highly unstable carbenoid species. This was evident from the  $^1\text{H}$  NMR analysis, which showed the formation of an equimolar amount of the corresponding alkene *via*  $\beta$ -hydride elimination (**Figure II-4**). Despite our best efforts, we were unable to reduce the occurrence of the  $\beta$ -hydride elimination product, even when we increased the catalytic amount of  $\text{PbCl}_2$  4 mol% (twice the typical amount used in our zincation process) and/or decreased the rate of addition of the *gem*-diiodo compound. This by-product might pose a challenge in the context of the *intramolecular* arylation step, as it consists of an aromatic iodide that could potentially lead to unintended *intermolecular* arylation.

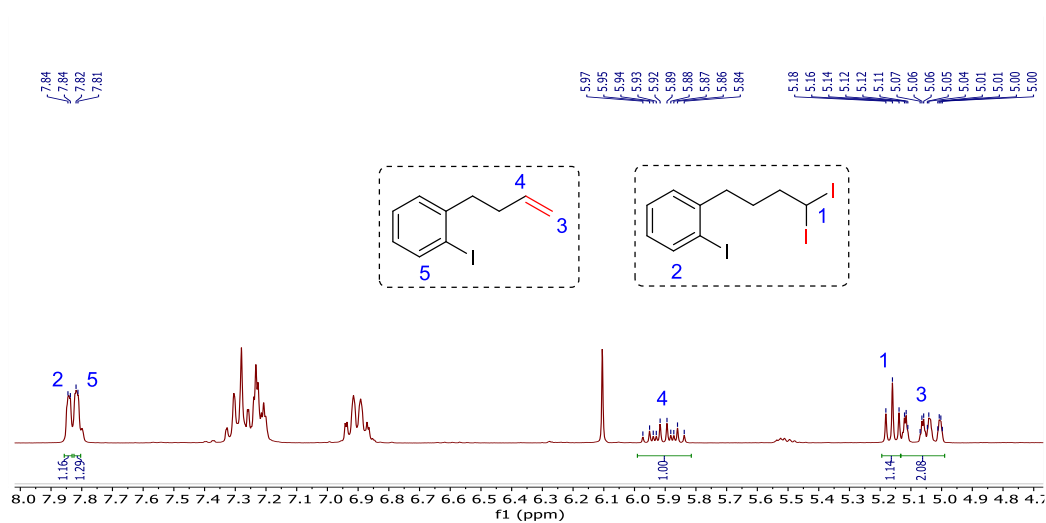
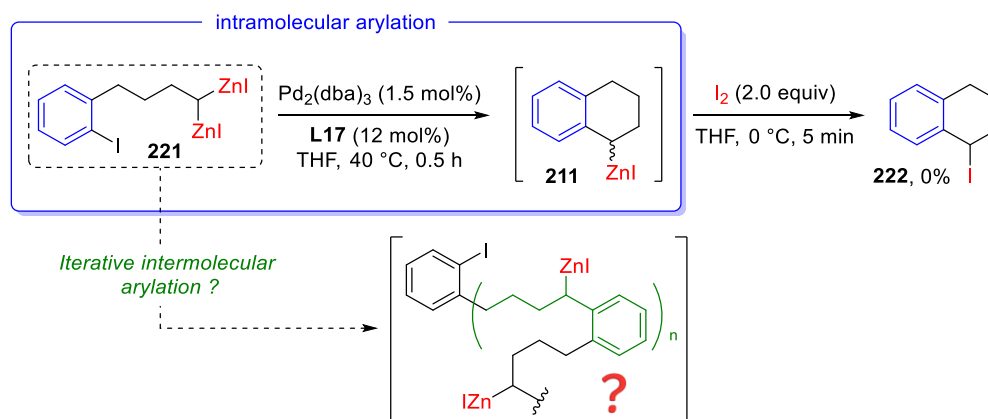


**Figure II-4.**  $^1\text{H}$  NMR spectra of the titration with iodine of gem-dizincio **221**.

With **221** in hand, we proceeded with the Pd-catalyzed intramolecular reaction using  $\text{Pd}_2(\text{dba})_3$  (1.5 mol%) and **L17** (12 mol%) in THF at 40 °C for 0.5 hour (**Scheme II-47**). To determine whether the intramolecular adduct had formed, we quenched the potential organomonozinc intermediate **211** with  $\text{I}_2$ .



**Scheme II-47.** Pd-catalyzed intramolecular arylation reaction with gem-dizinc **221**.

Regrettably, no product was obtained. The  $^1\text{H}$  NMR analysis indicated the presence of a high and disordered signals pattern, resembling some form of oligomer or polymer. Consequently, we conducted a TLC-MS (thin layer chromatography – mass spectrometer) analysis on the prominent spot visible on the TLC plate (**Figure II-5**). This analysis supported our hypothesis as it revealed an iterative loss of ~72 atomic mass units (a.m.u.), a characteristic pattern for oligomers or polymers that shed their monomeric units.

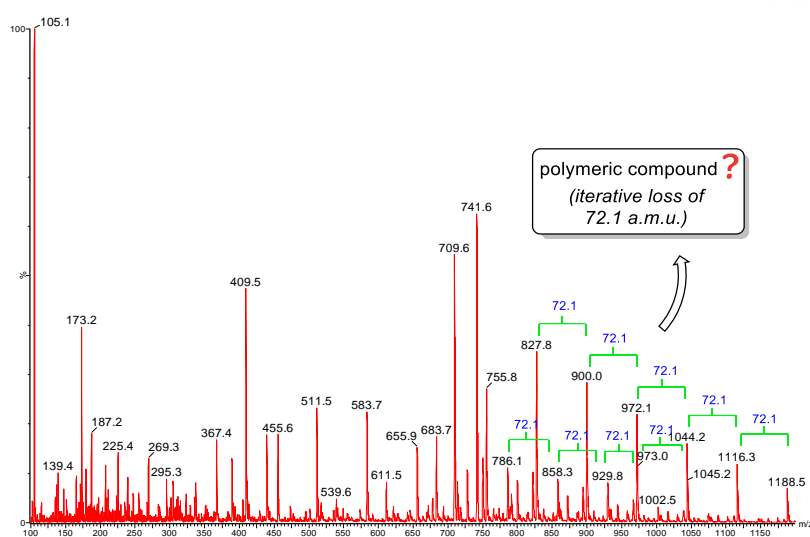
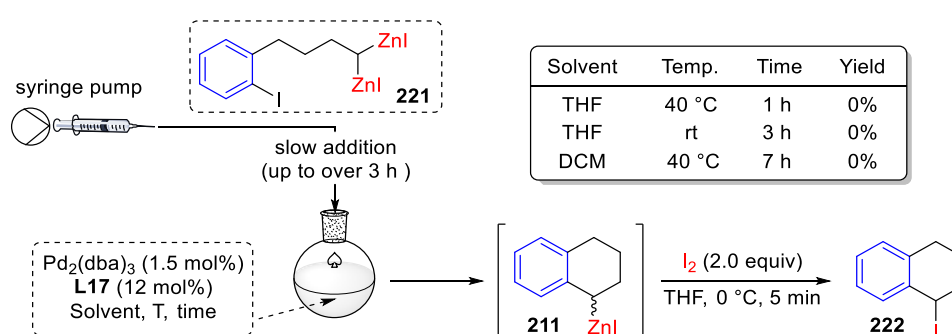


Figure II-5. TLC-MS spectra of the intramolecular arylation crude.

This outcome could be expected, as *gem*-dizincio compound **221** has the potential to engage in intermolecular arylation reactions with the aromatic iodide from another *gem*-dizincio molecule, and this process can occur multiple times. Consequently, we attempted to introduce the *gem*-dizinc into the THF solution of  $\text{Pd}_2(\text{dba})_3/\text{L17}$  very slowly, aiming to create a highly diluted mixture (**Scheme II-48**), with the intention of favouring the intramolecular reaction exclusively. However, despite the slow addition rate and the temperature, the final result remained identical to the previous attempt. This indicates that under these reaction conditions, **221** displays excessive reactivity, and achieving selective control over the intramolecular arylation is challenging.



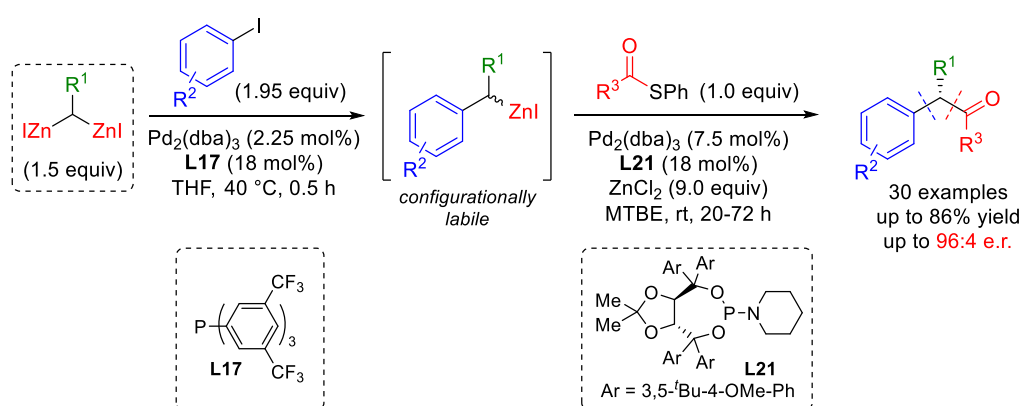
Scheme II-48. Diluted conditions for the Pd-catalyzed intramolecular arylation.

As a result, we decided to switch to dichloromethane as the solvent, as the intermolecular (mono)arylation with 1,1-bis(iodozincio)ethane was considerably slower (taking 4 h at 40 °C for complete conversion). Unfortunately, even with this solvent there was no substantial change in the final outcome, and no product was observed. In this particular case, it appears that achieving intramolecular arylation is not feasible under our current reaction conditions and with this substrate.

However, we are currently conducting additional experiments in our laboratories to try to address this issue.

## 1.14. Partial Conclusion

In conclusion, we have developed a one-pot sequential enantioselective double cross-coupling reaction of 1,1-bis(iodozincio)alkane reagents entailing arylation and acylation with two distinct Pd-based catalytic systems (**Scheme II-49**).<sup>[368]</sup> Mechanistically, the approach relies on a first step involving the (non-enantioselective) desymmetrization of an achiral geminated C(sp<sup>3</sup>)-dizinc reagent that delivers a stereolabile monometallic intermediate that undergoes efficient DKR during the subsequent second step. Our report represents the first example of implementation of such a strategy for asymmetric synthesis.



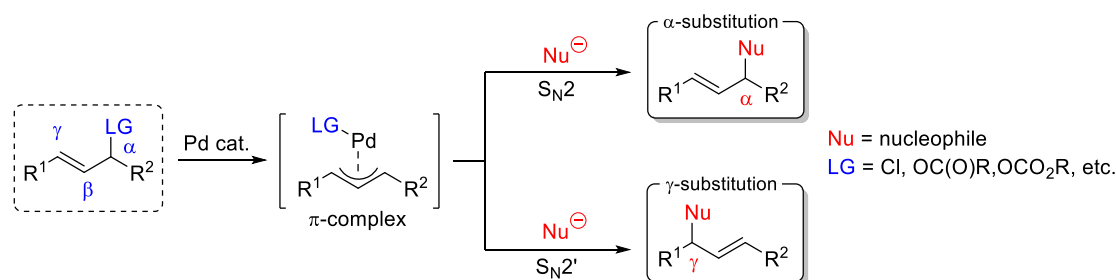
**Scheme II-49.** Enantioselective sequential catalytic arylation-Fukuyama cross-coupling of 1,1-bis(iodozincio)alkanes.

Synthetically, we disclosed a modular access to important enantioenriched 1-arylethyl (and 1-arylalkyl to a lesser extent) ketones, including products with electron-rich aryl units which had not been accessed previously through direct Fukuyama cross-coupling reactions. As part of this work, we also establish on the one hand that Matsubara's Pd-catalyzed (mono)arylation of *gem*-bisorganozinc reagents tolerates the presence of H-atoms  $\beta$  to the metal and can thus be used conveniently with 1,1-bis(iodozincio)alkanes other than 1,1-bis(iodozincio)methane, and on the other hand that asymmetric Fukuyama cross-coupling reactions can be extended beyond (1-arylethyl) organozincs.

## 2. Enantioselective Sequential Double Allylation of $\alpha$ -Silyl-Substituted *Gem*-Dizinc Reagents

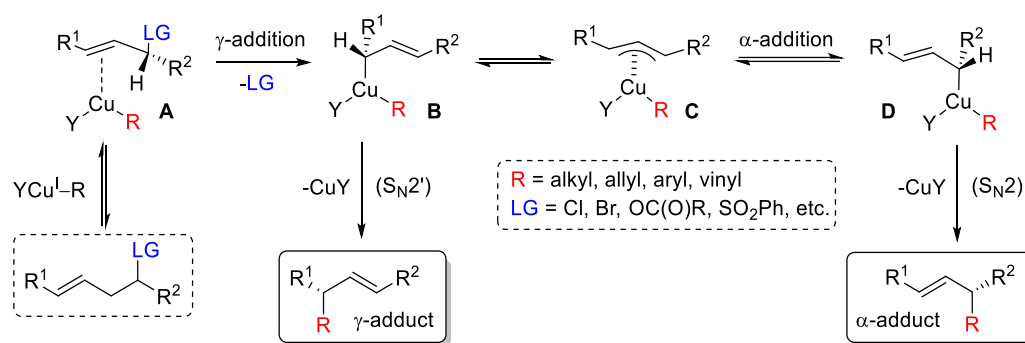
### 2.1. Asymmetric Allylation: Introduction

In the realm of organic chemistry, asymmetric allylation is prominently recognized as one of the most powerful transformations currently accessible for achieving enantioselective C–C bond formation.<sup>[369]</sup> This process has garnered extensive attention, and various metals, including Pd, Ni, Ir, Rh, and Ru, have been explored for its application.<sup>[370–373]</sup> Palladium, in particular, has been commonly employed, especially in the Tsuji–Trost reaction, using soft stabilized nucleophiles with notable success.<sup>[370]</sup> However, a significant hurdle in this domain has been the observed lack of regioselectivity in non-symmetrical allylic substrates, limiting the versatility of this approach. In fact, central to the intricacies of allylic substitution is the imperative aspect of regulating regiochemistry. This pivotal process hinges on the displacement of an allylic leaving group *via* two distinct pathways. The first pathway entails a direct attack on the carbon bearing the leaving group at the  $\alpha$ -position, akin to an  $S_N2$  reaction. The second one, known as  $\gamma$ -substitution or  $S_N2'$ , involves the ejection of the leaving group while simultaneously involving an allylic shift of the double bond (**Scheme II-50**). Consequently, a substrate with distinct substituents at the  $\alpha$ - and  $\gamma$ -positions of the allylic moiety can yield two different products, depending on the chosen pathway.



**Scheme II-50.** Proposed mechanism for Pd-catalyzed allylic substitution.

On the other hand, utilization of hard and non-stabilized nucleophiles, exemplified by organometallic species like organolithium,<sup>[374,375]</sup> Grignard,<sup>[376]</sup> and organozinc reagents,<sup>[377–379]</sup> has emerged as a highly advantageous alternative within this context, particularly through the application of copper-catalysis. In this commonly accepted mechanism, the regiochemistry is established at different levels of the reaction, which proceeds via a transient Cu(III) intermediate (**Scheme II-51**).<sup>[380]</sup>



**Scheme II-51.** Proposed mechanism for the Cu-catalyzed allylic substitution.

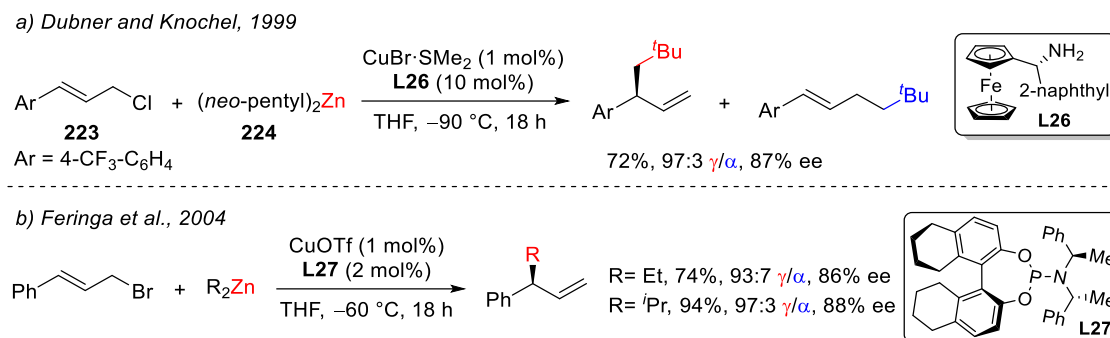
The starting formation of the  $\pi$ -Cu(I) complex **A** leads to the *anti* and regioselective oxidative addition in  $\gamma$ -position respect to the leaving group (LG), to furnish the  $\sigma$ -allyl Cu(III) complex **B**. The regiochemical outcome is contingent on the rate of the reductive elimination of **B** to give the  $\gamma$ -adduct and/or equilibration into the  $\pi$ -allyl Cu(III) complex **C**, later leading to the  $\sigma$ -complex **D**. Electron-withdrawing ligands **Y**, such as CN, Cl, etc., promote a fast reductive elimination of **B**. Conversely, when **Y** is alkyl and thus forms a more electron-rich Cu(III) species the equilibration becomes competitive, preferring the least sterically hindered carbon. It is important to note that Cu(III) complexes have been analytically detected,<sup>[381-384]</sup> and even isolated,<sup>[385]</sup> proving strong evidences for this mechanism. Moreover, the mechanism and the regioselectivity of the copper-catalyzed allylation has also been confirmed through DFT calculations by Nakamura.<sup>[386]</sup>

It is crucial to emphasize that the regioisomeric result of this transformation is intricately influenced by a multitude of factors. These encompass the inherent structural and electronic properties of the substrate, the characteristics of the leaving group, the choice of solvent, the temperature at which the reaction takes place, and the nature of the organometallic reagent employed, among various other variables.<sup>[378,379]</sup> Nevertheless, through meticulous adjustment and optimization of these conditions, it becomes feasible to attain a high degree of precision in regulating regioselectivity according to the specific requirements of the desired outcome.

## 2.2. Asymmetric Allylation of Organozinc Reagents

In the realm of enantioselective allylation of organozinc reagents, numerous instances have been documented in the literature with copper catalysis. A significant milestone was achieved by Dubner and Knochel in 1999 when they introduced a pioneering copper(I)-catalyzed allylic substitution reaction involving allylic chlorides **223** and diorganozinc reagents, employing a ferrocenyl-based chiral amine **L26** (**Scheme II-52a**).<sup>[387]</sup> This method yielded remarkable ee levels (up to 87%) and demonstrated excellent  $\gamma$ -selectivities, although it was limited to highly sterically hindered

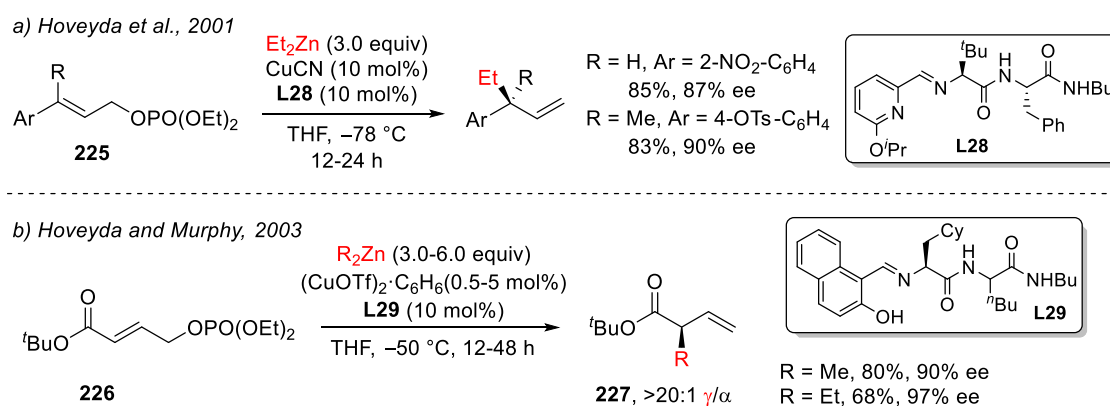
dineopentylzinc reagents **224** and required very low temperatures ( $-90\text{ }^{\circ}\text{C}$ ). Subsequently, improved conditions were developed for the same reaction by making modifications to the chiral ligand and implementing a simultaneous addition of substrate and organozinc reagent, leading to an impressive 98% ee at  $-30\text{ }^{\circ}\text{C}$  in 3 h, and expanding the scope.<sup>[388]</sup>



**Scheme II-52.** Copper-catalyzed enantioselective allylic  $\gamma$ -substitution of cinnamyl halides with dialkylzinc reagents.

Nonetheless, achieving highly copper-catalyzed enantioselective allylic alkylation using linear dialkylzinc compounds posed a significant obstacle. In this context, Feringa's works in the early 2000s unveiled their discoveries when employing chiral phosphoramidite ligands (**Scheme II-52b**).<sup>[389,390]</sup> Following a comprehensive study of the intrinsic impacts of leaving groups, temperature variations, ligands, and solvents, the optimal conditions outlined in **Scheme II-52b** promoted the allylic substitution of cinnamyl bromide with dialkylzinc compounds, up to 88% ee.<sup>[390]</sup>

In 2001, Hoveyda documented the use of peptide-based ligand **L28** to promote the copper-catalyzed enantioselective  $\gamma$ -substitution reaction of cinnamyl phosphates **225** with diethylzinc.<sup>[391]</sup> The transformation demonstrated high ee up to 90% (**Scheme II-53a**). Notably, this reaction marked the first instance of highly enantioselective substitution reaction involving  $\gamma$ -disubstituted allylic substrates, resulting in the formation of quaternary stereocenters. Furthermore, this represented the initial application of allylic phosphates in an asymmetric context.



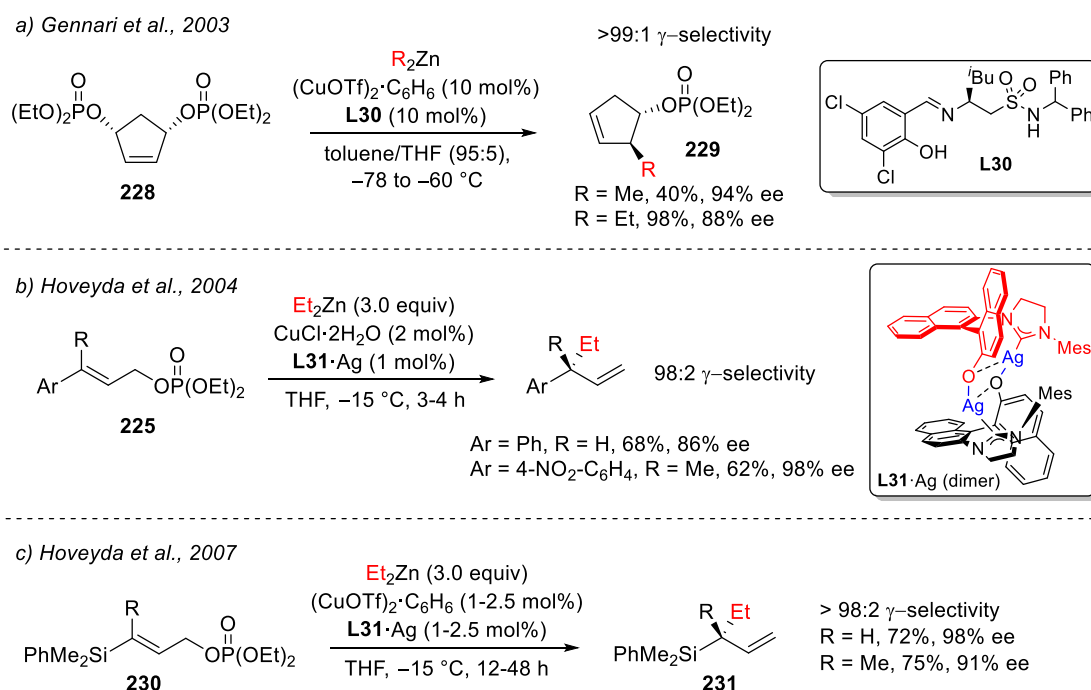


**Scheme II-53.** Peptide-based ligands promotion of Cu-catalyzed enantioselective  $S_N2'$ -substitution reaction with dialkylzinc reagents of: a) cinnamyl phosphates, b)  $\alpha$ -unsaturated esters bearing a phosphate group at the  $\gamma$ -position.

Through minor structural modifications of the peptide-based ligand, and the use of the copper salt  $(\text{CuOTf})_2 \cdot \text{C}_6\text{H}_6$ , Hoveyda and Murphy successfully extended the scope to  $\alpha$ -unsaturated esters **226** featuring a phosphate group at the  $\gamma$ -position (**Scheme II-53b**).<sup>[392]</sup> This expansion resulted in the production of **227** with excellent ee values up to 97%.

In 2003, Gennari introduced an innovative allylation reaction characterized by high levels of regio-, diastereo- and enantioselectivity.<sup>[393]</sup> This protocol involved the desymmetrization of *meso* cyclic allylic bisdiethylphosphates **228** using dialkylzinc reagents (**Scheme II-54a**). The catalytic allylic substitution was facilitated by a copper(I) complex formed with the chiral Schiff base ligand **L30**, resulting in the formation of the  $S_N2'$  product **229** through an *anti*-stereoselective mechanism. In the same year, Gennari and Feringa, published further advancements in this area. They utilized chiral phosphoramidite ligands, which induced outstanding enantioselectivities for the addition of diethylzinc to the *meso* bisdiethylphosphates derivatives of cyclohexene and cycloheptene (respectively 94%, and 98% ee).<sup>[394]</sup>

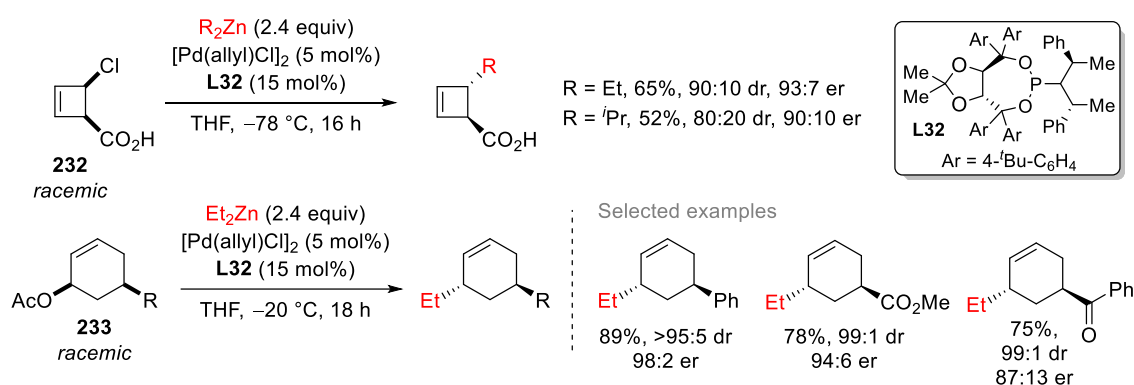
Hoveyda revealed that NHC ligands can serve as highly efficient chiral promoters in the copper-catalyzed allylation process (**Scheme II-54b**). This innovative catalyst system exhibited remarkable effectiveness, enabling the achievement of highly enantioselective substitutions on cinnamyl phosphates **225** with 2 mol% of chiral NHC catalyst loading.<sup>[395]</sup>



**Scheme II-54.** a) Desymmetrization of *meso* cyclic allylic bisdiethylphosphates using dialkylzinc reagents; b) NHC-catalyzed enantioselective allylation reaction of diethylzinc with allyl phosphates; c) NHC-catalyzed enantioselective allylic substitution reaction of vinyl silanes.

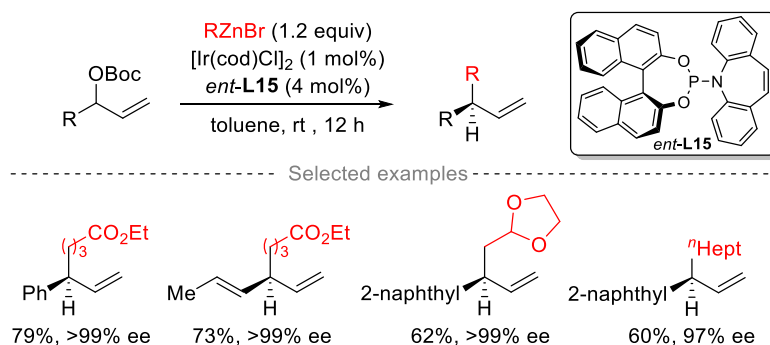
To enhance both the efficiency and selectivity of this procedure, a dinuclear silver(I) complex of the NHC ligand **L31** was synthesized. During the reaction, this silver-based carbene complex underwent a facile transmetalation with copper, resulting in the formation of the copper complex, which displayed exceptional enantioselectivity, with quaternary stereocenter formation reaching up to 98% ee. In 2007, Hoveyda also presented an innovative allylation reaction involving vinylsilanes **230** (Scheme II-54c).<sup>[396]</sup> By adding Et<sub>2</sub>Zn to these functionalized olefins, optically active allylic silanes **231** were obtained with high ee, reaching up to 98%.

While the majority of documented Pd-catalyzed allylation reactions have primarily focused on stabilized carbon nucleophiles, there has been few instances involving organozinc reagents that has emerged.<sup>[397]</sup> In this scenario, Maulide documented an interesting allylation through the adequate choice of the TADDOL-based phosphoramidite **L32** which enabled the achievement of highly diastereoselective and enantioselective allylic substitution of racemic cyclic compounds such as **232** and **233** (Scheme II-55).<sup>[398]</sup>



**Scheme II-55.** Pd-catalyzed asymmetric allylic substitution of cyclic compounds with dialkylzinc reagents.

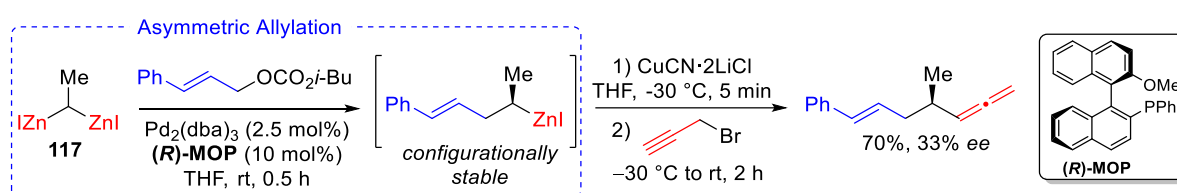
Within the domain of TM-catalyzed allylation reactions, a notable example emerges regarding iridium-catalyzed allylic substitution with organozinc reagents. This approach has been pioneered by Carreira, who has introduced an iridium-*ent*-**L15** complex as a catalyst (Scheme II-56).<sup>[399]</sup> The procedure enabled the allylic substitution of branched racemic carbonates using a broad spectrum of functionalized primary and secondary alkylzinc bromides, yielding remarkable regio- and enantioselectivities in the formation of the S<sub>N</sub>2-product.



**Scheme II-56.** Ir-catalyzed enantioselective allylic substitution of branched carbonates with functionalized organozinc halides.

## 2.3. Enantioselective Allylation of *Gem*-Dizinc Reagents

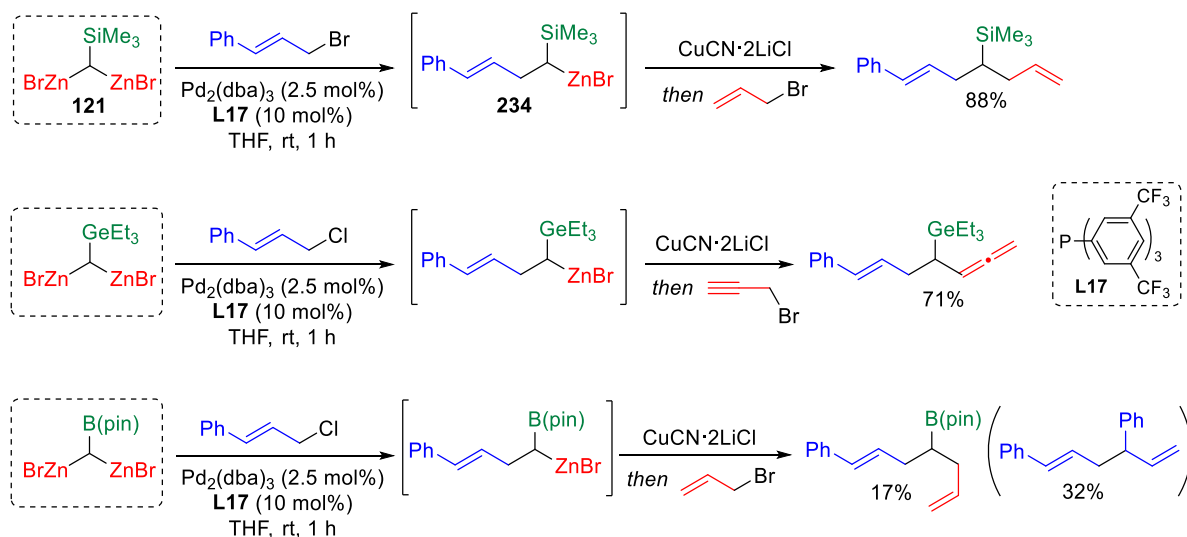
Despite numerous examples of allylation involving *mono*-organozinc compounds, there has been only one reported instance within the realm of *gem*-dizinc reagents. In this context, Matsubara embarked on the quest to synthesize a chiral organomonozinc compound through a desymmetrization strategy of a prochiral *gem*-dizinc compound.<sup>[289]</sup> Their approach involved a Pd-catalyzed enantioselective allylation reaction of cinnamyl electrophiles with 1,1-bis(iodozincio)ethane (**117**), resulting in a configurationally stable mono-organozinc intermediate. This intermediate was subsequently employed in a stereospecific copper(I)-mediated allenylation reaction with propargyl bromide (**Scheme II-57**). The best result was obtained by employing isobutyl cinnamate and the chiral monophosphine ligand (**R**)-MOP. However, the observed level of asymmetric induction in this endeavor reached only a modest 33% ee.<sup>[289]</sup>



**Scheme II-57.** Pd-catalyzed enantioselective allylation of 1,1-bis(iodozincio)ethane.

In addition to this, there have been other instances of allylic alkylation using hetero-substituted *gem*-dizinc reagents; however these reactions were performed only in a racemic fashion. In these particular cases, *gem*-dizinc compounds containing silyl or germyl substituents underwent Pd-catalyzed allylic substitution with cinnamyl halides, (**Scheme II-58**).<sup>[201,203]</sup> The resulting organomonozinc intermediates were then subjected to a subsequent copper-mediated allylation or allenylation with respectively allyl and propargyl bromides. Interestingly, when boryl-substituted *gem*-dizinc compounds were employed in conjunction with cinnamyl chloride, the reaction yielded only 17% of the desired adduct and was accompanied by the formation of the diene through a

homocoupling reaction.<sup>[202]</sup> This diene was believed to be formed as a result of the generation of allyl zinc from allyl palladium species and the *gem*-dizinc reagent.<sup>[400]</sup>

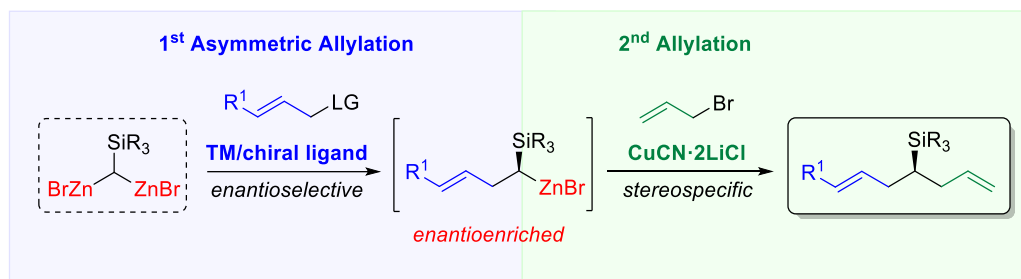


**Scheme II-58.** Pd-catalyzed racemic allylation of hetero-substituted *gem*-dizinc reagents, and subsequent copper-mediated cross-coupling with allyl and propargyl bromides.

## 2.4. Objectives and Purpose of the Project

As we have previously observed, the realm of *gem*-dizinc reagents has seen limited instances of allylation, with the solitary example involving the use of 1,1-bis(iodozincio)ethane. However, Matsubara's works has shed light on racemic allylic substitution with silyl- and germyl-substituted *gem*-dizinc compounds. These hetero-substituted *gem*-dizincio reagents can be viewed as *gem*-trimetallic compounds, presenting an intriguing avenue for three sequential cross-coupling for achieving highly functionalized compounds in a straightforward manner. Motivated by Matsubara's preliminary results, particularly those involving bis(bromozincio)trimethylsilylmethane **121**, we made a deliberate choice to concentrate our efforts on this compound. Our decision considered several factors. Firstly, germane-based compounds are not only scarce but also expensive, and moreover, the field of germanium chemistry remains relatively uncharted and underexplored.<sup>[401]</sup> In contrast, silicon-based compounds are more affordable, and silicon chemistry has enjoyed extensive exploration over recent decades. For instance, after bifunctionalizing the two C–Zn bonds in a silyl-substituted *gem*-dizinc compound, a trialkylsilyl group offers the exciting potential for subsequent post-functionalization reactions. These could encompass Hiyama cross-coupling reactions,<sup>[402]</sup> or Tamao-Fleming type oxidations,<sup>[403]</sup> further expanding the versatility of the resulting compounds.

In light of these considerations, this project aims to pioneer the development of an enantioselective sequential double allylation reaction of  $\alpha$ -silyl-substituted *gem*-dizinc compounds. This entails an initial step of TM-catalyzed asymmetric allylation, followed by a subsequent copper-mediated cross-coupling with allyl halides (**Scheme II-59**).

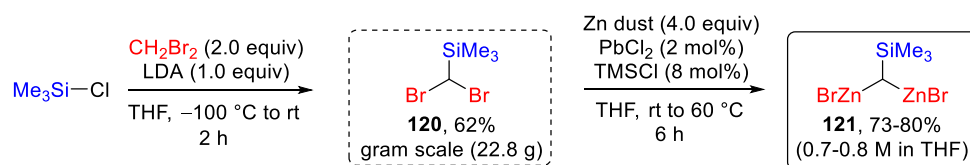


**Scheme II-59.** Project objective: enantioselective sequential double allylation of  $\alpha$ -silyl-substituted *gem*-dizinc reagents.

Our overarching goal is to unlock the full potential of these versatile reagents, possibly even performing a third functionalization step (optional), and thereby leverage their unique properties for the synthesis of valuable, highly functionalized, and optically active molecules in a straightforward manner.

## 2.5. Synthesis of 1,1-Bis(bromozincio)trimethylsilylmethane

As a benchmark, our choice fell upon the utilization of bis(bromozincio)trimethylsilylmethane **121**, which was prepared through an easy two-step process (**Scheme II-60**). In the initial step, (dibromomethyl)trimethylsilane **120** was synthesized by deprotonating dibromomethane with LDA (lithium diisopropylamide), followed by a nucleophilic substitution on trimethylsilyl chloride, according to the procedure outlined by Yoon and Son.<sup>[404]</sup> The resultant crude product was easily purified through distillation at reduced pressure to afford analytically pure (dibromomethyl)trimethylsilane in 62% yield. Notably, the advantage of this reaction lays in its scalability, allowing for the efficient production and long-term storage of large quantities (22.8 grams, ~93 mmol) of the di-halide, since this compound have proven to be stable over time.

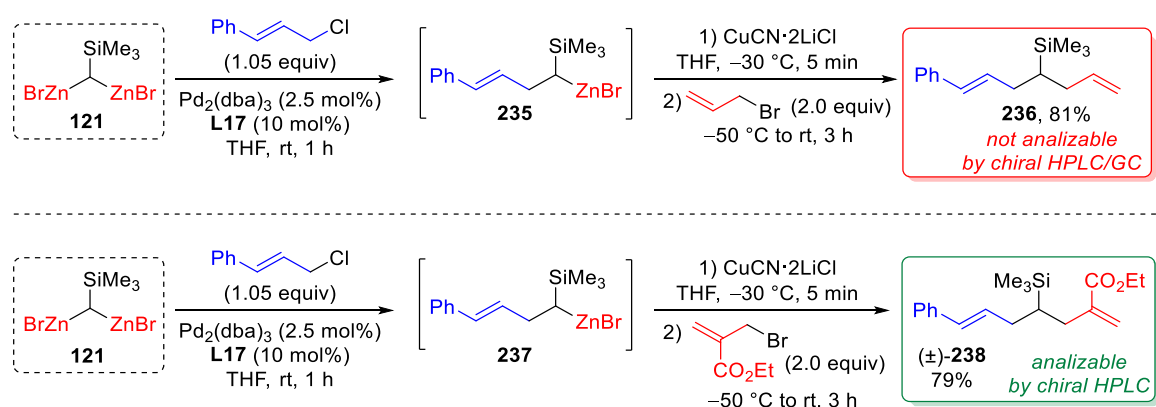


**Scheme II-60.** Preparation of bis(bromozincio)trimethylsilylmethane.

Subsequently, in accordance with a modified Matsubara's procedure,<sup>[201]</sup> **121** was prepared *via* direct reductive zincation, after activating zinc with trimethylsilyl chloride. To achieve this, (dibromomethyl)trimethylsilane was treated with zinc powder (4 equiv) and a catalytic amount (2 mol%) of PbCl<sub>2</sub> in THF at 60 °C for 6 hours (**Scheme II-60**). The presence of the silyl group not only significantly expedited the yield of the reduction of the C–Br bonds but also prevented  $\beta$ -hydride eliminations as a side reaction since no  $\beta$ -hydrogens were present. This contributed to the remarkable stability observed in the resultant silyl-substituted *gem*-dizinc compound. Consequently, the bimetallic species was obtained in 73–80% yield, representing a significant improvement compared to *gem*-dizincio alkanes. In this context, the determination of the bimetallic reagent's yield was accomplished by titration with I<sub>2</sub>, and concentrations of 0.73–0.8 M were routinely obtained. The solution could be stored under a positive pressure of argon at –20 °C for at least 3 weeks with no noticeable loss of title.

## 2.6. Preliminary Studies

The preliminary studies were undertaken with the primary objective of replicating Matsubara's outcomes to assess the reproducibility of the sequential di-allylation reaction with bis(bromozincio)trimethylsilylmethane (**121**).<sup>[201]</sup> Within this framework, a solution consisting of **121** in tetrahydrofuran was treated with cinnamyl chloride (commercially available) in the presence of a Pd<sub>2</sub>(dba)<sub>3</sub> catalyst and the achiral phosphine ligand P[3,5-(CF<sub>3</sub>)<sub>2</sub>C<sub>6</sub>H<sub>3</sub>]<sub>3</sub> (**L17**). Subsequently, the resultant solution containing homoallylzinc species **235** in THF was subjected to a copper-mediated allylation process involving allyl bromide, to furnish the successful production of the desired coupling adduct **236**, in 81% yield (**Scheme II-61, top**).



**Scheme II-61.** Sequential racemic di-allylation of Me<sub>3</sub>SiCH(ZnBr)<sub>2</sub> with cinnamyl chloride and: allyl bromide (top); ethyl 2-bromomethyl acrylate (bottom).

However, due to total apolar nature of the compound, it proved exceedingly challenging to identify suitable separation conditions using any of the chiral-phase GC or HPLC columns available in our

laboratories. Although the possibility of derivatizing the compound was considered, we aimed to streamline the optimization phase, avoiding unnecessary protraction. Hence, we opted to change the allyl bromide in the second step, replacing it with a more polar electrophile.

For this purpose, the commercially available ethyl 2-(bromomethyl)acrylate was selected (**Scheme II-61, bottom**). Utilizing this particular allyl bromide, the sequential di-allylation in a racemic manner resulted in a satisfactory 79% yield of the corresponding product ( $\pm$ )-**238**.

With this racemic sample, the ester motif displayed adequate polarity, facilitating the identification of favorable separation conditions using a chiral-phase HPLC column. This enabled us to measure an accurate enantiomeric excess for all reactions within the screening/optimization phase.

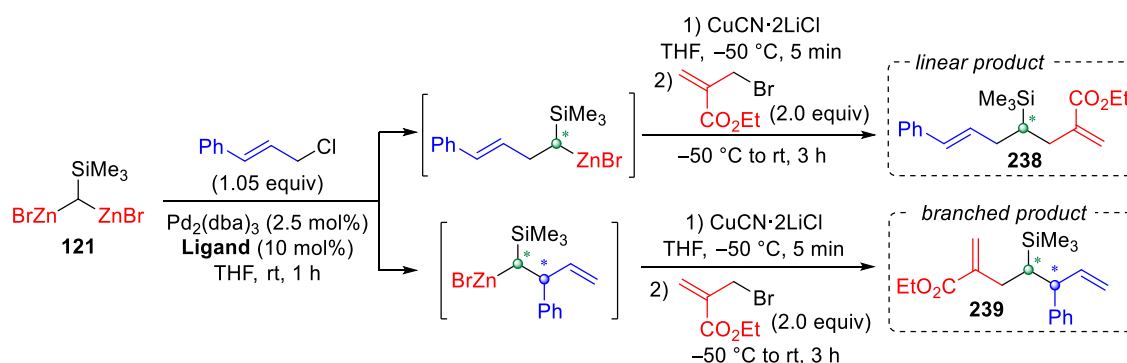
## 2.7. Screening of Chiral Ligands for the Pd-Catalyzed Allylation of $\text{Me}_3\text{SiCH}(\text{ZnBr})_2$ with Cinnamyl Chloride

Based on the preliminary results obtained in racemic fashion, we initiated a screening of various chiral ligands, as summarized in Table II-10. Naturally, we commenced with (**R**)-**MOP**, the chiral ligand utilized by Matsubara et al., which had previously exhibited the best (albeit mediocre) enantiomeric excess in the Pd-catalyzed enantioselective allylic alkylation of 1,1-bis(iodozincio)ethane with cinnamyl electrophiles.<sup>[289]</sup> This initial attempt yielded 37% of the desired product, although with no discernible ee (entry 1, **Table II-10**). In light of this result, an experiment was conducted using cinnamyl benzoate as the primary electrophile, as Matsubara had reported one of the highest ee they could achieve in their system with (**R**)-**MOP**.<sup>[289]</sup> Regrettably, this endeavor also led to a significantly reduced product formation, and, disappointingly, there was still no enantiomeric excess observed (entry 2, **Table II-10**). Subsequently, due to the extensive use of phosphoramidite ligands in enantioselective allylic alkylation with organozinc reagents,<sup>[379]</sup> we decided to test one. Specifically, we attempted the phosphoramidite ligand *ent*-**L21** developed in the previous section for the enantioconvergent Fukuyama cross-coupling with benzylzinc reagents, where very good enantioselectivity have been achieved.<sup>[368]</sup> However, this catalytic system deviated from expectations, failing to produce the expected product **238**. Instead, a different outcome emerged: the formation of the branched product **239**. This compound resulted from a formal  $\text{S}_{\text{N}}2'$  process, as opposed to a formal  $\text{S}_{\text{N}}2$  reaction in the initial step, followed by the subsequent copper-mediated allylation. This process introduced two stereocenters in the final product, resulting in the generation of two diastereoisomers. Nonetheless, this conversion resulted in a diastereoselective ratio that was either minimal or close to negligible (entry 3, **Table II-10**).

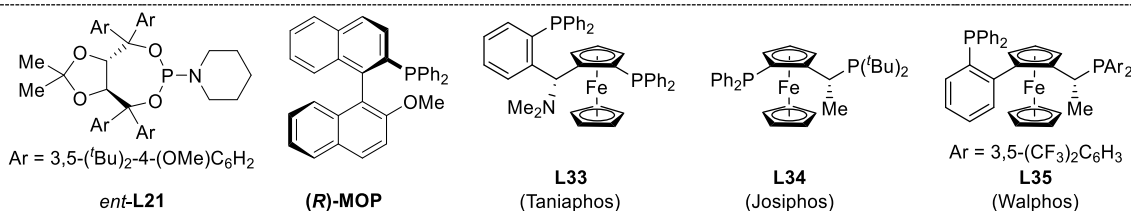
Moving forward, we explored various bidentate ligands from the ferrocene diphosphine family, including **L33**, **L34**, and **L35** (respectively, entries 4, 5, and 6, **Table II-10**), chosen for their commercial availability and the wide range of electronic properties and bite angles they offered.

However, even with these diverse chiral ligands, only the branched product was observed, with neither a satisfactory yield nor diastereoselectivity obtained. Interestingly, it is worth noting that the nucleophilic attack of the allylic alkylation exhibited a complete switch depending on the ligand employed, with the other pathway being entirely undetectable.

**Table II-10.** Screening of chiral ligands for the Pd-catalyzed enantioselective allylation of  $\text{Me}_3\text{SiCH}(\text{ZnBr})_2$  with cinnamyl chloride.



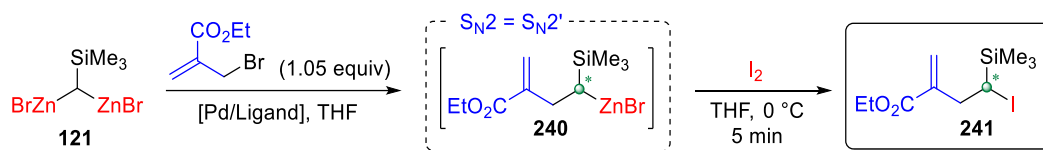
Entry	Ligand	238:239	Yield 238 <sup>[a]</sup>	ee <sup>[b]</sup>	dr <sup>[c]</sup>
1	<b>(R)-MOP</b>	1:0	37%	0%	-
2 <sup>[d]</sup>	<b>(R)-MOP</b>	1:0	13%	0%	-
3	<b>ent-L21</b>	0:1	18%	-	55:45
4	<b>L33</b>	0:1	29%	-	60:40
5	<b>L34</b>	0:1	32%	-	55:45
6	<b>L35</b>	0:1	21%	-	55:45



[a] Isolated yield. [b] The ee values were determined by chiral-phase HPLC analysis. [c] Diastereomeric ratio measured by <sup>1</sup>H NMR spectroscopy. [d] Cinnamyl benzoate was used instead of cinnamyl chloride.

To place a greater focus on the initial cross-coupling reaction, where stereodifferentiation occurs, we decided to change the electrophile used in the first step of our sequence, devising an easier approach (**Scheme II-62**). To begin with, we decided to deviate from our previous sequential reaction of using copper-mediated allylation as second step. Instead, we adopted a strategy where the intermediate from the first coupling reaction would be captured by iodine. This modification offers several advantages, as it is not only a straightforward and rapid transformation but also exhibits quantitative yield.<sup>[347]</sup>





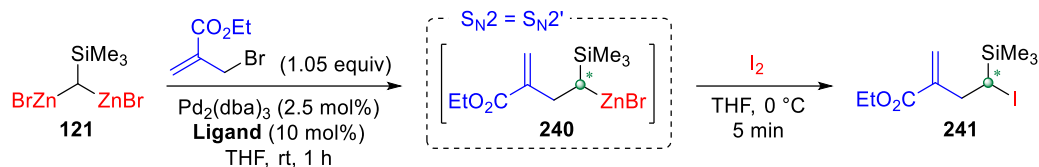
**Scheme II-62.** Simplified system for the study of the enantioselective allylic alkylation reaction with **121**.

In addition, we opted to use ethyl 2-(bromomethyl)acrylate as the electrophile for the initial step. Notably, in this way both the formal  $S_N2'$  and  $S_N2$  reactions on this substrate yield the same product, effectively bypassing the challenge of regioselectivity between linear and branched products. In summary, these strategic adjustments will allow us to focus more intently on the crucial first cross-coupling reaction, facilitating a more efficient and precise control of stereodifferentiation in our synthesis.

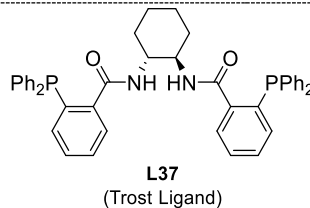
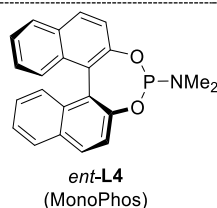
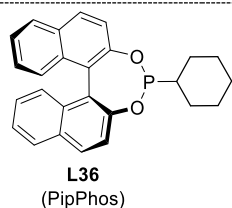
To test this new system, we initiated with an assessment of the efficacy of our previously established reaction conditions. Hence, we employed first  $\text{Pd}_2(\text{dba})_3$  (2.5 mol%) in conjunction with the achiral phosphine ligand  $\text{P}[3,5-(\text{CF}_3)_2\text{C}_6\text{H}_3]_3$  (10 mol%) in THF at room temperature. Following this step, we subjected the resulting organomonozinc intermediate to iodolysis, which yielded an impressive 89% of the desired product. Once again, with this racemic sample, we successfully identified good separation conditions using a chiral-phase HPLC column, allowing for the successive measurement of the enantiomeric excess for all reactions conducted within the screening and optimization phase.

## 2.8. Screening of Chiral Ligands for the Pd-Catalyzed Enantioselective Allylation of $\text{Me}_3\text{SiCH}(\text{ZnBr})_2$ with Ethyl 2-(Bromomethyl)acrylate

In the context of our new simplified sequential reaction, we first performed an enantioselective allylic alkylation of **121** with ethyl 2-(bromomethyl)acrylate. Next, the *mono*-organozinc intermediate was quenched with iodine to assess the stereodifferentiation that occurred during the initial cross-coupling. As a result, we conducted a thorough exploration of diverse chiral ligands. The outcomes from this ligand screening process are presented in **Table II-11**. In our initial experiment, we utilized ligand **(R)-MOP**, which had previously shown the highest yield among all the tested ligands. Under these reaction conditions, we achieved a 49% yield of the product. However, this attempt did not result in any ee (entry 1, **Table II-11**).

**Table II-11.** Screening of chiral ligands for the Pd-catalysed enantioselective allylation of  $\text{Me}_3\text{SiCH}(\text{ZnBr})_2$  with ethyl 2-(bromomethyl)acrylate.

Entry	Ligand	Yield <b>241</b> <sup>[a]</sup>	ee <sup>[b]</sup>
1	<b>(R)</b> -MOP	49%	0%
2	<i>ent</i> -L21	traces	-
3	<b>L36</b>	traces	-
4	<i>ent</i> -L9	traces	-
5	<b>L34</b>	traces	-
6	<b>L35</b>	traces	-
7	<b>L37</b>	42%	0%
8 <sup>[c]</sup>	<b>(R)</b> -MOP	24%	0%



[a] Isolated yield. [b] The ee values were determined by chiral-phase HPLC analysis. [c]  $\text{Pd}_2\text{Cl}_2(\text{allyl})_2$  was used instead of  $\text{Pd}_2(\text{dba})_3$ .

Having eliminated the issue of regioselectivity between the linear and branched organozinc intermediates in the initial coupling, we decided to investigate ligands that had previously only given  $\text{S}_{\text{N}}2'$  reactivity, forming exclusively the branched isomer. Our attention turned to phosphoramidite ligands, specifically, *ent*-L21, and the commercially available ligands **L36** and *ent*-L4 (entries 2, 3, and 4, **Table II-11**). Unfortunately, these ligands produced only trace amounts of the product, underscoring their ineffectiveness for this particular system. Similarly, ferrocene diphosphine ligands **L34** and **L35** also yielded disappointing results, with only minimal traces of the product observed (entries 5 and 6, **Table II-11**). Within the biphosphine ligand family, we tested also **L37** (known as the Trost ligand), which has a strong track record in palladium-catalyzed enantioselective allylic alkylations.<sup>[405–407]</sup> Nevertheless, when we employed this ligand, we achieved a 42% product yield, yet no ee was obtained.

Frustratingly, none of the ligands we tested yielded a product with a yield exceeding 50%, and more importantly, none showed any ee. In an attempt to shed light on this issue, we explored a different source of palladium. Until now, palladium had been introduced as Pd(0), specifically as  $\text{Pd}_2(\text{dba})_3$ , with its dibenzylideneacetone ligands, later exchanged *in situ* for the appropriate chiral ligand. Despite some initial concerns about this exchange process, it became evident that the absence of ee was not

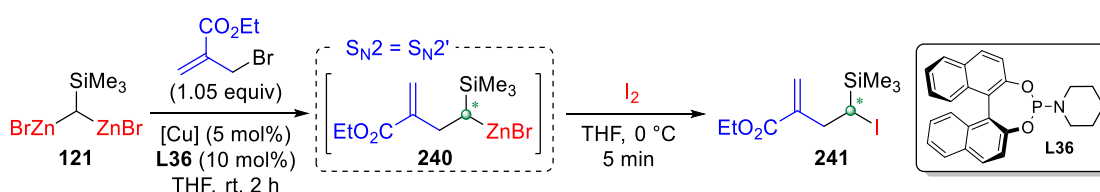
solely attributed to it, as we observed different results with various ligands. To explore further, we introduced  $\text{Pd}_2\text{Cl}_2(\text{allyl})_2$  as a palladium source alongside **(R)-MOP**. However, this combination yielded only a 35% yield with no ee (entry 8, **Table II-11**).

Given the unsatisfactory results with palladium catalysis despite experimenting with a fair range of different chiral ligands, we decided to explore an alternative transition-metal catalyst. In this context, we opted for copper, as its use in enantioselective catalyzed allylic substitutions has been extensively documented in the literature.<sup>[379,408]</sup>

## 2.9. Screening of Cu-Salts for the Enantioselective Allylation of $\text{Me}_3\text{SiCH}(\text{ZnBr})_2$ with Ethyl 2-(Bromomethyl)acrylate

Inspired by Feringa's paper,<sup>[389]</sup> we initiated the study on Cu-catalyzed enantioselective allylation using the *gem*-dizincio reagent and ethyl 2-(bromomethyl)acrylate (**Table II-12**). We employed copper(I) iodide, in conjunction with the commercially available phosphoramidite **L36**. The reaction was performed in THF, for a duration of 2 h at room temperature. Subsequently, we conducted the sequential iodination trapping of the organozinc intermediate, which resulted in a satisfactory 45% product recovery (entry 1, **Table II-12**). Regrettably, there were no traces of ee.

**Table II-12.** Screening of copper salts for the Cu-catalyzed enantioselective allylic alkylation of  $\text{Me}_3\text{SiCH}(\text{ZnBr})_2$  with ethyl 2-(bromomethyl)acrylate.



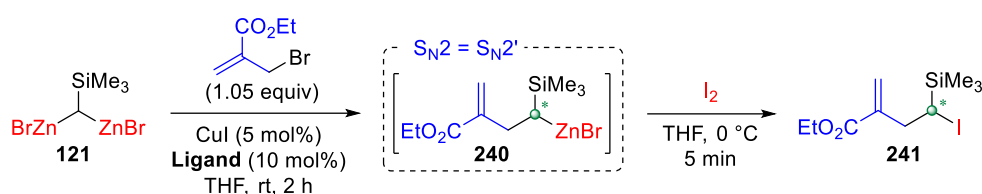
Entry	[Cu]	Yield <b>241</b> <sup>[a]</sup>	ee <sup>[b]</sup>
1	CuI	45%	0%
2	CuTC	<10% <sup>[c]</sup>	-
3	Cu(OTf) <sub>2</sub>	36%	0%
4	Cu(OAc) <sub>2</sub>	20%	0%

[a] Isolated yield. [b] The ee values were determined by chiral-phase HPLC analysis. [c] Yield measured by <sup>1</sup>H NMR analysis using 1,3,5-trimethoxybenzene as internal standard.

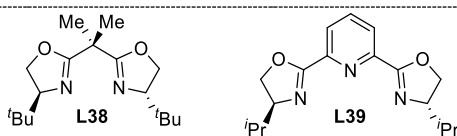
Based on this outcome, we conducted a brief screening of copper sources while consistently using **L36** as the chiral ligand. We tested both copper (I) and copper (II) sources. Copper thiophene-2-carboxylate (CuTC) proved to be highly ineffective for our system, yielding less than 10% (entry 2, **Table II-12**).

Copper (II) salts, specifically copper triflate and copper acetate, were also evaluated, yielding 36% and 20% respectively, but still, no enantiomeric excess was detected (entry 3 and 4, **Table II-12**). This initial screening indicated that CuI was the most suitable copper source for our specific system. Consequently, we proceeded to explore the reaction with different chiral ligands. To begin with, we attempted other chiral phosphoramidites, considering that the best results had been achieved with a ligand from this family. Phosphoramidite derivative *ent*-**L4**, yielded only 22% of the product with 0% of ee (entry 2, **Table II-13**), proving to be inferior to the initially tested ligand **L36**. Similarly, the TADDOL phosphoramidite derivative *ent*-**L21** did not promote the reaction's progress (entry 3, **Table II-13**), yielding identical results to when palladium was employed as the transition-metal catalyst.

**Table II-13.** Screening of chiral ligands for the Cu-catalyzed enantioselective allylation of  $\text{Me}_3\text{SiCH}(\text{ZnBr})_2$  with ethyl 2-(bromomethyl)acrylate.



Entry	Ligand	Yield <b>241</b> <sup>[a]</sup>	ee <sup>[b]</sup>
1	<i>ent</i> - <b>L4</b>	45%	0%
2	<b>L36</b>	<10% <sup>[c]</sup>	-
3	<i>ent</i> - <b>L21</b>	traces	-
4	<b>L37</b>	45%	0%
5	<b>L38</b>	24%	0%
6	<b>L39</b>	42%	0%



[a] Isolated yield. [b] The ee values were determined by chiral-phase HPLC analysis. [c] Yield measured by <sup>1</sup>H NMR analysis using 1,3,5-trimethoxybenzene as internal standard.

Since none of the phosphine ligands tested yielded even a slight ee, we opted to explore nitrogen-based ligands. In this context, inspired by the relatively good yield achieved using Trost Ligand **L37** in palladium-catalysis (entry 7, **Table II-13**), we decided to evaluate its performance, even though no prior instances had been documented in the literature for copper-catalyzed allylic substitution. We managed to achieve a reasonable 45% yield but still observed a 0% ee (entry 4, **Table II-13**).

Next, we turned our attention to bis(oxazoline) ligands. This class of highly regarded chiral ligands in copper asymmetric catalysis, featuring two oxazoline rings and typically C<sub>2</sub>-symmetric.<sup>[409,410]</sup>

They come in various forms, with structures based on CH<sub>2</sub> or pyridine linkers (often referred to as BOX and PyBOX, respectively). The appeal of these ligands lies in their easy synthesis,<sup>[409–412]</sup> allowing for extensive structural modifications that can significantly impact stereodifferentiation. Within this context, we tested **L38** and **L39**. Unfortunately, although both provided the desired product **241** in yields of 24% and 42%, respectively, complete racemates were obtained in both cases (entries 5 and 6, **Table II-13**).

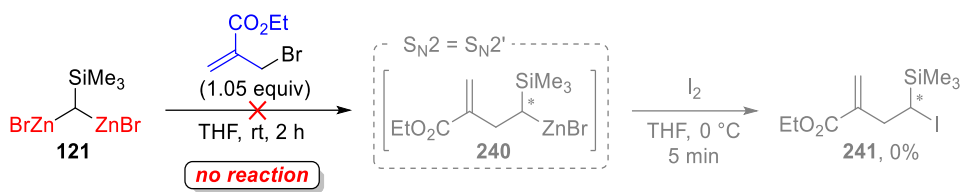
Even after exploring a variety of chiral ligand families, we were unable to attain any enantiomeric excess. This suggests that the issue may potentially reside within the system itself, rather than our inability to identify the correct chiral transition metal-ligand complex for the stereodifferentiation of the initial step.

## 2.10. Investigation on the Complete Absence of Enantiomeric Excess

The total absence of ee across all our experimental outcomes, despite employing various transition-metal catalysts and a range of chiral ligands, has led us to consider three potential reasons: 1) the allylation reaction might be metal- and/or ligand-free and thus no stereoinduction can be introduced in the catalytic cycle; 2) the level of stereospecificity in the iodolysis step involving our organometallic intermediate; 3) the possible configurational instability of the *mono*-organozinc intermediate under our reaction conditions. Hereafter, we will analyze and investigate both factors. It is important to note that these three studies have been conducted concurrently.

### 2.10.1. Investigation of the Metal/Ligand-Free Nature of Allylation Reaction of Me<sub>3</sub>SiCH(ZnBr)<sub>2</sub>

To begin with, it is conceivable that due to the high reactivity of the substrates themselves, the transformation could proceed without the need for a transition metal catalyst. In such a scenario, the catalyst would play a minimal or non-existent role in the mechanism, and the reaction would autonomously proceed, resulting in racemic outcomes since no stereoinduction from the chiral complex could occur. To examine this hypothesis, we exposed the *gem*-dizincio reagent to ethyl 2-(bromomethyl)acrylate without any transition-metal catalyst (**Scheme II-63**). The outcome revealed no conversion of the acrylate, conclusively demonstrating that the metal does indeed play a pivotal role in the reaction mechanism. Consequently, it remains plausible that the chiral ligand is also integral to the process.

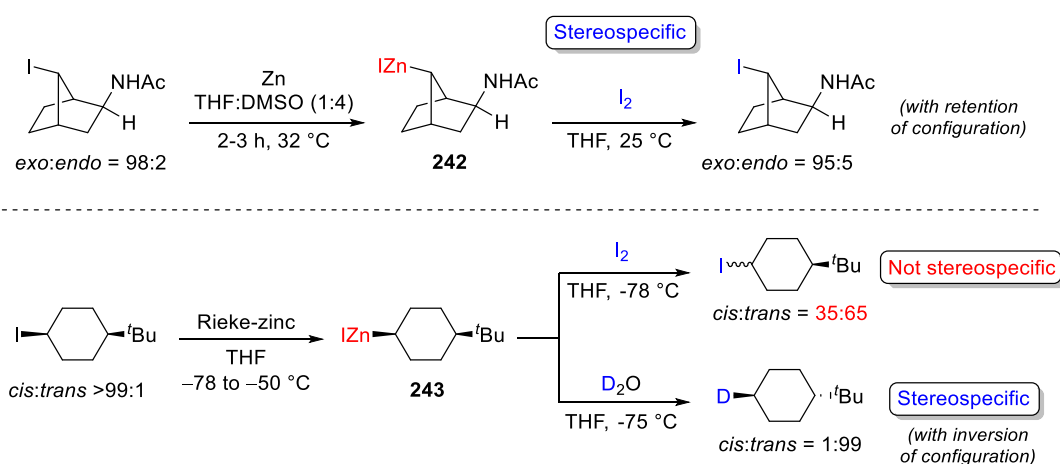


**Scheme II-63.** Allylation of ethyl 2-(bromomethyl)acrylate with **121** without any TM-catalyst.

Subsequently, we can rule out the possibility of the reaction being ligand-free. This conclusion is drawn from the significant variation in yield observed when different ligands were employed, sometimes even within the same ligand family. This variability indicates that the ligand is indeed coordinated effectively to the transition metal catalyst. To further support this hypothesis, we conducted the reaction with CuI in the absence of any ligands. This experimental approach resulted in a very low conversion rate of 14%, which is notably distinct from the superior outcomes achieved with *ent*-**L4** or **L37**, yielding 45% (entries 1 and 4, **Table II-13**) of the racemic product. This effectively refutes the notion of the ligand being excluded from the reaction mechanism. Consequently, it is reasonable to expect at least some degree of chiral induction at some point in the reaction pathway.

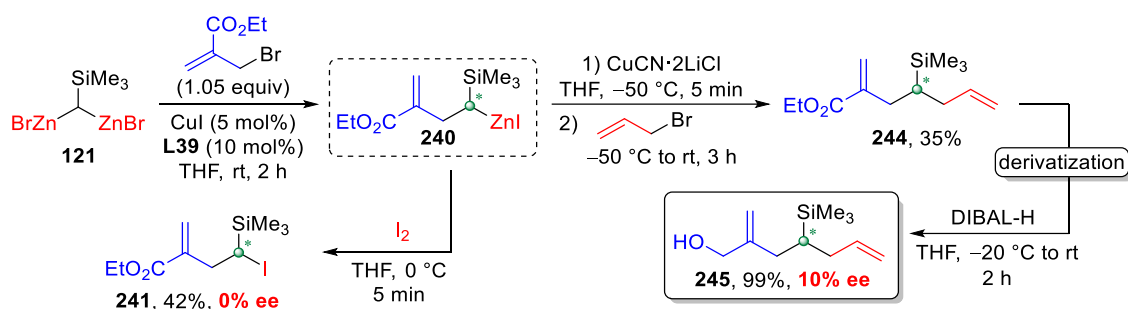
## 2.10.2. Investigation on the Stereospecificity of Iodination Reaction

Our study heavily relied on the iodination step being entirely stereospecific with no additional difficulty. However, in the literature a pivotal work of Knochel reports that this is not always the case (**Scheme II-64**).<sup>[413]</sup>



**Scheme II-64.** Stereospecificity level of iodolysis reaction with different diastereoselectively pure organozinc reagents.

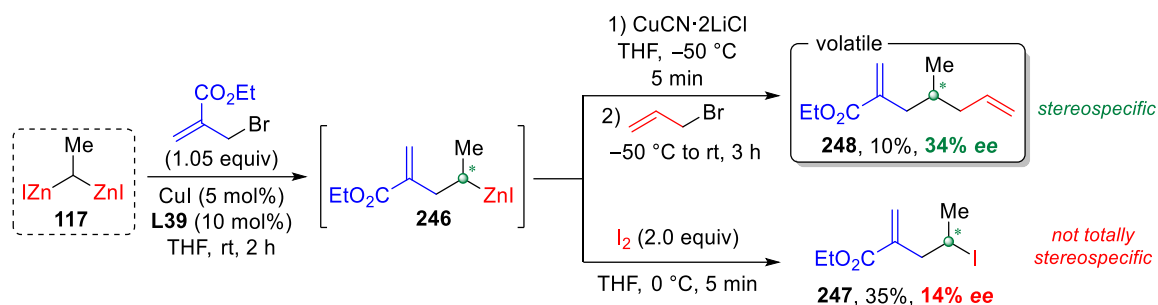
In the case of organozinc compound **242**, the iodolysis proceeds with a high degree of stereoselectivity, preserving the original configuration. However, the same iodination quenching method to the organozinc compound **243** at a temperature of  $-78\text{ }^{\circ}\text{C}$ , it resulted in a mixture of *cis* and *trans* isomers in a ratio of 35:65, indicating that the reaction was not stereospecific under those conditions. On the other hand, when the quench of the organozinc reagent was performed with deuterated water at  $-75\text{ }^{\circ}\text{C}$ , it exhibited total stereospecificity, but with an inversion of configuration. These findings suggest that both the nature of quenching reagent and the specific organometallic compound employed have a significant impact on the stereoselectivity of the reaction. To determine whether the iodolysis of our organozinc compound under our conditions was stereospecific or not, we conducted a study (**Scheme II-65**). Initially, we performed the enantioselective step using CuI and **L39** (which displayed one of the highest yields in the CuI-catalyzed allylic alkylation, see entry 6, **Table II-13**) in THF at room temperature for 2 h. Then, instead of iodination quenching, we carried out a copper-mediated allylation using simple allyl bromide, yielding the desired product in a 35% yield.



**Scheme II-65.** Comparison of the ee obtained with Cu-mediated allylation and iodolysis of **240**.

We encountered substantial challenges in attempting to find suitable separation conditions for this compound. None of the chiral-phase GC or HPLC columns available in our laboratories were able to provide a satisfactory separation of the two enantiomers. Consequently, we adopted a derivatization approach, converting the ester group (i.e. **244**) into the corresponding alcohol (i.e. **245**) through reduction with DIBAL-H. With the resulting alcohol, we identified optimal separation conditions using a chiral-phase HPLC column. Interestingly, the results revealed an enantiomeric excess of 10%, confirming our suspicion that under our specific conditions, the iodolysis reaction is not stereospecific.

In our pursuit of understanding the potential influence of the nature of the organometallic compound during the iodination step on the stereoselectivity of the reaction, we undertook an alternative experimental example. We set out to conduct an enantioselective allylic alkylation using 1,1-bis(iodozincio)ethane (**117**), all the while maintaining the same reaction conditions (**Scheme II-66**). Subsequently, we quenched the organozinc intermediate with iodine, which resulted in the desired product **247** with a yield of 35% and 14% ee.



**Scheme II-66.** Comparison of the ee obtained with Cu-mediated allylation and iodolysis of **246**.

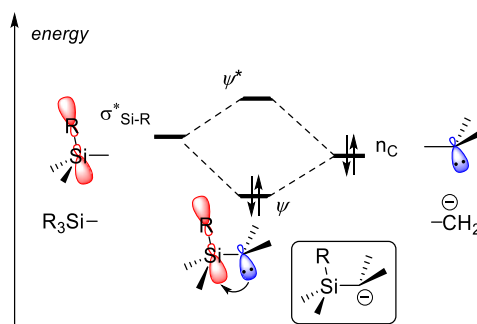
We thus replicated the same sequential reaction but replacing the iodolysis step with a copper-mediated allylation with allyl bromide. This particular reaction exhibited an NMR yield of 40%, but the isolated yield was a mere 10% due to the unexpected volatility of the product **248**. Intriguingly, the enantiomeric excess in this case measured at a modest but encouraging 34%. These findings unequivocally demonstrate that, even when dealing with the alkylic organozinc intermediate **246**, the iodolysis step has a pronounced effect, leading to a notable reduction in enantiomeric excess, amounting to a significant 20% decrease.

### 2.10.3. Investigation on the Configurational Stability of the $\alpha$ -Silyl Organozinc Intermediate

#### 2.10.3.1. Negative Hyperconjugation Effect

The absence of enantiomeric excess in our experimental outcomes has prompted us to consider a potential explanation: the configurational instability of the *mono*-organozinc intermediate within the confines of our specific reaction conditions (2 h at rt). While prior research has demonstrated that secondary alkylzinc compounds exhibit commendable configurational stability at room temperature,<sup>[294]</sup> our situation presents an intriguing departure from the norm. Indeed, in our case, the carbon atom bearing the metal functionality is substituted with a silicon group. This introduces an intriguing element, as third-period heteroatoms like silicon are known to stabilize adjacent carbanions through a phenomenon known as negative hyperconjugation,<sup>[414,415]</sup> making emerge critical considerations. The concept of silicon stabilising an anion can be understood by considering a qualitative molecular orbital diagram as depicted in **Scheme II-67**.





**Scheme II-67.** Qualitative stabilisation diagram of a carbanion by adjacent silicon group.

Electron donation from the carbanion's sp-type HOMO to the  $\sigma^*_{Si-R}$  orbital, is viable due to significant orbital overlap, matching energy levels, and symmetrical similarities between these orbitals. The interaction between anionic lone-pair electrons and adjacent antibonding orbitals becomes advantageous owing to the *relatively low energy level compared to the elevated energy of the anion*.<sup>[414,415]</sup> This effect allows silicon to exert its stabilizing influence on carbanions positioned in the  $\alpha$ -position relative to it, thereby promoting the formation of these carbanions. Within our context, this proposition presents an intriguing possibility: silicon may assume a pivotal role in stabilizing the negative charge on the  $\alpha$ -carbon, which arises from a C–Zn bond inversion, making our organozinc intermediate **240** less configurationally stable under our reaction conditions, which are rt for a period of 2 h.

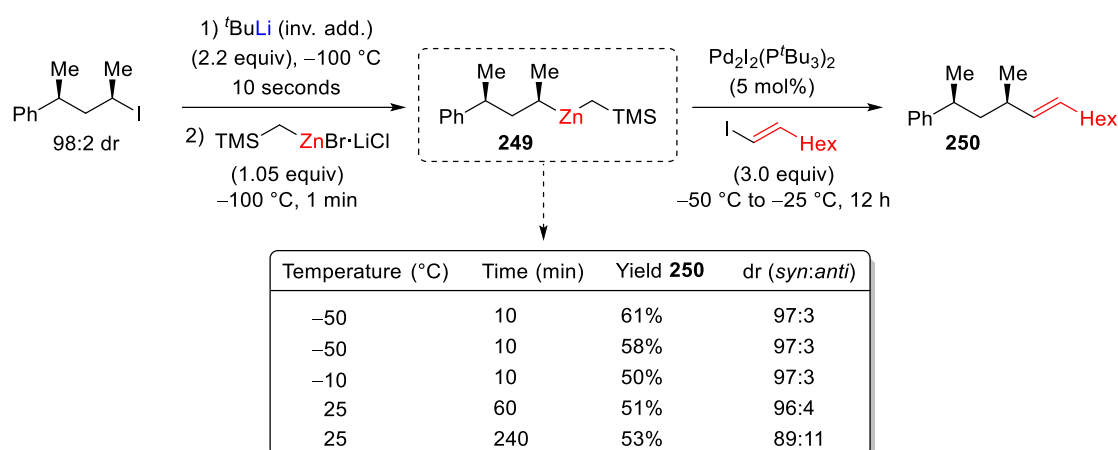
### 2.10.3.2. Effect of $\alpha$ -Heteroatoms on Configurational Stability in Organolithium and Organozinc Compounds

Before continuing it is crucial to remind the reader that the term "*configurationally stable*" lacks specificity on its own. This concept becomes meaningful only when linked to both a specific temperature and a specific timeframe. Typically, the lower the energy barrier for inversion in enantio- or diastereomerically enriched organometallic reagents at a given temperature, the quicker the inversion process occurs.

In the absence of general data concerning the stereochemical behaviour of zinc carbanions bearing a heteroatom in  $\alpha$ -position, it is interesting to overlook what is known concerning the corresponding *lithio* carbanions: the presence of a heteroatom in  $\alpha$ -position to a lithium-bearing carbon atom can significantly affect and modify the stereochemical behaviour. Oxygen-<sup>[416,417]</sup> and amino-substituted<sup>[418–421]</sup> lithium compounds maintain their configurational stability on a macroscopic time scale over minutes at  $-30\text{ }^\circ\text{C}$ , whereas sulfur-<sup>[422]</sup> selenium-<sup>[423–425]</sup> tellurium-<sup>[426]</sup> and silicon-substituted<sup>[426]</sup> alkyl lithium compounds exhibit configurational lability on the same timescale and temperature, due to the stabilization of the respective carbanion by negative hyperconjugation, resulting in similar enantiomerization barriers of  $\sim 11/12\text{ kcal mol}^{-1}$  at  $-10\text{ }^\circ\text{C}$  in

THF-*d*8 (with negligible reported solvent influence).<sup>[426]</sup> In contrast, secondary, unfunctionalized chiral organolithiums, like 1-methylheptyl lithium<sup>[427]</sup> or *s*-BuLi,<sup>[428]</sup> when in the presence of Et<sub>2</sub>O, demonstrate racemization half-lives of only seconds at -70 °C. However, without reported enantiomerization barriers, the quantification of the stabilization provided by the heteroatom like silicon in the  $\alpha$ -position remains undetermined.

Concerning zinc compounds, only one (but fundamental) example in literature of  $\alpha$ -silicon substituted alkylzinc compounds have been reported by Knochel (**Scheme II-68**).<sup>[306]</sup>



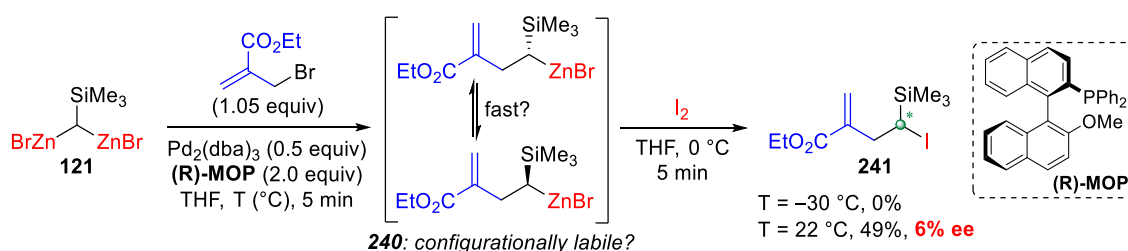
**Scheme II-68.** Study of the configurational stability of dialkylzinc **249**.

The dialkylzinc compound **249** exhibited lower configurational stability at room temperature compared to typical secondary alkylzinc compounds. Specifically, diastereomeric ratio of **250** changed from 97:3 to 89:11 after exposing **249** to room temperature for 4 hours, before performing the Pd-catalyzed cross-coupling with vinyl iodide. This example suggests to us that in our case silicon could play an analogous role, rendering our silyl-substituted organozinc intermediate configurationally labile at room temperature and thus losing some potential enantiomeric excess gained by the enantioinduction of the catalyst during the reaction.

### 2.10.3.3. Preliminary Studies

Initially, to explore this hypothesis, we attempted to minimize the required reaction time for the first step, ideally completing it within a few minutes before significant racemization occurs, by increasing the catalyst loading to a stoichiometric level. For these experiments, we have opted to start back with palladium catalysis. Hence, we selected (**R**)-**MOP** as chiral ligand, as it was the most efficient one. Working at room temperature for 5 minutes resulted in a 49% yield, and during this period, a minor ee of 6% was detected (**Scheme II-69**).

This observation raises the possibility of racemization occurring in the monozinc intermediate and a gradual loss of enantiomeric excess over time. However, these findings are not conclusive, as the 6% ee, while not negligible, remains relatively low and may potentially be attributed to the precision limitations of HPLC integration.



**Scheme II-69.** Initial investigation on the configurational stability of organozinc **240**: reactions with stoichiometric amount of chiral catalyst.

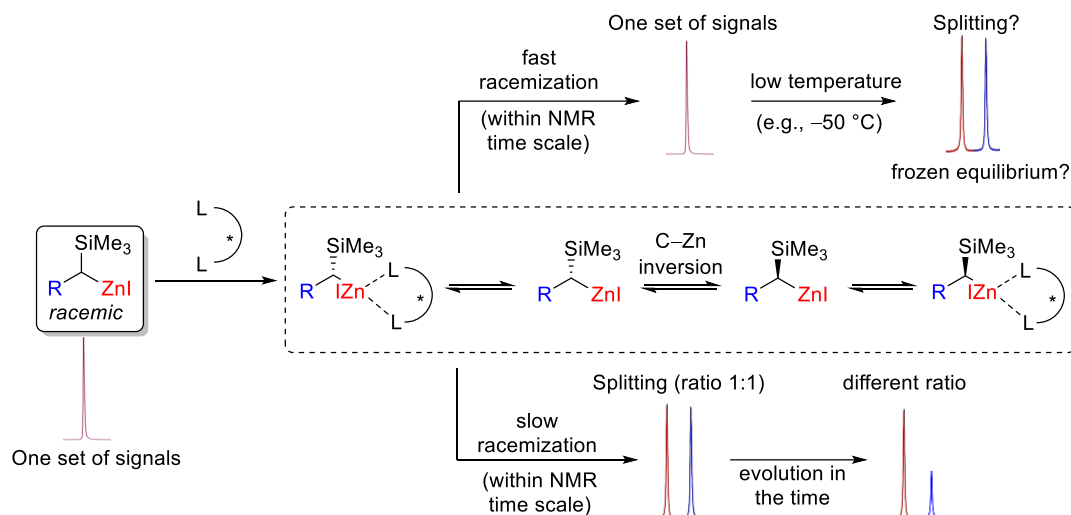
It is also conceivable that racemization could be occurring rapidly, and the 6% ee observed after 5 minutes at room temperature may represent the residual effect of a major stereodifferentiation. To explore this further, we attempted to conduct the same reaction at a temperature of  $-30\text{ }^{\circ}\text{C}$  to mitigate racemization, assuming our hypothesis holds true. Unfortunately, this low temperature had a detrimental impact on the overall reaction kinetics, resulting in no observable conversion.

### 2.10.3.4. Investigation Using NMR Spectroscopy and Chiral Solvating Agents

To gain further insights into the configurational behavior of the silyl-substituted organozinc intermediate, we opted to directly synthesize the racemic organometallic reagent and utilize NMR spectroscopy in conjunction with chiral solvating agents. Our objective with this approach was to replicate the methodology utilized by Guijarro and Rieke in their investigation of the configurational stability of secondary alkylzinc compounds,<sup>[308]</sup> with a particular focus on estimating an approximate racemization rate (see Part I: Bibliographic Overview, section 2.2.2).

As already mentioned, the fundamental principle behind this method is that when a racemic organometallic compound is complexed with an enantiomerically pure chiral ligand, diastereoisomeric complexes are formed, which are observable in NMR spectroscopy. Initially, the two sets of signals should exhibit a roughly equal ratio of approximately 1:1, reflecting the racemic nature of the organozinc compound (**Scheme II-70**). However, because this system is not static, the composition at equilibrium dynamically changes based on the rate of inversion of the C–Zn bond. This evolution continues until the system reaches its thermodynamic equilibrium configuration.

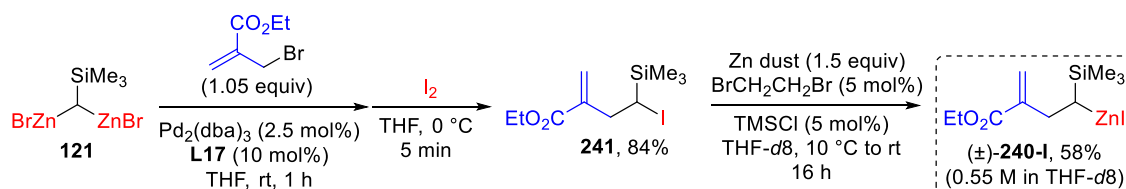
Consequently, the presence of the chiral ligand induces a shift in the composition of the initial racemic mixture of organozinc compounds, resulting in a different final outcome.



**Scheme II-70.** NMR spectra of a racemic secondary allylic organozinc compound in the presence of chiral solvating agents with fast or slow rates of C-Zn bond inversion (on the NMR timescale).

This value corresponds to the new thermodynamic equilibrium within the chiral environment. By deriving the equations governing the interconversion rate of both enantiomers, one can deduce the exponential progression towards the ultimate equilibrium state and approximate the racemization rate of the organometallic reagent. Nonetheless, if the organozinc species is in rapid equilibrium (within the NMR timescale), it will manifest a single set of signals, even when it forms two diastereoisomers in combination with the enantiopure ligand. However, conducting the identical NMR experiment at low temperature (e.g., -50 °C) can potentially halt or significantly slow down the equilibrium process, resulting in the appearance of two distinct signals. In such a scenario, it indicates that the inversion of the C-Zn bond is indeed rapid at room temperature.

Therefore, we synthesized the racemic silyl-substituted organozinc intermediate ( $\pm$ )-**240-I** using the procedure outlined in **Scheme II-71**.



**Scheme II-71.** Preparation of racemic organozinc ( $\pm$ )-**240-I** in THF-d<sub>8</sub>.

The reaction of **241** with zinc dust was carried out in deuterated THF (THF-*d*8) to produce the corresponding organozinc iodide ( $\pm$ )-**240-I**, which was titrated with iodine to determine its concentration. We found it to be  $\sim$ 0.55 M, equating to a 58% yield of zinc insertion under our conditions.

It is worth noting that ( $\pm$ )-**240-I** differs from the actual intermediate **240** in terms of the counteranion (iodide instead of bromide). However, this change is not expected to affect the configurational behavior, as demonstrated by Marek and Normant in their investigation of configurational stability in benzylzinc compounds (see Part I: Bibliographic Overview, section 2.2.3).<sup>[317,318]</sup>

Among the various chiral ligands, the  $C_2$  symmetrically substituted bis(oxazoline) ligand **L39** was selected, and after introducing a stoichiometric amount of the chiral ligand (1 equiv) into the THF-*d*8 solution containing a racemic organozinc compound, we recorded the initial  $^1\text{H}$  NMR spectrum approximately 20 minutes later (**Figure II-6**).

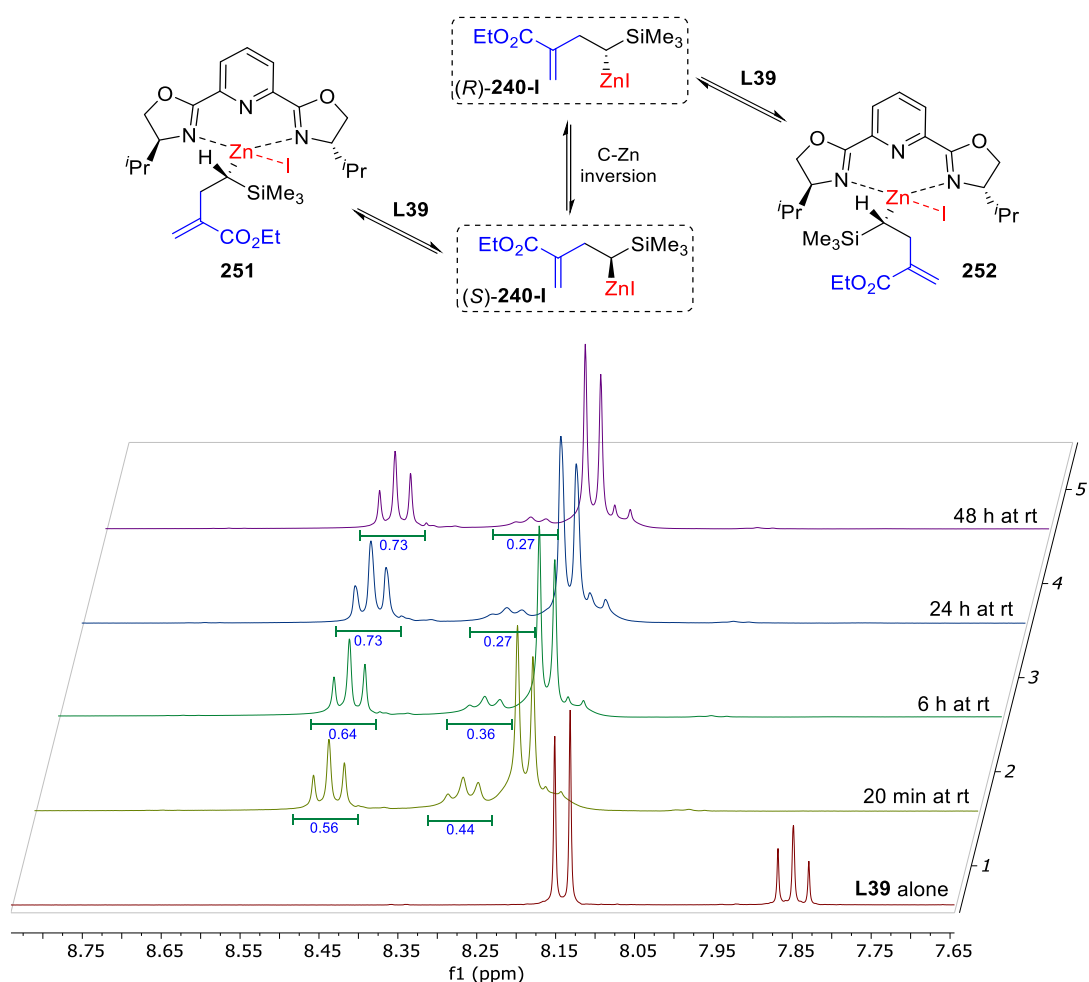
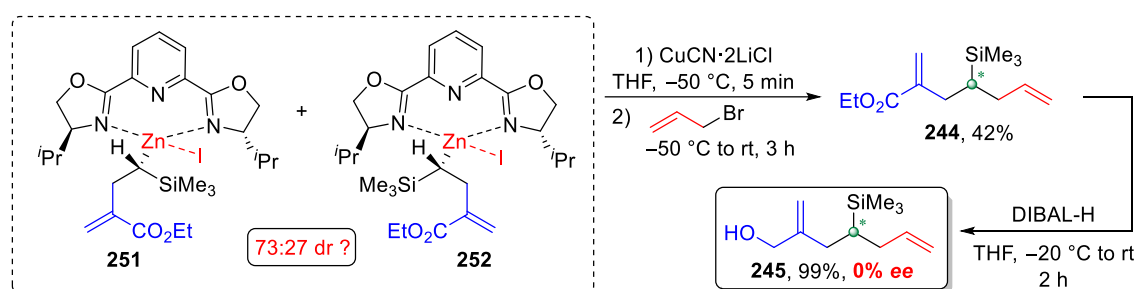


**Figure II-6.** Evolution of the  $^1\text{H}$  NMR spectra over time for racemic organozinc ( $\pm$ )-**240-I** in the presence of **L39**.

Our initial focus was on the disappearance of the signal set associated with both the organozinc compound and the chiral Pybox ligand, along with the emergence of a new signal. This new signal exhibited significant chemical shift changes compared to the previous two, confirming the successful complexation of the chiral solvating agent. Subsequently, our attention was directed to the triplet of **L39** within the aromatic region, where we detected two signals in a 56:44 ratio (approximately 1:1). This ratio, reflecting the nature of the racemic organozinc compound, likely resulted from the formation of two different complexes. If those complexes are the diastereomeric one reported in **Figure II-6** (**251** and **252**), a slight deviation from the 1:1 ratio would indicate that some racemization had occurred during the 20-minute interval. Continuing to monitor the ratio between these two signals over time, we observed a change in the ratio, eventually stabilizing at 73:27 after 24 hours. This observation could strongly support the occurrence of racemization within the NMR tube, leading to an equilibrium shift toward the more thermodynamically stable diastereoisomer. In order to further insight, we attempted to record the NMR spectrum at a temperature of  $-50\text{ }^{\circ}\text{C}$  with the aim of detecting any spectral changes. However, despite our effort, no discernible alterations manifested in the NMR data.

Given the potential diastereomeric enrichment of the organozinc compound in the NMR tube, which was estimated to be approximately 73:27, to validate our hypothesis it becomes necessary to utilize this possible diastereoisomeric enrichment in a stereoselective reaction. This concept was initially explored in a pioneering study involving  $\alpha$ -methylbenzyl lithium-sparteine complexes by Nozaki,<sup>[429]</sup> and later extended to configurationally labile benzyl- and allyllithium compounds,<sup>[430–432]</sup> as well as  $\alpha$ -sulfur<sup>[433]</sup> and  $\alpha$ -seleno<sup>[434,435]</sup> organolithium compounds. However, being aware of our precedent frustration with the lack of stereoselectivity through iodination reaction (see paragraph 2.10.2.), we opted a copper-mediated allylation using allyl bromide (**Scheme II-72**).



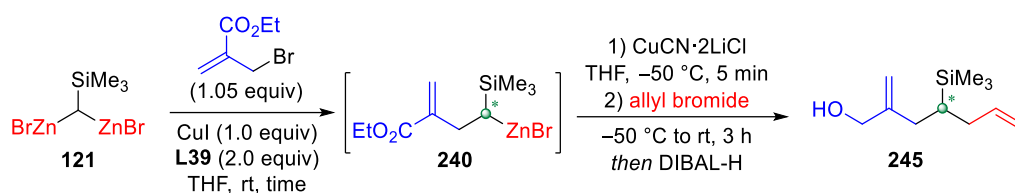
**Scheme II-72.** Exploring the (hypothesized) diastereomeric enrichment from the use of chiral enantiopure **L39** with racemic organozinc ( $\pm$ )-**240-I**.

The results of the allylation reaction yielded 42% of the desired product **244**. As already mentioned before, due to the impossibility of finding suitable separation conditions we had to perform a derivatization approach, transforming the ester group into the corresponding alcohol through reduction with DIBAL-H. However, the resulting alcohol **245** revealed an ee of 0%. This outcome

strongly contradicted our hypothesis and what we had observed in the spectra during the chiral ligand complexation. Therefore, we conducted a repetition of the experiment by combining **L39** with racemic organozinc compound ( $\pm$ )-**240-I**. Interestingly, in this iteration, there were no observed fluctuations in the signal ratio over time. Consequently, it is plausible that the variations noted in the NMR spectra may have arisen from some artifact introduced during the data recording process.

### 2.10.3.5. Racemisation Rate

Due to our observation of stereodifferentiation in the enantioselective allylation with CuI/**L39** illustrated before we sought to reexamine the configurational behaviour of the  $\alpha$ -silyl substituted organozinc intermediate **240**. In our prior experiment under Pd-catalysis, we were unable to conclusively confirm its configurational stability. To address this, we conducted the enantioselective allylation using a stoichiometric amount of the CuI/**L39** catalyst complex (**Table II-14**). This approach aimed to minimize the reaction time, allowing it to reach completion within a few minutes. Our objective was to determine if racemization occurred and, if so, to estimate its rate. Consequently, we carried out the reaction under stoichiometric conditions at room temperature for a duration of 10 minutes (entry 1, **Table II-14**). Subsequently, we performed the transmetallation at  $-50\text{ }^{\circ}\text{C}$  with CuCN $\cdot$ 2LiCl and proceeded with the second stereospecific allylation. The desired product **244** was obtained with a yield of 39%. After derivatization into the corresponding allylic alcohol **245**, we measured an ee of 18%. Based on these results, we can confidently assert that the organozinc intermediate lacks configurational stability and racemizes at room temperature. Notably, the racemization process does not occur at a rapid rate. This observation stems from the fact that our previous findings with 2 h duration (to be exact, 2 h and 20 min), the ee dropped to 10% (entry 3, **Table II-14**). This implies that over the course of approximately 2 h, there was an  $\sim$ 8% reduction in ee. Subsequently, we conducted a repetition of the experiment using stoichiometric quantities. However, in this iteration, we introduced varying time intervals before proceeding with the second cross-coupling step, as outlined in **Table II-14**. After 2 h reaction time, the ee was observed to be 14%, and after 6 h, it had reduced to just 4% (entries 2 and 4, **Table II-14**). Utilizing this dataset, we can construct a graphical representation of the racemization kinetic of our compound, which aligns quite neatly with a linear plot (**Figure II-7**). It is worth noting that the slight discrepancy observed in the experiment with 10% ee (entry 3, **Table II-14**) could potentially be attributed to minor fluctuations in room temperature (23-25  $^{\circ}\text{C}$ ) and/or the inherent precision limitations associated with HPLC integration.

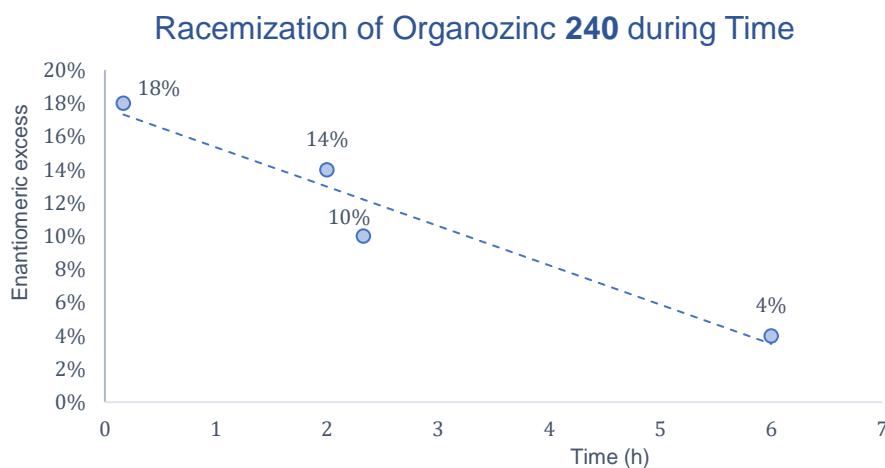
**Table II-14.** Racemization kinetic experiment for organozinc intermediate **240**.

Entry	Time	Yield <b>245</b> <sup>[a]</sup>	ee <sup>[b]</sup>
1	10 min	39%	18%
2	2 h	50%	14%
3 <sup>[c]</sup>	2 h 20 min	35%	10%
4	6 h	47%	4%

[a] Isolated yield over 2 steps, with quantitative yield of the derivatization step. [b] The ee values were determined by chiral-phase HPLC analysis. [c] CuI/L39 (5/10 mol%).

After 2 h reaction time, the ee was observed to be 14%, and after 6 h, it had reduced to just 4% (entries 2 and 4, **Table II-14**). Utilizing this dataset, we can construct a graphical representation of the racemization kinetic of our compound, which aligns quite neatly with a linear plot (**Figure II-7**). It is worth noting that the slight discrepancy observed in the experiment with 10% ee (entry 3, **Table II-14**) could potentially be attributed to minor fluctuations in room temperature (23-25 °C) and/or the inherent precision limitations associated with HPLC integration.

This racemization that we have detected, is in line (in timeframe and temperature) with the one reported by Knochel for his  $\alpha$ -silyl-substituted dialkylzinc species **249**.<sup>[306]</sup> Indeed, Knochel reported a loss of 16% diastereomeric excess (de) when the zinc species was exposed to 25 °C for 4 h, while we report a loss of 14% ee when we waited almost 6 h at rt (23-25 °C) before performing the 2<sup>nd</sup> coupling.

**Figure II-7.** Racemization of the secondary silyl-substituted alkylzinc **240** during time.



## 2.11. Partial Conclusion

In summary, based on the extensive experimentation presented in this study, we can now confidently assert that our initial assumption regarding the configurational stability of the secondary silyl-substituted alkylzinc intermediate **240** was incorrect. Contrary to our expectations, this  $\alpha$ -silyl organozinc intermediate exhibit racemization at rt. In this context, this study expanded our understanding of the configurational behavior of  $\alpha$ -silyl-substituted alkylzinc compounds, previously unexplored in the literature. Additionally, our investigations have revealed that the iodination quench method is not an ideal approach for capturing organozinc intermediates to evaluate its ee. Indeed, building upon Knochel's findings,<sup>[413]</sup> we have reaffirmed that the stereospecificity of this quenching is contingent on the nature of the organometallic reagent.

Nonetheless, there are several valuable takeaways and exciting experimental prospects stemming from this research. First and foremost, it is worth exploring strategies to mitigate racemization on this substrate. Lowering the reaction temperature could potentially slow down or even halt the racemization process. Of course, finding the right balance between preventing racemization without unduly delaying the allylic substitution reaction itself is a crucial consideration. Furthermore, numerous variables should be considered to optimize the enantioselectivity of the allylic substitution. For instance, different solvents and families of chiral ligands could be explored. Notably, chiral NHC carbenes were not investigated in this study, presenting a possible starting point for further research.

It is worth highlighting that we achieved a 34% ee in the allylation reaction using 1,1-bis(iodozincio)ethane. Importantly, this result was attained without any optimization of solvent, temperature, or the choice of a chiral catalyst. We just utilized **L39** as the chiral ligand, but the Pybox ligand family offers a wide array of structural possibilities. Significant modifications can be attempted given the relative ease of preparing these chiral ligands. This suggests the potential for achieving significantly higher enantiomeric excess than our current results. Furthermore, it is important to note that, to the best of our knowledge, PyBox ligands have not been previously reported for use in enantioselective allylic substitution reactions with organozinc reagents. This introduces a novel approach to this type of asymmetric transformation, potentially leading to improved yields and enantiomeric excesses compared to existing methods.



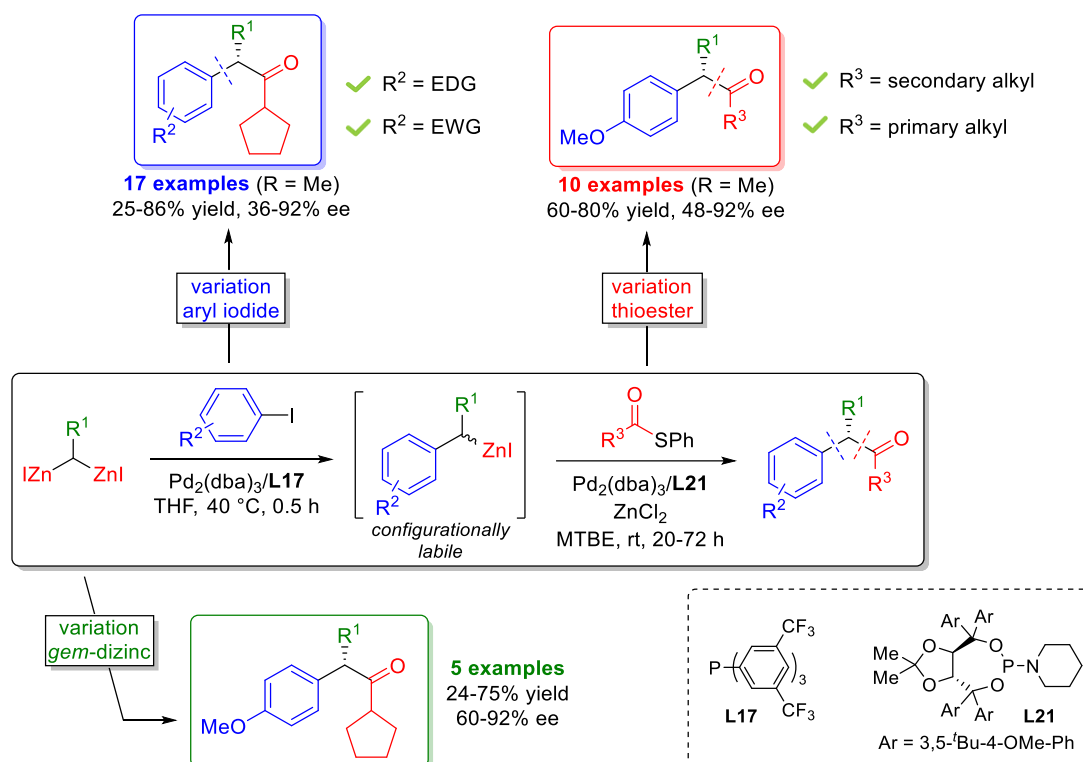
# **GENERAL CONCLUSION AND PERSPECTIVES**

---



The objective of this doctoral thesis was to develop novel, highly efficient enantioselective sequential cross-coupling reactions using prochiral *gem*-dizinc compounds.

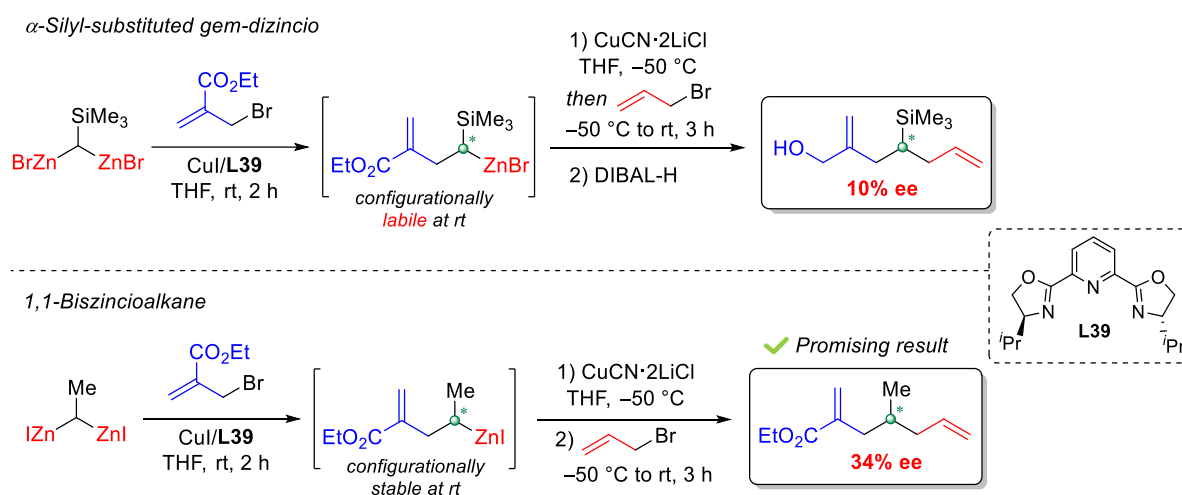
In the first part, we investigated two catalytic C–C bond-forming reactions employing prochiral 1,1-bis(iodozincio)alkanes, utilizing two distinct palladium-based catalytic systems. During these investigations, we successfully developed a new one-pot sequential enantioselective double cross-coupling reaction of 1,1-bis(iodozincio)alkane reagents entailing arylation and acylation (**Scheme GC-1**).<sup>[368]</sup> Mechanistically, the approach relies on a first step involving the (non-enantioselective) desymmetrization of a prochiral geminated C(sp<sup>3</sup>)-dizinc reagent that delivers a stereolabile benzylzinc intermediate that undergoes efficient DKR during the subsequent second step. Our report represents the first example of implementation of such a strategy for asymmetric synthesis.



**Scheme GC-1.** Enantioselective sequential catalytic arylation-Fukuyama cross-coupling of 1,1-bis(iodozincio)alkanes.

Through this protocol, we have disclosed a modular access to synthesize important enantioenriched 1-arylethyl (and 1-arylalkyl to a lesser extent) ketones, including products with electron-deficient and electron-rich aryl units. Specifically, the latter ones had not been accessed previously through direct Fukuyama cross-coupling reactions. Within this work, we also established that Matsubara's Pd-catalyzed (mono)arylation of *gem*-bisorganozinc reagents tolerates the presence of H-atoms  $\beta$  to the metal and can thus be used conveniently with 1,1-bis(iodozincio)alkanes other than 1,1-bis(iodozincio)methane, and additionally that asymmetric Fukuyama cross-coupling reactions can be extended beyond (1-arylethyl) organozincs.

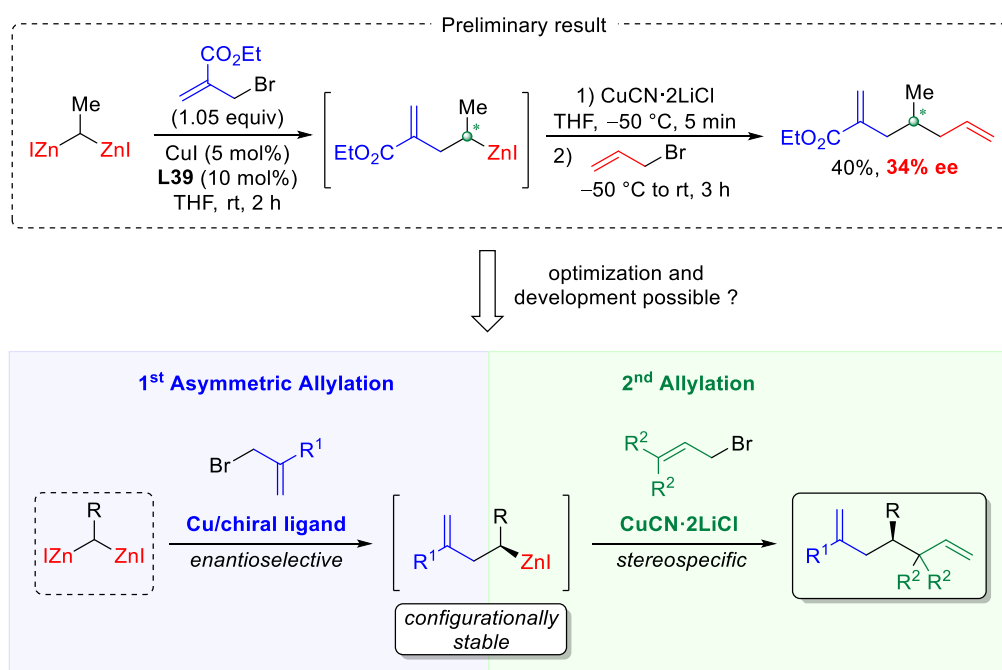
In the second section, we explored the desymmetrization of a prochiral  $\alpha$ -silyl-substituted *gem*-dizincio reagent through enantioselective allylic substitution. This aimed to create a configurationally stable mono-organozinc intermediate intended for use in a subsequent cross-coupling reaction. Based on the extensive investigation and experimentation presented in this study, we can conclude that our initial assumption regarding the configurational stability of the secondary silyl-substituted alkylzinc intermediate was incorrect. Contrary to our expectations, our  $\alpha$ -silyl organozinc intermediate exhibits racemization at rt. Nevertheless, this study significantly broadened our comprehension of the configurational behavior of  $\alpha$ -silyl-substituted alkylzinc compounds, which were previously underexplored in the literature, with only one documented example.<sup>[306]</sup> After the comprehensive screening of chiral catalyst, the enantioselective sequential double allylation of 1,1-bis(bromozincio)trimethylsilylmethane resulted in the desired adduct, yielding 35% with only 10% ee upon derivatization of the ester moiety (**Scheme GC-2**).



**Scheme GC-2.** Enantioselective sequential double allylation using 1,1-bis(bromozincio)trimethylsilylmethane or 1,1-bis(iodozincio)ethane.

However, performing this protocol under the same reaction conditions, we achieved a 34% ee when utilizing 1,1-bis(iodozincio)ethane as the *gem*-dizinc reagent (**Scheme GC-2**). This promising outcome was obtained without optimizing the solvent, temperature, nor the chiral catalyst, suggesting substantial potential for enhancing enantioselectivity.

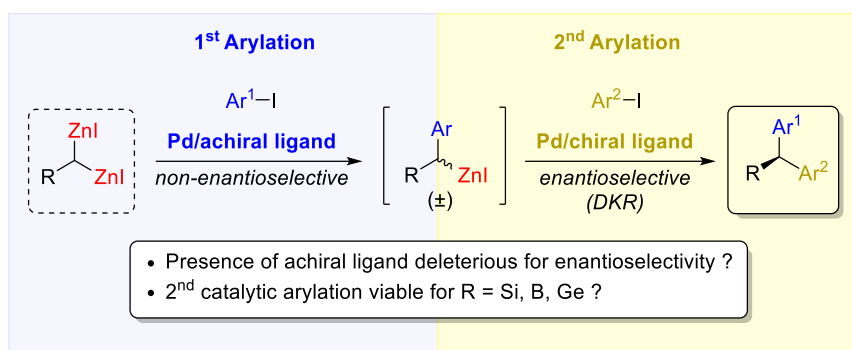
In the framework of this project, there are still several edges to explore. Firstly, the feasibility of performing enantioselective sequential cross-coupling reactions with prochiral 1,1-bis(iodozincio)alkanes through a desymmetrization strategy can be envisioned. In the course of our investigation into  $\alpha$ -silyl-substituted *gem*-dizincio reagents, we serendipitously uncovered novel conditions for the Cu-catalyzed asymmetric allylation of ethyl 2-(bromomethyl)acrylate using 1,1-bis(iodozincio)ethane. This led to a configurationally stable *mono*-organozinc intermediate that was enantiomerically enriched. Subsequent stereospecific copper-mediated cross-coupling with allyl bromide yielded a 40% yield of the desired product with 34% ee (**Scheme FP-1**). Notably, this initial outcome was obtained without optimizing solvent, temperature, or the chiral ligand. Regarding the latter one, only Pybox **L39** was tested. Considering the structural versatility within the Pybox ligand family, significant modifications can be explored, given the relative ease of preparing these chiral ligands. This suggests the potential for achieving a more general procedure with significantly higher enantiocontrol.



**Scheme FP-1.** Enantioselective sequential double allylation with prochiral 1,1-bis(iodozincio)alkanes via desymmetrization strategy with copper-catalysis.

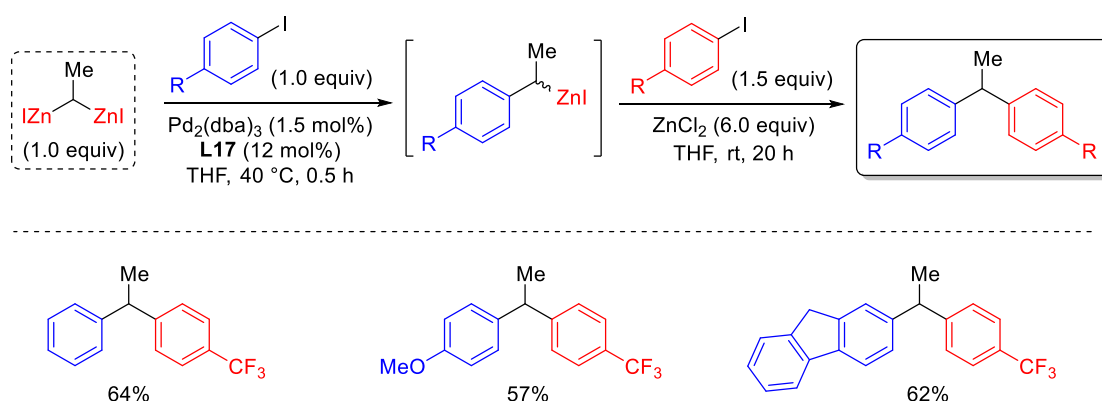
Secondly, an enantioselective sequential catalytic di-arylation can be explored. 1,1-Diarylalkanes represent crucial organic components found in various naturally occurring compounds, displaying a large spectrum of bioactivities that encompass antiviral, anticancer, antidepressant, antifungal properties, and beyond.<sup>[18,436]</sup> Consequently, developing efficient methods to obtain enantiomerically enriched diaryl structural motifs plays a pivotal role in both academic research and industrial applications. However, the creation of novel and straightforward synthetic approaches to access these

molecules remains challenging and highly sought after. Therefore, the pursuit of an enantioselective sequential di-arylation utilizing 1,1-bis(iodozincio)alkanes emerges as a promising and valuable process (**Scheme FP-2**).



**Scheme FP-2.** Pd-catalyzed enantioselective sequential di-arylation reaction and associated challenges.

Drawing from initial findings in our laboratories, we are highly optimistic about formulating a novel strategy for a streamlined synthesis of *gem*-diaryl compounds. Specifically, our discovery reveals that utilizing after the (mono)arylation process with a first aryl iodide (1 equiv) catalyzed by  $\text{Pd}_2(\text{dba})_3$  and **L17** in THF at 40 °C for 0.5 h, the addition of a second different aryl iodide along with  $\text{ZnCl}_2$  (6 equiv) leads to the formation of about 57-64% of the desired diarylated product within 20 hours at room temperature (**Scheme FP-3**).



**Scheme FP-3.** Pd-catalyzed sequential di-arylation reaction with 1,1-bis(iodozincio)ethane.

Building upon these initial racemic investigations, the next phase entails introducing a chiral ligand (or a chiral catalyst) for the second arylation step and aiming to leverage an efficient DKR to establish a highly enantioselective sequential diarylation protocol.





The background of the page features a simulated NMR spectrum. It consists of a horizontal baseline with several vertical peaks of varying heights. On the left side, there is a small multiplet. In the center, there is a single sharp peak. On the right side, there is a very tall, narrow peak, and further to the right, another smaller multiplet. The text is centered over the baseline.

**PART III:  
EXPERIMENTAL SECTION**



### 3.1. General Information

All reactions were carried out with magnetic stirring under argon atmosphere using oven-dried glassware and using standard Schlenk techniques. Unless otherwise stated, reagents and solvents were purchased from commercial sources and generally used without purification.

Ethereal solvents such as THF and methyl *tert*-butyl ether (MTBE) were distilled over sodium and benzophenone under argon atmosphere. MeCN, Et<sub>2</sub>O and CH<sub>2</sub>Cl<sub>2</sub> were dried using a solvent purification system (SPS) MBRAUN MB SPS-800.

Syringes which were used to transfer reagents and solvents were purged with argon prior to use and slow automatic additions were performed using a syringe pump.

NMR spectra (<sup>1</sup>H, <sup>13</sup>C, <sup>19</sup>F, <sup>31</sup>P) were recorded on a Bruker AM 300 MHz or a Bruker AVANCE 400 MHz spectrometer at room temperature. Chemical shifts are given in parts per million (ppm) using the CDCl<sub>3</sub> residual non-deuterated signals as reference ( $\delta$  <sup>1</sup>H = 7.26 ppm;  $\delta$  <sup>13</sup>C = 77.16 ppm). For the characterization of the observed signal multiplicities the following abbreviations were used: s (singlet), d (doublet), t (triplet), q (quartet), p (quintet), hept (heptaplet), m (multiplet) as well as br (broad) when the peak is broad, and the correct multiplicity cannot be assigned unambiguously.

IR spectra were recorded with a Tensor 27 (ATR diamond) Bruker spectrometer and reported as characteristic bands (cm<sup>-1</sup>).

High-resolution mass spectra (ESI-MS, APCI-MS) were acquired using an LTQ-Orbitrap XL from Thermo Scientific (Thermo Fisher Scientific, Courtaboeuf, France) operated in positive ionisation mode. Where ESI-MS and APCI-MS were not suitable, mass spectrometric chromatograms were acquired using a Shimadzu GCMS-QP2010 SE gas chromatograph mass spectrometer.

Thin layer chromatography (TLC) was performed on Merck 60 F-254 silica gel and the chromatograms were examined under UV light ( $\lambda$  = 254 nm) and/or by staining of the TLC plate with a specific colour reagent (KMnO<sub>4</sub> and *p*-anisaldehyde) followed by heating with a heat gun. Flash column chromatography was performed using the indicated solvents on silica gel Merck Geduran SI 60 (40-63  $\mu$ m).

Melting points (m.p.) were determined with Stuart Scientific SMP3 melting point apparatus and have not been corrected.

Specific optical rotations  $[\alpha]_D$  values reported in 10<sup>-1</sup> (°·cm<sup>2</sup>·g<sup>-1</sup>) were measured on JASCO P-2000 polarimeter at 20 °C in a 10 cm cell using the sodium D line ( $\lambda$  = 589 nm); the concentration *c* in CHCl<sub>3</sub> is given as g/100 mL.

Enantiomeric ratios were determined by chiral gas chromatography (GC) measurement on an Agilent GC 7890A (Injector: 220°C, split ratio 20, FID detector: 300°C, H<sub>2</sub> as vector gas), and by chiral high-performance liquid chromatography (HPLC) measurement on a Shimadzu SIL-20AHT instrument (with *n*-heptane/*i*-PrOH mixture as mobile phase) in comparison with authentic racemic materials. The absolute configuration was determined by comparison with known compounds and for the new products it was assigned by analogy.

Finally, all new compounds were named using the program *Chemdraw* by *Cambridgesoft*. In addition, the references of this chapter have been included as footnotes for the sake of simplicity.

## 3.2. Preparation of Inorganic Salts in THF Solution

### **Preparation of ZnCl<sub>2</sub> solution:**

ZnCl<sub>2</sub> solution (1.5 M in THF) was prepared by drying ZnCl<sub>2</sub> (1.362 g, 10 mmol) in a Schlenk tube under high vacuum at 450 °C for 15 min. After cooling, dry THF (6.65 mL) was added and stirring was continued until all salts were dissolved.

### **Preparation of LiCl solution:**

LiCl solution (0.5 M in THF) was prepared by drying LiCl (212 mg, 5 mmol) in a Schlenk tube under high vacuum at 450 °C for 10 min. After cooling, dry THF (10 mL) was added and stirring was continued until all salts were dissolved.

### **Preparation of CuCN·2LiCl solution:**

CuCN·2LiCl solution (1.0 M in THF) was prepared by drying LiCl (254 mg, 6 mmol) in a Schlenk tube under high vacuum at 450 °C for 10 min. After cooling, was added CuCN (269 mg, 3 mmol) and the mixture was dried under high vacuum at 140 °C for 10 min. After cooling, dry THF (3 mL) was added and stirring was continued until all salts were dissolved.

### 3.3. Preparation of 1,1-diiodo alkanes

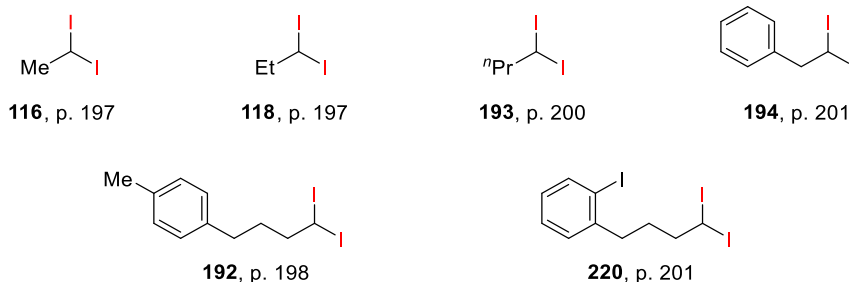
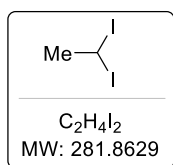


Chart of 1,1-diiodo alkanes prepared.

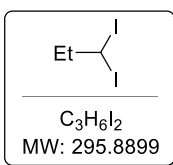
#### 1,1-diiodoethane (116):



According to a literature procedure,<sup>1</sup> 1,1-dichloroethane (15 mL, 177 mmol, 1.0 equiv) and iodoethane (43 mL, 531 mmol, 3.0 equiv) were added under argon atmosphere to a dry round-bottomed flask equipped with a stirring bar and reflux condenser. To this was added anhydrous  $AlCl_3$  (2.3 g, 17 mmol, 0.1 equiv), and the resulting mixture was refluxed heated at 80 °C for 30 min and then refluxed at 100 °C for 5 h. After that the mixture was cooled down to 0 °C and ~100 mL  $Et_2O$  were added, and the resulting mixture was washed with an aqueous satd. soln of  $Na_2S_2O_3$ . The biphasic mixture was separated, and the aqueous phase was extracted with diethyl ether (3×20 mL). The combined organic extracts were washed with brine, dried over  $MgSO_4$ , filtered, and concentrated under reduced pressure. Purification of the crude product by fractional distillation (75 °C at 25 mm Hg) afforded analytically pure **116** (36,0 g, 72% yield) as a pale-yellow liquid that rapidly turns red when exposed to light and/or heated.

<sup>1</sup>H NMR (400 MHz,  $CDCl_3$ )  $\delta$  5.2 (q,  $J = 6.7$  Hz, 1H), 2.9 (d,  $J = 6.7$  Hz, 3H). <sup>13</sup>C NMR (101 MHz,  $CDCl_3$ )  $\delta$  39.0, -38.5. Spectroscopic and physical properties are in good agreement with those previously reported.<sup>2</sup>

#### 1,1-diiodopropane (118):



According to a modified literature procedure,<sup>3</sup> a THF (4 mL) solution of  $CH_2I_2$  (1.2 mL, 15 mmol, 1.0 equiv) was added dropwise to NaHMDS (8 mL, ~ 1.9 M in THF, 15 mmol, 1.0 equiv) in  $Et_2O$  (12 mL) at -78 °C. After stirring 20 min at -78 °C, a THF (10

<sup>1</sup> R. L. Letsinger, C. W. Kammeyer, *J. Am. Chem. Soc.* **1951**, *73*, 4476.

<sup>2</sup> J. J. Mousseau, C. J. Morten, T. F. Jamison, *Chem. - Eur. J.* **2013**, *19*, 10004–10016.

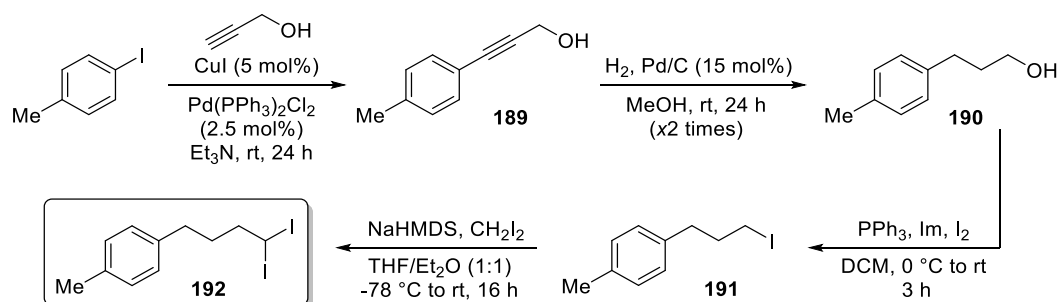
<sup>3</sup> J. A. Bull, A. B. Charette, *J. Org. Chem.* **2008**, *73*, 8097–8100.

mL) solution of iodoethane (6 mL, 75 mmol, 5.0 equiv) was added dropwise. The reaction mixture was allowed to warm slowly to rt over 16h in the dark. Water (80 mL) was added, and the mixture was extracted with CH<sub>2</sub>Cl<sub>2</sub> (3×40 mL). The combined organic layers were washed with aqueous sat. Na<sub>2</sub>S<sub>2</sub>O<sub>3</sub> solution, dried over MgSO<sub>4</sub>, filtered, and concentrated under reduced pressure. The residue was filtered through a plug of silica gel (pentane) and the filtrate reduced under reduced pressure to afford analytically pure **118** (3.6 g, 81% yield) as a pale-yellow liquid.

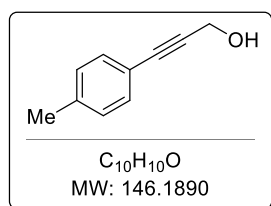
**<sup>1</sup>H NMR** (300 MHz, CDCl<sub>3</sub>) δ 5.14 (t, J = 6.0 Hz, 1H), 2.36 (qd, J = 7.1, 6.0 Hz, 2H), 0.96 (t, J = 7.1 Hz, 3H).  
**<sup>13</sup>C NMR** (75 MHz, CDCl<sub>3</sub>) δ 41.68, 16.65, -21.87. **IR** (ATR) 2967, 1451, 1377, 1327, 1262, 1200, 1095, 793, 621 cm<sup>-1</sup>. **MS** (EI, 70 eV) *m/z*: 296 (M<sup>+</sup>, 27%), 169 (100%), 127 (22%).

### Synthesis of 1-(4,4-diiodobutyl)-4-methylbenzene (**192**)

The following synthetic sequence was used:



### 3-(*p*-tolyl)prop-2-yn-1-ol (**189**):

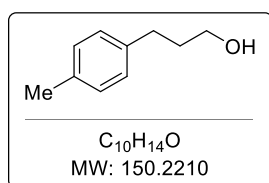


According to a literature procedure,<sup>4</sup> to a suspension of 4-iodotoluene (4.36 g, 20 mmol, 1.0 equiv), Pd(PPh<sub>3</sub>)<sub>2</sub>Cl<sub>2</sub> (351 mg, 0.5 mmol, 0.025 equiv), CuI (190 mg, 1 mmol, 0.05 equiv) in distilled Et<sub>3</sub>N (100 mL) was added dropwise propargyl alcohol (1.4 mL, 24 mmol, 1.2 equiv) under argon atmosphere and the reaction mixture was stirred 24 h at rt. Then to the reaction mixture was added aqueous sat. NH<sub>4</sub>Cl solution (30 mL) and extracted with CH<sub>2</sub>Cl<sub>2</sub> (3×30 mL). The combined organic layer was dried over MgSO<sub>4</sub>, filtered, and concentrated under reduced pressure. Purification of the crude material by flash column chromatography on silica gel (cyclohexane/EtOAc, 8:2) afforded analytically pure **189** (2.91 g, >99% yield) as yellow oil.

<sup>4</sup> N. Cabrera-Lobera, P. Rodríguez-Salamanca, J. C. Nieto-Carmona, E. Buñuel, D. J. Cárdenas, *Chem. Eur. J.* **2018**, *24*, 784–788.

**<sup>1</sup>H NMR** (300 MHz, CDCl<sub>3</sub>) δ 7.33 (d, *J* = 8.2 Hz, 2H), 7.12 (d, *J* = 7.9 Hz, 2H), 4.49 (d, *J* = 6.1 Hz, 2H), 2.35 (s, 3H), 1.67 (t, *J* = 6.1 Hz, 1H). **<sup>13</sup>C NMR** (CDCl<sub>3</sub>, 75 MHz) δ ppm 138.9, 131.9, 129.3, 119.7, 86.8, 86.1, 51.9, 21.7. The spectroscopic data are in good agreement with those reported previously in the literature.<sup>5</sup>

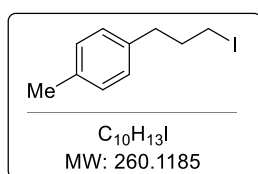
### 3-(*p*-tolyl)propan-1-ol (**190**):



According to a modified literature procedure,<sup>6</sup> a solution of **189** (2.915 g, 20 mmol, 1.0 equiv) and Pd/C (320 mg, 3 mmol 10 wt.% loading, 0.15 equiv) in methanol (100 mL) was stirred under a hydrogen atmosphere at rt for 24 h. Then the reaction mixture was filtered through celite and concentrated under reduced pressure. A mixture of the corresponding alkane and alkene was obtained. For this reason, the same reaction and work-up was repeated another time to afford analytically pure **3** (3.0 g, >99% yield) as brownish oil.

**<sup>1</sup>H NMR** (300 MHz, CDCl<sub>3</sub>) δ 7.10 (s, 4H), 3.68 (t, *J* = 6.4 Hz, 2H), 2.74 – 2.62 (m, 2H), 2.33 (s, 3H), 1.96 – 1.82 (m, 2H), 1.41 (bs, 1H). **<sup>13</sup>C NMR** (75 MHz, CDCl<sub>3</sub>): δ 138.6, 135.1, 128.9, 128.2, 61.9, 34.2, 31.5, 20.3. The spectroscopic data are in good agreement with those reported previously in the literature.<sup>7</sup>

### 1-(3-iodopropyl)-4-methylbenzene (**191**):



According to a literature procedure,<sup>8</sup> to a solution of **190** (3.0 g, 20 mmol, 1.0 equiv) in dichloromethane (80 mL) at 0 °C, were added in this order PPh<sub>3</sub> (5.5 g, 21 mmol, 1.05 equiv), imidazole (2.7 g, 40 mmol, 2.0 equiv) and finally I<sub>2</sub> (5.6 g, 22 mmol, 1.1 equiv). After 5 min at 0 °C, the mixture was stirred at rt for 3 h. The reaction was quenched by addition of an aqueous sat. Na<sub>2</sub>S<sub>2</sub>O<sub>3</sub> solution until loss of colour. Then the reaction mixture was extracted with CH<sub>2</sub>Cl<sub>2</sub> (3×30 mL), the combined organic phases were dried over MgSO<sub>4</sub>, filtered, and concentrated to 10 mL under reduced pressure. After addition of 100 mL of pentane the mixture was filtered through a plug silica gel, washed with pentane, and concentrated under reduced pressure to recover analytically pure **191** (4.16 g, 80% yield) as a colourless oil.

<sup>5</sup> C. B. Kelly, K. M. Lambert, M. A. Mercadante, J. M. Ovian, W. F. Bailey, N. E. Leadbeater, *Angew. Chem. Int. Ed.* **2015**, *54*, 4241–4245.

<sup>6</sup> D. J. Baek, N. MacRitchie, N. G. Anthony, S. P. Mackay, S. Pyne, N. Pyne, R. Bittman, *J. Med. Chem.* **2013**, *56*, 9310–9327.

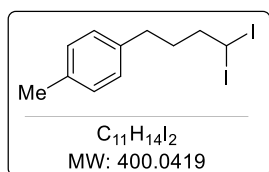
<sup>7</sup> H. Takakura, R. Kojima, M. Kamiya, E. Kobayashi, T. Komatsu, T. Ueno, T. Terai, K. Hanaoka, T. Nagano, Y. Urano, *J. Am. Chem. Soc.* **2015**, *137*, 4010–4013.

<sup>8</sup> B. R. Brutiu, W. A. Bubeneck, O. Cvetkovic, J. Li, N. Maulide, *Monatshefte Für Chemie* **2019**, *150*, 3–10.



**<sup>1</sup>H NMR** (300 MHz, CDCl<sub>3</sub>) δ 7.14 – 7.06 (m, 4H), 3.18 (t, *J* = 6.8 Hz, 2H), 2.70 (t, *J* = 7.3 Hz, 2H), 2.33 (s, 3H), 2.12 (p, *J* = 7.0 Hz, 2H). **<sup>13</sup>C NMR** (75 MHz, CDCl<sub>3</sub>): δ 137.5, 135.8, 129.3, 128.6, 35.9, 35.2, 21.2, 6.6. The spectroscopic data are in good agreement with those reported previously in the literature.<sup>5</sup>

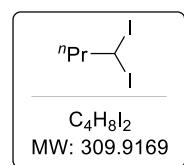
### 1-(4,4-diiodobutyl)-4-methylbenzene (**192**):



According to a modified literature procedure,<sup>3</sup> a THF (10 mL) solution of CH<sub>2</sub>I<sub>2</sub> (4 mL, 50 mmol, 5.0 equiv) was added dropwise to NaHMDS (26 mL, ~ 1.9 M in THF, 50 mmol, 5.0 equiv) in THF (54 mL) and ether (80 mL) at -78 °C. After stirring 20 min at -78 °C, a THF (20 mL) solution of **191** (2.6 g, 10 mmol, 1.0 equiv) was added dropwise. The reaction mixture was allowed to warm slowly to rt over 16 h in the dark. Water (100 mL) was added, and the mixture was extracted with CH<sub>2</sub>Cl<sub>2</sub> (3×50 mL). The combined organic layers were washed with brine, dried over MgSO<sub>4</sub>, filtered, and concentrated under reduced pressure. Purification of the crude product by flash column chromatography on silica gel (pentane) afforded analytically pure **192** (3.68 g, 92% yield) as a pale-orange solid.

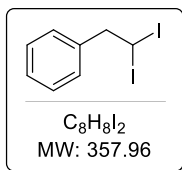
**<sup>1</sup>H NMR** (300 MHz, CDCl<sub>3</sub>) δ 7.16 – 7.03 (m, 4H), 5.11 (t, *J* = 6.5 Hz, 1H), 2.64 (t, *J* = 7.6 Hz, 2H), 2.44 – 2.30 (m, 5H), 1.84 – 1.68 (m, 2H). **<sup>13</sup>C NMR** (75 MHz, CDCl<sub>3</sub>) δ 138.1, 135.5, 129.2, 128.3, 47.6, 33.6, 33.4, 21.2, -25.3. **IR** (ATR) 2983, 2939, 2920, 1514, 1455, 1420, 1328, 1144, 1109, 1089, 947, 838, 800, 752, 741 cm<sup>-1</sup>. **MS** (EI, 70 eV) *m/z*: 400 (M<sup>+</sup>, 1%), 145 (51%), 105 (100%), 77 (19%).

### 1,1-diiodobutane (**193**):



According to a modified literature procedure,<sup>3</sup> a THF (4 mL) solution of CH<sub>2</sub>I<sub>2</sub> (1.2 mL, 15 mmol, 1.0 equiv) was added dropwise to NaHMDS (8 mL, ~ 1.9 M in THF, 15 mmol, 1.0 equiv) in Et<sub>2</sub>O (12 mL) at -78 °C. After stirring 20 min at -78 °C, a THF (5 mL) solution of 1-iodopropane (4.4 mL, 45 mmol, 3.0 equiv) was added dropwise. The reaction mixture was allowed to warm slowly to r.t. over 16h in the dark. Water (80 mL) was added, and the mixture was extracted with CH<sub>2</sub>Cl<sub>2</sub> (3×40 mL). The combined organic layers were washed with aqueous sat. Na<sub>2</sub>S<sub>2</sub>O<sub>3</sub> solution, dried over MgSO<sub>4</sub>, filtered, and concentrated under reduced pressure. The residue was filtered through a plug of silica gel (pentane) and the filtrate reduced under reduced pressure to afford 3.7 analytically pure **193** (3.7 g, 80% yield) as a yellow liquid.

**<sup>1</sup>H NMR** (300 MHz, CDCl<sub>3</sub>) δ 5.12 (t, *J* = 6.5 Hz, 1H), 2.39 – 2.29 (m, 2H), 1.44 (h, *J* = 7.4 Hz, 2H), 0.95 (t, *J* = 7.4 Hz, 3H). **<sup>13</sup>C NMR** (75 MHz, CDCl<sub>3</sub>) δ 50.3, 25.3, 12.2, -25.1. **IR** (ATR) 2957, 1460, 1248, 1190, 1102, 1072, 745, 616 cm<sup>-1</sup>. **MS** (EI, 70 eV) *m/z*: 310 (M<sup>+</sup>, 8%), 183 (27%), 127 (7%), 55 (100%).

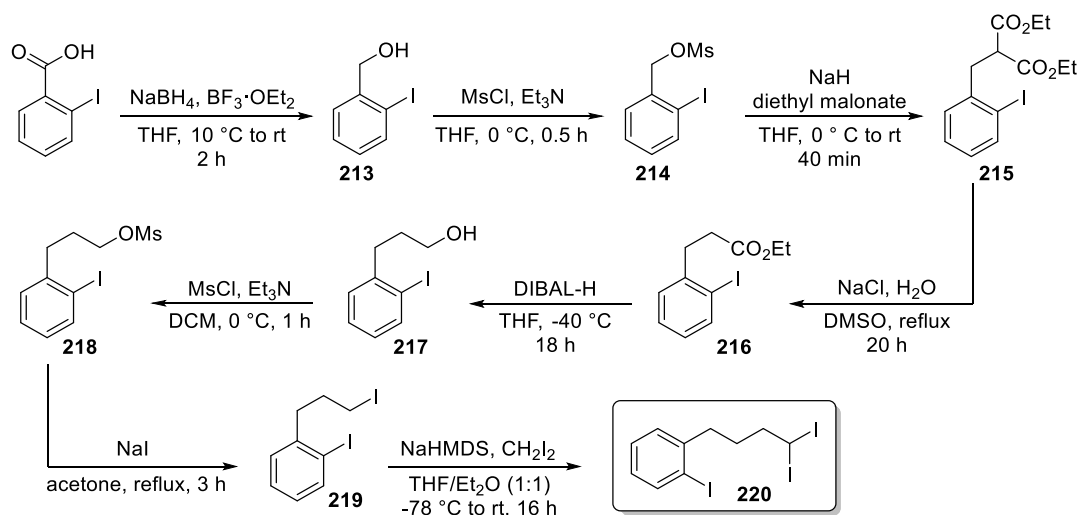
**(2,2-diiodoethyl)benzene (194):**

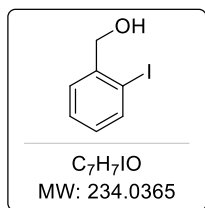
According to a literature procedure,<sup>3</sup> a THF (10 mL) solution of  $CH_2I_2$  (1.7 mL, 21 mmol, 2.05 equiv) was added dropwise to LiHMDS (20 mL, ~ 1.0 M in THF, 20 mmol, 2.0 equiv) in diethyl ether (20 mL) at  $-78\text{ }^\circ\text{C}$ . After stirring 20 min at  $-78\text{ }^\circ\text{C}$ , a THF (10 mL) solution of benzyl bromide (1.2 mL, 10 mmol, 1.0 equiv) was added dropwise. The reaction mixture was allowed to warm slowly to r.t. over 16 h in the dark. Water (70 mL) was added, and the mixture was extracted with  $CH_2Cl_2$  ( $3 \times 50$  mL). The combined organic layers were washed with brine, dried over  $MgSO_4$ , filtered, and concentrated under reduced pressure. Purification of the crude product by flash column chromatography on silica gel (pentane) afforded analytically pure **194** (3.02 g, 84% yield) as yellow viscous solid, which rapidly turns orange and then red when exposed to light and/or heated.

**$^1H$  NMR** (400 MHz,  $CDCl_3$ )  $\delta$  7.47 – 7.39 (m, 3H), 7.33 – 7.27 (m, 2H), 5.15 (t,  $J = 7.4$  Hz, 1H), 3.83 (d,  $J = 7.4$  Hz, 2H).  **$^{13}C$  NMR** (101 MHz,  $CDCl_3$ )  $\delta$  139.7, 128.9, 128.7, 127.6, 54.1,  $-25.6$ . The spectroscopic data are in good agreement with those reported previously in the literature.<sup>3</sup>

**Synthesis of 1-(4,4-diiodobutyl)-2-iodobenzene (220)**

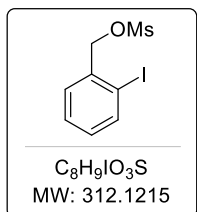
The following synthetic sequence was used:



**(2-iodophenyl)methanol (213):**

According to a modified literature procedure,<sup>9</sup> to a solution of 2-iodobenzoic acid (7.440 g, 30 mmol, 1.0 equiv) in THF (40 mL) was added in one portion NaBH<sub>4</sub> (2.270 g, 60 mmol, 2.0 equiv) at 10 °C and after was added slowly at the same temperature BF<sub>3</sub>·OEt<sub>2</sub> (7.4 mL, 60 mmol, 2.0 equiv). The mixture was vigorously stirred at 10 °C for 1 h and then 2 h at rt. Then the reaction mixture was cooled to 0 °C and MeOH (20 mL) was added slowly, followed by 1 M HCl (20 mL), and the aqueous layer was separated and extracted with EtOAc (3×30 mL). The combined organic extracts were washed with brine (20 mL), dried over MgSO<sub>4</sub>, filtered, and concentrated under reduced pressure to give a white solid as crude product, which was used directly in the next step without any further purification.

<sup>1</sup>H NMR (300 MHz, CDCl<sub>3</sub>) δ 7.82 (d, *J* = 7.9 Hz, 1H), 7.46 (d, *J* = 7.6 Hz, 1H), 7.36 (t, *J* = 7.5 Hz, 1H), 7.00 (t, *J* = 7.6 Hz, 1H), 4.67 (s, 2H), 2.18 (s, 1H). The spectroscopic data are in good agreement with those reported previously in the literature.<sup>10</sup>

**2-iodobenzyl methanesulfonate (214):**

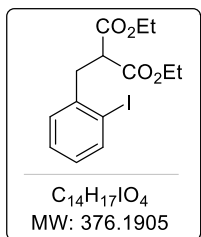
According to a literature procedure,<sup>11</sup> methanesulfonyl chloride (2.4 mL, 31 mmol) was added slowly at 0 °C to a solution of the above crude **213** (6.55 g, 28 mmol) and triethylamine (5.9 mL, 42 mmol) in THF (45 mL). After stirring for 30 min, the reaction was quenched with water (20 mL), the aqueous phase was separated and extracted with DCM (3×30 mL). The combined organic layers were washed dried over MgSO<sub>4</sub>, filtered, and concentrated under reduced pressure to give a yellow oil as crude product.

<sup>1</sup>H NMR (300 MHz, CDCl<sub>3</sub>) δ 7.92 – 7.83 (m, 1H), 7.52 – 7.43 (m, 1H), 7.44 – 7.33 (m, 1H), 7.13 – 7.02 (m, 1H), 5.26 (s, 2H), 3.02 (s, 3H). The spectroscopic data are in good agreement with those reported previously in the literature.<sup>11</sup> The crude product was used directly in the next step without any further purification.

<sup>9</sup> J. Bello-García, D. Padín, J. A. Varela, C. Saá, *Org. Lett.* **2021**, *23*, 5539–5544.

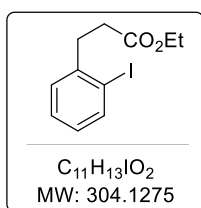
<sup>10</sup> T. V. Q. Nguyen, W.-J. Yoo, S. Kobayashi, *Adv. Synth. Catal.* **2016**, *358*, 452–458.

<sup>11</sup> H. Kim, K. Inoue, J.-I. Yoshida, *Angew. Chem. Int. Ed.* **2017**, *56*, 7863–7866.

**Diethyl 2-(2-iodobenzyl)malonate (215):**

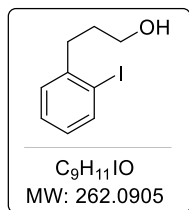
According to a literature procedure,<sup>11</sup> to a solution of NaH 60% dispersion in mineral oil (7.440 g, 31 mmol) in THF (55 mL) at 0 °C was added slowly diethyl malonate (4.965 g, 31 mmol). After 5 min stirring, the above crude 2-iodobenzyl methanesulfonate was added slowly at the same temperature and then the reaction mixture was stirred 40 min at room temperature. Then the reaction mixture was quenched with saturated  $NH_4Cl$  aqueous solution (30 mL) and water (30 mL). The aqueous layer was separated and extracted with EtOAc (3×30 mL). The combined organic extracts were dried over  $MgSO_4$ , filtered, and concentrated under reduced pressure to give a yellow oil as crude product.

**$^1H$  NMR** (400 MHz,  $CDCl_3$ )  $\delta$  7.85 – 7.79 (m, 1H), 7.28 – 7.22 (m, 2H), 6.96 – 6.87 (m, 1H), 4.25 – 4.13 (m, 4H), 3.83 (t,  $J = 7.8$  Hz, 1H), 3.33 (d,  $J = 7.8$  Hz, 2H), 1.22 (t,  $J = 7.1$  Hz, 6H). The spectroscopic data are in good agreement with those reported previously in the literature.<sup>11</sup> The crude product was used directly in the next step without any further purification.

**Ethyl 3-(2-iodophenyl)propanoate (216):**

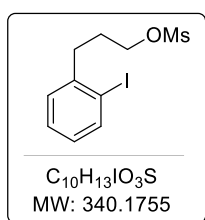
According to a literature procedure,<sup>11</sup> to a solution of the above crude **215** and NaCl (1.440 g, 59 mmol) was added water (1.1 mL, 59 mmol) and DMSO (36 mL) and the mixture was refluxed at 190 °C for 20 h. Then the reaction was cooled down to room temperature and was quenched with 1 M HCl (20 mL) and water (30 mL). The aqueous layer was separated and extracted with EtOAc (3×30 mL), and the combined organic extracts were dried over  $MgSO_4$ , filtered, and concentrated under reduced pressure to give an orange oil as crude product.

**$^1H$  NMR** (300 MHz,  $CDCl_3$ )  $\delta$  7.84 – 7.78 (m, 1H), 7.28 – 7.21 (m, 2H), 6.92 – 6.84 (m, 1H), 4.13 (q,  $J = 7.1$  Hz, 2H), 3.07 – 3.01 (m, 2H), 2.64 – 2.58 (m, 2H), 1.24 (t,  $J = 7.1$  Hz, 3H). The spectroscopic data are in good agreement with those reported previously in the literature.<sup>11</sup> The crude product was used directly in the next step without any further purification.

**3-(2-iodophenyl)propan-1-ol (217):**

According to a literature procedure,<sup>11</sup> to a solution of the above crude ethyl 3-(2-iodophenyl)propanoate in THF (35 mL) was added slowly DIBAL-H (85 mL, 1.0 M in toluene, 85 mmol) at -40 °C and the reaction mixture was stirred at the same temperature for 18 h. Then the reaction was quenched with cold 1 M HCl (30 mL), the aqueous layer was separated and extracted with EtOAc (3×20 mL), and the combined organic extracts were dried over MgSO<sub>4</sub>, filtered, and concentrated under reduced pressure. Purification of the crude product by flash column chromatography (pentane/EtOAc, 7:3) afforded analytically pure **217** (4.2 g, 53% yield over 5 steps) as a colourless oil.

**<sup>1</sup>H NMR** (400 MHz, CDCl<sub>3</sub>) δ 7.82 – 7.78 (m, 1H), 7.29 – 7.19 (m, 2H), 6.91 – 6.82 (m, 1H), 3.70 (t, *J* = 6.4 Hz, 2H), 2.84 – 2.76 (m, 2H), 2.06 (bs, 1H), 1.91 – 1.82 (m, 2H). **<sup>13</sup>C NMR** (101 MHz, CDCl<sub>3</sub>) δ 144.4, 139.6, 129.5, 128.4, 127.9, 100.7, 62.1, 37.1, 33.1. The spectroscopic data are in good agreement with those reported previously in the literature.<sup>12</sup>

**3-(2-iodophenyl)propyl methanesulfonate (218):**

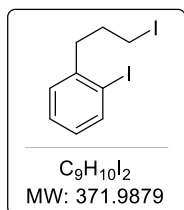
According to a literature procedure,<sup>13</sup> methanesulfonyl chloride (1.4 mL, 18 mmol) was added slowly at 0 °C to a solution of **217** (3.95 g, 15 mmol) and triethylamine (4.8 mL, 34.5 mmol) in dichloromethane (15 mL). After stirring for 30 min, the reaction was quenched with water (30 mL), the aqueous phase was separated and extracted with DCM (3×30 mL). The combined organic layers were washed dried over MgSO<sub>4</sub>, filtered, and concentrated under reduced pressure to give a yellow oil as crude product.

**<sup>1</sup>H NMR** (300 MHz, CDCl<sub>3</sub>) 7.84 – 7.77 (m, 1H), 7.32 – 7.17 (m, 2H), 6.95 – 6.84 (m, 1H), 4.26 (t, *J* = 6.3 Hz, 2H), 3.01 (s, 3H), 2.89 – 2.80 (m, 2H), 2.11 – 1.99 (m, 4H). The spectroscopic data are in good agreement with those reported previously in the literature.<sup>14</sup> The crude product was used directly in the next step without any further purification.

<sup>12</sup> J. Tummatorn, G. B. Dudley, *Org. Lett.* **2011**, *13*, 1572–1575.

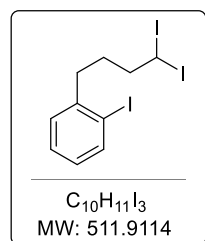
<sup>13</sup> A. Minatti, S. L. Buchwald, *Org. Lett.* **2008**, *10*, 2721–2724.

<sup>14</sup> R. Willand-Charnley, B. W. Puffer, P. H. Dussault, *J. Am. Chem. Soc.* **2014**, *136*, 5821–5823.

**1-iodo-2-(3-iodopropyl)benzene (219):**

According to a modified literature procedure,<sup>14</sup> to a solution of the above crude ethyl **218** in acetone (60 mL) was added NaI (11.24 g, 75 mmol) and the mixture was stirred at reflux for 3 h. Then the reaction mixture was cooled down to room temperature and was added water (30 mL). The aqueous layer was separated and extracted with EtOAc (3×20 mL), and the combined organic extracts were dried over MgSO<sub>4</sub>, filtered, and concentrated under reduced pressure and the crude material was purified by filtration through a plug silica gel (pentane) recovering analytically pure **219** (5.1 g, 91% yield over 2 steps) as a colourless oil.

<sup>1</sup>H NMR (300 MHz, CDCl<sub>3</sub>) 7.86 – 7.78 (m, 1H), 7.33 – 7.21 (m, 2H), 6.97 – 6.86 (m, 1H), 3.23 (t, *J* = 6.8 Hz, 2H), 2.89 – 2.80 (m, 2H), 2.13 (p, *J* = 7.0 Hz, 2H). <sup>13</sup>C NMR (75 MHz, CDCl<sub>3</sub>) δ 143.2, 139.8, 129.8, 128.5, 128.2, 100.7, 41.4, 33.7, 6.0. The spectroscopic data are in good agreement with those reported previously in the literature.<sup>15</sup>

**1-(4,4-diiodobutyl)-2-iodobenzene (220):**

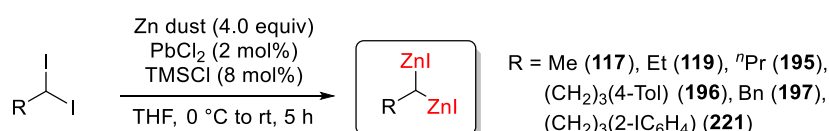
According to a modified procedure,<sup>3</sup> A solution of CH<sub>2</sub>I<sub>2</sub> (5.2 mmol, 65 mmol) in THF (15 mL) was added dropwise to a solution of NaHMDS (34.2 mL, ~ 1.9 M in THF, 65 mmol) in Et<sub>2</sub>O (60 mL) at –78 °C. After 20 min at –78 °C, a solution of **219** (4.85 g, 13 mmol) in THF (20 mL) was added dropwise at the same temperature. After complete addition the reaction mixture was allowed to warm slowly to room temperature over 16 h in the dark. Water (100 mL) was added, and the mixture was extracted with dichloromethane (3×50 mL). The combined organic layers were washed with saturated Na<sub>2</sub>S<sub>2</sub>O<sub>3</sub> aqueous solution (30 mL), dried over MgSO<sub>4</sub>, filtered, and concentrated under reduced pressure. Purification of the crude product by flash column chromatography (pentane) afforded analytically pure **220** (5.4 g, 81% yield) as a yellow-orange solid.

<sup>1</sup>H NMR (400 MHz, CDCl<sub>3</sub>) δ 7.86 – 7.80 (m, 1H), 7.33 – 7.27 (m, 1H), 7.24 – 7.19 (m, 1H), 6.95 – 6.88 (m, 1H), 5.15 (t, *J* = 6.4 Hz, 1H), 2.82 – 2.75 (m, 2H), 2.50 – 2.43 (m, 2H), 1.82 – 1.71 (m, 2H). <sup>13</sup>C NMR (101 MHz, CDCl<sub>3</sub>) δ 143.94, 139.72, 129.47, 128.58, 128.16, 100.70, 47.68, 38.81, 32.45, –26.22. IR (ATR) 2984, 2945, 1464, 1453, 1434, 1330, 1255, 1150, 1115, 1080, 1030, 1010 cm<sup>-1</sup>. MS (EI, 70 eV) *m/z*: 512 (M<sup>+</sup>, 0.2%), 386 (0.2%), 217 (15%), 131 (100%), 91 (39%), 51 (17%).

<sup>15</sup> L. Ripa, L. A. Hallberg, *J. Org. Chem.* **1996**, *61*, 7147–7155.

### 3.4. Preparation of 1,1-Bis(iodozincio)alkanes

#### 3.4.1. General Procedure for the preparation of 1,1-Bis(iodozincio) Alkanes (GP1)



To a THF (1 mL) suspension of Zn dust (1.3 g, 20 mmol, 4 equiv) and PbCl<sub>2</sub> (28 mg, 0.1 mmol, 0.02 equiv) under argon atmosphere, was added trimethylsilyl chloride (0.05 mL, 0.4 mmol), and the mixture was stirred for 10 minutes at rt. The mixture was cooled down to 0 °C and was added dropwise a THF (4 mL) solution of 1,1-diodoalkane (5 mmol) over 2 h. After complete addition, the resulting mixture was stirred for 3 h at rt. The excess of zinc was removed by centrifugation and the supernatant was transferred in an oven-dried flask and stored under a positive pressure of argon at -20 °C. The reagent was titrated with I<sub>2</sub> to determine the corresponding title.<sup>16</sup>

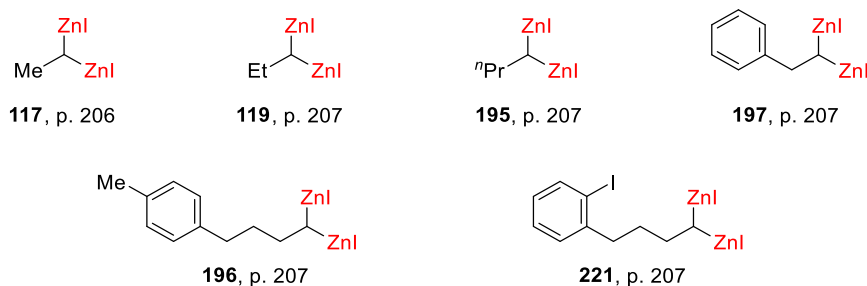
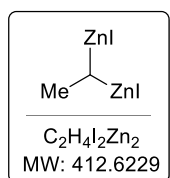


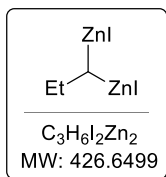
Chart of 1,1-(diiodozincio)alkanes synthesized via **GP1**.

#### 1,1-(diiodozincio)ethane (**117**):

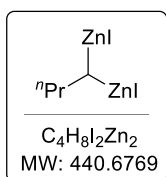


Prepared according to **GP1**, from 1,1-diodoethane **116** (1.409 g, 5 mmol, 1.0 equiv) as a pale-grey THF solution. Concentration of ~0.4 – 0.5 M was routinely obtained.

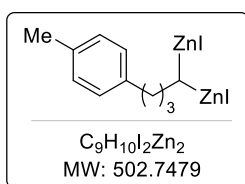
<sup>16</sup> A. Krasovskiy, P. Knochel, *Synthesis* **2006**, 2006, 890–891.

**1,1-(diiodozincio)propane (119):**

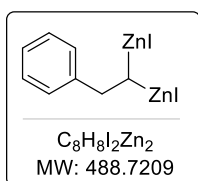
Prepared according to **GP1**, from 1,1-diiodopropane **118** (1.479 g, 5 mmol, 1.0 equiv) as a pale-grey THF solution. Concentration of ~0.4 – 0.5 M was routinely obtained.

**1,1-(diiodozincio)butane (195):**

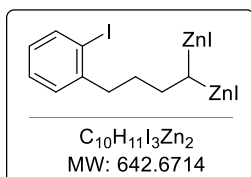
Prepared according to **GP1**, from 1,1-diiodobutane **193** (1.549 g, 5 mmol, 1.0 equiv) as a pale yellow-grey THF solution. Concentration of ~0.5 – 0.6 M was routinely obtained.

**1,1-(diiodozincio)-4-(4-methyl-phenyl)butane (196):**

Prepared according to **GP1**, from **192** (2.0 g, 5 mmol, 1.0 equiv) as an orange-red THF solution. Concentration of ~0.4 – 0.5 M was routinely obtained.

**1,1-(diiodozincio)-2-phenylethane (1):**

Prepared according to **GP1**, from (2,2-diiodoethyl)benzene (1.790 g, 5 mmol, 1.0 equiv) as an orange THF solution. Concentration of ~0.6 M was obtained.

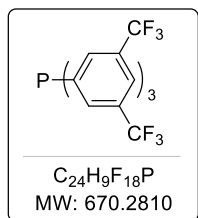
**1,1-(diiodozincio)-4-(2-iodophenyl)butane (221):**

Prepared according to **GP1**, from **220** (1.790 g, 5 mmol, 1.0 equiv) as an orange-red THF solution. Concentration of ~ 0.32 M was obtained.



### 3.5. Synthesis of Ligands

#### Tris(3,5-bis(trifluoromethyl)phenyl)phosphane (L17):



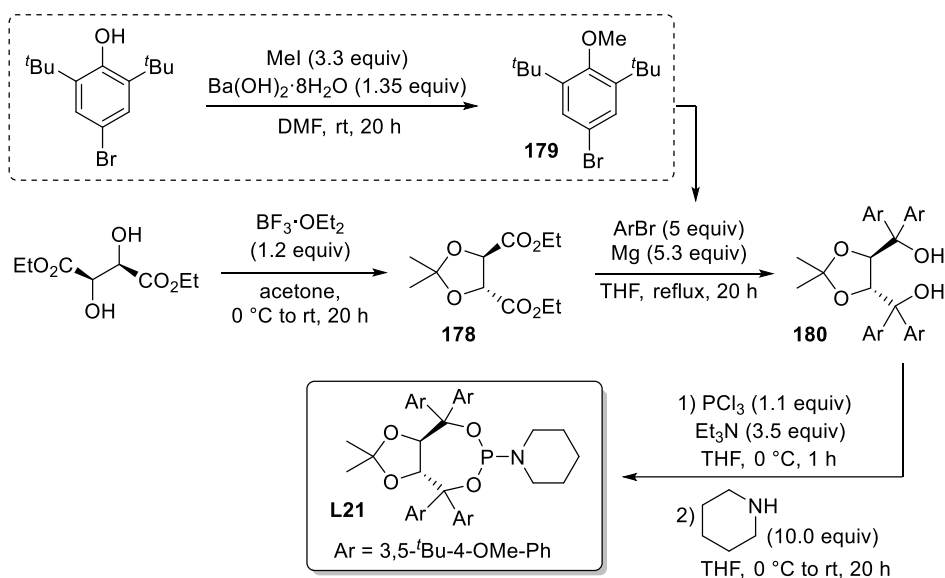
According to a literature procedure,<sup>17</sup> a solution of 1-bromo-3,5-bis(trifluoromethyl)benzene (3.620 mL, 21.0 mmol, 3.0 equiv) in anhydrous  $Et_2O$  (15 mL) was added dropwise to a suspension of magnesium turnings (730 mg, 30.0 mmol, 4.3 equiv) in anhydrous  $Et_2O$  (10 mL) and some grains of  $I_2$ . The reaction mixture was then refluxed for 2 h before cooling down to 0 °C. To the dark orange solution containing the Grignard reagent was carefully added dropwise a solution of phosphorus trichloride (0.610 mL, 7.0 mmol, 1.0 equiv) in anhydrous diethyl ether (10 mL). After complete addition, the mixture was refluxed for 1 h. Then the orange suspension obtained was cooled down to 0 °C and 10% aqueous HCl (30 mL) was added slowly. The aqueous phase was separated and extracted with  $Et_2O$  (3×15 mL). The organic fractions were combined and dried over anhydrous  $MgSO_4$ , filtered and concentrated under reduced pressure. Purification of the crude product by flash column chromatography on silica gel (pentane) afforded analytically pure **L17** (3.99 g, 85% yield) as a white solid.

**$^1H$  NMR** (400 MHz,  $CDCl_3$ )  $\delta$  7.98 (s, 3H), 7.75 (d,  $J = 7.0$  Hz, 6H).  **$^{13}C$  NMR** (101 MHz,  $CDCl_3$ )  $\delta$  137.6 (d,  $J = 17.5$  Hz), 133.4 (bd,  $J = 22.0$  Hz), 133.1 (qd,  $J = 33.9, 6.8$  Hz), 124.7–124.5 (m), 122.9 (q,  $J = 273.2$  Hz).  **$^{19}F$  NMR** (376 MHz,  $CDCl_3$ )  $\delta$  -63.3.  **$^{31}P$  NMR** (162 MHz,  $CDCl_3$ )  $\delta$  -4.1. Physical and spectroscopic data were in good agreement with those previously reported.<sup>17</sup>

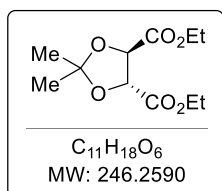
<sup>17</sup> D. Herrera, D. Peral, M. Córdón, J. C. Bayón, *Eur. J. Inorg. Chem.* **2021**, 354-363.

## Synthesis of enantiopure ligand L21

The following synthetic sequence was used:



### Diethyl (4*R*,5*R*)-2,2-dimethyl-1,3-dioxolane-4,5-dicarboxylate (178):

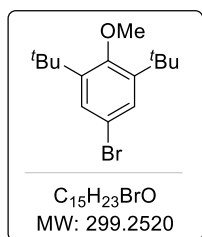


According to a literature procedure,<sup>18</sup> an oven-dried round-bottom flask was charged with (+)-diethyl *L*-tartrate (4.124 g, 20.0 mmol, 1.0 equiv, ee >99%) and 30 mL of acetone under argon atmosphere. A solution 46.5% of  $BF_3 \cdot Et_2O$  (6.4 mL, 24.0 mmol, 1.2 equiv) was added dropwise at 0 °C, and after complete addition the mixture was stirred at rt overnight. The reaction was quenched with 150 mL of sat. aqueous  $NaHCO_3$ , and the aqueous layer was extracted with EtOAc (3×40 mL). The combined organic fractions were washed with water, dried over anhydrous  $MgSO_4$ , filtered, and concentrated under reduced pressure. Purification of the crude product by flash column chromatography on silica gel (cyclohexane/EtOAc, 85:15) afforded analytically pure **178** (3.659 g, 74% yield) as a yellow oil.

**<sup>1</sup>H NMR** (400 MHz,  $CDCl_3$ )  $\delta$  4.75 (s, 2H), 4.27 (q,  $J = 7.1$  Hz, 4H), 1.49 (s, 6H), 1.30 (t,  $J = 7.1$  Hz, 6H).  
**<sup>13</sup>C NMR** (101 MHz,  $CDCl_3$ )  $\delta$  169.8, 113.9, 77.3, 62.0, 26.5, 14.2. The spectral data was in good agreement with that previously reported.<sup>19</sup>

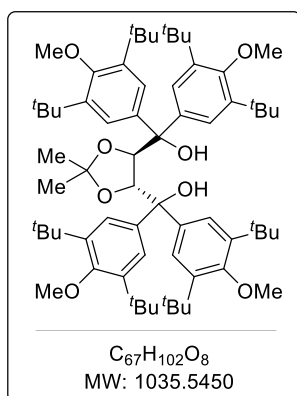
<sup>18</sup> Y.-X. Wang, S.-L. Qi, Y.-X. Luan, X.-W. Han, S. Wang, H. Chen, M. Ye, *J. Am. Chem. Soc.* 2018, 140, 5360–5364.

<sup>19</sup> R. A. Fernandes, *Eur. J. Org. Chem.* 2007, 5064–5070.

**5-Bromo-1,3-di-*tert*-butyl-2-methoxybenzene (179):**

According to a literature procedure,<sup>20</sup> an oven-dried flask equipped with stirring bar was charged with barium hydroxide octahydrate (4.26 g, 13.5 mmol, 1.35 equiv) and 4-bromo-2,6-di-*tert*-butylphenol (2.85 g, 10.0 mmol, 1.0 equiv) under argon atmosphere. Then was added DMF (35 mL) and the mixture was stirred at rt for 3 minutes. After that, iodomethane (2.05 mL, 33.0 mmol, 3.3 equiv) was added and the reaction was stirred at rt for 20 h. Then the insoluble salts were filtered off and washed with Et<sub>2</sub>O. The filtrate was washed with water, aq. NaOH 1 M (30 mL), brine, dried over MgSO<sub>4</sub>, filtered, and concentrated under reduced pressure. Purification of the crude product by flash column chromatography (pentane) afforded analytically pure **179** (2.09 g, 70% yield) as a colourless oil, which solidifies at rt.

<sup>1</sup>H NMR (400 MHz, CDCl<sub>3</sub>) δ 7.33 (s, 2H), 3.68 (s, 3H), 1.41 (s, 18H). <sup>13</sup>C NMR (101 MHz, CDCl<sub>3</sub>) δ 158.9, 146.2, 129.7, 116.5, 64.5, 36.1, 32.0. The spectral data was in good agreement with that previously reported.<sup>20</sup>

**((4*R*,5*R*)-2,2-dimethyl-1,3-dioxolane-4,5-diyl)-bis-(bis (3,5-di-*tert*-butyl-4 methoxyphenyl) methanol) (180):**

According to a literature procedure,<sup>21</sup> An oven-dried two-neck round bottom flask equipped with a magnetic stirring bar and a reflux condenser was charged with activated magnesium turnings (139 mg, 5.3 mmol), one grain of I<sub>2</sub> and anhydrous THF (2 mL). A solution of the aryl bromide **179** (1.496 g, 5 mmol, 5.0 equiv) in anhydrous THF (5 mL) was added dropwise to initiate the reaction (may need a warm of an oil bath or heat gun). When the colour of the solution disappeared, the remaining solution was added slowly, and the reaction mixture was refluxed for 2 h. After that the reaction mixture was cooled down to rt, and a solution of isopropylidene-protected diethyl tartrate **178** (246 mg, 1 mmol, 1.0 equiv) in anhydrous THF (4 mL) was added slowly. After complete addition, the reaction mixture was refluxed 20 h and then cooled down to rt. The reaction mixture was carefully quenched with sat. NH<sub>4</sub>Cl solution (4 mL), HCl (1 M, 1 mL) and water (5 mL). The aqueous layer was separated and extracted with diethyl ether (3×10 mL). The combined organic extracts were washed with brine, dried over MgSO<sub>4</sub>, filtered, and concentrated under reduced pressure. Purification of the

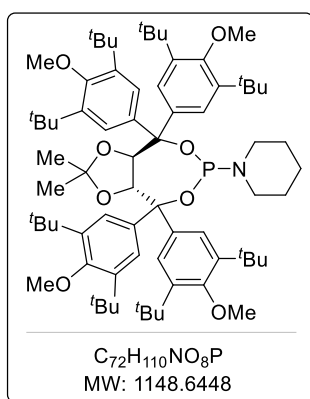
<sup>20</sup> N. Ukwitegetse, J. R. Sommer, P. J. G. Saris, R. Haiges, P. I. Djurovich, M. E. Thompson, *Chem. Eur. J.* **2019**, *25*, 1472–1475.

<sup>21</sup> Y.-X. Wang, S.-L. Qi, Y.-X. Luan, X.-W. Han, S. Wang, H. Chen, M. Ye, *J. Am. Chem. Soc.* **2018**, *140*, 5360–5364.

crude product by flash column chromatography in silica gel (cyclohexane/EtOAc, 98:2) afforde the corresponding TADDOL (970 mg, 94% yield) as yellow/orange solid.

**<sup>1</sup>H NMR** (300 MHz, CDCl<sub>3</sub>) δ 7.36 (s, 4H), 7.21 (s, 4H), 4.72 (s, 2H), 3.65 (s, 6H), 3.62 (s, 6H), 3.26 (bs, 2H), 1.41 (s, 36H), 1.31 (s, 36H), 0.93 (s, 6H). **<sup>13</sup>C NMR** (75 MHz, CDCl<sub>3</sub>) δ 158.6, 158.56, 158.52, 158.1, 157.9, 142.5, 142.3, 141.8, 141.7, 141.6, 141.3, 141.0, 140.9, 140.0, 137.0, 136.88, 136.85, 136.21, 136.20, 127.7, 127.2, 126.3, 125.9, 125.8, 109.9, 109.0, 83.5, 83.4, 83.3, 83.1, 82.1, 82.0, 81.7, 81.28, 81.26, 78.5, 77.4, 64.4, 64.24, 64.20, 64.1, 45.3, 45.0, 36.1, 35.98, 35.95, 35.89, 35.86, 32.44, 32.37, 32.32, 32.30, 32.22, 32.15, 27.9, 27.6, 27.5, 27.1, 25.5, 24.4. **IR** (ATR) 2960, 1448, 1416, 1214, 1117, 1015, 892, 789, 683 cm<sup>-1</sup>. **HRMS** (ESI) *m/z*: [M+Na]<sup>+</sup> calcd for C<sub>67</sub>H<sub>102</sub>O<sub>8</sub>Na 1057.7467, found 1057.7507.

**1-((3*aR*,8*aR*)-4,4,8,8-tetrakis(3,5-di-*tert*-butyl-4-methoxyphenyl)-2,2-dimethyl tetrahydro-[1,3]dioxolo[4,5-*e*][1,3,2]dioxaphosphepin-6-yl)piperidine (L21):**



According to a literature procedure,<sup>22</sup> an oven-dried round bottom flask equipped with a magnetic stirring bar was charged with the TADDOL **180** (932 mg, 0.9 mmol, 1.0 equiv) and anhydrous THF (5 mL) under argon atmosphere. Et<sub>3</sub>N (0.440 mL, 3.15 mmol, 3.5 equiv) was added at rt, and the reaction mixture was cooled to 0 °C before dropwise addition of phosphorous trichloride (0.090 mL, 1 mmol, 1.1 equiv). The mixture was stirred for 1 h at 0 °C, after which piperidine (0.890 mL, 9.0 mmol, 10.0 equiv) was added dropwise at 0 °C. Then the reaction was stirred overnight at rt, diluted with Et<sub>2</sub>O, and filtered. The filtrate was concentrated under reduced pressure and the resulting crude material was purified by flash column chromatography in silica gel (cyclohexane/EtOAc, 98:2) to afford the desired phosphoramidite **L21** analitically pure (880 mg, 85% yield) as a slightly yellow solid.

**<sup>1</sup>H NMR** (400 MHz, CDCl<sub>3</sub>) δ 7.65 (s, 2H), 7.58 (s, 2H), 7.31 (s, 2H), 7.20 (s, 2H), 5.22 (dd, *J* = 8.7, 2.5 Hz, 1H), 4.65 (d, *J* = 8.7 Hz, 1H), 3.68 (s, 3H), 3.67 (s, 3H), 3.65 (s, 3H), 3.60 (s, 3H), 3.44 – 3.25 (m, 4H), 1.72 – 1.58 (m, 6H), 1.46 (s, 3H), 1.44 (s, 18H), 1.41 (s, 18H), 1.39 (s, 18H), 1.38 (s, 18H), 0.23 (s, 3H). **<sup>13</sup>C NMR** (101 MHz, CDCl<sub>3</sub>) δ 158.7, 158.5, 158.2, 157.9, 142.3, 141.7, 141.6, 141.3, 141.0, 136.89, 136.87, 136.23, 136.22, 127.8, 126.0, 125.8, 109.9, 83.5, 83.4, 83.3, 83.1, 82.1, 82.0, 81.3, 81.3, 64.2, 64.1, 45.3, 45.1, 36.1, 36.0, 35.91, 35.88, 32.5, 32.34, 32.32, 32.2, 27.9, 27.6, 27.5, 27.1, 25.6, 24.4. **<sup>31</sup>P**

<sup>22</sup> D. M. Dalton, K. M. Oberg, R. T. Yu, E. E. Lee, S. Perreault, M. E. Oinen, M. L. Pease, G. Malik, T. Rovis, *J. Am. Chem. Soc.* **2009**, *131*, 15717–15728.

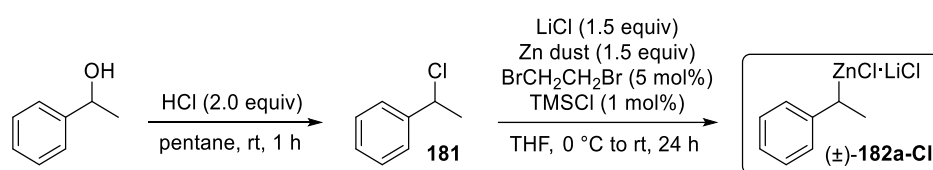
**NMR** (162 MHz, CDCl<sub>3</sub>)  $\delta$  136.5 (s). The spectroscopies properties are in good agreement with that previously reported.<sup>23</sup>

**NOTE:** 1-((3*aS*,8*aS*)-4,4,8,8-tetrakis(3,5-di-*tert*-butyl-4-methoxyphenyl)-2,2-dimethyltetrahydro[1,3]-dioxolo[4,5-*e*][1,3,2]dioxaphosphepin-6-yl)piperidine (*ent*-**L21**) was prepared from (-)-diethyl *D*-tartrate (*ee* >99%) in comparable yield using the same synthetic sequence. Racemic ( $\pm$ )-**L21** was obtained either by applying the same synthetic sequence to racemic ( $\pm$ )-diethyl tartrate or by mixing equimolar amounts of **L21** and *ent*-**L21**.

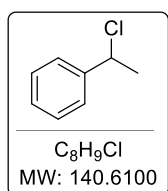
### 3.6. Preparation of secondary Benzylzinc Halides via Reductive Zincation

#### Synthesis of (1-phenylethyl)zinc chloride ( $\pm$ )-**182a-Cl**:

The following synthetic sequence was used:



#### (1-iodoethyl)benzene (**181**):

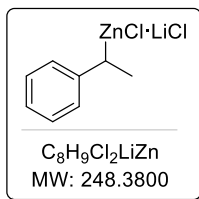


To a solution of 1-phenylethanol (1.833 g, 15 mmol, 1.0 equiv) in pentane (7 mL), was added HCl 12 M (2.5 mL, 30 mmol, 2.0 equiv), and the reaction mixture was stirred at rt for 1 h. The reaction was quenched by addition of a solution KOH 1 M until neutrality of the mixture. Then mixture was extracted with pentane (3×10 mL), and the combined organic phases were washed with brine, dried over MgSO<sub>4</sub>, filtered, and concentrated under reduced pressure. The crude material was filtered through a plug of silica gel, washed with pentane and concentrated under reduced pressure to recover analytically pure **181** (1.68 g, 80% yield) as colourless oil.

**<sup>1</sup>H NMR** (300 MHz, CDCl<sub>3</sub>)  $\delta$  7.49 – 7.29 (m, 5H), 5.13 (q, *J* = 6.8 Hz, 1H), 1.89 (d, *J* = 6.9 Hz, 3H). **<sup>13</sup>C NMR** (101 MHz, CDCl<sub>3</sub>)  $\delta$  142.8, 128.6, 128.2, 126.5, 58.7, 26.5. The spectral data was in good agreement with that previously reported.<sup>24</sup>

<sup>23</sup> R. Oost, A. Misale, N. Maulide, *Angew. Chem.* **2016**, *128*, 4663–4666.

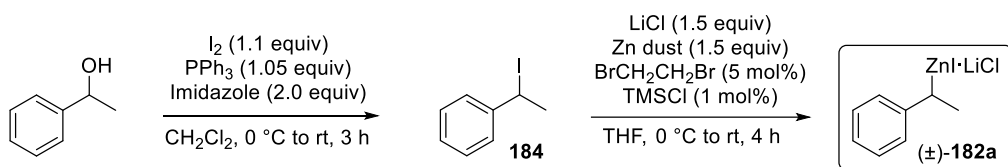
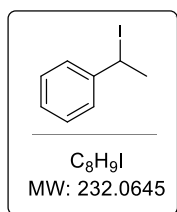
<sup>24</sup> P. H. Huy, S. Motsch, S. M. Kappler, *Angew. Chem. Int. Ed.* **2016**, *55*, 10145–10149.

**(1-phenylethyl)zinc chloride ((±)-182a-Cl):**

An oven dried flask was charged with anhydrous LiCl (318 mg, 7.5 mmol, 1.5 equiv) and it was dried under high vacuum at 450 °C for 10 min. After cooling, Zn dust was added (490 mg, 7.5 mmol, 1.5 equiv) and the flask was heated again for 10 minutes under high vacuum. Then, after cooling was added dry THF (1.2 mL) and the zinc was activated adding 1,2-dibromoethane (22  $\mu$ L, 0.25 mmol, 0.05 equiv) and heating the reaction mixture until ebullition occurred. After cooling to 25 °C, trimethylsilyl chloride (10  $\mu$ L, 0.05 mmol, 0.01 equiv) was added and the mixture was heated again until ebullition occurred. Then the mixture was cooled down to rt and a solution of **181** (703 mg, 5.0 mmol, 1.0 equiv) in THF (1.2 mL) was added dropwise over 1 h. After complete addition, the reaction mixture was stirred at rt for 23 h. The excess of zinc was removed by centrifugation and the liquid supernatant was transferred to another oven-dried flask under a positive pressure of argon and stored at -20 °C. The yield of the resulting benzylic zinc chloride was determined by titration with  $I_2$ .<sup>16</sup> Concentration of ~1.1 M was obtained.

**Synthesis of (1-phenylethyl)zinc iodide ((±)-182a)**

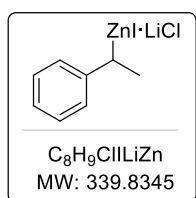
The following synthetic sequence was used:

**(1-iodoethyl)benzene (184):**

To a solution of 1-phenylethanol (1.833 g, 15 mmol, 1.0 equiv) in dichloromethane (40 mL) at 0 °C, were added in this order  $PPh_3$  (4.196 g, 16 mmol, 1.05 equiv), imidazole (2.042 g, 30 mmol, 2.0 equiv) and finally  $I_2$  (4.188 g, 16.5 mmol, 1.1 equiv). After 5 min at 0 °C, the mixture was stirred at rt for 3 h. The reaction was quenched by addition of an aqueous sat.  $Na_2S_2O_3$  solution until loss of colour. Then the reaction mixture was extracted with  $CH_2Cl_2$  (3×30 mL), the combined organic phases were dried over  $MgSO_4$ , filtered, and concentrated to 10 mL under reduced pressure. After addition of 70 mL of pentane the mixture was filtered through a plug silica gel, washed with pentane and concentrated under reduced pressure to recover analytically pure **184** (1.82 g, 52% yield) as yellow oil, which turns quickly to orange and then red if exposed to heat or light.

$^1\text{H NMR}$  (400 MHz,  $\text{CDCl}_3$ )  $\delta$  7.43 – 7.38 (m, 2H), 7.28 – 7.17 (m, 3H), 5.36 (q,  $J = 7.1$  Hz, 1H), 2.18 (d,  $J = 7.1$  Hz, 3H).  $^{13}\text{C NMR}$  (75 MHz,  $\text{CDCl}_3$ )  $\delta$  145.5, 128.9, 128.1, 126.8, 29.2, 26.6. The spectral data was in good agreement with that previously reported.<sup>25</sup>

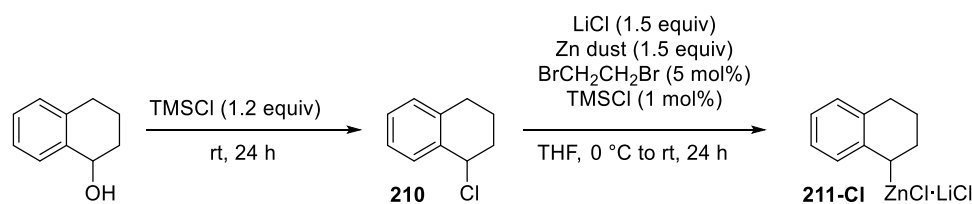
### (1-phenylethyl)zinc iodide ((±)-182a):



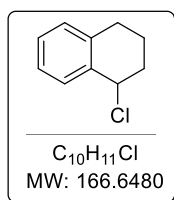
An oven dried flask was charged with anhydrous LiCl (191 mg, 4.5 mmol, 1.5 equiv) and it was dried under high vacuum at 450 °C for 10 min. After cooling, Zn dust was added (294 mg, 4.5 mmol, 1.5 equiv) and the flask was heated again for 10 minutes under high vacuum. Then, after cooling was added dry THF (2 mL) and the zinc was activated adding 1,2-dibromoethane (15  $\mu\text{L}$ , 0.15 mmol, 0.05 equiv) and heating the reaction mixture until ebullition occurred. After cooling to 25 °C, trimethylsilyl chloride (5  $\mu\text{L}$ , 0.03 mmol, 0.01 equiv) was added and the mixture was heated again until ebullition occurred. Then the mixture was cooled down to 0 °C and a solution of **184** (696 mg, 3.0 mmol, 1.0 equiv) in THF (1 mL) was added slowly over 1 h. After complete addition, the reaction mixture was stirred at rt for 3 h. The excess of zinc was removed by centrifugation and the liquid supernatant was transferred to another oven-dried flask under a positive pressure of argon and stored at –20 °C. The yield of the resulting benzylic zinc iodide was determined by titration with  $\text{I}_2$ .<sup>16</sup> Concentration of ~0.2 M was obtained.

### Synthesis of (1,2,3,4-tetrahydronaphthalen-1-yl)zinc chloride (211-Cl):

The following synthetic sequence was used:



### 1-Chloro-1,2,3,4-tetrahydronaphthalene (210):



According to a literature procedure,<sup>26</sup> an oven-dried flask equipped with stirring bar was charged with 1,2,3,4-tetrahydronaphthalen-1-ol (2.964 g, 20 mmol, 1.0 equiv) and trimethylsilyl chloride (3 mL, 24 mmol, 1.2 equiv) and the mixture was stirred vigorously at rt for 24 h. Upon completion of the reaction, the mixture was filtered

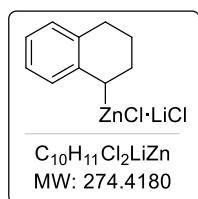
<sup>25</sup>A. K. Jha, S. Kishor, N. Jain, *RSC Adv.* **2015**, 5, 55218–55226.

<sup>26</sup>N. Ajvazi, S. Stavber, *Tetrahedron Lett.* **2016**, 57, 2430–2433.

through a plug of silica gel, washed with pentane and concentrated under reduced pressure to recover analytically pure **210** (3.0 g, 90% yield) as colourless oil.

**<sup>1</sup>H NMR** (300 MHz, CDCl<sub>3</sub>) δ 7.49 – 7.40 (m, 1H), 7.28 – 7.12 (m, 3H), 5.38 (t, *J* = 3.5 Hz, 1H), 3.02 – 2.76 (m, 2H), 2.43 – 2.20 (m, 3H), 1.99 – 1.87 (m, 1H). **<sup>13</sup>C NMR** (75 MHz, CDCl<sub>3</sub>) δ 136.7, 136.4, 130.4, 129.3, 128.3, 126.3, 58.7, 33.1, 28.9, 18.4. The spectral data was in good agreement with that previously reported.<sup>26</sup>

**(1,2,3,4-tetrahydronaphthalen-1-yl)zinc chloride (211-Cl):**

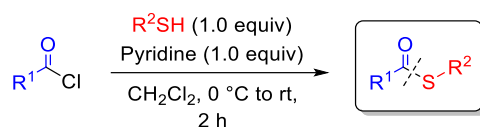


An oven dried flask was charged with anhydrous LiCl (318 mg, 7.5 mmol, 1.5 equiv) and it was dried under high vacuum at 450 °C for 10 min. After cooling, Zn dust was added (490 mg, 7.5 mmol, 1.5 equiv) and the flask was heated again for 10 minutes under high vacuum. Then, after cooling was added dry THF (1.5 mL) and the zinc was activated adding 1,2-dibromoethane (22 μL, 0.25 mmol, 0.05 equiv) and heating the reaction mixture until ebullition occurred. After cooling to 25 °C, trimethylsilyl chloride (10 μL, 0.05 mmol, 0.01 equiv) was added and the mixture was heated again until ebullition occurred. Then the mixture was cooled down to 0 °C and a solution of **210** (830 mg, 5.0 mmol, 1.0 equiv) in THF (1.5 mL) was added dropwise over 1 h. After complete addition, the reaction mixture was stirred at rt for 23 h. The excess of zinc was removed by centrifugation and the liquid supernatant was transferred to another oven-dried flask under a positive pressure of argon and stored at –20 °C. The yield of the resulting benzylic zinc chloride was determined by titration with I<sub>2</sub>.<sup>16</sup> Concentration of ~0.9 M was obtained.



## 3.7. Preparation of Thioesters

### 3.7.1. General Procedure for the Preparation of Thioesters (GP2)



According to a literature procedure,<sup>27</sup> an oven-dried round-bottomed flask equipped with stirring bar was charged with methylene chloride (7 mL), thiol (5 mmol, 1 equiv) and pyridine (0.4 mL, 5 mmol, 1 equiv) under argon atmosphere. The mixture was cooled to 0 °C in ice bath and the corresponding acyl chloride (5 mmol, 1 equiv) was added dropwise. The resulting suspension of white solid was stirred for an additional 5 min at 0 °C and at room temperature for 2 h. After that was added cold water (15 mL), the aqueous phase was separated and extracted with methylene chloride (3×10 mL), and the combined organic phases were dried over MgSO<sub>4</sub>, filtered, and concentrated under reduced pressure. The crude product was purified by flash chromatography in silica gel to afford the desired thioester.

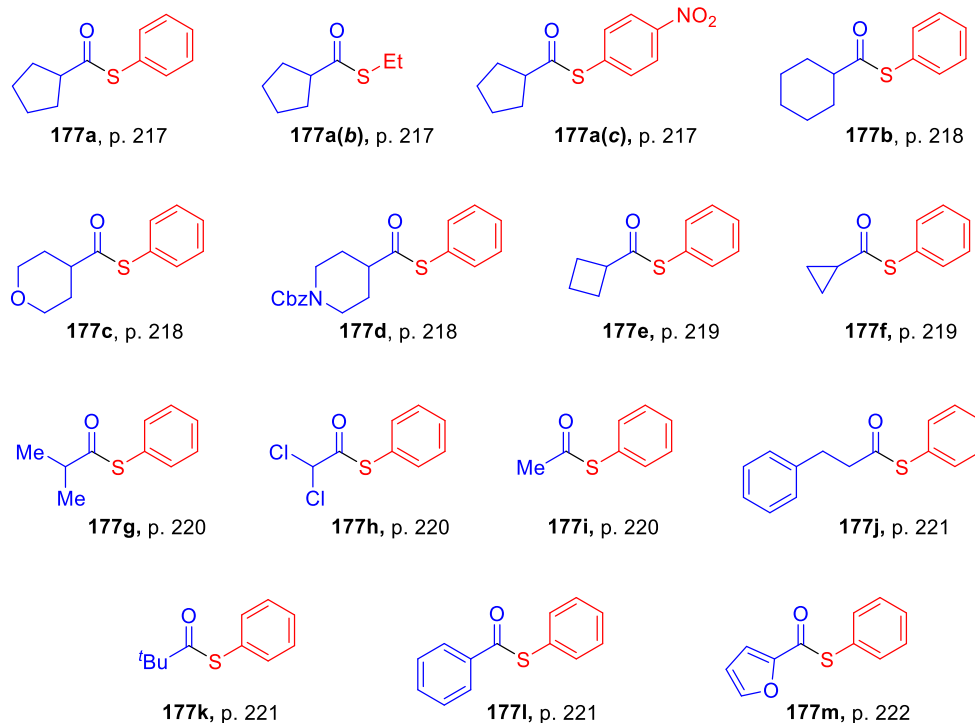
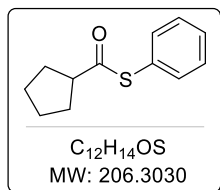


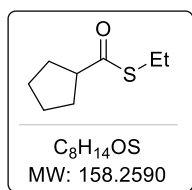
Chart of thioesters synthesized via GP2.

<sup>27</sup> C. L. Compton, K. R. Schmitz, R. T. Sauer, J. K. Sello, *ACS Chem. Biol.* **2013**, *8*, 2669–2677.

**S-phenyl cyclopentanecarbothioate (177a):**

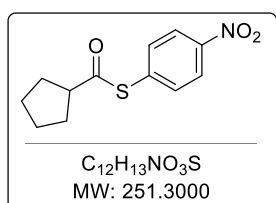
Prepared according to **GP2** from commercially available cyclopentanecarbonyl chloride (0.610 mL, 5 mmol, 1 equiv) and thiophenol (0.5 mL, 5 mmol, 1 equiv). Purification of the crude product by flash column chromatography (pentane/EtOAc, 98:2) afforded analytically pure **177a** (939 mg, 91% yield) as a colourless oil.

$^1H$  NMR (300 MHz,  $CDCl_3$ )  $\delta$  7.47 – 7.35 (m, 5H), 3.10 (p,  $J = 7.8$  Hz, 1H), 2.04 – 1.84 (m, 4H), 1.82 – 1.55 (m, 4H).  $^{13}C$  NMR (75 MHz,  $CDCl_3$ )  $\delta$  201.0, 134.7, 129.3, 129.2, 128.3, 53.1, 30.8, 26.1. Spectroscopic and physical properties match with those described in the literature.<sup>23</sup>

**S-ethyl cyclopentanecarbothioate (177a(b)):**

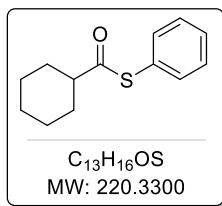
Prepared according to **GP2**, from commercially available cyclopentanecarbonyl chloride (0.610 mL, 5 mmol, 1 equiv) and ethanethiol (0.37 mL, 5 mmol, 1 equiv). Purification of the crude product by flash column chromatography (pentane/EtOAc, 98:2) afforded analytically pure **177a(b)** (695 mg, 91% yield) as yellow oil.

$^1H$  NMR (400 MHz,  $CDCl_3$ )  $\delta$  2.95 (p,  $J = 7.9$  Hz, 1H), 2.85 (q,  $J = 7.4$  Hz, 2H), 1.94 – 1.52 (m, 8H), 1.23 (t,  $J = 7.4$  Hz, 3H).  $^{13}C$  NMR (101 MHz,  $CDCl_3$ )  $\delta$  203.3, 53.4, 30.7, 26.0, 23.3, 14.9. IR (ATR) 2962, 2870, 1666, 1451, 1266, 1155, 1055, 1000, 867, 816  $cm^{-1}$ . HRMS (APCI)  $m/z$ :  $[M+H]^+$  calcd for  $C_8H_{14}OSH$  159.0838, found 159.0844.

**S-(4-nitrophenyl) cyclopentanecarbothioate (177a(c)):**

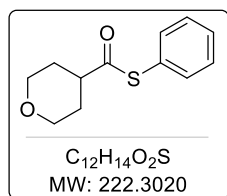
Prepared according to **GP2**, from commercially available cyclopentanecarbonyl chloride (0.610 mL, 5 mmol, 1 equiv) and commercially available 4-nitrobenzenethiol (780 mg, 5 mmol, 1 equiv). Purification of the crude product by flash column chromatography (pentane/EtOAc, 97:3) afforded analytically pure **177a(c)** (1.14 g, 91% yield) as a yellow oil.

$^1H$  NMR (400 MHz,  $CDCl_3$ )  $\delta$  8.25 – 8.21 (m, 2H), 7.62 – 7.57 (m, 2H), 3.11 (p,  $J = 8.1$  Hz, 1H), 2.05 – 1.85 (m, 4H), 1.81 – 1.59 (m, 4H).  $^{13}C$  NMR (101 MHz,  $CDCl_3$ )  $\delta$  198.8, 148.1, 137.0, 134.8, 124.0, 53.6, 30.7, 26.0. IR (ATR) 2980, 2971, 2882, 1716, 1708, 1598, 1577, 1514, 1346, 1310, 1174, 1109, 1077, 1008, 953, 850, 835, 775, 744, 731, 686  $cm^{-1}$ . HRMS (APCI)  $m/z$ :  $[M+H]^+$  calcd for  $C_{12}H_{13}NO_3SH$  252.0689, found 252.0684.

**S-phenyl cyclohexanecarbothioate (177b):**

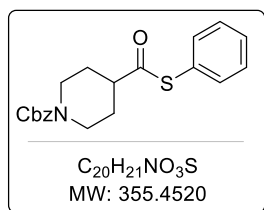
Prepared according to **GP2**, from commercially available cyclohexanecarbonyl chloride (0.67 mL, 5 mmol, 1 equiv) and thiophenol (0.5 mL, 5 mmol, 1 equiv). Purification of the crude product by flash column chromatography (pentane/EtOAc, 98:2) afforded analytically pure **177b** (1.020 g, 93% yield) as pale-yellow oil.

**$^1H$  NMR** (300 MHz,  $CDCl_3$ )  $\delta$  7.40 (s, 5H), 2.62 (tt,  $J = 11.4, 3.5$  Hz, 1H), 2.06–1.97 (m, 2H), 1.89–1.77 (m, 2H), 1.72–1.64 (m, 1H), 1.62–1.46 (m, 2H), 1.42–1.23 (m, 3H).  **$^{13}C$  NMR** (75 MHz,  $CDCl_3$ )  $\delta$  200.9, 134.7, 129.3, 129.2, 128.1, 52.6, 29.7, 25.7, 25.6. The spectroscopic properties are in good agreement with those previously reported.<sup>23</sup>

**S-phenyl tetrahydro-2H-pyran-4-carbothioate (177c):**

Prepared according to **GP2**, from commercially available tetrahydro-2H-pyran-4-carbonyl chloride (740 mg, 5 mmol, 1 equiv) and thiophenol (0.5 mL, 5 mmol, 1 equiv). Purification of the crude product by flash column chromatography (pentane/EtOAc, 9:1) afforded analytically pure **177c** (1.045 g, 94% yield) as white solid (m.p. 69–71 °C).

**$^1H$  NMR** (400 MHz,  $CDCl_3$ )  $\delta$  7.43 – 7.39 (m, 5H), 4.02 (ddd,  $J = 11.9, 4.1, 3.3$  Hz, 2H), 3.53 – 3.38 (m, 2H), 2.85 (tdd,  $J = 10.2, 6.6, 5.2$  Hz, 1H), 1.94 – 1.83 (m, 4H).  **$^{13}C$  NMR** (101 MHz,  $CDCl_3$ )  $\delta$  199.3, 134.7, 129.5, 129.3, 127.4, 67.1, 49.2, 29.2. **IR** (ATR) 2961, 2860, 2847, 1701, 1478, 1446, 1385, 1277, 1257, 1237, 1122, 1084, 1051, 1013, 972, 797, 755, 690  $cm^{-1}$ . **HRMS** (ESI)  $m/z$ :  $[M+H]^+$  calcd for  $C_{12}H_{14}O_2SH$  223.0787, found 223.0785.

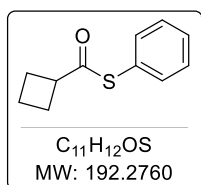
**Benzyl 4-((phenylthio)carbonyl)piperidine-1-carboxylate (177d):**

Prepared according to a modified procedure in literature,<sup>23</sup> from the corresponding 1-((benzyloxy)carbonyl)piperidine-4-carboxylic acid (1.315 g, 5 mmol, 1 equiv). This one was dissolved in DCM (5 mL) and after oxalyl chloride (0.51 mL, 6 mmol, 1.2 equiv) and 2 drops of anhydrous DMF were added at rt. The reaction was stirred 3 h at room temperature. After that, the reaction mixture was concentrated under reduced pressure and redissolved in DCM (7 mL). Then the thiophenol (0.5 mL, 5 mmol, 1 equiv) and pyridine (0.4 mL, 5 mmol, 1 equiv) were added slowly at 0 °C, and the reaction was stirred for 2 hours at room temperature. After this time, the solution was quenched with cold water (15 mL), the aqueous phase was separated and extracted with methylene

chloride (3×10 mL), and the combined organic phases were dried over MgSO<sub>4</sub>, filtered, and concentrated under reduced pressure. Purification of the crude product by flash column chromatography (pentane/EtOAc, from 10:1 to 8:2) afforded analytically pure **177d** (1.590 g, 89% yield) as a white solid (m.p. 89-91 °C).

**<sup>1</sup>H NMR** (400 MHz, CDCl<sub>3</sub>) δ 7.48 – 7.30 (m, 10H), 5.17 (s, 2H), 2.92 (t, *J* = 12.2 Hz, 2H), 2.77 (tt, *J* = 11.0, 3.8 Hz, 1H), 1.97 (d, *J* = 13.2 Hz, 2H), 1.76 (qd, *J* = 11.7, 4.1 Hz, 2H). **<sup>13</sup>C NMR** (101 MHz, CDCl<sub>3</sub>) δ 198.9, 154.9, 136.6, 134.4, 129.3, 129.1, 128.4, 127.9, 127.8, 127.1, 67.0, 49.7, 43.0, 28.3. **IR** (ATR) 2947, 1688, 1470, 1430, 1308, 1277, 1225, 1130, 1070, 1004, 969, 800, 748 cm<sup>-1</sup>. **HRMS** (ESI) *m/z*: [M+Na]<sup>+</sup> calcd for C<sub>20</sub>H<sub>21</sub>NO<sub>3</sub>SNa 378.1134, found 378.1132.

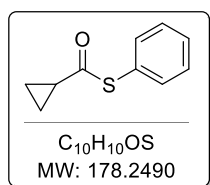
#### S-phenyl 2-methylpropanethioate (**177e**):



Prepared according to **GP2**, from commercially available cyclobutanecarbonyl chloride (0.57 mL, 5 mmol, 1 equiv) and thiophenol (0.5 mL, 5 mmol, 1 equiv). Purification of the crude product by flash column chromatography (pentane/EtOAc, 98:2) afforded analytically pure **177e** (830 mg, 86% yield) as a colourless oil.

**<sup>1</sup>H NMR** (400 MHz, CDCl<sub>3</sub>) δ 7.48–7.39 (m, 5H), 3.50 (p, *J* = 8.5 Hz, 1H), 2.50–2.37 (m, 2H), 2.35–2.22 (m, 2H), 2.09–1.89 (m, 2H). **<sup>13</sup>C NMR** (101 MHz, CDCl<sub>3</sub>) δ 199.4, 134.7, 129.3, 129.2, 128.0, 46.7, 26.2, 18.1. Spectroscopic and physical properties match with those described in the literature.<sup>28</sup>

#### S-phenyl cyclopropanecarbothioate (**177f**):

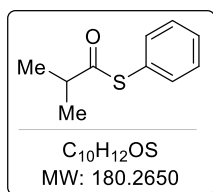


Prepared according to **GP2**, from commercially available cyclopropanecarbonyl chloride (0.45 mL, 5 mmol, 1 equiv) and thiophenol (0.5 mL, 5 mmol, 1 equiv). Purification of the crude product by flash column chromatography (pentane/EtOAc, 98:2) afforded analytically pure **177f** (884 mg, 99% yield) as a white solid.

**<sup>1</sup>H NMR** (400 MHz, CDCl<sub>3</sub>) δ 7.49 – 7.36 (m, 5H), 2.11 (tt, *J* = 7.9, 4.5 Hz, 1H), 1.26 – 1.17 (m, 2H), 1.01 (dq, *J* = 7.5, 4.3, 3.8 Hz, 2H). **<sup>13</sup>C NMR** (101 MHz, CDCl<sub>3</sub>) δ 197.6, 134.7, 129.4, 129.3, 128.0, 22.3, 11.3. Spectroscopic and physical properties match with those described in the literature.<sup>29</sup>

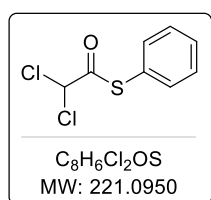
<sup>28</sup> K.S. Jeong, H.K. Oh, *Bull. Kor. Chem. Soc.* **2007**, *28*, 2535–2538.

<sup>29</sup> H. Keun Oh, J. Yun Lee, H. Whang Lee, I. Lee *New J. Chem.*, **2002**, *26*, 473–476.

**S-phenyl 2-methylpropanethioate (177g):**

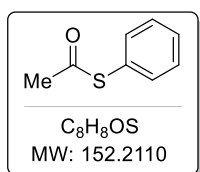
Prepared according to **GP2**, from commercially available isobutyryl chloride (0.52 mL, 5 mmol, 1 equiv) and thiophenol (0.5 mL, 5 mmol, 1 equiv). Purification of the crude product by flash column chromatography (pentane/EtOAc, 98:2) afforded analytically pure **177g** (840 mg, 93% yield) as colourless oil.

$^1H$  NMR (400 MHz,  $CDCl_3$ )  $\delta$  7.46–7.37 (m, 5H), 2.88 (hept,  $J = 6.9$  Hz, 1H), 1.28 (d,  $J = 6.9$  Hz, 6H).  $^{13}C$  NMR (101 MHz,  $CDCl_3$ )  $\delta$  201.9, 134.7, 129.3, 129.2, 128.0, 43.1, 19.5. The spectroscopic properties are in good agreement with those previously reported.<sup>30</sup>

**S-phenyl 2,2-dichloroethanethioate (177h):**

Prepared according to **GP2**, from commercially available 2,2-dichloroacetyl chloride (0.48 mL, 5 mmol, 1 equiv) and thiophenol (0.5 mL, 5 mmol, 1 equiv). Purification of the crude product by flash column chromatography (pentane/EtOAc, 98:2) afforded analytically pure **177h** (850 mg, 77% yield) as pale-yellow oil.

$^1H$  NMR (400 MHz,  $CDCl_3$ )  $\delta$  7.52 – 7.45 (m, 5H), 6.11 (s, 1H).  $^{13}C$  NMR (101 MHz,  $CDCl_3$ )  $\delta$  189.8, 134.7, 130.4, 129.7, 125.7, 69.6. The spectroscopic properties are in good agreement with those previously reported.<sup>31</sup>

**S-phenyl ethanethioate (177i):**

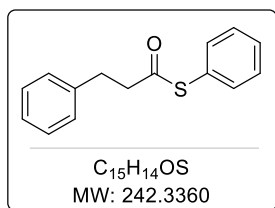
Prepared according to **GP2**, from commercially available acetyl chloride (0.360 mL, 5 mmol, 1 equiv) and thiophenol (0.5 mL, 5 mmol, 1 equiv). Purification of the crude product by flash column chromatography (pentane/EtOAc, 98:2) afforded analytically pure **177i** (686 mg, 90% yield) as a colourless oil.

$^1H$  NMR (400 MHz,  $CDCl_3$ )  $\delta$  7.45 – 7.40 (m, 5H), 2.43 (s, 3H).  $^{13}C$  NMR (101 MHz,  $CDCl_3$ )  $\delta$  194.1, 134.6, 129.5, 129.3, 128.1, 30.3. Spectroscopic and physical properties match with those described in the literature.<sup>32</sup>

<sup>30</sup> T. Böttcher, S. A. Sieber, *Angew. Chem. Int. Ed.* **2008**, *47*, 4600–4603.

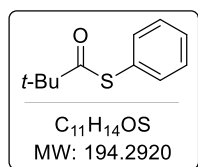
<sup>31</sup> G. Tabarelli, E. E. Albert, A. M. Deobald, G. Marin, O. E. D. Rodrigues, L. Dornelles, A. L. Braga, *Tetrahedron Lett.* **2010**, *51*, 5728–5731.

<sup>32</sup> S. T. Kadam, S. S. Kim, *Synthesis* **2008**, *2008*, 3307–3313.

**S-phenyl 3-phenylpropanethioate (177j):**

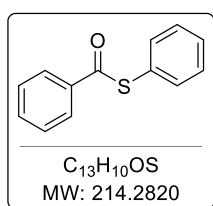
Prepared according to **GP2**, from commercially available 3-phenylpropanoyl chloride (0.74 mL, 5 mmol, 1 equiv) and thiophenol (0.5 mL, 5 mmol, 1 equiv). Purification of the crude product by flash column chromatography (pentane/EtOAc, 98:2) afforded analytically pure **177j** (1.06 g, 93% yield) as white crystals (m.p. 51-53 °C).

$^1H$  NMR (300 MHz,  $CDCl_3$ )  $\delta$  7.44 – 7.35 (m, 5H), 7.38 – 7.25 (m, 2H), 7.29 – 7.17 (m, 3H), 3.10 – 2.91 (m, 1H).  $^{13}C$  NMR (101 MHz,  $CDCl_3$ )  $\delta$  196.8, 140.1, 134.6, 129.5, 129.3, 128.7, 128.5, 127.8, 126.5, 45.3, 31.5. Spectroscopic properties match with those described in the literature.<sup>33</sup>

**S-phenyl 2,2-dimethylpropanethioate (177k):**

Prepared according to **GP2**, from commercially available pivaloyl chloride (0.62 mL, 5 mmol, 1 equiv) and thiophenol (0.5 mL, 5 mmol, 1 equiv). Purification of the crude product by flash column chromatography (pentane/EtOAc, 98:2) afforded analytically pure **177k** (880 mg, 91% yield) as a colourless oil.

$^1H$  NMR (300 MHz,  $CDCl_3$ )  $\delta$  7.44 – 7.37 (m, 5H), 1.33 (s, 9H).  $^{13}C$  NMR (75 MHz,  $CDCl_3$ )  $\delta$  204.7, 135.1, 129.2, 129.2, 128.3, 47.1, 27.6. Spectroscopic properties match with those described in the literature.<sup>34</sup>

**S-phenyl benzothioate (177l):**

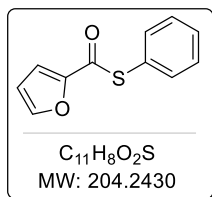
Prepared according to **GP2**, from commercially available benzoyl chloride (0.58 mL, 5 mmol, 1 equiv) and thiophenol (0.5 mL, 5 mmol, 1 equiv). Purification of the crude product by flash column chromatography (pentane/EtOAc, 98:2) afforded analytically pure **177l** (970 mg, 91% yield) as white crystals (m.p. 53-55 °C).

$^1H$  NMR (300 MHz,  $CDCl_3$ )  $\delta$  8.09 – 8.02 (m, 2H), 7.67 – 7.44 (m, 8H).  $^{13}C$  NMR (75 MHz,  $CDCl_3$ )  $\delta$  190.2, 136.8, 135.2, 133.8, 129.6, 129.4, 128.9, 127.6, 127.5. Spectroscopic properties match with those described in the literature.<sup>35</sup>

<sup>33</sup> L. Sancineto, C. Tidei, L. Bagnoli, F. Marini, V. Lippolis, M. Arca, E.J. Lenardão, C. Santi, *Eur. J. Org. Chem.*, **2016**, 2016, 2999-3005.

<sup>34</sup> J. B. Azeredo, M. Godoi, R. S. Schwab, G. V. Botteselle, A. L. Braga, *Eur. J. Org. Chem.* **2013**, 5188-5194.

<sup>35</sup> X. Pan, D. Curran, *Org. Lett.* **2014**, 16, 2728-2731.

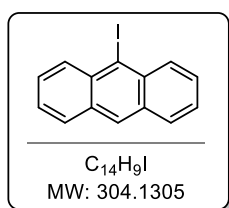
**S-phenyl furan-2-carbothioate (177m):**

Prepared according to **GP2**, from commercially available 2-furoyl chloride (0.49 mL, 5 mmol, 1 equiv) and thiophenol (0.5 mL, 5 mmol, 1 equiv). Purification of the crude product by flash column chromatography (pentane/EtOAc, 95:5) afforded analytically pure **177m** (980 mg, 96% yield) as a white solid.

**<sup>1</sup>H NMR** (400 MHz, CDCl<sub>3</sub>) δ 7.64 – 7.62 (m, 1H), 7.54 – 7.49 (m, 3H), 7.47 – 7.43 (m, 2H), 7.28 – 7.25 (m, 1H), 6.58 (dd, *J* = 3.6, 1.7 Hz, 1H). **<sup>13</sup>C NMR** (101 MHz, CDCl<sub>3</sub>) δ 178.8, 150.5, 146.6, 135.3, 129.8, 129.4, 126.3, 116.4, 112.6. Spectroscopic properties match with those described in the literature.<sup>36</sup>

### 3.8. Preparation of Aryl Iodides

Most aryl iodides were purchased from commercial suppliers, the following were prepared.

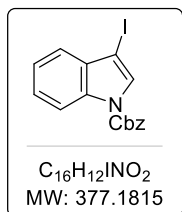
**9-iodoanthracene (A1):**

According to a literature procedure,<sup>37</sup> an oven-dried tube equipped with stirring bar was charged with CuI (76 mg, 0.4 mmol, 0.1 equiv), NaI (1.139 g, 7.6 mmol, 1.9 equiv), and 9-bromoranthracene (1.029 g, 4 mmol, 1.0 equiv), under argon atmosphere. Then was added anhydrous 1,4-dioxane (4 mL) and N,N'-dimethylethylene diamine (43 μL, 0.4 mmol, 0.1 equiv), the tube was sealed, and the reaction was stirred at 160 °C for 20 hours. The reaction mixture was then quenched with aqueous soln. of NH<sub>4</sub>OH, and the aqueous layer was extracted with ethyl acetate (3×15 mL). The combined organic phase was washed with water, brine, dried over MgSO<sub>4</sub>, and concentrated under reduced pressure to afford analytically pure **A1** (1.10 g, 90%) as a yellow solid.

**<sup>1</sup>H NMR** (400 MHz, CDCl<sub>3</sub>) δ 8.47 (d, *J* = 8.8 Hz, 2H), 8.42 (s, 1H), 7.94 (d, *J* = 8.4 Hz, 2H), 7.62 – 7.45 (m, 4H). **<sup>13</sup>C NMR** (101 MHz, CDCl<sub>3</sub>) δ 133.9, 133.3, 132.1, 128.9, 128.7, 127.8, 125.7, 104.9. The spectroscopic properties are in good agreement with those previously reported.<sup>31</sup>

<sup>36</sup> X. Zhu, Y. Shi, H. Mao, Y. Cheng, C. Zhu, *Adv. Synth. Catal.* **2013**, 355, 3558–3562.

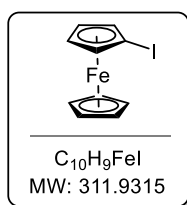
<sup>37</sup> A. J. McGrath, G. E. Garrett, L. Valgimigli, D. A. Pratt, *J. Am. Chem. Soc.* **2010**, 132, 16759–16761.

**Benzyl 3-iodo-1H-indole-1-carboxylate (A2):**

According to a literature procedure,<sup>38</sup> an oven-dried flask equipped with stirring bar was charged with 1*H*-indole (586 mg, 5 mmol, 1.0 equiv) and KOH (700 mg, 12.5 mmol, 2.5 equiv) and DMF (5 mL) under argon atmosphere. A solution of I<sub>2</sub> (1.330 g, 5.25 mmol, 1.05 equiv), in DMF (5 mL) was added at rt and the mixture was stirred at the same temperature for 2 h. After that the reaction mixture was poured into cold water (50 mL) containing 10% Na<sub>2</sub>S<sub>2</sub>O<sub>3</sub> and 0.5% ammonia. The aqueous layer was separated extracted with Et<sub>2</sub>O (3×15 mL) and the combined organic layers were washed with brine, dried over MgSO<sub>4</sub>, filtered, and concentrated under reduced pressure.

The residue was dissolved in DMF (8 mL) and was added NaH (60% in oil dispersion, 220 mg, 5.5 mmol, 1.1 equiv) at 0 °C. After being stirred for 2 h at 0 °C, the reaction mixture was quenched with a sat. soln of NaHCO<sub>3</sub>. The aqueous phase was separated and extracted with Et<sub>2</sub>O (3×15 mL). The combined organic layers were washed with brine, dried over MgSO<sub>4</sub>, filtered, and concentrated under reduced pressure. Purification of the crude product by flash column chromatography in silica gel (pentane/EtOAc, 97:3) afforded the desired **A2** (1.360 g, 72% yield over 2 steps) as a white solid.

<sup>1</sup>H NMR (400 MHz, CDCl<sub>3</sub>) δ 8.18 (d, J = 8.1 Hz, 1H), 7.78 (s, 1H), 7.53 – 7.31 (m, 8H), 5.46 (s, 2H). <sup>13</sup>C NMR (101 MHz, CDCl<sub>3</sub>) δ 150.0, 135.0, 134.9, 132.2, 129.7, 129.0, 129.0, 128.7, 125.8, 123.8, 121.7, 115.2, 69.2, 66.8. The spectral data was in good agreement with that previously reported.<sup>38</sup>

**Iodoferrocene (A3):**

According to a literature procedure,<sup>39</sup> an oven-dried flask equipped with stirring bar was charged with ferroceneboronic acid (690 mg, 3.0 mmol, 1.0 equiv) and N-iodosuccinimide (810 mg, 3.6 mmol) under argon atmosphere. Then was added anhydrous acetonitrile, and the mixture was stirred 20 h at rt. The mixture was extracted with pentane (3×80 mL). The combined extract was washed with aqueous soln of Na<sub>2</sub>S<sub>2</sub>O<sub>5</sub> (3×15 mL), water and brine, dried over MgSO<sub>4</sub>, and finally concentrated under reduced pressure. Purification of the crude product by flash chromatography on silica gel (pentane) afforded analytically pure **A3** (299 mg, 32% yield) as an orange solid.

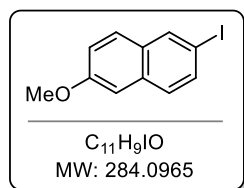
<sup>1</sup>H NMR (400 MHz, CDCl<sub>3</sub>) δ 4.44 – 4.41 (m, 2H), 4.21 (s, 5H), 4.18 – 4.15 (m, 2H). <sup>13</sup>C NMR (101 MHz, CDCl<sub>3</sub>) δ 74.6, 71.2, 68.9, 39.9. The spectroscopic properties are in good agreement with those previously reported.<sup>40</sup>

<sup>38</sup> T. Yokosaka, T. Nemoto, Y. Hamada, *Chem. Commun.* **2012**, 48, 5431–5433.

<sup>39</sup> Q. Shu, L. Birlenbach, M. Schmittel, *Inorg. Chem.* **2012**, 51, 13123–13127.

<sup>40</sup> M. Roemer, C. A. Nijhuis, *Dalton Trans.* **2014**, 43, 11815–11818.



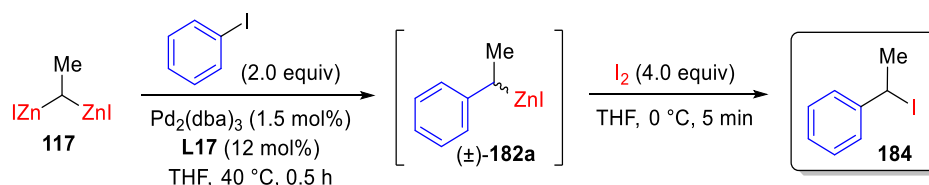
**2-iodo-6-methoxynaphthalene (A4):**

According to a literature procedure,<sup>41</sup> an oven-dried flask equipped with stirring bar was charged with 2-bromo-6-methoxynaphthalene (1.185 g, 5 mmol, 1.0 equiv) and THF (11 mL) under argon atmosphere. *t*-BuLi (1.7 M in pentane, 12 mL, 20 mmol, 4.0 equiv) was added dropwise at  $-78\text{ }^{\circ}\text{C}$  and the mixture was stirred 1 h at the same temperature. Then, a solution of I<sub>2</sub> (6.345 g, 25 mmol, 5.0 equiv) in THF (20 mL) was added slowly at  $-78\text{ }^{\circ}\text{C}$  and the mixture was then stirred at rt for 72 h. The reaction mixture was quenched with a sat. soln of Na<sub>2</sub>S<sub>2</sub>O<sub>3</sub> (30 mL), the aqueous layer was separated and extracted with dichloromethane (3×20 mL). The combined organic layers were dried over MgSO<sub>4</sub>, filtered, and concentrated under reduced pressure. Purification of the crude product by recrystallization (dichloromethane/methanol, 1:1) afforded the desired **A4** (1.05 g, 74% yield) as pale-yellow plates.

**<sup>1</sup>H NMR** (400 MHz, CDCl<sub>3</sub>)  $\delta$  8.14 (m, 1H), 7.68 – 7.59 (m, 2H), 7.47 (d, *J* = 8.7 Hz, 1H), 7.14 (dd, *J* = 8.9, 2.5 Hz, 1H), 7.08 (d, *J* = 2.5 Hz, 1H), 3.91 (s, 3H). **<sup>13</sup>C NMR** (101 MHz, CDCl<sub>3</sub>)  $\delta$  158.2, 136.4, 134.9, 133.5, 130.8, 128.53, 128.49, 119.7, 105.9, 88.2, 55.5. The spectroscopic properties are in good agreement with those previously reported.<sup>42</sup>

### 3.9. Racemic Sequential Catalytic Arylation–Electrophilic Substitution of 1,1-Bis(iodozincio)alkanes

#### 3.9.1 Catalytic Arylation–Iodolysis of 1,1-Bis(iodozincio)ethane



An oven-dried flask under argon was charged with Pd<sub>2</sub>(dba)<sub>3</sub> (2.7 mg, 0.003 mmol, 0.015) and **L17** (16.1 mg, 0.024 mmol, 0.12 equiv). A solution of iodobenzene (82 mg, 0.4 mmol, 2.0 equiv) in THF (0.5 mL) was added. The mixture was stirred for 5 min at rt before a solution of **117** (0.440 mL, ~0.45 M in THF, 0.2 mmol, 1.0 equiv) was added slowly. The resulting mixture was stirred for 0.5 h at 40 °C. Then the reaction mixture was cooled down to rt and was added slowly at 0 °C to a solution of I<sub>2</sub> (203

<sup>41</sup> J. M. Brown, S. J. Cook, R. Khan, *Tetrahedron* **1986**, *42*, 5105–5109.

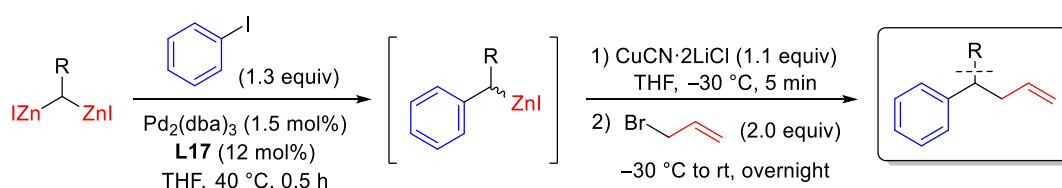
<sup>42</sup> W. B. Smith, *J. Org. Chem.* **1985**, *50*, 3649–3651.

mg, 0.8 mmol, 4 equiv) in THF (0.5 mL) under argon. The mixture was stirred at 0 °C for 5 minutes and 2 minutes at rt, after which was added a sat. soln of Na<sub>2</sub>S<sub>2</sub>O<sub>3</sub> until complete loss of colour. The reaction mixture was extracted with Et<sub>2</sub>O (3×5 mL), and the combined organic layers were dried over MgSO<sub>4</sub>, filtered, and concentrated under reduced pressure. Purification by flash column chromatography on silica gel (pentane) afforded **184** as a yellow oil (28 mg, 60% yield).

<sup>1</sup>H NMR (400 MHz, CDCl<sub>3</sub>) δ 7.43–7.38 (m, 2H), 7.28–7.17 (m, 3H), 5.36 (q, J = 7.1 Hz, 1H), 2.18 (d, J = 7.1 Hz, 3H). <sup>13</sup>C NMR (75 MHz, C<sub>6</sub>D<sub>6</sub>) δ 145.8, 128.8, 128.0, 126.8, 29.0, 25.9. The spectral data was in good agreement with that previously reported.<sup>43</sup>

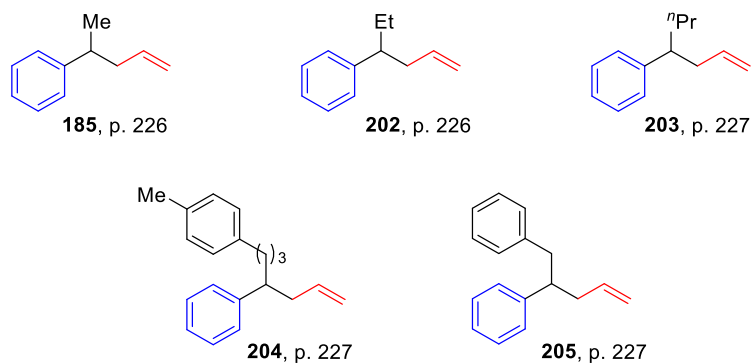
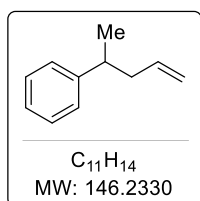
### 3.9.2. Catalytic Arylation–Cu-Mediated Allylation

#### 3.9.2.1. General Procedure for the Sequential Pd-Catalyzed Arylation–Cu-Mediated Allylation of 1,1- Bis(iodozincio)alkanes (GP3)



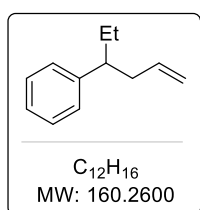
An oven-dried flask under argon was charged with Pd<sub>2</sub>(dba)<sub>3</sub> (2.7 mg, 0.003 mmol, 0.015) and **L17** (16.1 mg, 0.024 mmol, 0.12 equiv). A solution of iodoarene (0.26 mmol) in THF (0.5 mL) was added. The mixture was stirred for 5 min at rt. before a solution of 1,1-diiodozincioalkane in THF (0.2 mmol) was added slowly. The resulting mixture was stirred for 0.5 h at 40 °C. Then the reaction mixture was cooled down to –30 °C, a solution of CuCN·2LiCl (0.22 mL, 1.0 M in THF, 0.22 mmol, 1.1 equiv) was added dropwise and the resulting mixture was stirred at the same temperature for 20 minutes. After that, a THF (0.3 mL) solution of allyl bromide (48 mg, 0.40 mmol) was added dropwise at –30 °C and the reaction mixture was stirred overnight letting it return to rt slowly. The reaction was quenched with sat. soln of NH<sub>4</sub>Cl and extracted with Et<sub>2</sub>O (3×10 mL). The combined organic layers were dried over MgSO<sub>4</sub>, filtered, and concentrated under reduced pressure. The product was purified by flash column chromatography on silica gel.

<sup>43</sup> P. Wyatt, H. Eley, J. Charmant, B. J. Daniel, A. Kantacha, *Eur. J. Org. Chem.* **2003**, 2003, 4216–4226.

Chart of products synthesized via **GP3**.**Pent-4-en-2-ylbenzene (185):**

Prepared according to **GP3**, from **117** (0.44 mL, ~0.45 M in THF, 0.2 mmol, 1.0 equiv) and iodobenzene (53 mg, 0.26 mmol, 1.3 equiv). Purification of the crude product by flash column chromatography (pentane) afforded analytically pure **185** (22 mg, 75% yield) as a colourless oil.

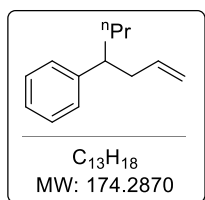
$^1\text{H NMR}$  (400 MHz,  $\text{CDCl}_3$ )  $\delta$  7.38 – 7.20 (m, 5H), 5.84 – 5.68 (m, 1H), 5.08 – 4.98 (m, 2H), 2.83 (h,  $J = 7.1$  Hz, 1H), 2.49 – 2.28 (m, 2H), 1.30 (d,  $J = 7.0$  Hz, 3H).  $^{13}\text{C NMR}$  (101 MHz,  $\text{CDCl}_3$ )  $\delta$  147.2, 137.3, 128.4, 127.1, 126.1, 116.0, 42.8, 39.9, 21.6. The spectral data was in good agreement with that previously reported.<sup>44</sup>

**Hex-5-en-3-ylbenzene (202):**

Prepared according to **GP3**, from **119** (0.40 mL, ~0.50 M in THF, 0.2 mmol, 1.0 equiv) and iodobenzene (53 mg, 0.26 mmol, 1.3 equiv). Purification of the crude product by flash column chromatography (pentane) afforded analytically pure **202** (27 mg, 84% yield) as colourless oil.

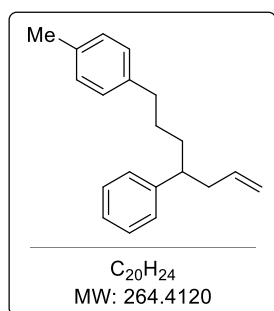
$^1\text{H NMR}$  (300 MHz,  $\text{CDCl}_3$ )  $\delta$  7.34 – 7.24 (m, 2H), 7.23 – 7.12 (m, 3H), 5.68 (ddt,  $J = 17.0, 10.1, 6.9$  Hz, 1H), 5.03 – 4.87 (m, 2H), 2.59 – 2.44 (m, 1H), 2.43 – 2.30 (m, 2H), 1.81 – 1.66 (m, 1H), 1.65 – 1.47 (m, 1H), 0.78 (t,  $J = 7.4$  Hz, 3H).  $^{13}\text{C NMR}$  (75 MHz,  $\text{CDCl}_3$ )  $\delta$  145.4, 137.4, 128.3, 127.9, 126.1, 115.8, 47.8, 41.1, 28.9, 12.2. The spectroscopic data are in good agreement with those reported.<sup>44</sup>

<sup>44</sup> D. Zhu, L. Lv, C.-C. Li, S. Ung, J. Gao, C.-J. Li, *Angew. Chem. Int. Ed.* **2018**, *57*, 16520–16524.

**Hept-6-en-4-ylbenzene (203):**

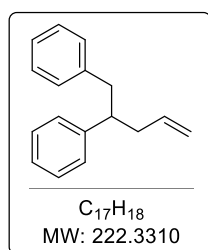
Prepared according to **GP3**, from **195** (0.30 mL, ~0.60 M in THF, 0.2 mmol, 1.0 equiv) and iodobenzene (53 mg, 0.26 mmol, 1.3 equiv). Purification of the crude product by flash column chromatography (pentane) afforded analytically pure **203** (28 mg, 77% yield) as a colourless oil.

**$^1H$  NMR** (300 MHz,  $CDCl_3$ )  $\delta$  7.35 – 7.27 (m, 2H), 7.24 – 7.14 (m, 3H), 5.70 (ddt,  $J = 17.1, 10.1, 7.0$  Hz, 1H), 5.03 – 4.91 (m, 2H), 2.70 – 2.58 (m, 1H), 2.44 – 2.32 (m, 2H), 1.75 – 1.50 (m, 2H), 1.27 – 1.13 (m, 2H), 0.88 (t,  $J = 7.3$  Hz, 3H).  **$^{13}C$  NMR** (75 MHz,  $CDCl_3$ )  $\delta$  145.6, 137.4, 128.3, 127.8, 126.1, 115.8, 45.8, 41.5, 38.4, 20.7, 14.2. The spectroscopic data are in good agreement with those reported.<sup>44</sup>

**1-methyl-4-(4-phenylhept-6-en-1-yl)benzene (204):**

Prepared according to **GP3**, from **196** (0.41 mL, ~0.49 M in THF, 0.2 mmol, 1.0 equiv) and iodobenzene (53 mg, 0.26 mmol, 1.3 equiv). Purification of the crude product by flash column chromatography (pentane/ $Et_2O$ ) afforded analytically pure **204** (46 mg, 87% yield) as a colourless oil.

**$^1H$  NMR** (300 MHz,  $CDCl_3$ )  $\delta$  7.38 – 7.30 (m, 2H), 7.28 – 7.02 (m, 7H), 5.72 (ddt,  $J = 17.1, 10.1, 7.0$  Hz, 1H), 5.07 – 4.93 (m, 2H), 2.75 – 2.50 (m, 3H), 2.46 – 2.34 (m, 5H), 1.87 – 1.45 (m, 4H).  **$^{13}C$  NMR** (75 MHz,  $CDCl_3$ )  $\delta$  145.3, 139.7, 137.2, 135.1, 129.0, 128.37, 128.35, 127.8, 126.1, 115.9, 46.0, 41.5, 35.8, 35.6, 29.5, 21.1. **IR** (ATR) 2923, 1516, 1452, 910, 805, 761, 734, 700  $cm^{-1}$ . **MS** (EI, 70 eV)  $m/z$ : 264 ( $M^+$ , 2%), 145 (79%), 131 (83%), 105 (100%), 91 (59%).

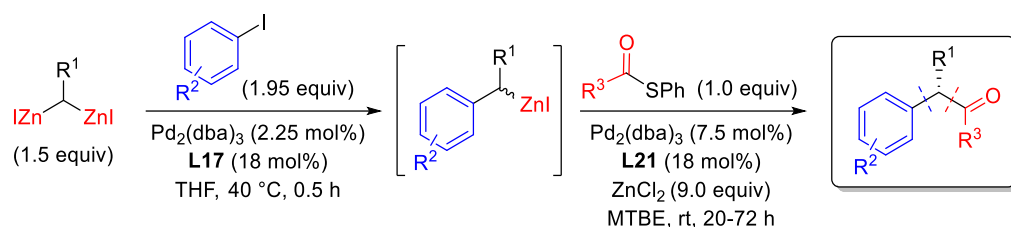
**Pent-4-ene-1,2-diyl dibenzene (205):**

Prepared according to **GP3**, from **197** (0.45 mL, ~0.45 M in THF, 0.2 mmol, 1.0 equiv) and iodobenzene (53 mg, 0.26 mmol, 1.3 equiv). Purification of the crude product by flash column chromatography (pentane) afforded analytically pure **205** (31 mg, 70% yield) as a colourless oil.

**$^1H$  NMR** (300 MHz,  $CDCl_3$ )  $\delta$  7.35 – 7.02 (m, 10H), 5.70 (ddt,  $J = 17.1, 10.2, 7.0$  Hz, 1H), 5.12 – 4.92 (m, 2H), 3.06 – 2.88 (m, 3H), 2.52 – 2.40 (m, 2H).  **$^{13}C$  NMR** (75 MHz,  $CDCl_3$ )  $\delta$  144.6, 140.6, 136.9, 129.3, 128.3, 128.2, 128.0, 126.3, 126.0, 116.3, 47.9, 42.9, 40.0. **IR** (ATR) 2977, 1714, 1657, 1448, 1369, 1255, 1157, 759, 697  $cm^{-1}$ . **MS** (EI, 70 eV)  $m/z$ : 222 ( $M^+$ , 5%), 181 (88%), 131 (100%), 91 (74%).

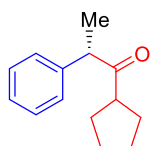
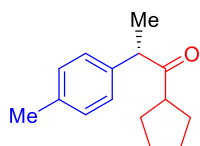
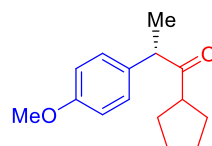
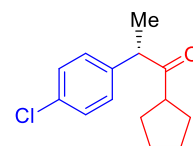
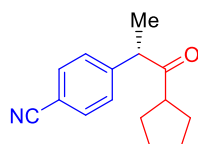
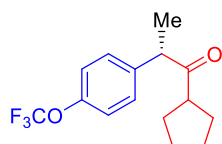
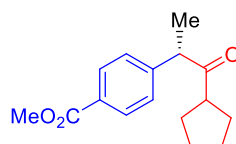
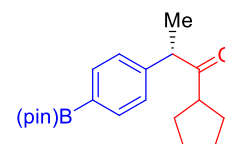
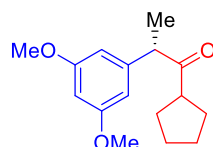
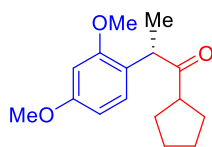
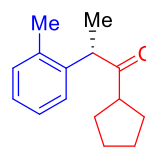
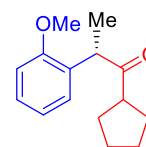
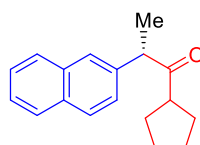
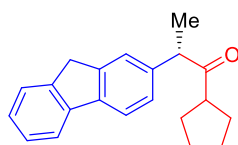
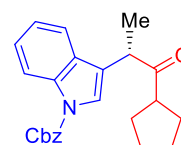
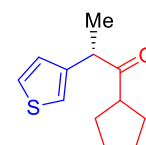
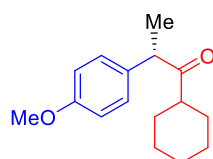
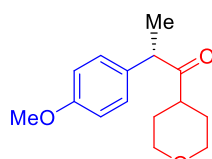
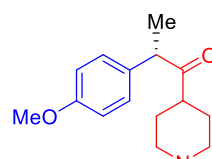
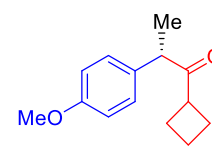
### 3.9.3. Synthesis of Enantioenriched $\alpha$ -Disubstituted ketones

#### 3.9.3.1. General Procedure for the Pd-Catalyzed Enantioselective Sequential Arylation–Fukuyama Cross-Coupling of 1,1-Bis(iodozincio)alkanes (GP4)

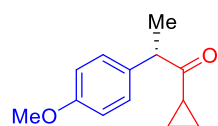
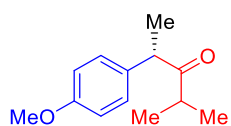
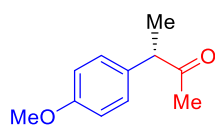
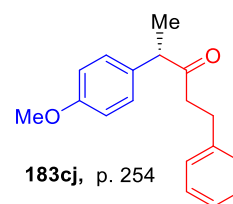
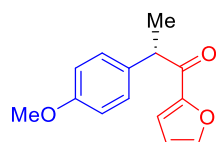
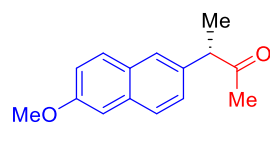
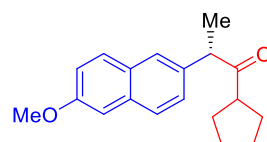
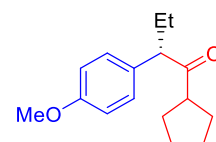
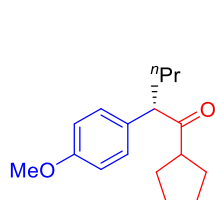
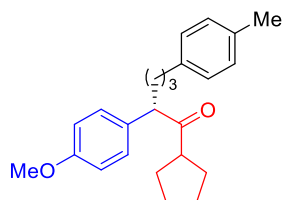
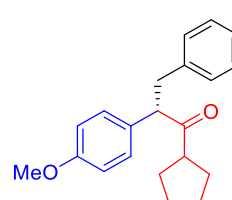


An oven-dried flask under argon was charged with  $\text{Pd}_2(\text{dba})_3$  (4.1 mg, 0.0045 mmol, 0.0225 equiv) and **L17** (24.1 mg, 0.036 mmol, 0.18 equiv) under argon atmosphere. A solution of aryl iodide (0.39 mmol, 1.95 equiv) in THF (0.5 mL) was added. The mixture was stirred for 5 min at rt before a solution of 1,1-diiodozincioalkane (0.4–0.6 M in THF, 0.3 mmol, 1.5 equiv) was added slowly. The resulting mixture was stirred for 0.5 h at 40 °C. Then the reaction mixture was cooled down to rt and was added  $\text{ZnCl}_2$  (1.2 mL, 1.5 M in THF, 1.8 mmol, 9 equiv) and the mixture was stirred for 30 minutes. After that, another oven-dried flask under argon was charged with  $\text{Pd}_2(\text{dba})_3$  (13.7 mg, 0.015 mmol, 0.075 equiv) and **L21** (41.4 mg, 0.036 mmol, 0.18) and MTBE (1.8 mL). The solution was stirred for 10 minutes at rt after which was added a solution of the appropriate thioester (0.2 mmol, 1 equiv) in THF (0.4 mL), and the reaction mixture from the first cross-coupling *via* cannula. The reaction was stirred at rt for 20–72 h, after which it was quenched with HCl (4 mL, 1.0 M) and extracted with EtOAc (3×10 mL). The combined organic layers were washed with NaOH (1.0 M) and brine, dried over  $\text{MgSO}_4$ , filtered, and concentrated under reduced pressure. The product was purified by flash column chromatography on silica gel.

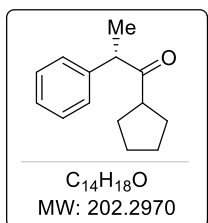
**NOTE:** All the target ketones were also obtained in racemic form for GC or HPLC analytic purposes by applying the same protocol using racemic ( $\pm$ )-**L21** as ligand for the second cross-coupling. No significant difference in yield was noted for these racemic reactions in comparison with the enantiopure reactions reported hereafter.

**183aa**, p. 231**183ba**, p. 232**183ca**, p. 233**183da**, p. 234**183ea**, p. 235**183fa**, p. 236**183ga**, p. 237**183ha**, p. 238**183ia**, p. 239**183ja**, p. 240**183ka**, p. 241**183la**, p. 242**183na**, p. 243**183pa**, p. 244**183qa**, p. 245**183ra**, p. 246**183cb**, p. 247**183cc**, p. 248**183cd**, p. 249**183ce**, p. 250

*Chart of the enantioenriched  $\alpha$ -disubstituted ketones synthesized via GP4.*

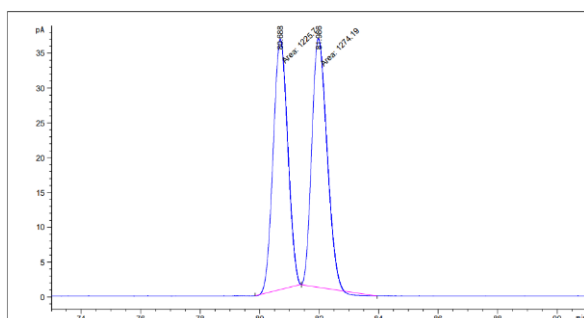
**183cf**, p. 251**183cg**, p. 252**183ci**, p. 253**183cj**, p. 254**183cm**, p. 255**183ti**, p. 256**183ta**, p. 257**206**, p. 258**207**, p. 259**208**, p. 260**209**, p. 261

*Chart of the enantioenriched  $\alpha$ -disubstituted ketones synthesized via GP4 (continue).*

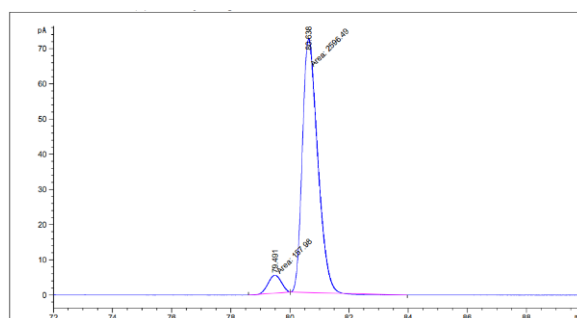
**(S)-1-cyclopentyl-2-phenylpropan-1-one (183aa):**

Prepared according to **GP4**, from **117** (0.7 mL, 0.43 M in THF, 0.3 mmol, 1.5 equiv), commercially available iodobenzene (80 mg, 0.39 mmol, 1.95 equiv) and thioester **177a** (41 mg, 0.2 mmol, 1.0 equiv) with a reaction time of 20 h for the second step. Purification of the crude product by flash column chromatography (pentane/EtOAc, 50:1) afforded analytically pure **183aa** (30 mg, 74% yield) as a pale-yellow oil.

**<sup>1</sup>H NMR** (400 MHz, CDCl<sub>3</sub>) δ 7.36–7.28 (m, 2H), 7.27–7.18 (m, 3H), 3.86 (q, *J* = 6.9 Hz, 1H), 2.89 (p, *J* = 7.6 Hz, 1H), 1.88–1.78 (m, 1H), 1.76–1.56 (m, 4H), 1.56–1.41 (m, 3H), 1.39 (d, *J* = 7.0 Hz, 3H). **<sup>13</sup>C NMR** (101 MHz, CDCl<sub>3</sub>) δ 213.7, 141.0, 129.0, 128.2, 127.1, 52.6, 50.1, 30.6, 29.2, 26.2, 18.1. **IR** (ATR) 2959, 2869, 1709, 1493, 1452, 1068, 1020, 986, 739, 700 cm<sup>-1</sup>. **HRMS** (ESI) *m/z*: [M+H]<sup>+</sup> calcd for C<sub>14</sub>H<sub>18</sub>OH 203.1430, found 203.1425. **Enantiomeric ratio** 94:6 was determined by chiral GC analysis with a Cyclosil-B column (isotherm at 105 °C, flow rate 1.4 mL/min, retention times (min): 79.49 (minor) and 80.64 (major)). [α]<sub>D</sub><sup>20</sup> = +148.2 (*c* = 0.90 in CHCl<sub>3</sub>). Spectroscopic properties match with those described in the literature.<sup>23</sup>

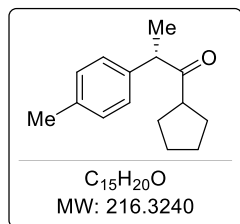


Peak #	RetTime [min]	Type	Width [min]	Area [pA*s]	Height [pA]	Area %
1	80.688	MM	0.5681	1225.70117	35.96008	49.03021
2	81.986	MM	0.5934	1274.18860	35.78614	50.96979



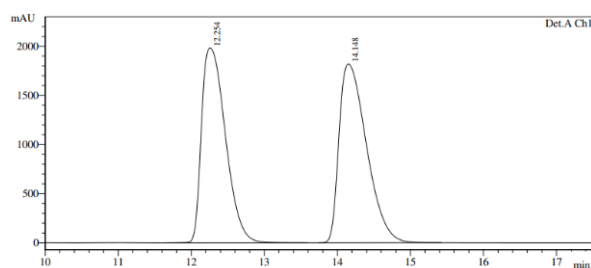
Peak #	RetTime [min]	Type	Width [min]	Area [pA*s]	Height [pA]	Area %
1	79.491	MM	0.5179	157.98010	5.08367	5.73541
2	80.638	MM	0.6001	2596.48926	72.10913	94.26459



**(S)-1-cyclopentyl-2-(p-tolyl)propan-1-one (183ba):**

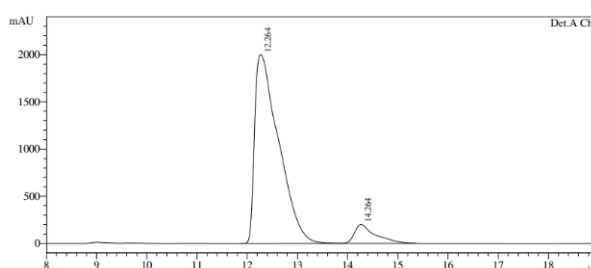
Prepared according to **GP4**, from **117** (0.7 mL, 0.43 M in THF, 0.3 mmol, 1.5 equiv), commercially available 1-iodo-4-methylbenzene (85 mg, 0.39 mmol, 1.95 equiv) and thioester **177a** (41 mg, 0.2 mmol, 1.0 equiv) with a reaction time of 20 h for the second step. Purification of the crude product by flash column chromatography (pentane/Et<sub>2</sub>O, 50:1) afforded analytically pure **183ba** (32 mg, 74% yield) as a pale-yellow oil.

**<sup>1</sup>H NMR** (400 MHz, Chloroform-*d*)  $\delta$  7.16 – 7.07 (m, 4H), 3.82 (q, *J* = 6.9 Hz, 1H), 2.89 (p, *J* = 7.4 Hz, 1H), 2.33 (s, 3H), 1.87 – 1.79 (m, 1H), 1.75 – 1.58 (m, 4H), 1.57 – 1.39 (m, 3H), 1.37 (d, *J* = 7.0 Hz, 3H). **<sup>13</sup>C NMR** (101 MHz, CDCl<sub>3</sub>)  $\delta$  213.8, 138.0, 136.7, 129.6, 128.0, 52.2, 50.0, 30.7, 29.2, 26.2, 21.2, 18.2. **IR** (ATR) 2956, 2868, 1708, 1513, 1450, 1372, 1359, 1314, 1128, 1110, 1064, 1020, 891, 820 cm<sup>-1</sup>. **HRMS** (ESI) *m/z*: [M+H]<sup>+</sup> calcd for C<sub>15</sub>H<sub>20</sub>OH 217.1587, found 217.1588. **Enantiomeric ratio** 92:8 was determined by chiral HPLC analysis with a Daicel Chiralcel OD-H column (0.2% isopropanol in *n*-heptane, 0.5 mL/min, 25 °C, detection at 220 nm, retention times (min): 12.26 (major), 14.26 (minor)).  **$[\alpha]_D^{20}$**  = +173.9 (*c* = 1.23 in CHCl<sub>3</sub>). Spectroscopic properties match with those described in the literature.<sup>23</sup>



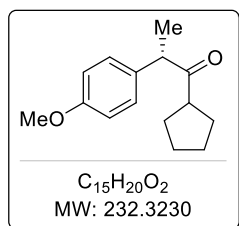
Detector A Ch1 220nm

Peak#	Ret. Time	Area	Height	Area %
1	12.254	45159770	1983009	48.701
2	14.148	47568187	1819430	51.299
Total		92727957	3802438	100.000



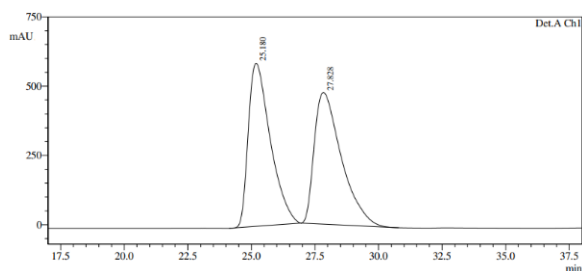
Detector A Ch1 220nm

Peak#	Ret. Time	Area	Height	Area %
1	12.264	66417278	1999960	92.124
2	14.264	5678316	198922	7.876
Total		72095594	2198882	100.000

**(S)-1-cyclopentyl-2-(4-methoxyphenyl)propan-1-one (183ca):**

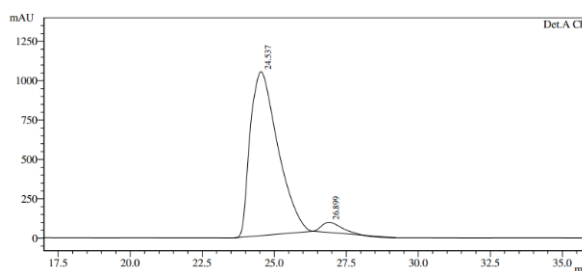
Prepared according to **GP4**, from **117** (0.7 mL, 0.43 M in THF, 0.3 mmol, 1.5 equiv), commercially available 1-iodo-4-methoxybenzene (91 mg, 0.39 mmol, 1.95 equiv) and thioester **177a** (41 mg, 0.2 mmol, 1.0 equiv) with a reaction time of 20 h for the second step. Purification of the crude product by flash column chromatography (pentane/EtOAc, 33:1) afforded analytically pure **183ca** (35 mg, 75% yield) as a pale-yellow oil.

**<sup>1</sup>H NMR** (400 MHz, CDCl<sub>3</sub>) δ 7.13 (d, *J* = 8.6 Hz, 2H), 6.85 (d, *J* = 8.7 Hz, 2H), 3.83 – 3.73 (s, 4H), 2.88 (p, *J* = 7.7 Hz, 1H), 1.86 – 1.77 (m, 1H), 1.72 – 1.56 (m, 4H), 1.55 – 1.41 (m, 3H), 1.35 (d, *J* = 6.9 Hz, 3H). **<sup>13</sup>C NMR** (101 MHz, CDCl<sub>3</sub>) δ 214.0, 158.7, 133.0, 129.1, 114.3, 55.3, 51.7, 49.9, 30.6, 29.2, 26.2, 18.2. **IR** (ATR) 2957, 2917, 2849, 1707, 1610, 1511, 1455, 1373, 1253, 1178, 1103, 1036, 833, 806 cm<sup>-1</sup>. **HRMS** (ESI) *m/z*: [M+H]<sup>+</sup> calcd for C<sub>15</sub>H<sub>20</sub>O<sub>2</sub>H 233.1536, found 233.1536. **Enantiomeric ratio** 96:4 was determined by chiral HPLC analysis with a Daicel Chiralcel OJ-column (0.5% isopropanol in *n*-heptane, 0.5 mL/min, 25 °C, detection at 230 nm, retention times (min): 24.54 (major), 26.90 (minor)). [α]<sub>D</sub><sup>20</sup> = +173.5 (c = 1.1 in CHCl<sub>3</sub>).



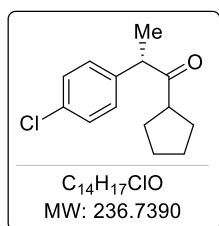
Detector A Ch1 230nm

Peak#	Ret. Time	Area	Height	Area %
1	25.180	35507073	588376	50.145
2	27.828	35301782	474981	49.855
Total		70808854	1063357	100.000



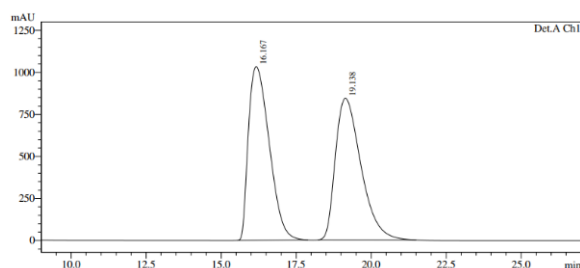
Detector A Ch1 230nm

Peak#	Ret. Time	Area	Height	Area %
1	24.537	69533724	1041067	95.965
2	26.899	2923799	64547	4.035
Total		72457523	1105614	100.000

**(S)-2-(4-chlorophenyl)-1-cyclopentylpropan-1-one (183da):**

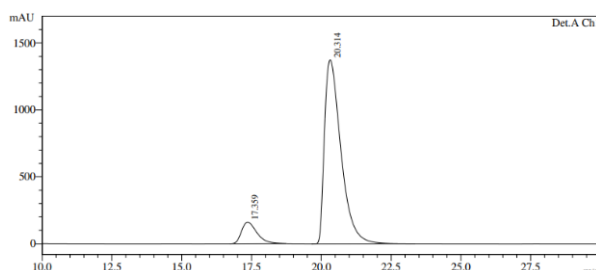
Prepared according to **GP4**, from **117** (0.7 mL, 0.43 M in THF, 0.3 mmol, 1.5 equiv), commercially available 1-iodo-4-chlorobenzene (93 mg, 0.39 mmol, 1.95 equiv) and thioester **177a** (41 mg, 0.2 mmol, 1.0 equiv) with a reaction time of 20 h for the second step. Purification of the crude product by flash column chromatography (pentane/EtOAc, 50:1) afforded analytically pure **183da** (37 mg, 78% yield) as a pale-orange oil.

**$^1H$  NMR** (400 MHz,  $CDCl_3$ )  $\delta$  7.29 (d,  $J = 8.4$  Hz, 2H), 7.15 (d,  $J = 8.4$  Hz, 2H), 3.84 (q,  $J = 6.9$  Hz, 1H), 2.85 (q,  $J = 7.5$  Hz, 1H), 1.88 – 1.75 (m, 1H), 1.72 – 1.57 (m, 4H), 1.57 – 1.43 (m, 3H), 1.37 (d,  $J = 7.0$  Hz, 3H).  
 **$^{13}C$  NMR** (101 MHz,  $CDCl_3$ )  $\delta$  214.0, 139.4, 133.0, 129.5, 129.1, 51.9, 50.2, 30.5, 29.3, 26.19, 26.18, 18.2.  
**IR** (ATR) 2958, 2931, 2869, 1709, 1649, 1492, 1451, 1409, 1282, 1125, 1093, 1015, 891, 832  $cm^{-1}$ .  
**HRMS** (APCI)  $m/z$ :  $[M+H]^+$  calcd for  $C_{14}H_{17}ClOH$  237.1041, found 237.1041. **Enantiomeric ratio** 90:10 was determined by chiral HPLC analysis with a Daicel Chiralcel OJ-H column (0.3% isopropanol in *n*-heptane, 0.5 mL/min, 25 °C, detection at 220 nm, retention times (min): 17.36 (minor), 20.31 (major)).  $[\alpha]_D^{20} = +129.1$  ( $c = 1.1$  in  $CHCl_3$ ). All the spectroscopic properties are in agreement with those described in the literature.<sup>[23]</sup>



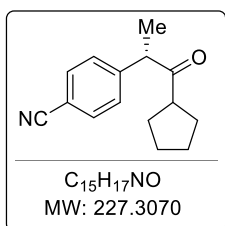
Detector A Ch1 220nm

Peak#	Ret. Time	Area	Height	Area %
1	16.167	49844202	1032364	49.890
2	19.138	50064210	842086	50.110
Total		99908412	1874450	100.000



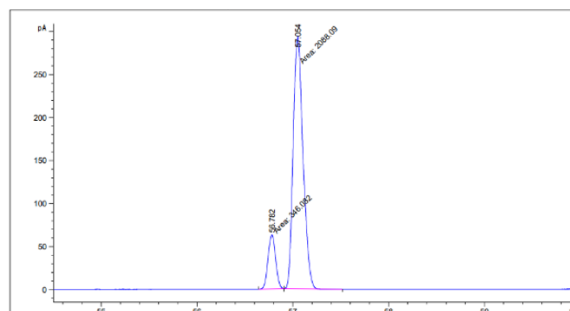
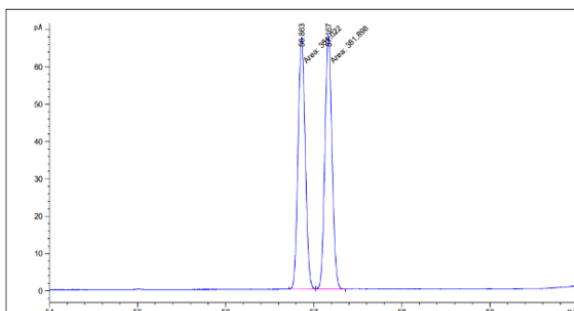
Detector A Ch1 220nm

Peak#	Ret. Time	Area	Height	Area %
1	17.359	6101324	160428	9.786
2	20.314	56247176	1374128	90.214
Total		62348500	1534556	100.000

**(S)-4-(1-cyclopentyl-1-oxopropan-2-yl)benzonitrile (183ea):**

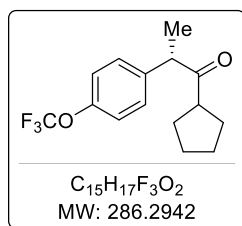
Prepared according to **GP4**, from **117** (0.7 mL, 0.43 M in THF, 0.3 mmol, 1.5 equiv), commercially available 4-iodobenzonitrile (89 mg, 0.39 mmol, 1.95 equiv) and thioester **177a** (41 mg, 0.2 mmol, 1.0 equiv) with a reaction time of 20 h for the second step. Purification of the crude product by flash column chromatography (pentane/EtOAc, 50:3) afforded analytically pure **183ea** (26 mg, 57% yield) as a pale-orange oil.

**<sup>1</sup>H NMR** (400 MHz, CDCl<sub>3</sub>) δ 7.60 (d, *J* = 8.3 Hz, 2H), 7.34 (d, *J* = 8.2 Hz, 2H), 3.93 (q, *J* = 6.9 Hz, 1H), 2.85 (p, *J* = 8.1 Hz, 1H), 1.87 – 1.77 (m, 1H), 1.71 – 1.56 (m, 4H), 1.56 – 1.45 (m, 3H), 1.39 (d, *J* = 7.0 Hz, 3H). **<sup>13</sup>C NMR** (101 MHz, CDCl<sub>3</sub>) δ 212.2, 146.2, 132.7, 128.9, 118.8, 111.1, 52.4, 50.6, 30.1, 29.2, 26.1, 18.2. **IR** (ATR) 2955, 2923, 2869, 2852, 2229, 1710, 1606, 1503, 1452, 1416, 1374, 1360, 1109, 1064, 1020, 890, 845 cm<sup>-1</sup>. **HRMS** (ESI) *m/z*: [M+Na]<sup>+</sup> calcd for C<sub>15</sub>H<sub>17</sub>NONa 250.1202, found 250.1203. **Enantiomeric ratio** 86:14 was determined by chiral GC analysis with a CP-Chirasil Dex CB column (initial temperature 70°C - temperature gradient 1°C/min - final temperature 200°C, retention times (min): 56.78 min (minor), 57.05 min (major)). [α]<sub>D</sub><sup>20</sup> = +104.3 (*c* = 0.95 in CHCl<sub>3</sub>).



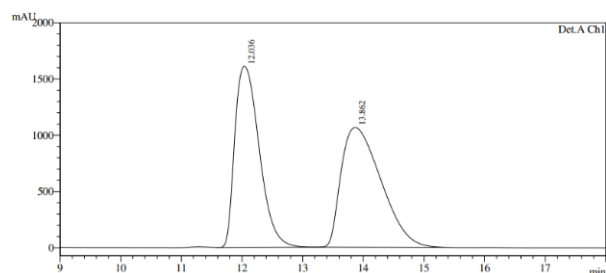
Peak #	RetTime [min]	Type	Width [min]	Area [pA*s]	Height [pA]	Area %
1	56.863	MM	0.0942	381.02203	67.44315	49.94258
2	57.167	MM	0.0936	381.89816	67.97682	50.05742

Peak #	RetTime [min]	Type	Width [min]	Area [pA*s]	Height [pA]	Area %
1	56.782	MM	0.0916	346.08246	62.97855	14.21769
2	57.054	MM	0.1186	2088.08545	293.54520	85.78231

**(S)-1-cyclopentyl-2-(4-(trifluoromethoxy)phenyl)propan-1-one (183fa):**

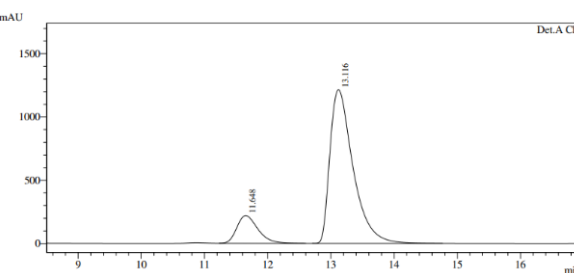
Prepared according to **GP4**, from **117** (0.7 mL, 0.43 M in THF, 0.3 mmol, 1.5 equiv), commercially available 1-iodo-4-(trifluoromethoxy)benzene (112 mg, 0.39 mmol, 1.95 equiv) and thioester **177a** (41 mg, 0.2 mmol, 1.0 equiv) with a reaction time of 20 h for the second step. Purification of the crude product by flash column chromatography (pentane/EtOAc, 50:1) afforded analytically pure **183fa** (36 mg, 63% yield) as a pale-orange oil.

**<sup>1</sup>H NMR** (400 MHz, CDCl<sub>3</sub>) δ 7.29 – 7.22 (m, 2H), 7.20 – 7.13 (m, 2H), 3.89 (q, *J* = 7.0 Hz, 1H), 2.88 (p, *J* = 7.8, 1H), 1.91 – 1.78 (m, 1H), 1.72 – 1.58 (m, 4H), 1.57 – 1.46 (m, 3H), 1.39 (d, *J* = 7.0 Hz, 3H). **<sup>13</sup>C NMR** (101 MHz, CDCl<sub>3</sub>) δ 213.2, 148.4 (q, *J* = 1.6 Hz), 139.6, 129.4, 121.4, 120.6 (q, *J* = 257.0 Hz), 51.7, 50.3, 30.4, 29.2, 26.2, 18.3. **<sup>19</sup>F NMR** (376 MHz, CDCl<sub>3</sub>) δ -57.9. **IR** (ATR) 2934, 2871, 1711, 1509, 1453, 1259, 1221, 1164, 1019, 891, 853 cm<sup>-1</sup>. **HRMS** (APCI) *m/z*: [M+H]<sup>+</sup> calcd for C<sub>15</sub>H<sub>17</sub>F<sub>3</sub>O<sub>2</sub>H 287.1253, found 287.1253. **Enantiomeric ratio** 86:14 was determined by chiral HPLC analysis with a Daicel Chiralcel OJ-H column (0.5% isopropanol in *n*-heptane, 0.5 mL/min, 25 °C, detection at 220 nm, retention times (min): 11.65 (minor), 13.12 (major)). [α]<sub>D</sub><sup>20</sup> = +90.8 (c = 1.11 in CHCl<sub>3</sub>).



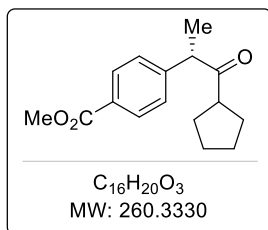
Detector A Ch1 220nm

Peak#	Ret. Time	Area	Height	Area %
1	12.036	45140959	1609599	48.116
2	13.862	48676026	1064412	51.884
Total		93816984	2674011	100.000



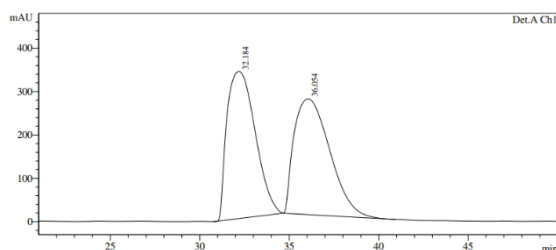
Detector A Ch1 220nm

Peak#	Ret. Time	Area	Height	Area %
1	11.648	5039037	218651	14.031
2	13.116	30873457	1213595	85.969
Total		35912495	1432246	100.000

**Methyl (S)-4-(1-cyclopentyl-1-oxopropan-2-yl)benzoate (183ga):**

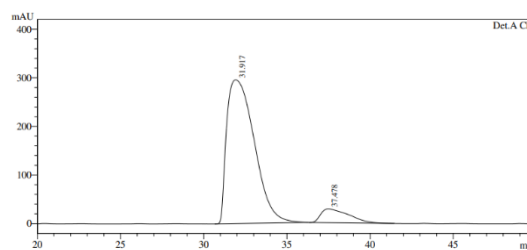
Prepared according to **GP4**, from **117** (0.7 mL, 0.43 M in THF, 0.3 mmol, 1.5 equiv), commercially available methyl 4-iodobenzoate (102 mg, 0.39 mmol, 1.95 equiv) and thioester **177a** (41 mg, 0.2 mmol, 1.0 equiv) with a reaction time of 20 h for the second step. Purification of the crude product by flash column chromatography (pentane/EtOAc, 20:1) afforded analytically pure **183ga** (32 mg, 61% yield) as a pale-orange oil.

<sup>1</sup>H NMR (400 MHz, CDCl<sub>3</sub>) δ 7.98 (d, *J* = 8.0 Hz, 2H), 7.29 (d, *J* = 8.0 Hz, 2H), 3.97 – 3.88 (m, 4H), 2.85 (p, *J* = 7.6 Hz, 1H), 1.87 – 1.76 (m, 1H), 1.70 – 1.55 (m, 4H), 1.56 – 1.40 (m, 3H), 1.39 (d, *J* = 6.9 Hz, 3H). <sup>13</sup>C NMR (101 MHz, CDCl<sub>3</sub>) δ 212.9, 167.0, 146.1, 130.2, 129.1, 128.2, 52.6, 52.2, 50.4, 30.4, 29.3, 26.2, 18.1. IR (ATR) 2953, 2980, 1723, 1610, 1436, 1359, 1280, 1181, 1112, 1019, 833, 705 cm<sup>-1</sup>. HRMS (ESI) *m/z*: [M+NH<sub>4</sub>]<sup>+</sup> calcd for C<sub>16</sub>H<sub>20</sub>O<sub>3</sub>NH<sub>4</sub> 278.1751, found 278.1750. **Enantiomeric ratio** 91:9 was determined by chiral HPLC analysis with a Daicel Chiralpak AD-H column (0.7% isopropanol in *n*-heptane, 0.5 mL/min, 25 °C, detection at 230 nm, retention times (min): 31.92 (major), 37.48 (minor)).  $[\alpha]_D^{20} = +89.4$  (*c* = 1.05 in CHCl<sub>3</sub>).



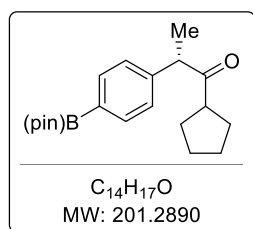
Detector A Ch1 230nm

Peak#	Ret. Time	Area	Height	Area %
1	32.184	37268608	338992	50.067
2	36.054	37169463	267065	49.933
Total		74438071	606057	100.000



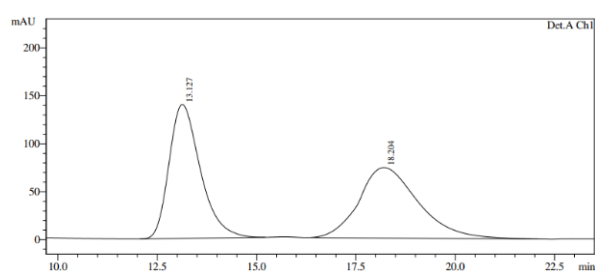
Detector A Ch1 230nm

Peak#	Ret. Time	Area	Height	Area %
1	31.917	34196087	295793	91.159
2	37.478	3316344	28512	8.841
Total		37512430	324304	100.000

**(S)-1-cyclopentyl-2-(4-(4,4,5,5-tetramethyl-1,3,2-dioxaborolan-2-yl)phenyl)propan-1-one (183ha):**

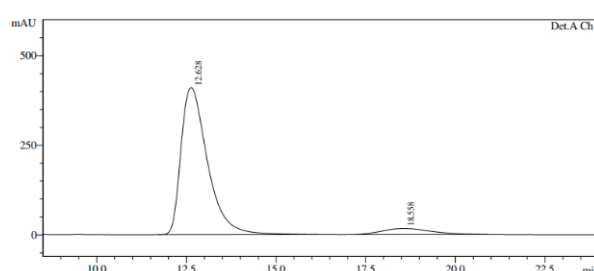
Prepared according to **GP4**, from **117** (0.7 mL, 0.43 M in THF, 0.3 mmol, 1.5 equiv), commercially available 2-(4-iodophenyl)-4,4,5,5-tetramethyl-1,3,2-dioxaborolane (129 mg, 0.39 mmol, 1.95 equiv) and thioester **177a** (41 mg, 0.2 mmol, 1.0 equiv) with a reaction time of 20 h for the second step. Purification of the crude product by flash column chromatography (pentane/acetone, 50:1) afforded analytically pure **183haa** (23 mg, 35% yield) as a pale-yellow oil.

**<sup>1</sup>H NMR** (400 MHz, CDCl<sub>3</sub>): δ 7.76 (d, *J* = 8.0 Hz, 2H), 7.22 (d, *J* = 8.1 Hz, 2H), 3.86 (q, *J* = 6.9 Hz, 1H), 2.85 (p, *J* = 7.8 Hz, 1H), 1.88 – 1.76 (m, 1H), 1.72 – 1.55 (m, 4H), 1.55 – 1.40 (m, 3H), 1.38 (d, *J* = 6.9 Hz, 3H), 1.33 (s, 12H). **<sup>13</sup>C NMR** (101 MHz, CDCl<sub>3</sub>): δ 213.5, 144.2, 135.5, 127.6, 83.9, 52.9, 50.2, 30.7, 29.2, 26.2, 25.01, 24.99, 18.0. **IR (ATR)** 2975, 2869, 1709, 1610, 1450, 1399, 1361, 1324, 1275, 1144, 1092, 1020, 963, 859, 659 cm<sup>-1</sup>. **HRMS (ESI)** *m/z*: [M+Na]<sup>+</sup> calcd for C<sub>20</sub>H<sub>29</sub>BO<sub>3</sub>Na 351.2102, found 351.2104. **Enantiomeric ratio** 93:7 was determined by chiral HPLC analysis with a Daicel Chiralcel OJ-H column (0.5% isopropanol in *n*-heptane, 0.5 mL/min, 25 °C, detection at 220 nm, retention times: 12.63 min (major), 18.56 min (minor)). **[α]<sub>D</sub><sup>20</sup>** = +115.2 (*c* = 0.95 in CHCl<sub>3</sub>).



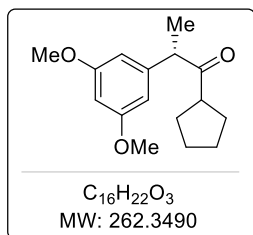
Detector A Ch1 220nm

Peak#	Ret. Time	Area	Height	Area %
1	13.127	7641531	139589	49.966
2	18.204	7651807	73532	50.034
Total		15293338	213121	100.000



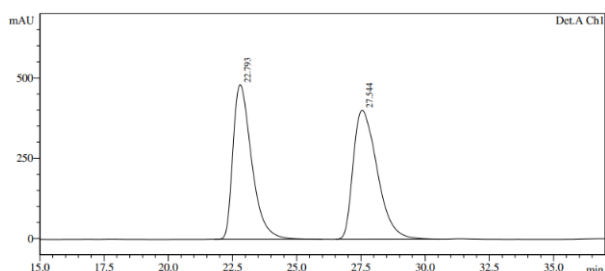
Detector A Ch1 220nm

Peak#	Ret. Time	Area	Height	Area %
1	12.628	21140203	410344	92.933
2	18.558	1607572	16909	7.067
Total		22747775	427253	100.000

**(S)-1-cyclopentyl-2-(3,5-dimethoxyphenyl)propan-1-one (183ia):**

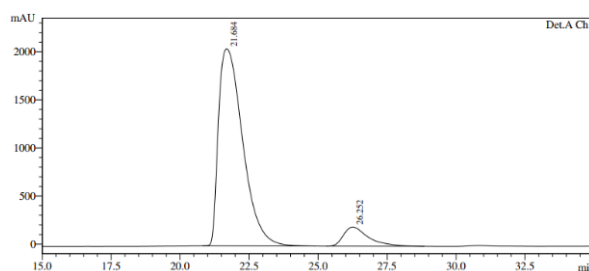
Prepared according to **GP4**, from **117** (0.7 mL, 0.43 M in THF, 0.3 mmol, 1.5 equiv), commercially available 1-iodo-3,5-dimethoxybenzene (103 mg, 0.39 mmol, 1.95 equiv) and thioester **177a** (41 mg, 0.2 mmol, 1.0 equiv) with a reaction time of 20 h for the second step. Purification of the crude product by flash column chromatography (pentane/EtOAc, 20:1) afforded analytically pure **183ia** (45 mg, 86% yield) as a yellow amorphous solid.

**$^1H$  NMR** (400 MHz,  $CDCl_3$ )  $\delta$  6.35 (s, 3H), 3.80 – 3.73 (m, 7H), 2.90 (p,  $J = 7.6$  Hz, 1H), 1.88 – 1.79 (m, 1H), 1.76 – 1.57 (m, 4H), 1.55 – 1.42 (m, 3H), 1.36 (d,  $J = 6.9$  Hz, 3H).  **$^{13}C$  NMR** (101 MHz,  $CDCl_3$ )  $\delta$  213.5, 161.2, 143.3, 106.2, 99.0, 55.4, 52.8, 49.9, 30.8, 29.3, 26.2, 17.9. **IR** (ATR) 2955, 2869, 1707, 1595, 1458, 1429, 1346, 1322, 1293, 1205, 1154, 1051, 1022, 928, 844, 696  $cm^{-1}$ . **HRMS** (ESI)  $m/z$ :  $[M+H]^+$  calcd for  $C_{16}H_{22}O_3H$  263.1642, found 263.1642. **Enantiomeric ratio** 91:9 was determined by chiral HPLC analysis with a Daicel Chiralcel OJ-H column (1.0% isopropanol in *n*-heptane, 0.5 mL/min, 25 °C, detection at 220 nm, retention times (min): 21.68 (major), 26.25 (minor)).  $[\alpha]_D^{20} = +125.7$  ( $c = 0.94$  in  $CHCl_3$ ).



Detector A Ch1 220nm

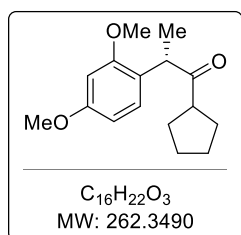
Peak#	Ret. Time	Area	Height	Area %
1	22.793	24416907	480995	48.265
2	27.544	26172248	401275	51.735
Total		50589155	882269	100.000



Detector A Ch1 220nm

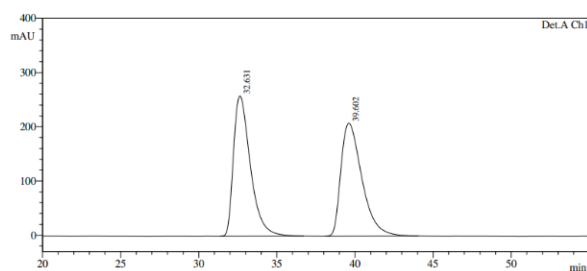
Peak#	Ret. Time	Area	Height	Area %
1	21.684	125360432	2049889	90.930
2	26.252	12504861	198744	9.070
Total		137865293	2248633	100.000



**(S)-1-cyclopentyl-2-(2,4-dimethoxyphenyl)propan-1-one (183ja):**

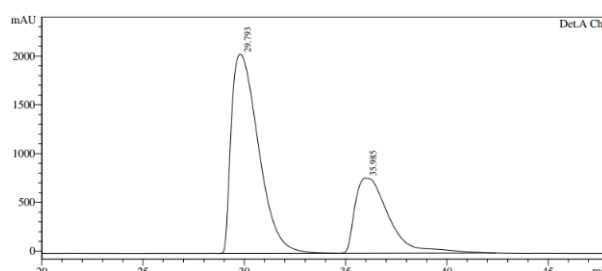
Prepared according to **GP4**, from **117** (0.7 mL, 0.43 M in THF, 0.3 mmol, 1.5 equiv), commercially available 1-iodo-2,4-dimethoxybenzene (103 mg, 0.39 mmol, 1.95 equiv) and thioester **177a** (41 mg, 0.2 mmol, 1.0 equiv) with a reaction time of 20 h for the second step. Purification of the crude product by flash column chromatography (pentane/EtOAc, 20:1) afforded analytically pure **183ja** (43 mg, 82% yield) as a pale-yellow amorphous solid.

**$^1H$  NMR** (400 MHz,  $CDCl_3$ )  $\delta$  6.99 (d,  $J = 9.0$  Hz, 1H), 6.48 – 6.41 (m, 2H), 4.12 (q,  $J = 7.0$  Hz, 1H), 3.80 (d,  $J = 2.2$  Hz, 3H), 2.84 (p,  $J = 8.3$  Hz, 1H), 1.84 – 1.68 (m, 2H), 1.67 – 1.54 (m, 3H), 1.53 – 1.40 (m, 3H), 1.30 (d,  $J = 6.9$  Hz, 3H).  **$^{13}C$  NMR** (101 MHz,  $CDCl_3$ )  $\delta$  214.9, 159.9, 157.8, 129.1, 122.2, 104.5, 98.8, 55.5, 55.4, 49.5, 44.9, 30.9, 29.3, 26.24, 26.21, 16.6. **IR** (ATR) 2955, 2868, 2837, 1706, 1612, 1587, 1506, 1454, 1419, 1293, 1263, 1209, 1158, 1136, 1037, 835, 608  $cm^{-1}$ . **HRMS** (ESI)  $m/z$ :  $[M+H]^+$  calcd for  $C_{16}H_{22}O_3H$  263.1642, found 263.1641. **Enantiomeric ratio** 68:32 was determined by chiral HPLC analysis with a Daicel Chiralcel OJ-H column (0.5% isopropanol in *n*-heptane, 0.5 mL/min, 25 °C, detection at 220 nm, retention times (min): 29.79 (major), 35.99 (minor)).  $[\alpha]_D^{20} = +63.3$  ( $c = 1.05$  in  $CHCl_3$ ).



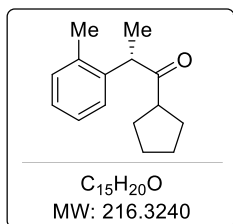
Detector A Ch1 220nm

Peak#	Ret. Time	Area	Height	Area %
1	32.631	19505122	258861	49.971
2	39.602	19527718	208362	50.029
Total		39032841	467223	100.000



Detector A Ch1 220nm

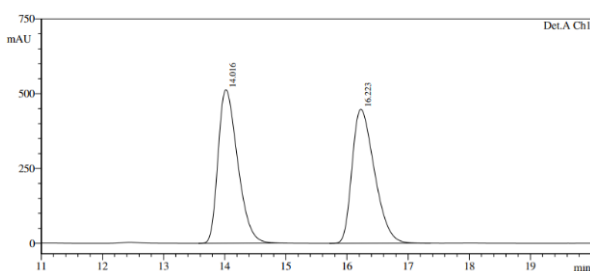
Peak#	Ret. Time	Area	Height	Area %
1	29.793	190603150	2041365	68.020
2	35.985	89611134	770699	31.980
Total		280214284	2812064	100.000

**(S)-1-cyclopentyl-2-(*o*-tolyl)propan-1-one (183ka):**

Prepared according to **GP4**, from **117** (0.7 mL, 0.43 M in THF, 0.3 mmol, 1.5 equiv), commercially available 1-iodo-2-methylbenzene (85 mg, 0.39 mmol, 1.95 equiv) and thioester **177a** (41 mg, 0.2 mmol, 1.0 equiv) with a reaction time of 20 h for the second step. Purification of the crude product by flash column chromatography (pentane/Et<sub>2</sub>O, 33:1) afforded analytically pure **183ka**

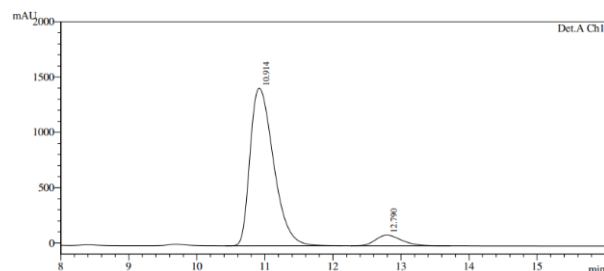
(23 mg, 53% yield) as a pale-orange oil.

**<sup>1</sup>H NMR** (400 MHz, CDCl<sub>3</sub>) δ 7.23 – 7.11 (m, 3H), 7.07 – 6.99 (m, 1H), 4.05 (d, J = 6.9 Hz, 1H), 2.77 (p, J = 8.0 Hz, 1H), 2.39 (s, 3H), 1.83 – 1.70 (m, 2H), 1.68 – 1.55 (m, 3H), 1.52 – 1.39 (m, 3H), 1.34 (d, J = 6.8 Hz, 3H). **<sup>13</sup>C NMR** (101 MHz, CDCl<sub>3</sub>) δ 214.2, 139.4, 135.8, 130.9, 127.4, 127.0, 126.7, 50.0, 48.6, 31.2, 29.3, 26.24, 26.20, 19.9, 17.3. **IR** (ATR) 2925, 2854, 1738, 1709, 1491, 1464, 1452, 1372, 1243, 1134, 1067, 1020, 756, 728 cm<sup>-1</sup>. **HRMS** (ESI) *m/z*: [M+NH<sub>4</sub>]<sup>+</sup> calcd for C<sub>15</sub>H<sub>20</sub>ONH<sub>4</sub> 234.1852, found 234.1853. **Enantiomeric ratio** 93:7 was determined by chiral HPLC analysis with a Daicel Chiralcel OD-H column (0.1% isopropanol in *n*-heptane, 0.5 mL/min, 25 °C, detection at 220 nm, retention times (min): 10.91 (major), 12.79 (minor)). [α]<sub>D</sub><sup>20</sup> = +152.9 (c = 0.9 in CHCl<sub>3</sub>).



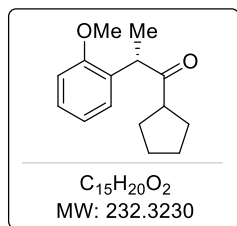
Detector A Ch1 220nm

Peak#	Ret. Time	Area	Height	Area %
1	14.016	11441765	513342	50.040
2	16.223	11423492	448070	49.960
Total		22865256	961412	100.000



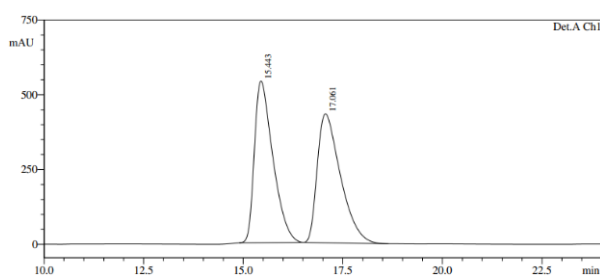
Detector A Ch1 220nm

Peak#	Ret. Time	Area	Height	Area %
1	10.914	34233268	1425033	93.015
2	12.790	2570604	96423	6.985
Total		36803872	1521455	100.000

**(S)-1-cyclopentyl-2-(2-methoxyphenyl)propan-1-one (183la):**

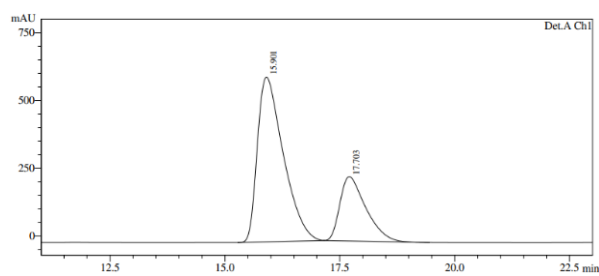
Prepared according to **GP4**, from **117** (0.7 mL, 0.43 M in THF, 0.3 mmol, 1.5 equiv), commercially available 1-iodo-2-methoxybenzene (91 mg, 0.39 mmol, 1.95 equiv) and thioester **177a** (41 mg, 0.2 mmol, 1 equiv) with a reaction time of 20 h for the second step. Purification of the crude product by flash column chromatography (pentane/EtOAc, 33:1) afforded analytically pure **183la** (26 mg, 56% yield) as a pale-orange oil.

**<sup>1</sup>H NMR** (400 MHz, CDCl<sub>3</sub>) δ 7.23 (td, *J* = 7.8, 1.8 Hz, 1H), 7.10 (dd, *J* = 7.6, 1.8 Hz, 1H), 6.98 – 6.85 (m, 2H), 4.21 (q, *J* = 6.9 Hz, 1H), 3.83 (s, 3H), 2.85 (p, *J* = 7.8 Hz, 1H), 1.84 – 1.70 (m, 2H), 1.69 – 1.55 (m, 3H), 1.54 – 1.41 (m, 3H), 1.33 (d, *J* = 7.0 Hz, 3H). **<sup>13</sup>C NMR** (101 MHz, CDCl<sub>3</sub>) δ 214.6, 156.9, 129.8, 128.7, 128.1, 121.0, 110.7, 55.5, 49.6, 45.5, 30.9, 29.3, 26.3, 26.2, 16.5. **IR** (ATR) 2919, 2850, 1709, 1597, 1493, 1439, 1415, 1246, 1030, 873, 754 cm<sup>-1</sup>. **HRMS** (ESI) *m/z*: [M+H]<sup>+</sup> calcd for C<sub>15</sub>H<sub>20</sub>O<sub>2</sub>H 233.1536, found 233.1542. **Enantiomeric ratio** 72:28 was determined by chiral HPLC analysis with a Daicel Chiralcel OJ column (0.5% isopropanol in *n*-heptane, 0.5 mL/min, 25 °C, detection at 220 nm, retention times (min): 15.90 (major), 17.70 (minor)). **[α]<sub>D</sub><sup>20</sup>** = +79.7 (*c* = 1.03 in CHCl<sub>3</sub>).



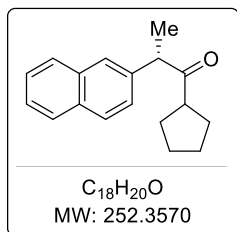
Detector A Chl 220nm

Peak#	Ret. Time	Area	Height	Area %
1	15.443	17451459	540246	49.933
2	17.061	17498423	430906	50.067
Total		34949883	971153	100.000



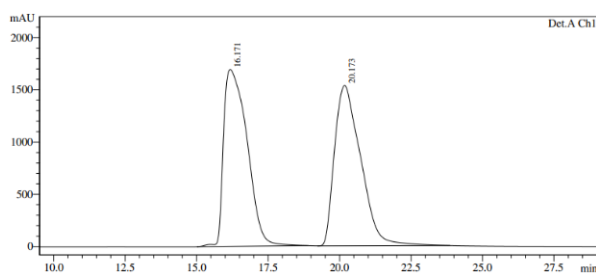
Detector A Chl 220nm

Peak#	Ret. Time	Area	Height	Area %
1	15.901	23876975	607406	71.930
2	17.703	9317540	237359	28.070
Total		33194514	844765	100.000

**(S)-1-cyclopentyl-2-(naphthalen-2-yl)propan-1-one (183na):**

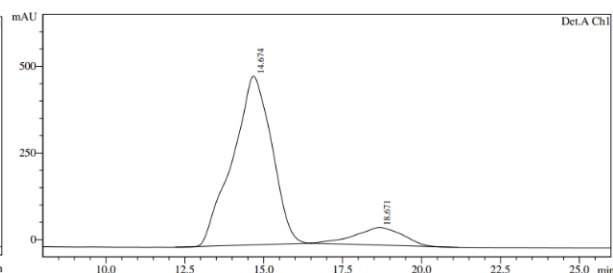
Prepared according to **GP4**, from **117** (0.7 mL, 0.43 M in THF, 0.3 mmol, 1.5 equiv), commercially available 2-iodonaphthalene (99 mg, 0.39 mmol, 1.95 equiv) and thioester **177a** (41 mg, 0.2 mmol, 1.0 equiv) with a reaction time of 20 h for the second step. Purification of the crude product by flash column chromatography (pentane/EtOAc, 50:1) afforded analytically pure **183na** (36 mg, 71% yield) as a pale-yellow viscous oil.

**<sup>1</sup>H NMR** (400 MHz, CDCl<sub>3</sub>) δ 7.85 – 7.79 (m, 3H), 7.69 (d, *J* = 1.7 Hz, 1H), 7.52 – 7.43 (m, 2H), 7.34 (dd, *J* = 8.5, 1.8 Hz, 1H), 4.04 (q, *J* = 6.9 Hz, 1H), 2.92 (q, *J* = 8.2 Hz, 1H), 1.91 – 1.82 (m, 1H), 1.77 – 1.56 (m, 4H), 1.55 – 1.38 (m, 6H). **<sup>13</sup>C NMR** (101 MHz, CDCl<sub>3</sub>) δ 213.7, 138.5, 133.8, 132.6, 128.7, 127.82, 127.80, 126.9, 126.4, 126.2, 126.0, 52.7, 50.2, 30.7, 29.21, 26.20, 18.2. **IR (ATR)** 3056, 2956, 2868, 1707, 1600, 1507, 1450, 1375, 1262, 1127, 1064, 1021, 949, 897, 857, 820, 746 cm<sup>-1</sup>. **HRMS (ESI)** *m/z*: [M+NH<sub>4</sub>]<sup>+</sup> calcd for C<sub>18</sub>H<sub>20</sub>ONH<sub>4</sub> 270.1852, found 270.1852. **Enantiomeric ratio** 89:11 was determined by chiral HPLC analysis with a Daicel Chiralpak AD-H column (0.3% isopropanol in *n*-heptane, 0.5 mL/min, 25 °C, detection at 220 nm, retention times (min): 14.67 (major), 18.67 (minor)). [α]<sub>D</sub><sup>20</sup> = +153.2 (c = 0.95 in CHCl<sub>3</sub>).



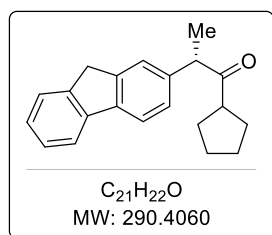
Detector A Ch1 220nm

Peak#	Ret. Time	Area	Height	Area %
1	16.171	96811571	1692202	49.750
2	20.173	97783387	1533688	50.250
Total		194594958	3225890	100.000



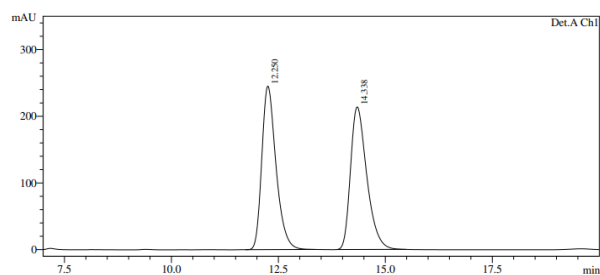
Detector A Ch1 220nm

Peak#	Ret. Time	Area	Height	Area %
1	14.674	42155285	487238	88.751
2	18.671	5343307	50907	11.249
Total		47498592	538144	100.000

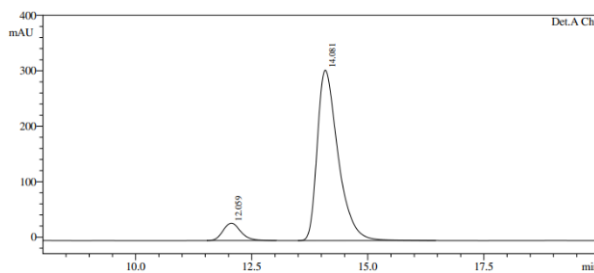
**(S)-1-cyclopentyl-2-(9H-fluoren-2-yl)propan-1-one (183pa):**

Prepared according to **GP4**, from **117** (0.7 mL, 0.43 M in THF, 0.3 mmol, 1.5 equiv), commercially available 2-iodo-9H-fluorene (114 mg, 0.39 mmol, 1.95 equiv) and thioester **177a** (41 mg, 0.2 mmol, 1.0 equiv) with a reaction time of 20 h for the second step. Purification of the crude product by flash column chromatography (pentane/EtOAc, 50:1) afforded analytically pure **183pa** (47 mg, 81% yield) as a pale-orange solid (m.p. 113-115 °C).

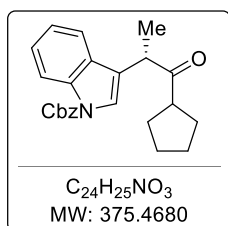
**$^1H$  NMR** (400 MHz,  $CDCl_3$ )  $\delta$  7.80 – 7.70 (m, 2H), 7.54 (d,  $J = 7.4$  Hz, 1H), 7.43 – 7.22 (m, 4H), 3.94 (q,  $J = 6.9$  Hz, 1H), 3.89 (s, 2H), 2.95 (p,  $J = 7.9$  Hz, 1H), 1.94 – 1.81 (m, 1H), 1.78 – 1.58 (m, 4H), 1.57 – 1.40 (m, 6H).  **$^{13}C$  NMR** (101 MHz,  $CDCl_3$ )  $\delta$  213.8, 144.0, 143.4, 141.5, 140.8, 139.5, 126.93, 126.89, 126.8, 125.1, 124.7, 120.2, 119.9, 52.7, 50.1, 37.0, 30.7, 29.3, 26.2, 18.3. **IR** (ATR) 2957, 2870, 1705, 1455, 1370, 1313, 1119, 1065, 1025, 866, 835, 766, 737  $cm^{-1}$ . **HRMS** (APCI)  $m/z$ :  $[M+H]^+$  calcd for  $C_{21}H_{22}OH$  291.1743, found 291.1744. **Enantiomeric ratio** 92:8 was determined by chiral HPLC analysis with a Daicel Chiralcel OD-H column (1.0% isopropanol in *n*-heptane, 0.5 mL/min, 25 °C, detection at 254 nm, retention times (min): 12.06 (minor), 14.08 (major)).  $[\alpha]_D^{20} = +118.5$  ( $c = 0.95$  in  $CHCl_3$ ).



Peak#	Ret. Time	Area	Height	Area %
1	12.250	5675839	245094	50.004
2	14.338	5674899	213893	49.996
Total		11350738	458988	100.000

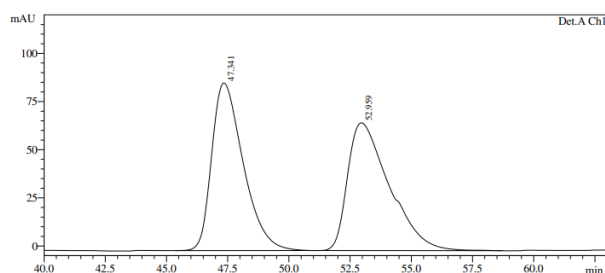


Peak#	Ret. Time	Area	Height	Area %
1	12.059	839268	31347	8.031
2	14.081	9611289	307438	91.969
Total		10450557	338785	100.000

**Benzyl (S)-3-(1-cyclopentyl-1-oxopropan-2-yl)-1H-indole-1-carboxylate (183qa):**

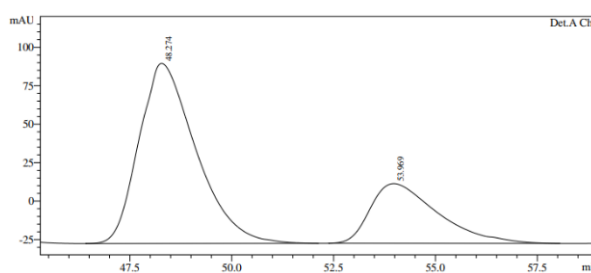
Prepared according to **GP4**, from **117** (0.7 mL, 0.43 M in THF, 0.3 mmol, 1.5 equiv), **A2** (147 mg, 0.39 mmol, 1.95 equiv) and thioester **177a** (41 mg, 0.2 mmol, 1.0 equiv) with a reaction time of 20 h for the second step. Purification of the crude product by flash column chromatography (pentane/Et<sub>2</sub>O, 10:1) afforded analytically pure **183qa** (19 mg, 25% yield) as a colourless oil.

**<sup>1</sup>H NMR** (300 MHz, CDCl<sub>3</sub>) δ 8.18 (d, J = 9.6 Hz, 1H), 7.56 – 7.19 (m, 9H), 5.45 (s, 2H), 4.05 (q, J = 7.0 Hz, 1H), 2.98 (p, J = 7.9 Hz, 1H), 1.87 – 1.43 (m, 11H). **<sup>13</sup>C NMR** (101 MHz, CDCl<sub>3</sub>) δ 213.6, 150.9, 135.2, 129.7, 128.9, 128.8, 125.1, 123.2, 123.1, 121.2, 119.4, 115.6, 68.9, 49.3, 43.6, 30.8, 29.6, 26.3, 16.9 (2 C signals are not visible). **IR** (ATR) 2969, 2918, 2869, 2037, 1935, 1738, 1712, 1455, 1397, 1354, 1236, 1219, 1118, 1097, 909, 763, 746, 733, 698 cm<sup>-1</sup>. **HRMS** (ESI) *m/z*: [M+NH<sub>4</sub>]<sup>+</sup> calcd for C<sub>24</sub>H<sub>25</sub>NO<sub>3</sub>NH<sub>4</sub> 393.2173, found 393.2172. **Enantiomeric ratio** 72:28 was determined by chiral HPLC analysis with a Daicel Chiralcel OD-H column (0.5% isopropanol in *n*-heptane, 0.5 mL/min, 25 °C, detection at 220 nm, retention times (min): 48.27 (major), 53.97 (minor)). **[α]<sub>D</sub><sup>20</sup>** = +23.7 (c = 0.56 in CHCl<sub>3</sub>).



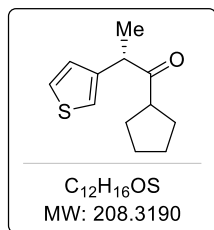
Detector A Ch1 220nm

Peak#	Ret. Time	Area	Height	Area %
1	47.341	7804373	86990	49.820
2	52.959	7860753	66290	50.180
Total		15665126	153280	100.000



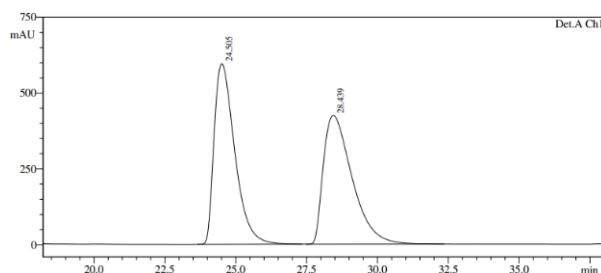
Detector A Ch1 220nm

Peak#	Ret. Time	Area	Height	Area %
1	48.274	11433034	117125	71.895
2	53.969	4469335	38843	28.105
Total		15902370	155969	100.000

**(S)-1-cyclopentyl-2-(thiophen-3-yl)propan-1-one (183ra):**

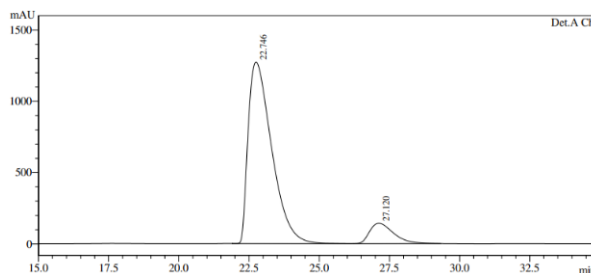
Prepared according to **GP4**, from **117** (0.7 mL, 0.43 M in THF, 0.3 mmol, 1.5 equiv), commercially available 3-iodothiophene (82 mg, 0.39 mmol, 1.95 equiv) and thioester **177a** (41 mg, 0.2 mmol, 1.0 equiv) with a reaction time of 20 h for the second step. Purification of the crude product by flash column chromatography (pentane/EtOAc, 50:2) afforded analytically pure **183ra** (14 mg, 34% yield) as a pale-orange oil.

**$^1H$  NMR** (400 MHz,  $CDCl_3$ )  $\delta$  7.29 – 7.26 (m, 1H), 7.07 (dd,  $J$  = 3.1, 1.3 Hz, 1H), 6.96 (dd,  $J$  = 5.0, 1.3 Hz, 1H), 3.99 (q,  $J$  = 6.9 Hz, 1H), 2.99 – 2.90 (m, 1H), 1.85 – 1.75 (m, 1H), 1.74 – 1.58 (m, 4H), 1.57 – 1.46 (m, 3H), 1.39 (d,  $J$  = 7.0 Hz, 3H).  **$^{13}C$  NMR** (101 MHz,  $CDCl_3$ )  $\delta$  213.5, 141.2, 127.3, 126.1, 121.6, 49.7, 47.8, 30.4, 29.3, 26.2, 17.8. **IR** (neat) 2953, 2918, 2850, 1709, 1452, 1372, 1260, 1104, 1022, 919, 861, 791, 764, 656  $cm^{-1}$ . **HRMS** (APCI)  $m/z$ :  $[M+H]^+$  calcd for  $C_{12}H_{16}OSH$  209.0995, found 209.0995. **Enantiomeric ratio** 90:10 was determined by chiral HPLC analysis with a Daicel Chiralcel OJ-H column (0.3% isopropanol in *n*-heptane, 0.5 mL/min, 25 °C, detection at 220 nm, retention times (min): 22.75 (major), 27.12 (minor)).  $[\alpha]_D^{20}$  = +110.4 ( $c$  = 0.55 in  $CHCl_3$ ).



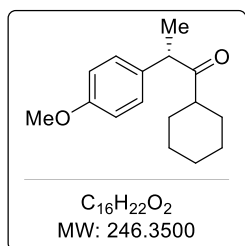
Detector A Ch1 220nm

Peak#	Ret. Time	Area	Height	Area %
1	24.505	30147335	595446	50.152
2	28.439	29964284	424330	49.848
Total		60111620	1019775	100.000



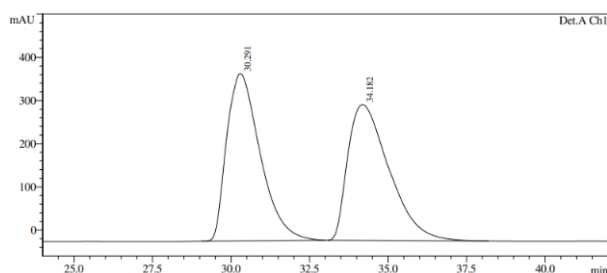
Detector A Ch1 220nm

Peak#	Ret. Time	Area	Height	Area %
1	22.746	74195637	1272337	89.793
2	27.120	8434139	142840	10.207
Total		82629776	1415177	100.000

**(S)-1-cyclohexyl-2-(4-methoxyphenyl)propan-1-one (183cb):**

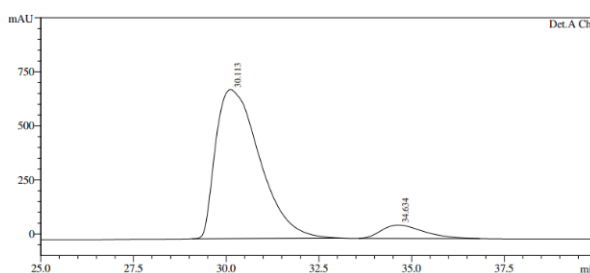
Prepared according to **GP4**, from **117** (0.7 mL, 0.43 M in THF, 0.3 mmol, 1.5 equiv), commercially available 1-iodo-4-methoxybenzene (91 mg, 0.39 mmol, 1.95 equiv) and thioester **177b** (44 mg, 0.2 mmol, 1 equiv) with a reaction time of 20 h for the second step. Purification of the crude product by flash column chromatography (pentane/Et<sub>2</sub>O, 25:1) afforded analytically pure **183cb** (37 mg, 75% yield) as a pale-yellow oil.

**<sup>1</sup>H NMR** (400 MHz, CDCl<sub>3</sub>) δ 7.12 (d, J = 8.7 Hz, 2H), 6.84 (d, J = 8.7 Hz, 2H), 3.84 (q, J = 6.9 Hz, 1H), 3.78 (s, 3H), 2.40 (tt, J = 11.3, 3.6 Hz, 1H), 1.87 – 1.56 (m, 4H), 1.50 – 1.03 (m, 9H). **<sup>13</sup>C NMR** (101 MHz, CDCl<sub>3</sub>) δ 214.2, 158.7, 132.9, 129.1, 114.3, 55.3, 50.4, 49.4, 29.6, 28.5, 26.0, 25.9, 25.4, 18.3. **IR** (ATR) 2930, 2854, 1707, 1610, 1511, 1449, 1372, 1247, 1178, 1145, 1036, 835 cm<sup>-1</sup>. **HRMS** (ESI) *m/z*: [M+H]<sup>+</sup> calcd for C<sub>16</sub>H<sub>22</sub>O<sub>2</sub>H 247.1693, found 247.1690. **Enantiomeric ratio** 92:8 was determined by chiral HPLC analysis with a Daicel Chiralcel OJ-H column (0.5% isopropanol in *n*-heptane, 0.5 mL/min, 25 °C, detection at 220 nm, retention times: 30.11 min (major), 34.63 min (minor)). [α]<sub>D</sub><sup>20</sup> = +144.3 (c = 1.0 in CHCl<sub>3</sub>).



Detector A Ch1 220nm

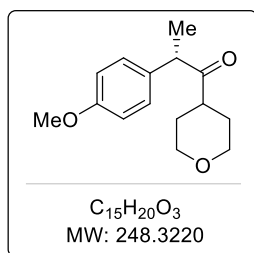
Peak#	Ret. Time	Area	Height	Area %
1	30.291	28750331	387466	50.007
2	34.182	28742498	314431	49.993
Total		57492828	701897	100.000



Detector A Ch1 220nm

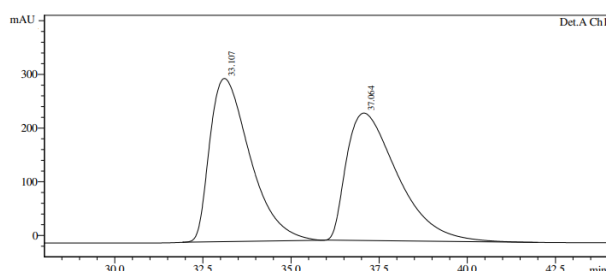
Peak#	Ret. Time	Area	Height	Area %
1	30.113	56930681	689354	92.105
2	34.634	4879812	61855	7.895
Total		61810494	751208	100.000



**(S)-2-(4-methoxyphenyl)-1-(tetrahydro-2H-pyran-4-yl)propan-1-one (183cc):**

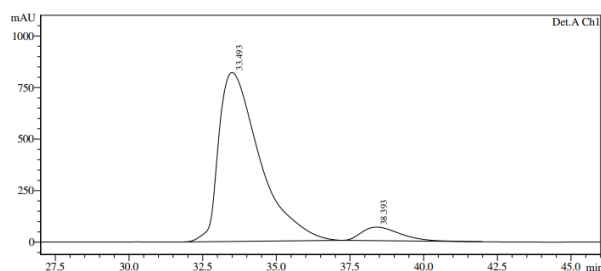
Prepared according to **GP4**, from **117** (0.7 mL, 0.43 M in THF, 0.3 mmol, 1.5 equiv), commercially available 1-iodo-4-methoxybenzene (91 mg, 0.39 mmol, 1.95 equiv) and thioester **177c** (44 mg, 0.2 mmol, 1.0 equiv) with a reaction time of 20 h for the second step. Purification of the crude product by flash column chromatography (pentane/EtOAc, 8:2) afforded analytically pure **183cc** (30 mg, 60% yield) as a yellow oil.

**<sup>1</sup>H NMR** (400 MHz, CDCl<sub>3</sub>) δ 7.11 (d, *J* = 8.7 Hz, 2H), 6.85 (d, *J* = 8.7 Hz, 2H), 3.99 – 3.76 (m, 6H), 3.34 (td, *J* = 11.5, 2.8 Hz, 1H), 3.25 (td, *J* = 11.8, 2.4 Hz, 1H), 2.61 (tt, *J* = 11.3, 4.0 Hz, 1H), 1.76 – 1.57 (m, 3H), 1.35 – 1.29 (m, 4H). **<sup>13</sup>C NMR** (101 MHz, CDCl<sub>3</sub>) δ 212.2, 158.9, 132.4, 129.1, 114.5, 67.4, 67.2, 55.4, 50.2, 46.1, 29.2, 28.3, 18.3. **IR** (ATR) 2951, 2929, 2839, 1706, 1609, 1511, 1444, 1365, 1281, 1249, 1179, 1124, 1033, 1019, 835 cm<sup>-1</sup>. **HRMS** (ESI) *m/z*: [M+H]<sup>+</sup> calcd for C<sub>15</sub>H<sub>20</sub>O<sub>3</sub>H 249.1485, found 249.1485. **Enantiomeric ratio** 93:7 was determined by chiral HPLC analysis with a Daicel Chiralcel OJ-H column (10% isopropanol in *n*-heptane, 0.5 mL/min, 25 °C, detection at 220 nm, retention times: 33.49 min (major), 38.39 min (minor)). **[α]<sub>D</sub><sup>20</sup>** = +126.1 (*c* = 1.0 in CHCl<sub>3</sub>).



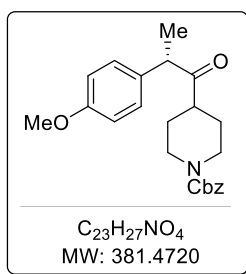
Detector A Ch1 220nm

Peak#	Ret. Time	Area	Height	Area %
1	33.107	24245769	304054	50.110
2	37.064	24139383	237463	49.890
Total		48385151	541517	100.000



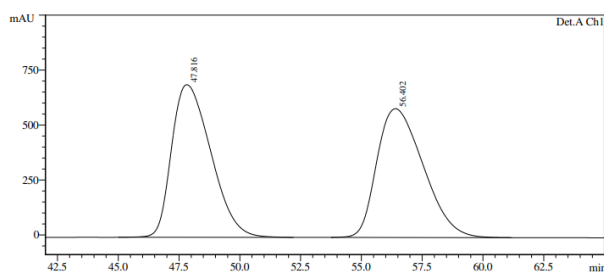
Detector A Ch1 220nm

Peak#	Ret. Time	Area	Height	Area %
1	33.493	79519525	819337	93.026
2	38.393	5961699	65497	6.974
Total		85481223	884834	100.000

**Benzyl (S)-4-(2-(4-methoxyphenyl)propanoyl)piperidine-1-carboxylate (183cd):**

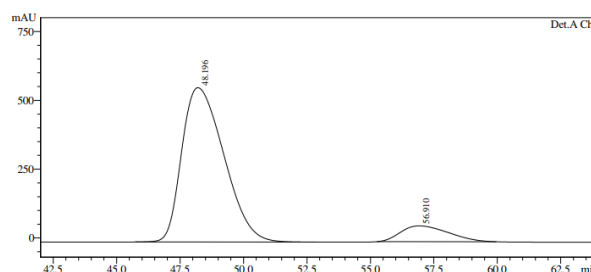
Prepared according to **GP4**, from **117** (0.7 mL, 0.43 M in THF, 0.3 mmol, 1.5 equiv), commercially available 1-iodo-4-methoxybenzene (91 mg, 0.39 mmol, 1.95 equiv) and thioester **177d** (71 mg, 0.2 mmol, 1.0 equiv) with a reaction time of 20 h for the second step. Purification of the crude product by flash column chromatography (pentane/Et<sub>2</sub>O, 1:1) afforded analytically pure **183cd** (48 mg, 63% yield) as yellow oil.

**<sup>1</sup>H NMR** (400 MHz, CDCl<sub>3</sub>) δ 7.40 – 7.28 (m, 5H), 7.11 (d, J = 8.7 Hz, 2H), 6.86 (d, J = 8.7 Hz, 2H), 5.10 (s, 2H), 4.23 – 3.99 (m, 2H), 3.84 (q, J = 6.9 Hz, 1H), 3.79 (s, 3H), 2.86 – 2.62 (m, 2H), 2.55 (tt, J = 11.3, 3.8 Hz, 1H), 1.78 (bs, 1H), 1.54 (dtd, J = 16.8, 13.1, 7.7 Hz, 2H), 1.44 – 1.37 (m, 1H), 1.34 (d, J = 6.9 Hz, 3H). **<sup>13</sup>C NMR** (101 MHz, CDCl<sub>3</sub>) δ 212.2, 158.9, 155.2, 136.9, 132.3, 129.0, 128.6, 128.1, 128.0, 114.5, 67.2, 55.4, 50.6, 46.9, 43.6, 43.3, 28.4, 27.6, 18.2. **IR** (ATR) 2930, 2858, 1698, 1609, 1511, 1467, 1445, 1430, 1365, 1279, 1251, 1224, 1179, 1133, 1020, 976, 911, 834, 764, 733, 699 cm<sup>-1</sup>. **HRMS** (ESI) *m/z*: [M+Na]<sup>+</sup> calcd for C<sub>23</sub>H<sub>27</sub>NO<sub>4</sub>Na 404.1832, found 404.1819. **Enantiomeric ratio** 90:10 was determined by chiral HPLC analysis with a Daicel Chiralpak AD-H column (10% isopropanol in *n*-heptane, 0.5 mL/min, 25 °C, detection at 220 nm, retention times: 48.20 min (major), 56.91 min (minor)). [ $\alpha$ ]<sub>D</sub><sup>20</sup> = +95.1 (c = 1.0 in CHCl<sub>3</sub>).



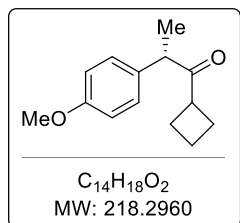
Detector A Ch1 220nm

Peak#	Ret. Time	Area	Height	Area %
1	47.816	78112079	694323	50.066
2	56.402	77906785	586044	49.934
Total		156018864	1280368	100.000



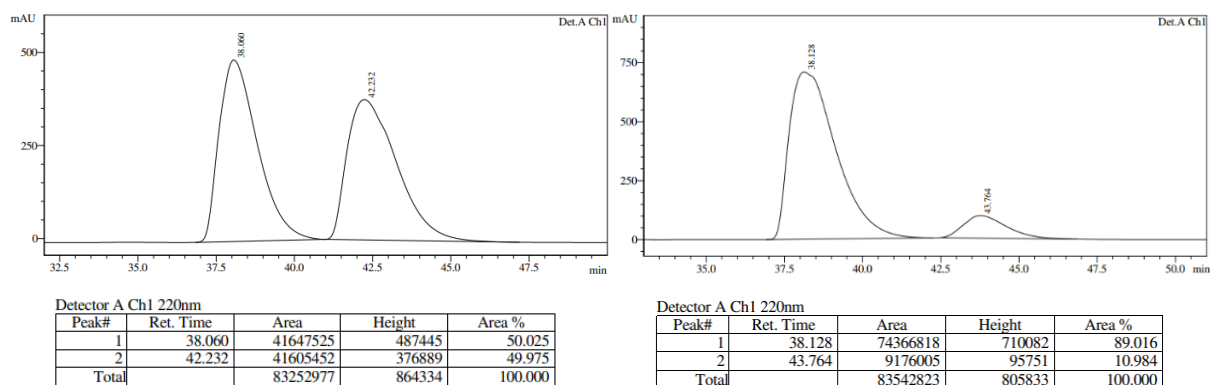
Detector A Ch1 220nm

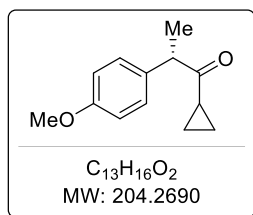
Peak#	Ret. Time	Area	Height	Area %
1	48.196	64790713	560458	89.648
2	56.910	7481671	57504	10.352
Total		72272384	617962	100.000

**(S)-1-cyclobutyl-2-(4-methoxyphenyl)propan-1-one (183ce):**

Prepared according to **GP4**, from **117** (0.7 mL, 0.43 M in THF, 0.3 mmol, 1.5 equiv), commercially available 1-iodo-4-methoxybenzene (91 mg, 0.39 mmol, 1.95 equiv) and thioester **177e** (39 mg, 0.2 mmol, 1.0 equiv) with a reaction time of 20 h for the second step. Purification of the crude product by flash column chromatography (pentane/Et<sub>2</sub>O, 25:1) afforded analytically pure **183ce** (33 mg, 76% yield) as a pale-yellow oil.

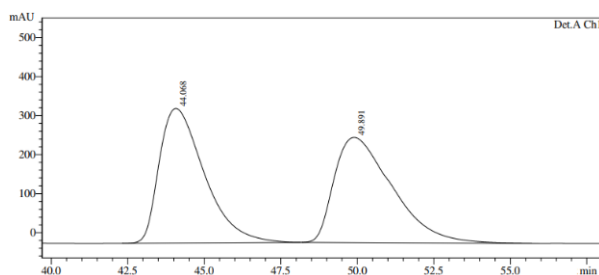
**<sup>1</sup>H NMR** (400 MHz, CDCl<sub>3</sub>) δ 7.09 (d, J = 8.7 Hz, 2H), 6.84 (d, J = 8.7 Hz, 2H), 3.78 (s, 3H), 3.68 (q, J = 7.0 Hz, 1H), 3.27 (p, J = 8.3 Hz, 1H), 2.21 – 1.99 (m, 3H), 1.91 – 1.67 (m, 3H), 1.35 (d, J = 7.0 Hz, 3H). **<sup>13</sup>C NMR** (101 MHz, CDCl<sub>3</sub>) δ 212.0, 158.7, 132.9, 129.0, 114.3, 55.3, 50.0, 44.2, 25.4, 24.6, 17.84, 17.79. **IR** (ATR) 2962, 1704, 1610, 1511, 1258, 1178, 1132, 1097, 1034, 833, 800 cm<sup>-1</sup>. **HRMS** (ESI) *m/z*: [M+H]<sup>+</sup> calcd for C<sub>14</sub>H<sub>18</sub>O<sub>2</sub>H 219.1380, found 219.138. **Enantiomeric ratio** 89:11 was determined by chiral HPLC analysis with a Daicel Chiralcel OJ-H column (0.5% isopropanol in *n*-heptane, 0.5 mL/min, 25 °C, detection at 220 nm, retention times: 38.13 min (major), 43.76 min (minor)). [ $\alpha$ ]<sub>D</sub><sup>20</sup> = +142.7 (c = 1.1 in CHCl<sub>3</sub>).



**(S)-1-cyclopropyl-2-(4-methoxyphenyl)propan-1-one (183cf):**

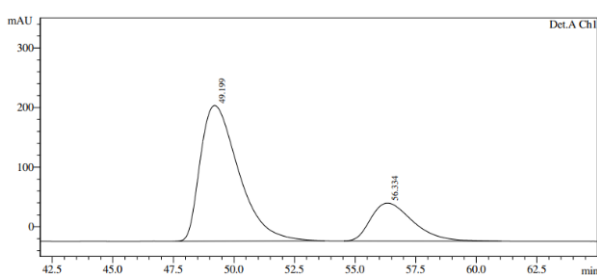
Prepared according to **GP4**, from **117** (0.7 mL, 0.43 M in THF, 0.3 mmol, 1.5 equiv), commercially available 1-iodo-4-methoxybenzene (91 mg, 0.39 mmol, 1.95 equiv) and thioester **177f** (36 mg, 0.2 mmol, 1.0 equiv) with a reaction time of 20 h for the second step. Purification of the crude product by flash column chromatography (pentane/Et<sub>2</sub>O, 25:1) afforded analytically pure **183cf** (31 mg, 76% yield) as a pale-yellow oil.

**<sup>1</sup>H NMR** (400 MHz, CDCl<sub>3</sub>) δ 7.15 (d, J = 8.7 Hz, 2H), 6.87 (d, J = 8.7 Hz, 2H), 3.85 (q, J = 7.0 Hz, 1H), 3.80 (s, 3H), 1.85 (tt, J = 7.8, 4.6 Hz, 1H), 1.38 (d, J = 7.0 Hz, 3H), 0.96 (tddd, J = 16.0, 9.6, 4.6, 2.9 Hz, 2H), 0.78 (dddd, J = 10.2, 8.1, 6.1, 2.6 Hz, 1H), 0.70 (dddd, J = 9.4, 7.9, 6.3, 2.6 Hz, 1H). **<sup>13</sup>C NMR** (101 MHz, CDCl<sub>3</sub>) δ 211.2, 158.3, 133.1, 129.2, 114.4, 55.4, 53.0, 19.7, 17.8, 11.4, 11.3. **IR** (ATR) 3007, 2966, 2932, 2836, 1698, 1611, 1582, 1511, 1444, 1380, 1302, 1250, 1179, 1132, 1036, 881, 765 cm<sup>-1</sup>. **HRMS** (ESI) *m/z*: [M+Na]<sup>+</sup> calcd for C<sub>13</sub>H<sub>16</sub>O<sub>2</sub>Na 227.1043, found 227.1048. **Enantiomeric ratio** 77:23 was determined by chiral HPLC analysis with a Daicel Chiralcel OJ-H column (0.5% isopropanol in *n*-heptane, 0.5 mL/min, 25 °C, detection at 220 nm, retention times: 49.20 min (major), 56.33 min (minor)). [α]<sub>D</sub><sup>20</sup> = +129.1 (c = 1.08 in CHCl<sub>3</sub>).



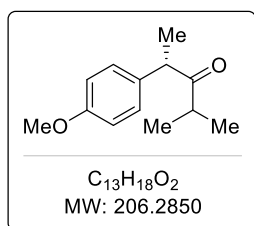
Detector A Ch1 220nm

Peak#	Ret. Time	Area	Height	Area %
1	44.068	35394693	345003	49.864
2	49.891	35587178	269622	50.136
Total		70981871	614624	100.000



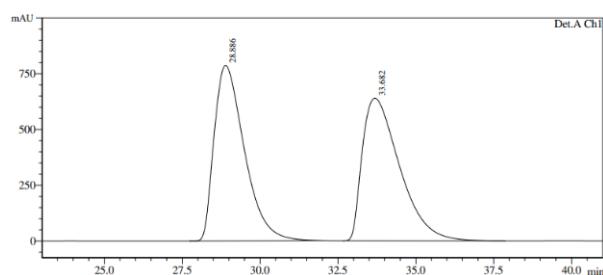
Detector A Ch1 220nm

Peak#	Ret. Time	Area	Height	Area %
1	49.199	25036270	227512	76.500
2	56.334	7691087	63573	23.500
Total		32727357	291084	100.000

**(S)-2-(4-methoxyphenyl)-4-methylpentan-3-one (183cg):**

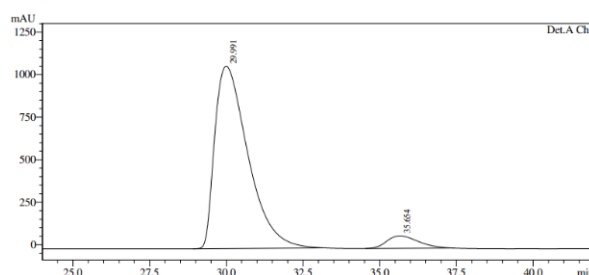
Prepared according to **GP4**, from **117** (0.7 mL, 0.43 M in THF, 0.3 mmol, 1.5 equiv), commercially available 1-iodo-4-methoxybenzene (91 mg, 0.39 mmol, 1.95 equiv) and thioester **177g** (36 mg, 0.2 mmol, 1.0 equiv) with a reaction time of 20 h for the second step. Purification of the crude product by flash column chromatography (pentane/Et<sub>2</sub>O, 25:1) afforded analytically pure **183cg** (33 mg, 80% yield) as a pale-yellow oil.

**<sup>1</sup>H NMR** (400 MHz, CDCl<sub>3</sub>)  $\delta$  7.13 (d, *J* = 8.7 Hz, 2H), 6.85 (d, *J* = 8.7 Hz, 2H), 3.86 (q, *J* = 6.9 Hz, 1H), 3.78 (s, 3H), 2.68 (p, *J* = 6.9 Hz, 1H), 1.34 (d, *J* = 6.9 Hz, 3H), 1.06 (d, *J* = 7.1 Hz, 3H), 0.91 (d, *J* = 6.7 Hz, 3H). **<sup>13</sup>C NMR** (101 MHz, CDCl<sub>3</sub>)  $\delta$  215.0, 158.8, 132.9, 129.1, 114.3, 55.34, 50.36, 39.1, 19.4, 18.4, 18.3. **IR** (ATR) 2969, 2932, 1710, 1611, 1511, 1465, 1445, 1252, 1179, 1035, 1017, 834 cm<sup>-1</sup>. **HRMS** (ESI) *m/z*: [M+H]<sup>+</sup> calcd for C<sub>13</sub>H<sub>18</sub>O<sub>2</sub>H 207.1380, found 207.1379. **Enantiomeric ratio** 94:6 was determined by chiral HPLC analysis with a Daicel Chiralcel OJ-H column (0.5% isopropanol in *n*-heptane, 0.5 mL/min, 25 °C, detection at 220 nm, retention times: 29.99 min (major), 35.65 min (minor)). [ $\alpha$ ]<sub>D</sub><sup>20</sup> = +252.6 (*c* = 0.9 in CHCl<sub>3</sub>).



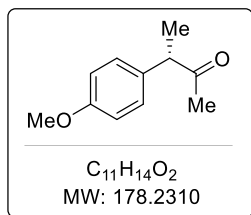
Detector A Ch1 220nm

Peak#	Ret. Time	Area	Height	Area %
1	28.886	53166529	786776	49.937
2	33.682	53301585	638744	50.063
Total		106468115	1425519	100.000



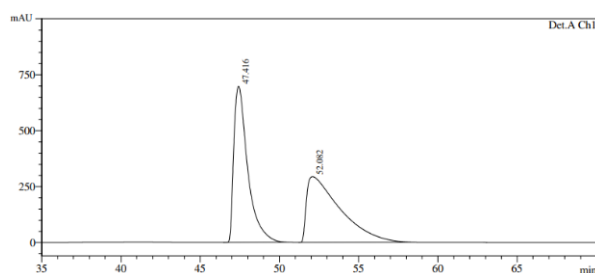
Detector A Ch1 220nm

Peak#	Ret. Time	Area	Height	Area %
1	29.991	80831378	1072136	93.922
2	35.654	5230477	73232	6.078
Total		86061855	1145368	100.000

**(S)-3-(4-methoxyphenyl)butan-2-one (183ci):**

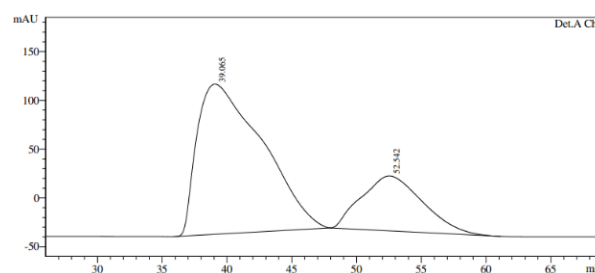
Prepared according to **GP4**, from **117** (0.7 mL, 0.43 M in THF, 0.3 mmol, 1.5 equiv), commercially available 1-iodo-4-methoxybenzene (91 mg, 0.39 mmol, 1.95 equiv) and thioester **177i** (30 mg, 0.2 mmol, 1.0 equiv) with a reaction time of 20 h for the second step. Purification of the crude product by flash column chromatography (pentane/acetone, 25:1) afforded analytically pure **183ci** (28 mg, 79% yield) as a pale-yellow oil.

**<sup>1</sup>H NMR** (400 MHz, CDCl<sub>3</sub>): δ 7.13 (d, J = 8.6 Hz, 2H), 6.87 (d, J = 8.8 Hz, 2H), 3.79 (s, 3H), 3.69 (q, J = 7.0 Hz, 1H), 2.03 (s, 3H), 1.36 (d, J = 7.0 Hz, 3H). **<sup>13</sup>C NMR** (101 MHz, CDCl<sub>3</sub>) δ 209.3, 158.9, 132.8, 128.9, 114.5, 55.4, 53.0, 28.3, 17.4. **IR** (ATR) 2932, 2838, 1713, 1611, 1511, 1457, 1355, 1303, 1248, 1178, 1166, 1067, 1037, 834, 811 cm<sup>-1</sup>. **HRMS** (ESI) *m/z*: [M+Na]<sup>+</sup> calcd for C<sub>11</sub>H<sub>14</sub>O<sub>2</sub>Na 201.0886, found 201.0891. **Enantiomeric ratio** 74:26 was determined by chiral HPLC analysis with a Daicel Chiralcel OD-H column (0.1% isopropanol in *n*-heptane, 0.5 mL/min, 25 °C, detection at 220 nm, retention times: 39.07 min (major), 52.54 min (minor)). **[α]<sub>D</sub><sup>20</sup>** = +108.3 (c = 1.05 in CHCl<sub>3</sub>).



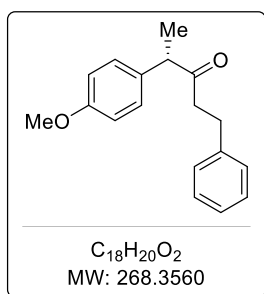
Detector A Ch1 220nm

Peak#	Ret. Time	Area	Height	Area %
1	47.416	42750420	698537	49.656
2	52.082	43343097	293783	50.344
Total		86093517	992320	100.000



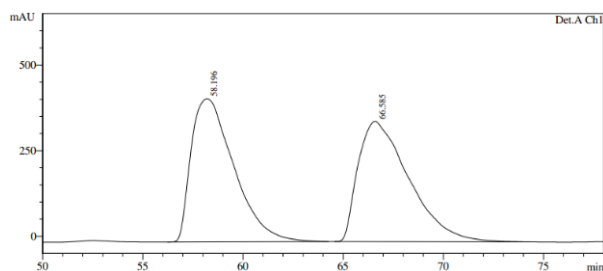
Detector A Ch1 220nm

Peak#	Ret. Time	Area	Height	Area %
1	39.065	53899864	153741	74.468
2	52.542	18480375	56140	25.532
Total		72380239	209881	100.000

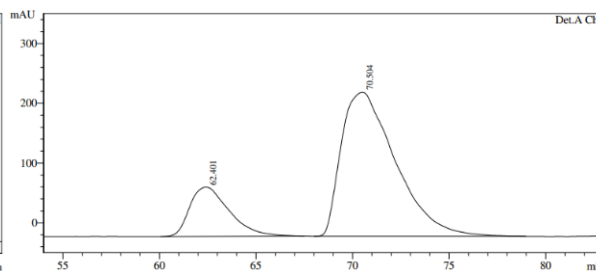
**(S)-4-(4-methoxyphenyl)-1-phenylpentan-3-one (183cj):**

Prepared according to **GP4**, from **117** (0.7 mL, 0.43 M in THF, 0.3 mmol, 1.5 equiv), commercially available 1-iodo-4-methoxybenzene (91 mg, 0.39 mmol, 1.95 equiv) and thioester **177j** (49 mg, 0.2 mmol, 1.0 equiv) with a reaction time of 20 h for the second step. Purification of the crude product by flash column chromatography (pentane/EtOAc, 50:3) afforded analytically pure **183cj** (42 mg, 78% yield) as a pale-yellow amorphous solid.

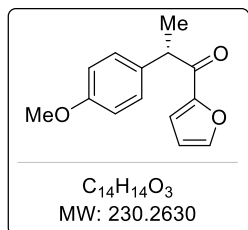
**<sup>1</sup>H NMR** (400 MHz, CDCl<sub>3</sub>): δ 7.29 – 7.14 (m, 3H), 7.12 – 7.09 (m, 4H), 6.87 (d, J = 8.7 Hz, 2H), 3.82 (s, 3H), 3.69 (q, J = 6.9 Hz, 1H), 2.93 – 2.62 (m, 4H), 1.38 (d, J = 6.9 Hz, 3H). **<sup>13</sup>C NMR** (101 MHz, CDCl<sub>3</sub>): δ 210.3, 158.8, 141.2, 132.6, 129.0, 128.5, 128.4, 126.1, 114.4, 55.4, 52.4, 42.5, 30.1, 17.5. **IR** (ATR) 3028, 2930, 2837, 1712, 1609, 1510, 1454, 1360, 1302, 1249, 1179, 1126, 1034, 833, 750, 700 cm<sup>-1</sup>. **HRMS** (ESI) *m/z*: [M+Na]<sup>+</sup> calcd for C<sub>18</sub>H<sub>20</sub>O<sub>2</sub>Na 291.1356, found 291.1363. **Enantiomeric ratio** 80:20 was determined by chiral HPLC analysis with a Daicel Chiralcel OJ-H column (4% isopropanol in *n*-heptane, 0.5 mL/min, 25 °C, detection at 220 nm, retention times: 62.40 min (minor), 70.50 min (major)). [α]<sub>D</sub><sup>20</sup> = +78.1 (c = 1.05 in CHCl<sub>3</sub>).



Detector A Ch1 220nm				
Peak#	Ret. Time	Area	Height	Area %
1	58.196	62059084	418181	50.032
2	66.585	61979165	351497	49.968
Total		124038249	769678	100.000

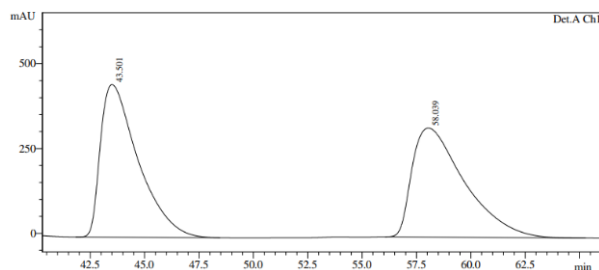


Detector A Ch1 220nm				
Peak#	Ret. Time	Area	Height	Area %
1	62.401	11706521	82310	19.917
2	70.504	47069156	240598	80.083
Total		58775677	322908	100.000

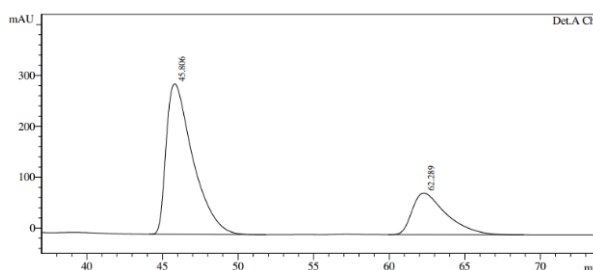
**(S)-1-(furan-2-yl)-2-(4-methoxyphenyl)propan-1-one (183cm):**

Prepared according to **GP4**, from **117** (0.7 mL, 0.43 M in THF, 0.3 mmol, 1.5 equiv), commercially available 1-iodo-4-methoxybenzene (91 mg, 0.39 mmol, 1.95 equiv) and thioester **177m** (41 mg, 0.2 mmol, 1.0 equiv) with a reaction time of 20 h for the second step. Purification of the crude product by flash column chromatography (pentane/EtOAc, 50:3) afforded analytically pure **183cm** (28 mg, 61% yield) as a colourless amorphous solid.

**$^1H$  NMR** (400 MHz,  $CDCl_3$ ):  $\delta$  7.52 (d,  $J$  = 1.6 Hz, 1H), 7.25 (d,  $J$  = 8.8 Hz, 2H), 7.13 (d,  $J$  = 3.6 Hz, 1H), 6.84 (d,  $J$  = 8.7 Hz, 2H), 6.45 (dd,  $J$  = 3.6, 1.7 Hz, 1H), 4.45 (d,  $J$  = 7.0 Hz, 1H), 3.76 (s, 3H), 1.50 (d,  $J$  = 7.0 Hz, 3H).  **$^{13}C$  NMR** (101 MHz,  $CDCl_3$ )  $\delta$  189.8, 158.8, 152.3, 146.4, 133.0, 129.0, 117.9, 114.3, 112.3, 55.3, 47.2, 18.4. **IR** (ATR) 3141, 3126, 3113, 2958, 1705, 1665, 1611, 1511, 1467, 1393, 1303, 1255, 1179, 1163, 1031, 1005, 958, 905, 881, 839, 815, 795, 780, 749, 702  $cm^{-1}$ . **HRMS** (ESI)  $m/z$ :  $[M+H]^+$  calcd for  $C_{14}H_{14}O_3H$  231.1016, found 231.1023. **Enantiomeric ratio** 74:26 was determined by chiral HPLC analysis with a Daicel Chiralcel OJ column (10% isopropanol in *n*-heptane, 0.5 mL/min, 25 °C, detection at 220 nm, retention times: 45.81 min (major), 62.29 min (minor)).  $[\alpha]_D^{20} = +28.8$  ( $c = 1.15$  in  $CHCl_3$ ).

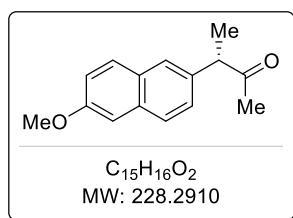


Detector A Ch1 220nm				
Peak#	Ret. Time	Area	Height	Area %
1	43.501	54224730	449759	50.206
2	58.039	53780604	321112	49.794
Total		108005335	770871	100.000



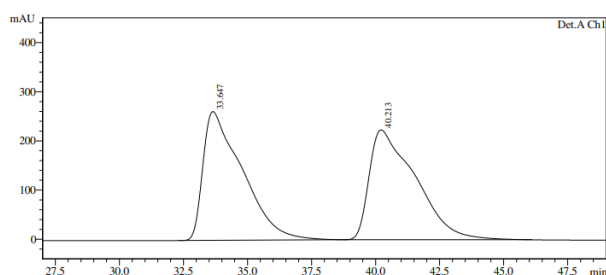
Detector A Ch1 220nm				
Peak#	Ret. Time	Area	Height	Area %
1	45.806	36272662	295851	73.812
2	62.289	12869484	81832	26.188
Total		49142146	377683	100.000



**(S)-3-(6-methoxynaphthalen-2-yl)butan-2-one (183ti):**

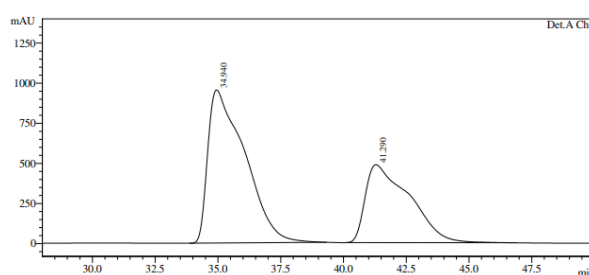
Prepared according to **GP4**, from **117** (0.7 mL, 0.43 M in THF, 0.3 mmol, 1.5 equiv), **A4** (111 mg, 0.39 mmol, 1.95 equiv) and thioester **177i** (30 mg, 0.2 mmol, 1.0 equiv) with a reaction time of 20 h for the second step. Purification of the crude product by flash column chromatography (pentane/EtOAc, 20:1) afforded analytically pure **183ti** (35 mg, 77% yield) as a pale-orange solid.

**<sup>1</sup>H NMR** (400 MHz, CDCl<sub>3</sub>) δ 7.71 (dd, *J* = 8.7, 4.6 Hz, 2H), 7.61 (s, 1H), 7.29 (dd, *J* = 8.5, 1.9 Hz, 1H), 7.19 – 7.12 (m, 2H), 3.92 (s, 3H), 3.87 (q, *J* = 7.0 Hz, 1H), 2.07 (s, 3H), 1.47 (d, *J* = 7.0 Hz, 3H). **<sup>13</sup>C NMR** (101 MHz, CDCl<sub>3</sub>) δ 209.1, 157.8, 135.8, 133.8, 129.3, 129.2, 127.7, 126.5, 126.4, 119.3, 105.7, 55.4, 53.8, 28.5, 17.3. **IR** (ATR) 2980, 2959, 2937, 2907, 1715, 1705, 1604, 1505, 1485, 1455, 1392, 1371, 1354, 1314, 1268, 1227, 1196, 1172, 913, 891, 856, 837, 818, 767, 739, 673 cm<sup>-1</sup>. **HRMS** (ESI) *m/z*: [M+Na]<sup>+</sup> calcd for C<sub>15</sub>H<sub>16</sub>O<sub>2</sub>Na 251.1043, found 251.1049. **Enantiomeric ratio** 62:38 was determined by chiral HPLC analysis with a Daicel Chiralpak AD-H column (0.5% isopropanol in *n*-heptane, 0.5 mL/min, 25 °C, detection at 220 nm, retention times: 34.94 min (major), 41.29 min (minor)). **[α]<sub>D</sub><sup>20</sup>** = +62.0 (*c* = 1.0 in CHCl<sub>3</sub>).



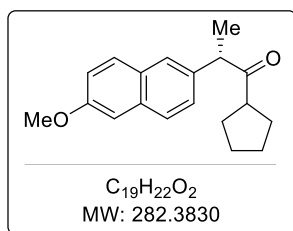
Detector A Ch1 220nm

Peak#	Ret. Time	Area	Height	Area %
1	33.647	28027342	261814	49.962
2	40.213	28069663	223263	50.038
Total		56097005	485077	100.000



Detector A Ch1 220nm

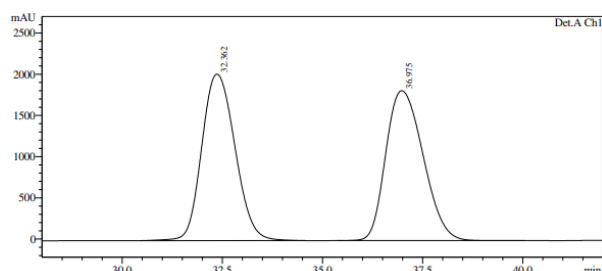
Peak#	Ret. Time	Area	Height	Area %
1	34.940	98011442	954180	62.206
2	41.290	59547065	485928	37.794
Total		157558507	1440107	100.000

**(S)-1-cyclopentyl-2-(6-methoxynaphthalen-2-yl)propan-1-one (183ta):**

Prepared according to **GP4**, from **117** (0.7 mL, 0.43 M in THF, 0.3 mmol, 1.5 equiv), **A4** (111 mg, 0.39 mmol, 1.95 equiv) and thioester **177a** (41 mg, 0.2 mmol, 1.0 equiv) with a reaction time of 20 h for the second step. Purification of the crude product by flash column chromatography (pentane/Et<sub>2</sub>O, 25:1) afforded analytically pure **183ta** (32 mg, 57% yield)

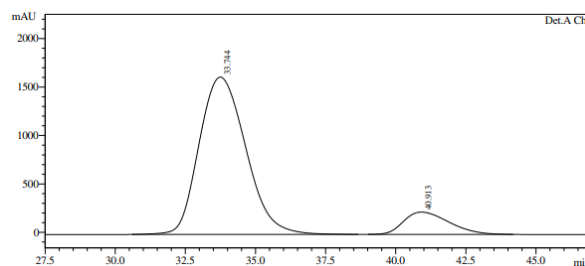
as a pale-orange oil.

**<sup>1</sup>H NMR** (400 MHz, CDCl<sub>3</sub>) δ 7.70 (d, *J* = 8.6 Hz, 2H), 7.61 (d, *J* = 1.8 Hz, 1H), 7.30 (dd, *J* = 8.4, 1.9 Hz, 1H), 7.20 – 7.08 (m, 2H), 3.99 (q, *J* = 6.9 Hz, 1H), 3.92 (s, 3H), 2.93 (p, *J* = 7.8 Hz, 1H), 1.90 – 1.80 (m, 1H), 1.76 – 1.56 (m, 4H), 1.53 – 1.38 (m, 6H). **<sup>13</sup>C NMR** (101 MHz, CDCl<sub>3</sub>) δ 213.9, 157.8, 136.1, 133.7, 129.3, 129.2, 127.5, 126.73, 126.71, 119.2, 105.8, 55.45, 52.54, 50.1, 30.7, 29.2, 26.2, 18.2. **IR** (ATR) 2957, 2868, 1706, 1605, 1505, 1484, 1391, 1266, 1229, 1174, 1032, 926, 892, 853, 812 cm<sup>-1</sup>. **HRMS** (ESI) *m/z*: [M+Na]<sup>+</sup> calcd for C<sub>19</sub>H<sub>22</sub>O<sub>2</sub>Na 305.1512, found 305.1513. **Enantiomeric ratio** 88:12 was determined by chiral HPLC analysis with a Daicel Chiralpak AD-H column (0.5% isopropanol in *n*-heptane, 0.5 mL/min, 25 °C, detection at 220 nm, retention times: 33.74 min (major), 40.91 min (minor)). **[α]<sub>D</sub><sup>20</sup>** = +124.4 (*c* = 1.1 in CHCl<sub>3</sub>).



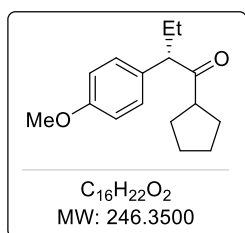
Detector A Ch1 220nm

Peak#	Ret. Time	Area	Height	Area %
1	32.362	116740538	2020083	49.758
2	36.975	117877973	1818459	50.242
Total		234618511	3838542	100.000



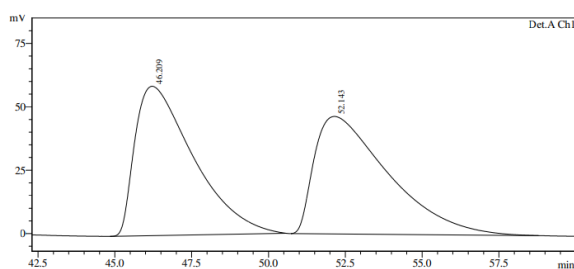
Detector A Ch1 220nm

Peak#	Ret. Time	Area	Height	Area %
1	33.744	187725524	1623824	87.889
2	40.913	25868880	229917	12.111
Total		213594404	1853741	100.000

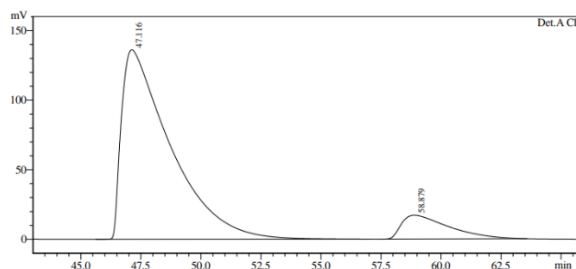
**(S)-1-cyclopentyl-2-(4-methoxyphenyl)butan-1-one (206):**

Prepared according to **GP4**, from **119** (0.6 mL, 0.54 M in THF, 0.3 mmol, 1.5 equiv), commercially available 1-iodo-4-methoxybenzene (91 mg, 0.39 mmol, 1.95 equiv) and thioester **177a** (41 mg, 0.2 mmol, 1.0 equiv), with a reaction time of 72 h for the second step. Purification of the crude product by flash column chromatography (pentane/Et<sub>2</sub>O, 25:1) afforded analytically pure **206** (34 mg, 69% yield) as a pale-yellow oil.

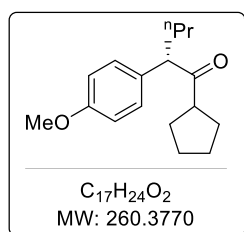
**<sup>1</sup>H NMR** (400 MHz, CDCl<sub>3</sub>) δ 7.15 – 7.08 (m, 2H), 6.88 – 6.80 (m, 2H), 3.78 (s, 3H), 3.56 (t, J = 7.4 Hz, 1H), 2.86 (p, J = 8.0 Hz, 1H), 2.02 (dt, J = 13.6, 7.2 Hz, 1H), 1.87 – 1.76 (m, 1H), 1.73 – 1.40 (m, 8H), 0.81 (t, J = 7.4 Hz, 3H). **<sup>13</sup>C NMR** (101 MHz, CDCl<sub>3</sub>) δ 213.4, S25 158.8, 131.4, 129.5, 114.2, 59.6, 55.4, 50.6, 30.2, 28.8, 26.2, 26.1, 25.9, 12.3. **IR** (ATR) 2944, 1516, 1454, 1422, 1329, 1259, 1146, 1110, 1088, 949, 809, 755 cm<sup>-1</sup>. **HRMS** (ESI) *m/z*: [M+H]<sup>+</sup> calcd for C<sub>16</sub>H<sub>22</sub>O<sub>2</sub>H 247.1693, found 247.1693. **Enantiomeric ratio** 89:11 was determined by chiral HPLC analysis with a Daicel Chiralcel OD-H column (0.1% isopropanol in *n*-heptane for 30 min, then gradient from 0.1% to 1% isopropanol in 5 min, and continue with 1% isopropanol, 0.5 mL/min, 25 °C, detection at 220 nm, retention times (min): 47.12 (major), 58.88 (minor)).  $[\alpha]_D^{20} = +147.1$  (c = 1.1 in CHCl<sub>3</sub>).



Detector A Ch1 220nm				
Peak#	Ret. Time	Area	Height	Area %
1	46.209	7810970	58899	50.145
2	52.143	7765683	46327	49.855
Total		15576653	105226	100.000

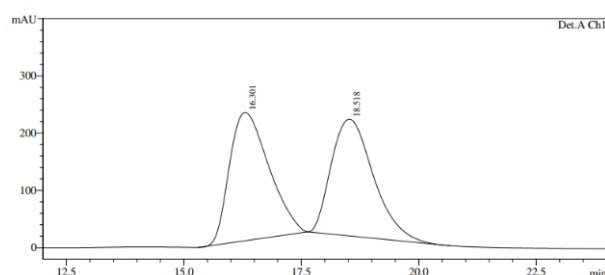


Detector A Ch1 220nm				
Peak#	Ret. Time	Area	Height	Area %
1	47.116	19380363	136092	89.182
2	58.879	2350934	17131	10.818
Total		21731297	153223	100.000

**(S)-1-cyclopentyl-2-(4-methoxyphenyl)pentan-1-one (207):**

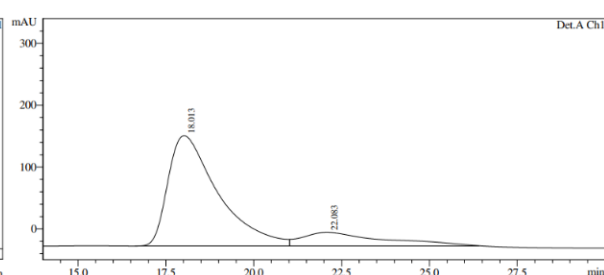
Prepared according to **GP4**, from **195** (0.5 mL, 0.6 M in THF, 0.3 mmol, 1.5 equiv), commercially available 1-iodo-4-methoxybenzene (91 mg, 0.39 mmol, 1.95 equiv) and thioester **177a** (41 mg, 0.2 mmol, 1 equiv), with a reaction time of 72 h for the second step. Purification of the crude product by flash column chromatography (pentane/Et<sub>2</sub>O, 50:1) afforded analytically pure **207** (26 mg, 50% yield) as a pale-yellow oil.

**<sup>1</sup>H NMR** (400 MHz, CDCl<sub>3</sub>) δ 7.16 – 7.08 (m, 2H), 6.86 – 6.82 (m, 2H), 3.78 (s, 3H), 3.67 (t, J = 7.4 Hz, 1H), 2.91 – 2.82 (m, 1H), 1.96 (dddd, J = 13.4, 9.6, 7.2, 6.2 Hz, 1H), 1.86 – 1.77 (m, 1H), 1.74 – 1.41 (m, 8H), 1.26 – 1.11 (m, 2H), 0.88 (t, J = 7.3 Hz, 3H). **<sup>13</sup>C NMR** (101 MHz, CDCl<sub>3</sub>) δ 213.5, 158.7, 131.6, 129.5, 114.2, 57.5, 55.4, 50.6, 35.0, 30.3, 28.9, 26.2, 26.1, 20.9, 14.2. **IR** (ATR) 2956, 2871, 1706, 1609, 1510, 1463, 1302, 1250, 1178, 1036, 831, 733 cm<sup>-1</sup>. **HRMS** (ESI) *m/z*: [M+H]<sup>+</sup> calcd for C<sub>17</sub>H<sub>24</sub>O<sub>2</sub>H 261.1849, found 261.1849. **Enantiomeric ratio** 83:17 was determined by chiral HPLC analysis with a Daicel Chiralcel OJ column (0.1% isopropanol in *n*-heptane, 0.5 mL/min, 25 °C, detection at 220 nm, retention times (min): 18.02 (major), 22.08 (minor)). **[α]<sub>D</sub><sup>20</sup>** = +83.7 (c = 0.95 in CHCl<sub>3</sub>).



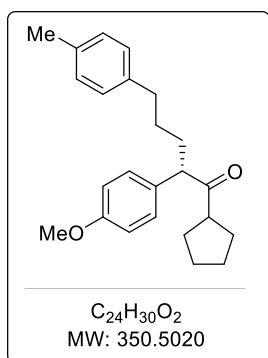
Detector A Ch1 220nm

Peak#	Ret. Time	Area	Height	Area %
1	16.301	13054011	224069	50.532
2	18.518	12778894	203713	49.468
Total		25832905	427782	100.000



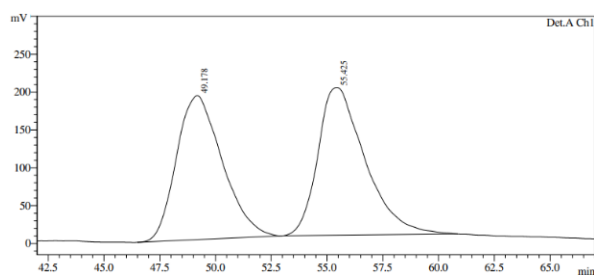
Detector A Ch1 220nm

Peak#	Ret. Time	Area	Height	Area %
1	18.013	17659545	178334	83.215
2	22.083	3562115	22067	16.785
Total		21221660	200401	100.000

**(S)-1-cyclopentyl-2-(4-methoxyphenyl)-5-(p-tolyl)pentan-1-one (208):**

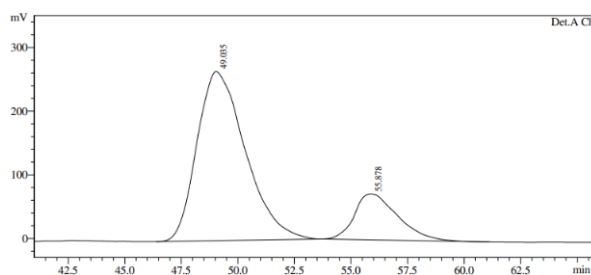
Prepared according to **GP4**, from **196** (0.6 mL, 0.49 M in THF, 0.3 mmol, 1.5 equiv), commercially available 1-iodo-4-methoxybenzene (91 mg, 0.39 mmol, 1.95 equiv) and thioester **177a** (41 mg, 0.2 mmol, 1.0 equiv), with a reaction time of 72 h for the second step. Purification of the crude product by flash column chromatography (pentane/acetone, 100:3) afforded analytically pure **208** (29 mg, 41% yield) as a pale-yellow oil.

$^1H$  NMR (400 MHz,  $CDCl_3$ )  $\delta$  7.15 – 6.99 (m, 6H), 6.88 – 6.80 (m, 2H), 3.79 (s, 3H), 3.66 (t,  $J = 7.4$  Hz, 1H), 2.85 (p,  $J = 7.6$  Hz, 1H), 2.64 – 2.46 (m, 2H), 2.31 (s, 3H), 2.11 – 1.97 (m, 1H), 1.86 – 1.77 (m, 1H), 1.75 – 1.38 (m, 10H).  $^{13}C$  NMR (101 MHz,  $CDCl_3$ )  $\delta$  213.3, 158.8, 139.3, 135.2, 131.4, 129.5, 129.1, 128.4, 114.3, 57.7, 55.4, 50.6, 35.6, 32.5, 30.3, 29.7, 28.9, 26.2, 26.1, 21.1. IR (ATR) 2943, 1705, 1514, 1456, 1250, 1146, 1111, 1086, 1037, 909, 809, 733, 643, 632, 624  $cm^{-1}$ . HRMS (ESI)  $m/z$ :  $[M+H]^+$  calcd for  $C_{24}H_{30}O_2H$  351.2319, found 351.2319. **Enantiomeric ratio** 80:20 was determined by chiral HPLC analysis with a Daicel Chiralcel OJ column (1% isopropanol in *n*-heptane for 30 min, then gradient from 1% to 5% isopropanol in 5 min, and continue with 5% isopropanol, 0.5 mL/min, 25 °C, detection at 230 nm, retention times (min): 49.04 (major), 55.88 (minor)).  $[\alpha]_D^{20} = +85.1$  ( $c = 1.0$  in  $CHCl_3$ ).



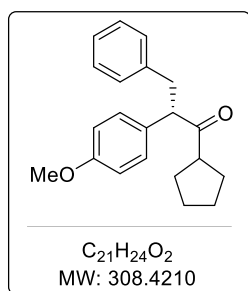
Detector A Ch1 230nm

Peak#	Ret. Time	Area	Height	Area %
1	49.178	27194053	190292	48.597
2	55.425	28764645	195078	51.403
Total		55958698	385370	100.000



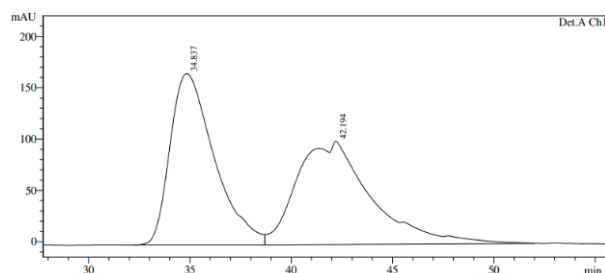
Detector A Ch1 230nm

Peak#	Ret. Time	Area	Height	Area %
1	49.035	39570750	265727	80.482
2	55.878	9596183	72034	19.518
Total		49166933	337761	100.000

**(S)-1-cyclopentyl-2-(4-methoxyphenyl)-3-phenylpropan-1-one (209):**

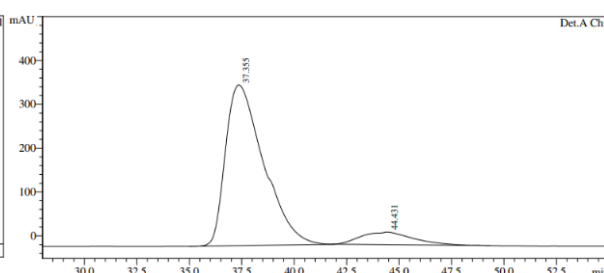
Prepared according to **GP4**, **197** (0.5 mL, 0.6 M in THF, 0.3 mmol, 1.5 equiv), commercially available 1-iodo-4-methoxybenzene (91 mg, 0.39 mmol, 1.95 equiv) and thioester **177a** (41 mg, 0.2 mmol, 1.0 equiv), with a reaction time of 72 h for the second step. Purification of the crude product by flash column chromatography (pentane/Et<sub>2</sub>O, 100:3) afforded analytically pure **209** (15 mg, 24% yield) as a pale-yellow oil.

**<sup>1</sup>H NMR** (400 MHz, CDCl<sub>3</sub>) δ 7.23 – 7.03 (m, 7H), 6.86 – 6.80 (m, 2H), 3.95 (dd, *J* = 8.0, 6.8 Hz, 1H), 3.79 (s, 3H), 3.38 (dd, *J* = 13.6, 8.0 Hz, 1H), 2.86 (dd, *J* = 13.6, 6.8 Hz, 1H), 2.78 (p, *J* = 7.8 Hz, 1H), 1.72 – 1.32 (m, 8H). **<sup>13</sup>C NMR** (101 MHz, CDCl<sub>3</sub>) δ 212.4, 158.9, 140.2, 130.9, 129.6, 129.2, 128.3, 126.2, 114.3, 59.8, 55.4, 51.0, 39.4, 29.8, 28.5, 26.1, 26.0. **IR** (ATR) 2952, 1705, 1608, 1510, 1454, 1251, 1178, 1109, 1035, 910, 832, 733, 700 cm<sup>-1</sup>. **HRMS** (ESI) *m/z*: [M+Na]<sup>+</sup> calcd for C<sub>21</sub>H<sub>24</sub>O<sub>2</sub>Na 331.1669, found 331.1666. **Enantiomeric ratio** 90:10 was determined by chiral HPLC analysis with a Daicel Chiralcel OJ-column (0.5% isopropanol in *n*-heptane, 0.5 mL/min, 25 °C, detection at 220 nm, retention times (min): 37.36 (major), 44.43 (minor)). [α]<sub>D</sub><sup>20</sup> = +127.1 (*c* = 0.45 in CHCl<sub>3</sub>).



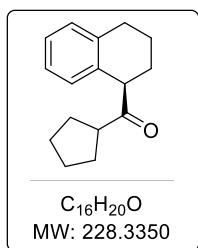
Detector A Ch1 220nm

Peak#	Ret. Time	Area	Height	Area %
1	34.837	25336261	166817	49.537
2	42.194	25810103	100639	50.463
Total		51146363	267455	100.000



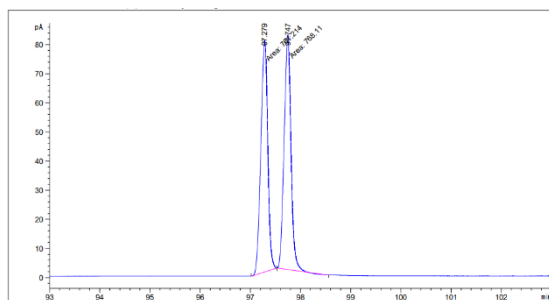
Detector A Ch1 220nm

Peak#	Ret. Time	Area	Height	Area %
1	37.355	46316558	366296	90.286
2	44.431	4983497	28768	9.714
Total		51300054	395064	100.000

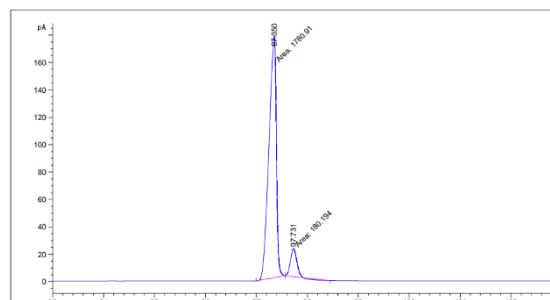
**(R)-cyclopentyl(1,2,3,4-tetrahydronaphthalen-1-yl)methanone (212):**

Prepared according to a modified literature procedure,<sup>23</sup> an oven-dried flask under argon was charged with Pd<sub>2</sub>(dba)<sub>3</sub> (13.7 mg, 0.015 mmol, 0.075 equiv) and *ent*-**L21** (41.4 mg, 0.036 mmol, 0.18) and MTBE (1.8 mL). The solution was stirred for 10 minutes at rt after which was added ZnCl<sub>2</sub> (1.2 mL, 1.5 M in THF, 1.8 mmol, 9 equiv) and a solution of **177a** (0.2 mmol, 1 equiv) in THF (0.4 mL). The reaction was stirred at rt for 48 h, after which it was quenched with HCl (4 mL, 1.0 M) and extracted with EtOAc (3×10 mL). The combined organic layers were washed with NaOH (1.0 M) and brine, dried over MgSO<sub>4</sub>, filtered, and concentrated under reduced pressure. Purification of the crude product by flash column chromatography (pentane/Et<sub>2</sub>O, 100:3) afforded analytically pure **212** (38 mg, 83% yield) as a pale-orange oil.

**<sup>1</sup>H NMR** (400 MHz, CDCl<sub>3</sub>) δ 7.19 – 7.09 (m, 3H), 6.97 – 6.90 (m, 1H), 3.95 (t, *J* = 6.8 Hz, 1H), 3.01 (p, *J* = 7.9 Hz, 1H), 2.88 – 2.73 (m, 2H), 2.10 – 1.51 (m, 12H). **<sup>13</sup>C NMR** (101 MHz, CDCl<sub>3</sub>) δ 215.9, 137.8, 134.1, 129.6, 129.4, 126.8, 125.9, 53.0, 49.3, 31.2, 30.4, 29.4, 26.3, 26.3, 21.0. **IR** (ATR) 2943, 2867, 1703, 1494, 1450, 1358, 744 cm<sup>-1</sup>. **HRMS (ESI)** *m/z*: [M+H]<sup>+</sup> calcd for C<sub>16</sub>H<sub>20</sub>OH 229.1587, found 229.1585. **Enantiomeric ratio** 91:9 was determined by chiral GC analysis with a Cyclosil-B column (initial temperature 70°C - temperature gradient 1 °C/min - final temperature 200 °C, retention times (min): 97.35 min (major), 97.73 min (minor)). [α]<sub>D</sub><sup>20</sup> = +44.3 (c = 0.95 in CHCl<sub>3</sub>).

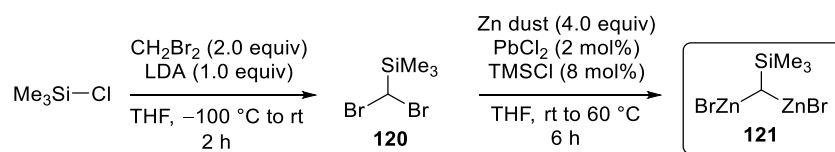


Peak #	RetTime [min]	Type	Width [min]	Area [pA*s]	Height [pA]	Area %
1	97.279	MM	0.1594	761.21429	79.56689	49.77455
2	97.747	MM	0.1589	768.10992	80.56012	50.22545

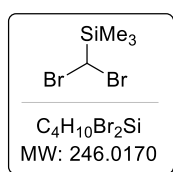


Peak #	RetTime [min]	Type	Width [min]	Area [pA*s]	Height [pA]	Area %
1	97.350	MM	0.1678	1780.91003	176.93320	90.81162
2	97.731	MM	0.1464	180.19362	20.51020	9.18838

### 3.10. Synthesis of Bis(bromozincio)trimethylsilylmethane



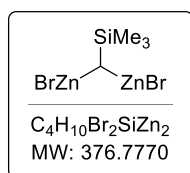
#### (Dibromomethyl)trimethylsilane (120):



According to a literature procedure,<sup>45</sup> in a 500-mL round-bottomed flask, diisopropylamine (21.1 mL, 150 mmol, 1.0 equiv) and anhydrous THF (100 mL) were added under argon atmosphere. Then the mixture was cooled down to 0 °C, and <sup>n</sup>BuLi (61 mL, 2.5 M in hexane, 150 mmol, 1.0 equiv) was added dropwise. After complete addition, the reaction mixture was stirred for 10 minutes at 0 °C, and then it was transferred slowly *via* cannula to another 500 mL round-bottomed flask loaded with trimethylsilyl chloride (19 mL, 150 mmol, 1.0 equiv), dibromomethane (21 mL, 300 mmol, 2.0 equiv) and anhydrous THF (20 mL) at -100 °C (the temperature was maintained for the whole duration of the transfer). After complete addition the mixture was allowed to return slowly to rt and then it was stirred 1 h. After this time, the reaction mixture was poured into a cold solution of saturated soln of NH<sub>4</sub>Cl. The aqueous phase was extracted with diethyl ether, and the combined organic layers were washed with brine, dried over MgSO<sub>4</sub>, and concentrated under reduced pressure. Purification of the crude product by distillation under reduced pressure (20 mmHg, 58 °C) afforded analytically pure **120** (22.8 g, 62% yield) as a colorless liquid.

<sup>1</sup>H NMR (300 MHz, CDCl<sub>3</sub>) δ 5.15 (s, 1H), 0.25 (s, 9H) <sup>13</sup>C NMR (75 MHz, CDCl<sub>3</sub>) δ 37.0, -3.1. IR (ATR) 1252, 842, 616 cm<sup>-1</sup>. MS (EI, 70 eV) *m/z*: 246 (M<sup>+</sup>, 1%), 203 (13%), 73 (100%).

#### Bis(bromozincio)trimethylsilylmethane (121):



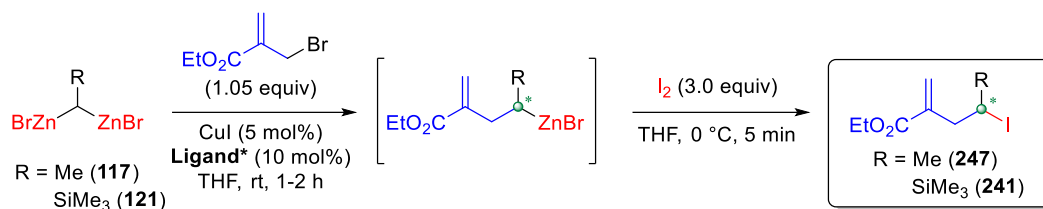
According to a modified literature procedure,<sup>46</sup> to a THF (1 mL) suspension of Zn dust (1.3 g, 20 mmol, 4 equiv) and PbCl<sub>2</sub> (28 mg, 0.1 mmol, 0.02 equiv) under argon atmosphere, was added trimethylsilyl chloride (0.05 mL, 0.4 mmol), and the mixture was stirred for 10 minutes at rt. After that, a THF (4 mL) solution of **120** (1.23 g, 5 mmol, 1.0 equiv) was added dropwise over 2 h. After complete addition, the resulting mixture was stirred for 4.5 h at 60 °C. Then the excess of zinc was removed by centrifugation and the supernatant was transferred in an oven-dried flask and stored under a positive pressure of argon at -20 °C. The reagent was titrated with I<sub>2</sub> to determine the corresponding title.<sup>16</sup>

<sup>45</sup> K. Yoon, D. Y. Son, *J. Organomet. Chem.* **1997**, 545–546, 185–189.

<sup>46</sup> S. Matsubara, Y. Otake, T. Morikawa, K. Utimoto, *Synlett* **1998**, 1998, 1315–1316

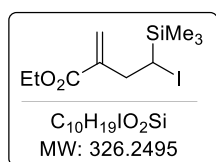


### 3.11. General Procedure for the Enantioselective Sequential Allylation–Iodolysis (GP5)



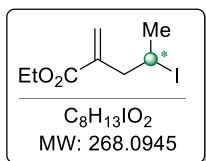
An oven-dried flask under argon was charged with CuI (3.8 mg, 0.02 mmol, 0.05 equiv) and chiral ligand (0.01 mmol, 0.1 equiv). A solution of ethyl 2-(bromomethyl)acrylate (81 mg, 0.42 mmol, 1.05 equiv) in THF (1.1 mL) was added. The mixture was stirred for 5 min at rt, before a solution of *gem*-dizincio (0.4 mmol, 1.0 equiv) was added slowly. The resulting mixture was stirred for 2 h at rt. Then the reaction mixture was added to a solution of I<sub>2</sub> (305 mg, 1.2 mmol, 3.0 equiv) in THF (0.5 mL) at 0 °C under argon. The mixture was stirred at 0 °C for 5 minutes and 3 minutes at rt, after which was added a sat. soln of Na<sub>2</sub>S<sub>2</sub>O<sub>3</sub> until complete loss of colour. The reaction mixture was extracted with Et<sub>2</sub>O (3×5 mL), and the combined organic layers were dried over MgSO<sub>4</sub>, filtered, and concentrated under reduced pressure. The product was purified by flash column chromatography on silica gel.

#### Ethyl 4-iodo-2-methylene-4-(trimethylsilyl)butanoate (241):



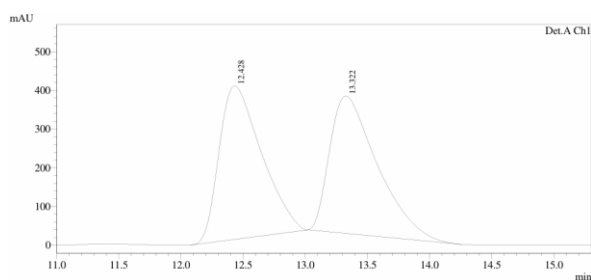
Prepared according to GP5, with L39 (12 mg, 0.04 mmol, 0.1 equiv), and 121 (0.5 mL, ~0.8 M in THF, 0.4 mmol, 1.0 equiv). Purification by flash column chromatography on silica gel (pentane/EtOAc, 100:3) afforded analytically pure 241 (55 mg, 89% yield) as a pale-yellow oil.

<sup>1</sup>H NMR (400 MHz, CDCl<sub>3</sub>) δ 6.31 (s, 1H), 5.61 (s, 1H); 4.20 (qd, J = 7.2, 2.2 Hz, 2H), 3.31 (dd, J = 12.4, 2.8 Hz, 1H), 2.88 (d, br., J = 15.1 Hz, 1H), 2.45 (dd, J = 15.1, 12.4 Hz, 1H), 1.30 (t, J = 7.1 Hz, 3H), 0.19 (s, 9H). <sup>13</sup>C NMR (101 MHz, CDCl<sub>3</sub>) δ 166.6, 139.1, 127.1, 60.9, 36.9, 20.7, 14.3, -2.0. IR (ATR) 1712, 1250, 1187, 1126, 855, 837, 741, 692 cm<sup>-1</sup>. HRMS (ESI) *m/z*: [M+H]<sup>+</sup> calcd for C<sub>10</sub>H<sub>19</sub>IO<sub>2</sub>SiH 327.0272, found 327.0286.

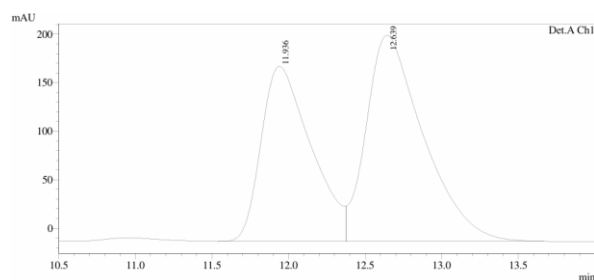
**Ethyl 4-iodo-2-methylenepentanoate (247), (enantioenriched):**

Prepared according to **GP5**, with CuI (2.9 mg, 0.015 mmol, 0.05 equiv), **L39** (9 mg, 0.03 mmol, 0.1 equiv), from ethyl 2-(bromomethyl)acrylate (60.8 mg, 0.3 mmol, 1.0 equiv) and **117** (0.9 mL, ~0.45 M in THF, 0.4 mmol, 1.33 equiv). Purification of the crude product by flash column chromatography (pentane/EtOAc, 33:1) afforded analytically pure **247** (28 mg, 35% yield) as a pale-yellow oil.

**<sup>1</sup>H NMR** (300 MHz, CDCl<sub>3</sub>) δ 6.31 (d, *J* = 1.3 Hz, 1H), 5.66 (d, *J* = 1.2 Hz, 1H), 4.43 – 4.30 (m, 1H), 4.22 (q, *J* = 7.1 Hz, 2H), 2.88 (ddd, *J* = 14.5, 8.4, 1.0 Hz, 1H), 2.75 (ddd, *J* = 14.5, 6.0, 1.2 Hz, 1H), 1.94 (d, *J* = 6.8 Hz, 3H), 1.31 (t, *J* = 7.1 Hz, 3H). **<sup>13</sup>C NMR** (75 MHz, CDCl<sub>3</sub>) δ 166.6, 138.6, 128.0, 61.0, 45.9, 28.7, 26.8, 14.3. **IR** (ATR) 2924, 2855, 1715, 1403, 1216, 1180, 1099, 759 cm<sup>-1</sup>. **HRMS** (APCI) *m/z*: [M+H]<sup>+</sup> calcd for C<sub>8</sub>H<sub>13</sub>IO<sub>2</sub>H 269.0033, found 269.0034. **Enantiomeric ratio** 57:43 was determined by chiral HPLC analysis with a Daicel Chiralcel OJ-column (0.1% isopropanol in *n*-heptane, 0.5 mL/min, 25 °C, detection at 220 nm, retention times (min): 11.94 (minor), 12.64 (major)). [α]<sub>D</sub><sup>20</sup> = [pending]

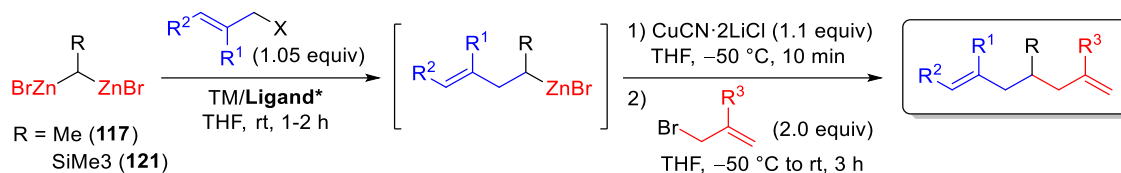


Peak#	Ret. Time	Area	Height	Area %
1	12.428	9373585	396247	49.726
2	13.322	9477017	353944	50.274
Total		18850602	750191	100.000



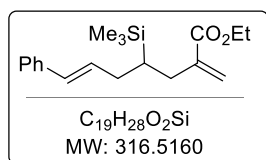
Peak#	Ret. Time	Area	Height	Area %
1	11.936	4088812	180206	42.663
2	12.639	5495096	212236	57.337
Total		9583908	392442	100.000

### 3.12. General Procedure for the Enantioselective Sequential Double Allylation (GP6)



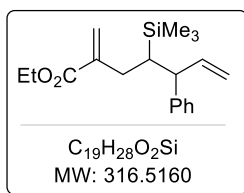
An oven-dried flask under argon was charged with **TM/Ligand** catalyst. A solution of allyl halide (0.42 mmol, 1.05 equiv) in THF (1.1 mL) was added. The mixture was stirred for 5 min at rt, before a solution of *gem*-dizincio (0.4 mmol, 1.0 equiv) was added slowly. The resulting mixture was stirred for 1-2 h at rt. Then the reaction mixture was cooled down to  $-50\text{ }^\circ\text{C}$ , a solution of CuCN·2LiCl (0.44 mL, 1.0 M in THF, 0.44 mmol, 1.1 equiv) was added dropwise and the resulting mixture was stirred at the same temperature for 10 minutes. After that, a THF (0.5 mL) solution of the allyl bromide (0.8 mmol, 2.0 equiv) was added dropwise at  $-50\text{ }^\circ\text{C}$  and the reaction mixture was stirred 3 h letting it return to rt slowly. The reaction was quenched with sat. soln of NH<sub>4</sub>Cl and extracted with Et<sub>2</sub>O (3×10 mL). The combined organic layers were dried over MgSO<sub>4</sub>, filtered, and concentrated under reduced pressure. The product was purified by flash column chromatography on silica gel.

#### Ethyl (*E*)-2-methylene-7-phenyl-4-(trimethylsilyl)hept-6-enoate ( $\pm$ -**238**):



Prepared according to **GP6**, using Pd<sub>2</sub>(dba)<sub>3</sub> (9.2 mg, 0.01 mmol, 0.025 equiv) and **L17** (26.8 mg, 0.04 mmol, 0.1 equiv) as catalytic system, from commercially available cinnamyl chloride (64 mg, 0.42 mmol, 1.05 equiv) and ethyl 2-(bromomethyl)acrylate (154 mg, 0.8 mmol, 2.0 equiv) respectively as first and second allyl halides, and from **121** (0.5 mL, ~0.8 M in THF, 0.4 mmol, 1.0 equiv) as *gem*-dizincio, with a reaction time of 1 h for the first step. Purification of the crude product by flash column chromatography (pentane/Et<sub>2</sub>O, 50:1) afforded analytically pure ( $\pm$ )-**238** (100 mg, 79% yield) as a colourless oil.

**<sup>1</sup>H NMR** (400 MHz, CDCl<sub>3</sub>)  $\delta$  7.32-7.24 (m, 4H), 7.18 (ddt, *J* = 8.6, 7.3, 1.9 Hz, 1H), 6.33 (d, *J* = 16.0 Hz, 1H), 6.20-6.11 (m, 2H), 5.52 (d, *J* = 1.3 Hz, 1H), 4.18 (qd, *J* = 7.1, 1.9 Hz, 2H), 2.56 (dd, *J* = 14.5, 3.0 Hz, 1H), 2.30 (q, *J* = 6.5 Hz, 2H), 2.20 (dd, *J* = 14.3, 10.6 Hz, 1H), 1.27 (t, *J* = 7.1 Hz, 3H), 1.08 (dtd, *J* = 10.5, 6.2, 4.2 Hz, 1H), 0.06 (s, 9H). **<sup>13</sup>C NMR** (101 MHz, CDCl<sub>3</sub>)  $\delta$  167.4, 140.9, 137.9, 130.9, 130.6, 128.6, 126.9, 126.0, 125.5, 60.7, 33.0, 32.3, 25.0, 14.3, -2.1. **IR** (ATR) 1716, 1248, 1185, 1128, 853, 834, 742, 692 cm<sup>-1</sup>. **HRMS** (ESI) *m/z*: [M+H]<sup>+</sup> calcd for C<sub>19</sub>H<sub>28</sub>O<sub>2</sub>SiH 317.1931, found 317.1931.

**Ethyl 2-methylene-5-phenyl-4-(trimethylsilyl)hept-6-enoate (239):**

Prepared according to **GP6**, using Pd<sub>2</sub>(dba)<sub>3</sub> (9.2 mg, 0.01 mmol, 0.025 equiv) and **L33** (27.5 mg, 0.04 mmol, 0.1 equiv) as catalytic system, from commercially available cinnamyl chloride (64 mg, 0.42 mmol, 1.05 equiv) and ethyl 2-(bromomethyl)acrylate (154 mg, 0.8 mmol, 2.0 equiv) respectively as first and second allyl halides, and from **121** (0.5 mL, ~0.8 M in THF, 0.4 mmol, 1.0 equiv) as *gem*-dizincio, with a reaction time of 1 h for the first step. Purification of the crude product by flash column chromatography (pentane/Et<sub>2</sub>O, 50:1) afforded **239** (37 mg, 29% yield) as a mixture of two diastereoisomer (60:40 dr) as a colourless oil.

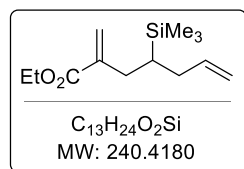
**Minor diastereoisomer:**

<sup>1</sup>H NMR: (400 MHz, CDCl<sub>3</sub>) δ 7.33–7.15 (m, 5H), 6.14 (m, 1H), 6.13–6.04 (m, 1H), 5.52 (d, J = 1.4 Hz, 1H), 5.22–5.07 (m, 2H), 4.18 (qd, J = 7.1, 1.8 Hz, 2H), 3.54 (t, J = 5.4 Hz, 1H), 2.59 (dd, J = 14.2, 3.9 Hz, 1H), 2.49 (t, J = 8.0 Hz, 1H), 1.68–1.55 (m, 1H), 1.34 (t, J = 7.2 Hz, 3H), –0.07 (s, 9H). <sup>13</sup>C NMR (101 MHz, CDCl<sub>3</sub>) δ 167.4, 145.0, 141.7, 140.7, 128.4, 128.1, 126.2, 125.2, 115.7, 60.6, 51.2, 30.9, 29.9, 14.4, –1.1 (3C).

**Major diastereoisomer:**

<sup>1</sup>H NMR: (400 MHz, CDCl<sub>3</sub>) δ 7.33–7.15 (m, 5H), 6.19 (d, J = 1.6 Hz, 1H), 6.13–6.04 (m, 1H), 5.52 (d, J = 1.4 Hz, 1H), 5.22–5.07 (m, 2H), 4.25 (qd, J = 7.1, 1.8 Hz, 2H), 3.57 (t, J = 5.4 Hz, 1H), 2.49 (t, J = 8.0 Hz, 1H), 2.31 (dd, J = 14.3, 9.0 Hz, 1H), 1.68–1.55 (m, 1H), 1.29 (t, J = 7.2 Hz, 3H), –0.06 (s, 9H). <sup>13</sup>C NMR (100 MHz, CDCl<sub>3</sub>) δ 167.4, 144.9, 141.0, 140.5, 128.2, 127.9, 126.0, 125.7, 116.8, 60.7, 50.2, 31.6, 30.8, 14.4, –0.5 (3C).

IR (ATR) 1716, 1249, 1186, 1129, 853, 835, 755, 700 cm<sup>-1</sup>. HRMS (ESI) *m/z*: [M+H]<sup>+</sup> calcd for C<sub>19</sub>H<sub>28</sub>O<sub>2</sub>SiH 317.1931, found 317.1931.

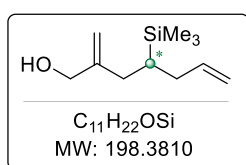
**Ethyl 2-methylene-4-(trimethylsilyl)hept-6-enoate (244), (enantioenriched):**

Prepared according to **GP6**, using CuI (57 mg, 0.3 mmol, 1.0 equiv) and **L39** (181 mg, 0.6 mmol, 2.0 equiv) as catalytic system, from commercially available ethyl 2-(bromomethyl)acrylate (81 mg, 0.315 mmol, 1.05 equiv) and allyl bromide (97 mg, 0.6 mmol, 2.0 equiv) respectively as first and second allyl halides, and from **121** (0.38 mL, ~0.8 M in THF, 0.3 mmol, 1.0 equiv) as *gem*-dizincio, with a reaction time of 10 min for the first step. Purification of the crude product by flash column chromatography (pentane/EtOAc, 100:3) afforded analytically pure **244** (28 mg, 39% yield) as a colourless oil.

**<sup>1</sup>H NMR** (400 MHz, CDCl<sub>3</sub>) δ 6.16 (d, *J* = 1.7 Hz, 1H), 5.75 (ddt, *J* = 17.1, 10.1, 7.1 Hz, 1H), 5.51 – 5.47 (m, 1H), 5.02 – 4.90 (m, 2H), 4.19 (qd, *J* = 7.1, 1.6 Hz, 2H), 2.48 (ddd, *J* = 14.3, 4.5, 1.4 Hz, 1H), 2.20 – 2.04 (m, 3H), 1.29 (t, *J* = 7.1 Hz, 3H), 0.96 (dtd, *J* = 10.5, 6.0, 4.5 Hz, 1H), 0.02 (s, 9H). **<sup>13</sup>C NMR** (101 MHz, CDCl<sub>3</sub>) δ 167.4, 140.7, 138.7, 125.3, 115.4, 60.6, 33.7, 32.0, 24.3, 14.3, -2.1 (3C). **IR** (ATR) 2979, 2905, 1718, 1299, 1249, 1180, 1132, 1115, 852, 834 cm<sup>-1</sup>. **HRMS** (ESI) *m/z*: [M+H]<sup>+</sup> calcd for C<sub>13</sub>H<sub>24</sub>O<sub>2</sub>SiH 241.1618, found 241.1619.

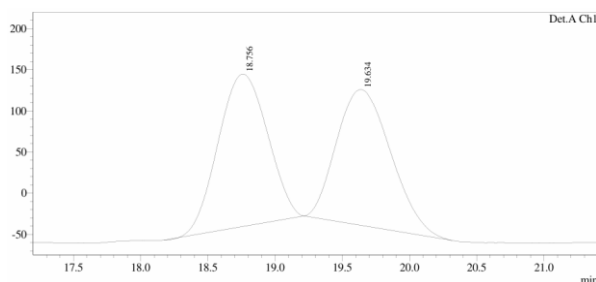
[Note: difficulty encountered in establishing effective separation conditions for the two enantiomers using chiral-phase GC/HPLC. Refer to the derivatization procedure to compound **245** (reported below) for the enantiomeric ratio]

### 2-Methylene-4-(trimethylsilyl)hept-6-en-1-ol (**245**), (*enantioenriched*):



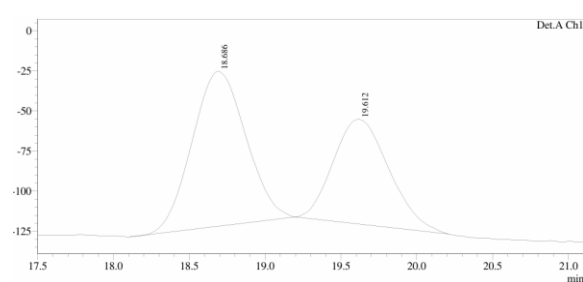
To a stirred solution of **244** (28 mg, 0.116 mmol, 1.0 equiv) in THF (1.0 mL) was slowly added DIBAL-H (1.2 M in toluene, 0.48 mL, 0.58 mmol, 5.0 equiv) at -20 °C. The resulting mixture was stirred at -20 °C for 10 min and then rt for 3 h. The reaction mixture was quenched with HCl 1 M (2.0 mL) at 0 °C, and the aqueous phase was extracted with EtOAc (3×5 mL). The combined organic layers were washed with brine, dried over MgSO<sub>4</sub>, and then filtered on a plug of silica gel (pentane/EtOAc, 1:1) to afford analytically pure **245** (27 mg, 97% yield).

**<sup>1</sup>H NMR** (300 MHz, CDCl<sub>3</sub>) δ 5.76 (ddt, *J* = 17.1, 10.1, 7.1 Hz, 1H), 5.09 – 4.86 (m, 4H), 4.04 (s, 2H), 2.23 – 1.94 (m, 4H), 1.77 (br s, 1H), 0.90 (dtd, *J* = 10.0, 6.2, 5.0 Hz, 1H), 0.00 (s, 9H). **<sup>13</sup>C NMR** (75 MHz, CDCl<sub>3</sub>) δ 148.5, 138.9, 115.4, 110.5, 65.6, 34.1, 33.1, 23.2, -2.1. **IR** (ATR) 3330, 3076, 2953, 2901, 1638, 1442, 1249, 1031, 906, 834, 752, 688 cm<sup>-1</sup>. **HRMS** (APCI) *m/z*: [M+H]<sup>+</sup> calcd for C<sub>11</sub>H<sub>22</sub>OSiH 199.1513, found 199.1513. **Enantiomeric ratio** 59:41 was determined by chiral HPLC analysis with a Daicel Chiralpak IA column (0.5% isopropanol in *n*-heptane until 8 min, then gradient up to 1% isopropanol in 1 min, and maintain at 1% isopropanol, 1.0 mL/min, 25 °C, detection at 210 nm, retention times: 18.69 min (major), 19.61 min (minor)). [α]<sub>D</sub><sup>20</sup> = [pending].



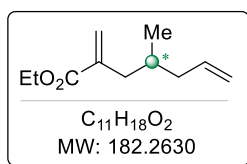
Detector A Ch1 210nm

Peak#	Ret. Time	Area	Height	Area %
1	18.756	4722563	185507	50.491
2	19.634	4630634	164787	49.509
Total		9353197	350294	100.000



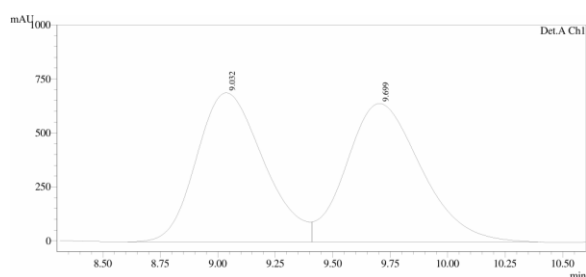
Detector A Ch1 210nm

Peak#	Ret. Time	Area	Height	Area %
1	18.686	2385100	96658	58.873
2	19.612	1666197	65239	41.127
Total		4051297	161897	100.000

**Ethyl 4-methyl-2-methylenehept-6-enoate (248), (enantioenriched):**

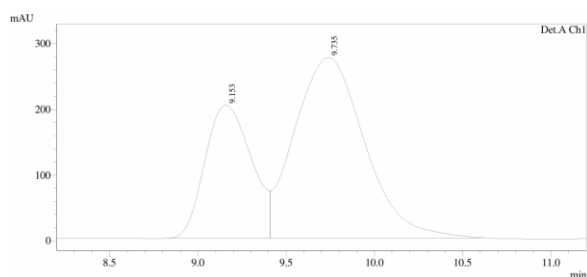
Prepared according to **GP6**, with CuI (2.9 mg, 0.015 mmol, 0.05 equiv) and the **L39** (9 mg, 0.03 mmol, 0.1 equiv), from commercially available ethyl 2-(bromomethyl)acrylate (60.8 mg, 0.3 mmol, 1.0 equiv) and allyl bromide (97 mg, 0.8 mmol, 2.0 equiv) respectively as first and second allyl halides, and **117** (0.9 mL, ~0.45 M in THF, 0.4 mmol, 1.33 equiv) as *gem*-dizincio, with a reaction time of 2 h for the first step. Purification of the crude product by flash column chromatography (pentane/EtOAc, 33:1) afforded analytically pure **248** (5 mg, 9% yield) as a colourless oil (*volatile compound*)

**$^1\text{H}$  NMR** (400 MHz,  $\text{CDCl}_3$ )  $\delta$  6.17 (d,  $J = 1.7$  Hz, 1H), 5.79 (ddt,  $J = 16.3, 10.8, 7.0$  Hz, 1H), 5.52 – 5.46 (m, 1H), 5.06 – 4.97 (m, 2H), 4.26 – 4.14 (m, 2H), 2.39 (ddd,  $J = 13.8, 5.9, 1.3$  Hz, 1H), 2.15 – 2.01 (m, 2H), 1.97 – 1.85 (m, 1H), 1.76 (dt,  $J = 12.8, 6.8$  Hz, 1H), 1.30 (t,  $J = 7.1$  Hz, 3H), 0.86 (d,  $J = 6.7$  Hz, 3H).  **$^{13}\text{C}$  NMR** (101 MHz,  $\text{CDCl}_3$ )  $\delta$  167.6, 139.9, 137.3, 125.9, 116.1, 60.7, 41.2, 39.3, 32.0, 19.2, 14.4. **IR** (ATR) 2979, 1718, 1630, 1280, 1160, 912, 735  $\text{cm}^{-1}$ . **HRMS** (APCI)  $m/z$ :  $[\text{M}+\text{H}]^+$  calcd for  $\text{C}_{11}\text{H}_{18}\text{O}_2\text{H}$  183.1380, found 183.1380. **Enantiomeric ratio** 67:33 was determined by chiral HPLC analysis with a Daicel Chiralcel OJ-H column (0.5% isopropanol in *n*-heptane until 8 min, then gradient up to 1% isopropanol in 1 min, and maintain at 1% isopropanol, 0.5 mL/min, 25 °C, detection at 220 nm, retention times: 9.15 min (minor), 9.74 min (major)).  $[\alpha]_D^{20} = [\text{pending}]$ .



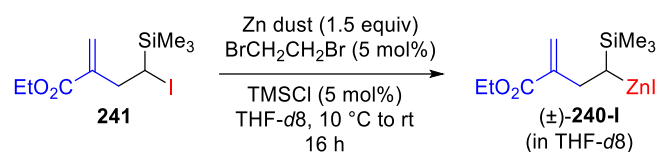
Detector A Ch1 220nm

Peak#	Ret. Time	Area	Height	Area %
1	9.032	14031015	690563	49.183
2	9.699	14497021	640933	50.817
Total		28528035	1331497	100.000



Detector A Ch1 220nm

Peak#	Ret. Time	Area	Height	Area %
1	9.153	3726283	202528	32.869
2	9.735	7610565	275166	67.131
Total		11336848	477695	100.000

3.13. Preparation of  $\alpha$ -Silyl Organozinc ( $\pm$ )-240-I in THF-*d*8

An oven dried flask was charged Zn dust (294 mg, 4.5 mmol, 1.5 equiv) and THF-*d*8 (0.7 mL) and the zinc was activated adding 1,2-dibromoethane (13  $\mu$ L, 0.15 mmol, 0.05 equiv) and heating the reaction mixture until ebullition occurred. After cooling to rt, trimethylsilyl chloride (19  $\mu$ L, 0.15 mmol, 0.05 equiv) was added and the mixture was heated again until ebullition occurred. Then the mixture was cooled down to rt and a solution of **241** (703 mg, 5.0 mmol, 1.0 equiv) [*prepared according to GP5 with Pd<sub>2</sub>(dba)<sub>3</sub>/L17*] in THF-*d*8 (2.1 mL) was added dropwise over 1 h at 10 °C. After complete addition, the reaction mixture was stirred at rt for 16 h. The excess of zinc was removed by centrifugation and the liquid supernatant was transferred to another oven-dried flask under a positive pressure of argon and stored at -20 °C. The title was determined by titration with I<sub>2</sub>.<sup>16</sup> Concentration of ~0.55 M was obtained.

## REFERENCES

- [1] I. Marek, J.-F. Normant, *Chem. Rev.* **1996**, *96*, 3241–3268.
- [2] G. Wittig, G. Harborth, *Berichte Dtsch. Chem. Ges. B Ser.* **1944**, *77*, 306–314.
- [3] Robert West, E. G. Rochow, *J. Org. Chem.* **1953**, *18*, 1739–1742.
- [4] K. Ziegler, K. Nagel, M. Patheiger, *Z. Für Anorg. Allg. Chem.* **1955**, *282*, 345–351.
- [5] N. J. R. van Eikema Hommes, F. Bickelhaupt, G. W. Klumpp, *Recl. Trav. Chim. Pays-Bas* **1987**, *106*, 514–515.
- [6] C. P. Vlaar, G. W. Klumpp, *Tetrahedron Lett.* **1991**, *32*, 2951–2952.
- [7] T. Cantat, L. Ricard, P. Le Floch, N. Mézailles, *Organometallics* **2006**, *25*, 4965–4976.
- [8] S. Harder, *Coord. Chem. Rev.* **2011**, *255*, 1252–1267.
- [9] M. Fustier-Boutignon, N. Nebra, N. Mézailles, *Chem. Rev.* **2019**, *119*, 8555–8700.
- [10] P. I. Dalko, L. Moisan, *Angew. Chem. Int. Ed.* **2001**, *40*, 3726–3748.
- [11] R. Noyori, *Angew. Chem. Int. Ed.* **2002**, *41*, 2008–2022.
- [12] P. I. Dalko, *Comprehensive Enantioselective Organocatalysis*, Wiley-VCH Verlag GmbH & Co. KGaA, Weinheim, **2013**.
- [13] D. G. Hall, *Boronic Acids: Preparation, Applications in Organic Synthesis and Medicine*, John Wiley & Sons, **2006**.
- [14] L. Xu, S. Zhang, P. Li, *Chem. Soc. Rev.* **2015**, *44*, 8848–8858.
- [15] N. Miralles, R. J. Maza, E. Fernández, *Adv. Synth. Catal.* **2018**, *360*, 1306–1327.
- [16] R. Nallagonda, K. Padala, A. Masarwa, *Org. Biomol. Chem.* **2018**, *16*, 1050–1064.
- [17] J. C. H. Lee, R. McDonald, D. G. Hall, *Nat. Chem.* **2011**, *3*, 894–899.
- [18] D. Ameen, T. J. Snape, *MedChemComm* **2013**, *4*, 893–907.
- [19] X. Liu, Y. Xiao, J.-Q. Li, B. Fu, Z. Qin, *Mol. Divers.* **2019**, *23*, 809–820.
- [20] P. Viereck, S. Krautwald, T. P. Pabst, P. J. Chirik, *J. Am. Chem. Soc.* **2020**, *142*, 3923–3930.
- [21] J. R. Coombs, L. Zhang, J. P. Morken, *J. Am. Chem. Soc.* **2014**, *136*, 16140–16143.
- [22] S. A. Murray, M. Z. Liang, S. J. Meek, *J. Am. Chem. Soc.* **2017**, *139*, 14061–14064.
- [23] S. A. Murray, E. C. M. Luc, S. J. Meek, *Org. Lett.* **2018**, *20*, 469–472.
- [24] Y. Lee, J. Park, S. H. Cho, *Angew. Chem. Int. Ed.* **2018**, *57*, 12930–12934.
- [25] W. J. Teo, S. Ge, *Angew. Chem.* **2018**, *130*, 13117–13121.
- [26] D. S. Matteson, R. J. Moody, *Organometallics* **1982**, *1*, 20–28.
- [27] D. S. Matteson, R. J. Moody, *J. Am. Chem. Soc.* **1977**, *99*, 3196–3197.
- [28] Z.-Q. Zhang, C.-T. Yang, L.-J. Liang, B. Xiao, X. Lu, J.-H. Liu, Y.-Y. Sun, T. B. Marder, Y. Fu, *Org. Lett.* **2014**, *16*, 6342–6345.
- [29] H. Ito, K. Kubota, *Org. Lett.* **2012**, *14*, 890–893.
- [30] T. C. Atack, S. P. Cook, *J. Am. Chem. Soc.* **2016**, *138*, 6139–6142.
- [31] G. Zweifel, H. Arzoumanian, *J. Am. Chem. Soc.* **1967**, *89*, 291–295.



- [32] H. C. Brown, C. G. Scouten, R. Liotta, *J. Am. Chem. Soc.* **1979**, *101*, 96–99.
- [33] R. Soundararajan, D. S. Matteson, *Organometallics* **1995**, *14*, 4157–4166.
- [34] G. Gao, J. Yan, K. Yang, F. Chen, Q. Song, *Green Chem.* **2017**, *19*, 3997–4001.
- [35] Z. Zuo, Z. Huang, *Org. Chem. Front.* **2016**, *3*, 434–438.
- [36] S. Lee, D. Li, J. Yun, *Chem. – Asian J.* **2014**, *9*, 2440–2443.
- [37] K. Endo, M. Hirokami, T. Shibata, *Synlett* **2009**, *2009*, 1331–1335.
- [38] J. H. Docherty, K. Nicholson, A. P. Dominey, S. P. Thomas, *ACS Catal.* **2020**, *10*, 4686–4691.
- [39] L. Zhang, Z. Huang, *J. Am. Chem. Soc.* **2015**, *137*, 15600–15603.
- [40] L. Li, T. Gong, X. Lu, B. Xiao, Y. Fu, *Nat. Commun.* **2017**, *8*, 345.
- [41] M. Hu, S. Ge, *Nat. Commun.* **2020**, *11*, 765.
- [42] L. Wang, T. Zhang, W. Sun, Z. He, C. Xia, Y. Lan, C. Liu, *J. Am. Chem. Soc.* **2017**, *139*, 5257–5264.
- [43] H. Zhao, M. Tong, H. Wang, S. Xu, *Org. Biomol. Chem.* **2017**, *15*, 3418–3422.
- [44] Z. He, Q. Zhu, X. Hu, L. Wang, C. Xia, C. Liu, *Org. Chem. Front.* **2019**, *6*, 900–907.
- [45] H. Abu Ali, I. Goldberg, M. Srebnik, *Organometallics* **2001**, *20*, 3962–3965.
- [46] H. Abu Ali, I. Goldberg, D. Kaufmann, C. Burmeister, M. Srebnik, *Organometallics* **2002**, *21*, 1870–1876.
- [47] A. J. Wommack, J. S. Kingsbury, *Tetrahedron Lett.* **2014**, *55*, 3163–3166.
- [48] H. Li, X. Shangguan, Z. Zhang, S. Huang, Y. Zhang, J. Wang, *Org. Lett.* **2014**, *16*, 448–451.
- [49] F.-P. Wu, X.-F. Wu, *Angew. Chem.* **2021**, *133*, 11836–11840.
- [50] W. J. Teo, X. Yang, Y. Y. Poon, S. Ge, *Nat. Commun.* **2020**, *11*, 5193.
- [51] M. L. Scheuermann, E. J. Johnson, P. J. Chirik, *Org. Lett.* **2015**, *17*, 2716–2719.
- [52] C. Sun, B. Potter, J. P. Morken, *J. Am. Chem. Soc.* **2014**, *136*, 6534–6537.
- [53] L. Nilvebrant, K.-E. Andersson, P.-G. Gillberg, M. Stahl, B. Sparf, *Eur. J. Pharmacol.* **1997**, *327*, 195–207.
- [54] B. Potter, A. A. Szymaniak, E. K. Edelstein, J. P. Morken, *J. Am. Chem. Soc.* **2014**, *136*, 17918–17921.
- [55] M. V. Joannou, B. S. Moyer, S. J. Meek, *J. Am. Chem. Soc.* **2015**, *137*, 6176–6179.
- [56] M. V. Joannou, B. S. Moyer, M. J. Goldfogel, S. J. Meek, *Angew. Chem. Int. Ed.* **2015**, *54*, 14141–14145.
- [57] S. A. Murray, J. C. Green, S. B. Tailor, S. J. Meek, *Angew. Chem. Int. Ed.* **2016**, *55*, 9065–9069.
- [58] J. Kim, K. Ko, S. H. Cho, *Angew. Chem.* **2017**, *129*, 11742–11746.
- [59] J. Kim, C. Hwang, Y. Kim, S. H. Cho, *Org. Process Res. Dev.* **2019**, *23*, 1663–1668.
- [60] J. Kim, M. Shin, S. H. Cho, *ACS Catal.* **2019**, *9*, 8503–8508.
- [61] Y. Shi, A. H. Hoveyda, *Angew. Chem. Int. Ed.* **2016**, *55*, 3455–3458.
- [62] M. Zhan, R.-Z. Li, Z.-D. Mou, C.-G. Cao, J. Liu, Y.-W. Chen, D. Niu, *ACS Catal.* **2016**, *6*, 3381–3386.
- [63] M. Kim, B. Park, M. Shin, S. Kim, J. Kim, M.-H. Baik, S. H. Cho, *J. Am. Chem. Soc.* **2021**, *143*, 1069–1077.
- [64] M. G. P. Buffat, *Tetrahedron* **2004**, *60*, 1701–1729.

- [65] D. Passarella, A. Barilli, F. Belinghieri, P. Fassi, S. Riva, A. Sacchetti, A. Silvani, B. Danieli, *Tetrahedron Asymmetry* **2005**, *16*, 2225–2229.
- [66] J. C. Green, J. M. Zanghi, S. J. Meek, *J. Am. Chem. Soc.* **2020**, *142*, 1704–1709.
- [67] J. M. Zanghi, S. J. Meek, *Angew. Chem. Int. Ed.* **2020**, *59*, 8451–8455.
- [68] M. Z. Liang, S. J. Meek, *J. Am. Chem. Soc.* **2020**, *142*, 9925–9931.
- [69] E. Wheatley, J. M. Zanghi, S. J. Meek, *Org. Lett.* **2020**, *22*, 9269–9275.
- [70] T. Miura, J. Nakahashi, M. Murakami, *Angew. Chem. Int. Ed.* **2017**, *56*, 6989–6993.
- [71] T. Miura, J. Nakahashi, W. Zhou, Y. Shiratori, S. G. Stewart, M. Murakami, *J. Am. Chem. Soc.* **2017**, *139*, 10903–10908.
- [72] T. Miura, N. Oku, M. Murakami, *Angew. Chem.* **2019**, *131*, 14762–14766.
- [73] T. Miura, N. Oku, Y. Shiratori, Y. Nagata, M. Murakami, *Chem. – Eur. J.* **2021**, *27*, 3861–3868.
- [74] S. Gao, M. Duan, Q. Shao, K. N. Houk, M. Chen, *J. Am. Chem. Soc.* **2020**, *142*, 18355–18368.
- [75] M. Shimizu, H. Kitagawa, T. Kurahashi, T. Hiyama, *Angew. Chem. Int. Ed.* **2001**, *40*, 4283–4286.
- [76] M. Shimizu, T. Kurahashi, H. Kitagawa, K. Shimono, T. Hiyama, *J. Organomet. Chem.* **2003**, *686*, 286–293.
- [77] C. Bomio, M. A. Kabeshov, A. R. Lit, S.-H. Lau, J. Ehlert, C. Battilocchio, S. V. Ley, *Chem. Sci.* **2017**, *8*, 6071–6075.
- [78] C. Wu, Z. Bao, X. Xu, J. Wang, *Org. Biomol. Chem.* **2019**, *17*, 5714–5724.
- [79] D. J. S. Tsai, D. S. Matteson, *Organometallics* **1983**, *2*, 236–241.
- [80] V. K. Aggarwal, M. Binanzer, M. C. de Ceglie, M. Gallanti, B. W. Glasspoole, S. J. F. Kendrick, R. P. Sonawane, A. Vázquez-Romero, M. P. Webster, *Org. Lett.* **2011**, *13*, 1490–1493.
- [81] A. Millán, P. D. Grigol Martinez, V. K. Aggarwal, *Chem. – Eur. J.* **2018**, *24*, 730–735.
- [82] T. Bootwicha, J. M. Feilner, E. L. Myers, V. K. Aggarwal, *Nat. Chem.* **2017**, *9*, 896–902.
- [83] R. W. Hoffmann, G. Dahmann, M. W. Andersen, *Synthesis* **1994**, *1994*, 629–638.
- [84] B. Cheng, D. Trauner, *J. Am. Chem. Soc.* **2015**, *137*, 13800–13803.
- [85] M. Chen, W. R. Roush, *J. Am. Chem. Soc.* **2012**, *134*, 3925–3931.
- [86] C. Allais, P. Nuhant, W. R. Roush, *Org. Lett.* **2013**, *15*, 3922–3925.
- [87] T. J. Harrison, S. Ho, J. L. Leighton, *J. Am. Chem. Soc.* **2011**, *133*, 7308–7311.
- [88] M. Chen, W. R. Roush, *Org. Lett.* **2013**, *15*, 1662–1665.
- [89] F. Meng, H. Jang, A. H. Hoveyda, *Chem. – Eur. J.* **2013**, *19*, 3204–3214.
- [90] B. Hu, S. Xing, J. Ren, Z. Wang, *Tetrahedron* **2010**, *66*, 5671–5674.
- [91] D. Sarkar, R. V. Venkateswaran, *Tetrahedron Lett.* **2011**, *52*, 3232–3233.
- [92] A. A. Szymaniak, C. Zhang, J. R. Coombs, J. P. Morken, *ACS Catal.* **2018**, *8*, 2897–2901.
- [93] E. Rémond, C. Martin, J. Martinez, F. Cavelier, *Chem. Rev.* **2016**, *116*, 11654–11684.
- [94] J. Cossrow, S. D. Rychnovsky, *Org. Lett.* **2002**, *4*, 147–150.
- [95] J. Park, Y. Jung, J. Kim, E. Lee, S. Y. Lee, S. H. Cho, *Adv. Synth. Catal.* **2021**, *363*, 2371–2376.
- [96] J. Kim, S. H. Cho, *ACS Catal.* **2019**, *9*, 230–235.

- [97] C. E. Masse, J. S. Panek, *Chem. Rev.* **1995**, *95*, 1293–1316.
- [98] L. Chabaud, P. James, Y. Landais, *Eur. J. Org. Chem.* **2004**, *2004*, 3173–3199.
- [99] T. Hayashi, M. Konishi, H. Ito, M. Kumada, *J. Am. Chem. Soc.* **1982**, *104*, 4962–4963.
- [100] T. Hayashi, Y. Okamoto, M. Kumada, *Tetrahedron Lett.* **1983**, *24*, 807–808.
- [101] T. Hayashi, M. Konishi, Y. Okamoto, K. Kabeta, M. Kumada, *J. Org. Chem.* **1986**, *51*, 3772–3781.
- [102] P. C. Wailes, H. Weigold, *J. Organomet. Chem.* **1970**, *24*, 405–411.
- [103] S. L. Buchwald, S. J. LaMaire, R. B. Nielsen, B. T. Watson, S. M. King, *Tetrahedron Lett.* **1987**, *28*, 3895–3898.
- [104] B. H. Lipshutz, R. Keil, E. L. Ellsworth, *Tetrahedron Lett.* **1990**, *31*, 7257–7260.
- [105] B. Zheng, M. Srebnik, *Tetrahedron Lett.* **1993**, *34*, 4133–4136.
- [106] S. Pereira, M. Srebnik, *J. Org. Chem.* **1995**, *60*, 4316–4317.
- [107] B. Zheng, L. Deloux, S. Pereira, E. Skrzypczak-Jankun, B. V. Cheesman, M. Sabat, M. Srebnik, *Appl. Organomet. Chem.* **1996**, *10*, 267–278.
- [108] S. Pereira, M. Srebnik, *Tetrahedron Lett.* **1995**, *36*, 1805–1808.
- [109] C. Yang, Y. Gao, S. Bai, C. Jiang, X. Qi, *J. Am. Chem. Soc.* **2020**, *142*, 11506–11513.
- [110] B. Zheng, M. Srebnik, *Tetrahedron Lett.* **1994**, *35*, 6247–6250.
- [111] M. M. Midland, S. Greer, A. Tramontano, S. A. Zderic, *J. Am. Chem. Soc.* **1979**, *101*, 2352–2355.
- [112] E. J. Corey, J. O. Link, *Tetrahedron Lett.* **1989**, *30*, 6275–6278.
- [113] D. Miyazaki, K. Nomura, H. Ichihara, Y. Ohtsuka, T. Ikeno, T. Yamada, *New J. Chem.* **2003**, *27*, 1164–1166.
- [114] H. C. Brown, B. Singaram, *Pure Appl. Chem.* **1987**, *59*, 879–894.
- [115] D. G. Hall, J. C. H. Lee, J. Ding, *Pure Appl. Chem.* **2012**, *84*, 2263–2277.
- [116] H. K. Scott, V. K. Aggarwal, *Chem. – Eur. J.* **2011**, *17*, 13124–13132.
- [117] C. Sandford, V. K. Aggarwal, *Chem. Commun.* **2017**, *53*, 5481–5494.
- [118] P. Knochel, *J. Am. Chem. Soc.* **1990**, *112*, 7431–7433.
- [119] M. J. Rozema, A. Sidduri, P. Knochel, *J. Org. Chem.* **1992**, *57*, 1956–1958.
- [120] M. Sakai, S. Saito, G. Kanai, A. Suzuki, N. Miyaoura, *Tetrahedron* **1996**, *52*, 915–924.
- [121] M. Nakamura, K. Hara, T. Hatakeyama, E. Nakamura, *Org. Lett.* **2001**, *3*, 3137–3140.
- [122] M. Nakamura, T. Hatakeyama, K. Hara, H. Fukudome, E. Nakamura, *J. Am. Chem. Soc.* **2004**, *126*, 14344–14345.
- [123] T. Hatakeyama, M. Nakamura, E. Nakamura, *J. Am. Chem. Soc.* **2008**, *130*, 15688–15701.
- [124] L. E. Wilbanks, H. E. Hennigan, C. D. Martinez-Brokaw, H. Lakkis, S. Thormann, A. S. Eggly, G. Buechel, E. I. Parkinson, *ACS Chem. Biol.* **2023**, *18*, 1624–1631.
- [125] R. R. A. Freund, P. Gobrecht, Z. Rao, J. Gerstmeier, R. Schlosser, H. Görls, O. Werz, D. Fischer, H.-D. Arndt, *Chem. Sci.* **2019**, *10*, 7358–7364.
- [126] S. Plunkett, C. H. Basch, S. O. Santana, M. P. Watson, *J. Am. Chem. Soc.* **2019**, *141*, 2257–2262.

- [127] R. R. A. Freund, M. van den Borg, D. Gaissmaier, R. Schlosser, T. Jacob, H.-D. Arndt, *Chem. – Eur. J.* **2020**, *26*, 8639–8650.
- [128] P. Guo, H. Jin, J. Han, L. Xu, P. Li, M. Zhan, *Org. Lett.* **2023**, *25*, 1268–1273.
- [129] P. Guo, M. Zhan, *J. Org. Chem.* **2021**, *86*, 9905–9913.
- [130] C. Zhang, W. Hu, G. J. Lovinger, J. Jin, J. Chen, J. P. Morken, *J. Am. Chem. Soc.* **2021**, *143*, 14189–14195.
- [131] L.-Q. Wang, *J. Chromatogr. B* **2002**, *777*, 289–309.
- [132] A. V. Mali, S. B. Padhye, S. Anant, M. V. Hegde, S. S. Kadam, *Eur. J. Pharmacol.* **2019**, *852*, 107–124.
- [133] N. Gulavita, A. Hori, Y. Shimizu, P. Laszlo, J. Clardy, *Tetrahedron Lett.* **1988**, *29*, 4381–4384.
- [134] C. E. Tucker, P. Knochel, *J. Am. Chem. Soc.* **1991**, *113*, 9888–9890.
- [135] D. W. Hart, J. Schwartz, *J. Am. Chem. Soc.* **1974**, *96*, 8115–8116.
- [136] J. Schwartz, J. A. Labinger, *Angew. Chem. Int. Ed. Engl.* **1976**, *15*, 333–340.
- [137] C. Yang, C. Jiang, X. Qi, *Synthesis* **2021**, *53*, 1061–1076.
- [138] V. M. Dembitsky, M. Srebnik, in *Titan. Zircon. Org. Synth.* (Ed.: I. Marek), Wiley-VCH Verlag GmbH & Co. KGaA, Weinheim, FRG, **2002**, pp. 230–281.
- [139] C. E. Tucker, B. Greve, W. Klein, P. Knochel, *Organometallics* **1994**, *13*, 94–101.
- [140] E. Frankland, *Liebigs Ann. Chem.* **1849**, *71*, 171–213.
- [141] Paul. Knochel, R. D. Singer, *Chem. Rev.* **1993**, *93*, 2117–2188.
- [142] E. Erdik, *Organozinc Reagents in Organic Synthesis*, CRC Press, **1996**.
- [143] Z. Rappoport, I. Marek, *The Chemistry of Organozinc Compounds: R-Zn*, John Wiley & Sons, **2007**.
- [144] P. Knochel, H. Leuser, L. Cong, S. Perrone, F. F. Kneisel, in *Handb. Funct. Organomet.* (Ed.: P. Knochel), Wiley, **2005**, pp. 251–346.
- [145] M. M. Heravi, E. Hashemi, N. Nazari, *Mol. Divers.* **2014**, *18*, 441–472.
- [146] A. Sidduri, J. W. Tilley, N. Fotouhi, *Synthesis* **2014**, *46*, 430–444.
- [147] J. H. Kim, Y. O. Ko, J. Bouffard, S. Lee, *Chem. Soc. Rev.* **2015**, *44*, 2489–2507.
- [148] M. Gaudemar, *C. R. Acad. Sci. Paris.* **1971**, *273*, 1669–1672.
- [149] I. Marek, J.-F. Normant, in *Met.-Catalyzed Cross-Coupling React.*, Stang, P. J., Diederich, J., Eds.; Wiley-VCH, Weinheim, **1998**, pp. 271–337.
- [150] J. F. Normant, *Acc. Chem. Res.* **2001**, *34*, 640–644.
- [151] P. Knochel, J. F. Normant, *Tetrahedron Lett.* **1986**, *27*, 1039–1042.
- [152] P. Knochel, J. F. Normant, *Tetrahedron Lett.* **1986**, *27*, 1043–1046.
- [153] P. Knochel, J. F. Normant, *Tetrahedron Lett.* **1986**, *27*, 4427–4430.
- [154] P. Knochel, J. F. Normant, *Tetrahedron Lett.* **1986**, *27*, 4431–4434.
- [155] P. Knochel, J. F. Normant, *Tetrahedron Lett.* **1986**, *27*, 5727–5730.
- [156] I. Marek, J.-M. Lefrancois, J.-F. Normant, *J. Org. Chem.* **1994**, *59*, 4154–4161.
- [157] Yoshinori. Yamamoto, Naoki. Asao, *Chem. Rev.* **1993**, *93*, 2207–2293.

- [158] I. Marek, P. R. Schreiner, J. F. Normant, *Org. Lett.* **1999**, *1*, 929–931.
- [159] A. Hirai, M. Nakamura, E. Nakamura, *J. Am. Chem. Soc.* **1999**, *121*, 8665–8666.
- [160] A. Hirai, M. Nakamura, E. Nakamura, *J. Am. Chem. Soc.* **2000**, *122*, 11791–11798.
- [161] P. C. Andrews, C. L. Raston, B. W. Skelton, A. H. White, *Organometallics* **1998**, *17*, 779–782.
- [162] D. Brasseur, I. Marek, J.-F. Normant, *Tetrahedron* **1996**, *52*, 7235–7250.
- [163] I. Marek, J. F. Normant, *Tetrahedron Lett.* **1991**, *32*, 5973–5976.
- [164] I. Marek, J.-M. Lefrancois, J. F. Normant, *ChemInform* **1994**, *131*, 910–918.
- [165] S. Cheramy, F. Ferreira, J. F. Normant, *Tetrahedron Lett.* **2004**, *45*, 4549–4552.
- [166] A. Bähr, I. Marek, J.-F. Normant, *Tetrahedron Lett.* **1996**, *37*, 5873–5876.
- [167] N. Bernard, F. Chemla, F. Ferreira, N. Mostefai, J.-F. Normant, *Chem. – Eur. J.* **2002**, *8*, 3139–3147.
- [168] D. Brasseur, H. Rezaei, A. Fuxa, A. Alexakis, P. Mangeney, I. Marek, J. F. Normant, *Tetrahedron Lett.* **1998**, *39*, 4821–4824.
- [169] D. Brasseur, I. Marek, J. F. Normant, *Comptes Rendus Académie Sci. - Ser. IIC - Chem.* **1998**, *1*, 621–625.
- [170] I. Marek, A. Alexakis, J.-F. Normant, *Tetrahedron Lett.* **1991**, *32*, 5329–5332.
- [171] J. F. Normant, J. Ch. Quirion, A. Alexakis, Y. Masuda, *Tetrahedron Lett.* **1989**, *30*, 3955–3958.
- [172] P. Knochel, C. Xiao, M. C. P. Yeh, *Tetrahedron Lett.* **1988**, *29*, 6697–6700.
- [173] F. Ferreira, J. F. Normant, *Eur. J. Org. Chem.* **2000**, *2000*, 3581–3585.
- [174] K. Fujita, K. Mori, *Biosci. Biotechnol. Biochem.* **2001**, *65*, 1429–1433.
- [175] H. E. Simmons, R. D. Smith, *J. Am. Chem. Soc.* **1958**, *80*, 5323–5324.
- [176] H. E. Simmons, T. L. Cairns, S. A. Vladuchick, C. M. Hoiness, in *Org. React.*, John Wiley & Sons, Ltd, **2011**, pp. 1–131.
- [177] P. Turnbull, K. Syhora, J. H. Fried, *J. Am. Chem. Soc.* **1966**, *88*, 4764–4766.
- [178] H. Hashimoto, M. Hida, S. Miyano, *Kogyo Kagaku Zasshi* **1966**, *69*, 174.
- [179] H. Hashimoto, M. Hida, S. Miyano, *J. Organomet. Chem.* **1967**, *10*, 518–520.
- [180] S. Miyano, M. Hida, H. Hashimoto, *J. Organomet. Chem.* **1968**, *12*, 263–268.
- [181] L. N. Nysted, *Methylenation Reagent*, **1975**, US3865848A.
- [182] L. N. Nysted, *Chem. Abstr.* **1975**, *83*, 10406q.
- [183] W. Tochtermann, S. Bruhn, M. Meints, C. Wolff, E.-M. Peters, K. Peters, H. G. von Schnering, *Tetrahedron* **1995**, *51*, 1623–1630.
- [184] S. Matsubara, M. Sugihara, K. Utimoto, *Synlett* **1998**, *09*, 313–315.
- [185] M. Tanaka, M. Imai, M. Fujio, E. Sakamoto, M. Takahashi, Y. Eto-Kato, X. M. Wu, K. Funakoshi, K. Sakai, H. Suemune, *J. Org. Chem.* **2000**, *65*, 5806–5816.
- [186] C. Aïssa, R. Riveiros, J. Ragot, A. Fürstner, *J. Am. Chem. Soc.* **2003**, *125*, 15512–15520.
- [187] J. S. Clark, F. Marlin, B. Nay, C. Wilson, *Org. Lett.* **2003**, *5*, 89–92.

- [188] L. A. Paquette, R. E. Hartung, J. E. Hofferberth, I. Vilotijevic, J. Yang, *J. Org. Chem.* **2004**, *69*, 2454–2460.
- [189] S. Hanessian, E. Mainetti, F. Lecomte, *Org. Lett.* **2006**, *8*, 4047–4049.
- [190] A. Haahr, Z. Rankovic, R. C. Hartley, *Tetrahedron Lett.* **2011**, *52*, 3020–3022.
- [191] B. Barnych, B. Fenet, J.-M. Vattelè, *Tetrahedron* **2013**, *69*, 334–340.
- [192] K. Takai, Y. Hotta, K. Oshima, H. Nozaki, *Tetrahedron Lett.* **1978**, *19*, 2417–2420.
- [193] J. Hibino, T. Okazoe, K. Takai, H. Nozaki, *Tetrahedron Lett.* **1985**, *26*, 5579–5580.
- [194] K. Takai, T. Kakiuchi, Y. Kataoka, K. Utimoto, *J. Org. Chem.* **1994**, *59*, 2668–2670.
- [195] S. Matsubara, T. Mizuno, T. Otake, M. Kobata, K. Utimoto, K. Takai, *Synlett* **1998**, *1998*, 1369–1371.
- [196] S. Matsubara, K. Oshima, H. Matsuoka, K. Matsumoto, K. Ishikawa, E. Matsubara, *Chem. Lett.* **2005**, *34*, 952–953.
- [197] S. Matsubara, H. Yoshino, Y. Yamamoto, K. Oshima, H. Matsuoka, K. Matsumoto, K. Ishikawa, E. Matsubara, *J. Organomet. Chem.* **2005**, *690*, 5546–5551.
- [198] G. Köbrich, A. Akhtar, F. Ansari, W. E. Breckoff, H. Büttner, W. Drischel, R. H. Fischer, K. Flory, H. Fröhlich, W. Goyert, H. Heinemann, I. Hornke, H. R. Merkle, H. Trapp, W. Zündorf, *Angew. Chem. Int. Ed. Engl.* **1967**, *6*, 41–52.
- [199] V. H. Gessner, *Chem. Commun.* **2016**, *52*, 12011–12023.
- [200] S. Matsubara, *J. Synth. Org. Chem. Jpn.* **2000**, *58*, 108–113.
- [201] S. Matsubara, Y. Otake, T. Morikawa, K. Utimoto, *Synlett* **1998**, *1998*, 1315–1316.
- [202] S. Matsubara, Y. Otake, Y. Hashimoto, K. Utimoto, *Chem. Lett.* **1999**, *28*, 747–748.
- [203] S. Matsubara, H. Yoshino, K. Utimoto, K. Oshima, *Synlett* **2000**, *2000*, 495–496.
- [204] A. B. Charette, A. Gagnon, J.-F. Fournier, *J. Am. Chem. Soc.* **2002**, *124*, 386–387.
- [205] J.-F. Fournier, S. Mathieu, A. B. Charette, *J. Am. Chem. Soc.* **2005**, *127*, 13140–13141.
- [206] S. Trippett, *Q. Rev. Chem. Soc.* **1963**, *17*, 406–440.
- [207] B. E. Maryanoff, A. B. Reitz, *Chem. Rev.* **1989**, *89*, 863–927.
- [208] A. Maercker, in *Org. React.*, John Wiley & Sons, Ltd, **2011**, pp. 270–490.
- [209] L. Lombardo, *Tetrahedron Lett.* **1982**, *23*, 4293–4296.
- [210] A. R. Hermes, G. S. Girolami, R. A. Andersen, in *Inorg. Synth.*, John Wiley & Sons, Ltd, **1998**, pp. 309–310.
- [211] K. Ukai, D. Arioka, H. Yoshino, H. Fushimi, H. Fushini, K. Oshima, K. Utimoto, S. Matsubara, *Synlett* **2001**, *2001*, 513–514.
- [212] S. Matsubara, K. Ukai, T. Mizuno, K. Utimoto, *Chem. Lett.* **1999**, *28*, 825–826.
- [213] H. Yoshino, M. Kobata, Y. Yamamoto, K. Oshima, S. Matsubara, *Chem. Lett.* **2004**, *33*, 1224–1224.
- [214] T. Okazoe, K. Takai, K. Oshima, K. Utimoto, *J. Org. Chem.* **1987**, *52*, 4410–4412.
- [215] K. Takai, O. Fujimura, Y. Kataoka, K. Utimoto, *Tetrahedron Lett.* **1989**, *30*, 211–214.
- [216] J. Pietruszka, *Chem. Rev.* **2003**, *103*, 1051–1070.

- [217] L. A. Wessjohann, W. Brandt, T. Thiemann, *Chem. Rev.* **2003**, *103*, 1625–1648.
- [218] W. A. Donaldson, *Tetrahedron* **2001**, *57*, 8589–8627.
- [219] D. Y.-K. Chen, R. H. Pouwer, J.-A. Richard, *Chem. Soc. Rev.* **2012**, *41*, 4631–4642.
- [220] N. R. O'Connor, J. L. Wood, B. M. Stoltz, *Isr. J. Chem.* **2016**, *56*, 431–444.
- [221] J. Liu, R. Liu, Y. Wei, M. Shi, *Trends Chem.* **2019**, *1*, 779–793.
- [222] A. B. Charette, A. Beauchemin, in *Org. React.*, John Wiley & Sons, Ltd, **2004**, pp. 1–415.
- [223] Z. Yang, J. C. Lorenz, Y. Shi, *Tetrahedron Lett.* **1998**, *39*, 8621–8624.
- [224] A. B. Charette, A. Beauchemin, S. Francoeur, *J. Am. Chem. Soc.* **2001**, *123*, 8139–8140.
- [225] S. E. Denmark, J. P. Edwards, *J. Org. Chem.* **1991**, *56*, 6974–6981.
- [226] A. B. Charette, S. Francoeur, J. Martel, N. Wilb, *Angew. Chem. Int. Ed.* **2000**, *39*, 4539–4542.
- [227] M.-C. Lacasse, C. Poulard, A. B. Charette, *J. Am. Chem. Soc.* **2005**, *127*, 12440–12441.
- [228] F. Ferreira, C. Herse, E. Riguet, J. F. Normant, *Tetrahedron Lett.* **2000**, *41*, 1733–1736.
- [229] J. D. White, M. S. Jensen, *J. Am. Chem. Soc.* **1993**, *115*, 2970–2971.
- [230] D. G. Nagle, W. H. Gerwick, *J. Org. Chem.* **1994**, *59*, 7227–7237.
- [231] J. D. White, M. S. Jensen, *J. Am. Chem. Soc.* **1995**, *117*, 6224–6233.
- [232] T. Nagasawa, Y. Onoguchi, T. Matsumoto, K. Suzuki, *Synlett* **1995**, *1995*, 1023–1024.
- [233] G. Kumaraswamy, M. Padmaja, *J. Org. Chem.* **2008**, *73*, 5198–5201.
- [234] K. Ota, N. Sugata, Y. Ohshiro, E. Kawashima, H. Miyaoka, *Chem. – Eur. J.* **2012**, *18*, 13531–13537.
- [235] D. Beruben, I. Marek, J.-F. Normant, N. Platzter, *Tetrahedron Lett.* **1993**, *34*, 7575–7578.
- [236] D. Beruben, I. Marek, J. F. Normant, N. Platzter, *J. Org. Chem.* **1995**, *60*, 2488–2501.
- [237] K. Ukai, K. Oshima, S. Matsubara, *J. Am. Chem. Soc.* **2000**, *122*, 12047–12048.
- [238] S. Matsubara, K. Ukai, H. Fushimi, Y. Yokota, H. Yoshino, K. Oshima, K. Omoto, A. Ogawa, Y. Hioki, H. Fujimoto, *Tetrahedron* **2002**, *58*, 8255–8262.
- [239] K. Nomura, K. Oshima, S. Matsubara, *Tetrahedron Lett.* **2004**, *45*, 5957–5959.
- [240] K. Nomura, K. Asano, T. Kurahashi, S. Matsubara, *Heterocycles* **2008**, *76*, 1381–1399.
- [241] Y. Takada, K. Nomura, S. Matsubara, *Org. Lett.* **2010**, *12*, 5204–5205.
- [242] R. Haraguchi, Y. Takada, S. Matsubara, *Chem. Lett.* **2012**, *41*, 628–629.
- [243] R. Haraguchi, Y. Takada, S. Matsubara, *Org. Biomol. Chem.* **2015**, *13*, 241–247.
- [244] K. Nomura, K. Oshima, S. Matsubara, *Angew. Chem.* **2005**, *117*, 6010–6013.
- [245] K. Li, L. G. Hamann, M. Koreeda, *Tetrahedron Lett.* **1992**, *33*, 6569–6570.
- [246] T. Sato, T. Kikuchi, H. Tsujita, A. Kaetsu, N. Sootome, K. Nishida, K. Tachibana, E. Murayama, *Tetrahedron* **1991**, *47*, 3281–3304.
- [247] K. Nomura, S. Matsubara, *Chem. Lett.* **2007**, *36*, 164–165.
- [248] K. Cheng, P. J. Carroll, P. J. Walsh, *Org. Lett.* **2011**, *13*, 2346–2349.
- [249] N. Halland, A. Braunton, S. Bachmann, M. Marigo, K. A. Jørgensen, *J. Am. Chem. Soc.* **2004**, *126*, 4790–4791.
- [250] M. P. Brochu, S. P. Brown, D. W. C. MacMillan, *J. Am. Chem. Soc.* **2004**, *126*, 4108–4109.

- [251] T. Hirayama, K. Oshima, S. Matsubara, *Angew. Chem.* **2005**, *117*, 3357–3360.
- [252] M. Sada, S. Matsubara, *J. Am. Chem. Soc.* **2010**, *132*, 432–433.
- [253] M. Sada, T. Furuyama, S. Komagawa, M. Uchiyama, S. Matsubara, *Chem. – Eur. J.* **2010**, *16*, 10474–10481.
- [254] R. Otto, H. Ostrop, *Ann. Chem. Pharm.* **1866**, *141*, 372.
- [255] F. Chemla, I. Marek, J.-F. Normant, *Synlett* **1993**, *1993*, 665–666.
- [256] T. Harada, D. Hara, K. Hattori, A. Oku, *Tetrahedron Lett.* **1988**, *29*, 3821–3824.
- [257] T. Harada, K. Hattori, T. Katsuhira, A. Oku, *Tetrahedron Lett.* **1989**, *30*, 6035–6038.
- [258] T. Harada, T. Katsuhira, D. Hara, Y. Kotani, K. Maejima, R. Kaji, A. Oku, *J. Org. Chem.* **1993**, *58*, 4897–4907.
- [259] T. Harada, T. Katsuhira, K. Hattori, A. Oku, *J. Org. Chem.* **1993**, *58*, 2958–2965.
- [260] T. Harada, T. Kaneko, T. Fujiwara, A. Oku, *Tetrahedron* **1998**, *54*, 9317–9332.
- [261] H. Yoshino, N. Toda, M. Kobata, K. Ukai, K. Oshima, K. Utimoto, S. Matsubara, *Chem. – Eur. J.* **2006**, *12*, 721–726.
- [262] J. M. Coxon, S. J. van Eyk, P. J. Steel, *Tetrahedron* **1989**, *45*, 1029–1041.
- [263] Y. Shimada, R. Haraguchi, S. Matsubara, *Synlett* **2015**, *26*, 2395–2398.
- [264] S. Matsubara, K. Ukai, N. Toda, K. Utimoto, K. Oshima, *Synlett* **2000**, *2000*, 995–996.
- [265] Z. Ikeda, K. Oshima, S. Matsubara, *Org. Lett.* **2005**, *7*, 4859–4861.
- [266] S. Matsubara, K. Kawamoto, K. Utimoto, *Synlett* **1998**, *09*, 267–268.
- [267] S. Matsubara, Y. Yamamoto, K. Utimoto, *Synlett* **1999**, *1999*, 1471–1473.
- [268] H. Tokuyama, S. Yokoshima, T. Yamashita, T. Fukuyama, *Tetrahedron Lett.* **1998**, *39*, 3189–3192.
- [269] S. Sikandar, A. F. Zahoor, S. Naheed, B. Parveen, K. G. Ali, R. Akhtar, *Mol. Divers.* **2022**, *26*, 589–628.
- [270] Z. Ikeda, T. Hirayama, S. Matsubara, *Angew. Chem.* **2006**, *118*, 8380–8383.
- [271] R. Haraguchi, Z. Ikeda, A. Ooguri, S. Matsubara, *Tetrahedron* **2015**, *71*, 8830–8837.
- [272] A. Ooguri, Z. Ikeda, S. Matsubara, *Chem. Commun.* **2007**, *0*, 4761–4763.
- [273] P. Brownbridge, *Synthesis* **1983**, *1983*, 1–28.
- [274] P. Brownbridge, *Synthesis* **1983**, *1983*, 85–104.
- [275] J.-M. Poirier, *Org. Prep. Proced. Int.* **1988**, *20*, 317–369.
- [276] S. Matsubara, D. Arioka, K. Utimoto, *Synlett* **1999**, *1999*, 1253–1254.
- [277] Y. Shimada, Z. Ikeda, S. Matsubara, *Org. Lett.* **2017**, *19*, 3335–3337.
- [278] R. Haraguchi, S. Matsubara, *Org. Lett.* **2013**, *15*, 3378–3380.
- [279] R. Haraguchi, S. Matsubara, *Synthesis* **2014**, *46*, 2272–2282.
- [280] M. L. Hlavinka, J. R. Hagadorn, *Organometallics* **2005**, *24*, 4116–4118.
- [281] S. Ueno, M. Sada, S. Matsubara, *Chem. Lett.* **2010**, *39*, 96–97.
- [282] M. Sada, K. Nomura, S. Matsubara, *Org. Biomol. Chem.* **2011**, *9*, 1389–1393.
- [283] S. Matsubara, H. Yamamoto, D. Arioka, K. Utimoto, K. Oshima, *Synlett* **2000**, *2000*, 1202–1204.



- [284] P. Beak, A. Basu, D. J. Gallagher, Y. S. Park, S. Thayumanavan, *Acc. Chem. Res.* **1996**, *29*, 552–560.
- [285] D. Hoppe, T. Hense, *Angew. Chem. Int. Ed. Engl.* **1997**, *36*, 2282–2316.
- [286] A. Boudier, P. Knochel, *Tetrahedron Lett.* **1999**, *40*, 687–690.
- [287] E. Hupe, M. I. Calaza, P. Knochel, *J. Organomet. Chem.* **2003**, *680*, 136–142.
- [288] R. W. Hoffmann, *Chem. Soc. Rev.* **2003**, *32*, 225–230.
- [289] S. Matsubara, N. Toda, M. Kobata, K. Utimoto, *Synlett* **2000**, *2000*, 987–988.
- [290] C. Zhang, W. Hu, J. P. Morken, *ACS Catal.* **2021**, *11*, 10660–10680.
- [291] C.-Y. Wang, J. Derosa, M. R. Biscoe, *Chem. Sci.* **2015**, *6*, 5105–5113.
- [292] L.-W. Xu, L. Li, G.-Q. Lai, J.-X. Jiang, *Chem. Soc. Rev.* **2011**, *40*, 1777–1790.
- [293] K. Igawa, K. Tomooka, in *Organosilicon Chem.*, John Wiley & Sons, Ltd, **2019**, pp. 495–532.
- [294] A. Guijarro, “Dynamic Behavior of Organozinc Compounds”, in *Chem. Organozinc Compd.*, John Wiley & Sons, Ltd, **2006**, pp. 193–236.
- [295] G. Binsch, E. L. Eliel, H. Kessler, *Angew. Chem. Int. Ed. Engl.* **1971**, *10*, 570–572.
- [296] M. Witanowski, J. D. Roberts, *J. Am. Chem. Soc.* **1966**, *88*, 737–741.
- [297] G. M. Whitesides, M. Witanowski, J. D. Roberts, *J. Am. Chem. Soc.* **1965**, *87*, 2854–2862.
- [298] M. Witanowski, J. D. Roberts, *J. Am. Chem. Soc.* **1966**, *88*, 737–741.
- [299] R. F. W. Jackson, R. J. Moore, C. S. Dexter, J. Elliott, C. E. Mowbray, *J. Org. Chem.* **1998**, *63*, 7875–7884.
- [300] M. Oki, “Applications of Dynamic NMR Spectroscopy to Organic Chemistry”, in *Methods Stereochem. Anal.*, Ed. A. P. Marchand, VCH, Deerfield Beach, FL, **1985**.
- [301] R. Duddu, M. Eckhardt, M. Furlong, H. P. Knoess, S. Berger, P. Knochel, *Tetrahedron* **1994**, *50*, 2415–2432.
- [302] C. Darcel, F. Flachsmann, P. Knochel, *Chem. Commun.* **1998**, *0*, 205–206.
- [303] A. Boudier, F. Flachsmann, P. Knochel, *Synlett* **1998**, *1998*, 1438–1440.
- [304] A. Boudier, C. Darcel, F. Flachsmann, L. Micouin, M. Oestreich, P. Knochel, *Chem. – Eur. J.* **2000**, *6*, 2748–2761.
- [305] P. Knochel, A. Boudier, L. O. Bromm, E. Hupe, J. A. Varela, A. Rodriguez, C. Koradin, T. Bunlaksananusorn, H. Laaziri, F. Lhermitte, *Pure Appl. Chem.* **2000**, *72*, 1699–1703.
- [306] J. Skotnitzki, A. Kremsmair, D. Keefer, Y. Gong, R. de Vivie-Riedle, P. Knochel, *Angew. Chem. Int. Ed.* **2020**, *59*, 320–324.
- [307] H. Liang, J. P. Morken, *J. Am. Chem. Soc.* **2023**, *145*, 9976–9981.
- [308] A. Guijarro, R. D. Rieke, *Angew. Chem. Int. Ed.* **2000**, *39*, 1475–1479.
- [309] D. Parker, *Chem. Rev.* **1991**, *91*, 1441–1457.
- [310] R. W. Hoffmann, W. Klute, R. K. Dress, A. Wenzel, *J. Chem. Soc. Perkin Trans. 2* **1995**, *0*, 1721–1726.
- [311] E. L. Eliel, N. L. Allinger, S. G. Angyal, G. A. Morrison, *Conformational Analysis*, Interscience Publishers, New York, **1965**.

- [312] J. A. Hirsch, *Topics in Stereochemistry*, John Wiley & Sons, Inc., **1967**.
- [313] C. Romers, C. Altona, H. R. Buys, E. Havinga, *Topics in Stereochemistry*, John Wiley & Sons, Inc., New York, **1969**.
- [314] E. L. Eliel, S. H. Wilen, L. N. Mander, *Stereochemistry of Organic Compounds*, Wiley, New York, **1994**.
- [315] A. Guijarro, R. D. Rieke, *Angew. Chem. Int. Ed.* **1998**, *37*, 1679–1681.
- [316] A. Guijarro, D. M. Rosenberg, R. D. Rieke, *J. Am. Chem. Soc.* **1999**, *121*, 4155–4167.
- [317] S. Klein, I. Marek, J.-F. Normant, *J. Org. Chem.* **1994**, *59*, 2925–2926.
- [318] S. Norsikian, I. Marek, S. Klein, J. F. Poisson, J. F. Normant, *Chem. – Eur. J.* **1999**, *5*, 2055–2068.
- [319] J. L. Wardell, in *Compr. Organomet. Chem.* (Eds.: G. Wilkinson, F.G.A. Stone, E.W. Abel), Pergamon, Oxford, **1982**, pp. 43–120.
- [320] R. W. Hoffmann, T. Rühl, F. Chemla, T. Zahneisen, *Liebigs Ann. Chem.* **1992**, *1992*, 719–724.
- [321] T. Kato, S. Marumoto, T. Sato, I. Kuwajima, *Synlett* **1990**, *1990*, 671–672.
- [322] S. Marumoto, I. Kuwajima, *Chem. Lett.* **1992**, *21*, 1421–1424.
- [323] Paul. Knochel, R. D. Singer, *Chem. Rev.* **1993**, *93*, 2117–2188.
- [324] T. Hayashi, T. Hagihara, Y. Katsuro, M. Kumada, *Bull. Chem. Soc. Jpn.* **1983**, *56*, 363–364.
- [325] R. Oost, A. Misale, N. Maulide, *Angew. Chem.* **2016**, *128*, 4663–4666.
- [326] D. Hoppe, A. Carstens, T. Krámer, *Angew. Chem. Int. Ed. Engl.* **1990**, *29*, 1424–1425.
- [327] H. D. Visser, J. P. Oliver, *J. Organomet. Chem.* **1972**, *40*, 7–14.
- [328] J. A. Marshall, P. Eidam, *Org. Lett.* **2004**, *6*, 445–448.
- [329] S. W. Hansen, T. D. Spawn, D. J. Burton, *J. Fluor. Chem.* **1987**, *35*, 415–420.
- [330] Q. Liu, D. J. Burton, *Tetrahedron Lett.* **2000**, *41*, 8045–8048.
- [331] E. G. Hoffmann, H. Nehl, H. Lehmkuhl, K. Seevogel, W. Stempfle, *Chem. Ber.* **1984**, *117*, 1364–1377.
- [332] K.-H. Thiele, D. Gaudig, *Z. Für Anorg. Allg. Chem.* **1969**, *365*, 301–307.
- [333] H. J. Reich, J. E. Holladay, T. G. Walker, J. L. Thompson, *J. Am. Chem. Soc.* **1999**, *121*, 9769–9780.
- [334] B. W. Gung, X. Xue, N. Knatz, J. A. Marshall, *Organometallics* **2003**, *22*, 3158–3163.
- [335] J.-F. Poisson, F. Chemla, J. F. Normant, *Synlett* **2001**, *2001*, 305–307.
- [336] J.-F. Poisson, J. F. Normant, *J. Am. Chem. Soc.* **2001**, *123*, 4639–4640.
- [337] J. A. Marshall, *J. Org. Chem.* **2007**, *72*, 8153–8166.
- [338] R. Unger, T. Cohen, I. Marek, *Tetrahedron* **2010**, *66*, 4874–4881.
- [339] J. Bejjani, C. Botuha, F. Chemla, F. Ferreira, S. Magnus, A. Pérez-Luna, *Organometallics* **2012**, *31*, 4876–4885.
- [340] T. Hayashi, T. Hagihara, Y. Katsuro, M. Kumada, *Bull. Chem. Soc. Jpn.* **1983**, *56*, 363–364.
- [341] T. Hayashi, A. Yamamoto, M. Hojo, Y. Ito, *J. Chem. Soc. Chem. Commun.* **1989**, *0*, 495–496.
- [342] T. Thaler, B. Haag, A. Gavryushin, K. Schober, E. Hartmann, R. M. Gschwind, H. Zipse, P. Mayer, P. Knochel, *Nat. Chem.* **2010**, *2*, 125–130.

- [343] T. Thaler, L.-N. Guo, P. Mayer, P. Knochel, *Angew. Chem. Int. Ed.* **2011**, *50*, 2174–2177.
- [344] A. H. Cherney, S. E. Reisman, *Tetrahedron* **2014**, *70*, 3259–3265.
- [345] R. Oost, A. Misale, N. Maulide, *Angew. Chem.* **2016**, *128*, 4663–4666.
- [346] R. L. Letsinger, C. W. Kammeyer, *J. Am. Chem. Soc.* **1951**, *73*, 4476.
- [347] A. Krasovskiy, P. Knochel, *Synthesis* **2006**, *2006*, 0890–0891.
- [348] C. L. Compton, K. R. Schmitz, R. T. Sauer, J. K. Sello, *ACS Chem. Biol.* **2013**, *8*, 2669–2677.
- [349] D. Herrera, D. Peral, M. Cordón, J. C. Bayón, *Eur. J. Inorg. Chem.* **2021**, *2021*, 354–363.
- [350] R. Appel, *Angew. Chem. Int. Ed. Engl.* **1975**, *14*, 801–811.
- [351] C. Han, S. L. Buchwald, *J. Am. Chem. Soc.* **2009**, *131*, 7532–7533.
- [352] C. Elschenbroich, *Organometallics*, Wiley-VCH, Weinheim, **2006**.
- [353] L. C. McCann, M. G. Organ, *Angew. Chem. Int. Ed.* **2014**, *53*, 4386–4389.
- [354] P. Eckert, S. Sharif, M. G. Organ, *Angew. Chem.* **2021**, *133*, 12332–12349.
- [355] G. T. Achonduh, N. Hadei, C. Valente, S. Avola, C. J. O'Brien, M. G. Organ, *Chem. Commun.* **2010**, *46*, 4109–4111.
- [356] L. C. McCann, H. N. Hunter, J. A. C. Clyburne, M. G. Organ, *Angew. Chem.* **2012**, *124*, 7130–7133.
- [357] P. Knochel, M. C. P. Yeh, S. C. Berk, J. Talbert, *J. Org. Chem.* **1988**, *53*, 2390–2392.
- [358] P. Knochel, N. Millot, A. L. Rodriguez, C. E. Tucker, in *Org. React.*, John Wiley & Sons, Ltd, **2004**, pp. 417–759.
- [359] Y. Mori, M. Seki, *Adv. Synth. Catal.* **2007**, *349*, 2027–2038.
- [360] R. Haraguchi, S. Tanazawa, N. Tokunaga, S. Fukuzawa, *Eur. J. Org. Chem.* **2018**, *2018*, 1761–1764.
- [361] C. Reichel, R. Brugger, H. Bang, G. Geisslinger, K. Brune, *Mol. Pharmacol.* **1997**, *51*, 576–582.
- [362] K. Williams, R. Day, R. Knihinicki, A. Duffield, *Biochem. Pharmacol.* **1986**, *35*, 3403–3405.
- [363] R. Kourist, P. D. de María, K. Miyamoto, *Green Chem.* **2011**, *13*, 2607–2618.
- [364] M.-W. Ha, S.-M. Paek, *Molecules* **2021**, *26*, 4792.
- [365] R. C. Fuson, B. A. Bull, *Chem. Rev.* **1934**, *15*, 275–309.
- [366] J. D. Brown, *Tetrahedron Asymmetry* **1992**, *3*, 1551–1552.
- [367] J. A. Bull, A. B. Charette, *J. Org. Chem.* **2008**, *73*, 8097–8100.
- [368] F. Banchini, B. Leroux, E. Le Gall, M. Presset, O. Jackowski, F. Chemla, A. Perez-Luna, *Chem. – Eur. J.* **2023**, *29*, e202301084.
- [369] I. Ojima, *Catalytic Asymmetric Synthesis*, John Wiley & Sons, **2010**.
- [370] B. M. Trost, M. L. Crawley, *Chem. Rev.* **2003**, *103*, 2921–2944.
- [371] W.-B. Liu, J.-B. Xia, S.-L. You, in *Transit. Met. Catalyzed Enantioselective Allylic Substit. Org. Synth.* (Ed.: U. Kazmaier), Springer, Berlin, Heidelberg, **2012**, pp. 155–207.
- [372] T. Hayashi, A. Okada, T. Suzuka, M. Kawatsura, *Org. Lett.* **2003**, *5*, 1713–1715.
- [373] B. M. Trost, C. A. Kalnals, D. Ramakrishnan, M. C. Ryan, R. W. Smaha, S. Parkin, *Org. Lett.* **2020**, *22*, 2584–2589.

- [374] M. Fañanás-Mastral, M. Pérez, P. H. Bos, A. Rudolph, S. R. Harutyunyan, B. L. Feringa, *Angew. Chem.* **2012**, *124*, 1958–1961.
- [375] V. Hornillos, S. Guduguntla, M. Fañanás-Mastral, M. Pérez, P. H. Bos, A. Rudolph, S. R. Harutyunyan, B. L. Feringa, *Nat. Protoc.* **2017**, *12*, 493–505.
- [376] A. Kar, N. P. Argade, *Synthesis* **2005**, *2005*, 2995–3022.
- [377] H. Yorimitsu, K. Oshima, *Angew. Chem. Int. Ed.* **2005**, *44*, 4435–4439.
- [378] Z. Rappoport, I. Marek, *The Chemistry of Organocopper Compounds*, John Wiley & Sons, **2009**.
- [379] C. A. Falciola, A. Alexakis, *Eur. J. Org. Chem.* **2008**, *2008*, 3765–3780.
- [380] E. S. M. Persson, M. van Klaveren, D. M. Grove, J. E. Bäckvall, G. van Koten, *Chem. – Eur. J.* **1995**, *1*, 351–359.
- [381] N. Yoshikai, E. Nakamura, *Chem. Rev.* **2012**, *112*, 2339–2372.
- [382] S. H. Bertz, S. Cope, M. Murphy, C. A. Ogle, B. J. Taylor, *J. Am. Chem. Soc.* **2007**, *129*, 7208–7209.
- [383] E. R. Bartholomew, S. H. Bertz, S. Cope, D. C. Dorton, M. Murphy, C. A. Ogle, *Chem. Commun.* **2008**, *0*, 1176–1177.
- [384] T. Gärtner, N. Yoshikai, M. Neumeier, E. Nakamura, R. M. Gschwind, *Chem. Commun.* **2010**, *46*, 4625–4626.
- [385] S. F. Hannigan, J. S. Lum, J. W. Bacon, C. Moore, J. A. Golen, A. L. Rheingold, L. H. Doerrer, *Organometallics* **2013**, *32*, 3429–3436.
- [386] M. Yamanaka, S. Kato, E. Nakamura, *J. Am. Chem. Soc.* **2004**, *126*, 6287–6293.
- [387] F. Dübner, P. Knochel, *Angew. Chem. Int. Ed.* **1999**, *38*, 379–381.
- [388] F. Dübner, P. Knochel, *Tetrahedron Lett.* **2000**, *41*, 9233–9237.
- [389] H. Malda, A. W. van Zijl, L. A. Arnold, B. L. Feringa, *Org. Lett.* **2001**, *3*, 1169–1171.
- [390] A. W. van Zijl, L. A. Arnold, A. J. Minnaard, B. L. Feringa, *Adv. Synth. Catal.* **2004**, *346*, 413–420.
- [391] C. A. Luchaco-Cullis, H. Mizutani, K. E. Murphy, A. H. Hoveyda, *Angew. Chem. Int. Ed.* **2001**, *40*, 1456–1460.
- [392] K. E. Murphy, A. H. Hoveyda, *J. Am. Chem. Soc.* **2003**, *125*, 4690–4691.
- [393] U. Piarulli, P. Daubos, C. Claverie, M. Roux, C. Gennari, *Angew. Chem.* **2003**, *115*, 244–246.
- [394] U. Piarulli, C. Claverie, P. Daubos, C. Gennari, A. J. Minnaard, B. L. Feringa, *Org. Lett.* **2003**, *5*, 4493–4496.
- [395] A. O. Larsen, W. Leu, C. N. Oberhuber, J. E. Campbell, A. H. Hoveyda, *J. Am. Chem. Soc.* **2004**, *126*, 11130–11131.
- [396] M. A. Kacprzynski, T. L. May, S. A. Kazane, A. H. Hoveyda, *Angew. Chem.* **2007**, *119*, 4638–4642.
- [397] J. A. Marshall, *Chem. Rev.* **2000**, *100*, 3163–3186.
- [398] A. Misale, S. Niyomchon, M. Luparia, N. Maulide, *Angew. Chem. Int. Ed.* **2014**, *53*, 7068–7073.
- [399] J. Y. Hamilton, D. Sarlah, E. M. Carreira, *Angew. Chem. Int. Ed.* **2015**, *54*, 7644–7647.
- [400] Y. Tamaru, S. Goto, A. Tanaka, M. Shimizu, M. Kimura, *Angew. Chem. Int. Ed. Engl.* **1996**, *35*, 878–880.

- [401] H. Yamamoto, K. Oshima, Eds. , *Main Group Metals in Organic Synthesis*, Wiley, **2004**.
- [402] Y. Nakao, T. Hiyama, *Chem. Soc. Rev.* **2011**, *40*, 4893–4901.
- [403] G. R. Jones, Y. Landais, *Tetrahedron* **1996**, *52*, 7599–7662.
- [404] K. Yoon, D. Y. Son, *J. Organomet. Chem.* **1997**, *545–546*, 185–189.
- [405] B. M. Trost, *J. Org. Chem.* **2004**, *69*, 5813–5837.
- [406] B. M. Trost, T. Zhang, J. D. Sieber, *Chem. Sci.* **2010**, *1*, 427–440.
- [407] I. Guerrero Rios, A. Rosas-Hernandez, E. Martin, *Molecules* **2011**, *16*, 970–1010.
- [408] A. Alexakis, C. Malan, L. Lea, K. Tissot-Croset, D. Polet, C. Falciola, *CHIMIA* **2006**, *60*, 124.
- [409] G. Desimoni, G. Faita, K. A. Jørgensen, *Chem. Rev.* **2006**, *106*, 3561–3651.
- [410] G. Desimoni, G. Faita, P. Quadrelli, *Chem. Rev.* **2003**, *103*, 3119–3154.
- [411] A. K. Ghosh, P. Mathivanan, J. Cappiello, *Tetrahedron Asymmetry* **1998**, *9*, 1–45.
- [412] A. Cornejo, J. M. Fraile, J. I. García, M. J. Gil, V. Martínez-Merino, J. A. Mayoral, E. Pires, I. Villalba, *Synlett* **2005**, 2321–2324.
- [413] R. Duddu, M. Eckhardt, M. Furlong, H. P. Knoess, S. Berger, P. Knochel, *Tetrahedron* **1994**, *50*, 2415–2432.
- [414] E. A. Brinkman, S. Berger, J. I. Brauman, *J. Am. Chem. Soc.* **1994**, *116*, 8304–8310.
- [415] D. M. Wetzel, J. I. Brauman, *J. Am. Chem. Soc.* **1988**, *110*, 8333–8336.
- [416] W. C. Still, C. Sreekumar, *J. Am. Chem. Soc.* **1980**, *102*, 1201–1202.
- [417] J. S. Sawyer, T. L. Macdonald, G. J. McGarvey, *J. Am. Chem. Soc.* **1984**, *106*, 3376–3377.
- [418] R. E. Gawley, G. C. Hart, L. J. Bartolotti, *J. Org. Chem.* **1989**, *54*, 175–181.
- [419] W. H. Pearson, A. C. Lindbeck, *J. Am. Chem. Soc.* **1991**, *113*, 8546–8548.
- [420] S. T. Kerrick, P. Beak, *J. Am. Chem. Soc.* **1991**, *113*, 9708–9710.
- [421] A. I. Meyers, G. Milot, *J. Am. Chem. Soc.* **1993**, *115*, 6652–6660.
- [422] P. G. Mcdougal, B. D. Condon, M. D. Jun. Laffosse, A. M. Lauro, D. Vanderveer, *ChemInform* **1988**, *19*, chin.198847065.
- [423] A. Krief, G. Evrard, E. Badaoui, V. De Beys, R. Dieden, *Tetrahedron Lett.* **1989**, *30*, 5635–5638.
- [424] H. J. Reich, M. D. Bowe, *J. Am. Chem. Soc.* **1990**, *112*, 8994–8995.
- [425] R. W. Hoffmann, M. Bewersdorf, *Liebigs Ann. Chem.* **1992**, *1992*, 643–653.
- [426] R. W. Hoffmann, R. K. Dress, T. Ruhland, A. Wenzel, *Chem. Ber.* **1995**, *128*, 861–870.
- [427] R. L. Letsinger, *J. Am. Chem. Soc.* **1950**, *72*, 4842–4842.
- [428] D. Y. Curtin, W. J. Koehl, *J. Am. Chem. Soc.* **1962**, *84*, 1967–1973.
- [429] H. Nozaki, T. Aratani, T. Toraya, R. Noyori, *Tetrahedron* **1971**, *27*, 905–913.
- [430] P. Beak, H. Du, *J. Am. Chem. Soc.* **1993**, *115*, 2516–2518.
- [431] S. Thayumanavan, S. Lee, C. Liu, P. Beak, *J. Am. Chem. Soc.* **1994**, *116*, 9755–9756.
- [432] D. Hoppe, O. Zschage, *Angew. Chem.* **1989**, *101*, 67–69.
- [433] B. Kaiser, D. Hoppe, *Angew. Chem. Int. Ed. Engl.* **1995**, *34*, 323–325.
- [434] W. Klute, R. Dress, R. W. Hoffmann, *J. Chem. Soc. Perkin Trans. 2* **1993**, *0*, 1409–1411.

[435] R. W. Hoffmann, W. Klute, R. K. Dress, A. Wenzel, *J. Chem. Soc. Perkin Trans. 2* **1995**, 0, 1721–1726.

[436] Md. Belal, Z. Li, X. Lu, G. Yin, *Sci. China Chem.* **2021**, 64, 513–533.







---

## Asymmetric Sequential Cross-Coupling Reactions with Prochiral Zinc-Based C(sp<sup>3</sup>)-Gem-Bimetallic Reagents

---

This thesis presents the development of asymmetric sequential cross-coupling reactions using prochiral C(sp<sup>3</sup>)-*gem*-dizinc reagents. While enantioselective consecutive cross-coupling reactions have been explored for various *gem*-bimetallics, a significant gap exists in the literature for 1,1-dizinc reagents. The motivation behind this work is the establishment of novel enantioselective sequential cross-coupling reactions employing these reagents to synthesize complex, optically active molecules in a modular fashion. The first part introduces a highly enantioselective palladium-catalyzed sequenced arylation/acylation of prochiral 1,1-bis(iodozinc)alkanes achieving  $\alpha$ -disubstituted ketones bearing enolizable tertiary stereocenters in excellent yields and enantiomeric ratios. In the second part, a significant advancement was attempted using silyl-substituted *gem*-dizinc reagents, potentially enabling three consecutive reactions in a single pot.

**Keywords:** *Gem*-Bimetallics, Cross-Coupling, Enantioselectivity, Sequential Reactions, Zinc

---

## Réactions de Couplage Croisé Séquentiel Asymétrique avec des Réactifs C(sp<sup>3</sup>)-Gem-Bimétalliques Prochiraux à Base de Zinc

---

Cette thèse présente le développement de réactions asymétriques de couplages croisés séquentiels à partir des réactifs prochiraux C(sp<sup>3</sup>)-*gem*-dizinc. Alors que la réalisation de deux couplages croisés consécutifs en version énantiosélective a été explorée pour divers composés *gem*-bimétalliques, dans la littérature, un manque significatif de travaux existe pour les réactifs 1,1-dizinc. Ce travail consiste ainsi en l'établissement de nouvelles réactions asymétriques de couplages croisés séquentiels en utilisant ces réactifs pour synthétiser des molécules complexes et optiquement actives de manière modulaire. La première partie présente une séquence arylation/acétylation pallado-catalysée hautement énantiosélective de 1,1-bis(iodozinc)alcanes prochiraux, conduisant à des cétones  $\alpha$ -disubstituées portant des centres stéréogènes tertiaires énoles avec d'excellents rendements et rapports énantiomériques. Dans la deuxième partie, une avancée significative a été tentée en utilisant des réactifs *gem*-dizinc silyl-substitués, permettant potentiellement trois réactions consécutives en une seule étape.

**Mots-clés:** *Gem*-Bimétalliques, Couplage Croisé, Énantiosélectivité, Réactions Séquentielles, Zinc